A STUDY OF PARAMETERS AFFECTING PROPERTIES OF TIRE TREAD COMPOUNDS

PUCHONG THAPTONG

A THESIS SUBMITTED IN PARTIAL FULFILLMENT
OF THE REQUIREMENTS FOR
THE DEGREE OF DOCTOR OF PHILOSOPHY
(POLYMER SCIENCE AND TECHNOLOGY)
FACULTY OF GRADUATE STUDIES
MAHIDOL UNIVERSITY
2016

Thesis
entitled

A STUDY OF PARAMETERS AFFECTING PROPERTIES OF TIRE TREAD COMPOUNDS

.....
Mr. Puchong Thaptong
Candidate

.....
Assoc. Prof. Chakrit Sirisinha,
Ph.D. (Rubber Engineering)
Major advisor

.....
Mr. Pongdhorn Sae-Oui,
Ph.D. (Rubber Engineering)
Co-advisor

.....
Mr. Pairote Jittham,
Ph.D. (Engineering)
Co-advisor

.....
Prof. Patcharee Lertrit,
M.D., Ph.D. (Biochemistry)
Dean
Faculty of Graduate Studies
Mahidol University

.....
Assoc. Prof. Sombat Thanawan,
Ph.D. (Polymer Materials and Composites)
Program Director
Doctor of Philosophy Program in
Polymer Science and Technology
Faculty of Science, Mahidol University

Thesis
entitled

A STUDY OF PARAMETERS AFFECTING PROPERTIES OF TIRE TREAD COMPOUNDS

was submitted to the Faculty of Graduate Studies, Mahidol University
for the degree of Doctor of Philosophy (Polymer Science and Technology)
on
December 6, 2016

Puchong Thaptong
.....
Mr. Puchong Thaptong
Candidate

Kanoktip Boonkerd
.....
Asst. Prof. Kanoktip Boonkerd,
Ph.D. (Polymer Science)
Chair

.....
Assoc. Prof. Chakrit Sirisinha,
Ph.D. (Rubber Engineering)
Member

Pongdhorn Saeoui
.....
Mr. Pongdhorn Sae-Oui,
Ph.D. (Rubber Engineering)
Member

.....
Mr. Pairote Jittham,
Ph.D. (Engineering)
Member

.....
Prof. Patcharee Lertrit,
M.D., Ph.D. (Biochemistry)
Dean
Faculty of Graduate Studies
Mahidol University

.....
Assoc. Prof. Sittiwat Lertsiri,
Ph.D. (Agricaltural Science)
Dean
Faculty of Science
Mahidol University

ACKNOWLEDGEMENTS

This dissertation could not have been completely successful without the kind supports of many people. Foremost, I would like to express my sincere appreciation to my supervisor, Assoc. Prof. Chakrit Sirisinha, for his excellent supervision, inspiring guidance and encouragement throughout the duration of my research work.

My profound gratitude is also expressed to the members of my advisory committees, Dr. Pongdhorn Sae-oui and Dr. Pairote Jittham, for their extremely valuable advices and comments for completion of this dissertation.

I would like to express my appreciation to Asst. Prof. Kanoktip Boonkerd, thesis defense chair, for her supervision, suggestion, and recommendation, which fulfill my dissertation.

I wish to express my gratefulness to Prof. Hiroshi Jinnai for his valuable suggestions and endless support during my staying at Tohoku University, Japan. He gave me the opportunity to learn about Transmission Electron Microtomography (TEMT) which surely fills my research career in colors. In addition, I would like to greatly thank Asst. Prof. Takeshi Higuchi for giving me his kindly support and friendship at any moment.

Sincere appreciation is also extended to Thailand Research Fund via Research and Researcher for Industries (RRi) and Siam Rubber Ltd., Part. for the financial support to this research (Grant No. PHD56I0074).

Special thankfulness is given to all technicians and staffs of Rubber Technology Research Centre (RTEC) and National Metal and Materials Technology Center (MTEC) for their helps and endless support throughout this research.

Finally, I am deeply grateful to my beloved parents and my family for their love, understanding, encouragement and inspiration in every way over my whole life.

Puchong Thaptong

A STUDY OF PARAMETERS AFFECTING PROPERTIES OF TIRE TREAD COMPOUNDS

PUCHONG THAPTONG 5537490 SCPO/D

Ph.D. (POLYMER SCIENCE AND TECHNOLOGY)

THESIS ADVISORY COMMITTEE: CHAKRIT SIRISINHA, Ph.D, PONGDHORN SAE-OUI, Ph.D., PAIROTE JITTHAM, Ph.D.

ABSTRACT

In this study, passenger car radial (PCR) tire tread compounds based on styrene butadiene rubber (SBR) were prepared. Two types of SBR, i.e., solution SBR (SSBR) and emulsion SBR (ESBR), and two types of silica, i.e., highly dispersible silica (HDSi) and conventional precipitated silica (CSi), were compared. Influences of silanization temperature, silane coupling agent (TESPT) content, silica/carbon black (CB) hybrid ratio, filler and processing oil loadings, as well as sulfur vulcanization system and crosslink density on properties of PCR tire tread compounds were investigated. Results showed that although the increase in silanization temperature resulted in the improvement in vulcanizate properties such as modulus, heat build-up (HBU), dynamic set, as well as tire performance, e.g., wet grip (WG), fuel saving efficiency (FSE), and abrasion resistance, great care must be taken to avoid the scorch phenomenon during the mixing at high temperature. It was also found that TESPT content of 10 wt% of silica offers the balanced compound and vulcanizate properties, including tire performance. In silica/CB hybrid filler system, the increase of CB ratio not only deteriorated the HBU and dynamic set, but also impaired the WG and FSE. On the other hand, the abrasion resistance was improved with increasing CB ratio up to 60-80 wt%. As SSBR gave greater degrees of rubber-filler interaction, crosslink density and T_g due to its higher vinyl and bound styrene contents, SSBR provides significantly better WG and abrasion resistance than ESBR. Despite the fact that the simultaneous increases of total filler and oil loadings, in order to keep hardness of the vulcanizate constant, are capable of reducing the material cost, the vulcanizate properties, e.g., tensile strength (TS), elongation at break (EB), HBU, dynamic set, and tire performance, are sacrificed. As expected, the increased curative content not only accelerated the vulcanization process, but also enhanced the crosslink density of the vulcanizates. Although there was an improvement in tire performance, HBU, and dynamic set were found when the crosslink density increased, the TS, EB, including thermal ageing resistance were impaired. Results also revealed that conventional vulcanization (CV) system provides better HBU, dynamic set, WG and FSE than semi-efficient vulcanization (semi-EV) system, attributed mainly to the greater crosslink density of the CV system. However, the semi-EV system imparts superior thermal ageing resistance, compared to the CV system, possibly due to the higher proportion of mono- and di-sulfidic linkages. Surprisingly, silica type played a little role in WG, FSE, and degree of filler dispersion in this study despite the fact that HDSi is claimed to offer greater dispersability. Results suggest that the HDSi could be replaced by the CSi when a sufficiently long mixing time is used. Compared to commercial PCR tires, the best compound formulation developed in this study demonstrates better WG and FSE, suggesting the potential for further development into commercially viable products.

KEY WORDS: STYRENE BUTADIENE RUBBER / SILANE COUPLING AGENT / SILICA-CARBON BLACK HYBRID FILLER / MECHANICAL AND DYNAMIC PROPERTIES / TIRE PERFORMANCE / TREAD

296 pages

การศึกษาตัวแปรที่มีผลต่อสมบัติของยางคอมพาวด์ที่ใช้ในการผลิตดอกยางล้อ

A STUDY OF PARAMETERS AFFECTING PROPERTIES OF TIRE TREAD COMPOUNDS

ภุชงค์ ทับทอง 5537490 SCPO/D

ปร.ด. (วิทยาศาสตร์และเทคโนโลยีพอลิเมอร์)

คณะกรรมการที่ปรึกษาวิทยานิพนธ์: ชาคริต สิริสิงห, Ph.D., พงษ์ธร แซ่อุย, Ph.D., ไพโรจน์ จิตรธรรม, Ph.D.

บทคัดย่อ

ในงานวิจัยนี้ ได้ทำการเตรียมยางคอมพาวด์ที่จะนำไปใช้ผลิตเป็นดอกยางล้อรถยนต์นั่งส่วนบุคคลจากยางสไตรีนบิวทาไดอีน โดยทำการเปรียบเทียบระหว่างยางสไตรีนบิวทาไดอีน 2 ชนิด (ยางโซลูชั่นสไตรีนบิวทาไดอีน (SSBR) และยางอีมัลชั่นสไตรีนบิวทาไดอีน (ESBR)) และซิลิกา 2 ชนิด (ซิลิกาชนิดที่สามารถแตกตัวได้ดี (HDSi) และซิลิกาชนิดทั่วไป (CSi)) นอกจากนี้ ยังได้ทำการศึกษาผลของตัวแปรต่างๆ ที่อาจส่งผลต่อสมบัติของยางคอมพาวด์อีกด้วย ซึ่งได้แก่ อุณหภูมิในขั้นตอนการทำไซลาไนเซชั่น ปริมาณสารคู่ควบไซเลน (TESPT) สัดส่วนสารตัวเติมผสมระหว่างซิลิกาและเขม่าดำ ปริมาณสารตัวเติมและน้ำมัน รวมทั้งระบบการวัลคาไนซ์ด้วยกำมะถันและระดับความหนาแน่นของการเชื่อมโยง จากการทดลองพบว่า แม้ว่าการเพิ่มอุณหภูมิในขั้นตอนการทำไซลาไนเซชั่นจะช่วยปรับปรุงสมบัติบางประการของยางวัลคาไนซ์ (เช่น มอดูลัส ความร้อนสะสม การเสียรูปถาวรหลังการกดอัดเชิงพลวัต) อีกทั้งยังช่วยเพิ่มสมรรถนะของดอกยางล้อ (เช่น สมบัติการยึดเกาะบนถนนเปียก การประหยัดเชื้อเพลิง และความทนทานต่อการสึกหรอ) อย่างไรก็ดี การใช้อุณหภูมิในขั้นตอนการทำไซลาไนเซชั่นที่สูงเกินไปอาจก่อให้เกิดปัญหายางตาย (สกอร์ช) ในระหว่างการผสมได้ ยังพบอีกว่าการใช้ TESPT ในปริมาณร้อยละ 10 โดยน้ำหนักของซิลิกา ส่งผลให้สมบัติของยางคอมพาวด์และยางวัลคาไนซ์ รวมถึงสมรรถนะของดอกยางล้ออยู่ในเกณฑ์ที่เหมาะสม เมื่อพิจารณาผลของระบบสารตัวเติมผสมระหว่างซิลิกาและเขม่าดำ พบว่าการเพิ่มสัดส่วนของเขม่าดำไม่เพียงแต่จะส่งผลเสียต่อความร้อนสะสมและการเสียรูปถาวรหลังการกดอัดเชิงพลวัต แต่ยังทำให้สมบัติการยึดเกาะบนถนนเปียกและการประหยัดเชื้อเพลิงมีแนวโน้มแย่ลงอีกด้วย ในทางตรงกันข้ามกลับพบว่าความทนทานต่อการสึกหรอของยางมีแนวโน้มสูงขึ้นตามการเพิ่มสัดส่วนของเขม่าดำจนถึงร้อยละ 60-80 โดยน้ำหนัก จากการที่ยาง SSBR มีปริมาณไวนิลและบาวด์สไตรีนที่สูงกว่า ส่งผลทำให้ยางมีอันตรกิริยากับสารตัวเติม ความหนาแน่นของการเชื่อมโยง และอุณหภูมิการเปลี่ยนสถานะคล้ายแก้วที่สูงกว่าตามไปด้วย จึงทำให้ยาง SSBR มีสมบัติการยึดเกาะบนถนนเปียกและความทนทานต่อการสึกหรอที่ดีกว่าเมื่อเปรียบเทียบกับยาง ESBR แม้ว่าการเพิ่มปริมาณสารตัวเติมไปพร้อมๆกับการเพิ่มปริมาณน้ำมัน (เพื่อที่จะรักษาความแข็งของยางให้คงที่) จะทำให้ต้นทุนวัตถุดิบลดลง แต่ก็ส่งผลทำให้ยางมีสมบัติบางประการที่แย่ลง (เช่น ความทนทานต่อแรงดึง การยืดตัว ณ จุดขาด ความร้อนสะสม การเสียรูปถาวรหลังการกดอัดเชิงพลวัต) นอกจากนี้ยังส่งผลเสียต่อสมรรถนะของดอกยางล้ออีกด้วย ผลการทดลองยังแสดงให้เห็นว่าการเพิ่มปริมาณสารที่ทำให้ยางวัลคาไนซ์ไม่เพียงแต่จะช่วยทำให้ยางเกิดการวัลคาไนซ์ได้เร็วขึ้น แต่ยังเพิ่มความหนาแน่นของการเชื่อมโยงให้สูงขึ้นอีกด้วย ซึ่งช่วยปรับปรุงสมรรถนะของดอกยางล้อ ความร้อนสะสม และการเสียรูปถาวรหลังการกดอัดเชิงพลวัตของยางให้ดีขึ้น อย่างไรก็ดี การเพิ่มความหนาแน่นของการเชื่อมโยงดังกล่าวก็ส่งผลเสียต่อความทนทานต่อแรงดึง การยืดตัว ณ จุดขาด และความทนทานต่อการเสื่อมสภาพจากความร้อนของยาง เมื่อทำการเปรียบเทียบระหว่างระบบการวัลคาไนซ์แบบดั้งเดิม (CV system) และระบบการวัลคาไนซ์แบบกึ่งประสิทธิภาพ (semi-EV system) พบว่าระบบการวัลคาไนซ์แบบดั้งเดิมจะทำให้ได้ยางที่มีค่าความร้อนสะสมและการเสียรูปถาวรหลังการกดอัดเชิงพลวัตต่ำกว่า อีกทั้งยังทำให้ยางสามารถยึดเกาะบนถนนเปียกและประหยัดเชื้อเพลิงได้ดีกว่าอีกด้วย ซึ่งคาดว่าเกิดจากการที่ยางมีความหนาแน่นของการเชื่อมโยงที่สูงกว่านั่นเอง ในทางตรงกันข้าม ระบบการวัลคาไนซ์แบบกึ่งประสิทธิภาพจะทำให้ยางมีความทนทานต่อการเสื่อมสภาพจากความร้อนที่สูงกว่า ซึ่งคาดว่าน่าจะเกิดจากการมีสัดส่วนของพันธะเชื่อมโยงกำมะถันอะตอมเดี่ยว (monosulfidic linkages) และกำมะถันอะตอมคู่ (disulfidic linkages) ที่สูงกว่า เป็นที่น่าประหลาดใจที่ผลการทดลองบ่งชี้ว่าชนิดของซิลิกาส่งผลน้อยมากต่อสมบัติการยึดเกาะบนถนนเปียก การประหยัดเชื้อเพลิง และระดับการแตกตัวของสารตัวเติมในยางทั้งๆ ที่มีการอ้างว่า HDSi สามารถแตกตัวได้ดีกว่าเมื่อเปรียบเทียบกับ CSi ผลการทดลองเผยให้เห็นว่าสามารถใช้ CSi แทนที่ HDSi ถ้าใช้ระยะเวลาในการผสมที่นานเพียงพอ เมื่อทำการเปรียบเทียบกับดอกยางล้อรถยนต์นั่งส่วนบุคคลที่จำหน่ายเชิงพาณิชย์ พบว่าสูตรดอกยางล้อรถยนต์นั่งส่วนบุคคลที่ดีที่สุดในงานวิจัยนี้จะให้สมบัติการยึดเกาะบนถนนเปียกและการประหยัดเชื้อเพลิงที่ดีกว่า แสดงให้เห็นถึงศักยภาพที่จะนำไปพัฒนาต่อยอดสำหรับการจำหน่ายเชิงพาณิชย์ต่อไป

CONTENTS

CONTENTS (cont.)

CONTENTS (cont.)

CONTENTS (cont.)

CONTENTS (cont.)

CONTENTS (cont.)

CONTENTS (cont.)

LIST OF TABLES

LIST OF TABLES (cont.)

LIST OF TABLES (cont.)

LIST OF TABLES (cont.)

LIST OF TABLES (cont.)

LIST OF TABLES (cont.)

LIST OF FIGURES

LIST OF FIGURES (cont.)

LIST OF FIGURES (cont.)

LIST OF FIGURES (cont.)

LIST OF FIGURES (cont.)

LIST OF FIGURES (cont.)

LIST OF FIGURES (cont.)

LIST OF FIGURES (cont.)

LIST OF ABBREVIATIONS

6PPD	*N*-(1,3-dimethylbutyl)-*N*′-phenyl-p-phenylenediamine
ABR	Acrylate-butadiene rubber
Amine-BSA	p-Aminobenzenesulfonyl azide
APTES	γ-Aminopropyl triethoxysilane
ASTM	American society for testing and materials
BPST	British pendulum skid tester
BR	Butadiene rubber
BRC	Bound rubber content
CB	Carbon black
CBS	*N*-Cyclohexyl-2-benzothiazole sulfonamide
CRI	Cure rate index
CSi	Conventional precipitated silica
CTAB	Cetyltrimethylammonium bromide
CV	Conventional vulcanization
dB	Decibel
DBP	Dibutylphthalate
DMTA	Dynamic mechanical thermal analyzer
DPG	Diphenyl guanidine
EB	Elongation at break
ESBR	Emulsion styrene butadiene rubber
EV	Efficient vulcanization
EU	European Union
FSE	Fuel saving efficiency
F-SSBR	Functionalized solution styrene butadiene rubber
GPC	Gel permeation chromatography
HDSi	Highly dispersible silica
HBU	Heat build-up

LIST OF ABBREVIATIONS (cont.)

IIR	Butyl rubber
ISO	International standardization and organization
log a_T	Shift factor
M10	Modulus at 10%strain
M100	Modulus at 100%strain
M300	Modulus at 300%strain
MBTS	2,2'-Dithiobis(benzothiazole)
MDR	Moving die rheometer
MWD	Molecular weight distribution
NR	Natural rubber
NXT	3-Octanoylthio-1-propyltriethoxysilane
OTES	Octyltrimethylsilane
PCR	Passenger car radial
phr	Parts per hundred rubber
RPA	Rubber process analyzer
rpm	Revolutions per minute
RR	Rolling resistance
S_8	Sulfur
SBR	Styrene butadiene rubber
SCA	Silane coupling agent
SEM	Scanning electron microscopy
Semi-EV	Semi-efficient vulcanization
SSBR	Solution styrene butadiene rubber
STM	Scanning tunneling microscopy
TBBS	*N*-tert-butyl-2-benzothiazole sulfenamide
TBzTD	Tetrabenzylthiuram disulfide
t_c90	Optimum cure time
TDAE	Treated distillate aromatic extract
TEM	Transmission electron microscopy

LIST OF ABBREVIATIONS (cont.)

TESPT	Bis[3-(triethoxysilyl)propyl] tetrasulfide
THF	Tetrahydrofuran
TMEDA	Tetramethylethylenediamine
TMQ	2,2,4-trimethyl-1,2-dihydroquinoline, polymerized
TS	Tensile strength
t_s1	Scorch time
VOC	Volatile organic compound
WG	Wet grip
WLF	The Williams-Landel-Ferry equation
WSR	Wet skid resistance
wt%	Weight percent
XIIR	Halogenated butyl rubber
ZnO	Zinc oxide
γ	Strain
γ_o	Maximum strain
ω	Angular frequency
t	Time
τ	Stress
δ	Phase lag
τ_0	Maximum stress
τ^*	Complex stress
τ'	In-phase with the displacement
τ''	90^o out-of-phase with the displacement
G^*	Complex modulus
G'	In-phase (or storage) modulus
G''	Out-of-phase (or loss) modulus
G_0	Modulus of rubber vulcanizates
ν	Number of elastically active chains per unit volume

LIST OF ABBREVIATIONS (cont.)

K	Bolzmann's constant
T	Absolute temperature
η	Viscous particle suspension
η_0	Viscosity of unfilled fluids
ϕ	Volume fraction of particles
f	Shape factor
T_g	Glass transition temperature
W_d	Weight of dry gel
F	Weight of filler in the test piece
R	Weight of rubber in the test piece
v_2	Volume fraction of polymer in the swollen test piece
χ_1	Polymer-solvent interaction parameter
V_1	Molar volume of the solvent
m_0	Weight of the test piece before swelling
m_1	Weight of the test piece after swelling
m_2	Weight of the test piece after drying
ϕ_1	Weight fraction of rubber in the vulcanized sheet
α	Weight loss fraction of the test piece after the swelling test
ρ_p	Density of rubber
ρ_s	Density of solvent
H_o	Original height of the specimen
H_f	Final height of the specimen

CHAPTER I
INTRODUCTION

Nowadays, tires play an important role in the life of human beings because they are not only crucial assemblies of vehicles, but also used in large numbers on automobiles, trucks, as well as aircrafts. Moreover, as tires play a key role in transportation, they strongly affect the economic growth of the world [1].

From 1st November 2012, a standard label of vehicle tires was introduced throughout European Union (EU), namely EU tire labelling regulation, based on three criteria concerning the environmental and safety characteristics of a tire, i.e., rolling resistance (RR), wet skid resistance or wet grip (WG), and outside rolling noise [2]. This standard label can help users making a decision before purchasing tire by considering the standard label information [3]. To avoid loss of competitive ability, tire manufacturers and exporters in Thailand have to adopt such regulation. In the meantime, the factors influencing on three criteria should be clearly understood in order to apply the obtained knowledge for tire technology development.

Among the parts of tire, tread is one of the most important parts because it not only contacts the road surface and protects the inner casing from road hazards, but also responds to main tire performance, e.g., RR, WG, wear resistance [4]. Although RR has recently gained much attention from many tire technologists because the reduction of RR leads to a decrease in the energy consumption during driving [5], WG is also one of the most important properties for tire. It is widely known that driving on a wet surface could be very dangerous due to a greater chance for loss of car control and longer stopping distance [6, 7]. To improve safety, driving at sufficiently slow speed and proper selection of tire are recommended.

Although tread pattern of the tire is known to play an important role in RR [8] and WG [9], tire tread formulation is also a key factor governing these properties [10]. Therefore, this research aims to investigate the parameters affecting WG and RR of the vulcanizates used for passenger car radial (PCR) tire tread. The main target is to

gain the compound formulation providing a high WG while still maintaining a low RR and sufficiently good mechanical properties, especially abrasion resistance. To achieve the main target, the optimal silanization temperature must be determined to be employed in the subsequent experiments. Other factors affecting WG and RR, i.e., silane coupling agent content, styrene butadiene rubber (SBR) type, filler type (highly dispersible silica (HDSi) and conventional precipitated silica (CSi)), silica/carbon black (CB) hybrid filler ratio, oil and reinforcing filler loadings including sulfur vulcanization system will also be studied and discussed.

CHAPTER II
OBJECTIVES

In this research, parameters affecting the properties of PCR tire tread compounds are studied. The main target of this work is to gain the compound formulation giving the optimum tire performance, i.e., low RR, high WG, and high abrasion resistance. The scopes of this work are composed of 5 main parts as follows:

2.1 Effects of silanization temperature and silica type on properties of silica-filled solution styrene butadiene rubber (SSBR)

In this part, the relationships among silanization temperature and processability, viscoelastic properties, mechanical properties, as well as dynamic properties of silica-filled SSBR were investigated. Also, properties of the compounds filled with 2 types of silica, namely, highly dispersed silica (HDSi) and conventional precipitated silica (CSi), were compared. The suitable silanization temperature providing the balanced properties was drawn from this part.

2.2 Effects of silane coupling agent content and silica type on properties of silica-filled SSBR

The present study aims to gain the optimum content of silane coupling agent (Bis[3-(triethoxysilyl)propyl] tetrasulfide (TESPT)) for each type of silica, i.e., HDSi and CSi. Influence of TESPT content on viscoelastic, mechanical, and dynamic properties was determined. The proper silanization temperature obtained from the previous part was employed in this part. The optimum TESPT content drawn from this part will be used in the subsequent sections of the study.

2.3 Effects of silica/CB hybrid filler and SBR type on properties of SBR

In this study, the ratio of silica/CB hybrid filler was varied and its influences on viscoelastic, mechanical, and dynamic properties were monitored. Two SSBR grades having comparable styrene content and Mooney viscosity, i.e., SSBR6450SL and SSBR3626 were used in this study. In addition to SSBR, another grade of emulsion styrene butadiene rubber (ESBR), namely ESBR1723, was employed and compared. The effect of silica type, i.e., HDSi and CSi, on properties of SBR compounds and vulcanizates was also studied.

2.4 Effects of filler and oil loadings on properties of SBR

The objective of this part is to investigate the effect of filler loading on vulcanizate properties. Only SSBR and 60/40 CSi/CB hybrid filler were used in this study (the decision was made based on the results obtained from the previous section). In order to keep hardness of vulcanizates constant, a total filler content was altered simultaneously with rubber process oil content. The viscoelastic, mechanical and dynamic properties, as well as the estimated relative cost of the compounds were evaluated. The optimum filler and oil loadings giving the best tire performance will be employed in the subsequent section.

2.5 Effects of sulfur vulcanization system and crosslink density on properties of SBR

This part focuses on two sulfur vulcanization systems, namely, conventional vulcanization (CV) system and semi-efficient vulcanization (semi-EV) system. The effect of crosslink density, by changing the amount of curatives (*N*-tert-butyl-2-benzothiazole sulfenamide (TBBS), tetrabenzylthiuram disulfide (TBzTD) and sulfur), on viscoelastic, mechanical, and dynamic properties was studied. Finally, the best PCR tire tread compound formulation for this research was gained.

CHAPTER III
LITERATURE REVIEW

3.1 Tire technology

Tire, a continuous band covering the rim of a wheel [11], is a necessary part for vehicles because it not only protects the wheel's rim and supports the load of vehicle, but also absorbs the shock from road imperfections providing a driving comfort. Tire was firstly invented by Robert W. Thomson [12], a Scottish engineer, in 1845, and has been continuously developed until the present. Tires are now produced worldwide and used in numerous types of vehicles, particularly in passenger cars, light trucks and trucks as shown in Figure 3.1 [13].

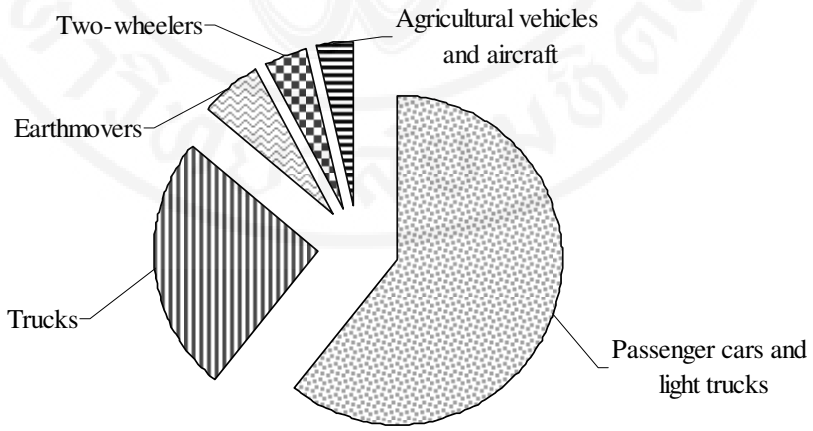

Figure 3.1 The use of various types of tire in 2000 [13]

3.1.1 Type of tire

Currently, there are 4 criteria widely used to classify tire type [1, 14]:

(i) *Classified by vehicles:* passenger car tire, light truck tire, truck and bus tire, off the road tire, motorcycle tire, air craft tire, etc.

(ii) *Classified by structure:* bias tire, radial tire, etc.

(iii) *Classified by target season:* all season tire, winter tire, etc.

(iv) *Classified by application:* regular tire, run flat tire, etc.

Figure 3.2 illustrates the construction of tire classified by structure, e.g., bias and radial tires. The main difference between bias and radial tire structure is the body ply cord characteristic. In the case of bias tire, the body ply cord is formed by laying ply cords diagonally from bead to bead at angle less than 90^{o} to the centerline of tread. Unlike bias tire, the body ply cord of radial tire is laid from bead to bead at angle 90^{o} with two or more belts diagonally laid on tread region [14, 15]. Since sidewall and tread of radial tire are not interdependent, all sidewall flex is not transmitted to the tread. This is the reason why radial tire offers greater footprint stability and high-speed performance, compared to bias tire [15, 16].

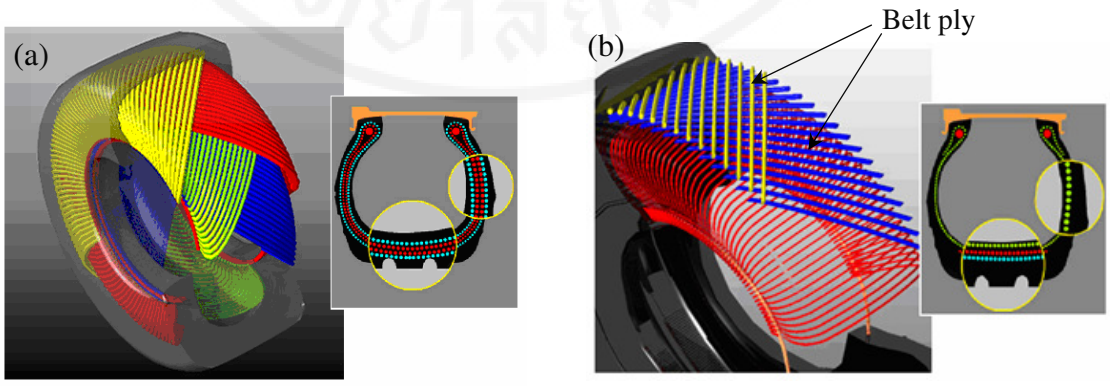

Figure 3.2 Structure of tire (a) bias tire and (b) radial tire [16]

3.1.2 Basic construction of tire

Tire is one of the most complex mass products because it is made from various components. Several types of raw materials, e.g., elastomers, textiles, and wires, are usually used to produce tire. Generally, tire structure can be divided into 2 parts, i.e., exterior and interior. A layer of rubber, e.g., bead, sidewall, shoulder, and tread, is classified into an exterior part of tire whereas a section of tire made from rubber reinforced by fibers or wires, i.e., carcass ply, belt ply, and bead wire, is normally categorized as an interior part [1]. A typical construction of PCR tire is depicted in Figure 3.3. The major parts and their functions are summarized as follows [1, 9, 17]:

(i) *Tread:* A filler-filled rubber vulcanizates. This part serves several functions such as to contact the road surface, to displace the water, to protect the inner casing from road hazards, and to respond to main tire performance, e.g., traction and fuel efficiency.

(ii) *Cap ply:* Layers of rubber-coated fabric enable tire to operate at high speed.

(iii) *Belt ply:* It is generally made from rubber-coated steel wire. It not only protects and restricts deformation of carcass, but also offers the rigidity to tread area, leading to improve handling properties and wear resistance.

(iv) *Carcass ply:* The main reinforcing layer of tire casing which is produced from rubber-coated steel wire or fabric. It maintains the shape of tire and also controls internal air pressure.

(v) *Side wall:* An outer layer of tire that protects the inner casing from damage. It is usually made from carbon black (CB)-filled natural rubber (NR)/butadiene rubber (BR) blends.

(vi) *Inner liner:* The layer which retains air inside the tire. Butyl rubber (IIR) or halogenated butyl rubber (XIIR) is generally used as the raw material for inner liner.

(vii) *Bead wire:* A ring of steel wire that locks the tire onto the rim or wheel.

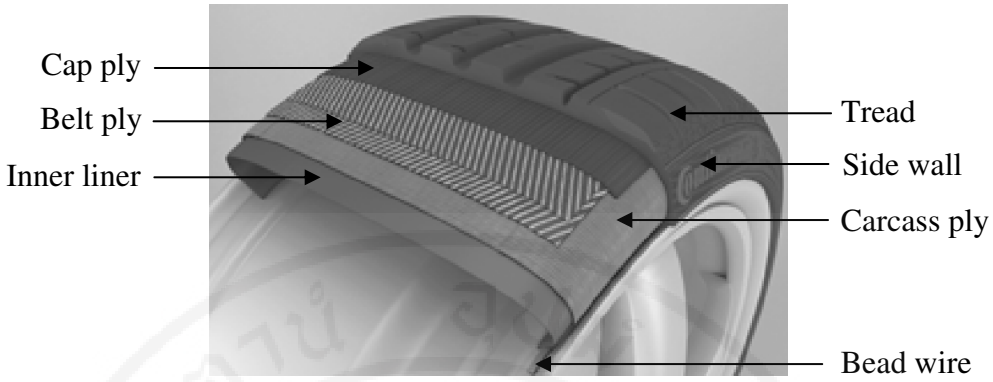

Figure 3.3 Typical construction of PCR tire [17]

3.1.3 Tire performance

Generally, tire performance should concern driving safety, comfortable mobility, and environmental friendliness as shown in Figure 3.4. Due to green revolution, tire is currently required to provide not only good performance, but also low environmental impact. To obtain a good tire for green revolution, these requirements illustrated in Figure 3.4 should be strongly aware.

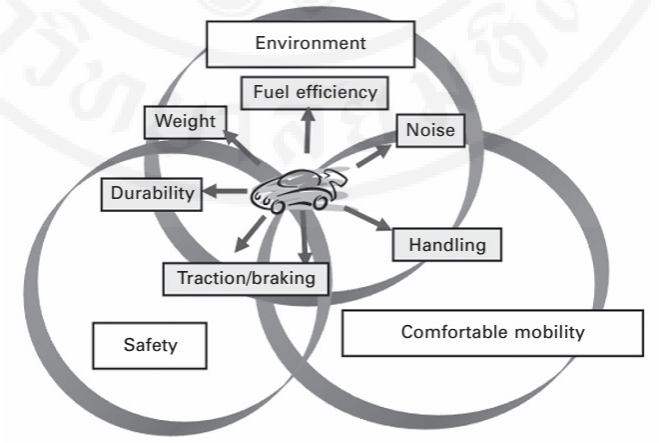

Figure 3.4 The main tire requirements [1]

According to Figure 3.4, tire performance can be generally evaluated based on 4 important properties, i.e., treadwear and durability, traction, fuel efficiency, and outside rolling noise. Details of each property are demonstrated as follows:

3.1.3.1 Treadwear and durability

Treadwear and durability are tire properties related to safety aspect and environmental perspective. In general, the degree of treadwear including the failure of tire casting, often called the carcass, are usually used as indicators for tire service life [4]. There are several factors affecting the tire service life, i.e., environment, road surface texture, driving habits, etc. To extend tire service life, several types of chemical ingredients, e.g. antioxidants, antiozonants, as well as reinforcing filler, are commonly added into tire compound [18]. By considering the preventive maintenance, keeping tires properly aligned and rotating tires every 6,000 miles (9,700 km) driven are also good ways to improve tire service life [19].

3.1.3.2 Traction

In tire application, traction is conceptualized as the resistance between tire and road surfaces in reaction to torque being exerted by the wheel axle under engine power [20]. Generally, the safety during driving under various conditions, i.e., dry, wet, and ice/snow conditions, is directly proportional to tire traction. It is widely known that, compared to dry condition, an accident can occur more easily in wet or ice/snow condition. This is due mainly to the water film generated between tread and road surface, leading to the reduction of friction, and, thus, the loss of car control ability [21]. It is also believed that tire traction depends on both tread pattern and tread compound formulation [21, 22].

3.1.3.3 Fuel efficiency

It is well known that the energy required to roll a tire along a road under a given vehicle load, namely RR [8, 23], is inversely related to the fuel efficiency of a vehicle. In general, the lower the RR, the better the fuel efficiency [24]. It has been reported that the reduction of RR for 10% can lead to the decrease in fuel consumption for approximately 2-3% [25, 26]. In addition, the replacement of CB by silica in tire tread compound is one of the efficiency methods to reduce the RR of tire [27].

3.1.3.4 Outside rolling noise

This property refers to noise generated by rolling a tire on road surface [28]. Generally, outside rolling noise is directly related to the level of sound pollution. For instance, the louder outside rolling noise indicates the greater level of sound pollution. The examples of parameters affecting the outside rolling noise such as vehicle speed [29], road surface texture [30], tire tread pattern [31], and tire damping ability [32].

3.1.4 Tire label

As previously mentioned, due to the great concern about the environmental and safety characteristics of a tire in Europe, the tire label offering the information on fuel efficiency, WG, and outside rolling noise is required (see Figure 3.5). The detail of properties depicted on the EU tire label is described as follows:

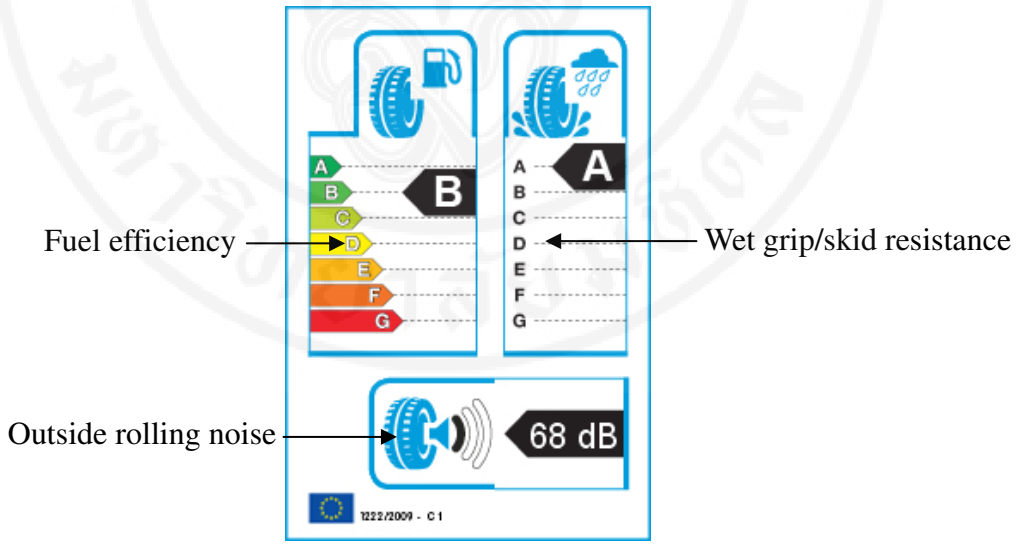

Figure 3.5 EU tire label [33]

3.1.4.1 Fuel efficiency

This property is inversely related to RR of tire, i.e., the lower the RR, the better the fuel efficiency. In EU tire label, the fuel efficiency is rated from A to G on a color-coded scale. “A (green)” represents the highest fuel efficiency rating whereas “G (red)” indicates the lowest fuel efficiency rating [34]. The test is carried

out following UNECE Reg.117.02. The value obtained from the test is then corrected in accordance with the alignment procedure according to EU Reg.1235/2011 to obtain the labelling scale [35].

3.1.4.2 Wet grip

Wet grip, sometimes called wet skid resistance (WSR), is typically defined as the tire's braking ability on road in wet conditions which is classed from A to G. When full brakes are applied, the shortest and longest braking distances on wet roads are represented in rating "A" and "G", respectively. However, rating "D" and "G" are not currently used for PCR tire [36]. For PCR tire, the test is performed as per EU Reg.228/2011. For light truck and truck & bus tires, the test is carried out following EU Reg.1235/2011 [35].

3.1.4.3 Outside rolling noise

This property is measured in decibel (dB). The level of outside rolling noise is graded in the number of black sound wave according to UNECE Reg.117.02 [35]. One black sound wave indicates the best noise performance (3dB or more below the EU limit). Two black sound waves represent the moderate noise performance (between the EU limit and 3dB below). Lastly, three black sound waves reveal the worst noise performance (above the EU limit) [36].

3.2 Tire performance predictors

It is wildly known that tire testing, i.e., drum test, WSR test, etc., is not only relatively expensive, but also sometimes time-consuming. Therefore, many attempts have been made to predict tire performance in laboratory. Nowadays, the prediction of tire performance by evaluating the viscoelastic properties of tire is one of the efficient methods [37] because this method offers several advantages such as low cost, small-sized test specimen, ease in specimen preparation, including short test time. This topic therefore aims to describe the relationship between viscoelastic properties of rubber and tire performance focusing on RR and WG.

3.2.1 Dynamic mechanical properties

Rubber is normally a viscoelastic material which is composed of two portions, i.e., elastic portion and viscous portion. When the rubber is deformed by an applied force, the elastic and viscous portions in rubber response inversely. The applied force (or energy) will be elastically stored in elastic portion. On contrary, in viscous portion, the applied force (or energy) will be dissipated and usually converted into heat or sound which is called hysteresis loss [38, 39].

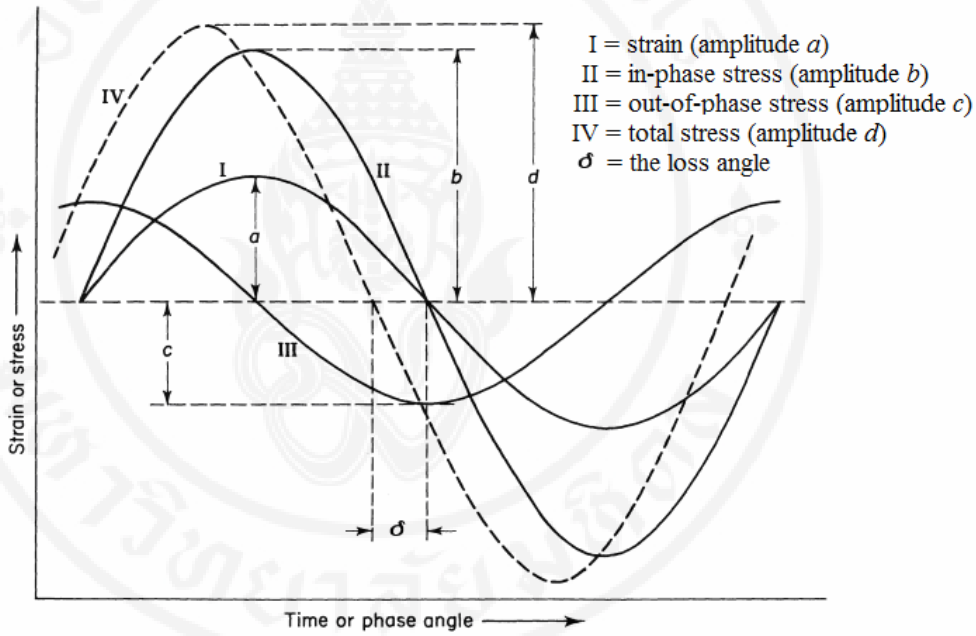

Figure 3.6 Sinusoidal strain and stress cycles [39]

The viscoelastic response of tire tread generally deals with cyclic deformation (see Figure 3.6). For sinusoidal strain, the relationship among strain (γ), maximum strain (γ_o), angular frequency (ω), and time (t) is described as follows [39, 40]:

$$\gamma = \gamma_o \sin \omega t \tag{1}$$

Since rubber is a viscoelastic material, the stress (τ) will not be in phase with the strain, i.e., there will be a phase lag (δ) between stress and strain which is sometimes

called loss angle. The relationship between stress and maximum stress (τ_0) can be represented as given below [39, 40]:

$$\tau = \tau_o \sin(\omega t + \delta) \quad (2)$$

If the stress is considered in terms of vector, the complex stress (τ^*) can be separated into two components, i.e., τ' (in-phase with the displacement) and τ'' (90^o out-of-phase with the displacement) [39, 41], as shown in Figure 3.7.

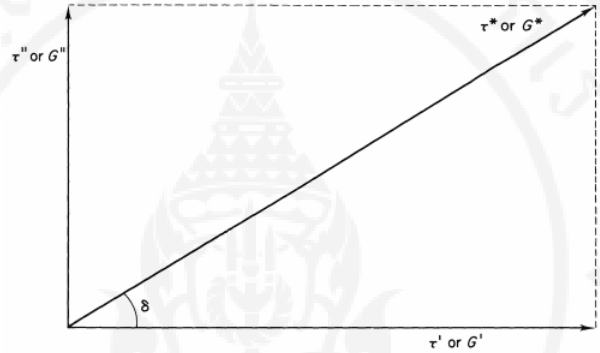

Figure 3.7 Diagram of stress or shear modulus vector [39]

In shear mode, the relationship among complex modulus (G^*), in-phase (or storage) modulus (G'), and out-of-phase (or loss) modulus (G'') is represented by [39]:

$$G^* = G' + iG'' \quad (3)$$

$$|G^*| = (G'^2 + G''^2)^{1/2} \quad (4)$$

Also, G' and G'' in term of G^* and δ can be written as follows:

$$G' = G^* \cos\delta \quad (5)$$

$$G'' = G^* \sin\delta \quad (6)$$

Finally, it can be shown that:

$$\tan\delta = \frac{G''}{G'} \quad (7)$$

In general, $\tan\delta$ is usually used to indicate the magnitude of energy dissipation in rubber vulcanizates. The higher the $\tan\delta$ value, the greater the magnitude of energy dissipation [42, 43].

3.2.2 Fuel efficiency

As previously mentioned, fuel consumption of a vehicle is directly related to RR of tire during driving. Therefore, the RR is usually used as an indicator for fuel efficiency of a vehicle.

When considering tire rotation during driving (see Figure 3.8), the tire rotates at low frequency, say $\approx 10^1$ Hz [1], while the temperature of tread could increase to 60-80°C due to the energy dissipation of rubber during the dynamic deformation. Since the $\tan\delta$ is associated with the magnitude of energy dissipation, the $\tan\delta$ value at 60°C is widely used to indicate RR and fuel efficiency of tire, as shown in Figure 3.9. In general, the lower $\tan\delta$ value at 60°C indicates the lower RR and, thus, the greater fuel efficiency [5, 44, 45]. As the tire tread is normally subjected to high strain during driving, the fuel efficiency is closely related to the $\tan\delta$ value at high strain, e.g., 5% [46], 6% [47], and 7.5% [48], where the transient filler-filler network is of great importance. At high strain, the filler-filler network, usually formed through physical interaction, e.g., van der Waals force (especially in the case of carbon black) and/or hydrogen bonds (especially in the case of silica), is greatly disrupted leading to the enhanced energy dissipation, and, thus, the increased $\tan\delta$ value.

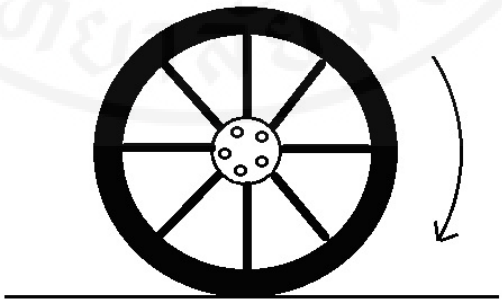

Figure 3.8 Rolling frequency during a complete rotation of a wheel

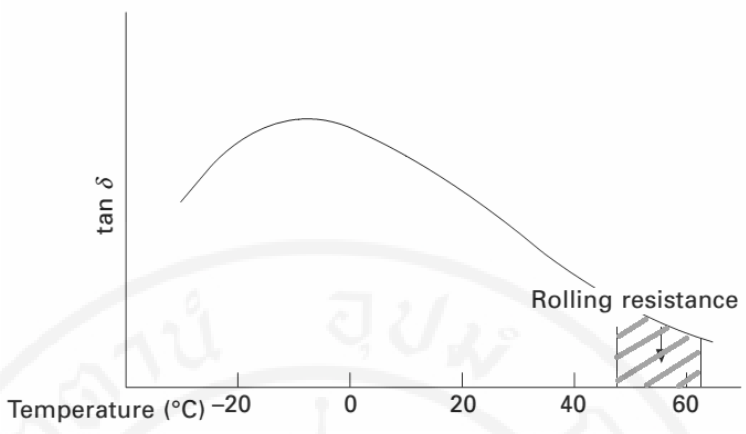

Figure 3.9 Dependence of the tanδ on temperature focusing on RR. Adapted from [1].

3.2.3 Wet grip

When full brakes are applied during driving on wet road, the tread will be subjected to periodical deformation at very high frequency ($\approx 10^4 - 10^5$ Hz) [1] due to the dynamic sliding contact on the asperity of the road surfaces, as illustrated in Figure 3.10. Even though a measurement of viscoelastic properties of rubber at such high frequency is almost impossible in practice due to the limitations of the test equipment, with the application of time-temperature superposition theory (the Williams-Landel-Ferry (WLF) equation), the viscoelastic properties at high frequency could be estimated by shifting the measured temperature towards lower temperature (see Figure 3.11) [1]. In most cases, value of tanδ at 0°C is employed to represent WG efficiency of tires, i.e., the higher the tanδ value at 0°C, the greater the WG [5, 44, 45, 49]. Since the tire tread is normally subjected to low strain during braking/skidding where the frequency is relatively high, the tanδ value at 0°C at relatively low strain (0.1%) is usually used to predict the WG efficiency [45, 50].

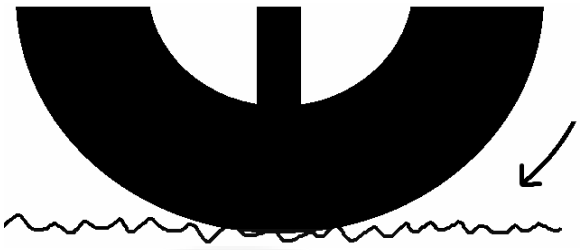

Frequency ≈ 10^4-10^5 Hz

Figure 3.10 Skidding frequency of tread on wet condition

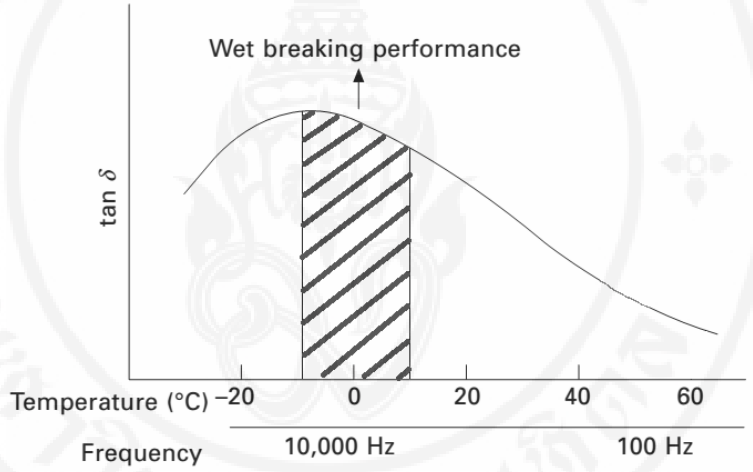

Figure 3.11 Dependence of the tanδ on temperature and frequency focusing on WG. Adapted from [1].

3.3 Tire tread compounds

It is widely known that tread pattern is one of the main factors affecting RR [8] and WG [9]. However, tire tread formula also plays a crucial role in these properties. Moreover, tire tread formula directly concerns with the cost of tire, not only raw material cost, but also processing cost. Tire tread formulation is therefore very important for tire industry.

In general, tire tread formula consists of several ingredients playing a different role in tire properties. In this topic, details of main ingredients used for tire

tread compound, i.e., SBR, silica, CB including silane coupling agents (SCAs), are therefore described. In addition, a briefly detail of sulfur curing system is given.

3.3.1 Tread compound formula

The examples of PCR tire tread compound formula designed for specific applications are tabulated in Table 3.1. It can be seen that blend of rubbers based on SBR as a main component, e.g. ESBR/NR, SSBR/BR, are usually used for PCR tread. Particulate reinforcing fillers such as CB and silica are also used. SCA is generally added when tread compound contains silica. In addition, sulfur curing system is widely applied for PCR tire tread compound.

Table 3.1 Tire tread compound formulas [51-53]

Ingredients	Content (phr)		
	1*	2**	3**
Natural rubber (NR)	50.0	-	-
Solution styrene butadiene rubber (SSBR)	-	75.0	70.0
Emulsion styrene butadiene rubber (ESBR)	50.0	-	-
Butadiene rubber (BR)	-	25.0	30.0
Zinc oxide (ZnO)	3.0	2.5	3.0
Stearic acid	3.0	1.0	2.0
Highly dispersible silica (HDSi)	-	80.0	80.0
Carbon black (CB)	45.0	-	-
Silane coupling agent (SCA)	-	12.8	9.0
Aromatic oil	9.0	32.5	36.0
Antioxidant	1.0	2.0	1.5
Antiozonant	2.0	-	-
Wax	1.0	1.5	1.0
Diphenyl guanidine (DPG)	0.4	2.0	0.25
Tetrabenzylthiuram disulfide (TBzTD)	-	-	0.5
N-Cyclohexyl-2-benzothiazole sulfenamide (CBS)	-	1.7	1.5
2,2'-Dithiobis(benzothiazole) (MBTS)	0.8	-	-
Sulfur	1.6	1.4	2.2

* Low rolling resistance PCR tire tread

** Silica-based PCR tire tread

3.3.2 Styrene butadiene rubber (SBR)

SBR is a synthetic rubber produced by copolymerization of styrene and butadiene monomers. The styrene content of SBR generally ranges from 23 to 40 wt% [54]. Two kinds of polymerization, i.e., emulsion polymerization and solution polymerization, are currently used for synthesis of SBR. As the polymerization condition affects the microstructure of butadiene unit, three possible configurations of butadiene unit in SBR, e.g., cis-, trans-, and vinyl-, are normally found [55, 56]. Figure 3.12 depicts the chemical structure of typical SBR and possible configurations of butadiene unit.

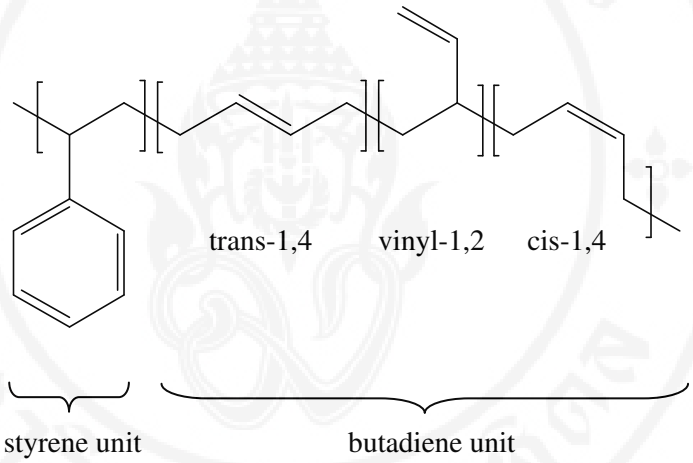

Figure 3.12 Chemical structure of typical SBR with three possible configurations of butadiene unit. Adapted from [56].

An Emulsion SBR (ESBR) is a type of SBR which is polymerized via free radical mechanism in emulsion form. The system is generally composed of a surfactant, an initiator, a chain transfer agent including styrene and butadiene monomers dispersed in water [56, 57]. According to a mechanism of emulsion polymerization [56], the microstructure of ESBR is uncontrollable, leading to the broad molecular weight distribution (MWD) and long chain branch [54].

Unlike ESBR, solution SBR (SSBR) is a type of SBR synthesized via living anionic polymerization mechanism in solution form. Typically, the styrene and butadiene monomers are dissolved in hydrocarbon solvent together with an alkyl lithium which acts as an initiator. Since SSBR is produced through anionic

polymerization, the MWD and butadiene configuration could be precisely controlled [58]. It has been reported that high vinyl SSBR is resulted when relatively low tetramethylethylenediamine (TMEDA)/Li ratio is used [59]. Compared to ESBR, SSBR generally provides narrower MWD and higher vinyl content. For vulcanizate properties, SSBR offers lower hysteresis and RR whereas still maintains wear and traction properties [56, 60]. However, the higher tensile strength is found when ESBR is used [60].

3.3.3 Filler

3.3.3.1 Carbon black (CB)

CB, a form of elemental carbon manufactured by the controlled vapor-phase pyrolysis and incomplete combustion of hydrocarbons, i.e., oils and gas [61-63], is used as the main reinforcing filler in tire industry for long decades because it can improve strength of several parts of tire such as tread and side wall. In general, primary particles of CB (diameter ≈ 10-90 nm) are not individually separated but, during the manufacturing process at high temperature, they are partially fused to form clusters of many primary particles, widely known as aggregates (diameter ≈ 100-300 nm), which play a key role in rubber reinforcement. These aggregates can later interact with each other through Van der Waals force during the quenching process to form agglomerates (diameter ≈ 10^4-10^6 nm), as illustrated in Figure 3.13(a) [62]. The aggregation of many spherical CB particles to form aggregates creates internal void of which its volume is used to define structure level of CB. If the number of aggregated particles is relatively high resulting in a more complex aggregate shape with greater void volume, this grade of CB will be classified as a high structure CB. On the contrary, if lower number of particles are densely aggregated (low void volume), this grade of CB will be classified as a low structure CB. Since these voids can be filled by rubber during the mixing process, structure of CB plays a very important role in many properties of CB-filled rubber.

Currently, CB can be classified into various grades depending on particle size, structure, and surface activity. According to the American Society for Testing and Materials (ASTM), a letter followed by a three-digit number, e.g., N330, S212, is normally used to represent the grade of CB. Letters N and S are used to define

normal and low vulcanization speeds, respectively. The first digit of three numbers indicates the average primary particle size of CB which is characterized by transmission electron microscopy (TEM) [63, 64], as shown in Figure 3.13(b). The last two digits are arbitrarily assigned by the CB manufacturers.

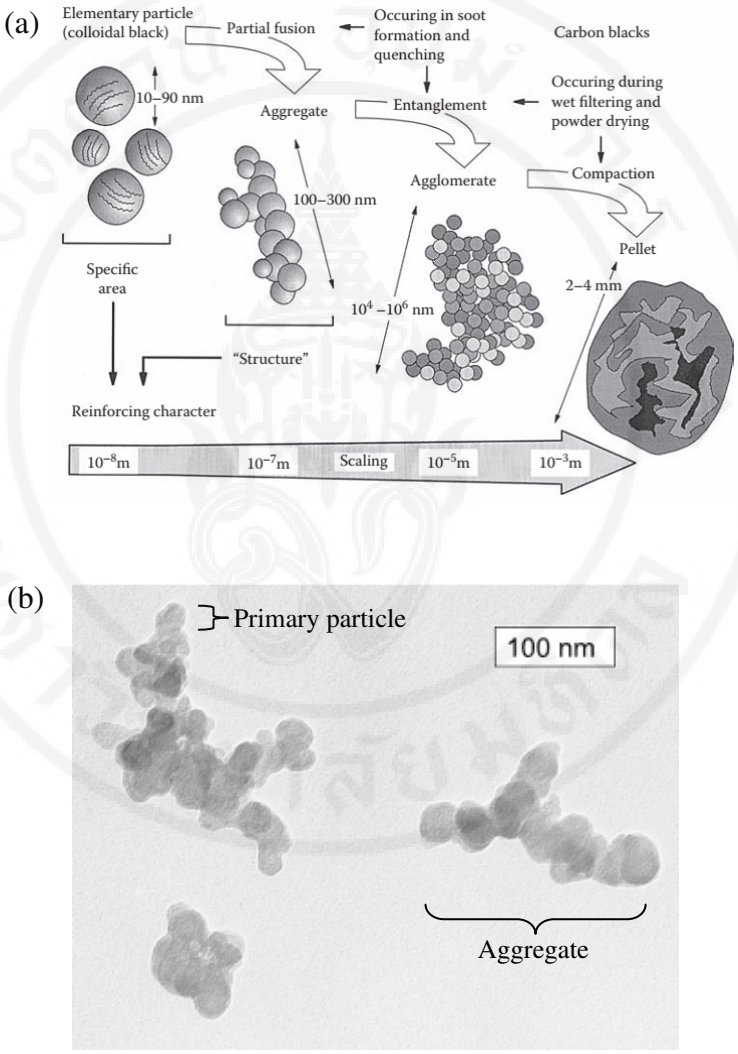

Figure 3.13 Structure of CB (a) illustrated by drawing [62] and (b) taken by TEM, Adapted from [61].

In general, particle size and specific surface area, structure, and specific surface activity are the three basic parameters affecting reinforcement of CB [65]. The specific surface area of CB, usually measured by nitrogen adsorption (N_2), iodine adsorption (I_2) or cetyltrimethylammonium bromide (CTAB), is inversely related to its primary particle size. The greater the specific surface area, the smaller the primary particle size. Generally, CB having high specific surface area provides greater reinforcement than that having low specific surface area. Structure of CB, usually determined by dibutylphthalate absorption (DBP), also greatly affects reinforcement. Generally, the higher CB structure leads to the greater viscosity of the compounds as well as higher modulus, hardness, and abrasion resistance of the vulcanizates [66]. For specific surface activity, it is widely known that the surface activity of filler plays a crucial role in rubber reinforcement. The higher surface activity leads to the better rubber-filler interaction and, thus, the greater rubber reinforcement. In the case of CB-filled rubber, it is believed that both physical adsorption of rubber molecules on CB surfaces and chemical interaction between rubber molecules and function groups on CB surfaces, e.g., carboxyls, phenols, quinone, lactol (see Figure 3.14), are responsible for the reinforcement [67].

Focusing on tire tread, several grades of CB are used for specific purpose. For example, N121 is produced for tire tread having high stiffness and wear resistance, N220 is suitable for making a good tear and wear resistance tread, and N234 is manufactured for tire tread offering excellent wear resistance [68].

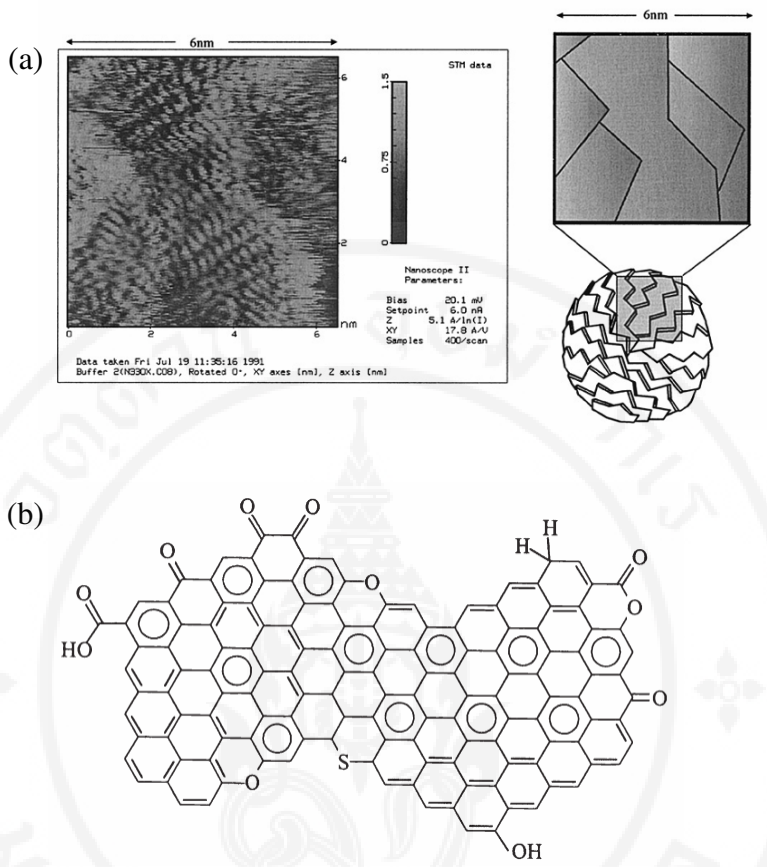

Figure 3.14 (a) CB surfaces taken by scanning tunneling microscope (STM) and (b) functional groups on CB surfaces [69].

3.3.3.2 Silica

The main disadvantage of using CB in tire tread includes high RR, resulting in high energy consumption [70]. For this reason, after the introduction of "green tire technology" by Michelin in the early 1990s, silica plays more crucial role in tire industry because the partial replacement of CB by silica in PCR tread leads to a significantly reduction of RR without sacrificing WG and wear resistance [71].

Silica can be generally divided into 2 main groups, i.e., natural (or crystalline) silica and synthetic (or amorphous) silica. For synthetic silica, fumed silica and precipitated silica are commonly used in rubber products [65]. Although fumed silica provides excellent degree of reinforcement due to its very small particle size, the mixing difficulty and high cost limit the use of fumed silica in tire industry. Precipitated silica, the major type of silica currently used in tire industry, is

manufactured by the controlled neutralization of alkali silicate, e.g., sodium silicate (water glass), by a mineral acid such as sulfuric acid and carbonic acid [72].

$$nSiO_2.Na_2O + H_2SO_4 \longrightarrow Na_2SO_4 + nSiO_2.H_2O$$

The reaction temperature plays a key role in primary particle size [65] while both drying time and pH control types of precipitated silica, as shown in Table 3.2.

Table 3.2 Dependence of pH and drying time on types of precipitated silica [73]

Drying time	pH	Dispersibility	Type of precipitated silica
long	high	poor	conventional
long	low	medium	semi highly dispersible
short	high	good	highly dispersible
short	optimized	excellent	highly dispersible

In general, the physical forms of precipitated silica are classified into three forms, i.e., powder, granule, and micro-pearl [74]. Powder form is an ordinary form obtained by a classical drying process whereas granule and micro-pearl forms, a dust-free form, are produced by mechanical process after drying and washing at the end of precipitation process [75]. Figure 3.15(a) and 3.15(b) depict scanning electron microscope (SEM) micrographs of precipitated silica in powder and micro-pearl forms, respectively.

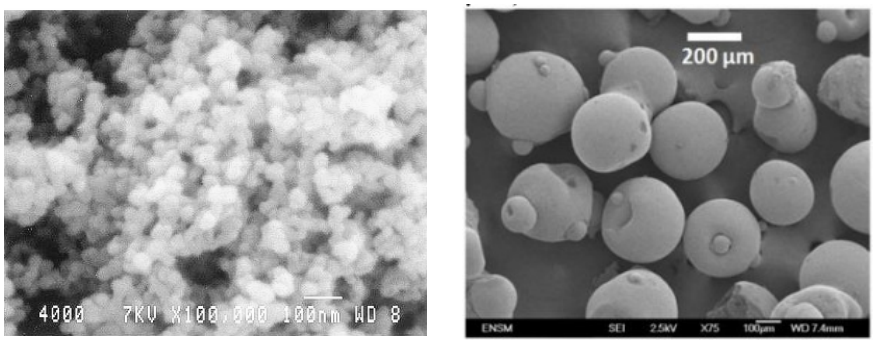

Figure 3.15 SEM micrograph of precipitated silica (a) powder form (Tokusil) [76] and (b) micropearl form (Rhodia Z1165MP) [77]

Like CB, primary particles of precipitated silica are not individually separated but they tend to form clusters and become aggregates. The aggregate structure of silica is formed via siloxane bonds which are very strong and cannot be broken by mechanical force during mixing. Since the surfaces of silica are densely covered by several kinds of polar silanol groups (see Figure 3.16), the silica aggregates can join together to form larger structure, called agglomerate, via hydrogen bonding or van der Waals force which can be destroyed by mechanical force [72, 75, 78]. In addition, it should be noted that the cluster of precipitated silica is usually in string of pearls or other tri-dimensional complex structure [62]. Figure 3.17 represents the structure and average size of typical precipitated silica.

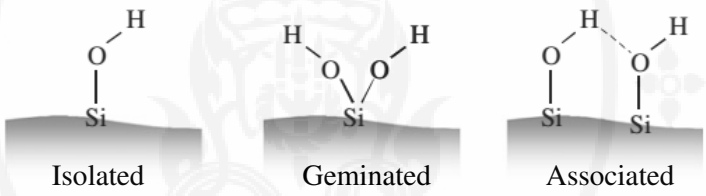

Figure 3.16 Several kinds of silanol group on silica surface [64].

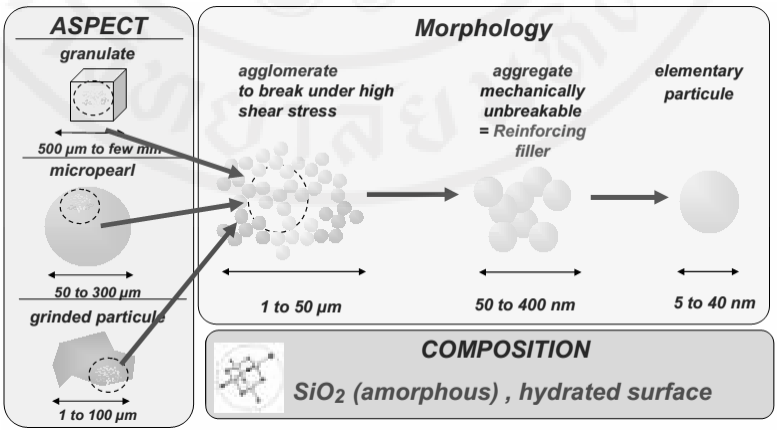

Figure 3.17 Structure of precipitated typical silica and average size [74].

In addition to the specific surface area and structure of precipitated silica, surface activity significantly affects the reinforcement of rubber vulcanizates. As previously mentioned, the surfaces of precipitated silica are densely covered by silanol groups, the compatibility between silica and low polarity rubbers, i.e., NR and SBR, is relatively low. Moreover, the polar silanol groups cause strong

filler-filler interaction through intermolecular hydrogen bond, resulting in poor filler dispersion and, thus, poor processability and degree of reinforcement as compared to CB [79]. In addition, since soluble zinc can be absorbed by silanol groups, both state of cure and cure rate of the silica-filled rubber compound are found to reduce [65, 80].

Focusing on tire technology, highly dispersible silica (HDSi) is currently put into commerce to replace the conventional silica (CSi) because it is claimed to offer better dispersion leading to the greater improvement in RR, wear, and other tire properties [4]. This is possibly explained from the fact that the HDSi provides higher shear force during the mixing process as a result of more branched structure and higher structure level as compared to CSi [75, 81, 82].

There are several grades of precipitated silica commercially available for producing tire tread compounds. For instance, Tokusil 255, a conventional powder grade, is manufactured for tire tread providing high fuel saving efficiency (FSE), high abrasion resistance, including high skid resistance [76], and Zeosil 1165MP, a highly dispersible micro-pearl grade, is suitable for producing high performance tire tread focusing on high FSE [83].

3.3.4 Silane coupling agents (SCAs)

As described above, the polar silanol groups covering on silica surfaces cause the decline of properties of the vulcanizate filled with silica. However, this problem has practically been overcome since SCA was discovered. SCAs are defined as silicon-based compounds possessing inorganic and organic moieties in their structure [84]. A general chemical structure of SCA is X_3SiRY, in which X is hydrolysable alkoxy group, R is alkyl group, and Y is organofunctional group, e.g., mercapto, amino and epoxy. In addition, SCAs are structurally divided into several groups, such as monofunctional, bifunctional, and non-sulfur bearing silane. Figure 3.18 demonstrates the chemical structure of SCAs.

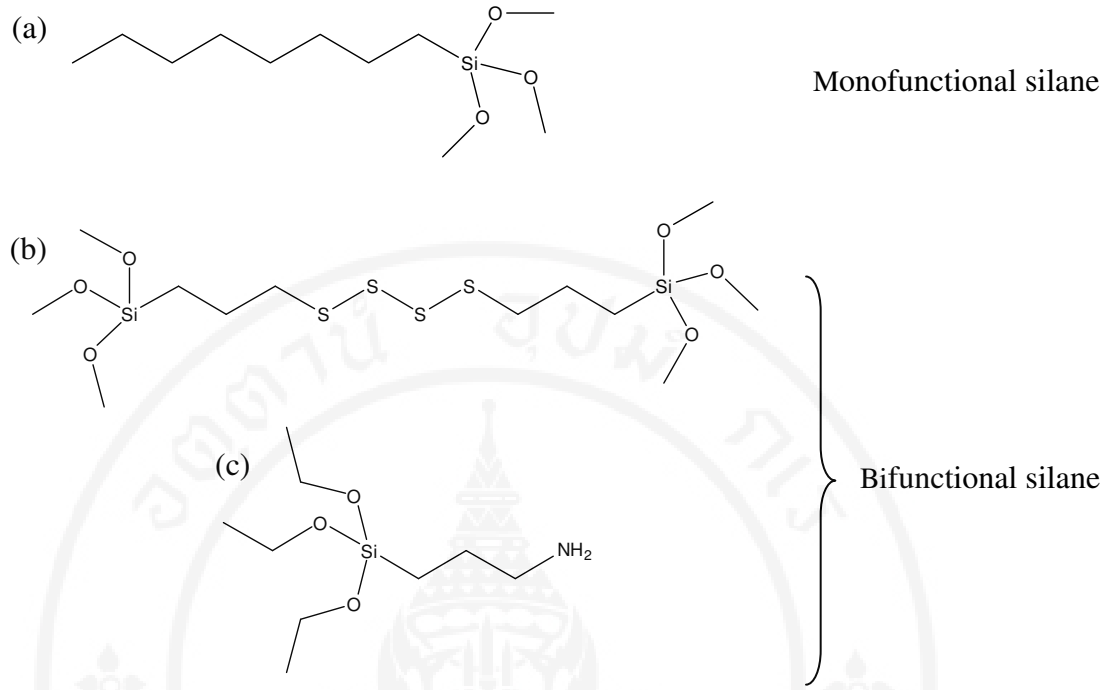

Figure 3.18 Chemical structure of SCAs (a) Octyltrimethylsilane (OTES); (b) bis-(3-(triethoxysilyl)-propyl)-tetrasulfide (TESPT); (c) γ-Aminopropyl triethoxysilane (APTES)

TESPT, a bifunctional SCA possessing a triethoxysilyl and a polysulfidic moieties in molecule, is widely used for not only general purpose rubber products, but also engineering rubber products including tire. Since the basic rubbers used for tire manufacturing, especially NR and SBR, have low polarity, the compatibility with silica covered by the polar silanol groups is relatively poor. This leads to a negative effect on degree of reinforcement including tire performance, as mentioned earlier. The addition of TESPT, into silica-filled tire tread compound, has been reported to improve significantly both RR and WG as a result of the enhanced degree of silica dispersion and rubber-silica interaction [85].

Brinke et al. proposed coupling reaction between silica and NR having TESPT as the bridge [86]. During mixing at sufficiently high temperature, two main chemical reactions occur, as shown in Figure 3.19. The primary reaction refers to the bonding of TESPT to the silica surface via the reaction between ethoxy groups of TESPT and silanol groups of silica, called silanization. Firstly, the ethoxy groups of

TESPT are hydrolyzed (+H_2O/-C_2H_5OH) followed by the condensation reaction (-H_2O) with the silanol groups of silica. Other ethoxy groups are then hydrolyzed and linked together through condensation reaction to form siloxane bonds. The secondary reaction involves the chemical reaction between polysulfidic moiety of TESPT and double bonds of NR to form sulfidic bond. From both primary and secondary reactions, the NR molecules can be bonded on silica surfaces through chemical linkage.

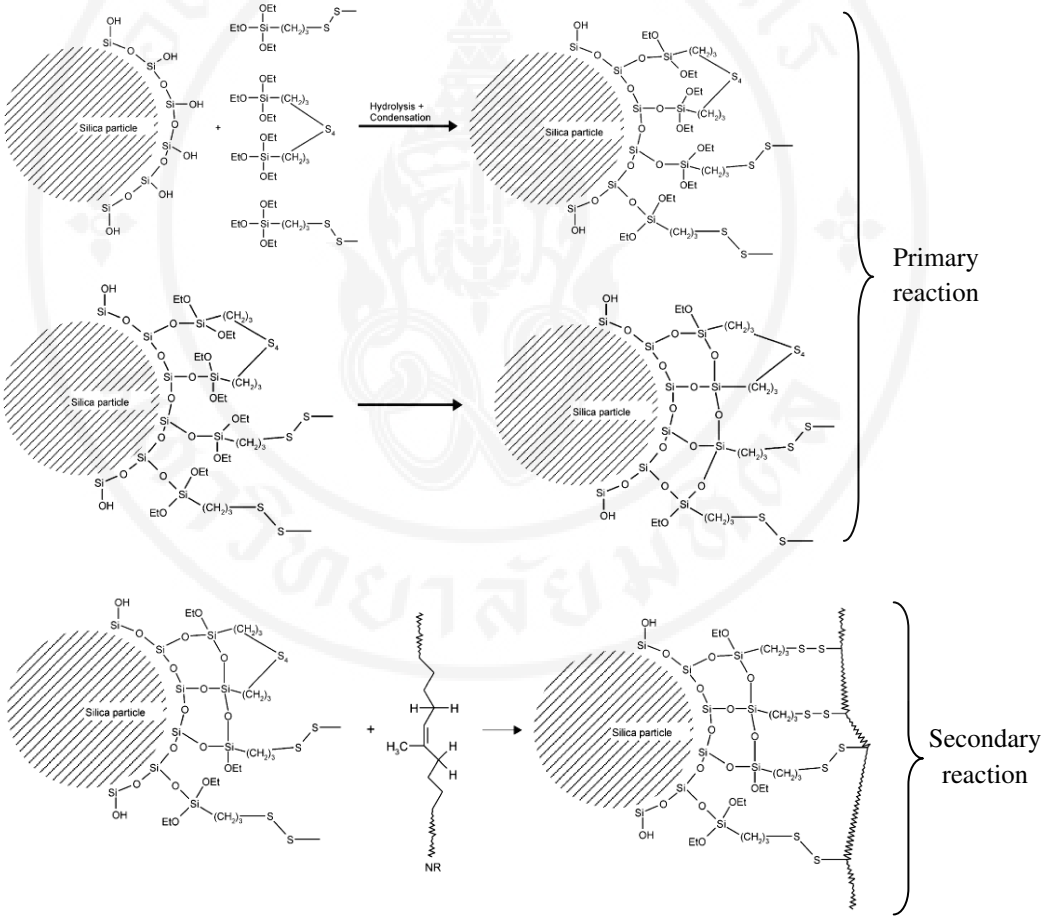

Figure 3.19 Coupling reaction between silica and NR by TESPT [86].

3.3.5 Sulfur curing system

As the major drawbacks of raw rubber are low strength, low elasticity, as well as high solubility in good solvent [38], the raw rubber needs to be vulcanized before being used in practice in order to overcome such drawbacks. Among curing systems used at present, sulfur curing system is widely used in tire technology because

it not only offers good mechanical and dynamic properties, but also eases the cure adjustment [87, 88]. In general, sulfur curing system consists of 3 groups of ingredients, i.e., sulfur, accelerator, and activator. Although unsaturated rubber can be vulcanized by sulfur without accelerator and activator, very long vulcanization time is required. The addition of activators and accelerators into the system leads to the profound reduction in vulcanization time and the significant enhancement in state-of-cure and cure rate [89].

Sulfur used in rubber technology is typically divided into 2 types, i.e., rhombic (or soluble) sulfur and amorphous (or insoluble) sulfur. Rhombic sulfur, a crown-shaped S_8 ring structure, is more preferable than amorphous sulfur due to its lower cost. However, when an excessive amount of rhombic sulfur is used, such sulfur can migrate to the surfaces of rubber compounds, leading to the bloom phenomenon, and, thus, the decline of tackiness [90]. This problem can be alleviated by the use of amorphous sulfur which is a highly polymeric form of sulfur. Although the bloom phenomenon is not found in this type of sulfur, great care must be taken to avoid the transformation of amorphous sulfur. It has been reported that amorphous sulfur can be transformed to rhombic sulfur at the temperature range from 100^{o}-130^{o}C [91]. In other words, the mixing temperature must be controlled with caution.

As the name implies, accelerator is an additive used to speed up the vulcanization rate. There are 9 main groups of accelerator usually employed in rubber industry, i.e., aldehyde amines (slow), guanidines (slow), thiazoles (medium), thiophosphates (ultra-fast), sulfenamides (fast-delayed action), thioureas (ultra-fast), thiurams (ultra-fast), dithiocarbamates (ultra-fast), and xanthates (ultra-fast) [92]. Figure 3.20 depicts the chemical structures of TBBS and TBzTD which are accelerators in sulfenamide and thiuram groups, respectively. Lastly, the combination of ZnO and fatty acid, e.g., stearic acid, is commonly used as effective activator for sulfur curing system [93].

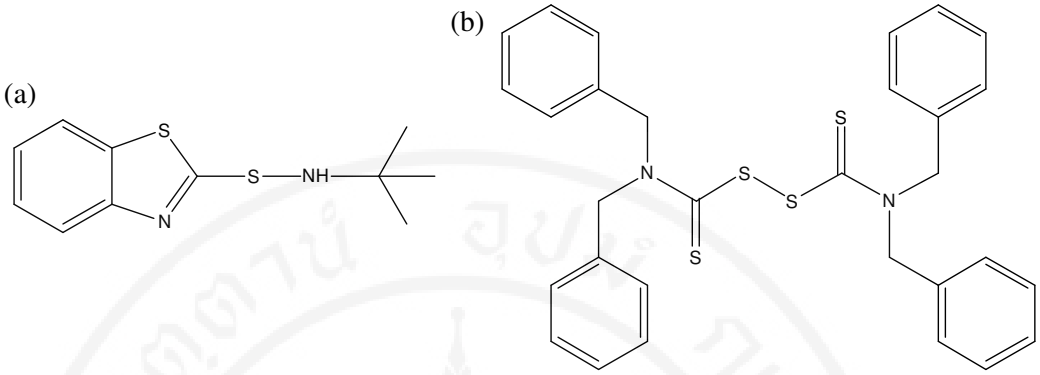

Figure 3.20 Examples of chemical structure of accelerators (a) TBBS, and (b) TBzTD

It has been widely accepted that properties of rubber vulcanizates strongly depend on the magnitude of crosslink density and type of linkage. In sulfur curing system, there are several types of sulfidic linkages typically formed during vulcanization process, as illustrated in Figure 3.21. The ratio of accelerator to sulfur greatly influences the types of sulfidic linkages in rubber vulcanizates. In general, three types of sulfur curing system, namely, conventional vulcanization (CV) system, efficient vulcanization (EV) system, and semi-efficient vulcanization (semi-EV) system, are classified based on the ratio of accelerator to sulfur [94, 95], as illustrated in Table 3.3. For the CV system, the ratio of accelerator to sulfur is relatively low and, thus, polysulfidic linkages (-S-S_x-S-; $x \geq 1$) are mainly formed providing the vulcanizate with good mechanical and dynamic properties. In the case of EV system, on the other hand, the vulcanizates are mainly crosslinked by monosulfidic linkages (-S-) and disulfidic linkages (-S-S-) as a result of a high accelerator/sulfur ratio. As the bond energy of C-S bond found in EV system is significantly higher than that of S-S bond mainly found in CV system, the EV system generally offers greater thermal ageing resistance but poorer mechanical and dynamic properties, compared to CV system. Finally, for the semi-EV system, the ratio of accelerator to sulfur is between that of CV and EV systems, leading to the balanced combination of poly-, di-, and monosulfidic linkages, and, thus, a compromise of properties obtained from CV and EV system is usually found [94].

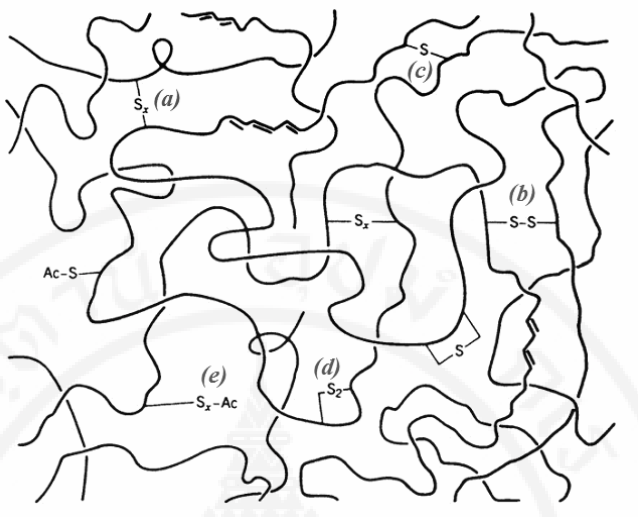

Figure 3.21 Several types of sulfidic linkages in rubber vulcanizate, Adapted from [89]: (a) polysulfidic linkages; (b) disulfidic linkages; (c) monosulfidic linkages; (d) cyclic sulfidic linkages; (e) sulfidic pendant groups

Table 3.3 Accelerator/sulfur ratio (A/S ratio) used in sulfur curing system [88, 96]

	CV system	**Semi-EV system**	**EV system**
Accelerator (phr)	1.2-0.4	2.5-1.2	5.0-2.0
Sulfur (phr)	2.0-3.5	1.0-1.7	0.4-0.8
A/S ratio	0.1-0.6	0.7-2.5	2.5-12.0

3.4 Rubber reinforcement

Fillers are usually added into rubber for several purposes such as cost reduction and reinforcement [38]. It is believed that the fillers added into rubber compounds play crucial roles in both static and dynamic behaviors. Figure 3.22 represents 4 main factors affecting complex modulus and reinforcing efficiency of filled rubber at various strains. These factors can be generally classified into strain-independent behavior, i.e., polymer network, hydrodynamic effects, as well as in-rubber structure, and strain-dependent behavior, i.e., filler-filler interaction [97].

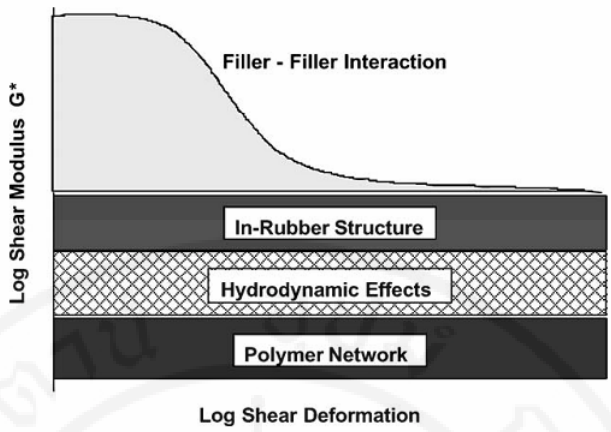

Figure 3.22 Complex shear modulus of filled rubber as a function of dynamic shear strain [98]

3.4.1 Polymer network

There are two types of network generally formed in polymer, i.e., physical and chemical networks. The former is formed through chain entanglement whereas the latter, a major network in vulcanized rubber, is generated during the vulcanization process via chemical reaction. Although the chemical network contribution is strain-independent behavior, it is directly proportional to modulus. Typically, the greater amount of polymer network leads to the higher modulus. The relationship among the modulus of rubber vulcanizates (G_0), number of elastically active chains per unit volume (ν), Bolzmann's constant (K), and absolute temperature (T) is shown as follows [99, 100]:

$$G_0 = \nu KT \tag{8}$$

3.4.2 Hydrodynamic effects

This contribution is considered as strain independent behavior involving the addition of filler (rigid phase) into fluid (deformable phase). Fröhlich et al. [97] mentioned that this contribution deals with strain amplification effect. When the force is applied, the polymer matrix is deformable whereas the filler cannot be deformed due to its rigidity. This leads to the higher deformation of polymer matrix, compared to the external deformation.

By considering the context of suspension, the viscosity of a viscous particle suspension (η) is related to the viscosity of unfilled fluids (η_0) and the volume fraction of particles (ϕ), as following equation [101, 102]:

$$\eta = \eta_0(1 + 2.5\phi) \tag{9}$$

However, this equation is suitable for low concentration of spherical particle system (non-interacting spherical filler). To apply for the modulus of filled rubber (G') usually containing high concentration of spherical particles (interacting spherical filler), the quadratic term (ϕ^2) dealing with the interaction between particles is added into the above equation and, thus, the Einstein-Guth-Gold equation is developed, as follows [103]:

$$G' = G'_0 (1 + 2.5\phi + 14.1\phi^2) \tag{10}$$

Since the shape of the main reinforcing fillers, particularly CB, is not fully spherical but is composed of complex branched structure, the influence of particle shape on modulus is considered. As a result, the Einstein-Guth-Gold equation is modified by introducing a shape factor (f) which refers to the ratio of the longest to the shortest side of the filler particles, as shown in following equation [104, 105]:

$$G' = G'_0 (1 + 0.67 f\phi + 1.62 f^2\phi^2) \tag{11}$$

3.4.3 In-rubber structure

This contribution is believed to be the combined consequences of: (i) the rubber occluded in the voids of filler aggregates and (ii) the rubber physically or chemically adsorbed on the filler surfaces acting as the shell of filler [97]. As these rubbers, or the so-called bound rubber, are considered to be a part of immobilizing fillers and/or shielded form deformation, the in-rubber structure not only is one of strain-independent contributions, but also increases effective filler volume.

Several models of bound rubber are proposed by researchers, for example, shell rubber model, occluded rubber model, including glassy rubber shell model. The shell rubber model is proposed by considering the physical or chemical adsorption of rubber on filler surfaces to form the layer of shell rubber (see Figure 3.23(a)) [106]. The occluded rubber model is proposed based on the occlusion of rubber which is around filler aggregates and shell rubber, as illustrated in Figure 3.23(b) [106]. Lastly,

the glassy rubber shell model is proposed based on CB particles shelled by a double layer of a glass-state and a rubber-state layer (see Figure 3.23(c)) [107].

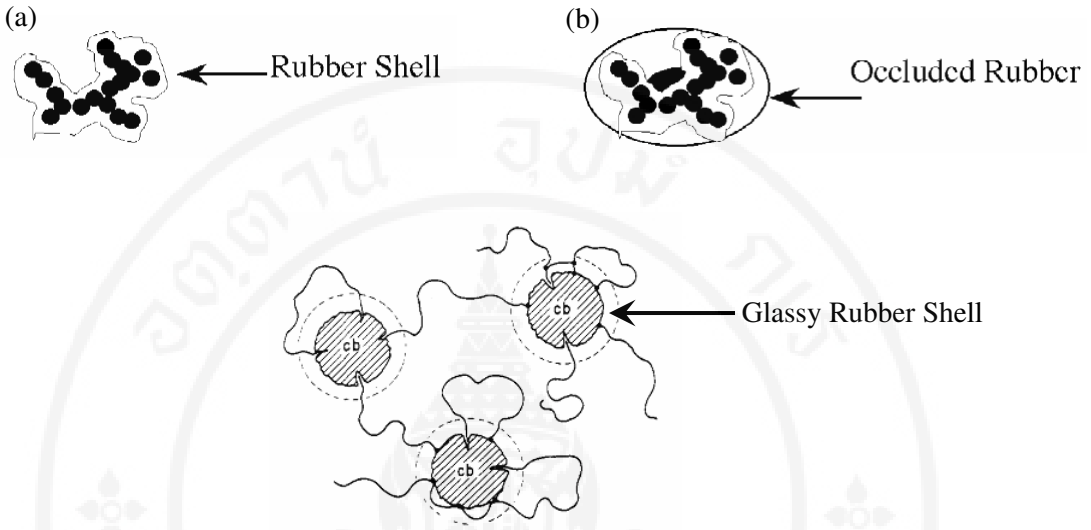

Figure 3.23 Bound rubber models: (a) shell rubber model; (b) occluded rubber model; (c) glassy rubber shell model [106, 107]

3.4.4 Filler-filler interaction

Among 4 main factors influencing the modulus of filled rubber, the filler-filler interaction is only a contribution classified as strain-dependent behavior. It is found that, originally demonstrated by Payne [108], the modulus of filled rubber is noticeably decreased under small deformation, attributed mainly to the breakdown of filler network (see Figure 3.24) which is usually formed through physical interaction, e.g., van der Waals force and/or hydrogen bonds. It is widely accepted that the magnitude of filler-filler interaction, namely Payne effect, can be used to predict the degree of filler dispersion in filled rubber, i.e., the lower the Payne effect, the greater the filler dispersion [109, 110]. Compared to CB, silica generally provides greater magnitude of filler-filler interaction because its surfaces are densely covered by hydrophilic silanol groups [108, 111].

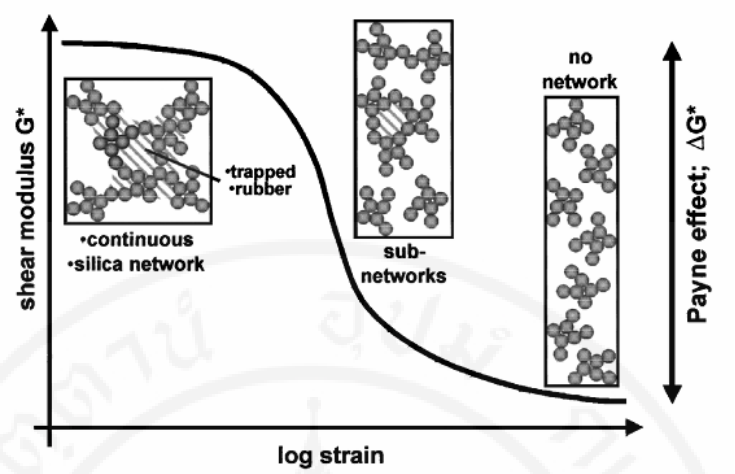

Figure 3.24 Payne effect model [78]

3.5 Previous studies on tire tread compounds

Many attempts have been made to investigate the relationship between viscoelastic properties and several properties including parameters affecting the mechanical properties, dynamic properties as well as tire performance, i.e., abrasion resistance, WG, and RR, of the tire tread compounds.

Grosch et al. [112] studied the friction of gum acrylate-butadiene rubber (ABR) against a clean dry silicon carbide surfaces as a function of temperature and sliding velocity. Results exhibited that the friction coefficient of gum ABR obtained from master curve increased with increasing the sliding velocity to a maximum value and then decreased afterwards. To obtain the master curve, the friction coefficients over a logarithmic range of sliding velocities at various temperatures were measured. The master curve was then established by shifting the curves obtained at various temperatures to the curve at room temperature by a shift factor (log a_T) calculated from the WLF equation (see Figure 3.25). It was also found that the relationship between viscoelastic properties and friction of the rubber arising from adhesion and deformation losses was found to be close.

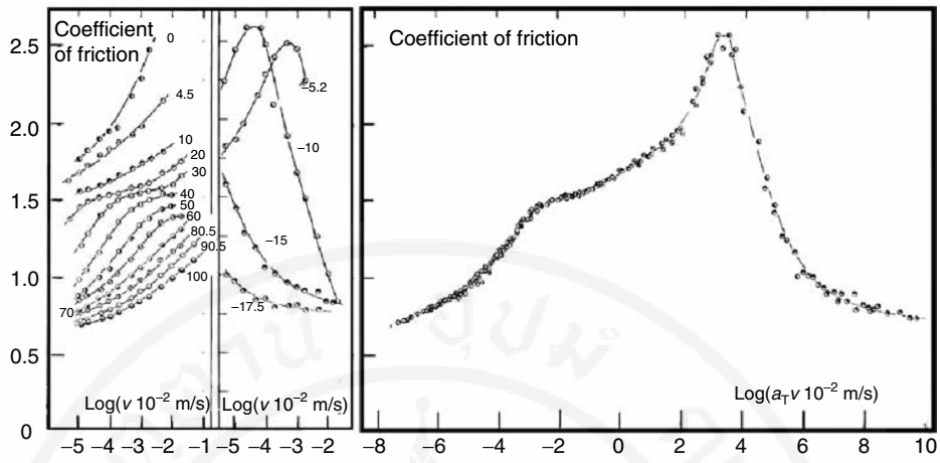

Figure 3.25 Friction coefficient over a range of sliding velocities at various temperatures (left) and a master curve referred to room temperature (right) of gum ABR [112]

Several researchers investigated the correlation between tanδ value at low temperature obtained from dynamic mechanical thermal analyzer (DMTA) and WG/WSR of the vulcanizates determined using a British Pendulum Skid Tester (BPST). They found a good correlation of tanδ at low temperature to WG/WSR values [113-115].

Nowadays, it has been widely accepted that the tanδ at low temperature could be used as the indicator for WG of the vulcanizates. Benito et al. [116] predicted WG of the CB-filled ESBR vulcanizates used for tire tread compound by considering tanδ at -15°C. Many researchers investigated the effects of several factors, e.g., SBR type [44, 110], filler type [49], SCA type [45, 51], including temperature used for modifying silica surfaces with TESPT [50], on WG property of the tire tread compounds by focusing on tanδ at 0°C. In addition, the tanδ at the temperature range from (-10) to 10°C is used as the indicator for WG of NR/BR blends filled with CSi/CB hybrid filler in truck tire tread application [117].

Also, RR of the vulcanizates is usually predicted by considering dynamic mechanical properties. Lee et al. [110] related the RR of the HDSi/CB-filled SBR/BR vulcanizates based on tire tread compound by estimating the tanδ at 70°C. Zafarmehrabian et al. [117] estimated the RR of truck tire tread compound by considering the tanδ in the temperature range from 50 to 80°C. It should be noted that

the RR of vulcanizates used for tire tread application, i.e., CB-filled ESBR [116], CSi-filled SSBR [44, 45], and HDSi-filled SSBR/BR [51], is usually predicted from the tanδ at 60°C.

Benito et al. [116] developed a coupling agent for CB-filled system. In this experiment, p-aminobenzenesulfonyl azide (Amine-BSA) was used as a coupling agent for CB-filled SBR. It has been found that, as Amine-BSA was added, not only the modulus at low strain, resilience, crosslink density, and T_g of the vulcanizates were increased, but tire performance, i.e., WG, RR, and abrasion resistance, was also improved. Explanation was given to the improvement in coupling behavior caused by azide moieties and amine groups of Amine-BSA reacting with rubber and carboxylic groups on CB surfaces, respectively (see Figure 3.26).

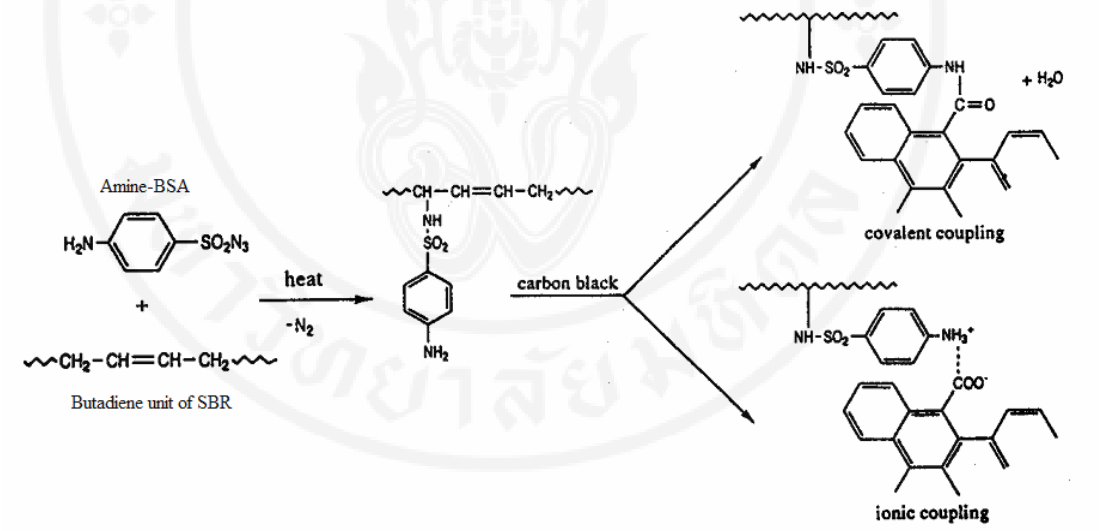

Figure 3.26 Proposed coupling reaction between CB and SBR by Amine-BSA [116]

The effect of SCAs on properties of silica-filled tire tread compounds based on SSBR was studied by Ko et al. [45]. In this study, four types of new SCAs, i.e., 1-[3-(octanoylthio)propyl]-1,1,3,3,3-pentaethoxy-1,3-disilapropane (S1), bis[3-(octanoylthio)-1-propyl]-diethoxysilane (S2), 5-(triethoxysilylpropylthia)-2 potassium-1,3,4-thiadiazolate (S3), as well as 2,5-(triethoxysilylpropylthia)-1,3,4-thiadiazole (S4), and two types of commercial SCAs, i.e., TESPT and 3-octanoylthio-1-propyltriethoxysilane (NXT), were compared. Figure 3.27 depicts chemical structure of SCAs used in this study. Results revealed that, among 6 types of SCAs, S3 and S4

gave the rubber compounds with shorter optimum cure time (t_c90) whereas WG (correlated with tanδ at 0°C) and RR (correlated with tanδ at 60°C) were slightly inferior compared to other SCAs. The results also revealed that NXT, S1, and S2 showed significant improvement of WG but with slight improvement in RR. Moreover, the greatest abrasion resistance together with moderate WG and RR could be found as TESPT was employed.

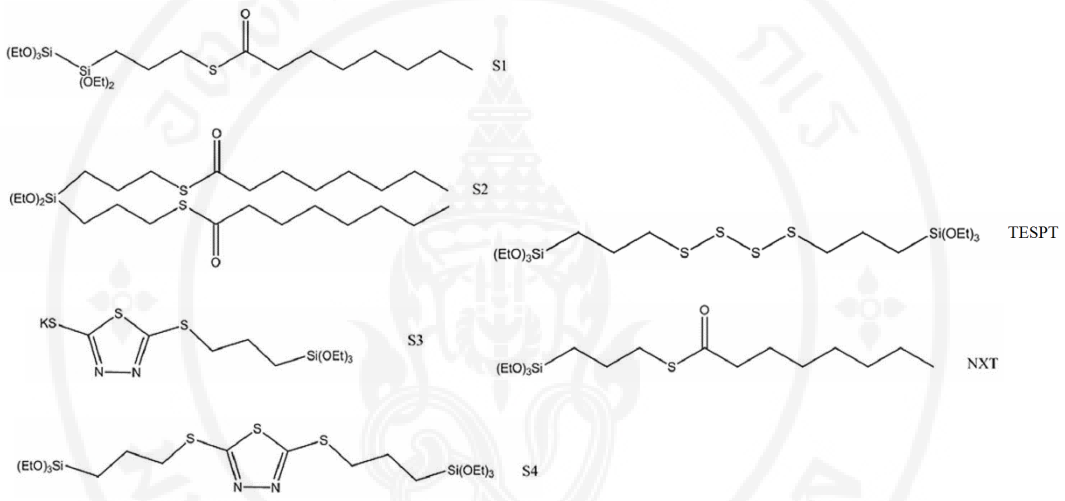

Figure 3.27 Chemical structure of S1, S2, S3, S4, TESPT, and NTX [45]

Although TESPT is widely used in tire industry, the optimum dosage of TESPT is still inconclusive because the results from published works are not congruous. Khorasani [118] demonstrated that, by considering cure characteristics and mechanical properties, e.g., tensile properties and tear strength, the optimum TESPT content of NR/CSi (30 phr) system was found at approximately 12 wt% of silica incorporated whereas 5 wt% of silica used was an appropriate value of TESPT for NR/CSi (50 phr) system. Qu et al. [119] showed that, for CSi-filled SSBR, the greatest degree of silica dispersion was found when 2.5 wt% of TESPT was added. Further increase in TESPT content led to not only a reappearance of silica agglomerates, but also a reduction of rubber-filler interaction which was indicated from bound rubber content (BRC).

A new type of SCA, namely VP Si 363, concerning about the environmental characteristics of a tire was developed by Klockmann et al [51]. The

comparison between VP Si 363 and TESPT was also studied. It was found that the silica-filled SSBR/BR containing 9 phr of Si VP 363 provided superior FSE (represented by tanδ at 60°C) to the silica-filled SSBR/BR containing 6.6 phr of TESPT. Moreover, the addition of 10 phr of Si VP 363 led to the lower volatile organic compound (VOC) emission, compared to the addition of 6.4 phr of TESPT. By considering the chemical structure of VP Si 363 (see Figure 3.28), its ethoxy group is capable of reacting with silanol groups on silica surfaces while its polymeric moieties possessing a polar part could attract and shield the silanol groups, resulting in silanization reaction with low VOC. In addition, a thiol moiety of VP Si 363 could react with double bond of rubber. This might be the reason why VP Si 363 is claimed as an eco-friendly SCA.

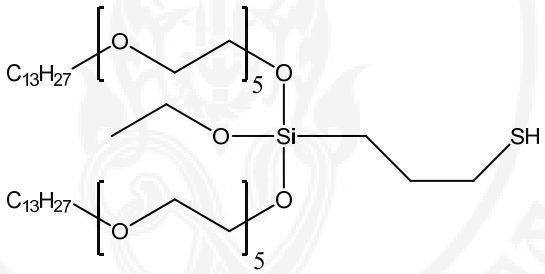

Figure 3.28 Chemical structure of VP Si 363

The effect of various parameters on the properties of N234 CB-filled SBR based tire tread compound was studied by Atashi et al. [120]. They reported that the partial substitution of SBR with NR resulted in improvement of mechanical properties, i.e., resilience, tear resistance, crack growth, and abrasion resistance, of the rubber vulcanizates. However, hardness and tensile properties of the blends were not significantly changed. Similar observation was found when SBR is partially substituted by BR with the exception of increased crack growth rate. It was also found that negative effects on the abrasion and tear resistance were found when N234 was partially replaced by N330. The results also revealed that crack growth rate tended to increase with increasing level of sulfur and accelerator.

Zhao et al. [44] successfully synthesized the functionalized SSBR (F-SSBR) by adding alkoxy-silane groups at 2 chain ends of SSBR. The effect of chain end functionalization on properties of CSi-filled SSBR was investigated. It was

found that the F-SSBR offered greater mechanical properties, e.g., tensile strength and tear strength, heat build-up (HBU), including WG (represented by tanδ at 0°C) and FSE (represented by tanδ at 60°C) than SSBR, attributed to the greater rubber-filler interaction indicated by BRC and degree of filler dispersion as compared to SSBR. Results also revealed that the above properties were significantly improved when small amount of CSi was added into F-SSBR solution and chemically interacted with alkoxy-silane groups at chain ends of F-SSBR during the synthesis (CSi/F-SSBR). Figure 3.29 illustrates the synthesis process of SSBR, F-SSBR, and CSi/F-SSBR.

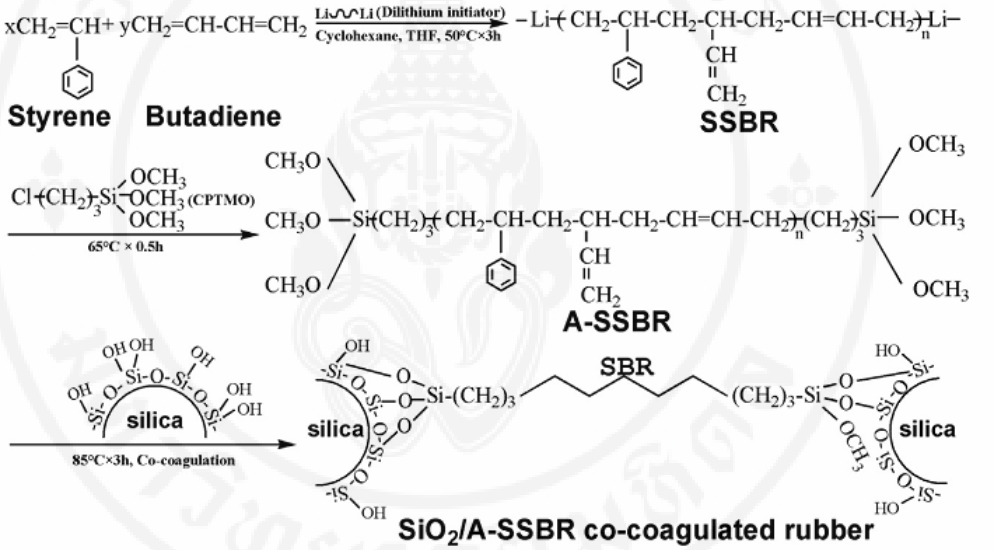

Figure 3.29 Synthesis process of SSBR, F-SSBR, and CSi/F-SSBR [44]

Effect of filler type, i.e., CSi, CB, and nano-diamond powder, on WSR of SSBR/BR blends measured by BPST was studied by Wu et al [49]. TESPT was added only into the system containing CSi. Results showed that the CSi provided higher WSR than CB, possibly owing to the greater hardness of CSi. Generally, the higher hardness of filler led to the greater micro-hardness of the composite, resulting in the higher WSR [121]. Moreover, the WSR of the CSi- and CB-filled vulcanizates measured on ground glass is significantly higher than that of the CSi- and CB-filled vulcanizates measured on smooth glass. Results revealed that the WSR of the vulcanizates strongly depended on both filler type and surfaces characteristics. Interestingly, the partial replacement of CSi and CB by nano-diamond particles led to

the improvement in WSR, because of the increased micro-hardness of the composite. Influence of strain amplitude on tanδ at 0°C of CSi- and CB-filled SSBR/BR blends was also investigated using DMTA. At low strain (< 0.344% strain), the CSi gave higher tanδ at 0°C as compared to CB. However, the opposite result was found when the strain amplitude was further increased, i.e., CB imparted higher tanδ at 0°C than CSi. Explanation was proposed via the greater magnitude of energy dissipation of CB caused by the higher magnitude of filler-filler network. Results revealed that the test strain should be specified when WSR of the vulcanizates was predicted by tanδ at 0°C.

Zafarmehrabian et al. [117] investigated the effects of CSi/CB ratio on properties of NR/BR blends with the presence of TESPT based on truck tire tread compounds. They found that the increased CSi ratio resulted in not only the improvement in HBU and RR (represented by tanδ at temperature range of 50-80°C) of the vulcanizates, but also enhancement in fatigue life. The improved fatigue resistance could be attributed to the reduced modulus at low strain caused by the decreased crosslink density. Results also represented that tensile strength, modulus at 300% strain (M300), including WG (represented by tanδ at temperature range of (-10) - (+10)°C of the vulcanizates tended to decrease with increasing silica ratio, possibly due to the dominant effect of the reduced crosslink density.

CHAPTER IV
MATERIALS AND METHODS

4.1 Materials

All materials were used as-received. The materials used in the present study are summarized in Table 4.1.

Table 4.1 List of materials used in the present study

Materials	Abbreviations	Grades/Suppliers
Solution styrene butadiene rubber: TDAE oil content = 27.1%; Bound styrene content = 34.6%; Vinyl content = 40.1%; ML(1+4 @100°C) = 54.5	SSBR	6450SL /Kumho Petrochemical Co., Ltd., South Korea
Solution styrene butadiene rubber: TDAE oil content = 27.3%; Bound styrene content = 36.0%; Vinyl content = 26.0%; ML(1+4 @100°C) = 52.0)	SSBR	3626 /LG Chemical, South Korea
Emulsion styrene butadiene rubber: TDAE oil content = 26.4%; Bound styrene content = 23.4%; ML(1+4 @100°C) = 44.6)	ESBR	1723 /Kumho Petrochemical Co., Ltd., South Korea

Table 4.1 List of materials used in the present study (continued)

Materials	Abbreviations	Grades/Suppliers
Zinc oxide	ZnO	White seal /Thai-Lysaght Co., Ltd., Thailand
Stearic acid	-	Kij Paiboon Chemical Ltd., Part., Thailand
N-(1,3-dimethylbutyl)-*N'*-phenyl-p-phenylenediamine	6PPD	Monflex Pte. Ltd., Singapore
2,2,4-trimethyl-1,2-dihydroquinoline, polymerized	TMQ	Monflex Pte. Ltd., Singapore
Paraffin wax	-	Petch Thai Chemical Co., Ltd., Thailand
Treated distillate aromatic extract oil	TDAE oil	PSP Specialties Co., Ltd., Thailand
Highly dispersible silica: BET surface area = 153 m^2/g; pH = 6.5	HDSi	Zeosil 1165MP /Rhodia Silica Korea Co., Ltd., South Korea
Conventional precipitated silica: BET surface area = 166 m^2/g; pH = 6.9	CSi	Tokusil 255 /OSC Siam Silica Co., Ltd., Thailand
Carbon black: BET surface area = 126 m^2/g	CB	N234 /Thai Carbon Black Public Co., Ltd., Thailand
Bis[3-(triethoxysilyl)propyl] tetrasulfide	TESPT	Si-69, Innova (Tianjin) Chemical Co., Ltd., China

Table 4.1 List of materials used in the present study (continued)

Materials	Abbreviations	Grades/Suppliers
N-tert-butyl-2-benzothiazole sulfenamide	TBBS	Monflex Pte. Ltd., Singapore
Tetrabenzylthiuram disulfide	TBzTD	Behn Meyer Chemicals (T) Co., Ltd., Thailand
Sulfur	S_8	The Siam Chemical Public Co., Ltd., Thailand

4.2 Equipment

The equipment used in the present study is tabulated in Table 4.2.

Table 4.2 List of equipment used in the present study

Equipment	Manufacturer or Supplier
Internal mixer	Brabender Plasticorder 350E, Germany
Two-roll mill	LabTech Model LRM150, Thailand
Hydraulic hot press	Wabash MPI Model G30-15-0X, USA
Mooney viscometer	TechPro ViscTECH+, USA
Moving die rheometer	TechPro MD+, USA
Rubber process analyzer	Alpha Technologies Model RPA2000, USA
Gel permeation chromatography Instrument	Waters 150-CV plus, USA

Table 4.2 List of equipment used in the present study (continued)

Equipment	Manufacturer or Supplier
Hardness tester	Wallace H17A, UK
Universal testing machine	Instron 3366 series, USA
Akron abrasion tester	Gotech Model GT-7012-A, Taiwan
Flexometer	BF Goodrich Model II, USA
Dynamic mechanical thermal analyzer	Gabo Qualimeter Model Eplexor 25N, Germany
Ultra-microtome	Leica EM FCS, Austria
Transmission electron microscope	Jeol JEM-2010, Japan
Scanning electron microscope	Hitachi 3400N, Japan
Atomic force microscope	Seiko SPA 400, Japan
Aging oven	Elastocon EB10, Sweden
Analytical balance	Kern ALJ 220-4, Germany
Bandknife splitting machine	Fortuna type AB 320 G, Germany

4.3 Experimental

4.3.1 Compounding design

4.3.1.1 Effects of silanization temperature and silica type on properties of silica-filled SSBR compounds and vulcanizates

To study the effects of silanization temperature and silica type, two types of silica (HDSi and CSi) were selected and silica loading was kept constant at 80 phr (parts per hundred rubber). The compound formulation used in this part is shown in Table 4.3.

Table 4.3 The compound formulation used in the study of silanization temperature and silica type effects

Ingredients	Content (phr)
SBR (SSBR6450SL)	137.5
ZnO	3.0
Stearic acid	2.0
6PPD	1.5
TMQ	1.0
Paraffin wax	2.0
TDAE oil	10.0
HDSi or CSi	80.0
TESPT (8 wt% of silica)	6.4
TBBS	1.2
TBzTD	0.2
S_8	2.2

4.3.1.2 Effects of TESPT content and silica type on properties of silica-filled SSBR compounds and vulcanizates

To study the effects of TESPT content and silica type, various TESPT contents were investigated: 0, 6, 8, 10 and 12 wt% of silica. Two types of silica (HDSi and CSi) were selected loading of at fixed of 80 phr. Table 4.4 represents the compound formulation used in this part.

Table 4.4 The compound formulations used in the study of TESPT content and silica type

Ingredients	Content (phr)				
	1	**2**	**3**	**4**	**5**
SBR (SSBR6450SL)	137.5	137.5	137.5	137.5	137.5
ZnO	3.0	3.0	3.0	3.0	3.0
Stearic acid	2.0	2.0	2.0	2.0	2.0
6PPD	1.5	1.5	1.5	1.5	1.5
TMQ	1.0	1.0	1.0	1.0	1.0
Paraffin wax	2.0	2.0	2.0	2.0	2.0
TDAE oil	10.0	10.0	10.0	10.0	10.0
HDSi or CSi	80.0	80.0	80.0	80.0	80.0
TESPT	0.0	4.8	6.4	8.0	9.6
TBBS	1.2	1.2	1.2	1.2	1.2
TBzTD	0.2	0.2	0.2	0.2	0.2
S_8	2.2	2.2	2.2	2.2	2.2

4.3.1.3 Effects of silica/CB hybrid filler and SBR type on properties of SBR compounds and vulcanizates

To study the effects of silica/CB hybrid filler and SBR type, two grades of SSBR having comparable styrene content and Mooney viscosity, i.e., SSBR6450SL and SSBR3626, and one grade of ESBR, i.e., ESBR1723, were selected. Two grades of silica (HDSi and CSi) and one grade of CB (N234) were used. The total amount of hybrid filler was kept constant at 80 phr. The ratio of silica to CB was varied as follows: 100/0, 80/20, 60/40, 40/60, 20/80 and 0/100. In this part, the TESPT dosage was kept constant at 10 wt% of silica incorporated. Details of compound formulations used in this part are given in Table 4.5.

Table 4.5 The compound formulations used in the study of silica/CB hybrid filler and SBR type

Ingredients	Content (phr)					
	100/0	**80/20**	**60/40**	**40/60**	**20/80**	**0/100**
SBR (SSBR6450SL or SSBR3626 or ESBR1723)	137.5	137.5	137.5	137.5	137.5	137.5
ZnO	3.0	3.0	3.0	3.0	3.0	3.0
Stearic acid	2.0	2.0	2.0	2.0	2.0	2.0
6PPD	1.5	1.5	1.5	1.5	1.5	1.5
TMQ	1.0	1.0	1.0	1.0	1.0	1.0
Paraffin wax	2.0	2.0	2.0	2.0	2.0	2.0
TDAE oil	10.0	10.0	10.0	10.0	10.0	10.0
HDSi or CSi	80.0	64.0	48.0	32.0	16.0	0.0
CB	0.0	16.0	32.0	48.0	64.0	80.0
TESPT	8.0	6.4	4.8	3.2	1.6	0.0
TBBS	1.2	1.2	1.2	1.2	1.2	1.2
TBzTD	0.2	0.2	0.2	0.2	0.2	0.2
S_8	2.2	2.2	2.2	2.2	2.2	2.2

4.3.1.4 Effects of filler and oil loadings on properties of SSBR compounds and vulcanizates

To study the effects of filler and oil loadings, a total filler content was altered simultaneously with rubber process oil content in order to keep the hardness constant. According to the results from the previous part, SSBR6450SL was selected as a rubber matrix in this part. The ratio of CSi to CB was kept constant at 60 to 40. The TESPT content was fixed at 10 wt% of CSi. Table 4.6 illustrates the compounding recipes and the estimated relative cost of the compounds used in this part.

Table 4.6 The compounding recipes and estimated relative cost of the compounds used in the study of filler and oil contents

Ingredients	Content (phr)			
	F1	**F2**	**F3**	**F4**
SBR (SSBR6450SL)	137.5	137.5	137.5	137.5
ZnO	3.0	3.0	3.0	3.0
Stearic acid	2.0	2.0	2.0	2.0
6PPD	1.5	1.5	1.5	1.5
TMQ	1.0	1.0	1.0	1.0
Paraffin wax	2.0	2.0	2.0	2.0
TDAE oil	0.0	10.0	20.0	30.0
CSi	42.6	48.0	53.4	59.4
CB	28.4	32.0	35.6	39.6
TESPT	4.3	4.8	5.3	5.9
TBBS	1.2	1.2	1.2	1.2
TBzTD	0.2	0.2	0.2	0.2
S_8	2.2	2.2	2.2	2.2
Estimated cost (%)	100.0	96.5	93.5	90.7

4.3.1.5 Effects of sulfur vulcanization system and crosslink density on properties of SSBR vulcanizates

To study the effects of sulfur vulcanization system and crosslink density, two sulfur vulcanization systems, i.e., CV system and semi-EV system were used. For each system, the relative amount of curatives (TBBS, TBzTD and sulfur) was varied from 100% to 140%. Similar to the experiment in section 4.3.1.4, only SSBR6450SL was selected as a rubber matrix. The ratio of CSi to CB was kept constant at 60 to 40. It should be noted that the total filler content in this part was reduced to 70 phr without any additional TDAE oil. The TESPT content was also fixed at 10 wt% of CSi filled. Details of compound formulations are represented in Table 4.7.

Table 4.7 The compound formulations used in the study of sulfur vulcanization system and crosslink density

Ingredients	Content (phr)					
	CV			semi-EV		
	100%	120%	140%	100%	120%	140%
SBR (SSBR6450SL)	137.5	137.5	137.5	137.5	137.5	137.5
ZnO	3.0	3.0	3.0	3.0	3.0	3.0
Stearic acid	2.0	2.0	2.0	2.0	2.0	2.0
6PPD	1.5	1.5	1.5	1.5	1.5	1.5
TMQ	1.0	1.0	1.0	1.0	1.0	1.0
Paraffin wax	2.0	2.0	2.0	2.0	2.0	2.0
CSi	42.0	42.0	42.0	42.0	42.0	42.0
CB	28.0	28.0	28.0	28.0	28.0	28.0
TESPT	4.2	4.2	4.2	4.2	4.2	4.2
TBBS	1.20	1.44	1.68	1.20	1.44	1.68
TBzTD	0.20	0.24	0.28	0.20	0.24	0.28
S_8	2.20	2.64	3.08	1.20	1.44	1.68

4.3.2 Preparation of rubber compounds

Rubber compounds were prepared using a laboratory internal mixer equipped with a pair of cam blade rotors. Rotor speed and fill factor were kept constant at 40 revolutions per minute (rpm) and 0.75, respectively. Mixing was carried out in 3 steps. In the first step, all ingredients, except for curatives (TBBS, TBzTD and sulfur), were mixed with SBR for 10 minutes at the mixing temperature of 60°C to achieve satisfactory degree of filler dispersion. The compounds were then sheeted on two-roll mill and cooled down to room temperature. In the second step, the so-called silanization step, the compounds were re-mixed at high temperature for 6 minutes to promote the silanization reaction between TESPT and silica. In the first part of this study where the effect of silanization temperature was investigated, the silanization temperature was varied from 120°C to 160°C. However, for the subsequent

experimental parts, only the optimum silanization temperature, i.e., 140°C, was employed for the compound preparation. After the silanization reaction, the compounds were then sheeted and cooled down to room temperature. Finally, the silanized compounds were mixed with the curatives in the final step for 3 minutes at the mixing temperature of 60°C. After mixing, the compounds were sheeted and kept overnight at room temperature prior to being vulcanized and tested.

4.3.3 Measurement of rubber compound properties

4.3.3.1 Mooney viscosity

Mooney viscosity (ML1+4@100°C) of rubber compounds was determined in accordance with ISO 289-1 using a Mooney viscometer at 100°C. Approximately 20 g of rubber compound was used for each test.

4.3.3.2 Cure characteristics

Cure characteristics of rubber compounds, i.e., t_s1, t_c90 and cure rate index (CRI), were investigated by the use of a moving die rheometer (MDR) at 160°C following ISO 6502. CRI is calculated using the following equation:

$$CRI = \frac{100}{(t_c 90 - t_s 1)} \tag{12}$$

4.3.3.3 Rheological properties

Payne effect was determined using a rubber process analyzer (RPA2000) at frequency of 1.7 Hz and temperature of 100°C. The dynamic strain was varied from 0.56 to 100.02%. The difference between storage shear moduli (G') at low strain (0.56%) and high strain (100.02%) is employed to predict the magnitude of Payne effect.

4.3.3.4 Bound rubber content (BRC)

Measurement of BRC was performed by extracting the unbound rubber with toluene. Approximately 0.5 g of rubber test piece was extracted by 100 ml of toluene for 168 hours at room temperature. After filtering with filter

paper, the insoluble part was dried for 2 days at ambient temperature and then placed in an oven at 70°C until a constant weight was gained. The total BRC was calculated by the following equation:

$$BRC(\%) = \frac{W_d - F}{R} x\,100 \quad (13)$$

where W_d is the weight of dry gel; F is the weight of filler in the test piece and R is the weight of rubber in the test piece. It is generally accepted that the BRC measured at room temperature is formed by both physical and chemical interactions [14]. As physically bound rubber could be destroyed at high temperature [122], the amount of chemically bound rubber could therefore be determined by the above procedure, except that, the extraction was performed at 85°C for 36 hours.

4.3.3.5 Molecular weight

Molecular weight of the rubber matrix was monitored by the use of gel permeation chromatography (GPC) technique. Approximately 5 mg of rubber compound was dissolved in 5 ml of tetrahydrofuran (THF) for 5 days. The solution of 100 μl was filtrated prior to being injected into the GPC instrument. The mobile phase and flow rate used in this experiment were THF and 1 mm/min, respectively.

4.3.4 Shaping and vulcanization of rubber compounds

Shaping and vulcanization of rubber compounds were carried out using a hydraulic hot press (via compression molding technique) at 160°C for a period of t_c90 as pre-determined from MDR, unless stated otherwise.

4.3.5 Determination of rubber vulcanizate properties

4.3.5.1 Crosslink density

Measurement of crosslink density was carried out by the use of an indirect method, namely, a swelling test with toluene employed as liquid medium. Three rubber test pieces with approximately 1×2×0.2 cm^3 in dimensions were swollen in toluene for 5 days at room temperature. The test pieces were then taken out, blotted

with filter paper and weighed. Finally, the test pieces were dried at 70°C until a constant weight was gained before reweighing. The crosslink density was calculated based on the Flory-Rehner equation as follows [123]:

$$-[\ln(1-\nu_2)+\nu_2+\chi_1\nu_2^{\,2}]=V_1 n(\nu_2^{1/3}-\frac{\nu_2}{2}) \quad (14)$$

where ν_2 is the volume fraction of polymer in the swollen test piece; χ_1 is the polymer-solvent interaction parameter (0.446 for SBR-toluene [124, 125]); V_1 is the molar volume of the solvent (106.3 cm^3/mol for toluene); n is the number of elastically active chains per unit volume; ν_2 is the volume fraction of polymer in the swollen test piece which is calculated as follows:

$$\nu_2=\frac{m_0\phi_1\frac{(1-\alpha)}{\rho_p}}{m_0\phi_1\frac{(1-\alpha)}{\rho_p}+\frac{(m_1-m_2)}{\rho_s}} \quad (15)$$

where m_0 is the weight of the test piece before swelling; m_1 is the weight of the test piece after swelling; m_2 is the weight of the test piece after drying; ϕ_1 is the weight fraction of rubber in the vulcanized sheet; α is the weight loss fraction of the test piece after the swelling test; ρ_p and ρ_s are densities of rubber and solvent, respectively.

4.3.5.2 Hardness

Hardness was measured using a Wallace Shore A durometer as per ISO 7619-1. The test specimen with approximately 6 mm in thickness was used. At least 5 measurements were carried out for each sample, and the average value was reported.

4.3.5.3 Tensile properties

Tensile properties such as tensile strength, elongation at break, and modulus were determined using a universal testing machine following ISO 37 at a crosshead speed of 500 mm/min with the load cell of 1 kN. The dumb-bell shaped specimens (die type 1) were stamped-cut from the approximately 2 mm. thickness vulcanized sheets. The specimen thickness was measured by a micrometer, and at least five specimens were tested for each sample.

4.3.5.4 Abrasion resistance

Measurement of abrasion resistance was performed by Akron abrasion tester according to BS 903: Part A9, Method B. The standard test specimens were vulcanized at 160°C for t_c90+10 minutes by compression molding technique. Abrasion resistance of the samples was reported in terms of the volume loss per 1,000 revolutions.

4.3.5.5 Heat build-up (HBU) and dynamic set

HBU was evaluated in terms of temperature rise as per ISO 4666-3 using Goodrich flexometer. A cylinder-shaped specimen, with a diameter of 17.8 mm and a height of 25 mm, was prepared at 160°C for t_c90+15 minutes by compression molding technique. The test was carried out under the following conditions: chamber temperature = 100°C; frequency = 30 Hz; initial load = 245 N; dynamic displacement (full stroke) = 4.45 mm. The temperature rise was recorded at the specimen base after testing for 25 minutes.

After the HBU test, the specimens were taken from the test chamber and left at room temperature for 30 minutes before measuring their final heights. The dynamic set was calculated from the following equation:

$$Dynamic\ set\ (\%) = \frac{H_o - H_f}{H_o} x\,100 \qquad (16)$$

where H_o and H_f are the original and final heights of the specimen, respectively.

4.3.5.6 Dynamic mechanical properties

Dynamic mechanical properties of the test specimens (approximately 3.5×0.6×0.2 cm^3 in dimensions) were evaluated in the tension mode by the use of a dynamic mechanical thermal analyzer (DMTA). For the temperature sweep test, the test conditions were as follows: static strain = 1%; dynamic strain = 0.15%; frequency = 10 Hz and heating rate = 2°C/min. The temperature was scanned from -60 to 80°C. For the strain sweep test, the test conditions were as follows: static strain = 12% and frequency = 10 Hz. The dynamic strain was varied from 0.03 to 10% at two test temperatures of 0°C and 60°C.

For preparation of commercial PCR tire test specimen, tread section was sliced using the bandknife splitting machine until the thickness of approximately 0.2 cm was gained. The specimens were then cut into 3.5×0.6×0.2 cm^3 in dimensions.

4.3.5.7 Thermal ageing properties

Investigation of thermal ageing resistance was carried out by ageing the specimens in an air-circulated oven at 100°C for 120 hours. The ratio of tensile properties after ageing to those before ageing, namely relative tensile properties, was used to represent the thermal ageing resistance of the rubber vulcanizates.

4.3.5.8 Degree of filler dispersion

The degree of filler dispersion was examined by TEM and SEM. For TEM, the images were taken on the ultra-thin sections of the specimens under an accelerating voltage of 200 kV. The ultra-thin sections were prepared under cryogenic condition at -70°C using an ultra-microtome. In the case of SEM, the SEM micrographs were taken under an accelerating voltage of 15 kV after the dried smooth surfaces were gold-coated to prevent charging on the surfaces. The smooth surfaces were prepared by glass knife under cryogenic condition at -70°C using an ultra-microtome.

4.3.6 Experimental scheme

The experimental scheme of each part is summarized as follows:

4.3.6.1 Effects of silanization temperature and silica type on properties of silica-filled SSBR compounds and vulcanizates

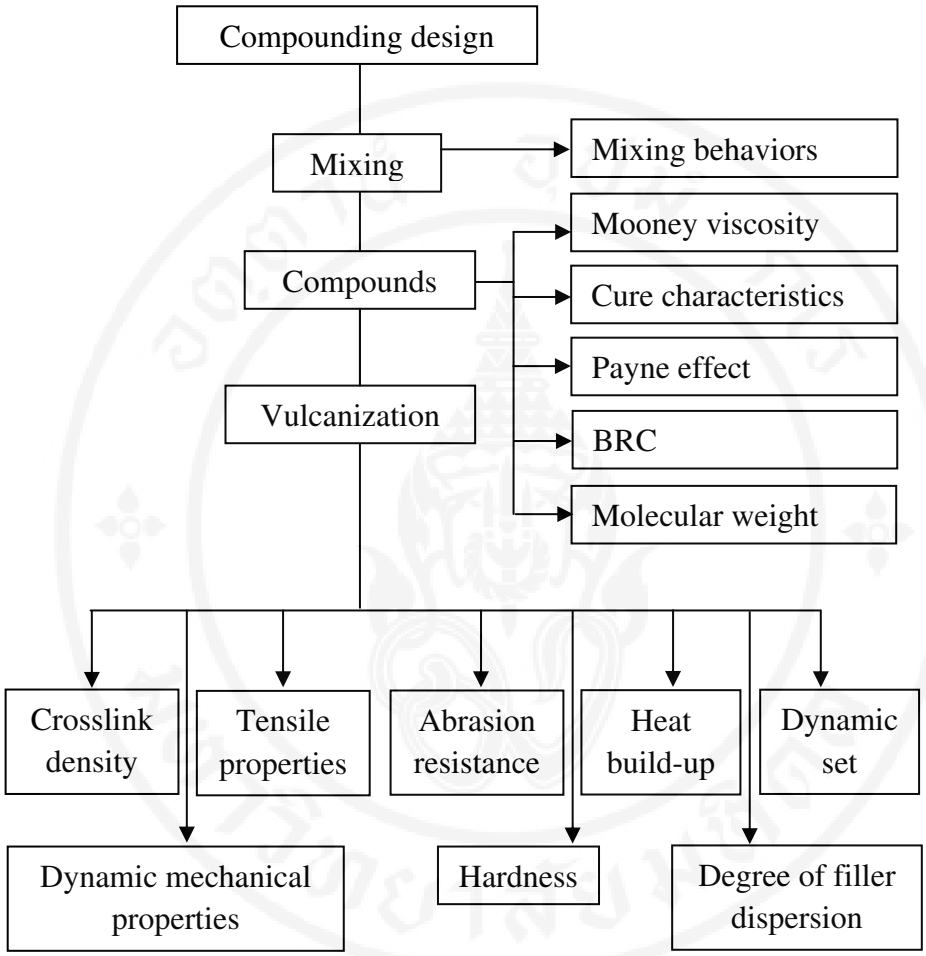

Figure 4.1 Experimental scheme for the study of silanization temperature and silica type

4.3.6.2 Effects of TESPT content and silica type on properties of silica-filled SSBR compounds and vulcanizates

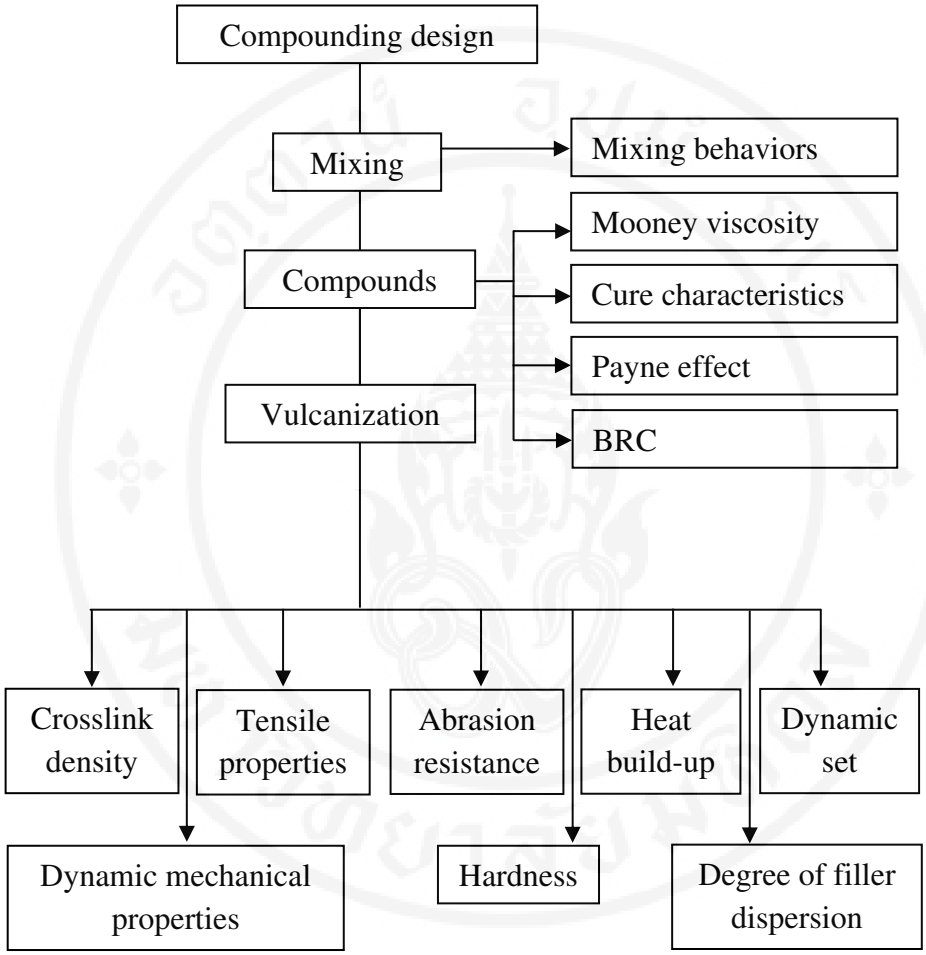

Figure 4.2 Experimental scheme for the study of TESPT content and silica type

4.3.6.3 Effects of silica/CB hybrid filler and SBR type on properties of SBR compounds and vulcanizates

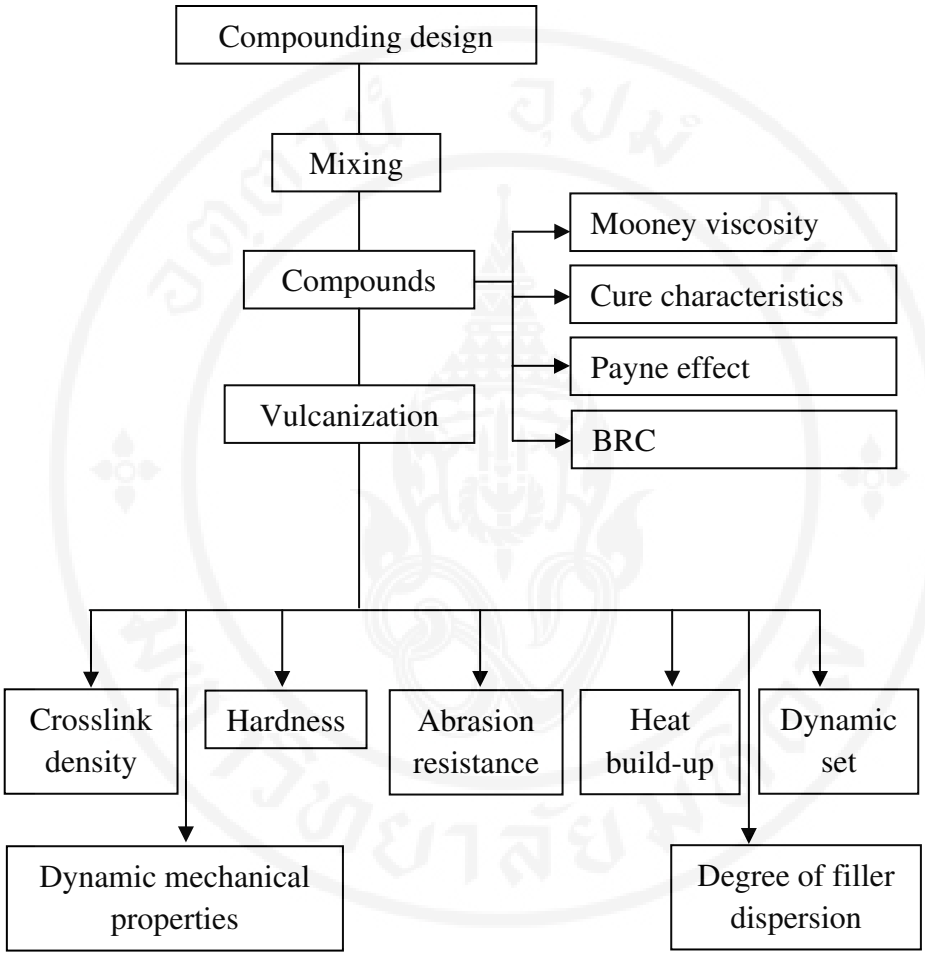

Figure 4.3 Experimental scheme for the study of silica/CB hybrid filler and SBR type

4.3.6.4 Effects of filler and oil loadings on properties of SSBR compounds and vulcanizates

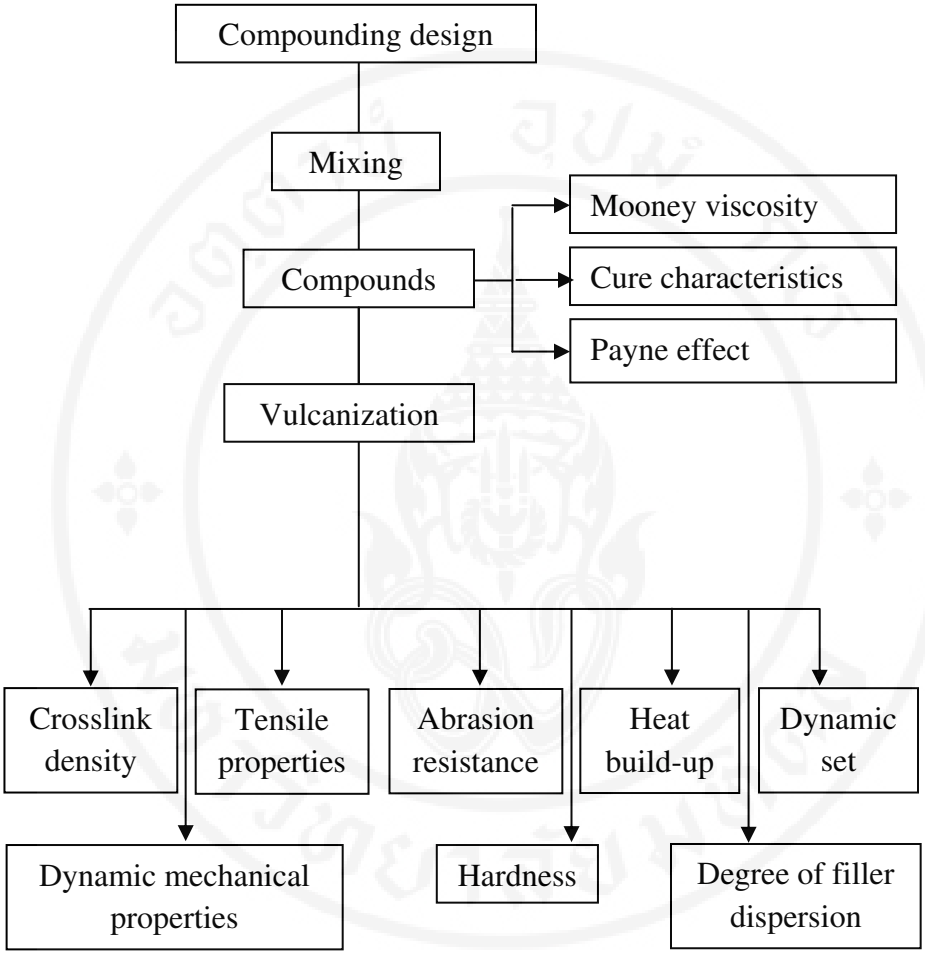

Figure 4.4 Experimental scheme for the study of filler and oil contents

4.3.6.5 Effects of sulfur vulcanization system and crosslink density on properties of SSBR vulcanizates

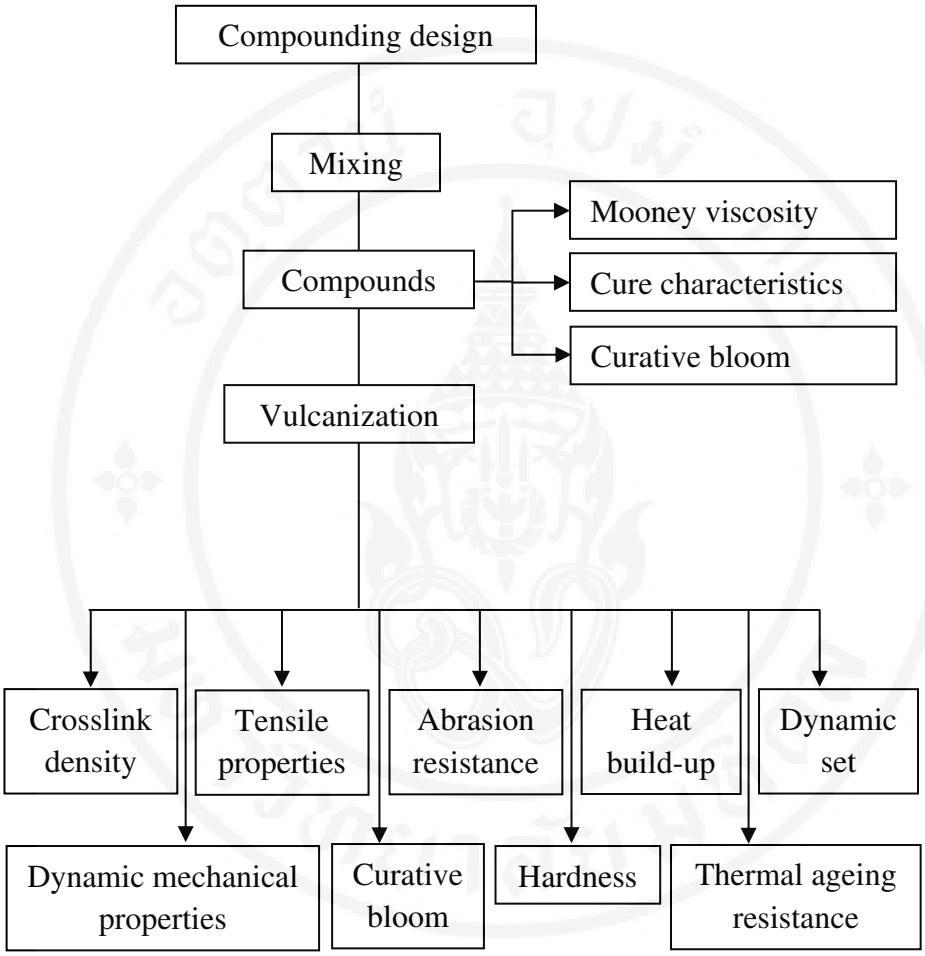

Figure 4.5 Experimental scheme for the study of sulfur vulcanization system and crosslink density

CHAPTER V
RESULTS AND DISCUSSION

Results and discussion can be divided into 5 main parts. In the first part, the compounds filled with HDSi and CSi were prepared under various silanization temperatures. The optimum silanization temperature was then employed in the second part in which the effect of TESPT content was determined. The proper TESPT content was used in the subsequent parts. The third part concerns the influences of SBR and silica types including silica/CB hybrid filler ratio on properties of SBR compounds and vulcanizates. Properties and raw material cost of the vulcanizates having similar hardness as controlled by simultaneously increasing filler and oil loadings were compared in the fourth part. Lastly, the final part is focused on effect of crosslink density on properties of the vulcanizates cured with CV and semi-EV systems.

5.1 Effects of silanization temperature and silica type on properties of silica-filled SSBR compounds and vulcanizates

In this part, the silanization temperature was varied from 120°C to 160°C. The SSBR6450SL was selected as the rubber matrix. The silica loading and TESPT content were kept constant at 80 phr and 8 wt% of silica, respectively. Viscoelastic, mechanical, and dynamic mechanical properties as well as processability of SSBR filled with two types of silica, i.e., HDSi and CSi, were compared.

5.1.1 Mixing behavior in silanization step

During the silanization step, dump temperature and temperature rise were recorded, and results are depicted in Figure 5.1. With increasing silanization temperature, the dump temperature is found to increase whereas the temperature rise noticeably reduces up to 140°C and level off thereafter. The reduction in temperature

rise with increasing silanization temperature is thought to arise from the decreased shear heating. With increasing silanization temperature, the bulk viscosity is reduced, leading to the decrease in shear heating during the mixing process and, thus, the temperature rise. It has previously been reported that scorch phenomenon could occur in the diene rubber when mixed with polysulfide silane (i.e., TESPT) at sufficiently high temperature [126]. This is understandable because the TESPT could contribute some sulfurs capable of reacting with rubber molecules at high temperatures, leading to the occurrence of three dimensional rubber network, and, thus, the increased bulk viscosity. Since the temperature rise of the compounds tends to level off at high silanization temperature (≥140°C), the counter-balance between the reduced bulk viscosity as a result of the increased silanization temperature and the enhanced bulk viscosity caused by scorching phenomenon could be a reasonable explanation for this finding. The results also imply that silica type does not significantly influence the dump temperature and temperature rise of the compounds.

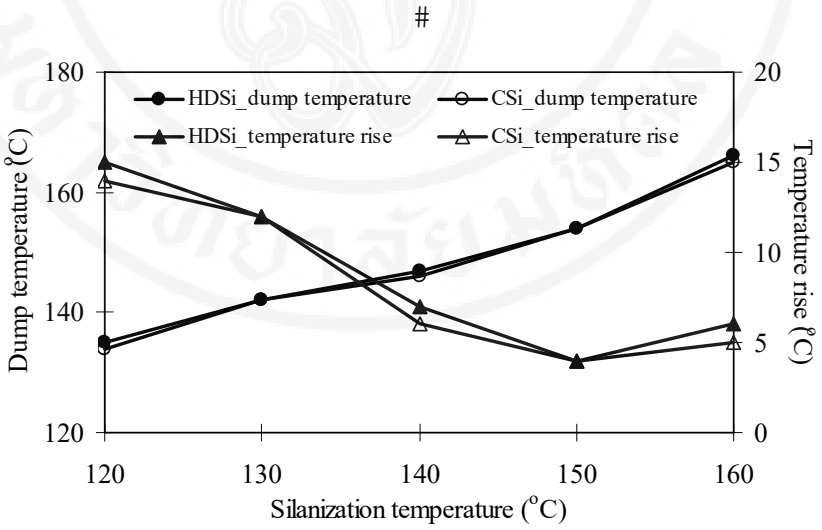

Figure 5.1 Dump temperature and temperature rise of the compounds during silanization step

To support the proposed statement that the scorch could take place at sufficiently high temperature even without the presence of curatives, further experiment was carried out. The rubber compounds (based on the formulation given in Table 4.3, except that no silica and curatives were added) were prepared. Mixing was

carried out in the internal mixer for 10 minutes at the mixing temperature of 60°C. After sheeting and cooling, the compounds were then re-mixed for 6 minutes at various silanization temperatures, i.e., 120°C, 130°C, 140°C, 150°C, and 160°C. Afterwards, the gel content of each compound, after being placed in toluene for 168 h at room temperature, was measured. Obviously, the compounds prepared at low silanization temperatures are completely dissolved in toluene as shown in Figure 5.2(a). However, at sufficiently high silanization temperature (160°C), rubber gel is clearly observed indicating the occurrence of scorch. Since it has been reported that SBR could form gel at high temperature possibly due to the presence of remaining stabilizers in the rubber during polymerization [127], additional experiment was carried out in order to ensure that the gel observed is the sole consequence from TESPT. The SSBR (without any ingredients) was mixed in an internal mixer at mixing temperature of 160°C for 6 minutes, and the investigation of gel content of the prepared SSBR was carried out. As expected, no gel is observed (see Figure 5.2(b)). The result clearly confirms that the gel found at high silanization temperature is resulted from crosslink induced by TESPT.

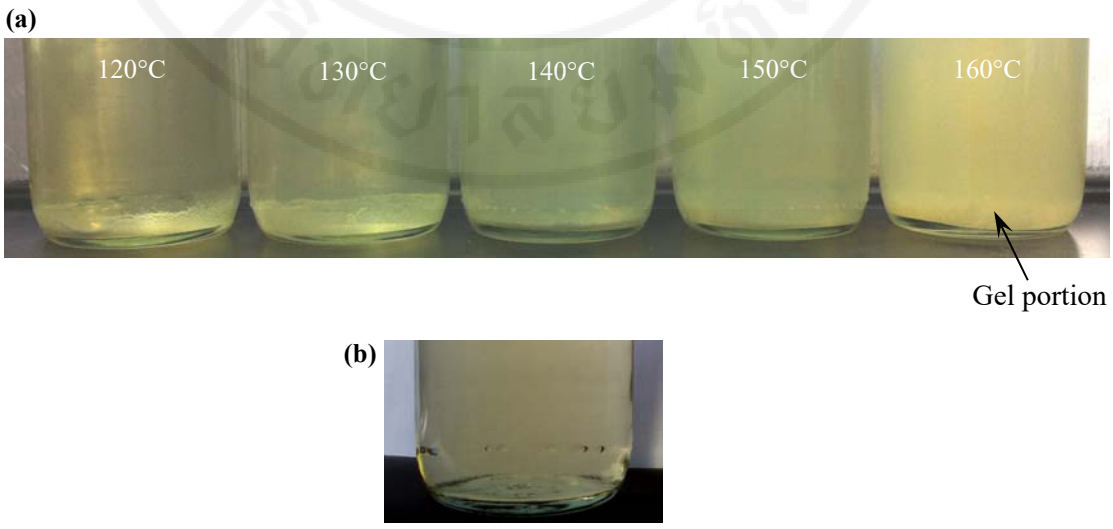

Figure 5.2 Gel test results of compounds: (a) compounds mixed at various silanization temperatures and (b) SSBR mixed at 160°C

5.1.2 Mooney viscosity and shear modulus at high strain of the rubber compounds

Mooney viscosity and storage modulus (G') at high strain (100%) results of the compounds are illustrated in Figure 5.3. Apparently, Mooney viscosity slightly increases with increasing silanization temperature up to 140°C. Further increase in silanization temperature causes a sharp increase in Mooney viscosity. This is probably due to the increased magnitude of rubber-filler interaction as evidenced from the BRC results (see Figure 5.4) and the scorch phenomenon induced by TESPT which is more pronounced at high temperature as previously mentioned.

Such increase in compound viscosity at high silanization temperature is supported by the results of G' at high strain (100%) as measured from RPA2000. The results reveal a slight change in G' as long as the silanization temperature is lower than 140°C. Above 140°C, the G' tends to increase rapidly with increasing silanization temperature. It is well known that the G' of filled rubber compound at high strain depends on 3 main factors, i.e., polymer network, hydrodynamic effect, and in-rubber structure involving bound rubber [97]. Since all compounds possess similar formulation and the measurement of G' was carried out at 100°C, the hydrodynamic effect and rubber network could be disregarded. However, as the rubber compounds contain TESPT molecules, from which sulfidic bonds could be cleaved, acting as sulfur donor, the initiation of crosslink in rubber phase could be expected as long as the mixing temperature is sufficiently high. The results suggest that the obvious increase in G' at high silanization temperature (≥140°C) could be resulted from the combination of the enhanced rubber-filler interaction and scorch phenomenon. It is also found that the Mooney viscosity and the G' at high strain of the compound filled with HDSi are considerably higher than those of the compound filled with CSi. The greater rubber-filler interaction and the higher structure level of HDSi are probably responsible for the results.

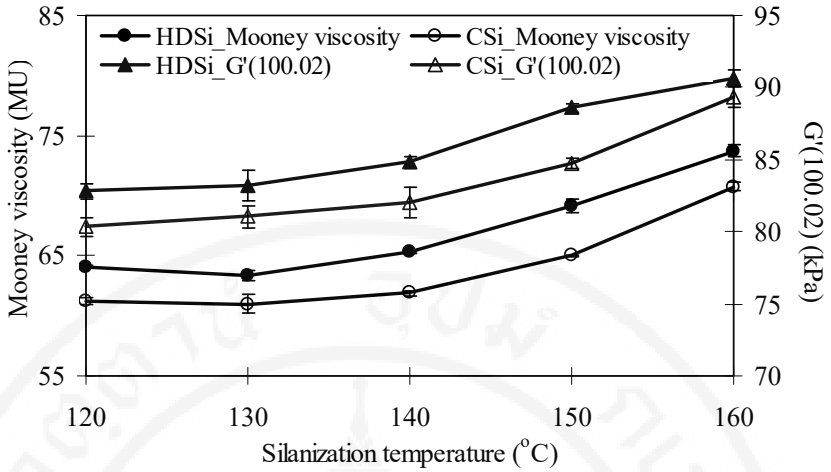

Figure 5.3 Mooney viscosity and storage modulus (G') at high strain of the compounds

5.1.3 Bound rubber content (BRC) of the compounds

Figure 5.4 exhibits BRC of the compounds as a function of silanization temperature. Clearly, both total BRC and chemical BRC tend to increase with increasing silanization temperature. Results also reveal that physical BRC of the compounds is independent of silanization temperature. As the portion of physical BRC is greatly lower than that of chemical BRC, the results suggest that the increase in silanization temperature leads to the improvement in rubber-filler interaction via the coupling reaction having TESPT acting as the bridge (see Figure 5.5). It is also found that the superior total BRC and chemical BRC are found in HDSi compounds, implying that the HDSi provides stronger rubber-filler interaction as compared to CSi.

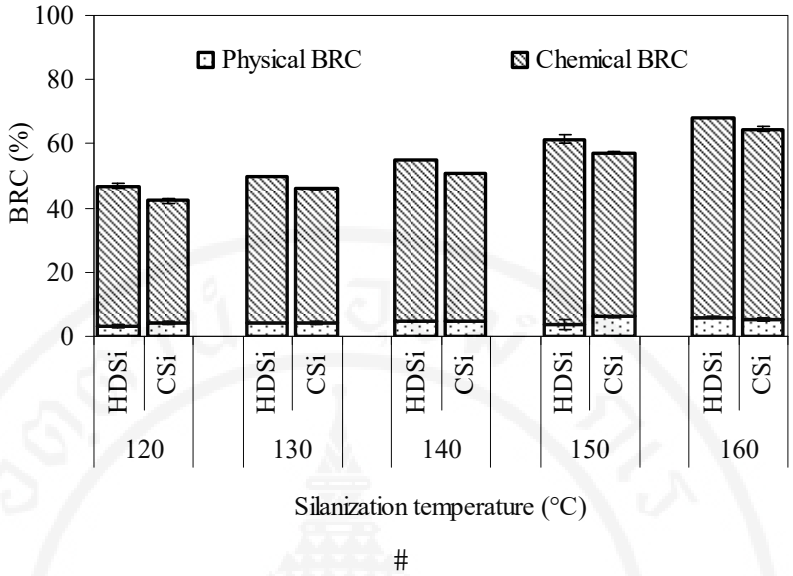

Figure 5.4 BRC of the compounds

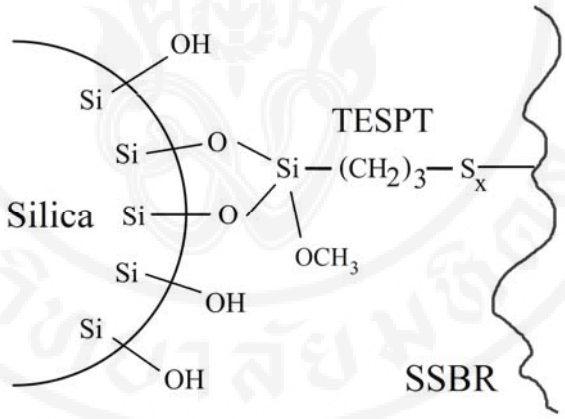

Figure 5.5 Coupling reaction between silica, TESPT, and SSBR

5.1.4 Payne effect of the compounds

It is widely known that, for filled compounds, the difference in storage moduli at low and high strains (ΔG'), or the so-called Payne effect, can be used to predict the magnitude of transient filler network. The lower the Payne effect magnitude, the lower the transient filler network level. The effect of silanization temperature on Payne effect is given in Figure 5.6. Regardless of the silica type, the magnitude of Payne effect is found to decrease with increasing silanization temperature, implying the reduced magnitude of transient filler network. This is

explained by the enhancement in silanization reaction between ethoxysilyl groups of TESPT and silanol groups on silica surface with increasing silanization temperature, resulting in a decreased hydrophilicity of silica surface and, hence, the reduction in filler-filler interaction. At any given silanization temperature, the magnitude of Payne effect of HDSi and CSi-filled compounds is comparable, suggesting comparable level of transient filler network in those compounds.

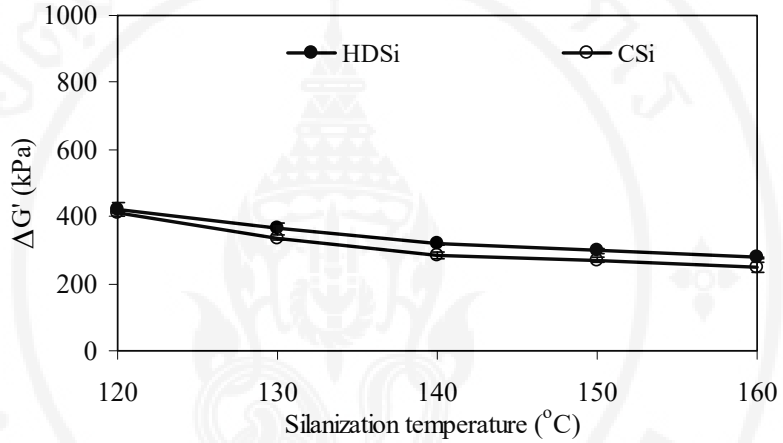

Figure 5.6 Payne effect of the compounds

5.1.5 Degree of filler dispersion of the vulcanizates

Figure 5.7 depicts TEM micrographs of the vulcanizates at magnification of 20,000x. As expected, the increased silanization temperature leads to the improvement in degree of filler dispersion, revealing a good accordance with the Payne effect results. Also, the enhanced hydrophobicity of silica surface with increasing silanization temperature is applied for explaining the results. In addition, the improvement in rubber-filler interaction after silanization reaction could be another reasonable explanation for this finding. Surprisingly, degree of filler dispersion of the vulcanizates filled with HDSi is comparable with that of the vulcanizates filled with CSi, despite the fact that HDSi is claimed to offer a greater dispersability. Results reveal that silica type plays a very minor role in degree of filler dispersion, as long as a sufficiently long mixing time is employed.

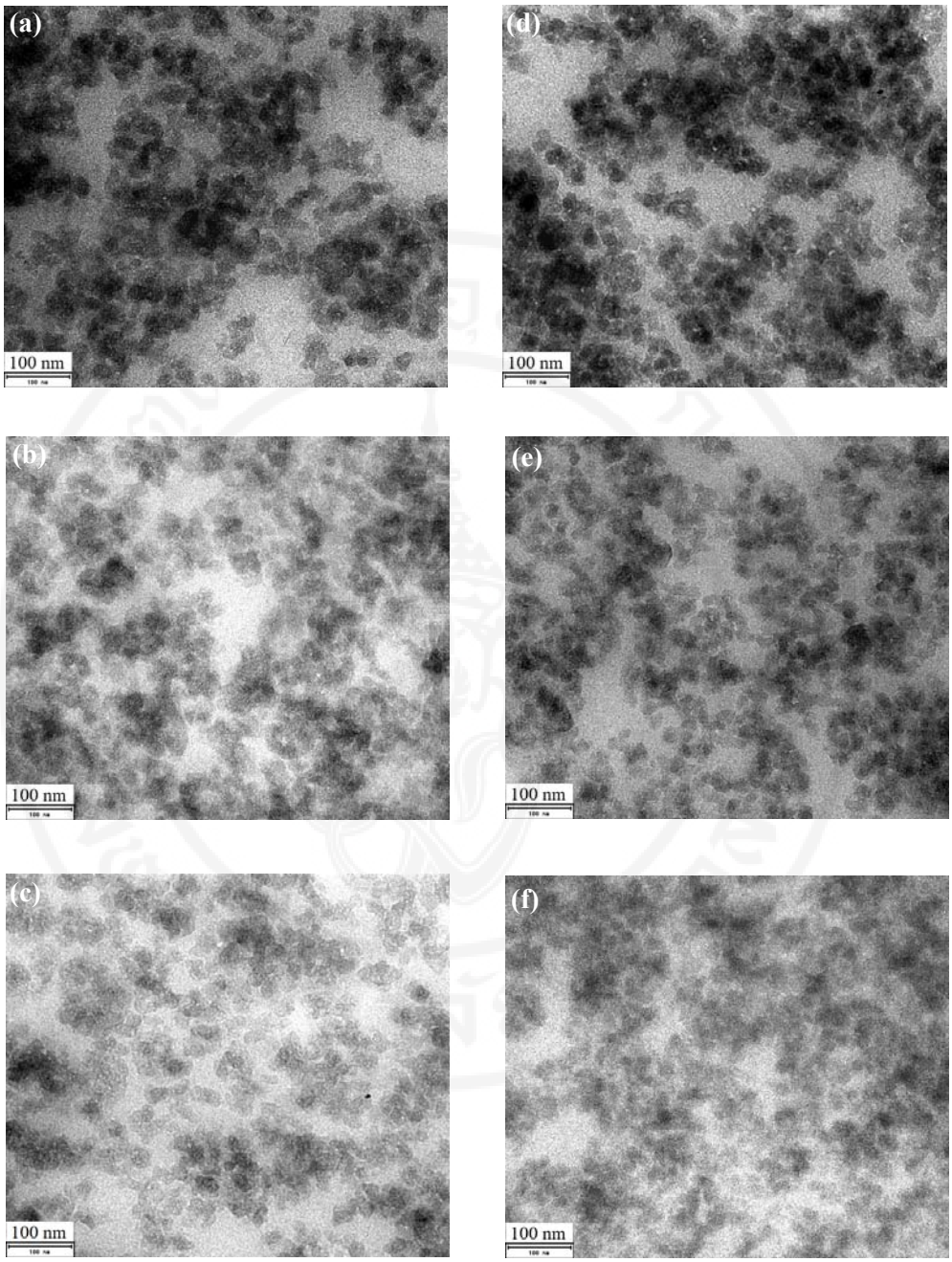

Figure 5.7 TEM micrographs (x20,000) of the silica-filled vulcanizates at various silanization temperatures: (a) HDSi_120°C, (b) HDSi_140°C, (c) HDSi_160°C, (d) CSi_120°C, (e) CSi_140°C, and (f) CSi_160°C.

5.1.6 Cure characteristics of the compounds

Figure 5.8 represents cure curves of the compounds at various silanization temperatures. Cure characteristics, i.e., t_s1, t_c90, and CRI, analyzed from Figure 5.8 are summarized in Table 5.1. With increasing silanization temperature, both t_s1 and t_c90 tend to increase whereas CRI is decreased continuously, revealing the reduced cure efficiency. Explanation is proposed based on a reduced amount of sulfur released from the TESPT during the curing process [125]. Referring to the chemical structure of TESPT, there are 4 sulfur atoms in its molecule which could be cleaved and participated during the curing process at sufficiently high temperature. Consequently, at high silanization temperature, some portion of sulfur atoms might deplete during the mixing process, giving rise to the decrease in sulfur atoms to be released during the curing process and thus the decrement in cure efficiency. As the two types of silica give comparable values of t_s1, t_c90, and CRI, it could be stated that silica type has little effect on cure characteristics of the compounds.

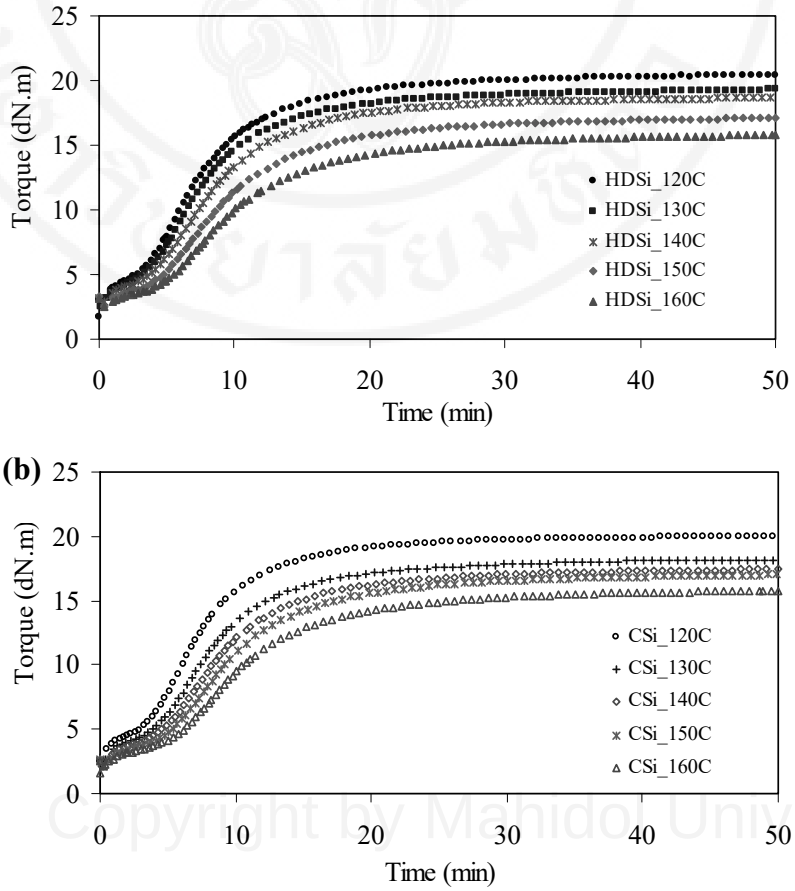

Figure 5.8 Cure curves of the compounds: (a) HDSi and (b) CSi

Table 5.1 Cure characteristics of the compounds

Silanization temperature (°C)	Silica type	t_s1 (min)	t_c90 (min)	CRI (min^{-1})
120	HDSi	0.85±0.04	15.45±0.16	6.80±0.03
130		0.86±0.02	16.55±0.06	6.37±0.01
140		1.11±0.04	17.56±0.05	6.08±0.00
150		1.43±0.09	19.40±0.06	5.56±0.01
160		2.46±0.01	20.88±0.08	5.43±0.02
120	CSi	0.54±0.04	15.02±0.12	6.91±0.04
130		0.82±0.03	16.63±0.45	6.33±0.17
140		1.00±0.04	18.26±0.28	5.79±0.08
150		1.26±0.05	19.32±0.49	5.54±0.14
160		2.03±0.06	21.60±0.59	5.11±0.14

5.1.7 Crosslink density of the vulcanizates

Crosslink density of the vulcanizates, measured from the swelling technique, as a function of silanization temperature is shown in Figure 5.9. It is found that silanization temperature does not significantly affect the crosslink density up to the silanization temperature of 140°C. At higher silanization temperatures, however, the crosslink density of the vulcanizates tends to increase with increasing silanization temperatures, due to the stronger rubber-filler interaction. It has been reported that the tightly bound rubber could restrict the rubber molecules from swelling and, thus, could behave as crosslink points in rubber vulcanizates [128]. Results also show that the crosslink density of vulcanizates filled with HDSi is greater than that of vulcanizates filled with CSi, owing again to the higher magnitude of rubber-filler interaction of HDSi [128].

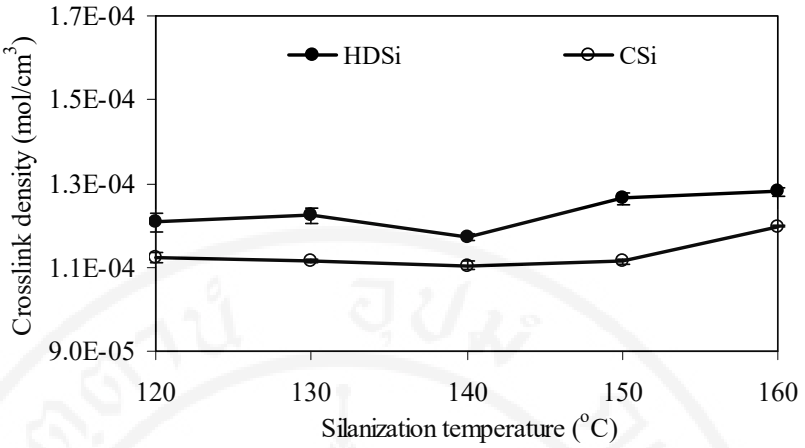

Figure 5.9 Crosslink density of the vulcanizates as measured from the swelling technique

5.1.8 Mechanical properties of the vulcanizates

Table 5.2 presents mechanical properties, i.e., hardness, modulus at 10% strain (M10), tensile strength (TS), and abrasion volume loss, of the vulcanizates. Results show that hardness of the vulcanizates decreases continuously with increasing silanization temperature, despite the enhancements in crosslink density (at silanization temperature >140°C) and rubber-filler interaction. Results suggest that the reductions in both transient filler network level and molecular weight of rubber matrix (see Table 5.3), as evaluated by a GPC technique, appear to govern the hardness of vulcanizates. Generally, molecular weight of rubber molecules could affect the properties of vulcanizates. In this case, the mixing was carried out under high temperature which could lead to degradation and/or chain scission of rubber molecules via thermo-oxidative breakdown, resulting in a reduction of mechanical properties. Obviously, GPC results illustrated in Table 5.3 reveal that the increased silanization temperature leads to the decrease in molecular weight of rubber in the compounds, implying the significantly high thermal degradation of rubber matrix at high silanization temperature. As expected, the higher hardness is observed in HDSi-filled vulcanizates which could be explained by the combined effects of greater crosslink density and rubber-filler interaction.

Since modulus at low strain of the vulcanizates is found to closely relate to hardness (to be discussed later), the effects of silanization temperature and silica type on M10 follow the same trend as the hardness, i.e., the M10 tends to decrease with increasing silanization temperature and HDSi offers higher M10 than CSi. The same explanation is applied.

Table 5.2 Mechanical properties of the vulcanizates

Silanization temperature (°C)	Silica type	Hardness (Shore A)	M10 (MPa)	TS (MPa)	Volume loss (mm^3)
120	HDSi	69.3±0.6	0.671±0.004	19.8±0.2	39.2±0.5
130		67.1±0.2	0.625±0.027	20.3±0.7	38.4±1.8
140		66.1±0.4	0.607±0.004	20.2±1.0	35.5±0.8
150		63.9±0.4	0.588±0.013	19.8±0.6	32.2±0.7
160		63.0±0.5	0.559±0.007	19.8±0.7	30.5±0.8
120	CSi	67.4±0.7	0.642±0.009	20.4±1.7	30.5±0.8
130		66.1±0.4	0.587±0.007	19.7±1.9	29.9±1.0
140		64.7±0.6	0.571±0.019	19.0±1.0	28.8±0.7
150		63.4±0.2	0.562±0.017	19.1±0.8	25.7±0.5
160		61.3±0.3	0.555±0.010	20.6±1.4	25.4±0.8

Table 5.3 Molecular weight as determined from GPC of rubber matrix in the compounds

Silanization temperature (°C)	Silica type	M_n (Daltons)	M_w (Daltons)	M_p (Daltons)
120	HDSi	440,709	713,072	855,512
130		405,666	691,584	846,044
140		347,774	630,732	799,340
150		341,641	616,347	758,408
160		325,272	541,949	667,836
120	CSi	447,183	708,343	859,915
130		411,515	710,093	870,939
140		356,733	670,704	840,166
150		354,700	640,499	804,040
160		361,976	635,933	756,510

Surprisingly, silanization temperature does not significantly influence TS of the vulcanizates, despite the fact that the increased rubber-filler interaction and degree of filler dispersion are found with increasing silanization temperature. Probably, the counter-balance between the increased rubber-filler interaction and degree of filler dispersion (giving the positive effect on TS) and the reduced molecular weight of rubber matrix caused by thermal degradation (giving the negative effect on TS) could be responsible for this finding. It is also found that TS of the vulcanizates is independent of silica type, which could be mainly explained by the dominant effect of the comparable degree of filler dispersion.

Results of abrasion resistance of the vulcanizates represented in terms of volume loss are shown in Table 5.2. As predicted, the volume loss tends to decrease with increasing silanization temperature. The improvement in abrasion resistance is due to the dominant effect of enhancement in rubber-filler interaction and degree of filler dispersion. At any given silanization temperature, the CSi gives better abrasion resistance as compared to HDSi. The greater specific surface area of CSi together with

the lower magnitude of thermal degradation of rubber matrix of CSi-filled compounds might be the possible explanations.

5.1.9 HBU and dynamic set of the vulcanizates

Table 5.4 shows the silanization temperature-dependent dynamic properties of the vulcanizates in terms of HBU and dynamic set. The HBU decreases slightly with increasing silanization temperature due to the combined consequences of: (i) the improved crosslink density; (ii) the enhanced rubber-filler interaction and (iii) the decreased transient filler network. Also, similarity in result trends is found in dynamic set of the vulcanizates, i.e., the dynamic set is reduced with increasing silanization temperature, implying the improved elasticity of the vulcanizates when silanization temperature is increased. The similar explanation could be applied. It is also found that silica type plays little role in HBU and dynamic set of the vulcanizates despite the fact that HDSi gives greater magnitude of rubber-filler interaction and crosslink density. The insignificant difference in degree of filler dispersion between HDSi- and CSi-filled vulcanizates might be the dominant factor controlling the HBU and dynamic set in this work.

Table 5.4 HBU and dynamic set of the vulcanizates

Silanization temperature (°C)	Silica type	HBU (°C)	Dynamic set (%)
120	HDSi	13.5±0.5	4.64±0.34
130		13.0±0.0	4.50±0.14
140		13.0±0.0	4.30±0.09
150		13.0±0.0	4.37±0.18
160		12.5±0.7	3.76±0.06
120	CSi	13.0±0.0	4.39±0.50
130		13.0±0.0	4.44±0.12
140		13.0±0.0	4.18±0.37
150		12.5±0.7	4.00±0.11
160		12.0±0.0	3.68±0.12

5.1.10 Dynamic mechanical properties of the vulcanizates

Figure 5.10 illustrates loss factor (tanδ) as a function of test temperature of the vulcanizates prepared at various silanization temperatures. Values of T_g, tanδ_{max} and tanδ area analyzed from Figure 5.10 are tabulated in Table 5.5. In general, the temperature at tanδ_{max} is used to indicate the T_g of polymer [129]. The results demonstrate that, regardless of the silica characteristics, the T_g of the vulcanizates is found to shift towards the higher temperature with increasing silanization temperature. This is owing to the enhanced restriction of molecular motion of the rubber molecules as a result of the improved rubber-filler interaction caused by the increased silanization temperature. Obviously, the tanδ_{max} value and tanδ area tend to increase with increasing silanization temperature. Results indicate that the amount of rubber chains participating in the glass transition is enhanced when the silanization temperature is increased, because of the improvement in degree of filler dispersion. It is also found that T_g and tanδ_{max} value of the vulcanizates filled with HDSi are comparable with those of the vulcanizates filled with CSi. However, the slightly lower

tanδ area is observed in HDSi-filled vulcanizates, possibly due to its higher structure and, hence, trapped (immobilized) rubber.

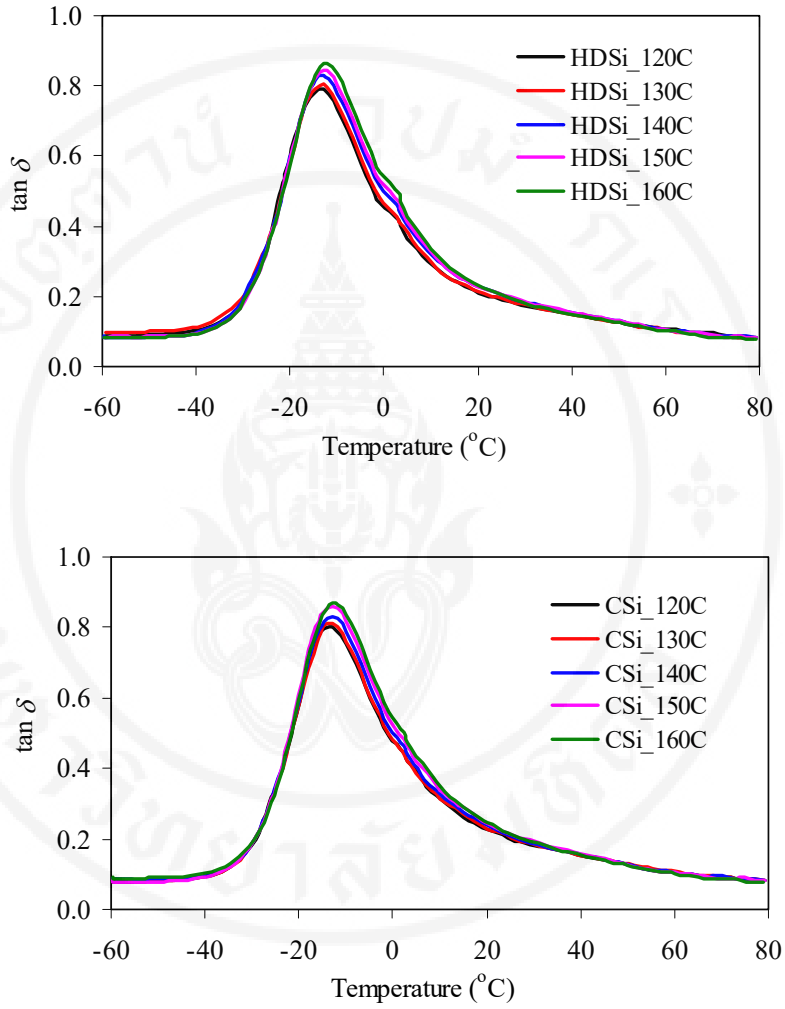

Figure 5.10 Effect of silanization temperature on loss factor (δ) as a function of test temperature of the vulcanizates: (a) HDSi and (b) CSi

Table 5.5 T_g, tanδ_{max} and tanδ area of the vulcanizates

Silanization temperature (°C)	Silica type	T_g (°C)	tanδ_{max}	tanδ area (°C)
120	HDSi	-14.0	0.787	15.36
130		-13.5	0.803	15.71
140		-12.9	0.828	16.35
150		-12.8	0.842	16.77
160		-12.2	0.862	17.35
120	CSi	-13.7	0.787	15.95
130		-13.3	0.802	16.06
140		-12.8	0.828	16.55
150		-12.6	0.840	17.42
160		-12.1	0.864	17.38

As previously mentioned, WG and RR (as an indication of FSE) of vulcanizates are closely related to the tanδ value at 0°C and 60°C, respectively. In many cases, the higher tanδ value at 0°C at 0.1% strain is referred to the better WG [44, 50]. Also, the lower tanδ value at 60°C at high strain, e.g., 5% [46] and 6% [47], is correlated to the lower RR and, thus, the higher FSE. It must be noted that, in this work, the tanδ value at 0°C at 0.1% strain and the tanδ value at 60°C at 5% strain are used as indication of WG and FSE, respectively.

Figure 5.11 depicts the tanδ of vulcanizates as a function of dynamic strain from 0.03-10% at 0°C. Results show that the tanδ value tends to increase with increasing dynamic strain up to 3% strain. Further increase in dynamic strain leads to the rapidly decreases of tanδ. The increased level of transient filler network destruction could be the reasonable explanation for the initial increase of tanδ whereas the disappearance of transient filler network is applied for the explanation of the decreased tanδ at high strains. At 0.1% strain, the tanδ value at 0°C is found to increase with increasing silanization temperatures implying the improved WG. This is

due to the shift of T_g towards higher temperature mainly as a result of the enhancement in rubber-filler interaction when the silanization temperature is increased. It is expected that, in tire technology, rubbers having higher T_g are prone to offer superior WG, explained from the fact that WG is directly related to the amount of energy dissipation which is high at transition zone [130]. Surprisingly, silica type imparts no profound effect on WG of the vulcanizates. Again, the comparable T_g of HDSi- and CSi-filled vulcanizates is applied to explain the results.

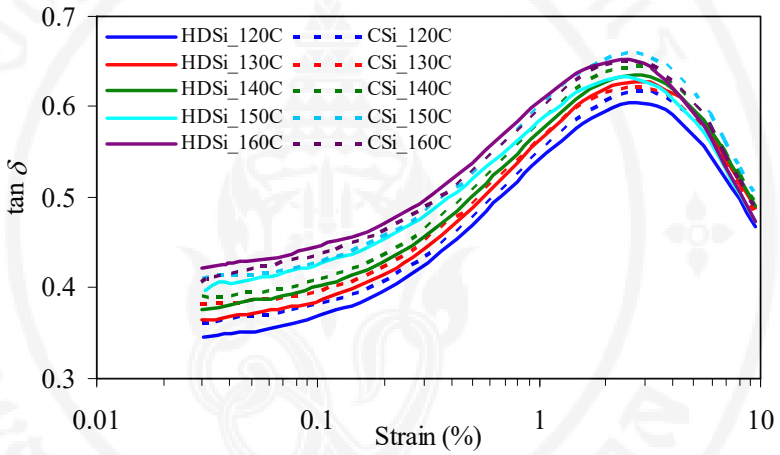

Figure 5.11 Loss factor (tanδ) at 0°C as a function of dynamic strain of the vulcanizates

Tanδ of the vulcanizates as a function of dynamic strain at 60°C is displayed in Figure 5.12. Results show that the tanδ value is not significantly changed up to approximately 0.2% strain and, then increases afterwards. Explanation for the increased tanδ value is given by the combined effects of the destruction of transient filler network and the increase in molecular slippage on filler surfaces with increasing dynamic strain. At 5% strain, RR of the vulcanizates as indicated from tanδ at 60°C decreases continuously with increasing silanization temperature, suggesting the improved FSE. This is evident from the reduced magnitude of transient filler network together with the improved level of rubber-filler interaction. The former leads to the reduced destruction of transient filler network while the latter causes the decreased slippage of rubber molecules on filler surface under being strained, and, thus, the

lowered energy dissipation is resulted. Similar to WG, the tanδ values at 60°C at 5% strain of the vulcanizates filled with HDSi and CSi are comparable. Results imply that the FSE is little affected by the silica type. In other words, the insignificant difference in degree of filler dispersion found in systems filled with HDSi and CSi might play dominant role on FSE in this work.

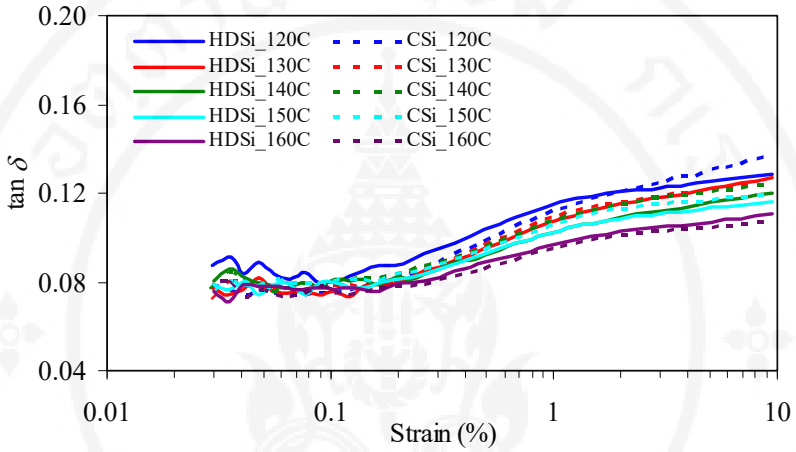

Figure 5.12 Loss factor (tanδ) at 60°C as a function of dynamic strain of the vulcanizates

Figure 5.13 discloses normalized graphs of processability (evaluated from Mooney viscosity) and tire performance at various silanization temperatures (reference line (100%): HDSi-filled system prepared at silanization temperature of 140°C). Although the silanization temperature of 160°C leads to the best tire performance, i.e., WG (indicated by tanδ at 0°C), FSE (indicated by tanδ at 60°C) and abrasion resistance, the worst processability caused by the scorch problem is found. It could be therefore summarized that the silanization temperature of 140°C seems to offer the best balanced tire performance and processability. Consequently, this silanization temperature is selected for the experiment in the subsequent sections.

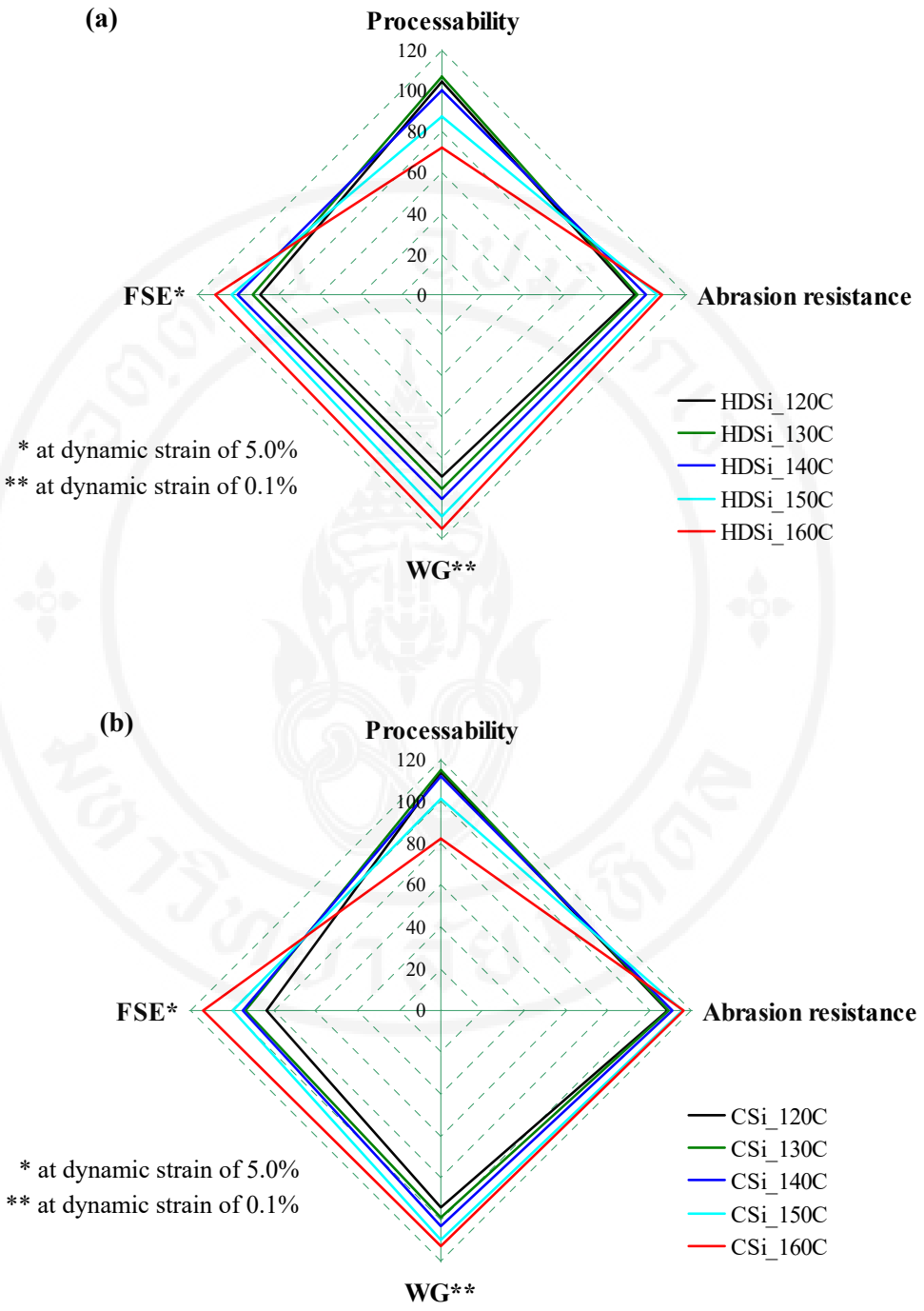

Figure 5.13 Influence of silanization temperature on processability and tire performance represented in terms of the normalized graph: (a) HDSi and (b) CSi

5.2 Effects of TESPT content and silica type on properties of silica-filled SSBR compounds and vulcanizates

In this study, various properties, i.e., processability, viscoelastic, mechanical, and dynamic mechanical properties, of the HDSi- and CSi-filled compounds and vulcanizates treated (6, 8, 10 and 12 wt% of silica) and untreated by TESPT were compared. The proper silanization temperature (140°C) obtained from the previous part was employed in this part of study.

5.2.1 Mixing energy and Mooney viscosity of the compounds

Table 5.6 illustrates the total mixing energy and Mooney viscosity of the compounds. Without TESPT, the compound demonstrates the highest mixing energy as expected. With the presence of TESPT, however, mixing energy is found to decrease with increasing TESPT content, possibly due to the reduced compound viscosity during the mixing process. In general, the silanization reaction between ethoxy groups of TESPT and silanol groups on silica surface could occur at sufficiently high temperature (≥130°C) [126, 131], leading to the improved degree of filler dispersion, resulting in the decreased effective filler volume fraction and, thus, the reduced compound viscosity. Moreover, at high TESPT contents, the plasticization effect as a result of excessive TESPT could be another reasonable explanation for the reduced compound viscosity [132]. At any given TESPT content, HDSi gives slightly greater mixing energy and Mooney viscosity than CSi. The superior magnitude of rubber-filler interaction indicated by BRC (see Figure 5.14) and the higher structure level of HDSi could be used to explain the results.

Table 5.6 Total mixing energy and Mooney viscosity of the compounds

TESPT content (wt% of silica)	Silica type	Total mixing energy (kN.m)	Mooney viscosity (MU)
0	HDSi	755.0	139.4±2.0
6		622.9	71.8±0.6
8		591.3	68.9±0.3
10		573.8	66.7±0.1
12		560.7	63.9±0.7
0	CSi	737.1	135.9±1.3
6		611.6	69.9±0.8
8		580.7	66.1±0.8
10		566.8	63.2±0.3
12		544.1	60.4±0.8

5.2.2 Bound rubber content (BRC) of the compounds

BRC of the compounds as a function of TESPT content is illustrated in Figure 5.14. Results show that TESPT content has little effect on physical BRC but plays an importance role in chemical BRC. Obviously, the addition of 6 wt% of TESPT leads to the significant increase in total BRC and chemical BRC. In other words, TESPT can promote the interaction between SSBR and silica. Surprisingly, the total BRC and chemical BRC are found to decrease with increasing TESPT content from 6 to 12 wt%, revealing the decline of rubber-filler interaction when an excess of TESPT content is used. Similar observation has also previously been reported by Qu, et al. [119]. It was proposed that, at high TESPT contents, TESPT could form chemical bonds with rubber during the mixing process. Hence, a diffusion of TESPT intentionally to react with the silanol groups on silica surface was restricted causing the decrease in BRC. Another explanation is given by Pickering, et al. [133], they found that the reaction between TESPT and -OH groups on iron sand particles decreased as TESPT content was beyond the optimum level (i.e., 6 wt% of the iron sand particles). It was explained that, at high TESPT contents, the polymeric siloxane

formed via the self-condensation of hydrolyzed TESPT led to the restriction of coupling reaction between TESPT and -OH groups on iron sand surfaces. In the present work, it is also found that the compound filled with HDSi possesses higher total BRC and chemical BRC than the compound filled with CSi, suggesting the stronger rubber-filler interaction of the HDSi-filled compound.

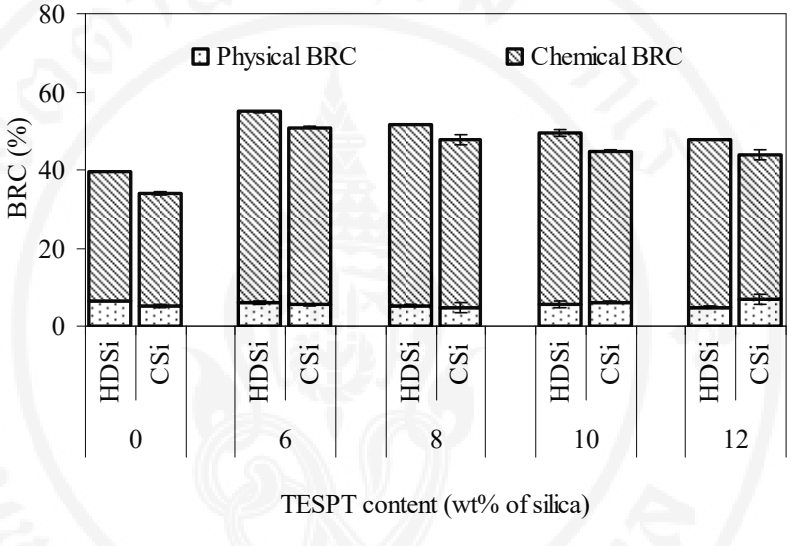

Figure 5.14 BRC results of the compounds

5.2.3 Cure characteristics of the compounds

Figure 5.15 represents cure curves of the compounds at various TESPT contents. Values of CRI analyzed from Figure 5.15 are shown in Figure 5.16. Clearly, the measured torque of the compounds is found to shift downward with the TESPT treatment. Possible explanation is mainly given by the increased amount of mobilized rubber caused by the improved degree of filler dispersion after the TESPT treatment (see Figure 5.18), leading to the decreased effective filler volume fraction and, hence, the torque of cure curves.

It is also found that, compared with the untreated system, the TESPT-treated system shows lower magnitude of marching, attributed probably to the decreased degree of filler flocculation by TESPT treatment. It is widely known that viscosity of the rubber compound filled with silica generally increases with storage time. This phenomenon is resulted from the reformation of transient filler network

facilitated by low rubber viscosity and high temperature [134]. TESPT treatment can lead to the reduction in hydrophilicity of silica surface, giving the decreased level of filler flocculation and, hence, the marching phenomenon.

Results also show that the CRI of the compounds is improved by TESPT treatment. Moreover, the CRI tends to increase with increasing TESPT content from 6 wt% to 12 wt%. The enhanced cure efficiency resulted from the decreased level of accelerator adsorption by silanol groups after the TESPT treatment could be applied for explaining this result. It is well known that the hydrophilicity of silanol groups can interact with the basic accelerators, causing the reduced cure efficiency in sulfur vulcanization system [135]. Since the TESPT possesses 4 sulfur atoms in its molecule which could be cleaved and participated in sulfur vulcanization at sufficiently high temperature, the increased sulfur atoms in the bulk brought about by the increased TESPT content could be another reasonable explanation for this finding. Results also show that silica type plays a little role in cure characteristics of the compounds.

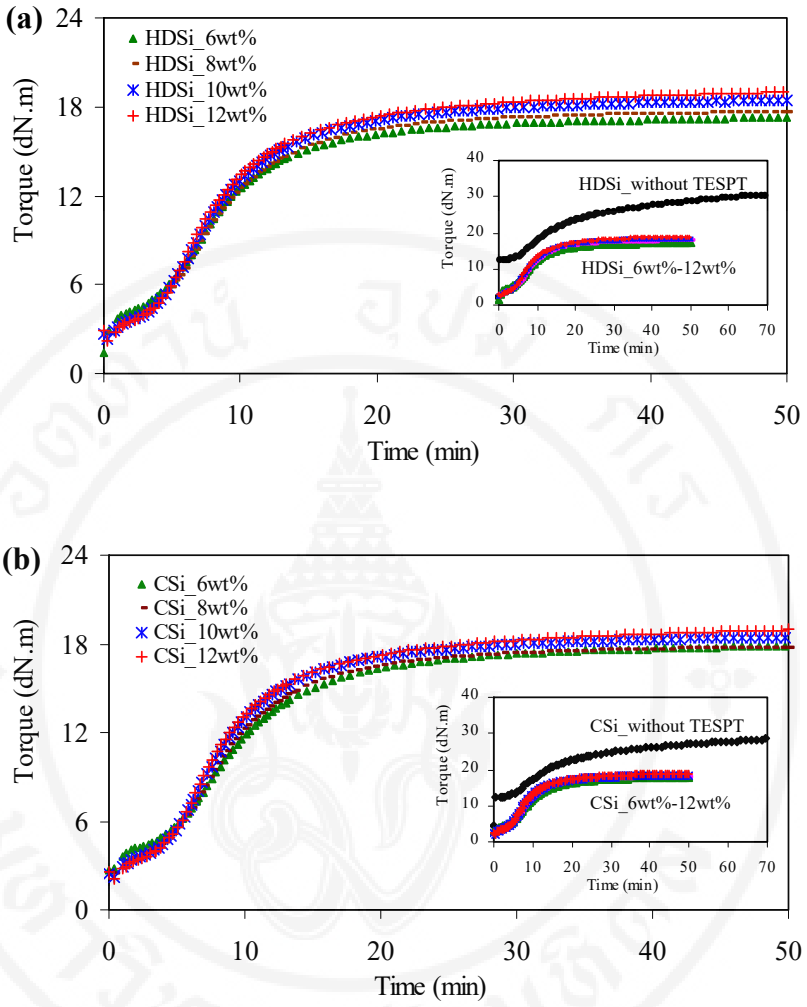

Figure 5.15 Cure curves of the compounds: (a) HDSi and (b) CSi

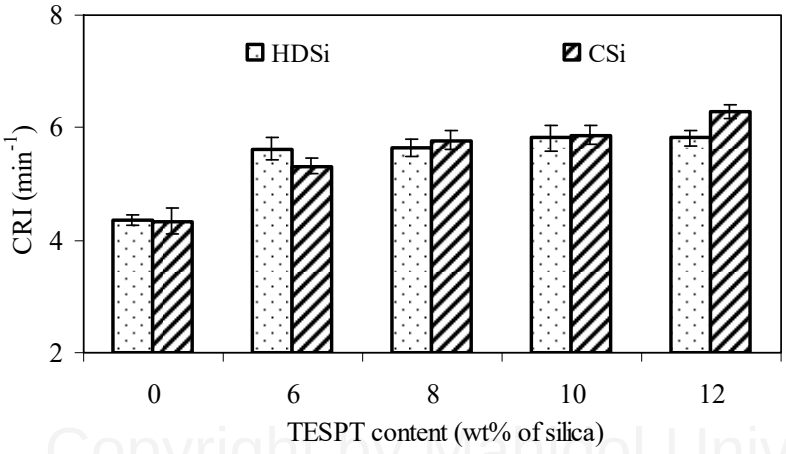

Figure 5.16 Cure rate index (CRI) of the compounds

5.2.4 Payne effect of the compounds

Figure 5.17 depicts Payne effect of the compounds at various TESPT contents. Obviously, the magnitude of Payne effect (ΔG') is significantly reduced when 6 wt% of TESPT is added. Results suggest that the addition of TESPT can significantly reduce the magnitude of transient filler network. This is explained by the reduced hydrophilicity of silica surface after silanization reaction which is induced by TESPT. Additionally, the increase of TESPT content beyond 6 wt% gives no profound effect on magnitude of Payne effect, implying the comparable magnitude of transient filler network. At any given TESPT content, Payne effect magnitude of HDSi and CSi-filled vulcanizates is found to be comparable, particularly in the presence of TESPT. Results suggest that silica type plays little role on magnitude of transient filler network.

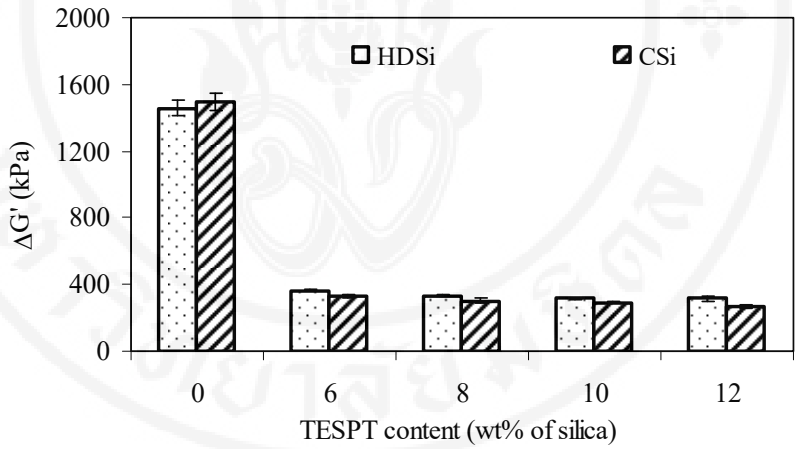

Figure 5.17 Payne effect results of the compounds

5.2.5 Degree of filler dispersion of the vulcanizates

TEM micrographs of the vulcanizates at magnification of 20,000x are represented in Figure 5.18. As expected, TESPT treatment gives a significant improvement in degree of filler dispersion, simply explained by the reduced hydrophilicity of silica surface together with the enhanced magnitude of rubber-filler interaction as evidenced from BRC results. It is also observed that the variation of TESPT content from 8 wt% to 12 wt% does not affect the degree of filler dispersion. Similar to the previous part, the degree of filler dispersion is independent of silica type. The same explanation could be applied.

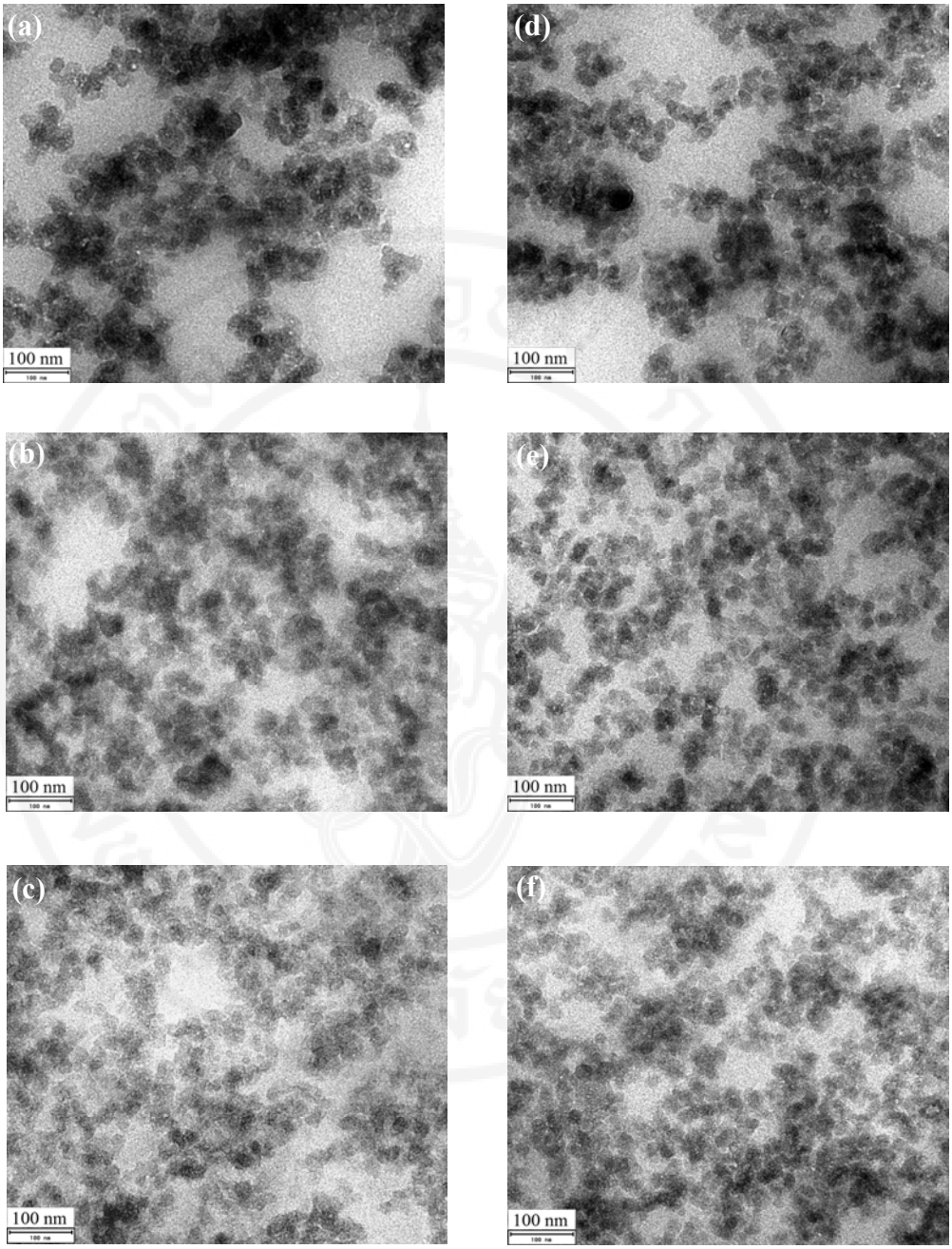

Figure 5.18 TEM micrographs (x20,000) of the silica-filled vulcanizates as a function of TESPT contents: (a) HDSi_without TESPT; (b) HDSi_8 wt%; (c) HDSi_12 wt%; (d) CSi_without TESPT; (e) CSi_8 wt%; (f) CSi_12 wt%

5.2.6 Crosslink density of the vulcanizates

Figure 5.19 exhibits the influence of TESPT content on crosslink density of the vulcanizates as measured from the swelling test. Apparently, the lowest crosslink density is found in the vulcanizates without TESPT treatment. This is because of the adsorption of basic accelerators by silanol groups densely covered on silica surface, leading to the negative effect on cure efficiency. Obviously, crosslink density increases with increasing TESPT content, possibly caused by the combined effects of: (i) the reduction in curative adsorption and (ii) the increase in sulfur atoms in the bulk. As mentioned earlier, TESPT possesses 4 sulfur atoms in its molecule which could be cleaved and participated in sulfur vulcanization at sufficiently high temperature. This explains why the enhanced crosslink density is observed when the TESPT content is increased. As previously mentioned, the magnitude of crosslink density as measured by swelling test can be enhanced when the tightly bound rubber behaving as crosslink points are increased. Referring to BRC results, HDSi imparts stronger rubber-filler interaction as compared to CSi. This could be the reason why the greater magnitude of crosslink density is found in the vulcanizates filled with HDSi.

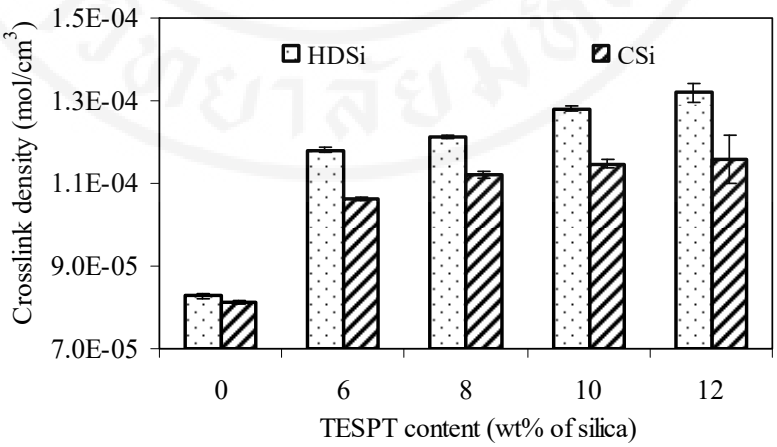

Figure 5.19 Crosslink density of the vulcanizates as measured from the swelling test

5.2.7 Mechanical properties of the vulcanizates

Generally, strain could affect the modulus of vulcanizates, especially in the materials having relatively high transient filler network such as silica-filled rubber. Modulus of the vulcanizates at various % strains as a function of TESPT content is disclosed in Figure 5.20. It is widely known that modulus at relatively low strain is mainly governed by the magnitude of transient filler network. As the vulcanizates without TESPT treatment possess the greatest magnitude of transient filler network, as compared with the TESPT-treated vulcanizates, the highest modulus at low strain (M10) is observed in the vulcanizates without TESPT treatment. It could be found that M10 tends to increase gradually with increasing TESPT content. This might be attributed to the increase of crosslink density with increasing TESPT content [119]. At high strains, i.e., 100% and 300% where the transient filler network is fully destroyed, modulus of the vulcanizates depend mainly on hydrodynamic effect, crosslink density and rubber-filler interaction. In this work, filler loading is kept constant at 80 phr and, thus, hydrodynamic effect is comparable for all vulcanizates. Consequently, modulus at high strain of the vulcanizates will mainly be controlled by crosslink density and rubber-filler interaction. Without TESPT treatment, the vulcanizate possesses the lowest crosslink density (see Figure 5.19) and rubber-filler interaction (see Figure 5.14). Both M100 and M300 of this vulcanizates are therefore the lowest. With increasing TESPT content from 6 wt% to 12 wt%, although rubber-filler interaction tends to gradually decrease as evidenced from the BRC results, both M100 and M300 appear to increase continuously which is in good accordance with the results of crosslink density. The results imply that modulus at high strain of the vulcanizates is mainly governed by crosslink density. Evidently, the superior modulus is found in the HDSi-filled vulcanizates, especially in the presence of TESPT. The higher crosslink density and the greater rubber-filler interaction as compared to the CSi-filled vulcanizates are used to explain the results.

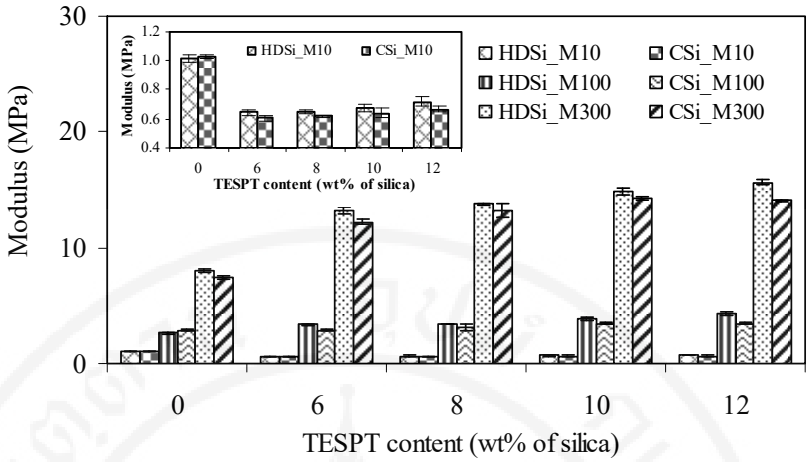

Figure 5.20 Modulus of the vulcanizates at 10% strain, 100% strain and 300% strain

Hardness of the vulcanizates is tabulated in Table 5.7. Apparently, the alteration in hardness with TESPT content follows the same trend as the change in M10, i.e., the hardness of vulcanizates decrease when 6 wt% of TESPT is added and then tends to increase gradually with increasing TESPT content. The results imply that hardness of the vulcanizates is closely related to the modulus at relatively low strain where transient filler network is still of great importance. Also, HDSi demonstrates the greater hardness than CSi. Similar explanation could be applied.

Results in Table 5.7 show that TS of the vulcanizates increases slightly in the presence of 6 wt% of TESPT, which could be explained by the combination of enhanced rubber-filler interaction, degree of filler dispersion and crosslink density. However, the increase in TESPT content from 6 to 12 wt% gives no profound effect on TS. Although crosslink density of the vulcanizates is enhanced with increasing TESPT content from 6 wt% to 12 wt%, this effect on TS could be cancelled out by the decreased rubber-filler interaction, causing no considerable change in TS. In addition, the insignificant change in degree of filler dispersion could be another reasonable explanation for this finding. Results also reveal that silica type does not significantly affect TS. The comparable degree of filler dispersion in both HDSi- and CSi-filled vulcanizates could be the possible explanation.

As expected, TESPT treatment leads to the decrease in abrasion volume loss of the vulcanizates (see also Table 5.7), meaning the improvement in abrasion resistance. The explanation is given by the enhancement in degree of filler dispersion,

rubber-filler interaction including crosslink density. It is also found that the abrasion resistance is improved with increasing TESPT content up to 8 wt%. Higher dosage of TESPT has little effect on the abrasion resistance, attributed to the counter-balancing effect of the increased crosslink density and the reduced rubber-filler interaction. Surprisingly, HDSi gives lower abrasion resistance, compared to CSi. The lower specific surface area of HDSi could probably be responsible for this finding.

Table 5.7 Mechanical properties of the vulcanizates

TESPT content (wt% of silica)	Silica type	Hardness (Shore A)	TS (MPa)	Volume loss (mm^3)
0	HDSi	72.8±0.4	18.1±0.7	72.9±1.7
6		64.1±0.5	19.7±1.5	32.2±2.2
8		65.9±0.4	19.4±0.7	28.5±1.3
10		66.9±0.5	20.1±0.4	28.6±1.1
12		67.9±0.7	19.3±0.5	27.6±1.3
0	CSi	72.9±0.7	17.7±0.2	66.8±1.3
6		63.4±1.0	19.4±0.7	26.2±0.8
8		65.0±0.5	18.9±1.0	24.3±0.5
10		66.0±0.5	19.6±1.2	24.8±0.5
12		66.4±0.2	18.5±1.1	25.1±1.0

5.2.8 HBU and dynamic set of the vulcanizates

Table 5.8 represents HBU and dynamic set of the vulcanizates. Clearly, the vulcanizates without TESPT treatment obviously shows high HBU. The addition of TESPT brings about the reduction in HBU, attributed to the improvement in magnitude of rubber-filler interaction, crosslink density and filler dispersion. It is also observed that the HBU decreases slightly with increasing TESPT content up to 10 wt% and then tends to level off, suggesting that 10 wt% of TESPT is sufficient for a purpose of HBU reduction in this experiment. It can also be found that the CSi demonstrates slightly lower HBU than HDSi. This could be explained by the dominant effect of the lower transient filler network of CSi.

Similar to the HBU, dynamic set of the vulcanizates is decreased noticeably by surface treatment of silica with TESPT, revealing the considerable improvement in elastic response under dynamic deformation. Similar explanation could be applied. It is also observed that the elastic response is gradually improved with increasing TESPT content from 6 to 12 wt%, possibly due to the dominant effect of the increased crosslink density. At any given TESPT content, dynamic set of the vulcanizates filled with HDSi and CSi is comparable. The dominant effect of the insignificant difference in magnitude of transient filler network could be applied for explaining the results.

Table 5.8 HBU and dynamic set of the vulcanizates

TESPT content (wt% of silica)	Silica type	HBU (°C)	Dynamic set (%)
0	HDSi	25.8±0.3	16.85±0.68
6		14.0±0.0	3.99±0.50
8		14.0±0.0	4.02±0.03
10		13.0±0.0	3.78±0.08
12		13.0±0.0	3.63±0.13
0	CSi	25.3±0.6	17.29±0.14
6		13.0±0.0	4.42±0.14
8		13.0±0.0	4.06±0.14
10		12.0±0.0	3.72±0.17
12		12.0±0.0	3.68±0.23

5.2.9 Dynamic mechanical properties of the vulcanizates

Loss factor (tanδ) as a function of test temperature of vulcanizates at various TESPT contents is illustrated in Figure 5.21. Values of T_g, tanδ_{max} and tanδ area analyzed from Figure 5.21 are summarized in Table 5.9. Regardless of the silica type, TESPT treatment reveals significant increase in T_g of the vulcanizates, arising from the improved rubber-filler interaction and crosslink density and thus the enhanced restriction of molecular motion of rubber molecules. Results also show that the increase of TESPT content from 6 to 12 wt% has little effect on T_g, attributed mainly to the counter-balancing effect of the reduced rubber-filler interaction and the increased crosslink density. Also, the vulcanizates treated by TESPT demonstrate obviously greater tanδ_{max} values and tanδ area than the vulcanizates without TESPT treatment. An explanation is given by the notable improvement in degree of filler dispersion after TESPT treatment, leading to the greater amount of rubber chains participating in the glass transition (or the reduced portion of immobilized rubber). It is also observed that the tanδ_{max} and tanδ area values are not significantly changed with increasing TESPT content from 6 to 10 wt%, possibly due to the same degree of filler dispersion. However, further increase in TESPT content from 10 to 12 wt% leads to the slight decrease in both tanδ_{max} and tanδ area values, suggesting the reduced number of rubber chains participating in the glass transition. Results also show that silica type has little effects on T_g, tanδ_{max}, and tanδ area of the vulcanizates.

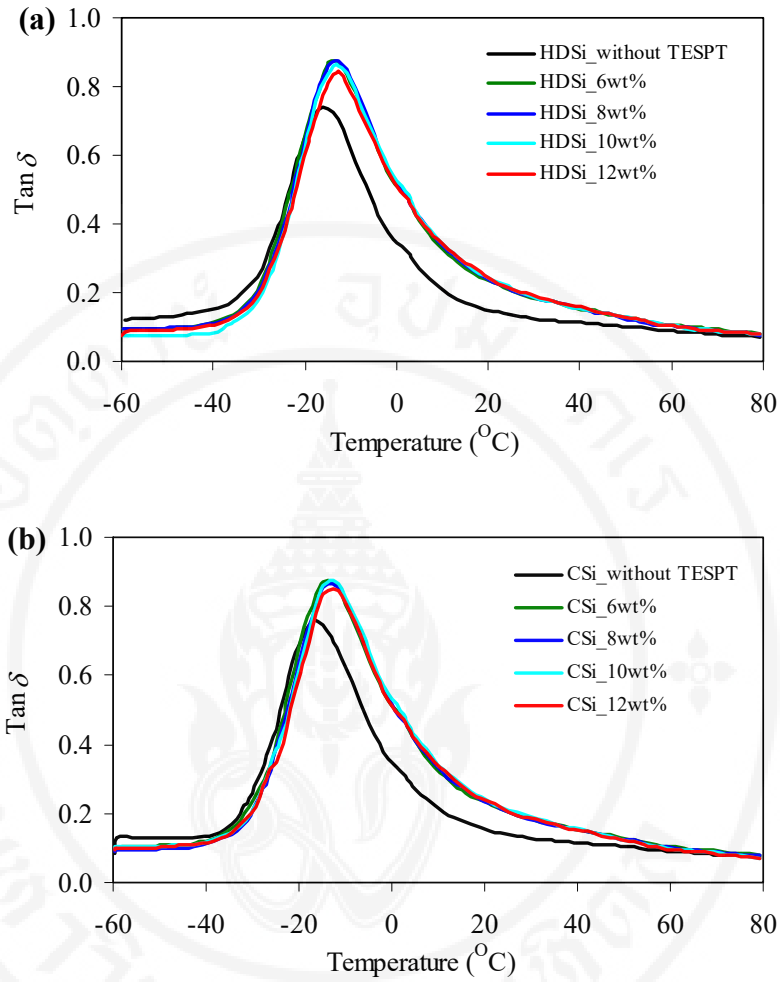

Figure 5.21 Effect of TESPT content on loss factor (δ) as a function of test temperature of the vulcanizates: (a) HDSi and (b) CSi

Table 5.9 T_g, $\tan\delta_{max}$ and $\tan\delta$ area of the vulcanizates

TESPT content (wt% of silica)	Silica type	T_g (°C)	$\tan\delta_{max}$	$\tan\delta$ area (°C)
0	HDSi	-15.8	0.737	12.89
6		-13.3	0.874	16.36
8		-13.3	0.876	16.36
10		-13.2	0.862	16.47
12		-13.0	0.840	15.75
0	CSi	-16.1	0.757	13.58
6		-13.4	0.871	16.41
8		-13.1	0.861	16.47
10		-13.1	0.874	16.58
12		-12.9	0.850	15.83

Dependence of $\tan\delta$ at 0°C on dynamic strain range of 0.03-10% of the vulcanizates is illustrated in Figure 5.22. Since the $\tan\delta$ at 0°C at 0.1% strain of the vulcanizates treated by TESPT is noticeably higher than that of the vulcanizates without TESPT treatment, it could be said that TESPT treatment leads to the significant improvement in WG. This is attributed to the higher T_g of the vulcanizates treated by TESPT. Results also show that WG of the vulcanizates is little influenced by the TESPT content ranging from 6 to 12 wt%. However, a thorough look at the results reveal that the best WG is obtained when approximately 8 to 10 wt% of TESPT content is used. Unexpectedly, silica type provides little effect on WG of the vulcanizates. The insignificant difference in T_g could be used to explain this result.

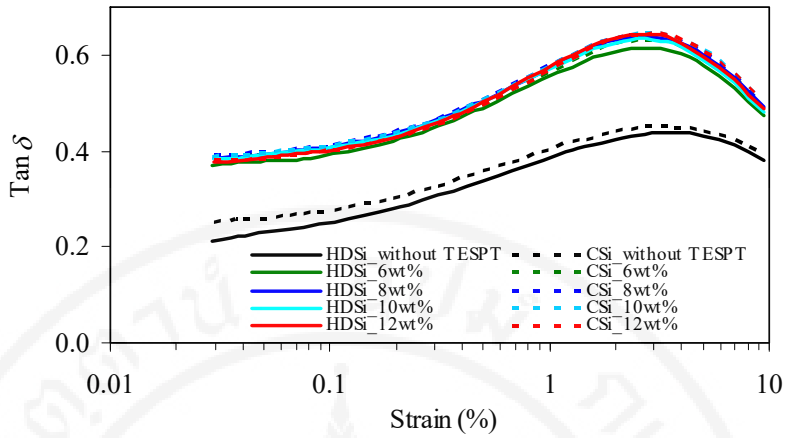

Figure 5.22 Loss factor (tanδ) at 0°C as a function of dynamic strain of the vulcanizates

Figure 5.23 represents the tanδ of vulcanizates as a function of dynamic strain from 0.03-10% at 60°C. Results show that the vulcanizates without TESPT treatment impart the lowest tanδ value at low strains (<2%), which could be explained by the effect of a strong transient filler network which still exists at low strain giving rise to the high elastic response. At higher applied strain (≥2%) where the disruption of transient filler network begins, however, the tanδ values of the vulcanizates without TESPT treatment sharply rise due to their strong magnitude of transient filler network and become higher than those of the vulcanizates treated by TESPT. Results reveal that the applied test strain plays an important role in the prediction of FSE (via tanδ value at 60°C), especially in the system containing relatively high transient filler network such as SSBR/silica nanocomposites without SCAs treatment. At 5% strain, TESPT treatment expectedly leads to the significantly reduced tanδ value at 60°C, indicating the decreased RR and, thus, the improved FSE. Results also show that the FSE tends to improve with increasing TESPT content from 6 to 10 wt%, possibly due to the dominant effect of the enhanced crosslink density. However, further increase of TESPT content beyond 10 wt% results in the negative effect on the FSE which could be owing to the more pronounced effect of reduced rubber-filler interaction. Results also suggest that the best FSE is achieved at 10 wt% of TESPT content for both HDSi-filled and CSi-filled systems.

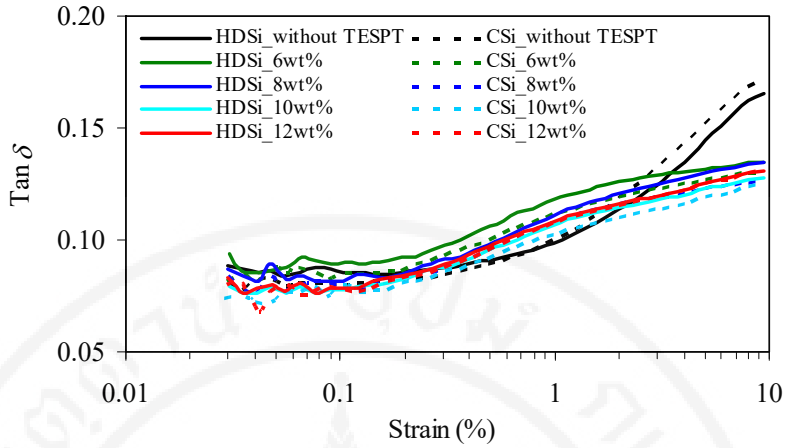

Figure 5.23 Loss factor (tanδ) at 60°C as a function of dynamic strain of the vulcanizates

The "magic triangle" of tire performance, including WG (indicated by tanδ at 0°C), FSE (indicated by tanδ at 60°C), and abrasion resistance, in terms of the normalized graph is depicted in Figure 5.24 (reference line (100%): HDSi-filled system treated with 8 wt% of TESPT). Obviously, the tire performance of the vulcanizates without TESPT treatment is not satisfactory. However, the significant improvement in tire performance can be achieved by TESPT treatment. As the best balance of tire performance is found in the vulcanizates treated with 10 wt% of TESPT, this TESPT content will be employed in the subsequent sections.

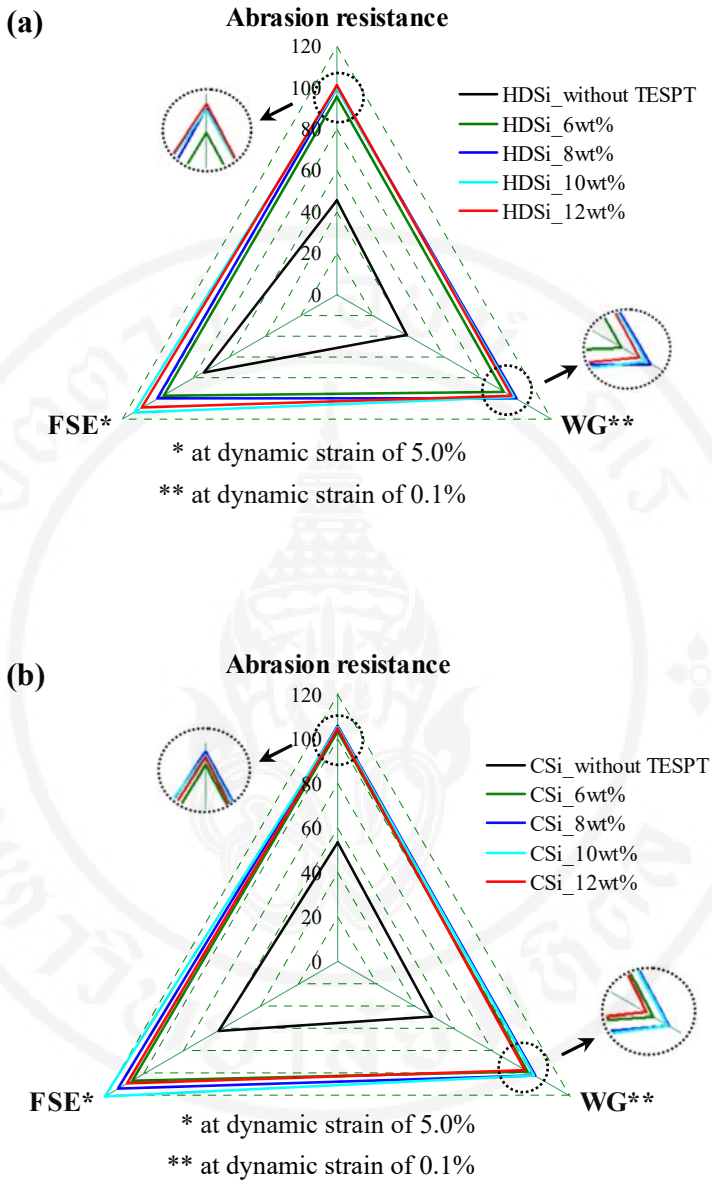

Figure 5.24 Effect of TESPT content on tire performance represented in terms of the normalized graph: (a) HDSi and (b) CSi

5.3 Effects of silica/CB hybrid filler and SBR type on properties of SBR compounds and vulcanizates

According to the results gained from the previous parts, the silanization temperature of 140°C and TESPT content of 10 wt% of silica were selected in this study. Properties of SBR (SSBR6450SL, SSBR3626, and ESBR1723) filled with silica (HDSi or CSi)/CB hybrid filler at various ratios (100/0, 80/20, 60/40, 40/60, 20/80 and 0/100) are investigated.

5.3.1 Mooney viscosity of the compounds

Mooney viscosity of the compounds is represented in Figure 5.25. Results show that Mooney viscosity is found to increase with increasing CB ratio. This is possibly due to the increase in effective filler volume fraction which arises from the decreased portion of mobilized rubber caused by the increased amount of rubber trapped in CB aggregates. It is widely known that the CB agglomerates are generally in an acini form (grape-like structure) [136] whereas silica clusters are typically in a string of pearl [62]. When filler is well dispersed in rubber matrix, the grape-like structure of CB could consume greater amount of rubber than silica leading to the greater effective filler volume fraction. The explanation is supported by the significant reduction of tanδ area with increasing CB ratio (to be subsequently discussed in details in section 5.3.9). It is widely known that tanδ area depends mainly on 2 main factors, i.e., the amount of mobilized rubber that can participate in transition and crosslink density. With increasing CB ratio, crosslink density of the rubber tends to decrease (see also the results in section 5.3.6) which shall in theory lead to the increased tanδ area. However, in practice, the tanδ area is found to decrease noticeably with increasing CB ratio. Such decrease is a solid evidence of the reduction of the mobilized rubber content and, thus, the increased effective filler volume fraction. At a given filler ratio, it is also observed that SSBR3626 imparts higher Mooney viscosity than SSBR6450SL. Possible explanation is given by the slightly better dispersion of filler in SSBR6450SL leading to the greater portion of mobilized rubber and, thus, lower effective filler volume fraction. Apparently, the greater Mooney viscosity is observed in SSBR compounds as compared to ESBR compounds, attributed mainly to

the combination of the higher native Mooney viscosity of raw rubber and the stronger rubber-filler interaction of SSBR. Results also show that Mooney viscosity of the compound filled with HDSi is higher than that of the compound filled with CSi, especially in SSBR compounds. The stronger rubber-filler interaction together with the higher structure of HDSi is applied for explaining the results.

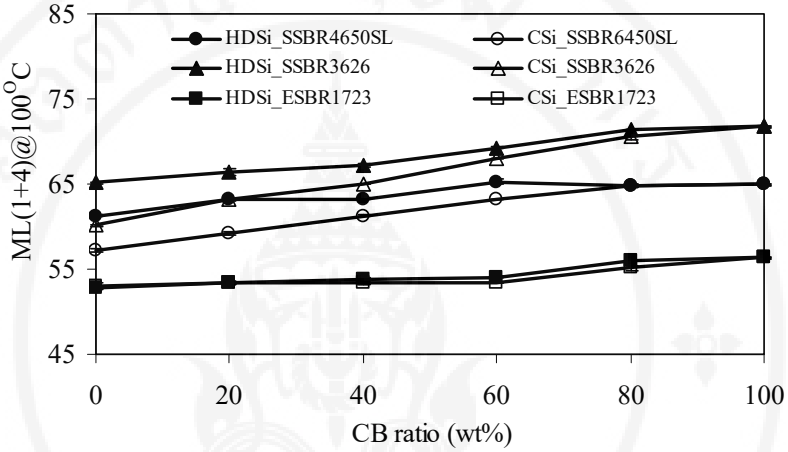

Figure 5.25 Mooney viscosity of the compounds

5.3.2 Bound rubber content (BRC) of the compounds

Figure 5.26 exhibits the relationship between BRC and CB ratio in hybrid filler. Clearly, the SSBR compounds reinforced by silica possess greater total BRC and chemical BRC than those reinforced by CB. Moreover, both total BRC and chemical BRC tend to decrease continuously with increasing CB ratio, indicating that the increased CB portion leads to the negative effect on rubber-filler interaction. The greater specific surface area of silica together with the high coupling efficiency of TESPT could be the reasonable explanation for this finding. Conversely, total BRC and chemical BRC of the ESBR compounds increases consecutively with increasing CB ratio, meaning that the improved rubber-filler interaction is gained when CB ratio is increased. It could also be observed that BRC of silica-filled ESBR is very low, compared with that of silica-filled SSBR, implying that the coupling efficiency of TESPT in ESBR is relatively low as compared to SSBR. It can also be seen that, at any given CB ratio, SSBR6450SL gives higher total BRC and chemical BRC than SSBR3626 and SSBR provides greater total BRC and chemical BRC than ESBR,

particularly in the silica-filled compounds. Since SSBR6450SL possesses significantly higher vinyl content as compared to SSBR3626, the results imply that the vinyl content in SBR considerably affects the rubber-silica interaction, especially in the system containing TESPT, i.e., the higher the vinyl content in SBR, the greater the rubber-silica interaction. This might be due to the higher reactivity of vinyl configuration in butadiene unit, compared to other configurations [137]. It is also found that both total BRC and chemical BRC of the compound filled with HDSi are greater than those of the compound filled with CSi, particularly in ESBR. Results indicate that HDSi provides stronger rubber-filler interaction than CSi having similar specific surface area.

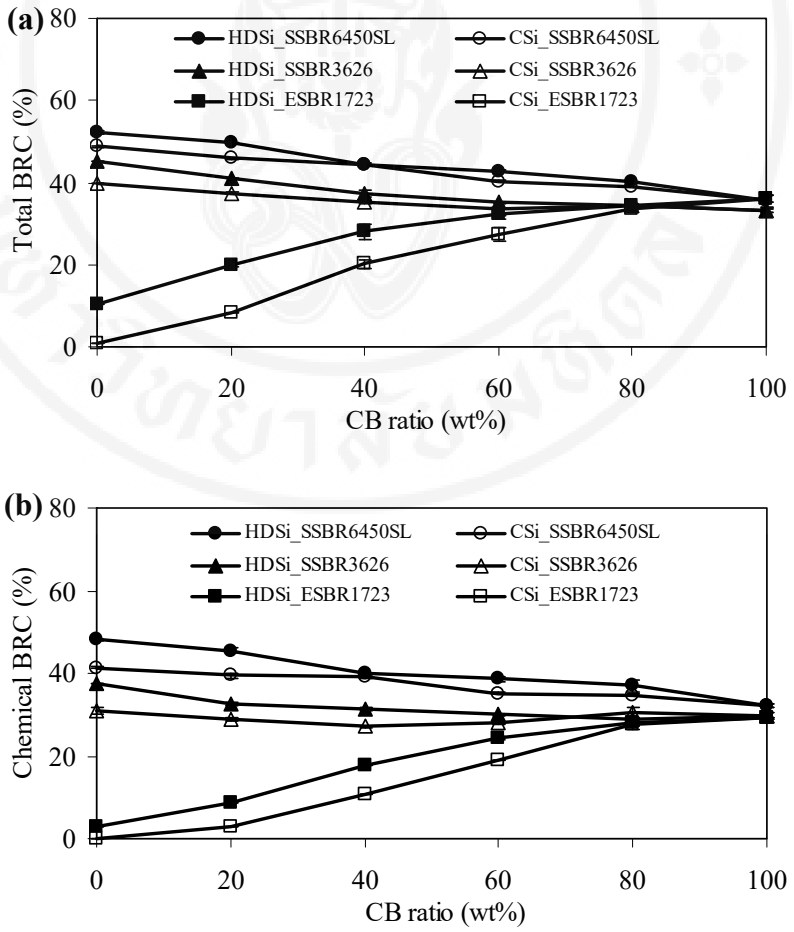

Figure 5.26 BRC of rubber compounds: (a) total BRC and (b) chemical BRC

5.3.3 Payne effect of the compounds

Payne effect of the compounds is depicted in Figure 5.27. Obviously, the magnitude of Payne effect (ΔG') is continuously increased with increasing CB ratio, implying the enhanced magnitude of transient filler network. This is because of the reduced portion of mobilized rubber as a result of the increased amount of rubber trapped in CB aggregates, leading to the increased probability of transient filler network formation. Since the magnitude of Payne effect of SSBR6450SL is not significantly different with that of SSBR3626 and the magnitude of Payne effect of SSBR is higher than that of ESBR, results suggest that both SSBR6450SL and SSBR3626 offer comparable magnitude of transient filler network while SSBR provides greater level of transient filler network than ESBR. Results also reveal that the magnitude of transient filler network of HDSi- and CSi- filled compounds is comparable.

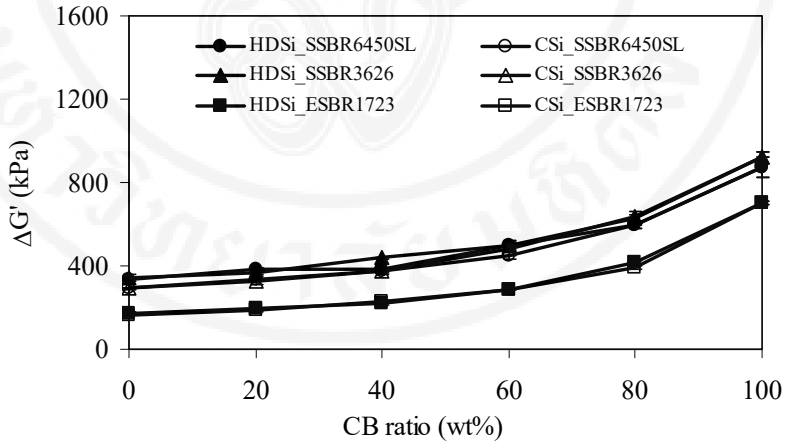

Figure 5.27 Payne effect of the compounds

5.3.4 Cure characteristics of the compounds

Figure 5.28 illustrates cure curves of the compounds. Cure characteristics, i.e., t_s1 and t_c90, analyzed from Figure 5.28 are represented in Figure 5.29. Apparently, both t_s1 and t_c90 of SSBR compounds are found to increase with increasing CB ratio up to approximately 60 wt% and then tends to decrease afterwards. Since the TESPT content is directly proportional to silica ratio, the increased CB ratio leads to the decreased TESPT content and, thus, the sulfur atoms released from the TESPT. As both t_s1 and t_c90 of the SBR vulcanizates are shorten when sulfur content is increased, this might the reason why the increased t_s1 and t_c90 of SSBR compounds is observed when CB ratio is increased up to 60 wt%. When CB ratio is further increased, contrary trend is observed, i.e., both t_s1 and t_c90 tend to decrease with increasing CB ratio which might arise from the reduction of mobilized rubber leading to the increase in curative concentration in rubber matrix. Unlike SSBR, both t_s1 and t_c90 of ESBR compounds decrease continuously with increasing CB ratio, attributed mainly to the enhanced curative concentration caused by the decreased portion of mobilized rubber. Results also reveal that both t_s1 and t_c90 of SSBR compounds are shorter than those of ESBR compounds at high silica ratio (>60 wt% of silica), probably due to the stronger interaction between silica and SSBR (higher BRC) leading to the reduction of mobilized rubber and, thus, the increased curative concentration. However, as both ESBR and SSBR show comparable level of interaction with CB, the values of t_s1 and t_c90 of ESBR and SSBR compounds are insignificantly different when CB ratio is higher than 60 wt%. As the HDSi and CSi impart insignificant difference in cure curves and, hence, both t_s1 and t_c90, it could be stated that silica type plays little role in cure characteristics of the compounds.

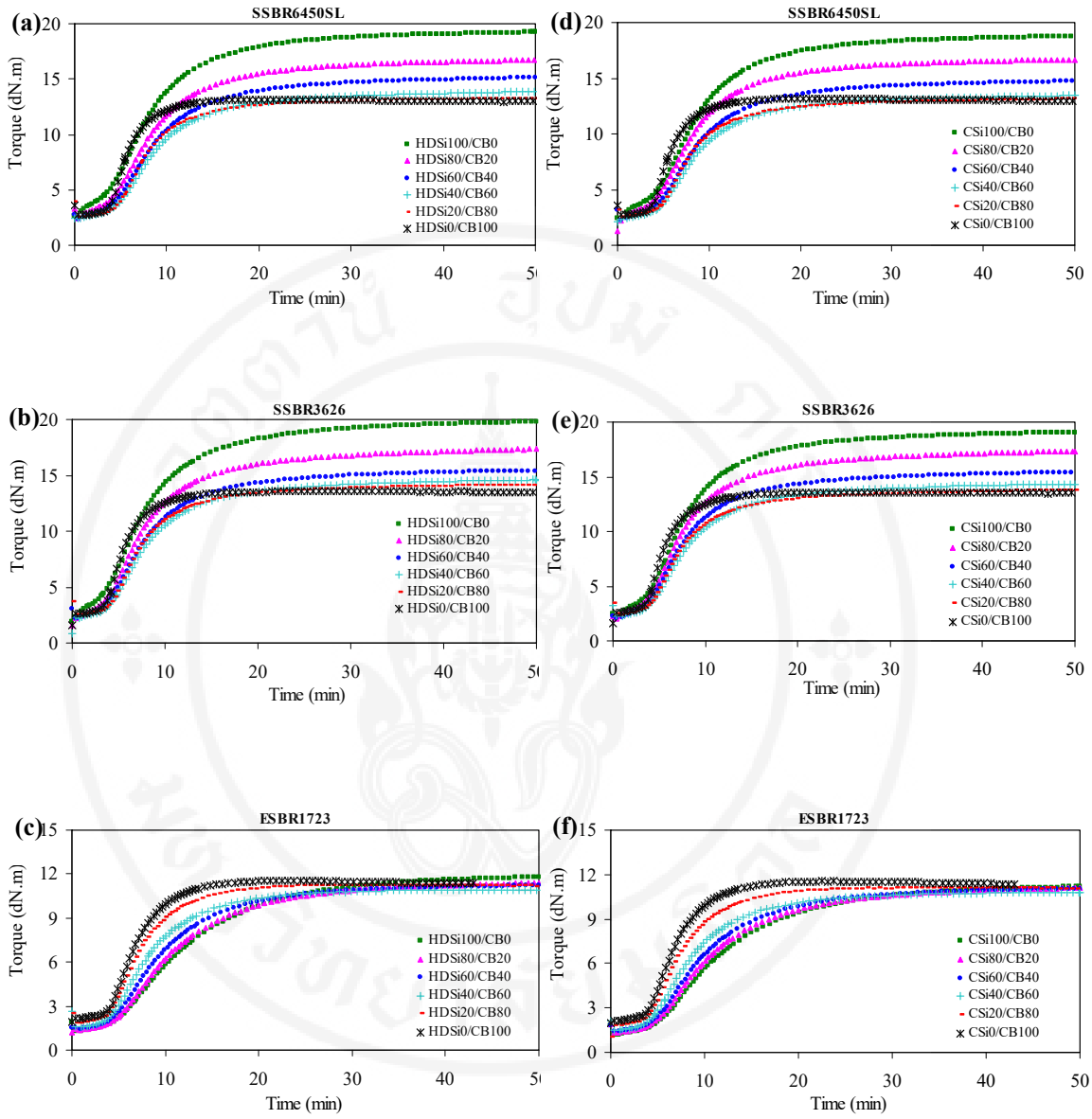

Figure 5.28 Cure curves of the compounds having various CB ratios:
(a) HDSi_SSBR6450SL (b) HDSi_SSBR3626 (c) HDSi_ESBR1723
(d) CSi_SSBR6450SL (e) CSi_SSBR3626 and (f) CSi_ESBR1723

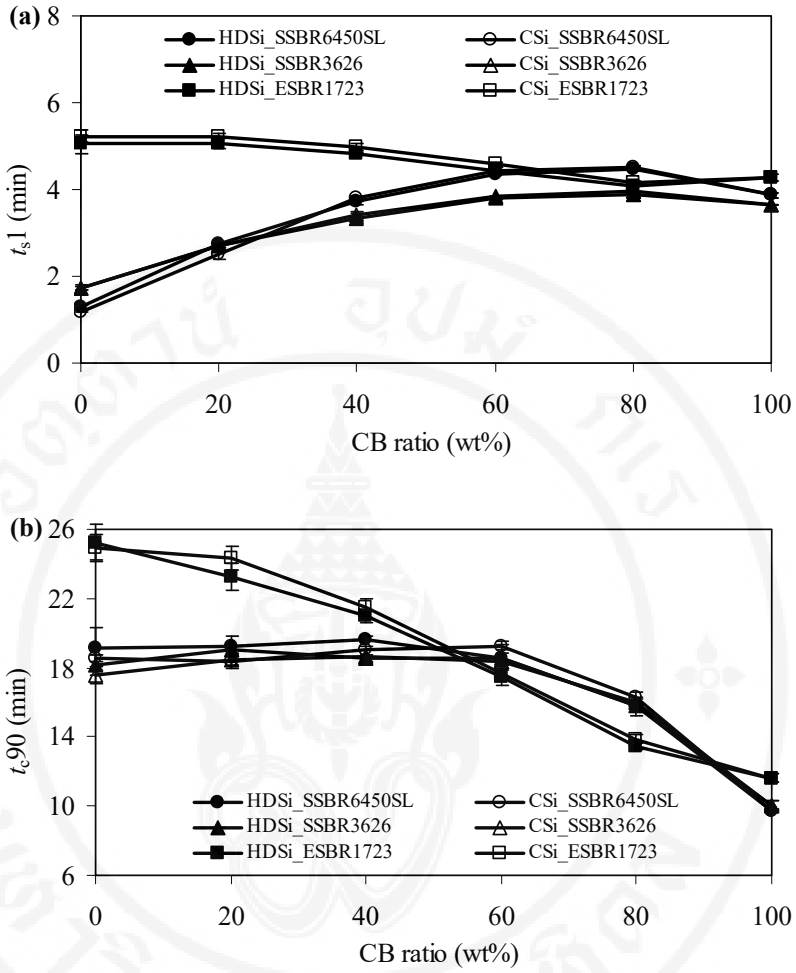

Figure 5.29 Values of t_s1 and t_c90 of the compounds as a function of CB ratio: (a) t_s1 and (b) t_c90

5.3.5 Degree of filler dispersion of the vulcanizates

It is well known that, in the case of rubber filled with hybrid filler, the properties of filled rubber strongly depend on both dispersion and distribution of each filler in the rubber matrix. In this study, the dispersion and the distribution of silica and/or CB in SBR matrix are primarily investigated by various types of microscopy techniques, i.e., TEM, AFM, and SEM-EDS. Since all above techniques cannot effectively distinguish the morphologies of silica and CB in rubber matrix (see Appendix A), only the overall degree of filler dispersion as investigated by SEM will be represented and discussed in this section.

Figure 5.30-5.32 displays SEM micrographs of the vulcanizates. Evidently, a high level of filler dispersion is observed in all vulcanizates, implying that the factors studied in this experiment, i.e., silica/CB ratio, SBR type, and silica type, play a minor role in degree of filler dispersion. Perhaps, the relatively long mixing time used in this experiment may override the effect of hybrid filler ratio including SBR and silica types. However, a thorough look at the results reveals that SSBR6450SL gives slightly better filler dispersion than SSBR3626 and ESBR1723 which is attributed to its highest initial Mooney viscosity providing the greatest shear field during the mixing process.

5.3.6 Crosslink density of the vulcanizates

Crosslink density of the vulcanizates, measured from the swelling technique, as a function of CB ratio in the hybrid filler is illustrated in Figure 5.33. Obviously, the crosslink density decreases consecutively with increasing CB ratio, possibly due to the reduced level of rubber-filler interaction [128] and/or the decreased number of sulfur atom released from TESPT. At any given CB ratio, SSBR6450SL gives higher crosslink density than SSBR3626 and ESBR1723, respectively. This is particularly pronounced in the vulcanizate filled with silica. The combined effects of the greater rubber-filler interaction and the higher reactivity towards chemical reaction of the vinyl configuration could be used to explain the result. Compared to the CSi-filled SSBR vulcanizates, the HDSi-filled SSBR vulcanizates possess higher crosslink density which could possibly owing to the greater rubber-filler interaction as previously mentioned. Surprisingly, silica type gives no profound effect on crosslink density of the ESBR vulcanizates.

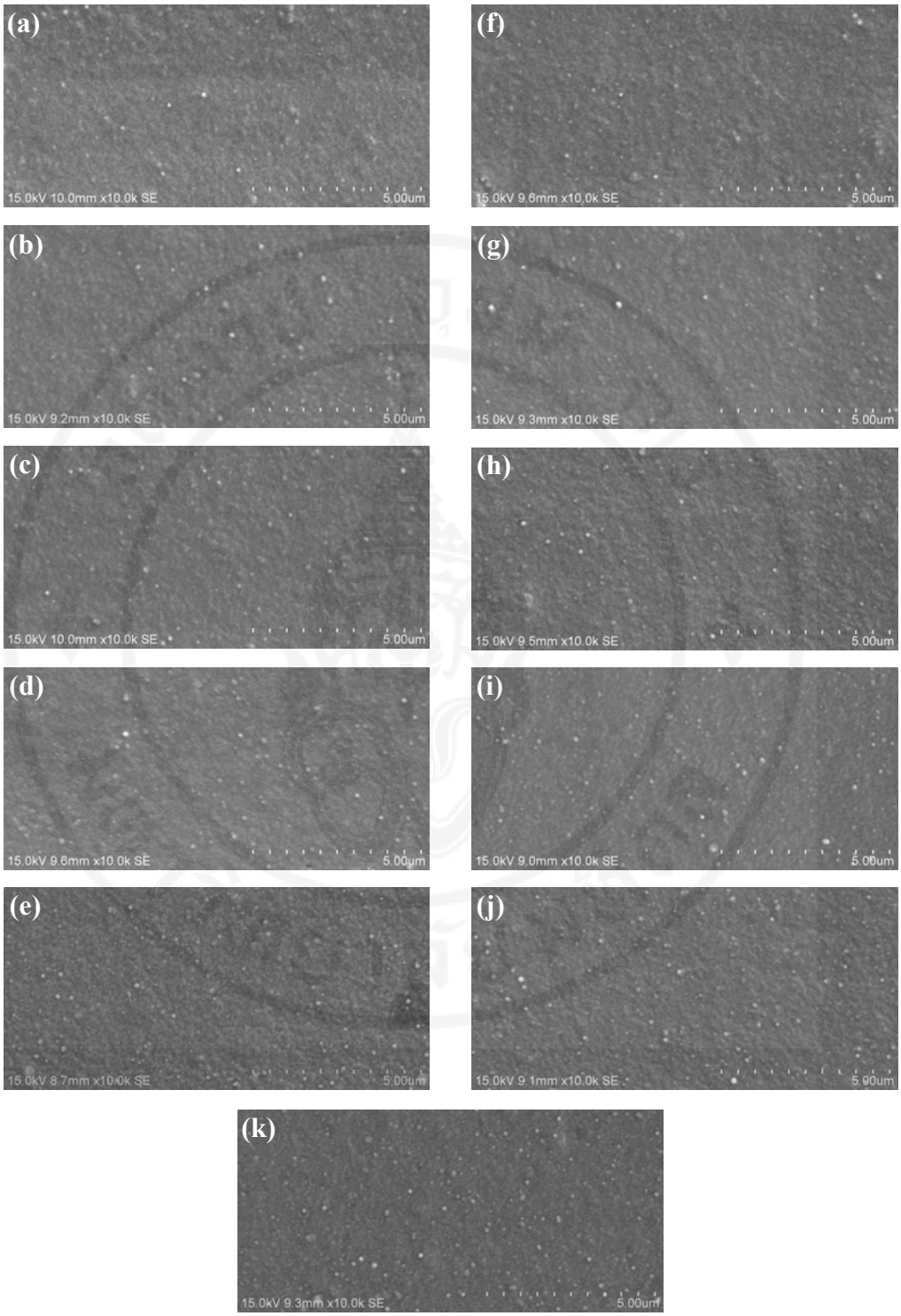

Figure 5.30 SEM micrographs (x10,000) of the filled SSBR6450SL vulcanizates at various CB ratios: (a) HDSi_CB 0 wt% (b) HDSi_CB 20 wt% (c) HDSi_CB 40 wt% (d) HDSi_CB 60 wt% (e) HDSi_CB 80 wt% (f) CSi_CB 0 wt% (g) CSi_CB 20 wt% (h) CSi_CB 40 wt% (i) CSi_CB 60 wt% (j) CSi_CB 80 wt% and (k) CB 100 wt%

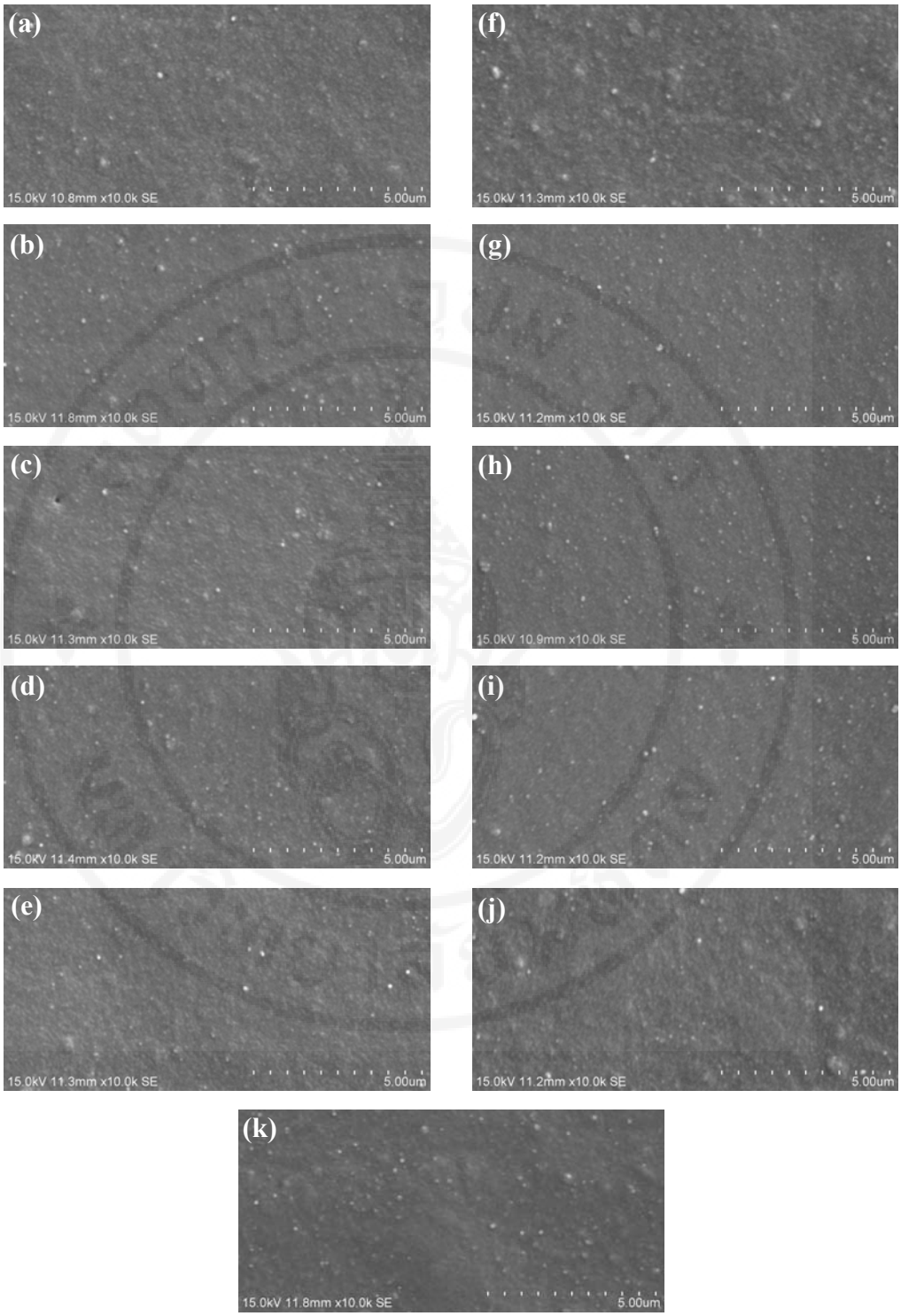

Figure 5.31 SEM micrographs (x10,000) of the filled SSBR3626 vulcanizates at various CB ratios: (a) HDSi_CB 0 wt% (b) HDSi_CB 20 wt% (c) HDSi_CB 40 wt% (d) HDSi_CB 60 wt% (e) HDSi_CB 80 wt% (f) CSi_CB 0 wt% (g) CSi_CB 20 wt% (h) CSi_CB 40 wt% (i) CSi_CB 60 wt% (j) CSi_CB 80 wt% and (k) CB 100 wt%

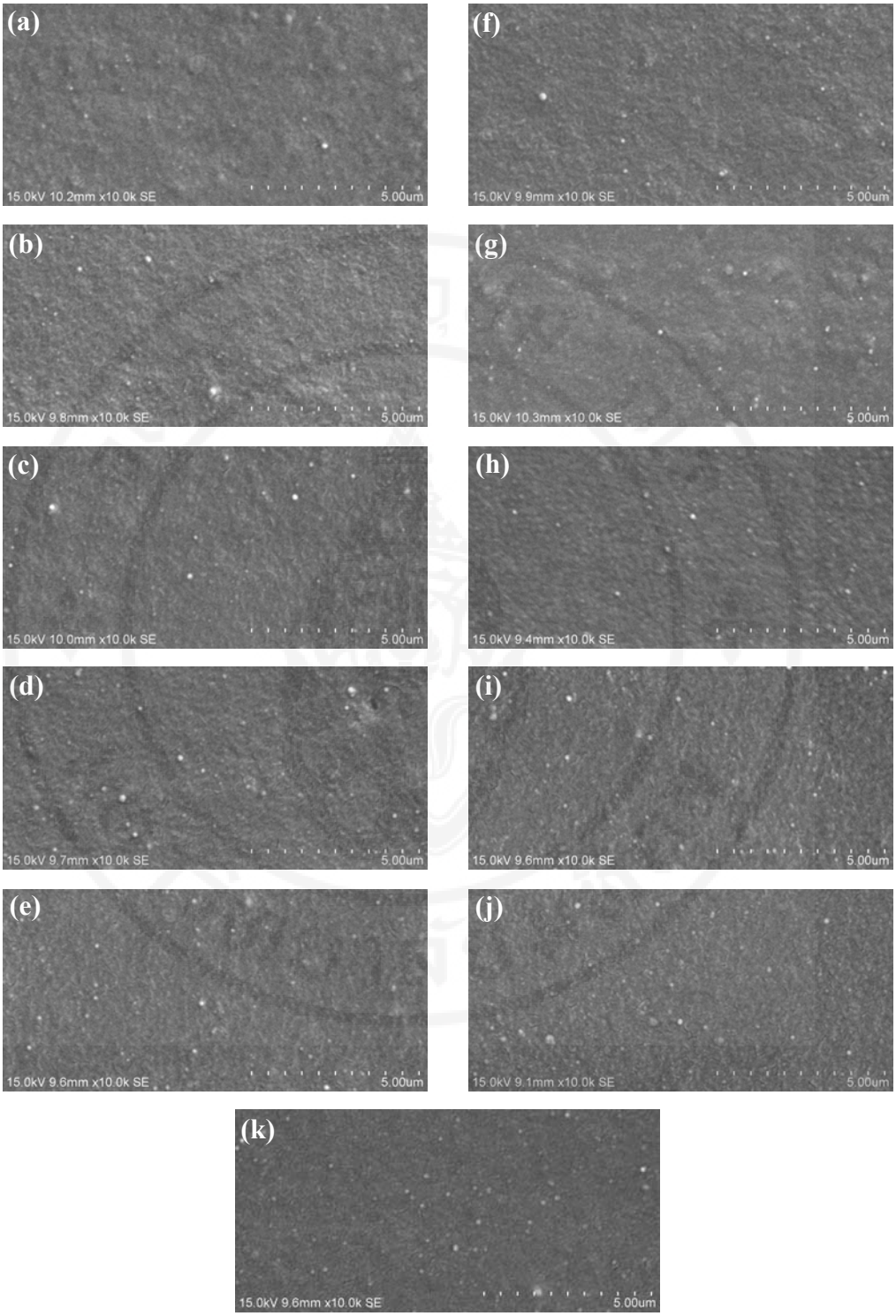

Figure 5.32 SEM micrographs (x10,000) of the filled ESBR1723 vulcanizates at various CB ratios: (a) HDSi_CB 0 wt% (b) HDSi_CB 20 wt% (c) HDSi_CB 40 wt% (d) HDSi_CB 60 wt% (e) HDSi_CB 80 wt% (f) CSi_CB 0 wt% (g) CSi_CB 20 wt% (h) CSi_CB 40 wt% (i) CSi_CB 60 wt% (j) CSi_CB 80 wt% and (k) CB 100 wt%

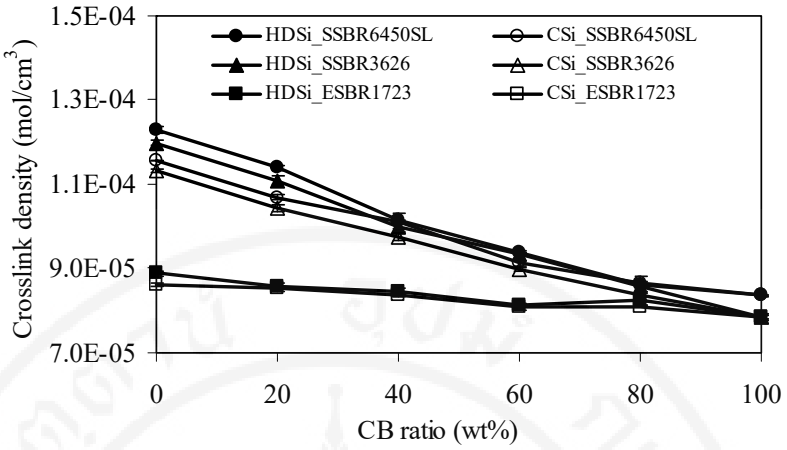

Figure 5.33 Crosslink density of the vulcanizates as measured from the swelling technique

5.3.7 Mechanical properties of the vulcanizates

Figure 5.34 represents hardness of the vulcanizates as a function of CB ratio in hybrid filler. For SSBR, the hardness of the vulcanizates decreases continuously with increasing CB ratio up to 60 wt%, attributed probably to the combination of: (i) the reduced crosslink density; (ii) the decreased level of rubber-filler interaction and (iii) the lower specific surface area of CB as compared to that of silica. At higher CB ratios, however, the increased CB ratio gives no considerable change in hardness of the vulcanizates which could be explained by the counter-balance between the decreased level of rubber-filler interaction together with crosslink density and the reduced portion of mobilized rubber. However, for ESBR, hardness of the vulcanizates is little influenced by the increase of CB ratio up to 60 wt%, possibly due to the counter-balance between the enhanced level of rubber-filler interaction and the decreased crosslink density. However, the hardness of ESBR vulcanizates tends to increase with increasing CB ratio beyond 60 wt%, due mainly to the combined effects of the increased rubber-filler interaction and the reduced portion of mobilized rubber. Surprisingly, regardless of the CB ratio and silica type, SSBR3626 provides slightly greater hardness than SSBR6450SL despite its lower level of rubber-filler interaction and crosslink density. The slightly poorer filler dispersion could be used to explain the results. As compared to SSBR, ESBR shows lower hardness because of its lower magnitude of rubber-filler interaction and crosslink density. As HDSi provides greater

crosslink density and level of rubber-filler interaction than CSi, the hardness of HDSi-filled SSBR vulcanizate is significantly higher than that of CSi-filled SSBR vulcanizate. However, due to the comparable crosslink density and degree of filler dispersion, silica type demonstrates little effect on hardness of the ESBR vulcanizates.

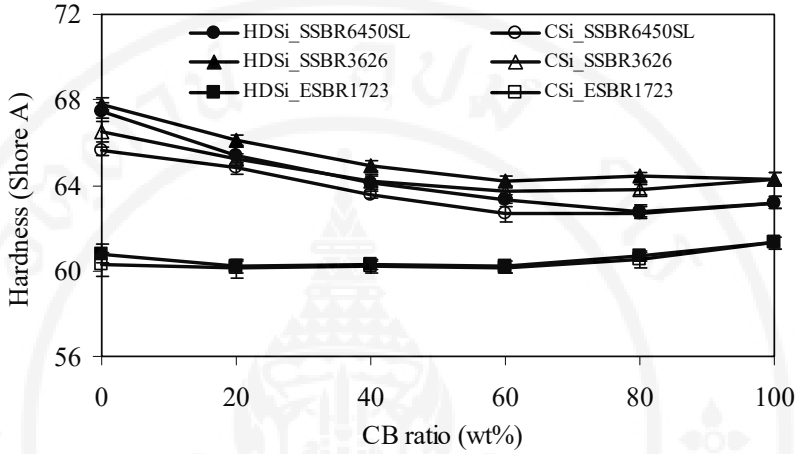

Figure 5.34 Hardness of the vulcanizates

Abrasion resistance represented in terms of volume loss of the vulcanizates is exhibited in Figure 5.35. For SSBR vulcanizates, volume loss is decreased with increasing CB ratio up to 80 wt%. The improvement in abrasion resistance is possibly because of the reduced mobilized rubber and the decreased friction coefficient of the vulcanizates when CB ratio is increased. It has been reported that the friction coefficient of the SSBR/BR filled with CB is lower than that of the SSBR/BR filled with CSi in the presence of TESPT [138]. In addition, the reduced sharpness of the abrasive wheel during the test might be another reasonable explanation for this finding. It is observed that the abraded debris becomes softer and stickier with increasing CB ratio, leading to the increased amount of abraded debris adhered on abrasive wheel and, thus, the reduced power of abrasion. The proposed statement is supported by Mokhtari, et al. [138]. They observed that the abraded debris of CB-filled SSBR/BR was sticky and prone to attach to the granite ball whereas the abraded debris of CSi-filled SSBR/BR is a dusty-like form. However, the volume loss increases again when CB is solely added, which could be explained by the dominant effects of the reduced crosslink density and the decreased level of rubber-filler

interaction. Similar to the case of SSBR, abrasion resistance of ESBR vulcanizates improves noticeably with increasing CB ratio up to 60 wt%. The same explanation is applied. Further increase in CB ratio, however, results in no considerable change in abrasion resistance. The counter-balance between the reduced crosslink density and the increased level of rubber-filler interaction could be used to explain this observation. Result also reveals that, compared to SSBR3626, SSBR6450SL gives higher abrasion resistance, possibly owing to the greater magnitude of rubber-filler interaction, better filler dispersion and higher crosslink density. Clearly, the abrasion resistance of the SSBR vulcanizates is superior to that of ESBR vulcanizates, particularly at low CB ratio. Again, the higher rubber-filler interaction and crosslink density of SSBR is applied for explaining the results. Moreover, the greater hardness of SSBR could also be taken into consideration, especially at high CB ratio, because it is well known that hard rubber usually offers greater abrasion resistance than soft rubber. In ESBR vulcanizates, the HDSi provides better abrasion resistance than the CSi, explained by the greater level of rubber-filler interaction. On the other hand, in SSBR vulcanizates, CSi gives superior abrasion resistance to HDSi, despite the fact that HDSi imparts greater magnitude of rubber-filler interaction, crosslink density and hardness as compared to CSi. The slightly higher specific surface area of CSi is believed to be responsible for this finding. In general, the filler possessing higher specific surface area usually provides better reinforcement including abrasion resistance due to its greater contact area with rubber [67].

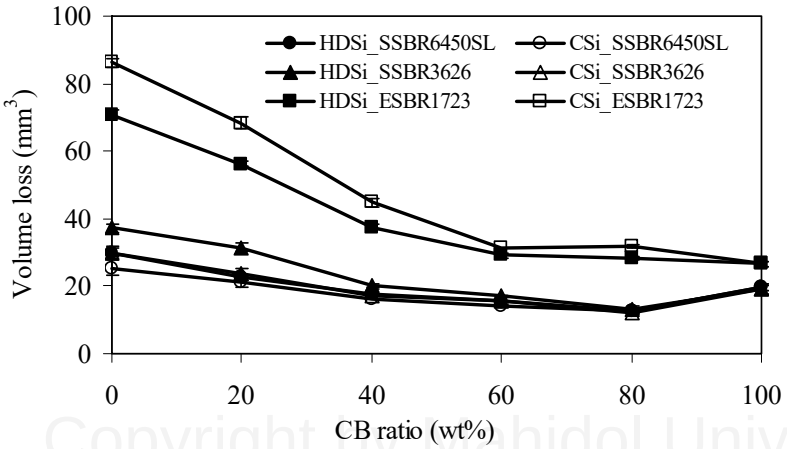

Figure 5.35 Volume loss of the vulcanizates

5.3.8 HBU and dynamic set of the vulcanizates

Figure 5.36 illustrates the relationships between CB ratio in hybrid filler and HBU and dynamic set of the vulcanizates. Regardless of SBR and silica type, both HBU and dynamic set tend to increase with increasing CB ratio. The results imply that the energy dissipation is enhanced whereas the elasticity of vulcanizates is impaired with increasing CB ratio. The negative effect on HBU and dynamic set could be attributed to the reduced level of rubber-filler interaction, the enhanced magnitude of transient filler network and/or the decreased crosslink density. It is also found that, in this experiment, silica type gives no profound effect on HBU and dynamic set. Compared to SSBR, ESBR demonstrates higher HBU and dynamic set because it possesses lower level of rubber-filler interaction and crosslink density.

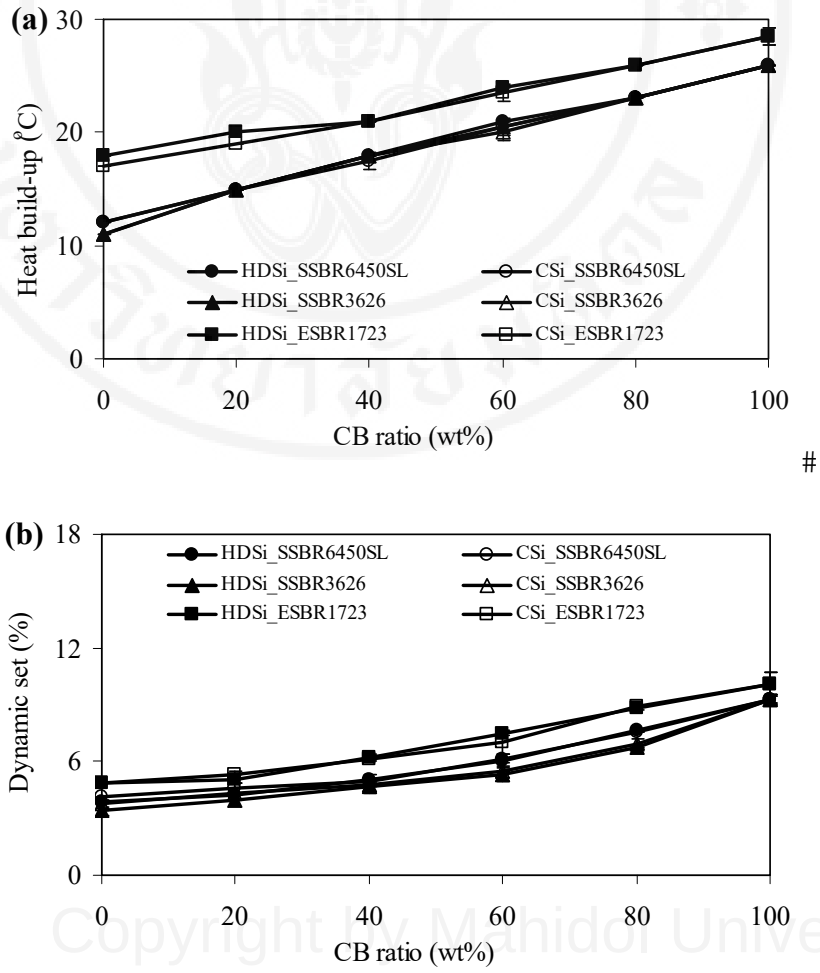

Figure 5.36 HBU and dynamic set of the vulcanizates

5.3.9 Dynamic mechanical properties of the vulcanizates

Figure 5.37 and 5.38 show the relationship between loss factor (tanδ) and test temperature of the vulcanizates having various CB ratios. Values of T_g, tanδ_{max} and tanδ area analyzed from Figure 5.37 and 5.38 are summarized in Table 5.10. Regardless of SBR and silica type, T_g of the vulcanizates is found to shift towards the left with increasing CB ratio. This is understandable because, in this work, the increased CB ratio leads to the reduced level of rubber-filler interaction and/or the decreased crosslink density, resulting in the reduced restriction of rubber molecular motion and, hence, T_g of the vulcanizates. It is also observed that values of tanδ_{max} and tanδ area decrease consecutively with increasing CB ratio, despite the reduced crosslink density, suggesting the reduced amount of rubber chains participating in the glass transition (or the reduced portion of mobilized rubber). This is explained by the increased amount of trapped (immobilized) rubber in CB aggregates resulted from its grape-like structure as previously discussed. At any given CB ratio, SSBR3626 provides higher T_g than SSBR6450SL despite its lower magnitude of rubber-filler interaction and crosslink density. Moreover, according to the chemical structure, SSBR3626 having lower vinyl content than SSBR6450SL should in theory exhibit lower T_g. Explanation is not known at present because there is no availability of detailed information concerning the difference in molecular structure (degree of branching) of the 2 rubbers. However, the slightly higher bound styrene content of SSBR3626 might be one of the reasons for its higher T_g. Obviously, ESBR shows noticeably lower T_g than SSBR, attributed mainly to the significantly lower vinyl content and bound styrene content of ESBR. In addition, the lower level of rubber-filler interaction and crosslink density, particularly at low CB ratio, might be another reasonable explanation. Although silica type has little effect on T_g of the vulcanizates, it demonstrates some influences on tanδ_{max} and tanδ area, i.e., CSi gives slightly higher tanδ_{max} and tanδ area as compared to HDSi, possibly due to its lower structure and, hence, trapped rubber.

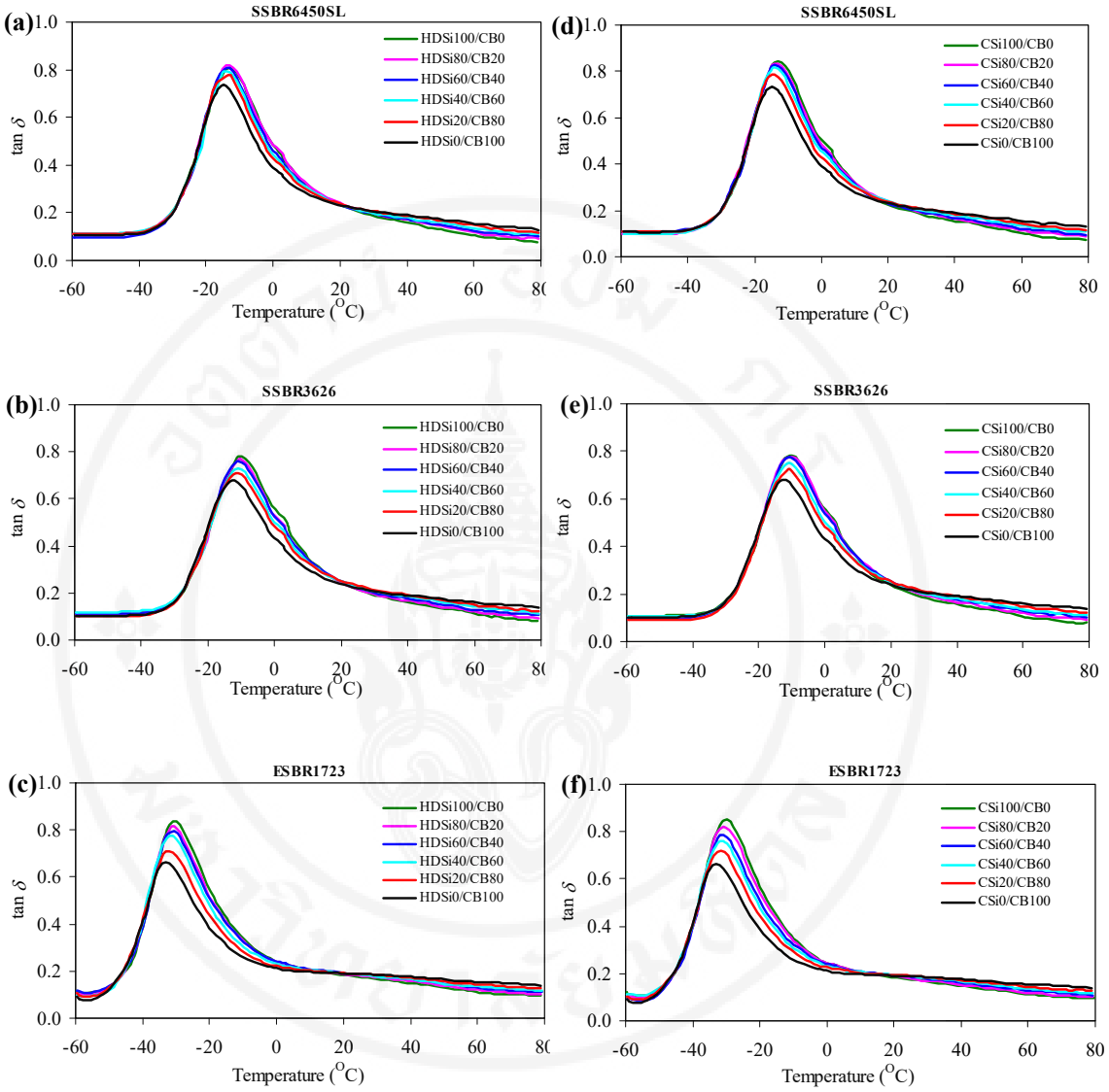

Figure 5.37 Loss factor (tanδ) as a function of test temperature of the vulcanizates having various CB ratios: (a) HDSi_SSBR6450SL (b) HDSi_SSBR3626 (c) HDSi_ESBR1723 (d) CSi_SSBR6450SL (e) CSi_SSBR3626 and (f) CSi_ESBR1723

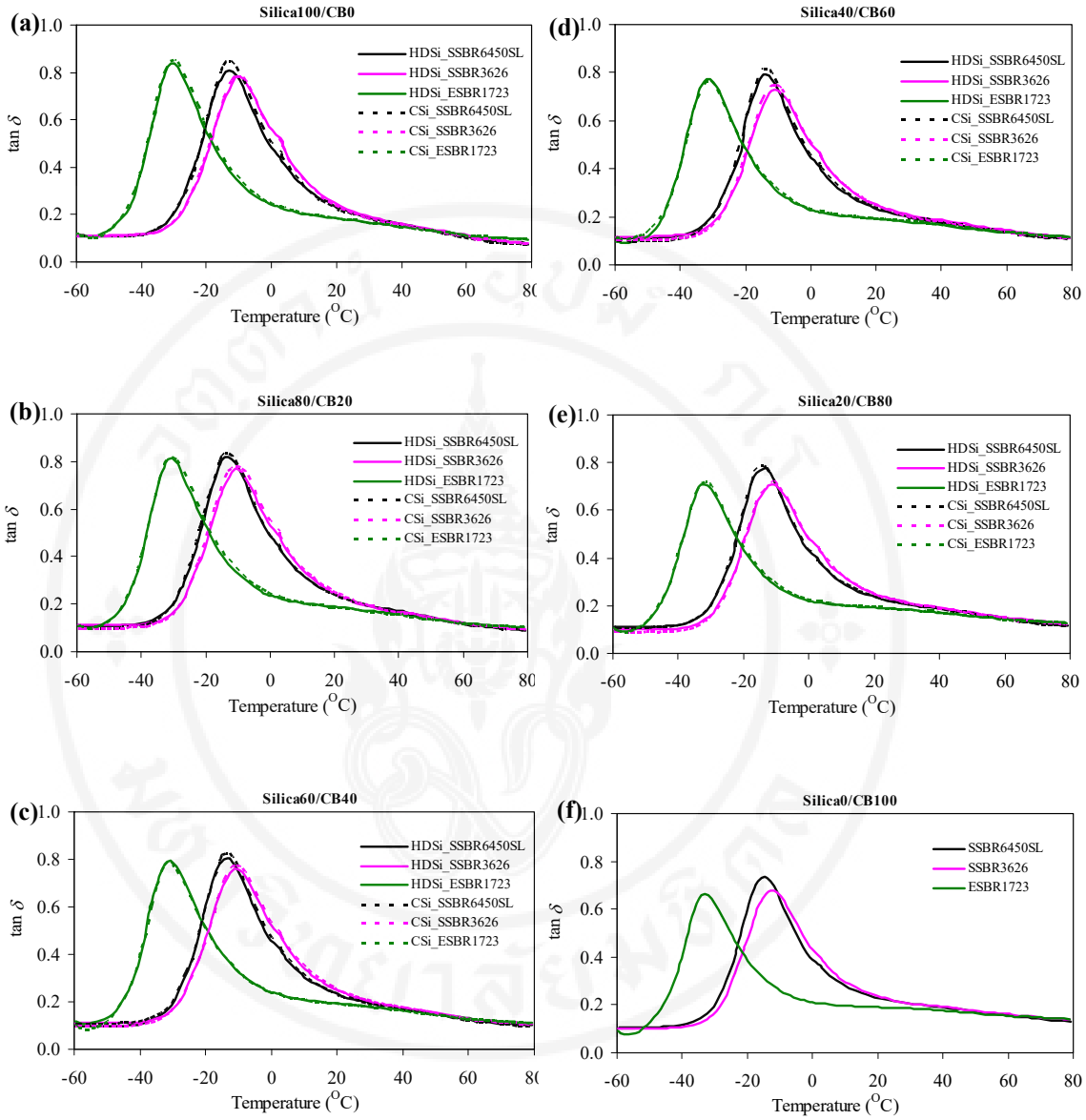

Figure 5.38 Loss factor (tanδ) as a function of test temperature of the vulcanizates: (a) CB 0 wt% (b) CB 20 wt% (c) CB 40 wt% (d) CB 60 wt% (e) CB 80 wt% and (f) CB 100 wt%

Table 5.10 T_g, tanδ_{max} and tanδ area of the vulcanizates

SBR type	CB ratio (wt%)	Silica type	T_g (°C)	tanδ_{max}	tanδ area (°C)
SSBR6450SL	0	HDSi	-12.8	0.808	15.59
	20		-13.2	0.819	15.41
	40		-13.5	0.806	15.16
	60		-13.9	0.792	14.31
	80		-14.3	0.774	13.86
	100		-14.9	0.735	12.78
	0	CSi	-12.8	0.845	16.18
	20		-13.1	0.834	16.06
	40		-13.8	0.824	15.41
	60		-13.8	0.814	15.08
	80		-14.5	0.786	14.07
	100		-14.9	0.735	12.78
SSBR3626	0	HDSi	-10.2	0.781	15.27
	20		-10.6	0.770	14.87
	40		-10.9	0.760	14.61
	60		-10.9	0.729	13.48
	80		-11.1	0.710	13.38
	100		-12.7	0.680	12.35
	0	CSi	-10.5	0.784	15.37
	20		-10.7	0.779	15.59
	40		-10.7	0.776	15.07
	60		-10.8	0.752	14.28
	80		-10.9	0.725	13.67
	100		-12.7	0.680	12.35
ESBR1723	0	HDSi	-30.6	0.835	15.48
	20		-30.8	0.812	14.98
	40		-30.7	0.794	14.56
	60		-31.5	0.773	14.32
	80		-32.2	0.710	12.71
	100		-32.8	0.661	11.57
	0	CSi	-29.9	0.845	16.14
	20		-30.7	0.820	15.47
	40		-30.8	0.783	14.68
	60		-31.0	0.762	13.67
	80		-31.9	0.718	12.85
	100		-32.8	0.661	11.57

Tanδ at 0°C of the vulcanizates as a function of dynamic strain from 0.03 to 10% is depicted in Figure 5.39 and 5.40. Regardless of SBR and silica type, at relatively low strains (<1% for SSBR and <0.3% for ESBR), the tanδ value at 0°C decreases continuously with increasing CB ratio whereas the opposite trend result is observed at high strains, i.e., the tanδ value at 0°C is found to increase with increasing CB proportion. At low strains where the transient filler network is not disrupted, the increase in CB ratio leads to the reduction of crosslink density and, thus, the shift of T_g towards lower temperature. Value of tanδ at 0°C (at the peak shoulder) therefore tends to decrease with increasing CB ratio. However, at relatively high strains where the destruction of transient filler network becomes more pronounced, value of tanδ will be strongly dependent on the magnitude of transient filler network because it is widely known that the breaking and reforming of the transient filler network are the main source of energy dissipation during the dynamic deformation [139]. As evidenced from the Payne effect results shown in Figure 5.27, CB network is much stronger than silica network. This explains why the increase of CB ratio would result in the increase of tanδ value at 0°C (or the decrease of rubber elasticity). Alternatively, one could say that, at relatively high strains, the destruction of transient filler network shows a greater effect on tanδ at 0°C than the T_g shift. Clearly, at 0.1% strain, the tanδ values at 0°C tend to decrease with increasing CB ratio particularly in SSBR, indicating the decreased WG. The reduced T_g with increasing CB ratio could be applied for explaining this result. The results also show that SSBR3626 gives the highest tanδ value at 0°C at 0.1% strain, possibly due to its highest T_g, and followed by SSBR6450SL and ESBR1723, respectively. It could be therefore stated that SSBR3626 provides better WG than SSBR6450SL and ESBR17232. Again, WG of the vulcanizates is independent of silica type, attributed probably to the comparable T_g of HDSi- and CSi-filled vulcanizates.

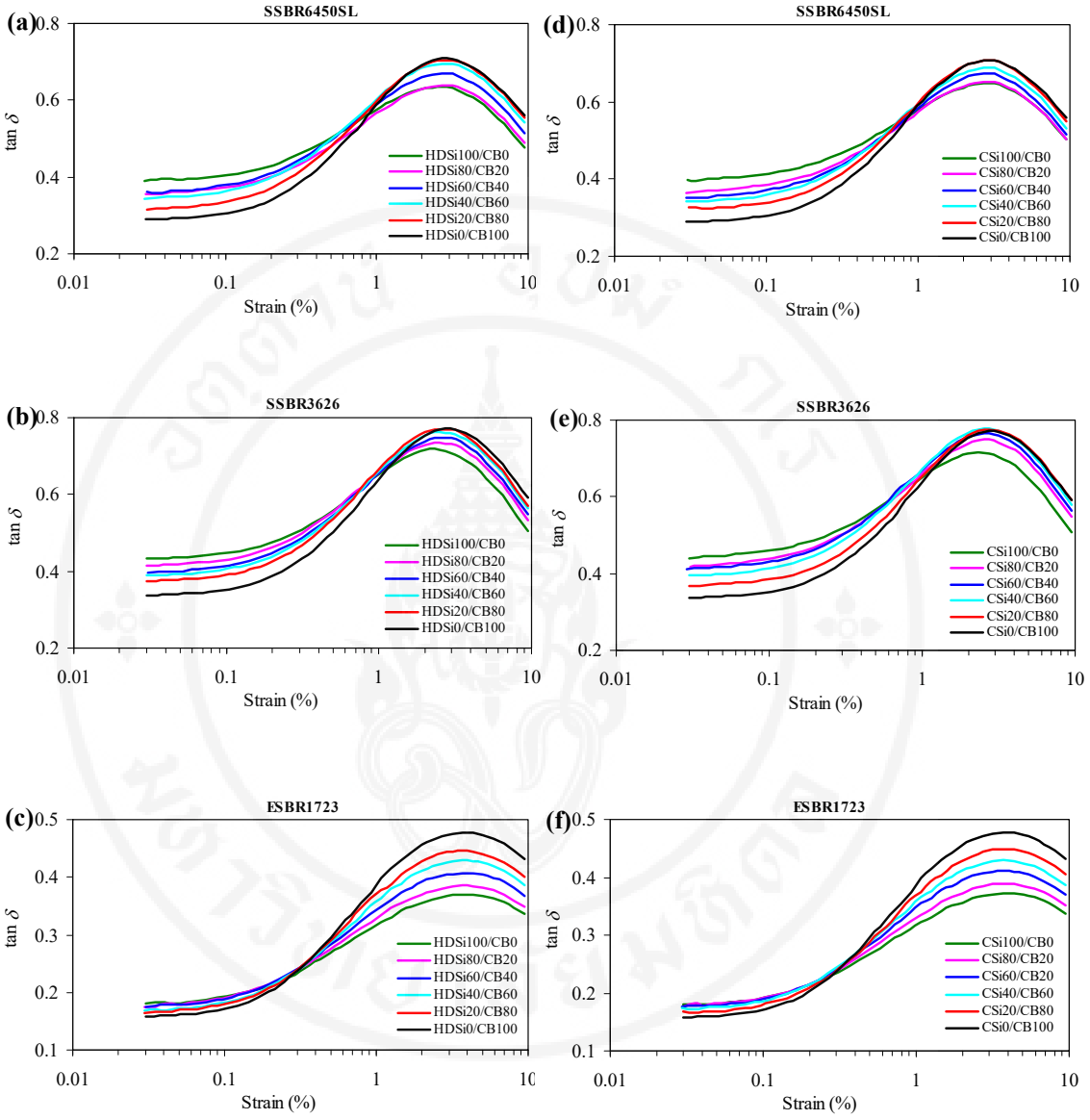

Figure 5.39 Loss factor (tanδ) as a function of dynamic strain at 0°C of the vulcanizates having various CB ratios: (a) HDSi_SSBR6450SL (b) HDSi_SSBR3626 (c) HDSi_ESBR1723 (d) CSi_SSBR6450SL (e) CSi_SSBR3626 and (f) CSi_ESBR1723

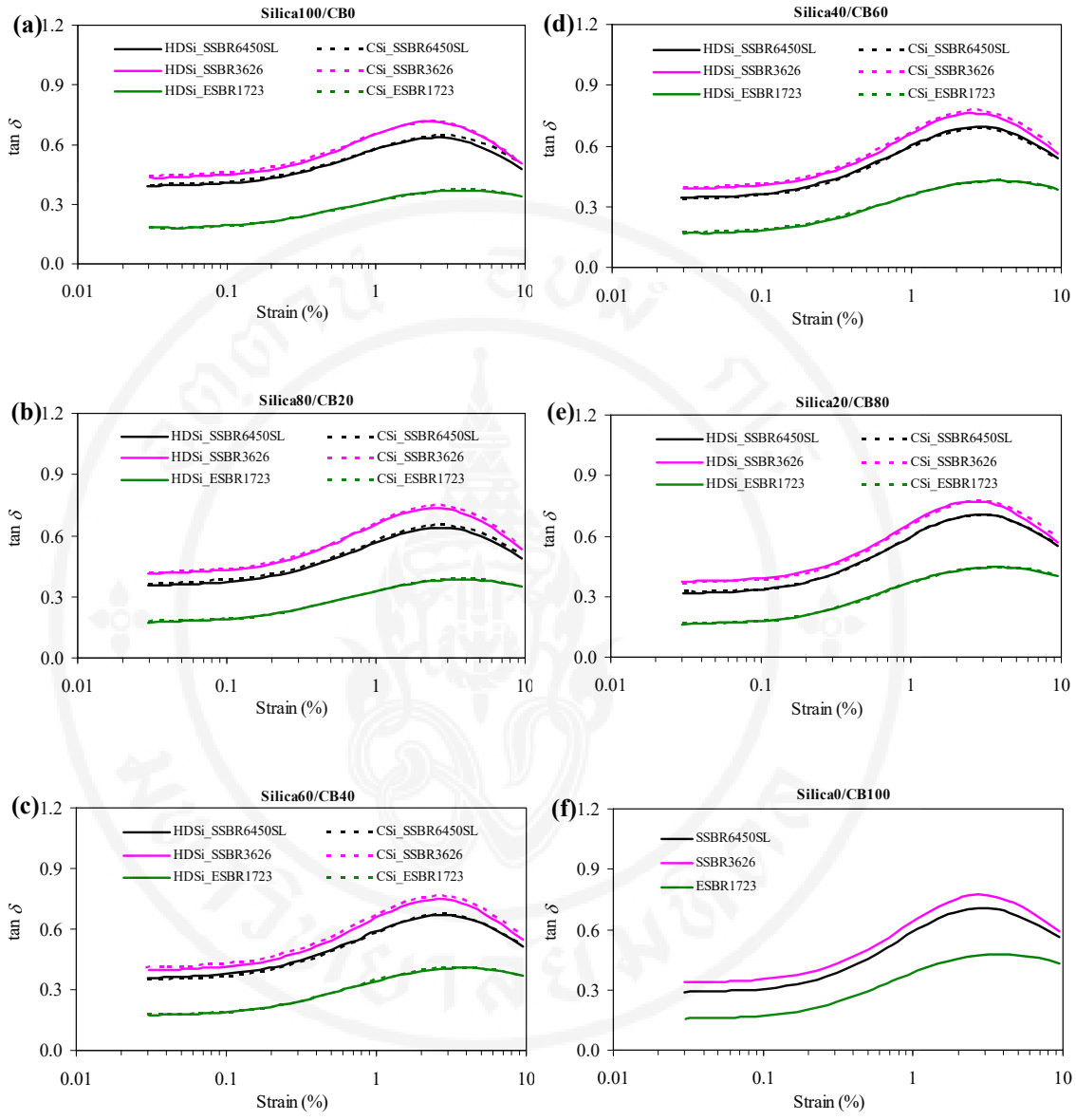

Figure 5.40 Loss factor (tanδ) as a function of dynamic strain at 0°C of the vulcanizates: (a) CB 0 wt% (b) CB 20 wt% (c) CB 40 wt% (d) CB 60 wt% (e) CB 80 wt% and (f) CB 100 wt%

Figure 5.41 and 5.42 represent the dependence of tanδ at 60°C on dynamic strain from 0.03 to 10% of the vulcanizates. Obviously, the tanδ value at 60°C tends to increase continuously with increasing CB ratio, probably due to the increased magnitude of transient filler network and the reduced crosslink density. At 5% strain, tanδ at 60°C tends to increase consecutively with increasing CB ratio, revealing the increased RR of the vulcanizates and, hence, the impaired FSE. Regardless of CB ratio and silica type, the tanδ values at 60°C at 5% strain of the SSBR6450SL are slightly lower than those of the SSBR3626, indicating the better FSE of SSBR6450SL. This is due to the combined consequences of: (i) the better filler dispersion; (ii) the greater level of rubber-filler interaction and (iii) the higher crosslink density. Surprisingly, both SSBR and ESBR vulcanizates show comparable FSE, despite the fact that ESBR has noticeably lower rubber-filler interaction and crosslink density than SSBR. Explanation is given by the lower magnitude of Payne effect in association with lower T_g value of ESBR which counterbalance the effects of rubber-filler interaction and crosslink density. Results also show that silica type demonstrates little role on the value of tanδ at 60°C (or FSE) since both silica types give comparable magnitude of transient filler network.

Normalized graphs of tire performance, i.e., abrasion resistance, WG (indicated by tanδ at 0°C), and FSE (indicated by tanδ at 60°C), at various CB ratio are illustrated in Figure 5.43 (reference line (100%): 60/40 CSi/CB-filled SSBR6450SL). Clearly, the balanced tire performance of 3 types of SBR, i.e., SSBR6450SL, SSBR3626, and ESBR1723, is found in 40 wt% of CB ratio. Focusing on 40 wt% of CB ratio (see Figure 5.44), it is found that ESBR shows the lowest tire performance (comparable FSE with poorest WG and abrasion resistance). For SSBR, although SSBR6450SL provides lower WG than SSBR3626, it imparts slightly better abrasion resistance and FSE. Thus, SSBR6450SL imparts better overall tire performance than SSBR3626. When the effect of silica type on tire performance of SSBR6450SL is concerned, CSi offers superior abrasion resistance to HDSi. It could be therefore summarized that the 60/40 CSi/CB-filled SSBR6450SL seems to give the best balanced tire performance. Consequently, this formula will be employed in the subsequent sections.

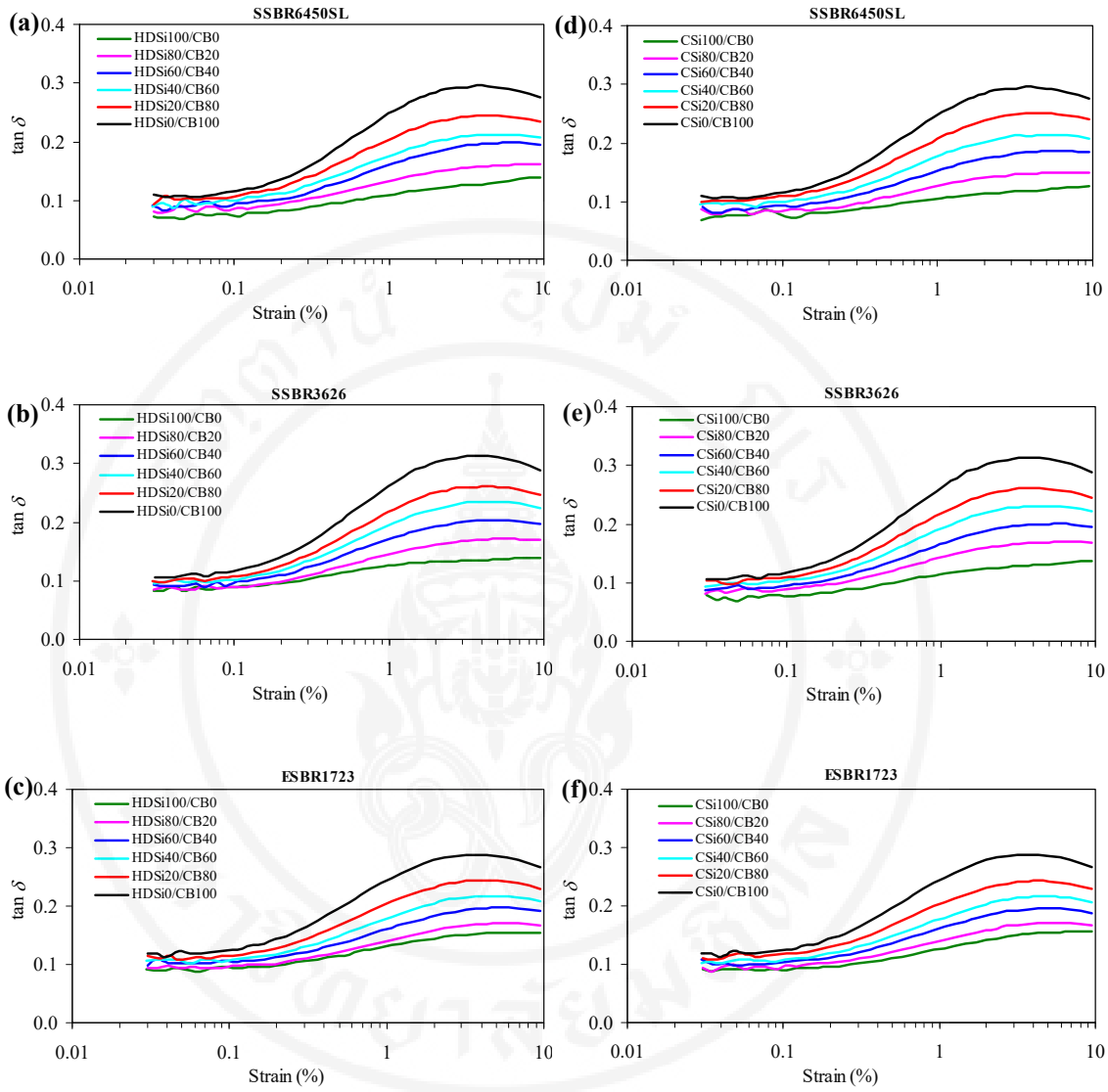

Figure 5.41 Loss factor (tanδ) as a function of dynamic strain at 60°C of the vulcanizates having various CB ratios (a) HDSi_SSBR6450SL (b) HDSi_SSBR3626 (c) HDSi_ESBR1723 (d) CSi_SSBR6450SL (e) CSi_SSBR3626 and (f) CSi_ESBR1723

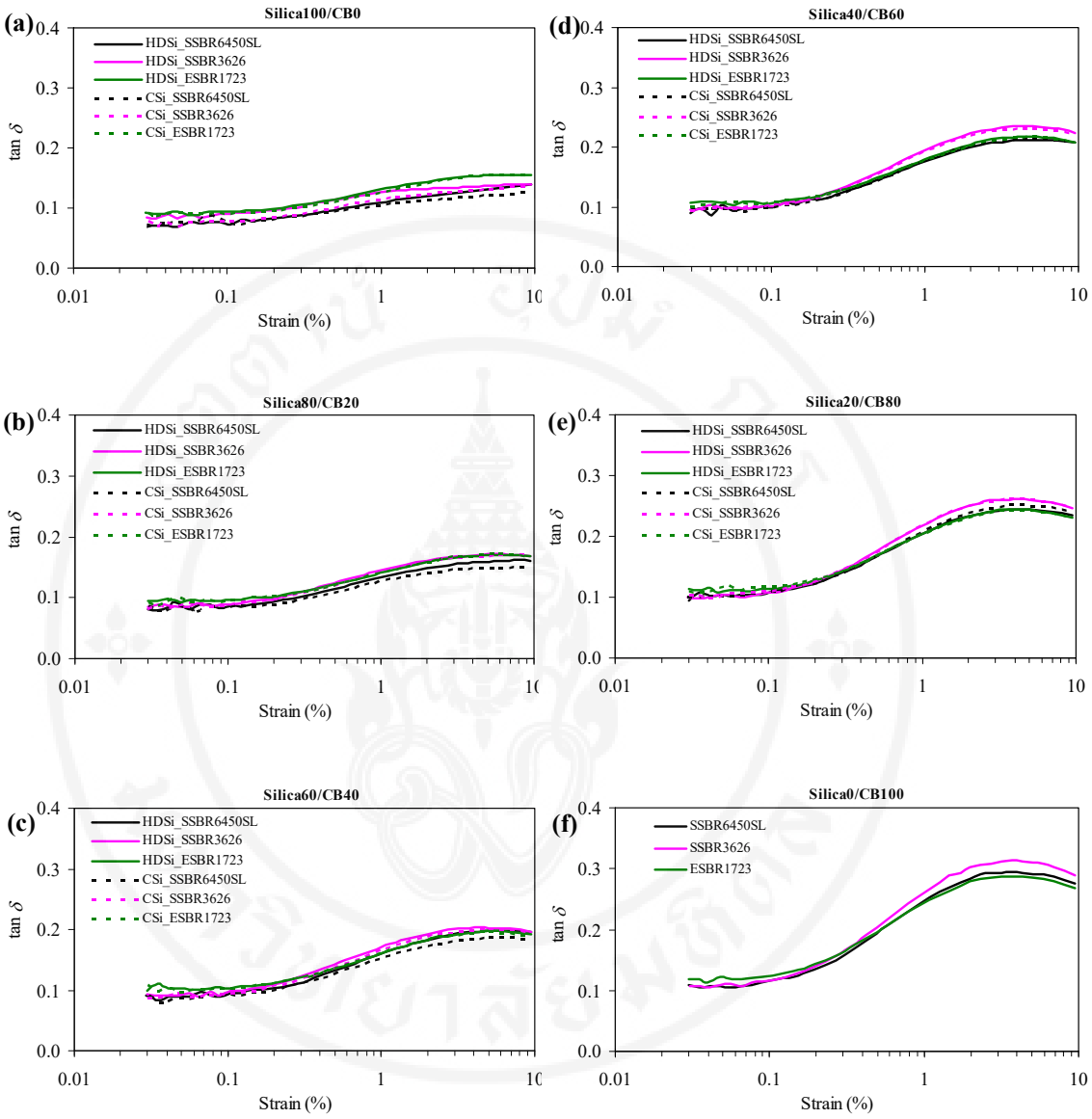

Figure 5.42 Loss factor (tanδ) as a function of dynamic strain at 60°C of the vulcanizates: (a) CB 0 wt% (b) CB 20 wt% (c) CB 40 wt% (d) CB 60 wt% (e) CB 80 wt% and (f) CB 100 wt%

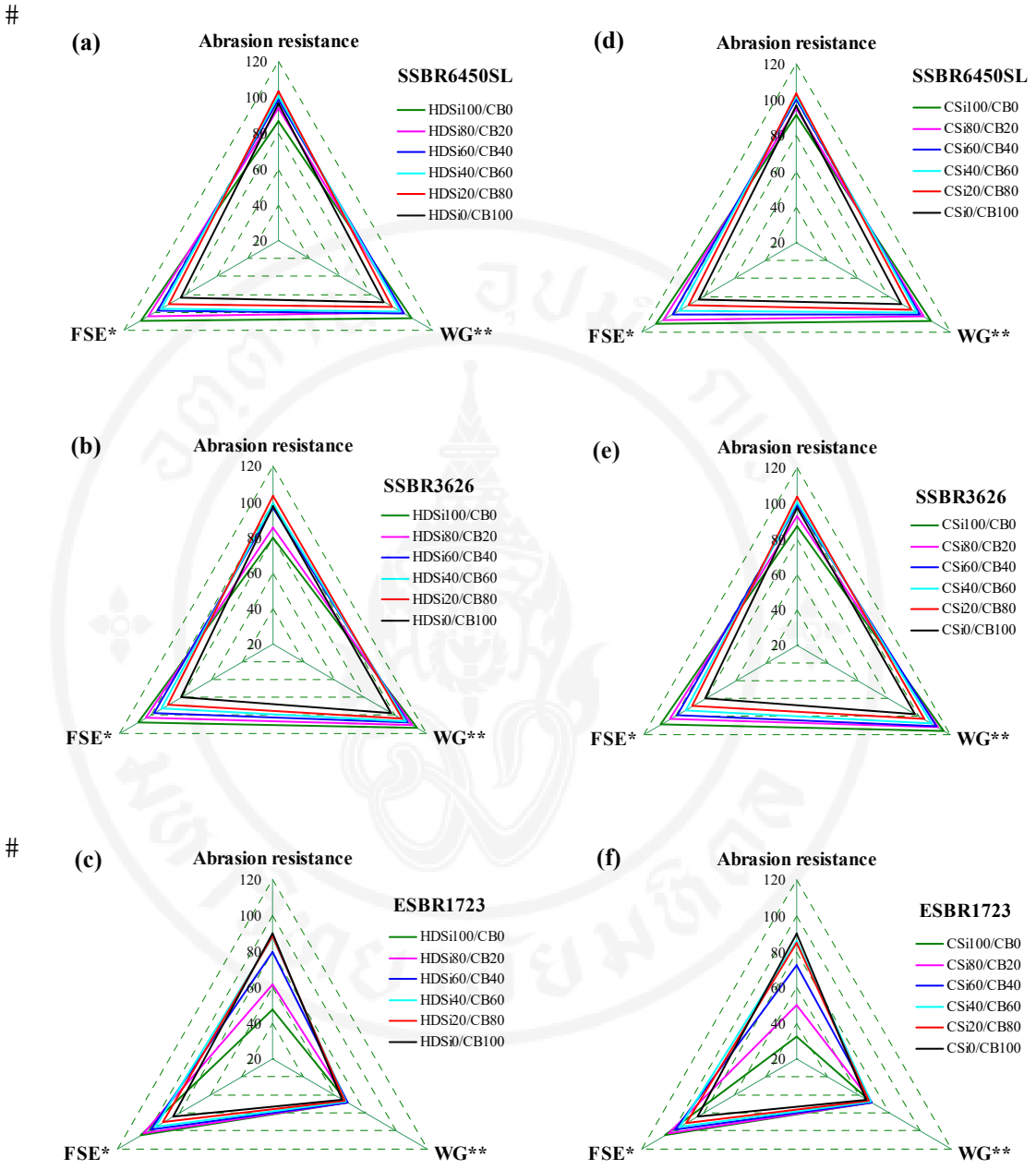

* at dynamic strain of 5.0%
** at dynamic strain of 0.1%

Figure 5.43 Normalized graphs of tire performance at various CB ratios: (a) HDSi_SSBR6450SL (b) HDSi_SSBR3626 (c) HDSi_ESBR1723 (d) CSi_SSBR6450SL (e) CSi_SSBR3626 and (f) CSi_ESBR1723

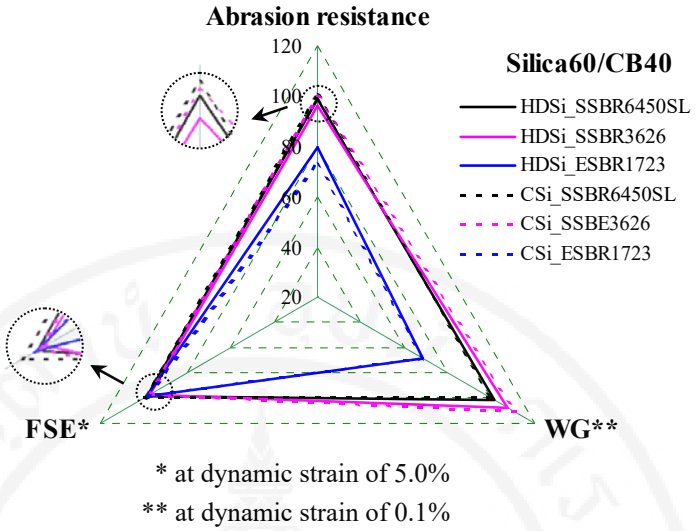

Figure 5.44 Normalized graphs of tire performance at 40 wt% of CB ratio

5.4 Effects of filler and oil loadings on properties of SSBR compounds and vulcanizates

In this section, the relationship between the estimated relative cost of the compounds and properties of the compounds and the vulcanizates having similar hardness is elucidated. A total filler loading was altered simultaneously with rubber process oil loading in order to keep hardness of the vulcanizates constant. According the balanced properties found in the previous parts, the 60/40 CSi/CB-filled SSBR6450SL-based formula is used in this study. The silanization temperature and the TESPT content are kept constant at 140°C and 10 wt% of CSi, respectively.

5.4.1 Mooney viscosity of the compounds

Figure 5.45 illustrates Mooney viscosity of the compounds. As filler particles can restrict the flowability of rubber chains, the increased filler loading generally leads to the increase in compound viscosity, widely known as “dilution effect”. On the other hand, the reduced compound viscosity is usually found with increasing oil loading as a result of “plasticization effect”. Since the compound viscosities decrease continuously from F1 to F4, it could be said that the plasticization effect might play a dominant role in controlling the compound viscosity.

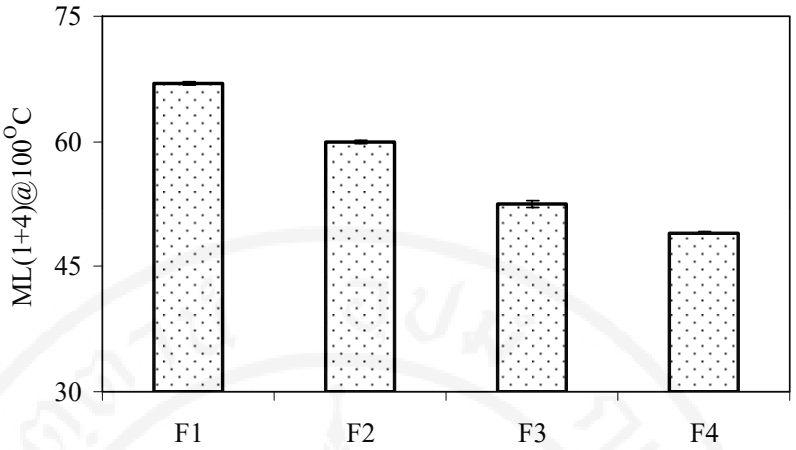

Figure 5.45 Mooney viscosity of the compounds

5.4.2 Payne effect of the compounds

Magnitude of Payne effect of the compounds is represented in Figure 5.46. As the lowered Payne magnitude (lowered ΔG') implies the reduced level of transient filler network, the results show that the magnitude of transient filler network increases continuously from F1 to F4. The reasonable explanation is given by the combination of increased filler loading resulting in the increased probability of transient filler network formation and the decreased shear force during the mixing process caused by the reduced compound viscosity as previously discussed. #

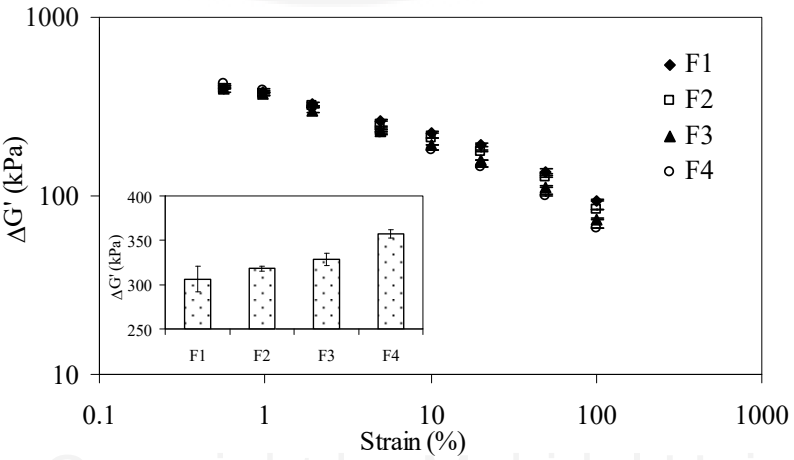

#

Figure 5.46 Payne effect of rubber compounds prepared

5.4.3 Cure characteristics of the compounds

Figure 5.47 shows the influence of filler and oil loadings on cure curves and CRI of the compounds. Clearly, CRI of the compounds is put in the following order; F1 > F2 > F3 > F4, revealing the decreased cure efficiency with increasing filler and oil loadings. This could arise from the depletion of some active chemicals for vulcanization into the oil phase giving rise to the decrease in concentration of such chemicals.

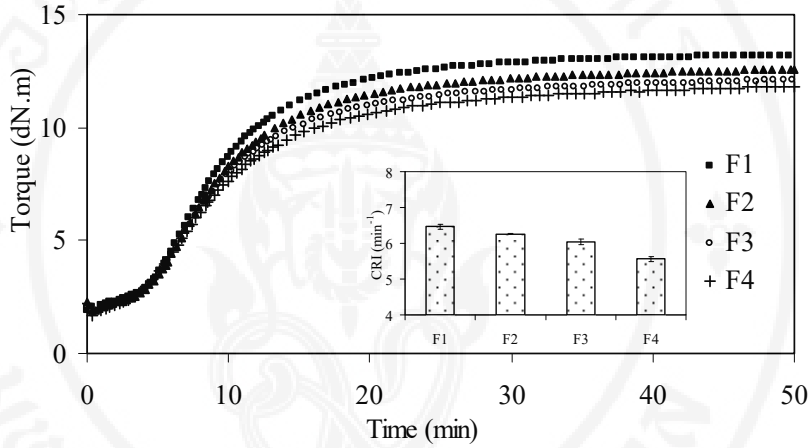

#

Figure 5.47 Cure curves and CRI of the compounds

5.4.4 Crosslink density of the vulcanizates

Crosslink density of the vulcanizates represented in terms of the number of elastically active chains per unit volume is depicted in Figure 5.48. Obviously, F1 provides the greatest degree of crosslink density, followed by F2, F3 and F4. The results reveal that the increased loadings of filler and rubber process oil lead to a detrimental effect on degree of crosslink density. Again, the reduced curative concentration caused by the depletion of some active chemicals into oil phase could be used to explain this result.

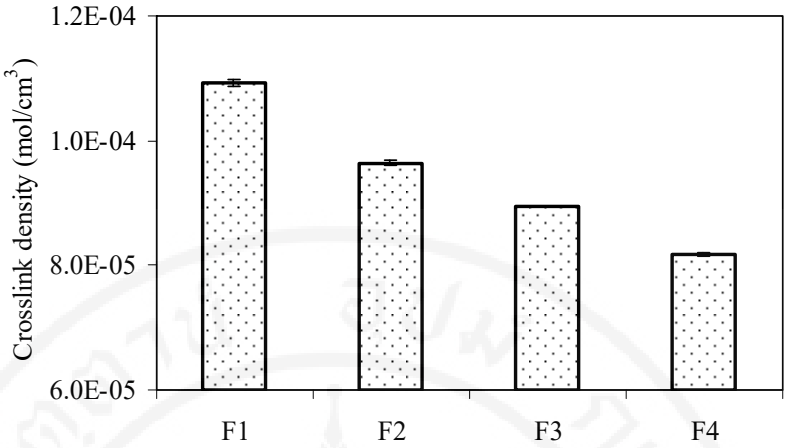

Figure 5.48 Crosslink density of the vulcanizates

5.4.5 Degree of filler dispersion of the vulcanizates

Figure 5.49 presents the SEM micrographs of the vulcanizates. Evidently, the degree of filler dispersion is impaired with increasing filler and oil loadings, i.e., F1 shows the highest degree of filler dispersion, whilst F4 shows the lowest degree of filler dispersion. With increasing filler and oil loadings, viscosity of the rubber compounds is decreased due to the dominant plasticization effect, as shown in Figure 5.45, leading to the reduced shear force during the mixing process and, thus, the reduced degree of filler dispersion.

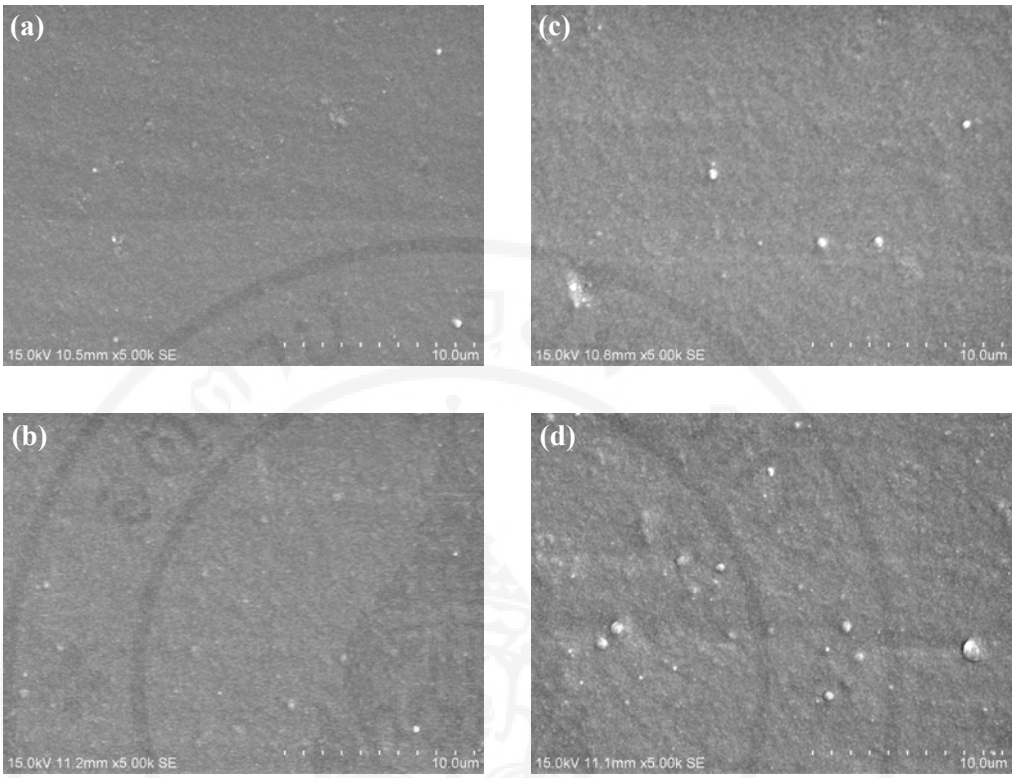

Figure 5.49 SEM micrographs (x5,000) of the vulcanizates:
(a) F1, (b) F2, (c) F3, and (d) F4

5.4.6 Mechanical properties of the vulcanizates

Hardness of the vulcanizates is exhibited in Figure 5.50. Clearly, all vulcanizates show similar hardness level (~62 Sh A). In other words, the effect of lowered crosslink density by increased filler and oil loadings is counterbalanced by the increased level of transient filler network.

Table 5.11 summarizes tensile properties of the vulcanizates. Similar to hardness result, modulus at 10% strain (M10) of all vulcanizates is not significantly different. The results support that hardness is directly proportional to the modulus at low strain. Similar explanation could therefore be applied. However, the moduli at 100% strain (M100) and 300% strain (M300) tend to decrease with increasing filler and oil loadings, i.e., F1 > F2 > F3 > F4. The dominant effects of the reduced crosslink density and plasticization from the increased oil loading might be responsible. It is also found that the increased loadings of filler and oil give detrimental effect on TS of the vulcanizates, e.g., F1 and F4 show the highest and

lowest TS, respectively. The decline of TS is attributed mainly to the combined consequences of: (i) the reduction in crosslink density (ii) the deterioration in degree of filler dispersion and (iii) the increase in plasticization effect. In addition, it is widely known that TS increases with increasing reinforcing filler loading up to a certain point and decreases thereafter. When filler loading exceeds an optimal point, the amount of rubber is not sufficient to accommodate filler, leading to the reduction in TS. Generally, the increase in filler loading causes the reduction in elongation at break (EB) due to the dilution of rubber matrix whereas the increase in oil loading causes contrary results due to the plasticization effect and the reduced crosslink density. Since the EB is not significantly changed when filler and oil loadings are increased in this study, results suggest that a counter-balance between effects of increased filler and oil loadings could be responsible for this observation.

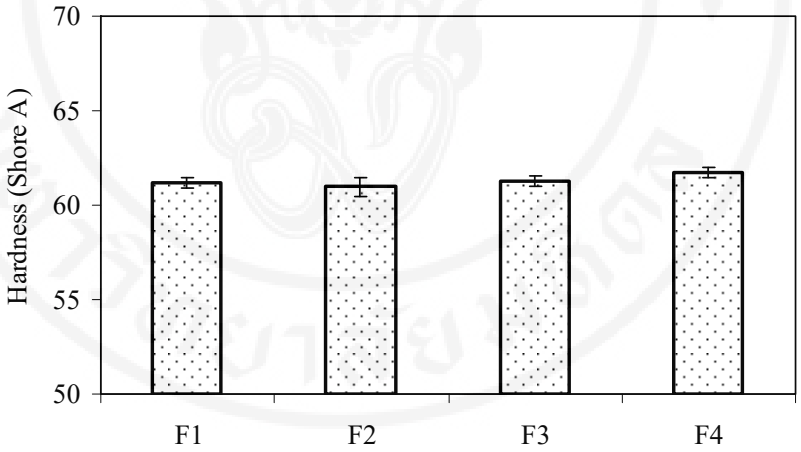

Figure 5.50 Hardness of the vulcanizates

Table 5.11 Tensile properties of the vulcanizates

Sample	M10 (%)	M100 (%)	M300 (%)	TS (MPa)	EB (%)
F1	0.545±0.010	3.05±0.08	13.4±0.3	20.8±0.9	456±9
F2	0.543±0.004	2.77±0.08	12.2±0.2	19.5±0.5	455±7
F3	0.538±0.010	2.78±0.05	11.9±0.1	19.1±0.9	467±13
F4	0.557±0.022	2.61±0.06	11.2±0.1	17.7±0.1	453±3

Abrasion resistance of the vulcanizates represented in terms of volume loss is illustrated in Figure 5.51. Results show that the volume loss is increased from F1 to F4. The combination of the decreased crosslink density and the reduced degree of filler dispersion is applied for explaining the impaired abrasion resistance with increasing filler and oil loadings.

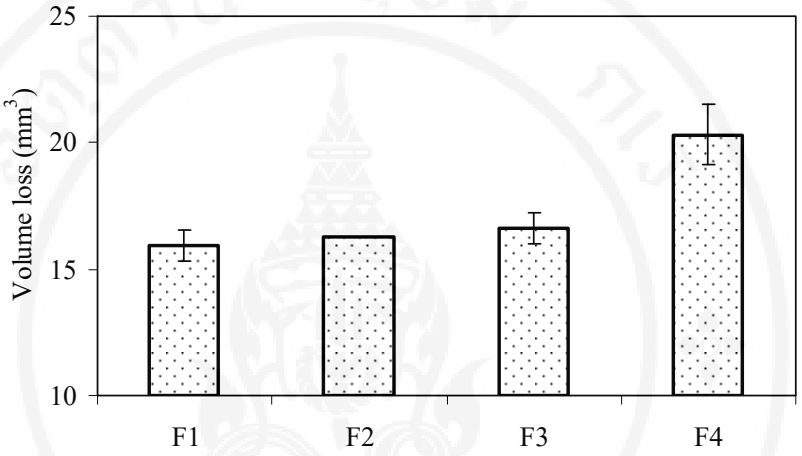

Figure 5.51 Abrasion loss of the vulcanizates

5.4.7 HBU and dynamic set of the vulcanizates

Figure 5.52 reveals the results of HBU and dynamic set of the vulcanizates. The increases in filler and oil loadings lead to the impaired dynamic properties, i.e., HBU and dynamic set of the vulcanizates tend to increase from F1 to F4. The results imply that the increases of filler and oil loadings give not only enhanced energy dissipation but also deteriorated elasticity of vulcanizates, possibly due to the decreased rubber portion (dilution effect), the reduced crosslink density and the decreased degree of filler dispersion as well as the increased level of transient filler network.

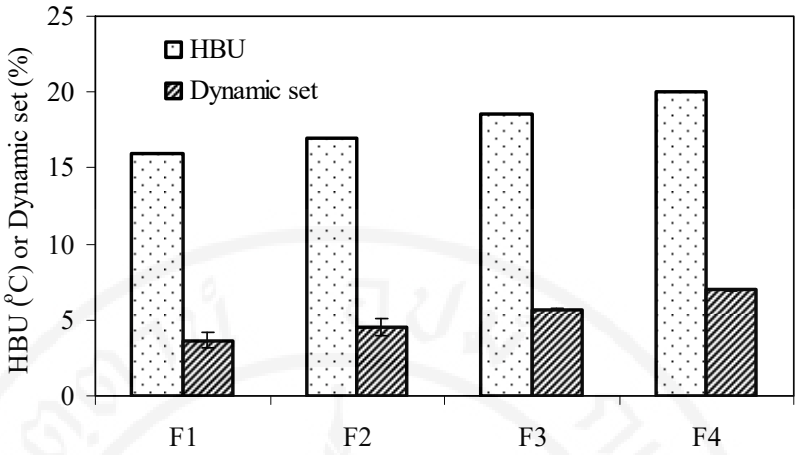

Figure 5.52 HBU and dynamic set of the vulcanizates

5.4.8 Dynamic mechanical properties of the vulcanizates

Figure 5.53 exhibits tanδ as a function of test temperature. T_g, tanδ_{max} and tanδ area analyzed from Figure 5.53 are shown in Table 5.12. As previously mentioned, the temperature at tanδ_{max} is related to the T_g of polymer. Therefore, Figure 5.53 demonstrates the decrease in T_g of the vulcanizates from F1 to F4. In this case, the reduction in crosslink density and the increase in magnitude of plasticization effect are responsible for the findings. Obviously, F1 provides the greatest tanδ_{max} value and tanδ area, followed by F2, F3 and F4. Results suggest that the increased filler and oil loadings lead to the decreased rubber chains participating in the glass transition, mainly owing to the decreased rubber portion which arises from the dilution effect. In addition, the reduction of rubber released from filler agglomerates as a result of the impaired degree of filler dispersion could be one of the reasons for this observation.

#

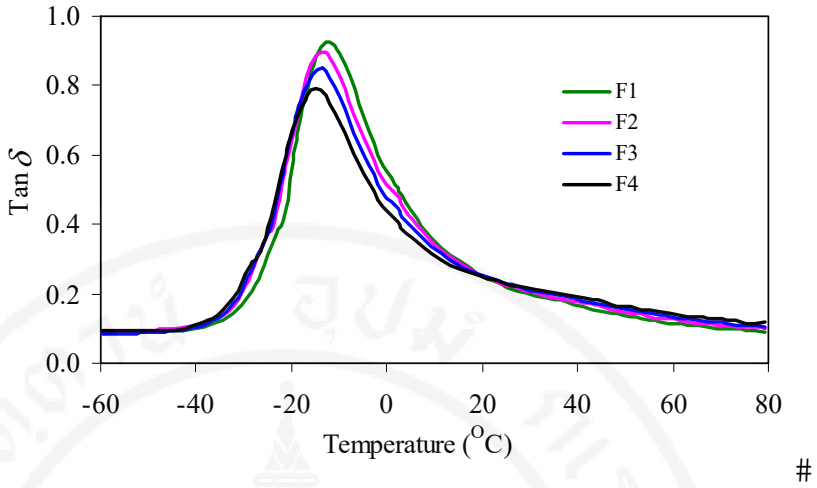

#

Figure 5.53 Tanδ as a function of test temperature of the vulcanizates#

#

Table 5.12 T_g, tanδ_{max} and tanδ area of the vulcanizates

Sample	T_g (°C)	tanδ_{max}	tanδ area (°C)
F1	-12.1	0.923	17.28
F2	-13.2	0.893	16.77
F3	-14.1	0.844	15.68
F4	-15.1	0.793	14.22

Tanδ at 0°C of the vulcanizates as a function of dynamic strain from 0.03-10% is depicted in Figure 5.54. The results show that, at low strains (<2%), the tanδ value at 0°C is found to increase from F4 to F1. This is simply due to the fact that, at low strains where filler network disruption is not significant, the increased filler and oil loadings lead to shift of T_g towards lower temperature due to the dominant plasticization effect. However, the opposite trend is observed at higher strains (2-10%), i.e., F1 < F2 < F3 < F4. Explanation is given by the dominant effects of the hysteretic transient filler network destruction in association with the reduced crosslink density and filler dispersion. Since the tanδ value at 0°C at 0.1% strain is decreased from F1 to F4, the results reveal that the increases of filler and oil loadings would lead to a negative effect on WG.

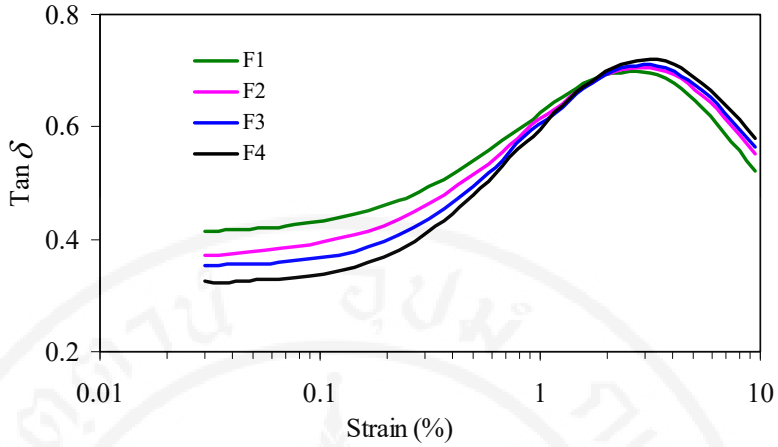

Figure 5.54 Tanδ at 0°C as a function of dynamic strain of the vulcanizates#

Figure 5.55 represents tanδ at 60°C of the vulcanizates as a function of dynamic strain from 0.03-10%. Regardless of the strain, the tanδ value at 60°C could be put in the following order; F1 < F2 < F3 < F4. As the RR is directly related to the tanδ value at 60°C at relatively high strains (5%), it could be summarized that the increased RR (reduced FSE) is resulted with the increases of filler and oil loadings. This is thought to arise from the combination of: (i) the dilution effect; (ii) the decreased crosslink density; (iii) the increased magnitude of transient filler network and (iv) the reduced degree of filler dispersion. These effects cause the increased energy dissipation during the cyclic deformation.

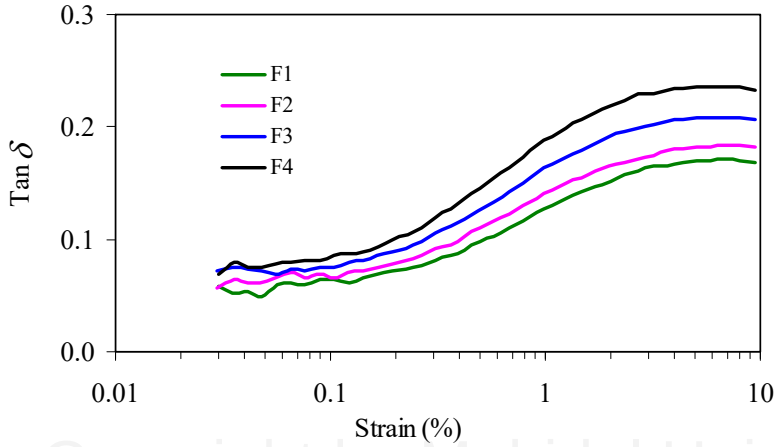

Figure 5.55 Tanδ at 60°C as a function of dynamic strain of the vulcanizates#

Normalized graph of the vulcanizates is exhibited in Figure 5.56 (reference line (100%): F1). Interestingly, although the increases in filler and oil loadings offer lowered compound cost, in the meantime, the tire performance, i.e., WG, FSE and abrasion resistance, is sacrificed. The results reveal that the art of balancing tire performance and cost is greatly important. Focusing on tire performance, the filler and oil loadings used in F1 give the best tire performance. Hence, the compound formulation based on F1 will be employed in the final section.

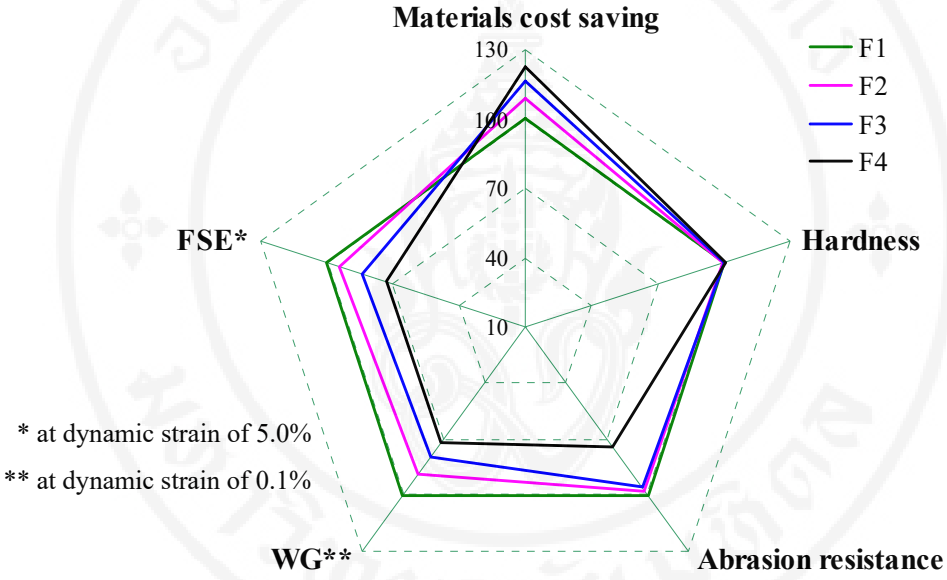

Figure 5.56 Normalized graph of raw material cost saving and tire performance at similar hardness of the vulcanizates

5.5 Effects of sulfur vulcanization system and crosslink density on properties of SSBR vulcanizates

In this part, the compounds based on F1 formula are prepared under silanization temperature of 140°C. The influences of sulfur vulcanization systems, i.e., CV system and semi-EV system, and crosslink density as a result of the alteration in relative amount of curatives (accelerators and sulfur), i.e., 100%, 120% and 140%, on compounds and vulcanizates properties are investigated.

5.5.1 Mooney viscosity of the compounds

Figure 5.57 illustrates the Mooney viscosity of the rubber compounds. Obviously, the relative amount of curatives does not significantly influence the viscosity of the compounds. Also, the compound viscosity is independent of vulcanization system. Results suggest that, in this experiment, the amount of curatives and vulcanization system play little role in processability of the compounds.

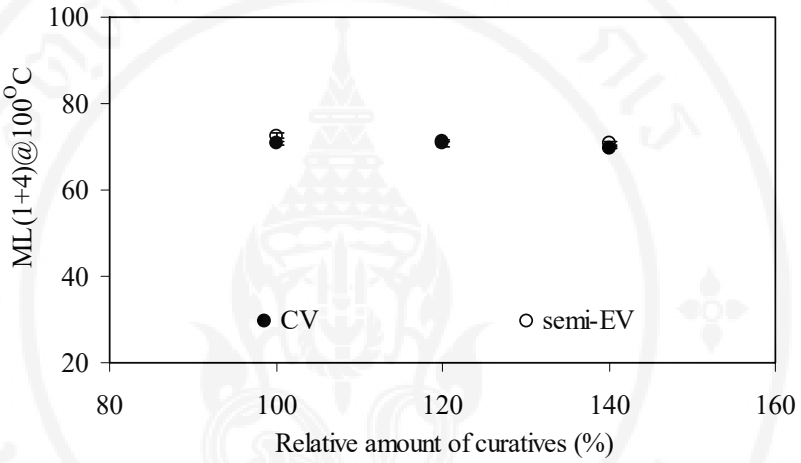

Figure 5.57 Mooney viscosity of the compounds

5.5.2 Cure characteristics of the compounds

Cure curves and cure characteristics, i.e., t_s1, t_c90, and CRI, of the rubber compounds are represented in Figure 5.58. As expected, both t_s1 and t_c90 decrease with increasing relative amount of curatives whereas CRI tends to increase. It is also found that, in this work, CV system provides shorter both t_s1 and t_c90 and higher CRI than semi-EV system. Results reveal that the vulcanization process can proceed more rapidly when the sulfur content [125] and/or the sulfur/accelerator ratio increase.

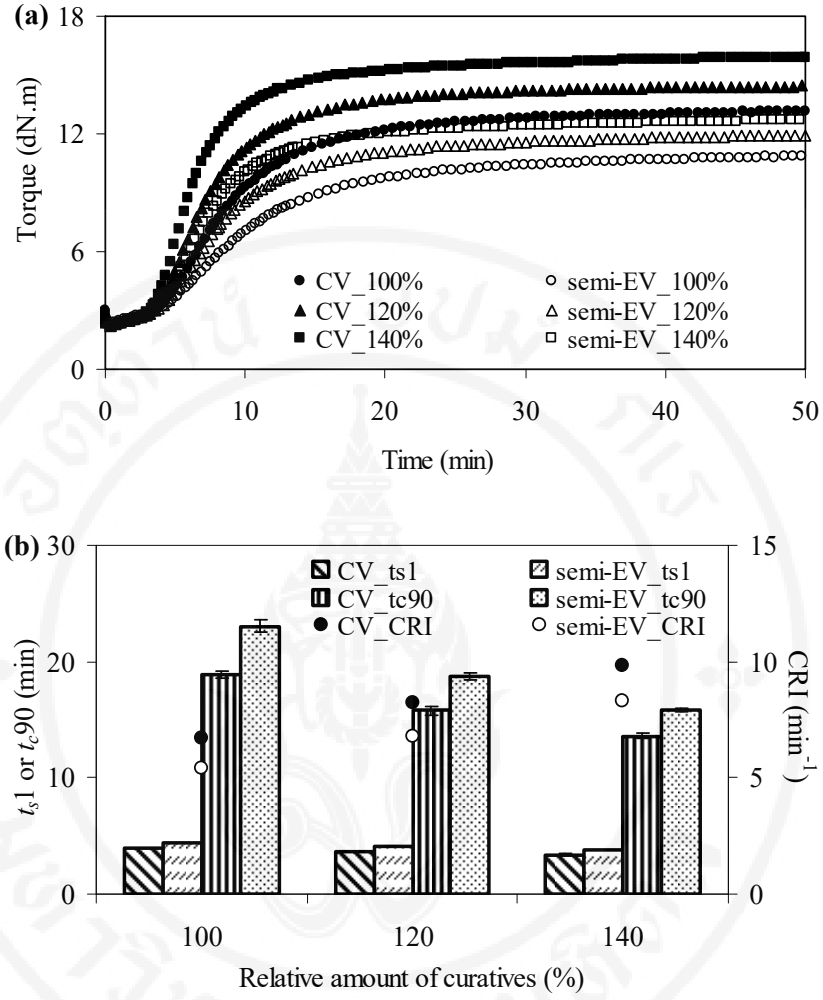

Figure 5.58 Cure curves and cure characteristics of the compounds

#

5.5.3 Crosslink density of the vulcanizates

Figure 5.59 depicts the crosslink density of the vulcanizates measured by the swelling technique. Clearly, the magnitude of crosslink density is found to increase with increasing relative amount of curatives, regardless of the vulcanization system. This is easily understandable because increasing of sulfur and accelerators would not only accelerate vulcanization rate, but also provide more crosslink points. At any given amount of curatives, CV system gives higher crosslink than semi-EV system. This is attributed to the greater sulfur content of the CV system (both CV and semi-EV systems possess the same content of accelerators).

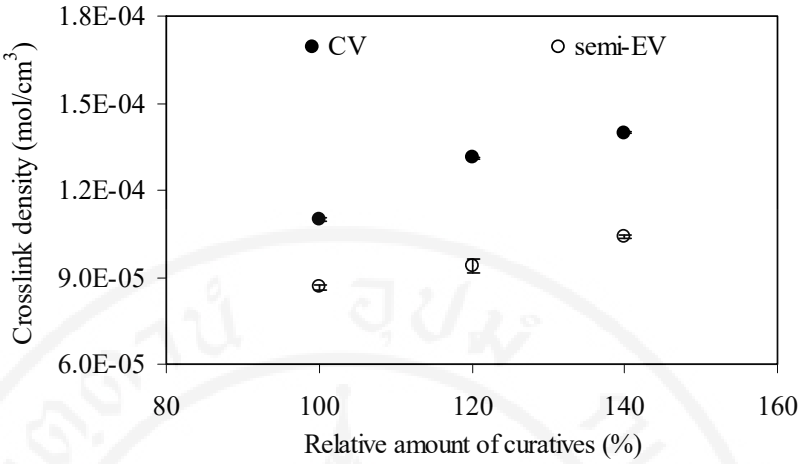

Figure 5.59 Crosslink density of the vulcanizates

5.5.4 Mechanical properties of the vulcanizates

The effects of relative amount of curatives and sulfur vulcanization system on hardness of the vulcanizates are illustrated in Figure 5.60. Regardless of the vulcanization system, the increase in hardness is found with increasing relative amount of curatives, attributed mainly to the enhancement in magnitude of crosslink density. Results also reveal that CV system gives greater hardness than semi-EV system. The higher magnitude of crosslink density of CV system, compared to semi-EV system, could be used to explain this result.

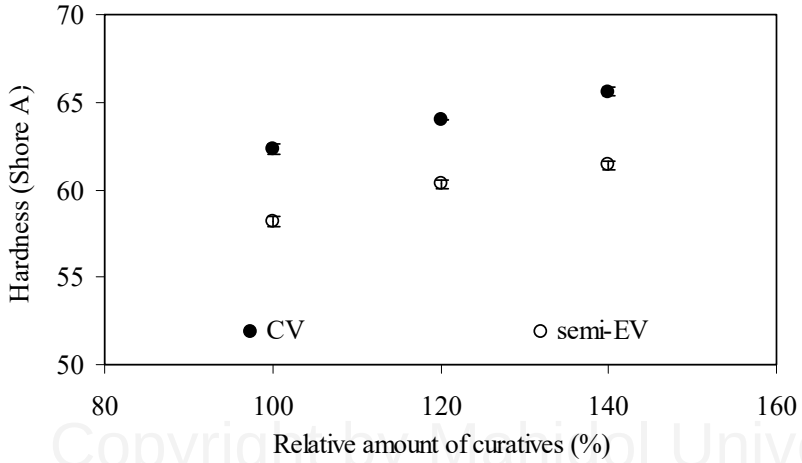

Figure 5.60 Hardness of the vulcanizates

Figure 5.61 displays the M10 and M300 of the vulcanizates. Referred to the results in previous part, modulus at low strain, i.e., M10, is directly proportional to the hardness. The effect of relative amount of curatives on M10 therefore follows the same trend as the change in hardness, i.e., the M10 increases with increasing relative amount of curatives. The same explanation could be applied. Also, as the modulus at high strain is governed mainly by crosslink density, the enhanced M300 is obtained when the relative amount of curatives is increased. As expected, at any given relative amount of curatives, the greater modulus is found in CV system. The higher magnitude of crosslink density could be the reasonable explanation for this finding.

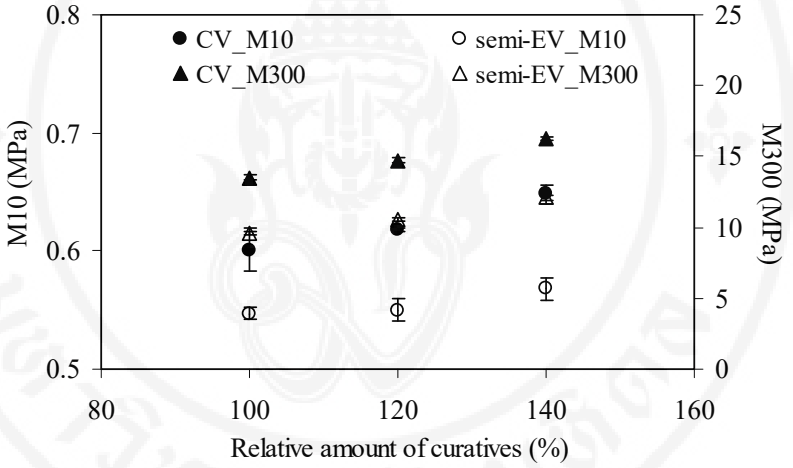

Figure 5.61 Moduli of the vulcanizates

Values of TS and EB of the vulcanizates as a function of relative amount of curatives are shown in Figure 5.62. Apparently, the increase in relative amount of curatives leads to the negative effect on TS. This is thought to arise from the fact that the magnitude of crosslink density might be higher than the optimum level and, thus, the brittle behavior of the vulcanizates is resulted [140]. Unexpectedly, CV system demonstrates slightly lower TS than semi-EV system despite the fact that CV system generally provides greater amount of polysulfidic linkages. It has been reported that TS of vulcanizates tends to increase with increasing amount of polysulfidic linkages, attributed to crosslink exchange under stress [141]. Compared to C-S bond usually found in efficient vulcanization (EV) system and semi-EV system, bond energy of S-S bond is lower, leading to better ability to break and reform, resulting in higher TS

[142]. However, in this case, the brittle behavior as a result of too high magnitude of crosslink density might override the crosslink structure effect. This is the reason why the lower TS is observed in CV system. As expected, increasing relative amount of curatives results in a decrease of EB. It is also found that EB of the vulcanizate in CV system is significantly lower than that of the vulcanizate in semi-EV system. The greater magnitude of crosslink density is applied for explaining the results.

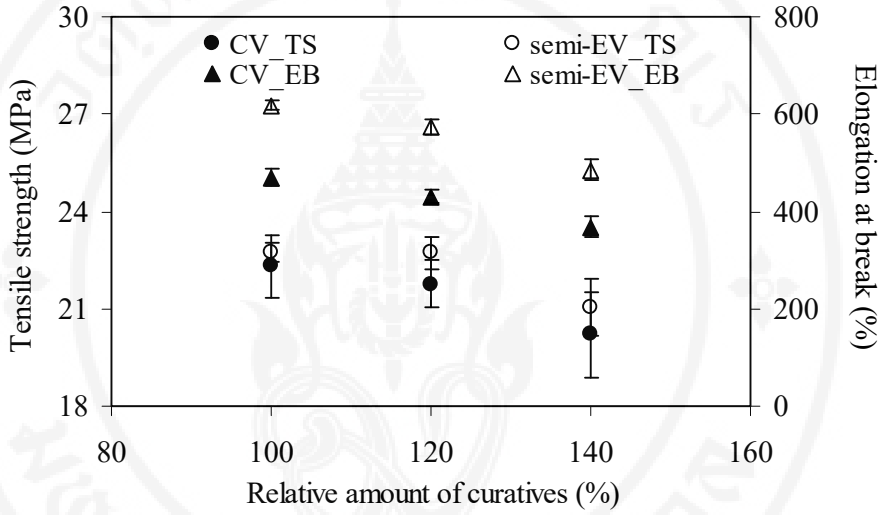

Figure 5.62 TS and EB of the vulcanizates

Figure 5.63 depicts abrasion resistance of the vulcanizates represented in terms of volume loss. Clearly, volume loss is reduced with increasing relative amount of curatives. The improved abrasion resistance arises from the enhanced magnitude of crosslink density. Since the lower volume loss is observed in semi-EV system, it could be said that, in this study, semi-EV system gives slightly better abrasion resistance than CV system. This is possibly due to the greater strength of the vulcanizates together with the lowered sharpness of the abrasive wheel during the test as a result of the greater amount of abraded debris stuck on abrasive wheel.

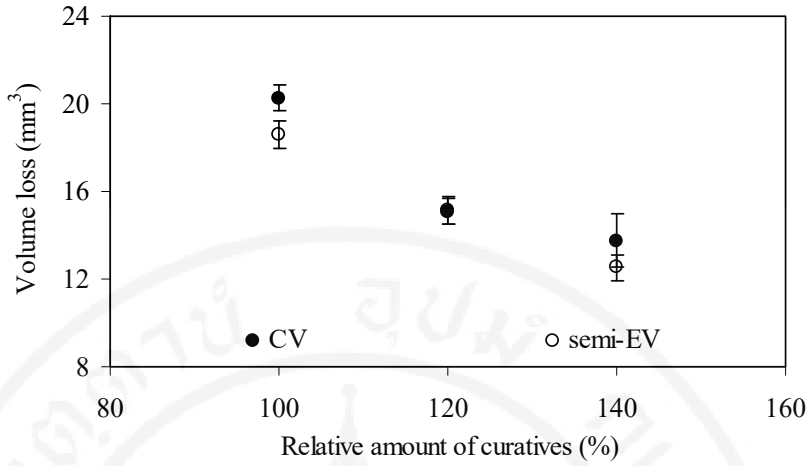

Figure 5.63 Abrasion loss of the vulcanizates

5.5.5 HBU and dynamic set of the vulcanizates

HBU and dynamic set of the vulcanizates are illustrated in Figure 5.64. As expected, increasing relative amount of curatives results in the reductions of HBU and dynamic set, revealing the positive effect on dynamic properties of the vulcanizates. The increase in magnitude of crosslink density is believed to be the main cause of this finding. Due to the greater amount of polysulfidic linkages which is relatively long and flexible [143], the lower HBU and dynamic set are found in CV system. The greater magnitude of crosslink density of the CV system also contributes to this observation.

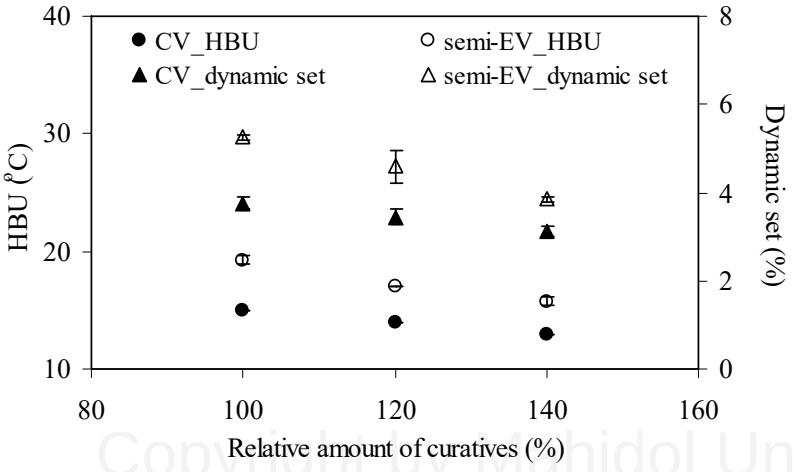

Figure 5.64 HBU and dynamic set of the vulcanizates

5.5.6 Dynamic mechanical properties of the vulcanizates

Figure 5.65 discloses the effects of relative amount of curatives and vulcanization system on loss factor (tanδ). T_g of the vulcanizates analyzed from Figure 5.65 is represented in Table 5.13. Results show that T_g is found to increase with increasing relative amount of curatives, regardless of vulcanization system. This is because of the enhanced magnitude of crosslink density, leading to the increase in restriction of the molecular motion and, thus, T_g of the vulcanizates [144]. Obviously, T_g of the vulcanizate in CV system is significantly higher than that of the vulcanizate in semi-EV system, mainly owing to its greater crosslink density.

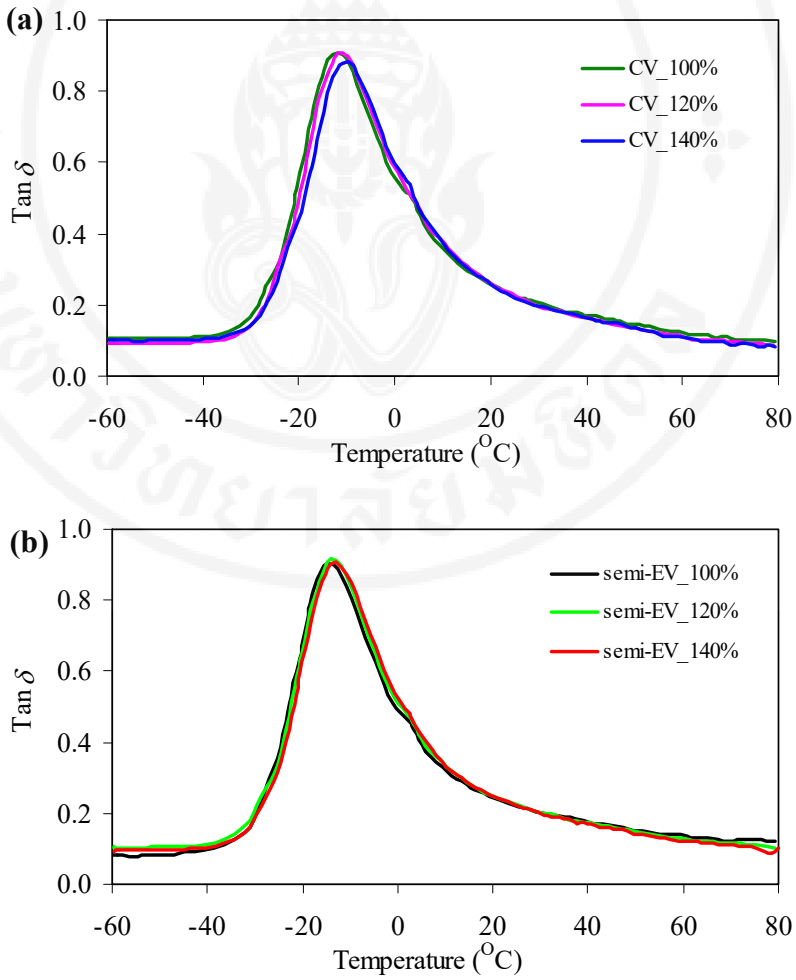

Figure 5.65 Tanδ as a function of test temperature of the vulcanizates: (a) CV system and (b) semi-EV system

Table 5.13 T_g of the vulcanizates#

Relative amount of curatives (%)	T_g (°C)	
	CV	Semi-EV
100	-11.9	-14.7
120	-10.8	-13.8
140	-9.8	-12.8

Figure 5.66 represents tanδ of the vulcanizates at 0°C as a function of dynamic strain from 0.03-10%. Results reveal that increasing relative amount of curatives leads to an improvement in WG, as indicated from the increased tanδ values at 0°C at 0.1% strain. This is explained by the shift of T_g towards higher temperature with increasing amount of curatives. It is also found that, at any given relative amount of curatives, CV system demonstrates better WG than semi-EV system. Again, the higher T_g, compared to semi-EV system, could be applied for explaining such finding.

The tanδ values at 60°C at 5% strain, as shown in Figure 5.67, decrease considerably with increasing amount of curatives, meaning the reduced RR of the vulcanizates. This is thought to arise from the enhanced magnitude of crosslink density when the amount of curatives is increased. Obviously, the lower tanδ values at 60°C at 5% strain are found in the CV system, indicating the lower RR (better FSE). This could be attributed to the greater magnitude of crosslink density, compared to the semi-EV system.

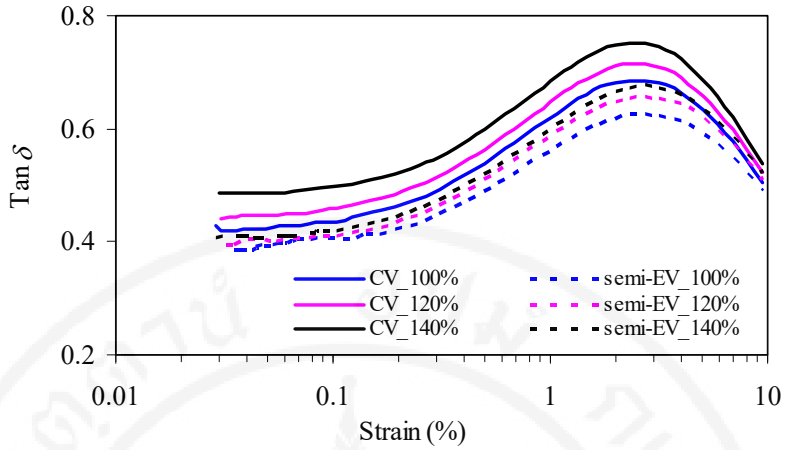

Figure 5.66 Tanδ at 0°C as a function of dynamic strain of the vulcanizates

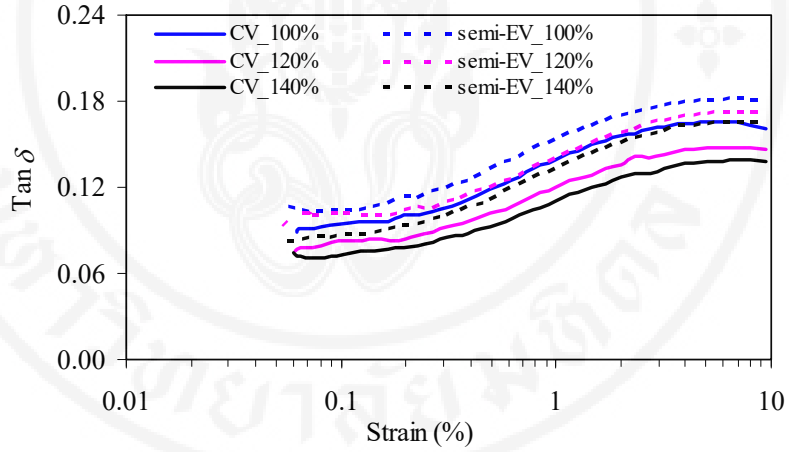

Figure 5.67 Tanδ at 60°C as a function of dynamic strain of the vulcanizates

5.5.7 Thermal ageing resistance of the vulcanizates

Dependence of thermal ageing resistance of the vulcanizates, represented in terms of the relative tensile properties after aging at 100°C for 120 hours, on relative amount of curatives and vulcanization system is shown in Figure 5.68. It is found that, in all cases, both relative TS and relative EB are lower than 1 whereas the relative M10 is greater than 1. Results indicate that both TS and EB of the vulcanizates are impaired after thermal ageing. Since modulus at low strain, i.e., M10, is directly proportional to the hardness, the increase in hardness of the vulcanizates could be found after thermal ageing. Obviously, the increasing relative amount of curatives

leads to the increase in relative M10. The results reveal that the enhancement of post-curing magnitude is obtained with increasing relative amount of curatives. Results also elucidates that CV system offers greater relative M10 than semi-EV system, indicating that post-curing is more prone to take place in CV system. Clearly, both relative TS and relative EB tend to decrease with increasing relative amount of curatives, revealing the adverse effect on thermal ageing resistance. This might be owing to the enhanced magnitude of post-curing when the amount of curatives is increased, leading to the reduction of both relative TS and relative EB. As expected, the vulcanizates in semi-EV system have higher relative TS and relative EB, compared to those in CV system, suggesting the better thermal ageing resistance. It is well known that bond energy of C-S bond usually found in semi-EV system is significantly higher than that of S-S bond generally found in CV system. This could be the reason why semi-EV system provides better thermal ageing resistance than CV system. In addition, the lower magnitude of post-curing found in semi-EV system might be one of the reasonable explanations for this finding.

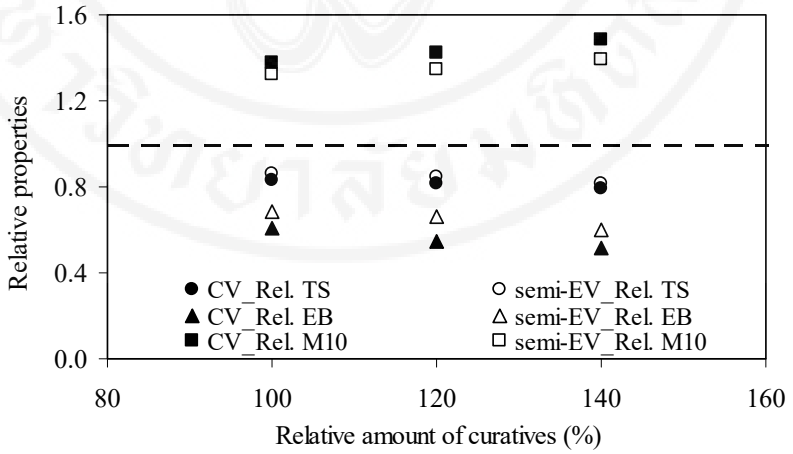

Figure 5.68 Thermal ageing resistance of the vulcanizates

5.5.8 Curative bloom

Figure 5.69 represents influence of relative amount of curatives and vulcanization system on curative bloom after keeping compounds and vulcanizates for 14 days at room temperature. Clearly, no curative bloom is observed on the specimen surfaces of all compounds and vulcanizates. The results reveal that, in this experiment, the relative amount of curatives and vulcanization system#do not significantly affect the curative bloom of the compounds and vulcanizates.

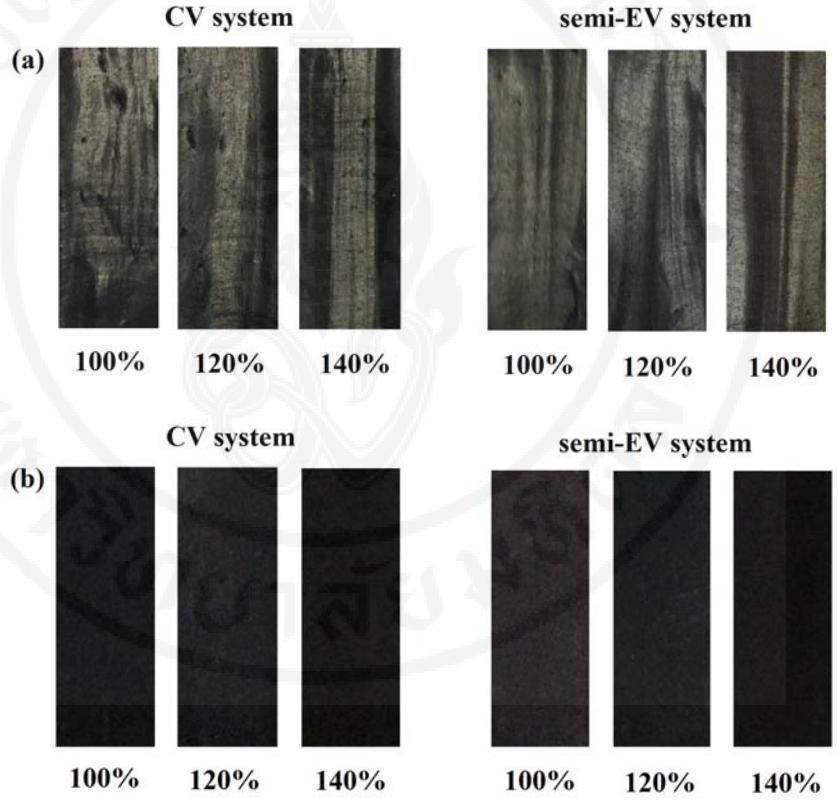

Figure 5.69 Photographs demonstrating effects of relative amount of curatives and vulcanization system on curative bloom: (a) compounds and (b) vulcanizates

Figure 5.70 depicts thermal ageing resistance (evaluated from relative TS) and tire performance, i.e., WG, FSE and abrasion resistance, of the vulcanizates in terms of normalized graph (reference line (100%): CV system with relative amount of curatives of 140%). Although the amount of curatives of 140% in CV system provides the worst thermal ageing resistance, it gives the excellent tire performance. Focusing on tire performance, the best PCR tire tread formulation for this research can be therefore summarized in Table 5.14.

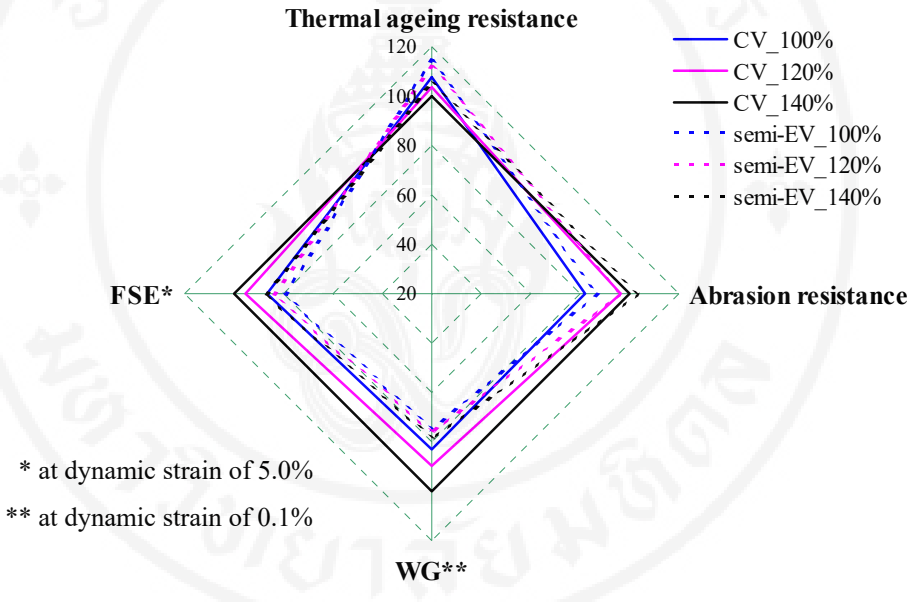

#

Figure 5.70 Normalized graph of thermal ageing resistance and tire performance at various relative amounts of curatives and vulcanization system

Table 5.14 The best PCR tire tread compound formulation for this research

Ingredients	Content (phr)
SBR (SSBR6450SL)	137.5
ZnO	3.0
Stearic acid	2.0
6PPD	1.5
TMQ	1.0
Paraffin wax	2.0
CSi	42.0
CB	28.0
TESPT (10 wt% of silica)	4.2
TBBS	1.68
TBzTD	0.28
S_8	3.08

5.5.9 Comparison of WG and FSE between the developed PCR tire tread compound and commercial PCR tire treads

Due to the limitation of specimen preparation of the commercial PCR tires (Michelin (Energy XM2), Bridgestone (Ecopia EP100), Goodyear (Assurance Fuel Max), Vee rubber (Zilent), and Deestone (NAKARA R301), only dynamic mechanical properties, i.e., tanδ at 0°C and 60°C respectively related to WG and RR, were tested and compared.

The tanδ values at 0°C and 60°C of the vulcanizates as a function of dynamic strain from 0.03-10% are shown in Figure 5.71 and 5.72, respectively. The WG and FSE, respectively related to the tanδ value at 0°C at 0.1% strain and the tanδ value at 60°C at 5% strain, analyzed from Figure 5.71 and 5.72 are summarized in Figure 5.73. Obviously, the developed PCR tire compound formulation offers better WG and FSE as compared to all commercial PCR tires. Results reveal that the developed PCR tire compound formulation obtained in this research has a potential for further development into commercially viable products.

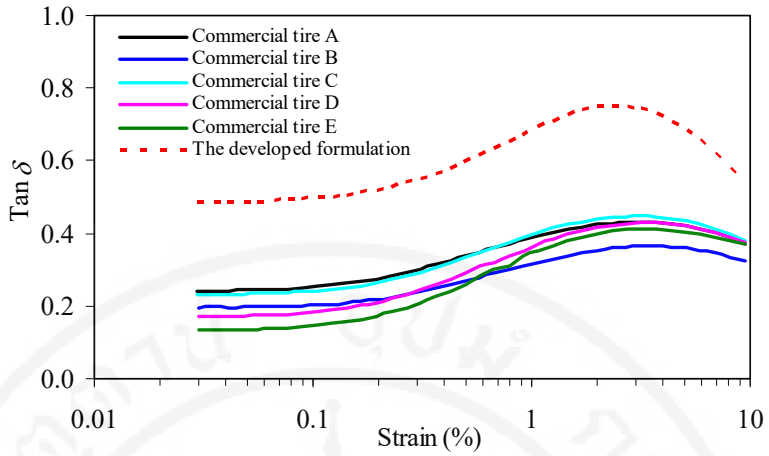

Figure 5.71 Tanδ at 0°C as a function of dynamic strain of the vulcanizates

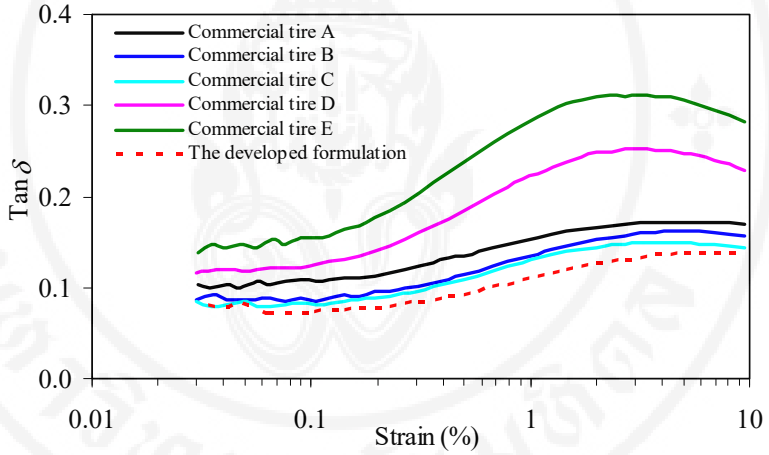

Figure 5.72 Tanδ at 60°C as a function of dynamic strain of the vulcanizates

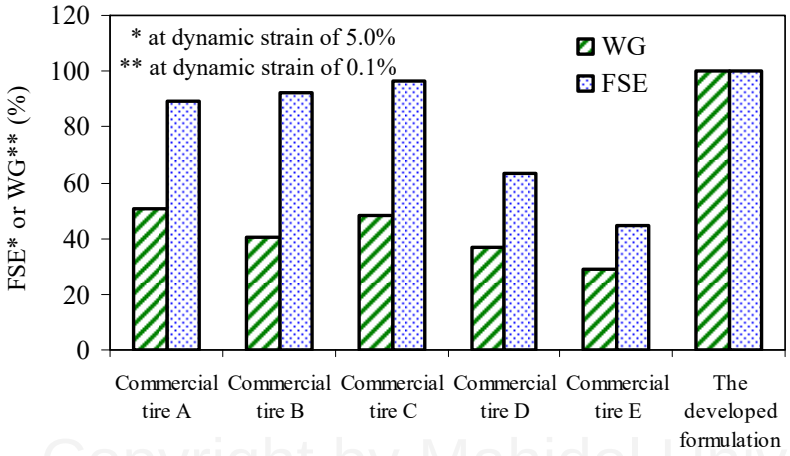

#

Figure 5.73 WG and FSE of the developed PCR compound formulation and commercial PCR tire treads

CHAPTER VI
CONCLUSIONS

In this work, various parameters (i.e., silanization temperature, TESPT content, silica/CB hybrid filler ratio, SBR and silica types, filler and oil loadings, including sulfur vulcanization system and crosslink density) influencing properties of SBR-based compounds used for PCR tire tread application were studied. The goal of this work is to gain the compound formulation offering the best balanced tire performance, i.e., WG, FSE, and abrasion resistance. The following conclusions can be drawn:

6.1 Effects of silanization temperature and silica type on properties of silica-filled SSBR compounds and vulcanizates

1. Although the improvement in compound and vulcanizate properties, e.g., rubber-filler interaction, degree of filler dispersion, and tire performances, is found with increasing silanization temperature, great care must be taken to avoid the undesirable scorch problem during the mixing at high temperature.

2. The increased silanization temperature leads to the improved rubber-filler interaction via the coupling reaction as indicated from the enhanced chemical BRC.

3. Focusing on tire performance, silica type (HDSi and CSi) gives no profound effect on WG and FSE, possibly due to: (i) the insignificant difference in T_g of the HDSi-filled and CSi-filled vulcanizates and (ii) the comparable degree of filler dispersion caused by the relatively long mixing time. However, silica type plays an important role in abrasion resistance, i.e., CSi provides better abrasion resistance than HDSi.

4. The balanced tire performance and processability are observed at the silanization temperature of 140°C.

6.2 Effects of TESPT content and silica type on properties of silica-filled SSBR compounds and vulcanizates

1. The addition of TESPT results in the positive effect on processability, mechanical properties (e.g., TS and hardness), dynamic properties (i.e., HBU and dynamic set), and tire performance. Explanation is given by the combined effects of enhanced rubber-filler interaction, improved degree of filler dispersion and increased crosslink density.

2. With increasing TESPT content from 6 wt% to 12 wt%, some properties are continuously improved, i.e., processability, CRI, crosslink density, hardness, and dynamic set. Surprisingly, such increase of TESPT content has very little effect on TS. However, tire performance is optimized at 10 wt% of TESPT content.

3. Focusing on tire performance, WG and FSE are little affected by the silica type employed in this study, as long as the sufficiently long mixing time during the compound preparation is used.

6.3 Effects of silica/CB hybrid filler and SBR type on properties of SBR compounds and vulcanizates

1. Despite the fact that the increased CB ratio in hybrid filler leads to the impaired WG, FSE, and dynamic mechanical properties, i.e., HBU and dynamic set, the best abrasion resistance is found at CB ratio of 60-80 wt%. Results reveal that the silica/CB ratio of 60/40 provides a good balance of tire performance.

2. Compared to ESBR, the two grades of SSBR give greater WG, better abrasion resistance, lower HBU and dynamic set with comparable FSE. Due to the higher vinyl content, SSBR6450SL provides higher crosslink density and rubber-filler interaction than SSBR3626, resulting in better FSE and abrasion resistance.

SSBR3626, however, imparts superior WG than SSBR6450SL, probably due to its higher T_g.

3. In this experiment, silica type has little effect on cure characteristics, degree of filler dispersion, HBU and dynamic set, WG, as well as FSE.

4. Degree of filler dispersion is independent of silica/CB hybrid ratio, SBR type, and silica type, as long as a sufficiently long mixing time is employed.

5. The best balance of tire performance is found in the 60/40 CSi/CB-filled SSBR6450SL.

6.4 Effects of filler and oil loadings on properties of SSBR compounds and vulcanizates

1. Although the economic benefit could be obtained by the increases of both filler and oil loadings, such increases lead to not only the deterioration of the vulcanizate properties such as TS, EB, M100, HBU and dynamic set, but also the impaired tire performance. Explanation is given by the declined degree of filler dispersion and crosslink density. The results suggest that the art of property-and-cost balancing is greatly important.

2. Taken as a whole, the F1 formula containing the lowest filler and oil loading is selected to employ in the final section because it provides the best mechanical properties, dynamic mechanical properties as well as tire performance.

6.5 Effects of sulfur vulcanization system and crosslink density on properties of SSBR vulcanizates

1. Compared to the semi-EV system, the CV system imparts negative effects on TS, EB, as well as thermal ageing resistance. However, it offers positive effects on WG, FSE, hardness, modulus, HBU and dynamic set, attributed mainly to the greater magnitude of crosslink density.

2. In this study, the increased curative content results in the improvements of both cure efficiency (CRI) and crosslink density without significant effect on Mooney viscosity and curative bloom.

3. Although the increased curative content causes negative effects on TS, EB and thermal ageing resistance, it gives beneficial effects on both tire performance and mechanical and dynamic properties of the vulcanizates, i.e., hardness, M10, M300, HBU and dynamic set.

4. In this study, the CV system with relative amount of curatives of 140% seems to give the excellent tire performance. The best PCR tire tread formula for this research is therefore summarized as follows:

Table 6.1 The best PCR tire tread formulation developed in this research

Ingredients	Content (phr)
SBR (SSBR6450SL)	137.5
ZnO	3.0
Stearic acid	2.0
6PPD	1.5
TMQ	1.0
Paraffin wax	2.0
CSi	42.0
CB	28.0
TESPT (10 wt% of silica)	4.2
TBBS	1.68
TBzTD	0.28
S_8	3.08

5. The best PCR tire tread developed in this study provides better WG and FSE than the commercial PCR tire treads, suggesting the great potential for further development into commercially viable products.

REFERENCES

1. Hirata Y, Kondo H, Ozawa Y. Natural Rubber (NR) for the Tyre Industry. In: Kohjiya S, Ikeda Y, editors. Chemistry, Manufacture and Applications of Natural Rubber. UK: Woodhead Publishing; 2014. p. 341.
2. Michelin Presents the Performance of Its Tire Ranges and Explains the New European Tire Labeling Regulation [press release]. 2012.
3. http://www.contionline.com/generator/www/de/en/continental/automobile/themes/tirelabel/download/european_tyre_labelling_regulation_en.pdf.
4. Evans MS. Tyre Compounding for Improved Performance: Smithers Rapra; 2002.
5. Muraki T, Ishikawa Y, inventors; Google Patents, assignee. Rubber Composition for Tire Tread patent 5,500,482. 1996.
6. Rao GV, Mouli SC, Boddeti NK. Anti Skid Methods and Materials-Skid Effects and Their Remedial Methods. International Journal of Engineering and Technology. 2010;2(2):87-92.
7. Brodsky H, Hakkert AS. Risk of a Road Accident in Rainy Weather. Accident Analysis & Prevention. 1988;20(3):161-76.
8. Burke E. High-tech Cycling: Human Kinetics; 2003.
9. Rodgers MB, Tracey DS, Waddell WH. Tire Applications of Elastomers: 1. Treads. 2004.
10. Ferrandino MP, Hong SW, McKenzir GT, inventors;Tire Tread Composition patent US 5,569,697. 1996.
11. https://www.britannica.com/technology/tire.
12. Hadland T, Lessing HE, Clayton N, Sanderson GW. Bicycle Design: An Illustrated History: MIT Press; 2014. 564 p.
13. Michelin É. The Tyre Digest: Michelin; 2002. 111 p.
14. Wolff S, Wang M-J, Tan E-H. Filler-Elastomer Interactions. Part VII. Study on Bound Rubber. Rubber Chemistry and Technology. 1993;66(2):163-77.

15. Lindenmuth BE. An Overview of Tire Technology. In: Gent AN, Walter JD, editors. The Pneumatic Tire. Washington DC2005.
16. http://www.michelinag.com/Innovating/Radial-vs.-Bias-technology.
17. Zarei M, Naderi G, Bakhshandeh GR, Shokoohi S. Ternary Elastomer Nanocomposites Based on NR/BR/SBR: Effect of Nanoclay Composition. Journal of Applied Polymer Science. 2013;127(3):2038-45.
18. Study NRCTRBCftNTE. Tires and Passenger Vehicle Fuel Economy: Informing Consumers, Improving Performance: Transportation Research Board; 2006.
19. http://www.wikihow.com/Extend-the-Life-of-Your-Car-Tires.\
20. Ladouce-Stelandre L, Bomal Y, Flandin L, Labarre D. Dynamic Mechanical Properties of Precipitated Silica Filled Rubber: Influence of Morphology and Coupling Agent. Rubber Chemistry and Technology. 2003;76(1):145-59.
21. Byrne FJ, inventorApparatus and Method for Enhancing Tire Traction patent US 7,370,888 B2. 2008.
22. Hess WM, Klamp WK. The Effects of Carbon Black and Other Compounding Variables on Tire Rolling Resistance and Traction. Rubber Chemistry and Technology. 1983;56(2):390-417.
23. Persson B. Sliding Friction: Physical Principles and Applications: Springer Berlin Heidelberg; 2000.
24. Bond R, Morton GF, Krol LH. A Tailor-Made Polymer for Tyre Applications. Polymer. 1984;25(1):132-40.
25. Payne GA. Managing Energy in Commerce and Industry: Butterworths; 1984.
26. Agency IE. Saving Oil in a Hurry: OECD/IEA; 2005.
27. Prasanth R, Owuor PS, Shankar r, Joyner J, Kosolwattana S, Jose SP, et al. Eco-Friendly Polymer-Layered Silicate Nanocomposite-Preparation, Chemistry, Properties, and Applications. In: Thakur VK, Thakur MK, editors. Eco-friendly Polymer Nanocomposites: Chemistry and Applications: Springer; 2015. p. 576.
28. Müller G, Möser M. Handbook of Engineering Acoustics: Springer Berlin Heidelberg; 2012.

29. Iwao K, Yamazaki I. A Study on the Mechanism of Tire/Road Noise. JSAE Review. 1996;17.
30. Oshino Y. Change of Sound Power Level of Running Vehicle Caused by the Differences of Road Surfaces (in Japan). Journal of the Acoustical Society of Japan. 1991;10.
31. Yamada H. On the Influence of Tire Characteristics on Tire Noise (in Japanese). JSAE Symposium No 9301. 1993.
32. Arteaga IL. Tyre/Rode Noise and Vibration: Understanding their Interaction and Contribution to Vehicle Noise and Fuel Consumtion. The 21th International Congress on Sound and Vibration; 13-17 July, 2014; Beijing, China2014.
33. http://www.reifenapp.com/.
34. https://www.goodyear.eu/en_gb/consumer/learn/eu-tire-label-explained.html.
35. http://www.etrma.org/uploads/Modules/Documentsmanager/2012-07-05--industry-guideline-on-tyre-labelling-(vers4).pdf.
36. https://www.dunlop.eu/en_gb/consumer/learn/eu-tire-label-explained.html.
37. Terrill ER, Centea M, Evans LR, Jr JDM. Dynamic Mechanical Properties Of Passenger and Light Truck Tire Treads. Akron Rubber Development Laboratory, Inc.: 2010 Contract No.: DOT HS 811 270.
38. Ciesielski A. An Introduction to Rubber Technology: iSmithers Rapra Publishing; 1999.
39. Brown RP. Physical Testing of Rubber. 3rd ed: Chapman and Hall 1996.
40. Nagi KL, Capaccioli S, Plazek DJ. The Viscoelastic Behavior of Rubber and Dynamics of Blends. In: Erman B, Mark JE, Roland CM, editors. The Science and Technology of Rubber. Fourth Edition ed. USA: Elsevier; 2013.
41. Wetton RE. Thermal analysis. In: Hunt BJ, Jame MI, editors. Polymer Characterisation: Chapman & Hall; 1993.
42. Sasikumar K, Manoj NR, Mukundan T, Khastgir D. Hysteretic Damping in XNBR – MWNT Nanocomposites at Low and High Compressive Strains. Composites Part B: Engineering. 2016;92:74-83.

43. Wessels RM, Fieten B, Amato L, inventors; Google Patents, assignee. Impact Resistant Freight Container patent US20120298657 A1. 2012.
44. Liu X, Zhao S, Zhang X, Li X, Bai Y. Preparation, Structure, and Properties of Solution-Polymerized Styrene-Butadiene Rubber with Functionalized End-Groups and its Silica-Filled Composites. Polymer. 2014;55(8):1964-76.
45. Ko JY, Prakashan K, Kim JK. New Silane Coupling Agents for Silica Tire Tread Compounds. Journal of Elastomers and Plastics. 2012;44(6):549-62.
46. Wang M-J. The Role of Filler Networking in Dynamic Properties of Filled Rubber. Rubber Division, American Chemical Society; May 5-8, 1998; Indiana1998.
47. Cichomski E, Dierkes WK, Noordermeer JWM, Tolpekina TV, Schultz S. Influence of Physical and Chemical Polymer-filler Bonds on Wet Skid Resistance and Related Properties of Passenger Car Tire Treads. DKT 2012; 2-5 July, 2012; Deutsche Kautschuk Tagung, Nürnberg.
48. Bomo F. Very High Structure Carbon Blacks for Low Rolling Resistance Tires. Tyretech 94 Conference; 24th-25th October 1994; Munich, Germany: iSmithers Rapra Publishing; 1994.
49. Wang Y-X, Wu Y-P, Li W-J, Zhang L-Q. Influence of Filler Type on Wet Skid Resistance of SSBR/BR Composites: Effects from Roughness and Micro-Hardness of Rubber Surface. Applied Surface Science. 2011;257(6):2058-65.
50. Li Y, Han B, Wen S, Lu Y, Yang H, Zhang L, et al. Effect of the Temperature on Surface Modification of Silica and Properties of Modified Silica Filled Rubber Composites. Composites Part A: Applied Science and Manufacturing. 2014;62(0):52-9.
51. Klockmann O. Processing of New Rubber Silane VP Si 363. ITEC 2006; The International Tire Exhibition & Conference: Rubber & Plastics News; 2006.
52. Rauline R, inventor; Google Patents, assignee. Copolymer Rubber Composition with Silica Filler, Tires having a Base of Said Composition and Method of Preparing Same patent US5227425. 1993.

53. Waddell WH, Bhakunl RS, Barbin WW, Sandstrom PH. Pneumatic Tire Compounding: Norwalk CT; 1990.
54. Hofmann W. Rubber Technonlogy Handbook: Hanser Publishers; 1989.
55. Rodgers B, Waddell W. The Science of Rubber Compounding. In: Mark JE, Erman B, Roland M, editors. The Science and Technology of Rubber: Elsevier Science; 2013.
56. Colvin H. General-Purpose Elastomers. In: Rodgers B, editor. Rubber Compounding: Chemistry and Applications. Nwe York, USA: Marcel Dekker, Inc; 2004.
57. http://www.iisrp.com/WebPolymers/09E-SBRPolymerSummaryJuly16.pdf.
58. Inagaki K, Hayashi M, Imai A. Development of the Solution SBRs for High-performance Tires. 2004.
59. Langer AW, inventor; Google Patents, assignee. Polymerization Catalyst and Uses Thereof patent US3,451,988. 1969.
60. Moore D, Day G. Comparison of Emulsion vs. Solution SBR on Tire Performance. Meeting of ACS Rubber Division; Washington DC1985.
61. Wampler WA, Carlson TF, Jones WR. Carbon Black. In: Rodgers B, editor. Rubber Compounding: Chemistry and Applications. New York, USA: Marcel Dekker, Inc; 2004.
62. Leblanc JL. Filled Polymers: Science and Industrial Applications. New York, USA: CRC Press; 2009. 428 p.
63. https://monographs.iarc.fr/ENG/Monographs/vol93/mono93-6.pdf.
64. Donnet J-B, Custodero E. Reinforcement of Elastomers by Particulate Fillers. In: Mark JE, Erman B, Roland CM, editors. The Science and Technology of Rubber. Fourth Edition ed. USA: Elsevier Inc.; 2013.
65. Hewitt N. Compounding Precipitated Silica in Elastomers: Theory and Practice. Norwich, NY, USA: William Andrew Publishing; 2007.
66. Horn JB. Rubber and Plastics Age. 1969.
67. Skelhorn D. Particulate Fillers in Elastomers. In: Rothon RN, editor. Particulate-filled Polymer Composites: Rapra Technology; 2003.
68. http://www.cabotcorp.com/solutions/products-plus/carbon-blacks-for-elastomer-reinforcement/reinforcing.

69. Bueche F. Molecular Basis for the Mullins Effect. Journal of Applied Polymer Science. 1960;4(10):107-14.

70. Bauer RG, Burlett DJ, Johnny DMII, Sandstrom PH, Segatta TJ, Verthe JJA, inventorsTires Having Improved Rolling Resistance patent US 5,378,754. 1995.

71. Rauline R, inventor; Rubber Compound and Tires Based on Such a Compound patent EP 0 501227 A1. 1992.

72. Waddell WH, Evans LR. Precipitated Silica and Non-Black Fillers. In: Dick JS, editor. Rubber Technology: Compounding and Testing for Performance. Munich: Hanser Publishers; 2001. p. 325-43.

73. Okel TA. Precipitated Silica: Fundamental Technology, Production, Compounding and Applications. the Spring 167th Technical Meeting of the Rubber Division, American Chemical Society; May 16-18; San Antonio, Texas2005.

74. Daudey S, Guy L, editors. Silica System to Modulate the Compromise Reinforcement/Hysteresis for the Silica Filled Elastomers. RIEG 2011; 2011; London, UK.

75. Chakraborty S, Shah D, Silica M. Precipitated Silica in Tires. Rubber World. 2013:37-41.

76. http://vchemchemicalandmachine.com/upload/images/Document/%E0%B8%AB%E0%B8%99%E0%B9%89%E0%B8%B2%E0%B9%81%E0%B8%A3%E0%B8%81/TOKUSIL%20Profile.pdf.

77. Grosseau P, Dumas Te, Bonnefoy O, Barriquand L, Guy L, Thomas Ge, editors. Internal Structure and Fragmentation Kinetics of Silica Granules. Powders and Grains 2013; 2013; Sydney, Australia: American Institut of Physics Publishing LLC.

78. Meon W, Blume A, Luginsland H-D, Uhrlandt S. Silica and Silanes. In: Rodgers B, editor. Rubber Compounding: Chemistry and Applications. New York, USA: Marcel Dekker, Inc; 2004.

79. Tohsan A, Ikeda Y. Generating Particulate Silica Fillers in situ to Improve the Mechanical Properties of Natural Rubber (NR). In: Kohjiya S, Ikeda Y, editors. Chemistry, Manufacture and Applications of Natural Rubber. UK: Woodhead Publishing; 2014. p. 168.
80. Pongdong W, Kummerlöwe C, Vennemann N, Thitithammawong A, Nakason C. A Comparative Study of Rice Husk Ash and Siliceous Earth as Reinforcing Fillers in Epoxidized Natural Rubber Composites. Polymer Composites. 2016:n/a.
81. Luginsland H-D, editor Chemistry and Physics of Network Formation of Silica/Silane Filled Rubber Compounds. 161st Spring Technical Meeting, American Chemical Society; 2002 April 29 - May 1 Savannah, Georgia.
82. Schaefer DW, Rieker T, Agamalian M, Lin JS, Fischer D, Sukumaran S, et al. Multilevel Structure of Reinforcing Silica and Carbon. Journal of Applied Crystallography. 2000;33:5.
83. http://www.rhodia.com/en/markets_and_products/product_finder/product_details.tcm?productCode=90035818&productName=Zeosil%C2%AE+1165MP.
84. https://www.xiameter.com/en/ExploreSilicones/Documents/Silane%20Chemistry-2a-95-719-01-F2.pdf.
85. Goerl U, Hunsche A, Mueller A, Koban HG. Investigations into the Silica/Silane Reaction System. Rubber Chemistry and Technology. 1997;70(4):608-23.
86. Brinke JWt, Debnath SC, Reuvekamp LAEM, Noordermeer JWM. Mechanistic Aspects of the Role of Coupling Agents in Silica–Rubber Composites. Composites Science and Technology. 2003;63(8):1165-74.
87. Nagdi K. Rubber as an Engineering Materials: Guideline for Users: Hanser Publishers; 1993.
88. Datta RN. Rubber Curing Systems: Shropshire: Rapra Technology Limited; 2002.
89. Coran AY. Vulcanization. In: Mark JE, Erman B, Roland CM, editors. The Science and Technology of Rubber. Fourth Edition ed. USA: Elsevier Inc.; 2013.

90. Li J, Wang S, Liu H, Liu N, You L. Preparation and Application of Poly(melamine-urea-formaldehyde) Microcapsules Filled with Sulfur. Polymer-Plastics Technology and Engineering. 2011;50(7):689-97.
91. http://interquimica.com.br/content/produtos/Crystex%20HD%20OT%2020.pdf.
92. http://www.nocil.com/Downloadfile/DTechnicalNote-Vulcanization-Dec10.pdf.
93. Datta RN, Ingham FAA. Rubber Additives - Compounding Ingredients. In: De SK, White JR, editors. Rubber Technologist's Handbook: Rapra Technology Limited; 2001.
94. Akiba M, Hashim AS. Vulcanization and Crosslinking in Elastomers. Progress in Polymer Science. 1997;22.
95. Aprem AS, Thomas S, Joseph K, Barkoula NM, Kocsis JK. Sulphur Vulcanisation of Styrene Butadiene Rubber using New Binary Accelerator Systems. Journal of Elastomers and Plastics. 2003;35.
96. Quirk RP. Overview of Curing and Crosslinking of Elastomers. Progress in Rubber Plastics and Recycling Technology. 1988;4(1).
97. Fröhlich J, Niedermeier W, Luginsland HD. The Effect of Filler–Filler and Filler–Elastomer Interaction on Rubber Reinforcement. Composites Part A: Applied Science and Manufacturing. 2005;36(4):449-60.
98. Luginsland H-D, Fröhlich J, Wehmeier A. Influence of Different Silanes on the Reinforcement of Silica-Filled Rubber Compounds. Rubber Chemistry and Technology. 2002;75(4):563-79.
99. Mihara S. Reactive Processing of Silica-Reinforced Tire Rubber: New Insight into the Time- and Temperature-Dependence of Silica Rubber Interaction: University of Twente; 2009.
100. Varkey JK. Epoxidised Natural Rubber as a Reinforcement Modifier for Silica Filled Natural Rubber and Acrylonitrile Butadiene Rubber: Mahatma Gandhi University; 2005.
101. Einstein A. Eine neue Bestimmung der Molekul-dimensionen. Annalen der Physik (Leipzig). 1906;19:289.
102. Einstein A. Berichtigungzu Meiner Arbeit: Eine neue Bestimmungder Molekuldimensionen. Annalen der Physik (Leipzig). 1911;34:591.

103. Guth E, Gold O. On the Hydrodynamical Theory of the Viscosity of Suspensions. Physical Review. 1938;53:322.
104. Guth E. Theory of Filler Reinforcement. Journal of Applied Physics. 1945(16):20.
105. Galimberti M, Cipolletti V, Kumar V. Nanofillers in Natural Rubber. In: Thomas S, Chan CH, Pothen LA, Joy J, Maria H, editors. Natural Rubber Materials: Volume 2: Composites and Nanocomposites: Royal Society of Chemistry; 2013.
106. Kohls DJ, Beaucage G. Rational Design of Reinforced Rubber. Current Opinion in Solid State and Materials Science. 2002;6(3):183-94.
107. O'Brien J, Cashell E, Wardell GE, McBrierty VJ. An NMR Investigation of the Interaction between Carbon Black and cis-Polybutadiene. Macromolecules. 1976;9(4):653-60.
108. Payne AR, Whittaker RE. Low Strain Dynamic Properties of Filled Rubbers. Rubber Chemistry and Technology. 1971;44(2):440-78.
109. Reuvekamp LAEM, Brinke JWt, Swaaij PJv, Noordermeer JWM. Effects of Time and Temperature on the Reaction of Tespt Silane Coupling Agent During Mixing with Silica Filler and Tire Rubber. Rubber Chemistry and Technology. 2002;75(2):187-98.
110. Lee HG, Kim HS, Cho ST, Jung IT, Cho CT. Characterization of Solution Styrene Butadiene Rubber (SBR) Through the Evaluation of Static and Dynamic Mechanical Properties and Fatigue in Silica-Filled Compound. Asian Journal of Chemistry. 2013;25(9):5251-6.
111. Medalia AI. Filler Aggregates and Their Effect on Reinforcement. Rubber Chemistry and Technology. 1974;47(2):411-33.
112. Grosch KA. Sliding Friction and Abrasion of Rubbers [Ph.D thesis]. London: University of London; 1963.
113. Heinrich G. The Dynamics of Tire Tread Compounds and Their Relationship to Wet Skid Behavior. Physics of Polymer Networks. Darmstadt: Steinkopff; 1992. p. 16-26.

114. Wang Y-X, Ma J-H, Zhang L-Q, Wu Y-P. Revisiting the Correlations between Wet Skid Resistance and Viscoelasticity of Rubber Composites via Comparing Carbon Black and Silica Fillers. Polymer Testing. 2011;30(5):557-62.
115. Takino H, Nakayama R, Yamada Y, Kohjiya S, Matsuo T. Viscoelastic Properties of Elastomers and Tire Wet Skid Resistance. Rubber Chemistry and Technology. 1997;70(4):584-94.
116. Benito JLd, González Hernández L, Marcos-Fernández Á, Rodríguez Díaz A. A New Carbon Black-Rubber Coupling Agent to Improve Wet Grip and Rolling Resistance of Tires. Rubber Chemistry and Technology. 1996;69:266-72.
117. Zafarmehrabian R, Gangali ST, Ghoreishy MHR, Davallu M. The Effects of Silica/Carbon Black Ratio on the Dynamic Properties of the Tread compounds in Truck Tires. E-Journal of Chemistry. 2012;9(3).
118. Salimi D, Khorasani SN, Abadchi MR, Veshare SJ. Optimization of Physico-Mechanical Properties of Silica-Filled NR/SBR Compounds. Advances in Polymer Technology. 2009;28(4):224-32.
119. Qu L, Yu G, Xie X, Wang L, Li J, Zhao Q. Effect of Silane Coupling Agent on Filler and Rubber Interaction of Silica Reinforced Solution Styrene Butadiene Rubber. Polymer Composites. 2013;34(10):1575-82.
120. Shiva M, Atashi H. Failure Optimization and Curing Properties of a Passenger Tire Tread Compound. Iranian Journal of Polymer Science and Technology (Persian). 2010;23(3)(107):187-201.
121. Bhushan B. Principles and Applications of Tribology: John Wiley & Sons; 2013.
122. Wolff S. Chemical Aspects of Rubber Reinforcement by Fillers. Rubber Chemistry and Technology. 1996;69(3):325-46.
123. Flory PJ, Rehner J. Statistical Mechanics of Cross-Linked Polymer Network II. Swelling. The Journal of Chemical Physics. 1943;11(11):521-6.
124. Deng JS, Isayev AI. Injection Molding of Rubber Compounds: Experimentation and Simulation. Rubber Chemistry and Technology. 1991;64(2):296-324.

125. Salgueiro W, Marzocca A, Somoza A, Consolati G, Cerveny S, Quasso F, et al. Dependence of the Network Structure of Cured Styrene Butadiene Rubber on the Sulphur Content. Polymer. 2004;45(17):6037-44.
126. Reuvekamp LAEM, Brinke JWt, Swaaij PJv, Noordermeer JWM. Effects of Mixing Conditions: Reaction of TESPT Silane Coupling Agent During Mixing with Silica Filler and Tire Rubber. Kautschuk Gummi Kunststoffe. 2002;55:41-7.
127. Mazzeo RA. Preventing Polymer Degradation During Mixing. Rubber World. 1995.
128. Valentín JL, Mora-Barrantes I, Carretero-González J, López-Manchado MA, Sotta P, Long DR, et al. Novel Experimental Approach To Evaluate Filler−Elastomer Interactions. Macromolecules. 2010;43(1):334-46.
129. Geethamma VG, Kalaprasad G, Groeninckx G, Thomas S. Dynamic Mechanical Behavior of Short Coir Fiber Reinforced Natural Rubber Composites. Composites Part A: Applied Science and Manufacturing. 2005;36(11):1499-506.
130. Roland CM. Mechanical Behavior of Rubber at High Strain Rates. Rubber Chemistry and Technology. 2006;79(3):429-59.
131. Dierkes W, Noordermeer JWM, Rinker M, Pol CVd. Increasing the Silanisation Efficiency of Silica Compounds: Upscaling. KGK Kautschuk Gummi Kunststoffe 2003;56:338-44.
132. Sae-oui P, Sirisinha C, Hatthapanit K, Thepsuwan U. Comparison of Reinforcing Efficiency between Si-69 and Si-264 in an Efficient Vulcanization System. Polymer Testing. 2005;24(4):439-46.
133. Pickering KL, Raa Khimi S, Ilanko S. The Effect of Silane Coupling Agent on Iron Sand for Use in Magnetorheological Elastomers Part 1: Surface Chemical Modification and Characterization. Composites Part A: Applied Science and Manufacturing. 2015;68:377-86.
134. Stöckelhuber KW, Das A, Jurk R, Heinrich G. Contribution of Physico-Chemical Properties of Interfaces on Dispersibility, Adhesion and Flocculation of Filler Particles in Rubber. Polymer. 2010;51(9):1954-63.

135. Rattanasom N, Saowapark T, Deeprasertkul C. Reinforcement of Natural Rubber with Silica/Carbon Black Hybrid Filler. Polymer Testing. 2007;26(3):369-77.

136. Semaan ME, Quarles CA, Nikiel L. Carbon Black and Silica as Reinforcers of Rubber Polymers: Doppler Broadening Spectroscopy Results. Polymer Degradation and Stability. 2002;75(2):259-66.

137. Brydson JA. Plastics Materials. Seventh ed. Great Britain: Biddles Ltd.; 1999.

138. Mokhtari M, Schipper DJ, Tolpekina TV. On the Friction of Carbon Black- and Silica-Reinforced BR and S-SBR Elastomers. Tribology Letters. 2014;54(3):297-308.

139. Sadasivuni KK, Grohens Y. Nonlinear Viscoelasticity of Two Dimensional Filler Reinforced Rubber Nanocomposites. In: Ponnamma D, Thomas S, editors. Non-Linear Viscoelasticity of Rubber Composites and Nanocomposites. Advances in Po;ymer Science: Springer International Publishing; 2014. p. 309.

140. Ignatz-Hoover F, To BH. Vulcanization. In: Rodgers B, editor. Rubber Compounding Chemistry and Applications: Taylor & Francis; 2004.

141. Bhowmick AK, Mangaraj D. Vulcanization and Curing Techniques. In: Bhowmick AK, Hall MM, Bernary HA, editors. Rubber Products Manufacturing Technology: Marcel Dekker, Inc.; 1994. p. 324.

142. Amara Y. Comparison of Rubber Curing - Peroxide-Coagent vs Sulfur-Accelerator in Polyisiprene (IR). Rubberchem 2001 - The International Rubber Chemicals, Compounding and Mixing Conference; 3rd-4th April 2001; Brussels, Belgium: iSmithers Rapra Publishing; 2001. p. 6.

143. Sae-oui P, Thepsuwan U, Hatthapanit K. Effect of Curing System on Reinforcing Efficiency of Silane Coupling Agent. Polymer Testing. 2004;23(4):397-403.

144. Hagen R, Salmén L, Stenberg B. Effects of the Type of Crosslink on Viscoelastic Properties of Natural Rubber. Journal of Polymer Science Part B: Polymer Physics. 1996;34(12):1997-2006.

145. Jinnai H, Shinbori Y, Kitaoka T, Akutagawa K, Mashita N, Nishi T. Three-Dimensional Structure of a Nanocomposite Material Consisting of Two Kinds of Nanofillers and Rubbery Matrix Studied by Transmission Electron Microtomography. Macromolecules. 2007;40(18):6758-64.

APPENDICES

APPENDIX A
INVESTIGATION OF MORPHOLOGY OF SILICA/CB HYBRID FILLER IN RUBBER VULCANIZATES

In this study, the morphology of silica and CB in the rubber vulcanizates filled with silica/CB hybrid filler was investigated using 3 techniques, i.e., AFM, TEM, and SEM-EDS.

A1 Atomic force microscopy (AFM)

Figure A1 demonstrates the AFM micrographs of (60/40) CSi/CB-filled SSBR6450SL vulcanizates at 3 magnification levels investigated in the tapping mode. Although the difference between SBR phase (yellow area) and fillers phase (red area) can be discriminated by this technique, the particles or aggregates of CSi and CB cannot be distinguished. Results suggest that the use of AFM in tapping mode may not be suitable for discrimination between silica and CB filled in rubber vulcanizates.

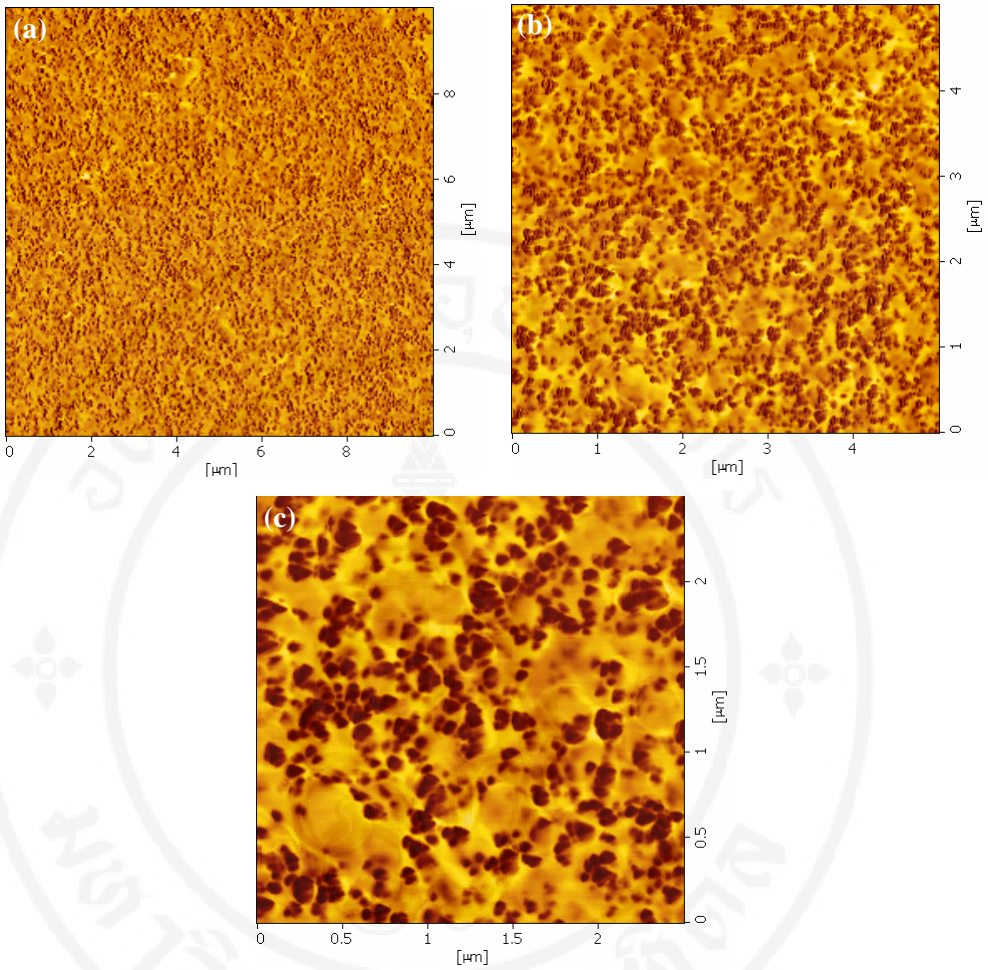

Figure A1 AFM micrographs of the (60/40) CSi/CB-filled SSBR6450SL vulcanizates at 3 magnifications: (a) low magnification; (b) medium magnification and (c) high magnification

A2 Transmission electron microscopy (TEM)

Since the electron densities of CB and silica are different (5.42×10^{23} cm^{-3} and 5.87×10^{23} cm^{-3}, respectively [145]), it is possible to distinguish the morphology of silica and CB in rubber vulcanizates filled with silica/CB hybrid filler by the use of TEM. Figure A2 represents the TEM micrographs of (60/40) CSi/CB-filled SSBR6450SL vulcanizates at 2 magnification levels. Evidently, some filler particles show a little darker than others, suggesting the greater electron density. In addition, the overlap along the depth direction of filler particles might be another reason for this

finding. For these reasons, it could be said that the morphology of CSi and CB in the vulcanizates cannot be clearly distinguished by conventional TEM.

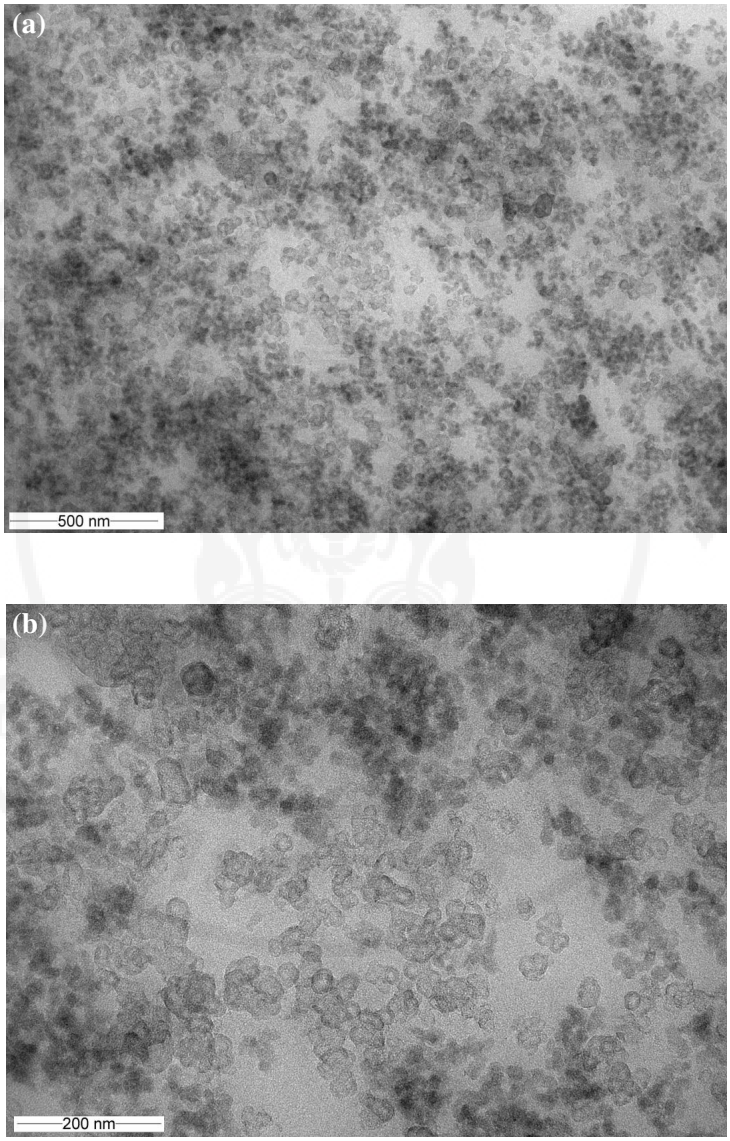

Figure A2 TEM micrographs of the (60/40) CSi/CB-filled SSBR6450SL vulcanizates at 2 magnifications: (a) low magnification and (b) high magnification

A3 Scanning electron microscopy equipped with energy dispersive x-ray spectroscopy (SEM-EDS)

As this technique can provide chemical information of materials by identifying the particular elements and their relative proportions at specific area, the morphology of silica and CB in the SSBR6450SL vulcanizates filled with CSi/CB hybrid filler was also investigated using this technique. Figure A3 depicts SEM micrographs and its elemental mapping, i.e., zinc, silicon, and carbon, at the same area of (20/80) CSi/CB-filled SSBR6450SL vulcanizates. Although the ratio of silica in the vulcanizates is ca. 20 wt%, the high amount of silicon element is found. Results suggest that silicon detected by SEM-EDS might be the combination of the silicon which is on the surface and the silicon embedded under the surface, revealing that the morphology of CSi and CB in the vulcanizates cannot be effectively distinguished by this technique.

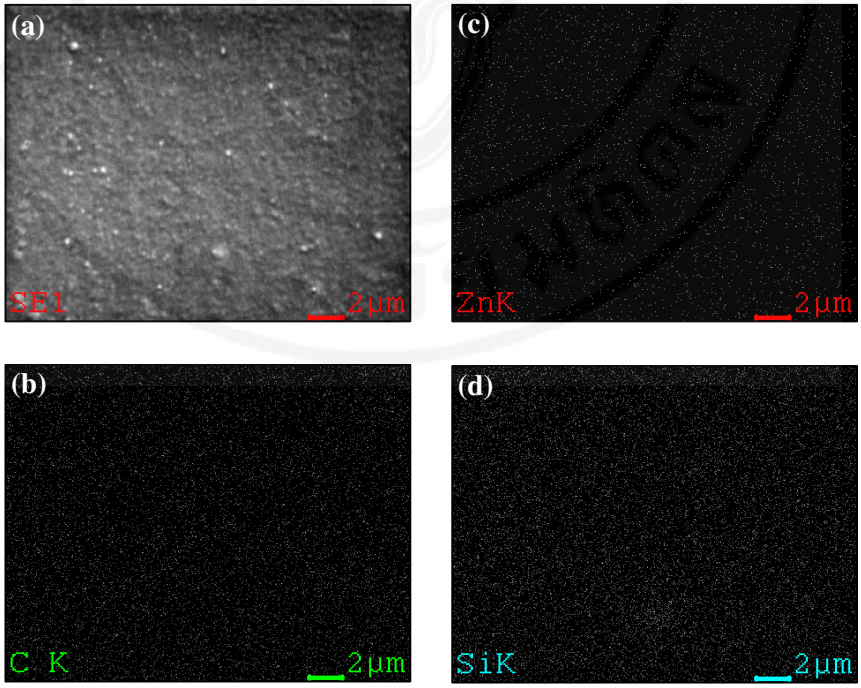

Figure A3 SEM micrograph and its elemental mapping of the (20/80) CSi/CB-filled SSBR6450SL vulcanizates: (a) SEM micrograph (b) Carbon mapping (c) Zinc mapping and (d) Silicon mapping

APPENDIX B
CURE CHARACTERISTICS OF THE RUBBER COMPOUNDS

Table B1 Cure characteristics of the compounds prepared at various silanization temperatures: (a) HDSi

HDSi_120°C		HDSi_130°C		HDSi_140°C		HDSi_150°C		HDSi_160°C	
Time (min)	Torque (dN.m)	Time (min)	Torque (dN.m)	Time (min)	Torque (dN.m)	Time (min)	Torque (dN.m)	Time (min)	Torque (dN.m)
0.02	1.75	0.02	3.01	0.02	3.12	0.02	3.27	0.02	3.13
0.34	3.10	0.14	2.52	0.34	2.87	0.34	2.44	0.34	2.49
0.66	3.60	0.26	2.66	0.66	3.29	0.66	2.85	0.66	2.73
0.82	3.76	0.58	3.21	0.98	3.58	0.98	3.12	0.98	2.93
0.98	3.91	0.90	3.58	1.30	3.78	1.30	3.32	1.30	3.08
1.30	4.12	1.22	3.83	1.62	3.93	1.62	3.46	1.62	3.20
1.62	4.28	1.54	4.01	1.94	4.04	1.94	3.56	1.94	3.29
1.94	4.43	1.86	4.16	2.26	4.14	2.26	3.65	2.26	3.37
2.26	4.59	2.18	4.29	2.58	4.27	2.58	3.77	2.42	3.42
2.58	4.81	2.50	4.45	2.90	4.41	2.90	3.86	2.58	3.45
2.90	5.05	2.82	4.64	3.22	4.59	3.22	3.99	2.90	3.53
3.22	5.36	3.14	4.88	3.54	4.81	3.54	4.14	3.22	3.63
3.54	5.69	3.46	5.17	3.86	5.08	3.86	4.32	3.54	3.73
3.86	6.08	3.78	5.49	4.18	5.40	4.18	4.54	3.86	3.87
4.18	6.53	4.10	5.86	4.50	5.74	4.50	4.75	4.18	4.02
4.50	7.02	4.42	6.28	4.82	6.14	4.82	5.03	4.50	4.18
4.82	7.59	4.74	6.74	5.14	6.55	5.14	5.39	4.82	4.41
4.90	7.77	5.06	7.26	5.46	7.02	5.46	5.74	4.86	4.43
4.98	7.90	5.22	7.54	5.78	7.51	5.78	6.13	4.90	4.46
5.30	8.54	5.38	7.82	6.10	8.01	6.10	6.53	5.22	4.71
5.62	9.21	5.70	8.43	6.42	8.54	6.42	6.98	5.54	5.00
5.94	9.86	6.02	9.03	6.74	9.07	6.70	7.36	5.86	5.31
6.27	10.50	6.34	9.64	7.06	9.59	6.98	7.75	6.18	5.65
6.59	11.10	6.66	10.23	7.38	10.09	7.30	8.20	6.50	6.01
6.91	11.67	6.98	10.79	7.70	10.59	7.62	8.63	6.82	6.40
7.23	12.19	7.30	11.34	8.02	11.06	7.94	9.06	7.14	6.79
7.55	12.69	7.62	11.83	8.34	11.49	8.26	9.48	7.46	7.17
7.87	13.14	7.94	12.29	8.66	11.92	8.58	9.90	7.66	7.42
8.19	13.59	8.26	12.72	8.98	12.30	8.90	10.28	7.86	7.67

Table B1 Cure characteristics of the compounds prepared at various silanization temperatures (cont.): (a) HDSi

HDSi_120°C		HDSi_130°C		HDSi_140°C		HDSi_150°C		HDSi_160°C	
Time (min)	Torque (dN.m)	Time (min)	Torque (dN.m)	Time (min)	Torque (dN.m)	Time (min)	Torque (dN.m)	Time (min)	Torque (dN.m)
8.51	13.97	8.58	13.12	9.30	12.66	9.22	10.64	8.18	8.06
8.83	14.36	8.90	13.51	9.62	13.00	9.54	10.96	8.50	8.43
9.15	14.70	9.22	13.86	9.94	13.32	9.86	11.28	8.82	8.80
9.47	15.02	9.54	14.17	10.26	13.61	10.18	11.59	9.14	9.14
9.79	15.33	9.86	14.46	10.58	13.86	10.50	11.87	9.46	9.47
10.11	15.61	10.18	14.75	10.90	14.14	10.82	12.13	9.78	9.78
10.43	15.86	10.50	14.99	11.22	14.38	11.14	12.37	10.10	10.07
10.75	16.12	10.82	15.25	11.54	14.60	11.46	12.61	10.42	10.34
11.07	16.34	11.14	15.46	11.86	14.81	11.78	12.82	10.74	10.60
11.39	16.54	11.46	15.68	12.18	15.03	12.10	13.02	11.06	10.85
11.71	16.75	11.78	15.86	12.50	15.21	12.42	13.21	11.38	11.07
12.03	16.93	12.10	16.05	12.82	15.38	12.74	13.41	11.70	11.29
12.35	17.11	12.42	16.22	13.14	15.54	13.06	13.57	12.02	11.51
12.67	17.27	12.74	16.38	13.46	15.69	13.38	13.76	12.34	11.70
12.99	17.43	13.06	16.51	13.78	15.84	13.70	13.89	12.66	11.88
13.31	17.57	13.38	16.64	14.10	15.99	14.02	14.04	12.98	12.05
13.63	17.71	13.70	16.75	14.42	16.11	14.33	14.17	13.30	12.23
13.95	17.84	14.02	16.90	14.74	16.22	14.65	14.28	13.62	12.38
14.27	17.96	14.34	17.01	15.06	16.33	14.97	14.42	13.94	12.53
14.59	18.06	14.66	17.12	15.38	16.46	15.29	14.54	14.26	12.68
14.91	18.17	14.98	17.21	15.70	16.57	15.61	14.65	14.58	12.81
15.23	18.27	15.30	17.32	16.02	16.66	15.93	14.76	14.90	12.93
15.55	18.36	15.62	17.40	16.34	16.75	16.25	14.86	15.22	13.05
15.87	18.47	15.94	17.46	16.66	16.84	16.57	14.93	15.54	13.17
16.19	18.54	16.26	17.54	16.98	16.93	16.89	15.03	15.86	13.27
16.51	18.61	16.58	17.63	17.30	17.00	17.21	15.13	16.18	13.38
16.83	18.70	16.90	17.70	17.62	17.09	17.53	15.22	16.50	13.47
17.15	18.77	17.22	17.75	17.94	17.14	17.85	15.29	16.82	13.57
17.47	18.83	17.54	17.82	18.26	17.21	18.17	15.35	17.14	13.66
17.79	18.89	17.86	17.88	18.58	17.28	18.49	15.42	17.46	13.74
18.11	18.95	18.18	17.93	18.90	17.33	18.81	15.50	17.78	13.82
18.43	19.02	18.50	17.99	19.22	17.39	19.13	15.57	18.10	13.89
18.75	19.08	18.82	18.04	19.54	17.44	19.45	15.62	18.42	13.97
19.07	19.13	19.14	18.09	19.86	17.49	19.77	15.69	18.74	14.04
19.39	19.17	19.46	18.15	20.18	17.55	20.09	15.73	19.06	14.10

Table B1 Cure characteristics of the compounds prepared at various silanization temperatures (cont.): (a) HDSi

HDSi_120°C		HDSi_130°C		HDSi_140°C		HDSi_150°C		HDSi_160°C	
Time (min)	Torque (dN.m)	Time (min)	Torque (dN.m)	Time (min)	Torque (dN.m)	Time (min)	Torque (dN.m)	Time (min)	Torque (dN.m)
19.71	19.19	19.78	18.17	20.50	17.58	20.41	15.78	19.38	14.17
20.03	19.27	20.10	18.22	20.82	17.62	20.73	15.84	19.70	14.23
20.36	19.30	20.42	18.26	21.14	17.66	21.05	15.89	20.02	14.29
20.68	19.36	20.74	18.28	21.46	17.69	21.37	15.93	20.34	14.35
21.00	19.42	21.06	18.32	21.78	17.74	21.69	15.96	20.66	14.40
21.32	19.41	21.38	18.36	22.10	17.76	22.01	16.01	20.98	14.45
21.64	19.46	21.70	18.38	22.42	17.80	22.33	16.06	21.30	14.49
21.96	19.49	22.02	18.42	22.74	17.85	22.65	16.09	21.62	14.54
22.28	19.52	22.34	18.47	23.06	17.86	22.97	16.12	21.94	14.58
22.60	19.56	22.66	18.49	23.38	17.90	23.29	16.17	22.26	14.63
22.92	19.58	22.98	18.53	23.70	17.93	23.61	16.20	22.58	14.67
23.24	19.61	23.30	18.54	24.02	17.96	23.93	16.25	22.90	14.71
23.56	19.65	23.62	18.56	24.34	17.98	24.25	16.25	23.22	14.74
23.88	19.67	23.94	18.56	24.66	18.01	24.57	16.28	23.54	14.78
24.20	19.68	24.26	18.59	24.98	18.02	24.89	16.31	23.86	14.81
24.52	19.70	24.58	18.62	25.30	18.04	25.21	16.35	24.18	14.85
24.84	19.74	24.90	18.65	25.62	18.06	25.53	16.36	24.50	14.88
25.16	19.75	25.22	18.68	25.94	18.09	25.85	16.40	24.82	14.90
25.48	19.80	25.54	18.69	26.26	18.11	26.17	16.42	25.14	14.94
25.80	19.79	25.86	18.71	26.58	18.12	26.49	16.44	25.46	14.97
26.12	19.82	26.18	18.73	26.90	18.13	26.81	16.45	25.78	15.00
26.44	19.84	26.50	18.73	27.22	18.16	27.13	16.48	26.10	15.01
26.75	19.85	26.82	18.76	27.54	18.18	27.45	16.49	26.42	15.06
27.07	19.88	27.14	18.76	27.86	18.20	27.77	16.51	26.74	15.08
27.39	19.90	27.46	18.78	28.18	18.21	28.09	16.54	27.06	15.10
27.71	19.91	27.78	18.76	28.50	18.23	28.41	16.56	27.38	15.12
28.03	19.93	28.10	18.80	28.82	18.25	28.73	16.58	27.70	15.14
28.35	19.95	28.42	18.82	29.14	18.25	29.05	16.59	28.02	15.16
28.67	19.96	28.74	18.84	29.46	18.28	29.37	16.60	28.34	15.19
28.99	19.96	29.06	18.86	29.78	18.29	29.69	16.63	28.66	15.21
29.31	19.97	29.38	18.87	30.10	18.29	30.01	16.64	28.98	15.23
29.63	19.97	29.70	18.86	30.42	18.31	30.33	16.65	29.31	15.22
29.95	19.98	30.02	18.89	30.74	18.31	30.65	16.66	29.63	15.26
30.27	20.02	30.34	18.89	31.05	18.33	30.97	16.68	29.95	15.28
30.59	20.03	30.66	18.90	31.37	18.34	31.29	16.69	30.27	15.29

Table B1 Cure characteristics of the compounds prepared at various silanization temperatures (cont.): (a) HDSi

HDSi_120°C		HDSi_130°C		HDSi_140°C		HDSi_150°C		HDSi_160°C	
Time (min)	Torque (dN.m)	Time (min)	Torque (dN.m)	Time (min)	Torque (dN.m)	Time (min)	Torque (dN.m)	Time (min)	Torque (dN.m)
30.91	20.03	30.98	18.91	31.69	18.36	31.61	16.71	30.59	15.30
31.23	20.03	31.30	18.92	32.01	18.35	31.93	16.72	30.91	15.32
31.55	20.05	31.62	18.94	32.33	18.37	32.25	16.73	31.23	15.34
31.87	20.07	31.94	18.94	32.65	18.37	32.57	16.74	31.55	15.35
32.19	20.07	32.26	18.95	32.97	18.39	32.89	16.75	31.87	15.36
32.51	20.09	32.58	18.96	33.29	18.39	33.21	16.75	32.19	15.38
32.83	20.12	32.90	18.97	33.61	18.41	33.53	16.77	32.51	15.39
33.15	20.12	33.22	18.98	33.93	18.42	33.85	16.78	32.83	15.41
33.47	20.12	33.54	18.98	34.25	18.43	34.17	16.80	33.15	15.41
33.79	20.12	33.86	18.99	34.57	18.43	34.49	16.80	33.47	15.43
34.11	20.14	34.18	19.00	34.89	18.45	34.81	16.81	33.79	15.42
34.43	20.15	34.50	19.00	35.21	18.45	35.13	16.82	34.11	15.45
34.75	20.16	34.82	19.02	35.53	18.46	35.45	16.84	34.43	15.45
35.07	20.17	35.14	19.04	35.85	18.44	35.77	16.83	34.75	15.47
35.39	20.18	35.46	19.05	36.17	18.47	36.09	16.85	35.07	15.48
35.71	20.17	35.78	19.06	36.49	18.47	36.41	16.85	35.39	15.48
36.03	20.20	36.10	19.05	36.81	18.48	36.73	16.86	35.71	15.49
36.35	20.20	36.42	19.06	37.13	18.49	37.05	16.86	36.03	15.51
36.67	20.21	36.74	19.08	37.45	18.48	37.37	16.88	36.35	15.51
36.99	20.21	37.06	19.07	37.77	18.48	37.69	16.88	36.67	15.53
37.31	20.21	37.38	19.06	38.09	18.51	38.01	16.89	36.99	15.53
37.63	20.21	37.70	19.10	38.41	18.52	38.32	16.90	37.31	15.55
37.95	20.24	38.02	19.09	38.73	18.51	38.64	16.90	37.63	15.57
38.27	20.23	38.34	19.09	39.05	18.52	38.96	16.91	37.95	15.57
38.59	20.24	38.66	19.11	39.37	18.54	39.28	16.91	38.27	15.57
38.91	20.25	38.98	19.13	39.69	18.53	39.60	16.92	38.59	15.59
39.23	20.27	39.30	19.12	40.01	18.54	39.92	16.94	38.91	15.59
39.55	20.28	39.62	19.12	40.33	18.55	40.24	16.94	39.23	15.60
39.87	20.28	39.94	19.14	40.65	18.54	40.56	16.93	39.55	15.61
40.19	20.28	40.26	19.14	40.97	18.56	40.88	16.94	39.87	15.62
40.51	20.29	40.58	19.14	41.29	18.56	41.20	16.95	40.19	15.63
40.83	20.28	40.90	19.16	41.61	18.56	41.52	16.95	40.51	15.62
41.15	20.30	41.22	19.14	41.93	18.57	41.84	16.96	40.83	15.64
41.47	20.30	41.53	19.13	42.25	18.58	42.16	16.97	41.15	15.64
41.79	20.29	41.85	19.15	42.57	18.58	42.48	16.97	41.47	15.64

Table B1 Cure characteristics of the compounds prepared at various silanization temperatures (cont.): (a) HDSi

HDSi_120°C		HDSi_130°C		HDSi_140°C		HDSi_150°C		HDSi_160°C	
Time (min)	Torque (dN.m)	Time (min)	Torque (dN.m)	Time (min)	Torque (dN.m)	Time (min)	Torque (dN.m)	Time (min)	Torque (dN.m)
42.11	20.31	42.17	19.16	42.89	18.57	42.80	16.98	41.79	15.65
42.43	20.32	42.49	19.17	43.21	18.57	43.12	16.99	42.11	15.64
42.75	20.31	42.81	19.17	43.53	18.57	43.44	17.00	42.43	15.66
43.07	20.33	43.13	19.19	43.85	18.57	43.76	16.98	42.75	15.67
43.39	20.31	43.45	19.19	44.17	18.59	44.08	17.00	43.07	15.67
43.71	20.32	43.77	19.20	44.49	18.59	44.40	17.00	43.39	15.68
44.03	20.32	44.09	19.21	44.81	18.58	44.72	17.00	43.71	15.69
44.35	20.34	44.41	19.22	45.13	18.59	45.04	17.02	44.03	15.69
44.67	20.34	44.74	19.21	45.45	18.62	45.36	17.02	44.35	15.69
44.99	20.34	45.06	19.21	45.77	18.62	45.68	17.03	44.67	15.70
45.31	20.33	45.38	19.21	46.09	18.63	46.00	17.03	44.99	15.70
45.63	20.35	45.69	19.22	46.41	18.62	46.32	17.05	45.32	15.72
45.95	20.35	46.01	19.21	46.73	18.62	46.64	17.05	45.64	15.72
46.27	20.36	46.33	19.22	47.05	18.63	46.96	17.04	45.96	15.72
46.59	20.36	46.65	19.24	47.37	18.64	47.28	17.05	46.28	15.72
46.91	20.36	46.97	19.23	47.69	18.63	47.60	17.05	46.60	15.73
47.23	20.37	47.29	19.23	48.01	18.63	47.92	17.03	46.92	15.74
47.55	20.37	47.61	19.25	48.33	18.62	48.24	17.04	47.24	15.74
47.91	20.36	47.93	19.25	48.65	18.64	48.56	17.04	47.56	15.74
48.23	20.37	48.25	19.26	48.97	18.64	48.88	17.05	47.88	15.74
48.55	20.38	48.57	19.25	49.29	18.63	49.20	17.06	48.20	15.74
48.87	20.38	48.89	19.25	49.61	18.64	49.52	17.06	48.52	15.75
49.19	20.38	49.21	19.27	49.99	18.65	49.84	17.06	48.84	15.74
49.52	20.39	49.54	19.28			50.00	17.07	49.16	15.77
49.84	20.38	49.86	19.27					49.48	15.76
50.00	20.39	50.00	19.28					49.80	15.77
								50.00	15.77

Table B2 Cure characteristics of the compounds prepared at various silanization temperatures: (b) CSi

CSi_120°C		CSi_130°C		CSi_140°C		CSi_150°C		CSi_160°C	
Time (min)	Torque (dN.m)	Time (min)	Torque (dN.m)	Time (min)	Torque (dN.m)	Time (min)	Torque (dN.m)	Time (min)	Torque (dN.m)
0.02	2.49	0.02	2.78	0.02	2.67	0.02	2.68	0.02	1.63
0.10	2.47	0.34	2.66	0.14	2.14	0.22	2.10	0.06	2.52
0.18	2.61	0.66	3.15	0.26	2.24	0.42	2.30	0.10	2.31
0.50	3.38	0.98	3.48	0.58	2.71	0.74	2.67	0.22	2.15
0.82	3.79	1.30	3.71	0.90	3.08	1.06	2.93	0.34	2.21
1.14	4.05	1.62	3.87	0.98	3.15	1.30	3.11	0.66	2.46
1.46	4.22	1.94	3.99	1.06	3.22	1.54	3.23	0.98	2.71
1.78	4.36	2.26	4.10	1.38	3.42	1.86	3.36	1.30	2.90
2.02	4.47	2.58	4.22	1.70	3.57	2.18	3.46	1.62	3.03
2.26	4.57	2.90	4.36	2.02	3.69	2.50	3.55	1.94	3.14
2.58	4.74	3.23	4.53	2.34	3.79	2.82	3.65	1.98	3.15
2.90	4.96	3.55	4.74	2.66	3.89	3.14	3.75	2.02	3.15
3.22	5.23	3.87	5.01	2.98	4.01	3.46	3.87	2.34	3.24
3.54	5.54	4.19	5.29	3.30	4.12	3.78	3.99	2.66	3.32
3.86	5.93	4.52	5.63	3.62	4.31	4.10	4.14	2.98	3.40
4.18	6.34	4.84	5.99	3.94	4.50	4.42	4.33	3.30	3.49
4.50	6.84	5.18	6.40	4.26	4.72	4.74	4.55	3.62	3.56
4.82	7.37	5.50	6.85	4.58	5.01	5.06	4.79	3.94	3.67
5.14	7.98	5.82	7.35	4.90	5.31	5.38	5.09	4.26	3.79
5.46	8.64	6.14	7.87	5.22	5.64	5.70	5.40	4.58	3.92
5.78	9.32	6.46	8.41	5.54	6.00	6.02	5.76	4.90	4.07
6.10	10.02	6.78	8.98	5.86	6.41	6.34	6.15	5.02	4.15
6.42	10.69	7.10	9.52	6.18	6.86	6.66	6.56	5.14	4.20
6.74	11.34	7.42	10.06	6.38	7.14	6.98	6.98	5.46	4.42
7.06	11.92	7.74	10.57	6.58	7.46	7.30	7.43	5.78	4.67
7.38	12.50	8.06	11.05	6.90	7.96	7.62	7.90	6.10	4.94
7.70	13.01	8.38	11.51	7.22	8.35	7.94	8.33	6.42	5.23
8.02	13.49	8.70	11.92	7.54	8.92	8.26	8.79	6.74	5.56
8.34	13.94	9.02	12.32	7.86	9.39	8.58	9.22	7.06	5.90
8.66	14.33	9.34	12.67	8.18	9.87	8.90	9.64	7.38	6.29
8.98	14.70	9.66	13.00	8.50	10.33	9.22	10.03	7.70	6.67
9.30	15.05	9.98	13.31	8.82	10.73	9.54	10.42	8.02	7.07
9.62	15.35	10.30	13.59	9.14	11.10	9.86	10.77	8.10	7.18
9.94	15.65	10.62	13.86	9.46	11.46	10.18	11.10	8.18	7.28
10.26	15.92	10.94	14.11	9.78	11.80	10.50	11.41	8.50	7.68

Table B2 Cure characteristics of the compounds prepared at various silanization temperatures (cont.): (b) CSi

CSi_120°C		CSi_130°C		CSi_140°C		CSi_150°C		CSi_160°C	
Time (min)	Torque (dN.m)	Time (min)	Torque (dN.m)	Time (min)	Torque (dN.m)	Time (min)	Torque (dN.m)	Time (min)	Torque (dN.m)
10.58	16.17	11.26	14.32	10.10	12.12	10.82	11.70	8.82	8.07
10.90	16.40	11.58	14.55	10.42	12.43	11.14	11.97	9.14	8.47
11.22	16.60	11.90	14.75	10.74	12.72	11.46	12.24	9.47	8.85
11.54	16.81	12.22	14.92	11.06	12.98	11.78	12.47	9.79	9.19
11.86	16.98	12.54	15.11	11.38	13.22	12.09	12.67	10.11	9.53
12.18	17.15	12.86	15.27	11.70	13.45	12.41	12.91	10.43	9.86
12.50	17.31	13.18	15.42	12.02	13.67	12.73	13.12	10.75	10.16
12.82	17.48	13.50	15.56	12.34	13.85	13.05	13.31	11.07	10.43
13.14	17.58	13.82	15.69	12.66	14.04	13.37	13.48	11.39	10.69
13.46	17.71	14.14	15.80	12.98	14.22	13.69	13.64	11.71	10.94
13.78	17.84	14.46	15.93	13.30	14.38	14.01	13.81	12.03	11.18
14.10	17.97	14.78	16.03	13.62	14.53	14.33	13.96	12.35	11.40
14.42	18.04	15.10	16.13	13.94	14.69	14.65	14.09	12.67	11.61
14.74	18.14	15.42	16.23	14.27	14.81	14.97	14.24	12.99	11.80
15.06	18.23	15.74	16.31	14.59	14.94	15.29	14.35	13.31	11.99
15.38	18.30	16.06	16.39	14.91	15.06	15.61	14.46	13.63	12.17
15.70	18.38	16.38	16.48	15.23	15.14	15.93	14.58	13.95	12.33
16.02	18.47	16.70	16.56	15.55	15.24	16.25	14.69	14.27	12.48
16.34	18.54	17.02	16.63	15.87	15.36	16.57	14.79	14.59	12.63
16.66	18.62	17.34	16.69	16.19	15.46	16.89	14.87	14.91	12.76
16.98	18.68	17.66	16.75	16.51	15.55	17.23	14.99	15.23	12.90
17.30	18.75	17.98	16.81	16.83	15.63	17.55	15.06	15.55	13.03
17.62	18.79	18.30	16.87	17.15	15.71	17.87	15.14	15.87	13.13
17.94	18.83	18.62	16.92	17.47	15.78	18.19	15.22	16.19	13.24
18.26	18.88	18.94	16.97	17.79	15.85	18.51	15.29	16.51	13.36
18.58	18.95	19.26	17.01	18.11	15.92	18.83	15.36	16.83	13.44
18.90	18.99	19.58	17.07	18.43	15.98	19.15	15.41	17.15	13.54
19.22	19.02	19.90	17.10	18.75	16.03	19.47	15.48	17.47	13.64
19.54	19.07	20.22	17.15	19.07	16.08	19.79	15.55	17.79	13.72
19.86	19.10	20.54	17.20	19.39	16.14	20.11	15.60	18.11	13.80
20.18	19.13	20.86	17.23	19.71	16.20	20.43	15.66	18.43	13.88
20.50	19.17	21.18	17.27	20.03	16.24	20.75	15.70	18.75	13.94
20.82	19.19	21.50	17.31	20.35	16.27	21.07	15.75	19.07	14.02
21.14	19.23	21.82	17.34	20.67	16.31	21.39	15.80	19.39	14.09
21.46	19.26	22.14	17.37	20.99	16.36	21.71	15.84	19.71	14.14

Table B2 Cure characteristics of the compounds prepared at various silanization temperatures (cont.): (b) CSi

CSi_120°C		CSi_130°C		CSi_140°C		CSi_150°C		CSi_160°C	
Time (min)	Torque (dN.m)	Time (min)	Torque (dN.m)	Time (min)	Torque (dN.m)	Time (min)	Torque (dN.m)	Time (min)	Torque (dN.m)
21.78	19.30	22.46	17.38	21.31	16.40	22.03	15.87	20.03	14.22
22.10	19.31	22.78	17.41	21.63	16.45	22.35	15.93	20.35	14.26
22.42	19.34	23.10	17.45	21.95	16.48	22.67	15.98	20.67	14.32
22.74	19.36	23.42	17.47	22.27	16.53	22.99	16.01	20.99	14.37
23.06	19.39	23.74	17.50	22.59	16.54	23.31	16.02	21.31	14.42
23.38	19.39	24.06	17.52	22.91	16.60	23.63	16.07	21.63	14.47
23.70	19.44	24.38	17.53	23.23	16.61	23.95	16.10	21.95	14.52
24.02	19.46	24.70	17.55	23.55	16.65	24.27	16.13	22.27	14.56
24.34	19.47	25.02	17.58	23.87	16.67	24.59	16.17	22.59	14.61
24.66	19.48	25.34	17.60	24.19	16.69	24.91	16.21	22.91	14.64
24.98	19.51	25.66	17.62	24.51	16.72	25.23	16.23	23.23	14.68
25.30	19.52	25.98	17.64	24.83	16.72	25.55	16.26	23.55	14.72
25.62	19.54	26.30	17.64	25.15	16.77	25.87	16.27	23.87	14.76
25.94	19.54	26.62	17.65	25.47	16.80	26.19	16.30	24.19	14.79
26.26	19.58	26.94	17.69	25.79	16.82	26.51	16.32	24.51	14.83
26.58	19.58	27.26	17.70	26.11	16.83	26.83	16.34	24.83	14.85
26.90	19.61	27.58	17.71	26.43	16.87	27.15	16.37	25.15	14.88
27.22	19.60	27.90	17.73	26.75	16.88	27.47	16.40	25.47	14.92
27.54	19.62	28.22	17.74	27.07	16.89	27.79	16.42	25.79	14.95
27.86	19.65	28.54	17.75	27.39	16.91	28.11	16.45	26.11	14.97
28.18	19.64	28.86	17.75	27.71	16.93	28.43	16.45	26.43	15.00
28.50	19.65	29.18	17.78	28.03	16.95	28.75	16.48	26.75	15.02
28.82	19.66	29.50	17.80	28.35	16.96	29.07	16.50	27.07	15.04
29.14	19.68	29.82	17.81	28.67	16.97	29.39	16.51	27.39	15.08
29.46	19.72	30.14	17.81	28.99	16.98	29.71	16.52	27.71	15.11
29.78	19.69	30.46	17.83	29.31	17.01	30.03	16.56	28.03	15.12
30.10	19.71	30.78	17.85	29.63	17.03	30.35	16.56	28.35	15.15
30.42	19.73	31.10	17.84	29.95	17.03	30.67	16.56	28.67	15.17
30.74	19.73	31.42	17.86	30.28	17.06	30.99	16.59	28.99	15.18
31.06	19.74	31.74	17.86	30.60	17.07	31.31	16.60	29.31	15.21
31.38	19.75	32.06	17.87	30.92	17.08	31.63	16.62	29.63	15.23
31.70	19.75	32.38	17.89	31.24	17.09	31.95	16.62	29.95	15.24
32.02	19.78	32.70	17.91	31.56	17.11	32.27	16.64	30.27	15.25
32.34	19.79	33.02	17.92	31.88	17.12	32.59	16.65	30.59	15.29
32.66	19.78	33.34	17.93	32.20	17.11	32.91	16.66	30.91	15.31

Table B2 Cure characteristics of the compounds prepared at various silanization temperatures (cont.): (b) CSi

CSi_120°C		CSi_130°C		CSi_140°C		CSi_150°C		CSi_160°C	
Time (min)	Torque (dN.m)	Time (min)	Torque (dN.m)	Time (min)	Torque (dN.m)	Time (min)	Torque (dN.m)	Time (min)	Torque (dN.m)
32.98	19.80	33.66	17.93	32.52	17.13	33.23	16.68	31.23	15.32
33.30	19.80	33.98	17.95	32.84	17.12	33.55	16.69	31.55	15.32
33.62	19.80	34.30	17.94	33.16	17.15	33.87	16.70	31.87	15.35
33.94	19.80	34.62	17.97	33.48	17.14	34.19	16.72	32.19	15.37
34.26	19.81	34.94	17.96	33.80	17.16	34.51	16.71	32.51	15.37
34.58	19.81	35.26	17.97	34.12	17.17	34.83	16.73	32.85	15.39
34.90	19.81	35.58	17.98	34.44	17.18	35.15	16.75	33.17	15.41
35.22	19.82	35.90	18.01	34.76	17.21	35.47	16.74	33.49	15.42
35.54	19.82	36.22	17.99	35.08	17.21	35.79	16.76	33.81	15.42
35.86	19.83	36.55	18.00	35.40	17.23	36.11	16.76	34.13	15.44
36.18	19.83	36.87	18.01	35.72	17.22	36.43	16.77	34.45	15.44
36.50	19.85	37.19	18.01	36.04	17.24	36.75	16.79	34.77	15.46
36.82	19.83	37.51	18.02	36.36	17.22	37.07	16.77	35.09	15.48
37.14	19.86	37.83	18.04	36.68	17.22	37.38	16.80	35.41	15.47
37.46	19.86	38.15	18.03	37.00	17.24	37.70	16.79	35.73	15.49
37.78	19.86	38.47	18.05	37.32	17.24	38.02	16.83	36.05	15.51
38.10	19.88	38.79	18.06	37.64	17.26	38.34	16.83	36.37	15.53
38.42	19.88	39.11	18.07	37.96	17.28	38.66	16.82	36.69	15.54
38.74	19.88	39.43	18.07	38.28	17.28	38.98	16.84	37.01	15.56
39.06	19.88	39.75	18.07	38.60	17.28	39.30	16.84	37.33	15.51
39.38	19.88	40.07	18.07	38.92	17.30	39.62	16.85	37.65	15.60
39.70	19.88	40.39	18.07	39.24	17.31	39.94	16.86	37.97	15.57
40.02	19.89	40.71	18.08	39.56	17.31	40.26	16.85	38.29	15.56
40.34	19.88	41.03	18.09	39.88	17.31	40.58	16.86	38.61	15.57
40.66	19.89	41.35	18.11	40.20	17.29	40.90	16.87	38.93	15.57
40.98	19.89	41.67	18.10	40.52	17.31	41.22	16.87	39.25	15.59
41.30	19.92	41.99	18.11	40.84	17.33	41.54	16.88	39.57	15.60
41.62	19.92	42.31	18.10	41.16	17.34	41.86	16.88	39.89	15.60
41.94	19.93	42.63	18.11	41.48	17.35	42.18	16.90	40.21	15.64
42.26	19.94	42.95	18.11	41.80	17.33	42.50	16.90	40.53	15.63
42.58	19.92	43.27	18.12	42.12	17.35	42.82	16.90	40.85	15.61
42.90	19.94	43.59	18.12	42.44	17.33	43.14	16.91	41.17	15.62
43.22	19.92	43.91	18.13	42.76	17.37	43.46	16.91	41.49	15.64
43.54	19.94	44.23	18.12	43.08	17.35	43.78	16.91	41.81	15.65
43.86	19.95	44.55	18.12	43.40	17.36	44.10	16.93	42.13	15.65

Table B2 Cure characteristics of the compounds prepared at various silanization temperatures (cont.): (b) CSi

CSi_120°C		CSi_130°C		CSi_140°C		CSi_150°C		CSi_160°C	
Time (min)	Torque (dN.m)	Time (min)	Torque (dN.m)	Time (min)	Torque (dN.m)	Time (min)	Torque (dN.m)	Time (min)	Torque (dN.m)
44.18	19.95	44.87	18.13	43.72	17.38	44.42	16.93	42.45	15.66
44.50	19.94	45.19	18.13	44.04	17.38	44.74	16.93	42.77	15.66
44.82	19.94	45.51	18.12	44.36	17.36	45.06	16.93	43.09	15.67
45.14	19.94	45.83	18.14	44.68	17.37	45.38	16.95	43.41	15.67
45.46	19.94	46.15	18.15	45.00	17.38	45.70	16.95	43.73	15.68
45.78	19.96	46.47	18.16	45.32	17.38	46.02	16.97	44.05	15.68
46.10	19.95	46.79	18.16	45.64	17.40	46.34	16.99	44.37	15.69
46.42	19.96	47.11	18.16	45.96	17.38	46.66	16.98	44.69	15.70
46.74	19.95	47.43	18.17	46.28	17.39	46.98	16.98	45.01	15.70
47.06	19.95	47.75	18.17	46.60	17.39	47.30	16.98	45.33	15.70
47.38	19.95	48.07	18.18	46.92	17.41	47.62	16.99	45.65	15.71
47.70	19.97	48.39	18.16	47.24	17.40	47.94	16.99	45.97	15.72
48.02	19.97	48.71	18.17	47.56	17.40	48.26	16.97	46.29	15.72
48.34	19.97	49.03	18.17	47.88	17.42	48.58	16.98	46.61	15.72
48.66	19.97	49.35	18.18	48.20	17.41	48.90	17.00	46.93	15.73
48.98	19.96	49.67	18.18	48.52	17.42	49.22	17.01	47.25	15.74
49.30	19.98	49.99	18.20	48.84	17.42	49.54	17.01	47.57	15.73
49.62	19.96			49.16	17.42	49.86	17.01	47.93	15.74
49.98	19.98			49.48	17.41	50.00	17.01	48.25	15.75
				49.80	17.43			48.57	15.74
				49.98	17.45			48.89	15.75
								49.21	15.76
								49.53	15.76
								49.85	15.76
								49.99	15.77

Table B3 Cure characteristics of the compounds treated by various TESPT contents: (a) HDSi

HDSi_without TESPT		HDSi_6wt%		HDSi_8wt%		HDSi_10wt%		HDSi_12wt%	
Time (min)	Torque (dN.m)	Time (min)	Torque (dN.m)	Time (min)	Torque (dN.m)	Time (min)	Torque (dN.m)	Time (min)	Torque (dN.m)
0.02	1.99	0.02	1.37	0.02	2.83	0.02	2.71	0.02	2.95
0.66	12.22	0.34	2.95	0.34	2.65	0.22	2.33	0.26	2.24
1.30	12.38	0.66	3.43	0.66	3.04	0.42	2.49	0.53	2.48
1.58	12.42	0.98	3.73	0.98	3.32	0.74	2.85	0.85	2.84
1.70	12.37	1.30	3.96	1.22	3.48	1.06	3.14	1.17	3.12
2.18	12.40	1.62	4.10	1.46	3.60	1.34	3.33	1.37	3.24
2.82	12.54	1.94	4.21	1.78	3.71	1.62	3.47	1.57	3.35
3.46	12.69	2.26	4.31	2.10	3.82	1.94	3.60	1.89	3.48
4.10	12.91	2.58	4.43	2.42	3.93	2.26	3.72	2.21	3.62
4.74	13.19	2.90	4.56	2.74	4.04	2.58	3.85	2.53	3.74
5.38	13.57	3.22	4.71	3.06	4.20	2.91	4.00	2.85	3.89
6.02	14.05	3.54	4.94	3.38	4.39	3.23	4.19	3.17	4.07
6.66	14.56	3.86	5.19	3.50	4.48	3.55	4.41	3.41	4.24
7.30	15.19	4.18	5.43	3.62	4.57	3.87	4.70	3.65	4.44
7.94	15.77	4.50	5.71	3.94	4.82	4.19	5.02	3.97	4.75
8.58	16.35	4.82	6.01	4.26	5.12	4.51	5.39	4.29	5.10
9.22	16.93	5.14	6.38	4.58	5.45	4.83	5.78	4.61	5.50
9.70	17.38	5.46	6.74	4.90	5.81	5.15	6.23	4.93	5.94
10.18	17.83	5.78	7.14	5.22	6.21	5.47	6.71	5.25	6.46
10.82	18.34	6.10	7.56	5.54	6.65	5.79	7.22	5.57	7.00
11.46	18.90	6.42	8.05	5.86	7.12	6.11	7.76	5.89	7.58
12.11	19.33	6.62	8.33	6.10	7.49	6.43	8.31	6.21	8.18
12.75	19.80	6.82	8.63	6.34	7.86	6.75	8.86	6.53	8.78
13.39	20.23	7.14	9.08	6.66	8.38	7.07	9.39	6.85	9.35
14.03	20.64	7.46	9.58	6.98	8.87	7.39	9.92	7.17	9.90
14.67	20.98	7.78	10.08	7.30	9.36	7.71	10.41	7.49	10.39
15.31	21.36	8.10	10.47	7.62	9.83	8.03	10.86	7.81	10.87
15.95	21.66	8.42	10.86	7.94	10.27	8.35	11.29	8.13	11.32
16.59	21.95	8.74	11.22	8.28	10.73	8.67	11.69	8.45	11.73
17.23	22.28	9.06	11.60	8.60	11.14	8.99	12.06	8.77	12.11
17.87	22.56	9.38	11.92	8.92	11.52	9.31	12.41	9.09	12.46
18.51	22.82	9.70	12.26	9.24	11.86	9.63	12.73	9.41	12.79
19.15	23.04	10.02	12.54	9.56	12.18	9.95	13.03	9.73	13.11
19.79	23.29	10.34	12.76	9.88	12.49	10.27	13.31	10.05	13.41
20.43	23.50	10.65	13.03	10.20	12.77	10.59	13.57	10.37	13.69

Table B3 Cure characteristics of the compounds treated by various TESPT contents (cont.): (a) HDSi

HDSi_without TESPT		HDSi_6wt%		HDSi_8wt%		HDSi_10wt%		HDSi_12wt%	
Time (min)	Torque (dN.m)	Time (min)	Torque (dN.m)	Time (min)	Torque (dN.m)	Time (min)	Torque (dN.m)	Time (min)	Torque (dN.m)
21.07	23.78	10.97	13.24	10.52	13.02	10.91	13.81	10.69	13.95
21.71	23.94	11.29	13.45	10.84	13.27	11.23	14.06	11.01	14.19
22.35	24.12	11.61	13.66	11.16	13.51	11.55	14.28	11.34	14.42
22.99	24.29	11.93	13.83	11.48	13.73	11.87	14.48	11.66	14.62
23.63	24.49	12.25	14.02	11.80	13.93	12.19	14.68	11.98	14.83
24.27	24.65	12.57	14.19	12.12	14.11	12.51	14.85	12.30	15.01
24.91	24.82	12.89	14.33	12.44	14.29	12.83	15.03	12.62	15.18
25.55	24.98	13.21	14.45	12.76	14.46	13.16	15.20	12.94	15.34
26.19	25.05	13.53	14.60	13.08	14.62	13.48	15.34	13.26	15.48
26.83	25.30	13.85	14.72	13.40	14.76	13.80	15.48	13.58	15.64
27.47	25.43	14.17	14.86	13.72	14.89	14.12	15.61	13.90	15.77
28.11	25.50	14.49	14.95	14.04	15.03	14.44	15.74	14.22	15.88
28.75	25.63	14.81	15.05	14.36	15.17	14.76	15.86	14.54	16.02
29.39	25.79	15.13	15.15	14.68	15.28	15.08	15.97	14.86	16.13
30.03	25.86	15.45	15.25	15.00	15.39	15.40	16.08	15.18	16.23
30.67	25.97	15.77	15.33	15.32	15.48	15.72	16.18	15.50	16.33
31.31	26.06	16.09	15.41	15.64	15.58	16.04	16.27	15.82	16.42
31.95	26.24	16.41	15.49	15.96	15.68	16.36	16.36	16.14	16.51
32.59	26.35	16.73	15.58	16.28	15.77	16.68	16.44	16.46	16.62
33.23	26.39	17.05	15.65	16.60	15.85	17.00	16.53	16.78	16.69
33.87	26.55	17.37	15.72	16.92	15.92	17.32	16.60	17.10	16.78
34.51	26.60	17.69	15.77	17.24	16.01	17.64	16.66	17.42	16.84
35.15	26.71	18.01	15.84	17.56	16.08	17.98	16.74	17.74	16.92
35.79	26.79	18.33	15.88	17.88	16.12	18.30	16.82	18.06	16.99
36.43	26.87	18.65	15.95	18.20	16.20	18.62	16.86	18.38	17.05
37.07	27.00	18.97	15.98	18.52	16.25	18.94	16.93	18.70	17.10
37.71	27.12	19.29	16.03	18.84	16.30	19.26	16.98	19.02	17.17
38.35	27.14	19.61	16.07	19.16	16.37	19.58	17.03	19.34	17.23
38.99	27.29	19.93	16.11	19.48	16.43	19.90	17.09	19.66	17.29
39.63	27.36	20.25	16.16	19.80	16.47	20.22	17.13	19.98	17.34
40.27	27.45	20.57	16.19	20.12	16.51	20.54	17.17	20.30	17.39
40.92	27.58	20.89	16.23	20.44	16.57	20.86	17.23	20.62	17.44
41.56	27.55	21.21	16.28	20.76	16.59	21.18	17.27	20.94	17.48
42.20	27.69	21.53	16.32	21.08	16.64	21.50	17.30	21.26	17.52
42.84	27.75	21.85	16.34	21.40	16.67	21.82	17.34	21.58	17.57

Table B3 Cure characteristics of the compounds treated by various TESPT contents (cont.): (a) HDSi

HDSi_without TESPT		HDSi_6wt%		HDSi_8wt%		HDSi_10wt%		HDSi_12wt%	
Time (min)	Torque (dN.m)	Time (min)	Torque (dN.m)	Time (min)	Torque (dN.m)	Time (min)	Torque (dN.m)	Time (min)	Torque (dN.m)
43.48	27.89	22.17	16.36	21.72	16.71	22.15	17.38	21.90	17.62
44.12	27.99	22.49	16.41	22.04	16.75	22.47	17.42	22.22	17.65
44.76	28.05	22.81	16.45	22.36	16.78	22.79	17.45	22.54	17.70
45.40	28.13	23.13	16.44	22.68	16.83	23.11	17.48	22.86	17.72
46.04	28.19	23.45	16.50	23.00	16.84	23.43	17.51	23.18	17.77
46.68	28.29	23.77	16.53	23.32	16.89	23.75	17.54	23.50	17.81
47.32	28.29	24.09	16.57	23.64	16.90	24.07	17.57	23.82	17.82
47.96	28.35	24.41	16.59	23.96	16.93	24.39	17.59	24.14	17.87
48.60	28.45	24.73	16.61	24.28	16.94	24.71	17.61	24.46	17.90
49.24	28.56	25.05	16.62	24.60	16.97	25.03	17.66	24.78	17.93
49.88	28.69	25.37	16.64	24.92	17.00	25.35	17.69	25.10	17.95
50.52	28.67	25.69	16.66	25.24	17.02	25.67	17.69	25.42	17.99
51.15	28.71	26.01	16.68	25.56	17.04	25.99	17.72	25.74	18.01
51.78	28.84	26.33	16.70	25.88	17.05	26.31	17.74	26.06	18.04
52.43	28.85	26.65	16.70	26.20	17.09	26.63	17.76	26.38	18.07
53.07	28.91	26.97	16.71	26.52	17.09	26.95	17.78	26.70	18.10
53.72	28.98	27.29	16.73	26.84	17.13	27.27	17.80	27.04	18.12
54.35	29.11	27.61	16.76	27.16	17.12	27.59	17.83	27.36	18.14
54.98	29.10	27.93	16.78	27.48	17.13	27.91	17.85	27.68	18.16
55.63	29.16	28.25	16.79	27.80	17.18	28.23	17.87	28.00	18.19
56.27	29.27	28.57	16.82	28.12	17.18	28.55	17.90	28.32	18.22
56.92	29.38	28.89	16.82	28.44	17.20	28.87	17.89	28.64	18.25
57.55	29.38	29.21	16.84	28.76	17.21	29.19	17.94	28.96	18.25
58.18	29.39	29.53	16.84	29.08	17.23	29.51	17.94	29.28	18.28
58.83	29.45	29.85	16.86	29.40	17.24	29.83	17.94	29.60	18.29
59.47	29.54	30.17	16.88	29.72	17.26	30.15	17.96	29.92	18.31
60.12	29.54	30.49	16.88	30.04	17.25	30.47	17.95	30.24	18.33
60.75	29.60	30.81	16.90	30.36	17.26	30.79	17.99	30.56	18.36
61.38	29.68	31.13	16.90	30.68	17.29	31.11	18.02	30.88	18.36
62.03	29.84	31.45	16.92	31.01	17.31	31.43	18.02	31.20	18.38
62.67	29.79	31.77	16.92	31.33	17.31	31.75	18.04	31.52	18.40
63.32	29.90	32.08	16.94	31.65	17.32	32.07	18.06	31.84	18.42
63.95	29.83	32.40	16.94	31.97	17.33	32.39	18.07	32.16	18.44
64.58	29.94	32.72	16.95	32.29	17.33	32.71	18.09	32.48	18.45
65.23	30.03	33.04	16.96	32.61	17.33	33.03	18.08	32.80	18.47

Table B3 Cure characteristics of the compounds treated by various TESPT contents (cont.): (a) HDSi

HDSi_without TESPT		HDSi_6wt%		HDSi_8wt%		HDSi_10wt%		HDSi_12wt%	
Time (min)	Torque (dN.m)	Time (min)	Torque (dN.m)	Time (min)	Torque (dN.m)	Time (min)	Torque (dN.m)	Time (min)	Torque (dN.m)
65.87	30.03	33.36	16.97	32.93	17.35	33.35	18.10	33.12	18.49
66.52	30.04	33.68	16.98	33.25	17.35	33.67	18.09	33.44	18.50
67.15	30.20	34.00	17.00	33.57	17.37	33.99	18.13	33.76	18.51
67.78	30.25	34.32	17.02	33.89	17.38	34.31	18.12	34.08	18.53
68.43	30.28	34.64	17.01	34.21	17.40	34.63	18.14	34.40	18.54
69.07	30.30	34.96	17.01	34.53	17.41	34.95	18.14	34.72	18.54
69.70	30.33	35.28	17.00	34.85	17.42	35.27	18.15	35.04	18.57
70.35	30.43	35.60	17.03	35.17	17.43	35.59	18.17	35.36	18.58
70.98	30.49	35.92	17.02	35.49	17.42	35.91	18.17	35.68	18.57
71.63	30.62	36.24	17.06	35.81	17.43	36.23	18.18	36.00	18.58
72.27	30.60	36.56	17.06	36.13	17.44	36.55	18.19	36.32	18.61
72.90	30.58	36.88	17.08	36.45	17.45	36.87	18.20	36.64	18.62
73.55	30.67	37.20	17.07	36.77	17.47	37.19	18.21	36.96	18.64
74.18	30.70	37.52	17.06	37.09	17.45	37.51	18.21	37.28	18.65
74.83	30.89	37.84	17.09	37.41	17.47	37.83	18.22	37.60	18.66
75.47	30.85	38.16	17.08	37.73	17.49	38.15	18.23	37.92	18.67
76.10	30.88	38.48	17.09	38.05	17.48	38.47	18.25	38.24	18.67
76.75	30.90	38.80	17.10	38.37	17.49	38.79	18.26	38.56	18.69
77.38	30.94	39.12	17.10	38.69	17.48	39.11	18.27	38.87	18.70
78.03	30.97	39.44	17.12	39.01	17.49	39.43	18.27	39.19	18.72
78.67	31.05	39.76	17.11	39.33	17.51	39.75	18.28	39.51	18.73
79.30	31.11	40.08	17.12	39.65	17.50	40.07	18.28	39.83	18.73
79.98	31.12	40.40	17.12	39.97	17.52	40.39	18.28	40.15	18.74
		40.72	17.15	40.29	17.53	40.71	18.29	40.47	18.77
		41.04	17.14	40.61	17.53	41.03	18.29	40.79	18.78
		41.36	17.14	40.93	17.54	41.35	18.30	41.11	18.76
		41.68	17.16	41.25	17.55	41.67	18.30	41.43	18.78
		42.00	17.17	41.57	17.53	41.99	18.33	41.75	18.79
		42.32	17.16	41.89	17.54	42.31	18.35	42.07	18.81
		42.64	17.17	42.21	17.55	42.63	18.33	42.39	18.80
		42.96	17.17	42.53	17.56	42.95	18.33	42.71	18.83
		43.28	17.19	42.85	17.57	43.27	18.33	43.03	18.83
		43.60	17.18	43.17	17.56	43.59	18.35	43.35	18.84
		43.92	17.19	43.49	17.58	43.91	18.35	43.67	18.85
		44.24	17.19	43.81	17.56	44.23	18.35	43.99	18.85

Table B3 Cure characteristics of the compounds treated by various TESPT contents (cont.): (a) HDSi

HDSi_without TESPT		HDSi_6wt%		HDSi_8wt%		HDSi_10wt%		HDSi_12wt%	
Time (min)	Torque (dN.m)	Time (min)	Torque (dN.m)	Time (min)	Torque (dN.m)	Time (min)	Torque (dN.m)	Time (min)	Torque (dN.m)
		44.55	17.21	44.13	17.57	44.55	18.35	44.31	18.87
		44.87	17.20	44.45	17.58	44.87	18.39	44.63	18.89
		45.19	17.20	44.77	17.59	45.19	18.37	44.95	18.88
		45.51	17.21	45.09	17.59	45.51	18.37	45.27	18.88
		45.83	17.21	45.41	17.61	45.83	18.39	45.59	18.90
		46.15	17.22	45.73	17.60	46.15	18.38	45.91	18.91
		46.47	17.21	46.05	17.60	46.47	18.39	46.23	18.91
		46.79	17.23	46.38	17.61	46.79	18.40	46.55	18.91
		47.11	17.23	46.70	17.62	47.11	18.43	46.87	18.93
		47.43	17.23	47.02	17.61	47.43	18.40	47.19	18.95
		47.75	17.24	47.34	17.62	47.75	18.42	47.51	18.94
		48.07	17.24	47.66	17.63	48.08	18.42	47.83	18.95
		48.39	17.23	47.98	17.63	48.40	18.42	48.15	18.96
		48.71	17.25	48.30	17.63	48.72	18.43	48.47	18.97
		49.03	17.26	48.62	17.63	49.04	18.44	48.79	18.99
		49.35	17.28	48.94	17.63	49.36	18.43	49.11	18.99
		49.67	17.27	49.26	17.64	49.68	18.43	49.43	19.02
		49.99	17.27	49.58	17.63	50.00	18.44	49.75	19.01
				49.90	17.64			49.99	19.01
				50.00	17.65				

Table B4 Cure characteristics of the compounds treated by various TESPT contents: (b) CSi

CSi_without TESPT		CSi_6wt%		CSi_8wt%		CSi_10wt%		CSi_12wt%	
Time (min)	Torque (dN.m)	Time (min)	Torque (dN.m)	Time (min)	Torque (dN.m)	Time (min)	Torque (dN.m)	Time (min)	Torque (dN.m)
0.02	4.54	0.02	2.72	0.02	2.52	0.02	2.41	0.02	2.53
0.66	12.23	0.34	2.80	0.34	2.41	0.34	2.19	0.34	2.04
1.30	12.39	0.66	3.32	0.66	2.81	0.66	2.60	0.66	2.44
1.62	12.44	0.98	3.64	0.98	3.10	0.98	2.92	0.98	2.77
1.94	12.41	1.30	3.88	1.30	3.30	1.18	3.09	1.22	2.97
2.06	12.37	1.62	4.04	1.62	3.47	1.38	3.20	1.46	3.11
2.18	12.40	1.94	4.14	1.94	3.60	1.70	3.37	1.78	3.28
2.82	12.50	2.26	4.25	2.26	3.71	2.02	3.49	2.10	3.40
3.46	12.61	2.58	4.34	2.58	3.80	2.34	3.63	2.42	3.49
4.10	12.86	2.90	4.44	2.90	3.94	2.66	3.74	2.74	3.61
4.74	13.12	3.22	4.57	3.22	4.09	2.98	3.87	3.06	3.79
5.38	13.48	3.54	4.71	3.50	4.26	3.30	4.02	3.38	3.95
6.02	13.93	3.86	4.90	3.78	4.45	3.62	4.21	3.42	3.97
6.66	14.45	4.18	5.12	4.10	4.69	3.94	4.45	3.46	3.98
7.30	15.01	4.50	5.36	4.42	4.98	4.26	4.72	3.78	4.22
7.94	15.56	4.82	5.62	4.74	5.30	4.58	5.05	4.10	4.49
8.58	16.15	5.14	5.90	5.06	5.65	4.90	5.40	4.42	4.84
9.22	16.69	5.46	6.22	5.38	6.03	5.22	5.82	4.74	5.17
9.86	17.26	5.78	6.56	5.70	6.46	5.54	6.26	5.06	5.60
10.02	17.39	6.10	6.93	6.02	6.93	5.86	6.75	5.38	6.10
10.18	17.52	6.42	7.32	6.34	7.42	6.06	7.09	5.70	6.63
10.82	18.02	6.50	7.45	6.66	7.92	6.26	7.44	6.02	7.22
11.46	18.44	6.58	7.53	6.98	8.43	6.58	8.02	6.34	7.87
12.10	18.98	6.90	7.97	7.30	8.95	6.90	8.60	6.66	8.49
12.74	19.31	7.22	8.41	7.62	9.43	7.22	9.18	6.98	9.05
13.38	19.72	7.54	8.83	7.94	9.89	7.54	9.71	7.30	9.62
14.02	20.14	7.86	9.27	8.26	10.35	7.86	10.25	7.62	10.15
14.66	20.50	8.18	9.68	8.58	10.77	8.18	10.73	7.94	10.71
15.30	20.78	8.50	10.08	8.90	11.16	8.50	11.18	8.26	11.14
15.94	21.08	8.82	10.47	9.22	11.54	8.82	11.61	8.58	11.59
16.58	21.34	9.14	10.85	9.54	11.88	9.14	12.02	8.90	11.99
17.22	21.60	9.46	11.21	9.86	12.19	9.46	12.40	9.22	12.36
17.86	21.86	9.78	11.55	10.18	12.51	9.78	12.73	9.54	12.71
18.50	22.11	10.10	11.86	10.50	12.79	10.10	13.05	9.86	13.04
19.14	22.35	10.42	12.16	10.82	13.05	10.41	13.37	10.18	13.33

Table B4 Cure characteristics of the compounds treated by various TESPT contents (cont.): (b) CSi

CSi_without TESPT		CSi_6wt%		CSi_8wt%		CSi_10wt%		CSi_12wt%	
Time (min)	Torque (dN.m)	Time (min)	Torque (dN.m)	Time (min)	Torque (dN.m)	Time (min)	Torque (dN.m)	Time (min)	Torque (dN.m)
19.78	22.56	10.74	12.44	11.14	13.31	10.73	13.64	10.50	13.60
20.42	22.73	11.06	12.71	11.46	13.54	11.05	13.90	10.82	13.86
21.06	22.90	11.38	12.96	11.78	13.75	11.37	14.14	11.14	14.10
21.70	23.12	11.70	13.21	12.10	13.97	11.70	14.38	11.46	14.34
22.34	23.23	12.02	13.43	12.42	14.14	12.02	14.57	11.78	14.55
22.98	23.41	12.34	13.62	12.74	14.35	12.34	14.76	12.10	14.75
23.62	23.57	12.66	13.82	13.06	14.52	12.66	14.94	12.42	14.94
24.27	23.73	12.98	14.02	13.38	14.67	12.98	15.12	12.74	15.12
24.91	23.85	13.30	14.19	13.70	14.83	13.29	15.27	13.06	15.28
25.55	24.04	13.62	14.36	14.02	14.97	13.61	15.42	13.38	15.44
26.19	24.12	13.94	14.51	14.34	15.09	13.93	15.57	13.70	15.58
26.83	24.32	14.26	14.66	14.66	15.22	14.25	15.70	14.02	15.71
27.47	24.34	14.58	14.79	14.98	15.34	14.57	15.82	14.34	15.84
28.11	24.47	14.90	14.93	15.30	15.45	14.89	15.94	14.66	15.96
28.75	24.59	15.22	15.06	15.62	15.56	15.21	16.05	14.98	16.09
29.39	24.65	15.54	15.18	15.94	15.66	15.53	16.16	15.30	16.19
30.03	24.75	15.86	15.28	16.26	15.74	15.85	16.26	15.62	16.29
30.67	24.84	16.18	15.40	16.58	15.84	16.17	16.35	15.94	16.39
31.31	24.95	16.50	15.52	16.90	15.91	16.49	16.43	16.26	16.47
31.95	25.09	16.82	15.61	17.22	15.97	16.81	16.52	16.58	16.56
32.59	25.17	17.14	15.70	17.54	16.07	17.13	16.59	16.90	16.64
33.23	25.29	17.46	15.78	17.86	16.13	17.45	16.68	17.22	16.71
33.87	25.38	17.78	15.86	18.18	16.19	17.77	16.75	17.54	16.78
34.51	25.49	18.10	15.95	18.50	16.27	18.09	16.81	17.86	16.85
35.15	25.46	18.42	16.04	18.82	16.31	18.41	16.86	18.18	16.92
35.79	25.56	18.74	16.10	19.14	16.38	18.73	16.92	18.50	16.99
36.43	25.62	19.06	16.16	19.46	16.44	19.05	17.00	18.82	17.05
37.07	25.70	19.38	16.22	19.77	16.50	19.37	17.03	19.14	17.11
37.71	25.77	19.70	16.30	20.09	16.55	19.69	17.09	19.46	17.16
38.35	25.86	20.02	16.37	20.41	16.59	20.01	17.14	19.78	17.21
38.99	25.94	20.34	16.39	20.73	16.64	20.33	17.18	20.10	17.27
39.63	25.97	20.66	16.46	21.05	16.68	20.65	17.22	20.42	17.32
40.27	26.11	20.98	16.52	21.37	16.72	20.97	17.27	20.74	17.37
40.91	26.09	21.30	16.56	21.69	16.77	21.29	17.33	21.06	17.42
41.55	26.22	21.62	16.60	22.01	16.80	21.61	17.36	21.38	17.45

Table B4 Cure characteristics of the compounds treated by various TESPT contents (cont.): (b) CSi

CSi_without TESPT		CSi_6wt%		CSi_8wt%		CSi_10wt%		CSi_12wt%	
Time (min)	Torque (dN.m)	Time (min)	Torque (dN.m)	Time (min)	Torque (dN.m)	Time (min)	Torque (dN.m)	Time (min)	Torque (dN.m)
42.19	26.31	21.94	16.64	22.33	16.84	21.93	17.38	21.70	17.48
42.83	26.30	22.26	16.70	22.65	16.88	22.25	17.43	22.02	17.54
43.47	26.38	22.58	16.71	22.97	16.90	22.57	17.45	22.34	17.59
44.11	26.43	22.90	16.74	23.29	16.93	22.89	17.49	22.66	17.62
44.75	26.52	23.22	16.79	23.61	16.95	23.21	17.52	22.98	17.65
45.39	26.56	23.54	16.82	23.93	16.99	23.53	17.56	23.30	17.70
46.03	26.67	23.86	16.87	24.25	17.01	23.85	17.58	23.62	17.72
46.67	26.73	24.18	16.88	24.57	17.04	24.17	17.59	23.94	17.76
47.31	26.80	24.50	16.94	24.89	17.06	24.49	17.62	24.26	17.79
47.95	26.87	24.83	16.96	25.21	17.09	24.81	17.65	24.58	17.82
48.59	26.87	25.15	16.99	25.53	17.12	25.13	17.67	24.90	17.84
49.23	26.97	25.47	17.00	25.85	17.14	25.45	17.71	25.22	17.87
49.87	27.00	25.79	17.03	26.17	17.16	25.77	17.72	25.54	17.90
50.50	27.04	26.11	17.05	26.49	17.18	26.09	17.76	25.86	17.95
51.15	27.12	26.43	17.09	26.81	17.20	26.41	17.76	26.18	17.98
51.78	27.12	26.75	17.11	27.13	17.21	26.73	17.78	26.50	17.98
52.42	27.18	27.07	17.13	27.45	17.24	27.05	17.81	26.82	18.01
53.07	27.28	27.39	17.16	27.77	17.25	27.37	17.84	27.14	18.05
53.70	27.30	27.71	17.17	28.09	17.27	27.69	17.85	27.46	18.06
54.35	27.32	28.03	17.20	28.41	17.28	28.01	17.85	27.78	18.09
54.98	27.35	28.35	17.21	28.73	17.30	28.33	17.89	28.10	18.11
55.62	27.48	28.67	17.23	29.05	17.31	28.65	17.90	28.42	18.14
56.27	27.49	28.99	17.25	29.37	17.34	28.97	17.92	28.74	18.16
56.90	27.51	29.31	17.29	29.69	17.35	29.29	17.93	29.06	18.18
57.55	27.61	29.63	17.29	30.01	17.35	29.60	17.94	29.38	18.21
58.18	27.64	29.95	17.32	30.33	17.38	29.92	17.97	29.70	18.22
58.82	27.67	30.27	17.32	30.65	17.39	30.24	17.99	30.02	18.24
59.47	27.66	30.59	17.35	30.97	17.39	30.56	18.01	30.34	18.26
60.10	27.75	30.91	17.37	31.29	17.41	30.88	18.01	30.66	18.28
60.75	27.78	31.23	17.38	31.61	17.41	31.20	18.02	30.98	18.28
61.38	27.80	31.55	17.39	31.93	17.42	31.52	18.04	31.30	18.30
62.02	27.87	31.87	17.41	32.25	17.44	31.84	18.05	31.62	18.33
62.67	27.91	32.19	17.41	32.57	17.46	32.16	18.07	31.94	18.35
63.30	27.94	32.51	17.43	32.89	17.46	32.48	18.08	32.26	18.37
63.95	28.02	32.83	17.45	33.21	17.48	32.80	18.10	32.58	18.39

Table B4 Cure characteristics of the compounds treated by various TESPT contents (cont.): (b) CSi

CSi_without TESPT		CSi_6wt%		CSi_8wt%		CSi_10wt%		CSi_12wt%	
Time (min)	Torque (dN.m)	Time (min)	Torque (dN.m)	Time (min)	Torque (dN.m)	Time (min)	Torque (dN.m)	Time (min)	Torque (dN.m)
64.58	28.05	33.15	17.47	33.53	17.48	33.12	18.09	32.90	18.39
65.22	28.11	33.47	17.47	33.85	17.49	33.44	18.11	33.22	18.40
65.87	28.16	33.79	17.48	34.17	17.51	33.76	18.12	33.54	18.43
66.50	28.19	34.11	17.50	34.49	17.52	34.08	18.15	33.86	18.43
67.15	28.25	34.43	17.50	34.81	17.52	34.40	18.14	34.18	18.45
67.78	28.26	34.75	17.52	35.13	17.54	34.72	18.15	34.50	18.48
68.42	28.35	35.07	17.54	35.45	17.53	35.04	18.17	34.82	18.49
69.07	28.33	35.39	17.54	35.77	17.54	35.36	18.18	35.14	18.49
69.70	28.41	35.71	17.55	36.09	17.56	35.68	18.18	35.46	18.50
70.35	28.41	36.03	17.56	36.41	17.55	36.00	18.19	35.78	18.53
70.98	28.51	36.37	17.56	36.73	17.57	36.32	18.21	36.10	18.54
71.62	28.55	36.69	17.57	37.05	17.56	36.64	18.21	36.41	18.54
72.27	28.60	37.01	17.58	37.37	17.59	36.96	18.21	36.73	18.58
72.90	28.60	37.33	17.60	37.69	17.58	37.28	18.21	37.05	18.58
73.55	28.61	37.65	17.62	38.01	17.60	37.60	18.24	37.37	18.58
74.18	28.65	37.97	17.62	38.33	17.60	37.92	18.25	37.69	18.59
74.82	28.67	38.29	17.63	38.65	17.59	38.25	18.26	38.01	18.61
75.47	28.79	38.61	17.63	38.97	17.62	38.57	18.25	38.33	18.61
76.10	28.78	38.93	17.64	39.29	17.62	38.89	18.26	38.65	18.63
76.75	28.83	39.25	17.65	39.61	17.62	39.20	18.27	38.97	18.65
77.38	28.85	39.57	17.65	39.93	17.63	39.52	18.26	39.29	18.66
78.02	28.89	39.89	17.66	40.25	17.64	39.84	18.29	39.61	18.67
78.67	29.00	40.21	17.67	40.57	17.63	40.16	18.31	39.93	18.68
79.30	29.00	40.53	17.69	40.89	17.65	40.49	18.30	40.25	18.69
79.98	29.05	40.85	17.69	41.21	17.64	40.81	18.32	40.57	18.69
		41.17	17.69	41.53	17.66	41.13	18.30	40.89	18.71
		41.49	17.69	41.85	17.66	41.45	18.32	41.21	18.72
		41.80	17.71	42.17	17.66	41.77	18.32	41.53	18.72
		42.12	17.72	42.49	17.67	42.09	18.33	41.85	18.73
		42.44	17.70	42.81	17.67	42.41	18.34	42.17	18.74
		42.76	17.70	43.13	17.66	42.73	18.35	42.49	18.76
		43.08	17.73	43.45	17.69	43.05	18.35	42.81	18.76
		43.40	17.73	43.77	17.68	43.37	18.35	43.13	18.77
		43.72	17.74	44.09	17.68	43.69	18.35	43.45	18.76
		44.04	17.74	44.41	17.69	44.01	18.38	43.77	18.78

Table B4 Cure characteristics of the compounds treated by various TESPT contents (cont.): (b) CSi

CSi_without TESPT		CSi_6wt%		CSi_8wt%		CSi_10wt%		CSi_12wt%	
Time (min)	Torque (dN.m)	Time (min)	Torque (dN.m)	Time (min)	Torque (dN.m)	Time (min)	Torque (dN.m)	Time (min)	Torque (dN.m)
		44.36	17.74	44.73	17.70	44.33	18.37	44.09	18.81
		44.68	17.76	45.05	17.70	44.65	18.37	44.41	18.80
		45.00	17.77	45.37	17.72	44.97	18.38	44.73	18.80
		45.32	17.77	45.69	17.71	45.29	18.39	45.05	18.82
		45.64	17.77	46.01	17.71	45.61	18.39	45.37	18.83
		45.96	17.78	46.33	17.72	45.93	18.39	45.69	18.83
		46.28	17.78	46.65	17.73	46.25	18.40	46.01	18.84
		46.60	17.78	46.97	17.73	46.57	18.38	46.33	18.85
		46.92	17.79	47.29	17.73	46.89	18.42	46.65	18.85
		47.24	17.81	47.61	17.73	47.21	18.41	46.97	18.87
		47.56	17.81	47.93	17.72	47.53	18.42	47.29	18.88
		47.88	17.83	48.25	17.74	47.85	18.43	47.61	18.89
		48.20	17.82	48.57	17.75	48.17	18.43	47.93	18.87
		48.52	17.82	48.89	17.75	48.49	18.44	48.25	18.88
		48.84	17.83	49.21	17.75	48.81	18.44	48.57	18.90
		49.16	17.82	49.53	17.74	49.13	18.45	48.89	18.90
		49.48	17.83	49.85	17.75	49.45	18.45	49.21	18.92
		49.80	17.83	49.99	17.76	49.77	18.45	49.53	18.92
		49.98	17.83			49.99	18.45	49.85	18.93
								49.99	18.94

Table B5 Cure characteristics of the compounds filled with various silica/CB hybrid ratios: (a) SSBR6450SL_HDSi

SSBR6450SL											
HDSi100/CB0		HDSi80/CB20		HDSi60/CB40		HDSi40/CB60		HDSi20/CB80		Silica0/CB100	
Time (min)	Torque (dN.m)	Time (min)	Torque (dN.m)	Time (min)	Torque (dN.m)	Time (min)	Torque (dN.m)	Time (min)	Torque (dN.m)	Time (min)	Torque (dN.m)
0.02	2.68	0.02	3.25	0.02	2.76	0.02	2.46	0.02	3.89	0.02	3.57
0.22	2.47	0.34	2.48	0.34	2.35	0.34	2.46	0.34	2.57	0.34	2.74
0.42	2.67	0.66	2.66	0.66	2.41	0.50	2.45	0.66	2.54	0.62	2.70
0.74	3.03	0.98	2.85	0.98	2.53	0.66	2.48	0.98	2.57	0.90	2.74
1.06	3.29	1.30	3.00	1.30	2.63	0.98	2.55	1.30	2.62	1.22	2.76
1.34	3.47	1.62	3.10	1.62	2.72	1.30	2.61	1.64	2.66	1.54	2.78
1.62	3.61	1.94	3.20	1.94	2.78	1.62	2.69	1.96	2.68	1.86	2.83
1.94	3.75	2.26	3.28	2.26	2.85	1.94	2.72	2.28	2.73	2.18	2.87
2.26	3.89	2.58	3.38	2.58	2.92	2.26	2.76	2.60	2.77	2.50	2.92
2.58	4.03	2.70	3.44	2.90	3.02	2.58	2.82	2.92	2.83	2.82	3.00
2.90	4.20	2.82	3.48	3.22	3.12	2.90	2.88	3.24	2.90	3.14	3.10
3.22	4.43	3.14	3.62	3.54	3.27	3.22	2.94	3.56	3.01	3.46	3.27
3.26	4.47	3.46	3.79	3.86	3.44	3.54	3.05	3.88	3.15	3.78	3.54
3.30	4.50	3.78	4.03	4.18	3.67	3.86	3.18	4.20	3.33	4.10	3.98
3.62	4.79	4.10	4.31	4.50	3.94	4.18	3.34	4.52	3.58	4.42	4.71
3.94	5.11	4.42	4.63	4.82	4.24	4.50	3.55	4.85	3.92	4.74	5.69
4.26	5.47	4.74	4.97	5.14	4.59	4.82	3.82	5.17	4.33	5.06	6.67
4.58	5.89	5.06	5.37	5.46	4.97	5.14	4.14	5.33	4.57	5.38	7.50
4.90	6.35	5.38	5.77	5.78	5.37	5.42	4.45	5.49	4.81	5.46	7.70
5.22	6.84	5.70	6.25	6.10	5.79	5.70	4.78	5.81	5.34	5.54	7.89
5.54	7.39	6.02	6.73	6.42	6.21	6.02	5.18	6.13	5.85	5.86	8.56
5.58	7.47	6.34	7.23	6.74	6.67	6.34	5.60	6.45	6.39	6.18	9.12
5.62	7.54	6.66	7.69	7.06	7.12	6.66	6.02	6.77	6.92	6.50	9.64
5.94	8.12	6.98	8.22	7.22	7.34	6.98	6.46	7.09	7.42	6.82	10.05
6.26	8.71	7.30	8.71	7.38	7.56	7.30	6.90	7.17	7.53	7.14	10.42
6.58	9.29	7.62	9.14	7.70	7.96	7.62	7.30	7.25	7.65	7.46	10.74
6.90	9.86	7.94	9.59	8.02	8.35	7.94	7.69	7.57	8.08	7.78	11.02
7.22	10.40	8.26	9.98	8.34	8.72	8.26	8.06	7.89	8.46	8.10	11.27
7.54	10.88	8.58	10.39	8.66	9.08	8.58	8.41	8.21	8.82	8.42	11.47
7.86	11.37	8.90	10.70	8.98	9.39	8.90	8.73	8.53	9.13	8.74	11.64
8.18	11.82	9.22	11.05	9.30	9.71	9.22	9.03	8.85	9.44	9.06	11.81
8.50	12.22	9.54	11.35	9.62	10.01	9.54	9.31	9.17	9.68	9.38	11.95
8.82	12.60	9.86	11.64	9.94	10.28	9.86	9.56	9.49	9.92	9.70	12.09
9.14	12.98	10.18	11.90	10.26	10.52	10.18	9.80	9.81	10.14	10.02	12.21
9.46	13.31	10.50	12.15	10.58	10.76	10.50	10.03	10.13	10.36	10.34	12.31

Table B5 Cure characteristics of the compounds filled with various silica/CB hybrid ratios (cont.): (a) SSBR6450SL_HDSi

SSBR6450SL											
HDSi100/CB0		HDSi80/CB20		HDSi60/CB40		HDSi40/CB60		HDSi20/CB80		Silica0/CB100	
Time (min)	Torque (dN.m)	Time (min)	Torque (dN.m)	Time (min)	Torque (dN.m)	Time (min)	Torque (dN.m)	Time (min)	Torque (dN.m)	Time (min)	Torque (dN.m)
9.78	13.62	10.82	12.39	10.90	10.97	10.82	10.24	10.45	10.56	10.66	12.40
10.10	13.91	11.14	12.61	11.22	11.19	11.14	10.42	10.77	10.72	10.98	12.48
10.42	14.20	11.46	12.81	11.54	11.39	11.46	10.61	11.09	10.88	11.30	12.57
10.74	14.44	11.78	12.99	11.86	11.58	11.78	10.77	11.41	11.02	11.62	12.63
11.06	14.68	12.10	13.19	12.18	11.74	12.10	10.93	11.73	11.15	11.94	12.68
11.38	14.92	12.43	13.36	12.50	11.91	12.42	11.07	12.05	11.27	12.25	12.75
11.70	15.13	12.75	13.53	12.82	12.06	12.74	11.20	12.37	11.38	12.57	12.79
12.02	15.32	13.07	13.68	13.14	12.21	13.06	11.34	12.69	11.48	12.89	12.82
12.34	15.52	13.39	13.82	13.46	12.34	13.38	11.46	13.01	11.56	13.21	12.87
12.66	15.69	13.71	13.95	13.78	12.46	13.70	11.59	13.33	11.65	13.53	12.89
12.98	15.86	14.03	14.07	14.10	12.57	14.02	11.67	13.65	11.75	13.85	12.93
13.30	16.02	14.35	14.20	14.42	12.69	14.34	11.78	13.97	11.83	14.17	12.96
13.62	16.17	14.67	14.29	14.74	12.79	14.66	11.87	14.29	11.90	14.49	12.99
13.94	16.30	14.99	14.40	15.06	12.90	14.98	11.95	14.61	11.96	14.81	13.01
14.26	16.43	15.30	14.51	15.38	12.99	15.30	12.05	14.93	12.03	15.13	13.05
14.58	16.54	15.62	14.59	15.70	13.09	15.62	12.11	15.25	12.09	15.45	13.06
14.90	16.67	15.94	14.69	16.02	13.17	15.94	12.19	15.57	12.15	15.77	13.06
15.22	16.76	16.26	14.77	16.34	13.25	16.26	12.25	15.89	12.19	16.09	13.08
15.54	16.89	16.58	14.84	16.66	13.32	16.58	12.33	16.21	12.25	16.41	13.10
15.86	16.98	16.90	14.93	16.98	13.39	16.90	12.39	16.53	12.29	16.73	13.10
16.18	17.08	17.22	14.99	17.30	13.47	17.21	12.44	16.85	12.33	17.05	13.11
16.50	17.16	17.54	15.06	17.62	13.53	17.53	12.50	17.17	12.36	17.37	13.11
16.82	17.23	17.86	15.11	17.94	13.59	17.85	12.54	17.49	12.40	17.69	13.11
17.14	17.32	18.18	15.17	18.26	13.64	18.17	12.60	17.81	12.45	18.01	13.14
17.46	17.40	18.50	15.24	18.58	13.71	18.49	12.65	18.13	12.48	18.33	13.14
17.78	17.46	18.82	15.29	18.90	13.76	18.81	12.67	18.45	12.52	18.65	13.15
18.10	17.53	19.14	15.34	19.22	13.81	19.13	12.72	18.78	12.54	18.97	13.15
18.42	17.60	19.46	15.40	19.54	13.84	19.45	12.77	19.10	12.57	19.29	13.13
18.74	17.66	19.78	15.45	19.86	13.89	19.77	12.81	19.42	12.61	19.61	13.14
19.06	17.73	20.10	15.49	20.18	13.93	20.09	12.84	19.74	12.62	19.93	13.14
19.38	17.78	20.42	15.54	20.50	13.97	20.41	12.88	20.06	12.64	20.25	13.13
19.70	17.83	20.74	15.58	20.82	14.01	20.73	12.91	20.38	12.68	20.57	13.14
20.02	17.89	21.06	15.62	21.14	14.05	21.05	12.95	20.70	12.71	20.89	13.13
20.34	17.93	21.38	15.65	21.46	14.09	21.37	12.99	21.02	12.72	21.21	13.14
20.66	17.99	21.70	15.68	21.78	14.13	21.69	13.00	21.34	12.74	21.53	13.15

Table B5 Cure characteristics of the compounds filled with various silica/CB hybrid ratios (cont.): (a) SSBR6450SL_HDSi

SSBR6450SL											
HDSi100/CB0		HDSi80/CB20		HDSi60/CB40		HDSi40/CB60		HDSi20/CB80		Silica0/CB100	
Time (min)	Torque (dN.m)	Time (min)	Torque (dN.m)	Time (min)	Torque (dN.m)	Time (min)	Torque (dN.m)	Time (min)	Torque (dN.m)	Time (min)	Torque (dN.m)
20.98	18.04	22.02	15.72	22.10	14.15	22.01	13.03	21.66	12.74	21.85	13.15
21.30	18.08	22.34	15.76	22.42	14.20	22.33	13.06	21.98	12.76	22.17	13.14
21.62	18.12	22.66	15.78	22.74	14.23	22.65	13.09	22.30	12.78	22.49	13.16
21.94	18.18	22.98	15.82	23.06	14.25	22.97	13.11	22.62	12.80	22.81	13.16
22.26	18.19	23.30	15.84	23.38	14.28	23.29	13.14	22.94	12.82	23.13	13.15
22.58	18.24	23.62	15.88	23.70	14.31	23.61	13.17	23.26	12.84	23.45	13.13
22.90	18.25	23.94	15.90	24.02	14.33	23.93	13.18	23.58	12.84	23.77	13.14
23.22	18.28	24.26	15.93	24.34	14.37	24.25	13.22	23.90	12.85	24.09	13.14
23.54	18.32	24.58	15.94	24.66	14.38	24.57	13.21	24.23	12.86	24.41	13.12
23.86	18.37	24.90	15.97	24.97	14.40	24.89	13.25	24.55	12.88	24.74	13.14
24.20	18.38	25.22	15.99	25.29	14.42	25.21	13.25	24.87	12.89	25.06	13.12
24.52	18.41	25.54	16.02	25.61	14.45	25.53	13.28	25.19	12.90	25.38	13.13
24.84	18.43	25.86	16.03	25.93	14.49	25.84	13.30	25.51	12.90	25.70	13.13
25.16	18.48	26.18	16.07	26.25	14.50	26.16	13.33	25.83	12.92	26.02	13.12
25.48	18.48	26.50	16.09	26.57	14.51	26.48	13.33	26.15	12.92	26.34	13.11
25.80	18.50	26.82	16.11	26.89	14.53	26.80	13.35	26.47	12.91	26.66	13.11
26.12	18.54	27.14	16.12	27.21	14.54	27.12	13.37	26.79	12.94	26.98	13.12
26.44	18.57	27.46	16.14	27.53	14.55	27.44	13.37	27.11	12.95	27.30	13.12
26.76	18.58	27.78	16.15	27.85	14.58	27.76	13.38	27.43	12.96	27.62	13.12
27.08	18.60	28.10	16.16	28.17	14.58	28.08	13.41	27.75	12.95	27.94	13.12
27.40	18.62	28.42	16.19	28.49	14.60	28.40	13.40	28.07	12.96	28.26	13.10
27.72	18.64	28.74	16.21	28.81	14.62	28.72	13.42	28.39	12.96	28.58	13.11
28.04	18.66	29.06	16.22	29.13	14.64	29.04	13.44	28.71	12.97	28.90	13.11
28.36	18.69	29.38	16.23	29.45	14.66	29.36	13.45	29.03	12.97	29.22	13.11
28.68	18.70	29.70	16.25	29.77	14.66	29.68	13.46	29.35	12.98	29.54	13.11
29.00	18.72	30.02	16.27	30.09	14.68	30.00	13.47	29.67	12.99	29.86	13.10
29.32	18.74	30.34	16.28	30.41	14.69	30.32	13.49	29.99	13.00	30.18	13.09
29.64	18.75	30.66	16.30	30.73	14.70	30.64	13.50	30.31	13.02	30.50	13.10
29.96	18.76	30.98	16.31	31.05	14.73	30.96	13.51	30.63	13.01	30.82	13.10
30.28	18.78	31.30	16.32	31.37	14.73	31.28	13.53	30.95	13.01	31.14	13.08
30.60	18.79	31.62	16.32	31.69	14.74	31.60	13.52	31.27	13.03	31.46	13.08
30.92	18.80	31.94	16.34	32.01	14.75	31.92	13.54	31.59	13.04	31.78	13.08
31.24	18.82	32.26	16.34	32.33	14.78	32.24	13.54	31.91	13.04	32.10	13.08
31.56	18.83	32.58	16.36	32.65	14.77	32.56	13.55	32.23	13.05	32.42	13.07
31.88	18.85	32.90	16.36	32.97	14.79	32.88	13.55	32.55	13.07	32.74	13.06

Table B5 Cure characteristics of the compounds filled with various silica/CB hybrid ratios (cont.): (a) SSBR6450SL_HDSi

SSBR6450SL											
HDSi100/CB0		HDSi80/CB20		HDSi60/CB40		HDSi40/CB60		HDSi20/CB80		Silica0/CB100	
Time (min)	Torque (dN.m)	Time (min)	Torque (dN.m)	Time (min)	Torque (dN.m)	Time (min)	Torque (dN.m)	Time (min)	Torque (dN.m)	Time (min)	Torque (dN.m)
32.20	18.86	33.24	16.39	33.29	14.79	33.20	13.56	32.87	13.06	33.06	13.06
32.52	18.87	33.56	16.39	33.61	14.80	33.52	13.57	33.19	13.06	33.38	13.06
32.84	18.87	33.88	16.40	33.93	14.81	33.84	13.58	33.51	13.07	33.70	13.06
33.16	18.89	34.20	16.41	34.25	14.82	34.16	13.59	33.83	13.07	34.02	13.06
33.48	18.91	34.52	16.44	34.57	14.83	34.48	13.59	34.15	13.06	34.34	13.06
33.80	18.92	34.84	16.44	34.89	14.85	34.80	13.61	34.47	13.07	34.66	13.06
34.12	18.93	35.16	16.43	35.21	14.85	35.12	13.61	34.79	13.07	34.98	13.05
34.44	18.94	35.48	16.46	35.53	14.85	35.44	13.62	35.11	13.10	35.30	13.06
34.76	18.96	35.80	16.46	35.85	14.87	35.76	13.63	35.43	13.11	35.62	13.04
35.08	18.96	36.12	16.46	36.17	14.87	36.08	13.64	35.75	13.11	35.94	13.05
35.40	18.97	36.44	16.48	36.49	14.89	36.40	13.64	36.07	13.12	36.26	13.04
35.72	18.98	36.76	16.49	36.81	14.90	36.72	13.66	36.39	13.11	36.58	13.05
36.04	18.99	37.08	16.49	37.13	14.90	37.04	13.66	36.71	13.12	36.90	13.03
36.36	19.00	37.40	16.49	37.45	14.90	37.36	13.67	37.03	13.12	37.22	13.03
36.68	19.00	37.72	16.50	37.77	14.91	37.68	13.68	37.35	13.13	37.54	13.03
37.00	18.99	38.04	16.51	38.09	14.92	38.00	13.68	37.67	13.13	37.86	13.02
37.32	19.00	38.36	16.52	38.41	14.92	38.32	13.68	37.99	13.14	38.18	13.01
37.64	19.01	38.68	16.52	38.73	14.94	38.64	13.69	38.31	13.16	38.50	13.01
37.96	19.03	39.00	16.53	39.05	14.94	38.96	13.69	38.63	13.15	38.82	13.02
38.28	19.03	39.32	16.55	39.37	14.96	39.28	13.69	38.95	13.14	39.14	13.02
38.60	19.04	39.64	16.55	39.69	14.96	39.60	13.68	39.27	13.14	39.46	13.02
38.92	19.05	39.96	16.56	40.01	14.96	39.92	13.71	39.59	13.15	39.78	13.02
39.24	19.06	40.28	16.56	40.33	14.97	40.24	13.70	39.91	13.16	40.10	13.01
39.56	19.07	40.60	16.57	40.65	14.98	40.56	13.71	40.23	13.16	40.42	13.01
39.88	19.07	40.92	16.57	40.97	14.97	40.88	13.72	40.55	13.16	40.74	13.01
40.20	19.09	41.24	16.59	41.29	14.99	41.20	13.74	40.87	13.16	41.06	13.00
40.52	19.09	41.56	16.59	41.61	14.98	41.52	13.75	41.19	13.17	41.38	13.00
40.84	19.08	41.88	16.59	41.93	15.00	41.84	13.74	41.51	13.17	41.70	13.01
41.16	19.09	42.20	16.59	42.25	15.01	42.16	13.75	41.83	13.17	42.02	13.02
41.48	19.10	42.52	16.61	42.57	15.00	42.48	13.75	42.15	13.17	42.34	13.02
41.80	19.10	42.84	16.62	42.91	15.02	42.80	13.75	42.47	13.17	42.66	13.02
42.12	19.09	43.16	16.62	43.23	15.01	43.12	13.75	42.79	13.19	42.98	13.01
42.44	19.11	43.48	16.63	43.55	15.01	43.44	13.76	43.11	13.19	43.30	13.01
42.76	19.12	43.80	16.63	43.87	15.01	43.76	13.77	43.43	13.19	43.62	13.01
43.08	19.12	44.12	16.63	44.19	15.02	44.08	13.77	43.75	13.20	43.94	12.99

Table B5 Cure characteristics of the compounds filled with various silica/CB hybrid ratios (cont.): (a) SSBR6450SL_HDSi

SSBR6450SL											
HDSi100/CB0		HDSi80/CB20		HDSi60/CB40		HDSi40/CB60		HDSi20/CB80		Silica0/CB100	
Time (min)	Torque (dN.m)	Time (min)	Torque (dN.m)	Time (min)	Torque (dN.m)	Time (min)	Torque (dN.m)	Time (min)	Torque (dN.m)	Time (min)	Torque (dN.m)
43.40	19.14	44.44	16.64	44.51	15.04	44.40	13.77	44.07	13.19	44.26	13.00
43.72	19.13	44.76	16.64	44.83	15.05	44.72	13.78	44.39	13.20	44.58	13.00
44.04	19.15	45.08	16.65	45.15	15.06	45.04	13.79	44.71	13.21	44.90	13.01
44.36	19.15	45.40	16.64	45.47	15.06	45.36	13.80	45.03	13.20	45.22	13.01
44.68	19.14	45.72	16.65	45.79	15.07	45.68	13.81	45.35	13.21	45.54	13.00
45.00	19.16	46.04	16.65	46.11	15.07	46.00	13.80	45.67	13.20	45.86	12.98
45.32	19.15	46.36	16.67	46.43	15.07	46.32	13.80	45.99	13.20	46.18	12.96
45.64	19.17	46.68	16.67	46.75	15.06	46.64	13.81	46.31	13.21	46.50	12.96
45.96	19.16	47.00	16.69	47.07	15.07	46.96	13.81	46.63	13.22	46.82	12.97
46.28	19.17	47.32	16.68	47.39	15.09	47.28	13.82	46.95	13.22	47.14	12.99
46.60	19.20	47.64	16.67	47.71	15.08	47.60	13.82	47.27	13.22	47.46	12.98
46.92	19.18	47.96	16.69	48.03	15.09	47.92	13.84	47.59	13.23	47.78	12.98
47.24	19.19	48.28	16.69	48.34	15.09	48.24	13.84	47.91	13.23	48.10	13.00
47.56	19.19	48.60	16.69	48.66	15.09	48.56	13.84	48.23	13.23	48.42	12.98
47.88	19.19	48.92	16.69	48.98	15.10	48.88	13.85	48.55	13.24	48.74	12.97
48.20	19.20	49.24	16.71	49.30	15.10	49.20	13.85	48.87	13.24	49.06	12.98
48.52	19.21	49.56	16.72	49.62	15.12	49.52	13.86	49.19	13.24	49.38	12.97
48.84	19.21	49.88	16.72	49.98	15.12	49.84	13.85	49.51	13.24	49.70	12.97
49.16	19.21	50.00	16.71			50.00	13.86	49.83	13.25	49.98	12.97
49.48	19.21							49.99	13.26		
49.80	19.23										
50.00	19.23										

Table B6 Cure characteristics of the compounds filled with various silica/CB hybrid ratios: (b) SSBR6450SL_CSi

SSBR6450SL											
CSi100/CB0		CSi80/CB20		CSi60/CB40		CSi40/CB60		CSi20/CB80		Silica0/CB100	
Time (min)	Torque (dN.m)	Time (min)	Torque (dN.m)	Time (min)	Torque (dN.m)	Time (min)	Torque (dN.m)	Time (min)	Torque (dN.m)	Time (min)	Torque (dN.m)
0.02	2.43	0.02	1.23	0.02	3.13	0.02	2.09	0.02	3.19	0.02	3.57
0.34	2.23	0.34	2.21	0.34	2.24	0.34	2.32	0.34	2.55	0.34	2.74
0.66	2.60	0.66	2.43	0.66	2.32	0.66	2.34	0.66	2.55	0.62	2.70
0.98	2.93	0.98	2.64	0.98	2.43	0.98	2.42	0.98	2.58	0.90	2.74
1.30	3.18	1.30	2.80	1.30	2.54	1.30	2.49	1.30	2.63	1.22	2.76
1.62	3.35	1.62	2.94	1.62	2.61	1.62	2.54	1.62	2.66	1.54	2.78
1.94	3.49	1.94	3.03	1.94	2.68	1.94	2.59	1.94	2.70	1.86	2.83
2.26	3.60	2.26	3.13	2.26	2.74	2.26	2.63	2.26	2.74	2.18	2.87
2.58	3.72	2.42	3.18	2.58	2.81	2.58	2.69	2.58	2.79	2.50	2.92
2.90	3.87	2.58	3.22	2.90	2.88	2.90	2.76	2.90	2.84	2.82	3.00
3.22	4.01	2.90	3.34	3.22	2.98	3.22	2.81	3.22	2.91	3.14	3.10
3.54	4.20	3.22	3.48	3.54	3.11	3.54	2.90	3.54	3.01	3.46	3.27
3.86	4.43	3.54	3.67	3.82	3.24	3.86	3.04	3.86	3.12	3.78	3.54
4.18	4.70	3.86	3.90	4.10	3.40	4.18	3.18	4.18	3.30	4.10	3.98
4.52	5.01	4.18	4.17	4.42	3.63	4.38	3.31	4.50	3.52	4.42	4.71
4.84	5.38	4.50	4.48	4.74	3.92	4.58	3.45	4.54	3.55	4.74	5.69
5.16	5.77	4.82	4.84	5.06	4.24	4.90	3.72	4.58	3.59	5.06	6.67
5.48	6.21	5.14	5.25	5.38	4.60	5.22	4.04	4.90	3.90	5.38	7.50
5.80	6.69	5.46	5.69	5.70	5.00	5.54	4.40	5.22	4.30	5.46	7.70
6.12	7.23	5.78	6.17	6.02	5.40	5.86	4.79	5.54	4.77	5.54	7.89
6.44	7.75	6.10	6.69	6.34	5.82	6.18	5.16	5.86	5.26	5.86	8.56
6.76	8.32	6.42	7.20	6.66	6.27	6.50	5.60	6.18	5.77	6.18	9.12
7.08	8.90	6.74	7.72	6.98	6.71	6.82	6.00	6.50	6.29	6.50	9.64
7.40	9.46	7.06	8.24	7.30	7.16	7.14	6.44	6.82	6.79	6.82	10.05
7.72	9.99	7.38	8.73	7.38	7.26	7.46	6.84	7.14	7.27	7.14	10.42
8.04	10.50	7.70	9.19	7.46	7.37	7.78	7.24	7.46	7.72	7.46	10.74
8.36	10.97	8.02	9.63	7.78	7.79	8.10	7.61	7.78	8.11	7.78	11.02
8.68	11.42	8.34	10.05	8.10	8.18	8.42	7.95	8.09	8.47	8.10	11.27
9.00	11.84	8.66	10.43	8.42	8.56	8.74	8.28	8.41	8.80	8.42	11.47
9.32	12.23	8.98	10.79	8.74	8.90	9.06	8.59	8.73	9.11	8.74	11.64
9.64	12.59	9.30	11.15	9.06	9.23	9.38	8.86	9.05	9.37	9.06	11.81
9.96	12.94	9.62	11.45	9.38	9.54	9.70	9.12	9.37	9.63	9.38	11.95
10.28	13.24	9.94	11.75	9.70	9.81	10.02	9.37	9.69	9.86	9.70	12.09
10.60	13.53	10.26	12.04	10.02	10.07	10.34	9.60	10.01	10.06	10.02	12.21
10.92	13.82	10.58	12.27	10.34	10.32	10.66	9.81	10.33	10.24	10.34	12.31

Table B6 Cure characteristics of the compounds filled with various silica/CB hybrid ratios (cont.): (b) SSBR6450SL_CSi

SSBR6450SL											
CSi100/CB0		CSi80/CB20		CSi60/CB40		CSi40/CB60		CSi20/CB80		Silica0/CB100	
Time (min)	Torque (dN.m)	Time (min)	Torque (dN.m)	Time (min)	Torque (dN.m)	Time (min)	Torque (dN.m)	Time (min)	Torque (dN.m)	Time (min)	Torque (dN.m)
11.24	14.07	10.90	12.52	10.66	10.55	10.98	9.99	10.65	10.41	10.66	12.40
11.56	14.31	11.22	12.75	10.98	10.77	11.30	10.18	10.97	10.59	10.98	12.48
11.88	14.54	11.54	12.95	11.30	10.96	11.62	10.36	11.29	10.73	11.30	12.57
12.20	14.74	11.86	13.15	11.62	11.17	11.94	10.50	11.61	10.87	11.62	12.63
12.52	14.94	12.18	13.32	11.94	11.33	12.26	10.66	11.93	10.99	11.94	12.68
12.84	15.14	12.50	13.49	12.26	11.52	12.58	10.81	12.25	11.11	12.25	12.75
13.16	15.31	12.82	13.65	12.58	11.67	12.90	10.93	12.57	11.22	12.57	12.79
13.48	15.48	13.14	13.79	12.90	11.80	13.22	11.05	12.89	11.30	12.89	12.82
13.80	15.64	13.46	13.93	13.22	11.94	13.54	11.16	13.21	11.41	13.21	12.87
14.12	15.77	13.80	14.08	13.54	12.08	13.86	11.27	13.53	11.49	13.53	12.89
14.44	15.91	14.12	14.22	13.86	12.20	14.18	11.38	13.85	11.58	13.85	12.93
14.76	16.04	14.44	14.31	14.18	12.31	14.50	11.46	14.17	11.65	14.17	12.96
15.08	16.16	14.76	14.41	14.50	12.41	14.82	11.55	14.49	11.70	14.49	12.99
15.40	16.28	15.08	14.52	14.82	12.52	15.14	11.63	14.81	11.78	14.81	13.01
15.72	16.38	15.40	14.62	15.14	12.61	15.46	11.72	15.13	11.83	15.13	13.05
16.04	16.49	15.72	14.70	15.46	12.70	15.78	11.79	15.47	11.91	15.45	13.06
16.36	16.60	16.04	14.80	15.78	12.79	16.10	11.86	15.79	11.96	15.77	13.06
16.68	16.69	16.36	14.87	16.10	12.87	16.41	11.92	16.11	12.01	16.09	13.08
17.00	16.77	16.68	14.97	16.42	12.97	16.73	12.00	16.43	12.06	16.41	13.10
17.31	16.85	17.00	15.01	16.74	13.03	17.05	12.05	16.75	12.10	16.73	13.10
17.63	16.93	17.32	15.09	17.06	13.08	17.37	12.11	17.07	12.14	17.05	13.11
17.95	17.00	17.64	15.15	17.38	13.14	17.69	12.17	17.39	12.18	17.37	13.11
18.27	17.08	17.96	15.21	17.70	13.21	18.01	12.19	17.71	12.22	17.69	13.11
18.59	17.13	18.28	15.25	18.02	13.27	18.33	12.26	18.03	12.26	18.01	13.14
18.91	17.20	18.59	15.32	18.34	13.32	18.65	12.28	18.35	12.29	18.33	13.14
19.23	17.26	18.91	15.37	18.66	13.37	18.97	12.34	18.66	12.33	18.65	13.15
19.55	17.33	19.23	15.42	18.98	13.42	19.29	12.37	18.98	12.35	18.97	13.15
19.87	17.38	19.55	15.45	19.30	13.48	19.61	12.42	19.30	12.38	19.29	13.13
20.19	17.43	19.87	15.50	19.62	13.51	19.93	12.45	19.62	12.40	19.61	13.14
20.51	17.48	20.19	15.53	19.94	13.56	20.25	12.49	19.94	12.42	19.93	13.14
20.83	17.53	20.51	15.58	20.26	13.60	20.57	12.52	20.26	12.45	20.25	13.13
21.15	17.57	20.83	15.61	20.58	13.64	20.89	12.55	20.58	12.48	20.57	13.14
21.47	17.61	21.15	15.64	20.90	13.67	21.21	12.58	20.90	12.51	20.89	13.13
21.79	17.64	21.47	15.69	21.22	13.71	21.53	12.62	21.22	12.52	21.21	13.14
22.11	17.69	21.79	15.73	21.54	13.75	21.85	12.65	21.54	12.55	21.53	13.15

Table B6 Cure characteristics of the compounds filled with various silica/CB hybrid ratios (cont.): (b) SSBR6450SL_CSi

SSBR6450SL											
CSi100/CB0		CSi80/CB20		CSi60/CB40		CSi40/CB60		CSi20/CB80		Silica0/CB100	
Time (min)	Torque (dN.m)	Time (min)	Torque (dN.m)	Time (min)	Torque (dN.m)	Time (min)	Torque (dN.m)	Time (min)	Torque (dN.m)	Time (min)	Torque (dN.m)
22.43	17.73	22.11	15.77	21.86	13.77	22.17	12.67	21.86	12.57	21.85	13.15
22.75	17.76	22.43	15.80	22.18	13.81	22.49	12.69	22.18	12.57	22.17	13.14
23.07	17.79	22.75	15.82	22.50	13.84	22.81	12.72	22.50	12.60	22.49	13.16
23.39	17.82	23.07	15.83	22.82	13.87	23.13	12.73	22.82	12.61	22.81	13.16
23.71	17.86	23.39	15.87	23.14	13.88	23.45	12.76	23.14	12.63	23.13	13.15
24.03	17.90	23.71	15.89	23.46	13.92	23.77	12.77	23.46	12.64	23.45	13.13
24.35	17.93	24.03	15.92	23.78	13.94	24.09	12.81	23.78	12.67	23.77	13.14
24.67	17.95	24.35	15.93	24.10	13.96	24.41	12.83	24.10	12.68	24.09	13.14
24.99	17.96	24.67	15.97	24.42	13.99	24.73	12.85	24.42	12.70	24.41	13.12
25.31	18.00	24.99	15.99	24.74	14.03	25.05	12.87	24.74	12.71	24.74	13.14
25.63	18.03	25.31	16.00	25.06	14.04	25.37	12.87	25.06	12.71	25.06	13.12
25.95	18.06	25.63	16.03	25.38	14.06	25.69	12.88	25.38	12.72	25.38	13.13
26.27	18.07	25.95	16.04	25.70	14.08	26.01	12.90	25.70	12.73	25.70	13.13
26.59	18.09	26.27	16.07	26.02	14.09	26.33	12.91	26.02	12.73	26.02	13.12
26.91	18.11	26.59	16.07	26.33	14.11	26.65	12.93	26.34	12.74	26.34	13.11
27.23	18.14	26.91	16.10	26.65	14.13	26.97	12.95	26.66	12.76	26.66	13.11
27.55	18.16	27.23	16.11	26.97	14.17	27.29	12.96	26.98	12.77	26.98	13.12
27.87	18.17	27.55	16.14	27.29	14.17	27.61	12.97	27.30	12.79	27.30	13.12
28.19	18.20	27.87	16.14	27.61	14.20	27.93	12.98	27.62	12.78	27.62	13.12
28.51	18.22	28.19	16.16	27.93	14.21	28.25	12.99	27.94	12.80	27.94	13.12
28.83	18.23	28.51	16.17	28.25	14.22	28.57	13.00	28.26	12.81	28.26	13.10
29.15	18.25	28.83	16.18	28.57	14.23	28.89	13.02	28.58	12.81	28.58	13.11
29.47	18.27	29.15	16.21	28.89	14.26	29.21	13.03	28.90	12.83	28.90	13.11
29.79	18.27	29.47	16.22	29.21	14.27	29.53	13.04	29.22	12.83	29.22	13.11
30.11	18.29	29.79	16.23	29.53	14.28	29.85	13.05	29.54	12.84	29.54	13.11
30.43	18.32	30.11	16.24	29.85	14.29	30.17	13.07	29.86	12.85	29.86	13.10
30.75	18.33	30.43	16.24	30.17	14.32	30.49	13.09	30.18	12.86	30.18	13.09
31.07	18.34	30.75	16.26	30.49	14.31	30.81	13.11	30.50	12.86	30.50	13.10
31.39	18.36	31.07	16.27	30.81	14.33	31.13	13.10	30.82	12.86	30.82	13.10
31.71	18.37	31.39	16.30	31.13	14.35	31.45	13.11	31.14	12.89	31.14	13.08
32.03	18.37	31.71	16.30	31.45	14.35	31.77	13.11	31.46	12.90	31.46	13.08
32.35	18.39	32.03	16.30	31.77	14.36	32.09	13.12	31.78	12.89	31.78	13.08
32.67	18.40	32.35	16.32	32.09	14.37	32.41	13.14	32.10	12.89	32.10	13.08
32.99	18.41	32.67	16.33	32.41	14.39	32.72	13.15	32.42	12.90	32.42	13.07
33.31	18.42	32.99	16.34	32.73	14.40	33.04	13.15	32.74	12.90	32.74	13.06

Table B6 Cure characteristics of the compounds filled with various silica/CB hybrid ratios (cont.): (b) SSBR6450SL_CSi

SSBR6450SL											
CSi100/CB0		CSi80/CB20		CSi60/CB40		CSi40/CB60		CSi20/CB80		Silica0/CB100	
Time (min)	Torque (dN.m)	Time (min)	Torque (dN.m)	Time (min)	Torque (dN.m)	Time (min)	Torque (dN.m)	Time (min)	Torque (dN.m)	Time (min)	Torque (dN.m)
33.63	18.45	33.31	16.35	33.05	14.41	33.38	13.16	33.06	12.91	33.06	13.06
33.95	18.46	33.63	16.35	33.37	14.41	33.70	13.18	33.38	12.92	33.38	13.06
34.27	18.46	33.95	16.36	33.69	14.43	34.02	13.18	33.70	12.94	33.70	13.06
34.59	18.47	34.27	16.37	34.01	14.44	34.34	13.18	34.02	12.92	34.02	13.06
34.91	18.47	34.59	16.38	34.33	14.44	34.66	13.21	34.34	12.93	34.34	13.06
35.23	18.48	34.91	16.39	34.65	14.47	34.98	13.19	34.66	12.94	34.66	13.06
35.55	18.50	35.23	16.40	34.97	14.46	35.30	13.21	34.98	12.95	34.98	13.05
35.87	18.53	35.55	16.40	35.29	14.47	35.62	13.21	35.30	12.96	35.30	13.06
36.19	18.51	35.87	16.44	35.61	14.46	35.94	13.23	35.62	12.97	35.62	13.04
36.51	18.52	36.19	16.43	35.93	14.48	36.26	13.23	35.94	12.97	35.94	13.05
36.83	18.52	36.51	16.43	36.25	14.48	36.58	13.23	36.26	12.99	36.26	13.04
37.15	18.53	36.83	16.44	36.57	14.49	36.90	13.23	36.58	12.99	36.58	13.05
37.47	18.54	37.15	16.44	36.89	14.49	37.22	13.24	36.90	12.97	36.90	13.03
37.79	18.55	37.47	16.45	37.21	14.51	37.54	13.26	37.22	12.99	37.22	13.03
38.11	18.57	37.79	16.46	37.53	14.52	37.86	13.25	37.54	12.98	37.54	13.03
38.43	18.57	38.11	16.47	37.85	14.53	38.18	13.26	37.86	12.99	37.86	13.02
38.75	18.57	38.43	16.48	38.17	14.53	38.50	13.27	38.18	13.00	38.18	13.01
39.07	18.59	38.75	16.49	38.49	14.53	38.82	13.27	38.49	13.00	38.50	13.01
39.39	18.59	39.07	16.48	38.81	14.56	39.14	13.28	38.81	13.00	38.82	13.02
39.71	18.59	39.39	16.49	39.13	14.56	39.46	13.28	39.13	13.00	39.14	13.02
40.03	18.58	39.71	16.52	39.45	14.56	39.78	13.29	39.45	13.01	39.46	13.02
40.35	18.61	40.03	16.52	39.77	14.57	40.10	13.30	39.77	13.01	39.78	13.02
40.67	18.62	40.35	16.52	40.09	14.57	40.42	13.31	40.09	13.02	40.10	13.01
40.99	18.64	40.67	16.52	40.41	14.58	40.74	13.32	40.41	13.02	40.42	13.01
41.31	18.64	40.99	16.53	40.73	14.60	41.06	13.31	40.73	13.05	40.74	13.01
41.63	18.63	41.31	16.54	41.05	14.61	41.38	13.32	41.05	13.06	41.06	13.00
41.95	18.64	41.63	16.55	41.37	14.60	41.70	13.33	41.37	13.05	41.38	13.00
42.27	18.65	41.95	16.54	41.69	14.60	42.02	13.32	41.69	13.05	41.70	13.01
42.59	18.66	42.27	16.55	42.01	14.62	42.34	13.33	42.01	13.05	42.02	13.02
42.91	18.67	42.59	16.57	42.33	14.63	42.66	13.34	42.33	13.06	42.34	13.02
43.23	18.67	42.91	16.56	42.65	14.62	42.98	13.34	42.65	13.06	42.66	13.02
43.55	18.67	43.23	16.57	42.97	14.62	43.30	13.34	42.97	13.08	42.98	13.01
43.87	18.67	43.55	16.58	43.29	14.62	43.62	13.36	43.29	13.08	43.30	13.01
44.19	18.69	43.87	16.58	43.61	14.64	43.94	13.36	43.61	13.07	43.62	13.01
44.51	18.68	44.19	16.59	43.93	14.62	44.25	13.36	43.93	13.07	43.94	12.99

Table B6 Cure characteristics of the compounds filled with various silica/CB hybrid ratios (cont.): (b) SSBR6450SL_CSi

SSBR6450SL											
CSi100/CB0		CSi80/CB20		CSi60/CB40		CSi40/CB60		CSi20/CB80		Silica0/CB100	
Time (min)	Torque (dN.m)	Time (min)	Torque (dN.m)	Time (min)	Torque (dN.m)	Time (min)	Torque (dN.m)	Time (min)	Torque (dN.m)	Time (min)	Torque (dN.m)
44.83	18.68	44.51	16.59	44.25	14.65	44.57	13.36	44.25	13.08	44.26	13.00
45.15	18.69	44.83	16.59	44.57	14.65	44.89	13.38	44.57	13.09	44.58	13.00
45.47	18.70	45.15	16.60	44.89	14.65	45.21	13.38	44.89	13.09	44.90	13.01
45.79	18.71	45.47	16.60	45.21	14.67	45.53	13.38	45.21	13.08	45.22	13.01
46.11	18.71	45.79	16.61	45.53	14.66	45.85	13.38	45.53	13.09	45.54	13.00
46.43	18.70	46.11	16.60	45.85	14.68	46.17	13.40	45.85	13.09	45.86	12.98
46.75	18.72	46.43	16.61	46.17	14.68	46.49	13.39	46.17	13.10	46.18	12.96
47.07	18.71	46.75	16.62	46.49	14.68	46.81	13.39	46.49	13.10	46.50	12.96
47.39	18.72	47.07	16.63	46.81	14.69	47.13	13.40	46.81	13.10	46.82	12.97
47.71	18.73	47.39	16.62	47.13	14.68	47.45	13.41	47.13	13.10	47.14	12.99
48.03	18.73	47.71	16.62	47.45	14.70	47.77	13.41	47.45	13.10	47.46	12.98
48.35	18.74	48.03	16.64	47.77	14.70	48.09	13.42	47.77	13.12	47.78	12.98
48.67	18.72	48.35	16.64	48.09	14.70	48.41	13.42	48.09	13.11	48.10	13.00
48.99	18.74	48.67	16.65	48.41	14.70	48.73	13.43	48.41	13.11	48.42	12.98
49.31	18.76	48.99	16.66	48.73	14.72	49.05	13.42	48.73	13.12	48.74	12.97
49.63	18.75	49.31	16.65	49.05	14.73	49.37	13.43	49.05	13.14	49.06	12.98
49.99	18.76	49.63	16.66	49.37	14.72	49.69	13.44	49.37	13.13	49.38	12.97
		49.99	16.65	49.69	14.72	49.99	13.45	49.69	13.14	49.70	12.97
				49.99	14.72			49.99	13.13	49.98	12.97

Table B7 Cure characteristics of the compounds filled with various silica/CB hybrid ratios: (c) SSBR3626_HDSi

SSBR3626											
HDSi100/CB0		**HDSi80/CB20**		**HDSi60/CB40**		**HDSi40/CB60**		**HDSi20/CB80**		**Silica0/CB100**	
Time (min)	**Torque (dN.m)**	**Time (min)**	**Torque (dN.m)**	**Time (min)**	**Torque (dN.m)**	**Time (min)**	**Torque (dN.m)**	**Time (min)**	**Torque (dN.m)**	**Time (min)**	**Torque (dN.m)**
0.02	1.86	0.02	1.53	0.02	3.07	0.02	0.88	0.02	3.69	0.02	1.59
0.34	2.32	0.34	2.17	0.34	2.16	0.34	2.31	0.34	2.56	0.34	2.61
0.66	2.59	0.66	2.29	0.50	2.14	0.66	2.27	0.66	2.49	0.62	2.55
0.98	2.84	0.98	2.46	0.66	2.18	0.70	2.26	0.98	2.52	0.90	2.59
1.30	3.05	1.30	2.62	0.98	2.28	0.74	2.28	1.30	2.56	1.22	2.64
1.62	3.22	1.62	2.74	1.30	2.40	1.06	2.34	1.62	2.62	1.54	2.68
1.78	3.29	1.94	2.84	1.62	2.48	1.38	2.41	1.94	2.68	1.86	2.75
1.94	3.37	2.26	2.95	1.94	2.57	1.70	2.48	2.26	2.72	2.18	2.79
2.26	3.52	2.58	3.10	2.26	2.66	2.02	2.54	2.58	2.79	2.50	2.88
2.58	3.69	2.74	3.19	2.58	2.75	2.34	2.60	2.90	2.89	2.82	2.98
2.90	3.91	2.90	3.27	2.90	2.86	2.66	2.68	3.22	3.00	3.14	3.13
3.22	4.19	3.22	3.50	3.22	3.03	2.98	2.78	3.54	3.16	3.46	3.36
3.34	4.30	3.54	3.77	3.54	3.24	3.30	2.92	3.86	3.39	3.78	3.77
3.46	4.43	3.86	4.10	3.86	3.53	3.62	3.10	4.18	3.72	4.10	4.45
3.78	4.80	4.18	4.50	4.18	3.86	3.82	3.26	4.50	4.15	4.14	4.55
4.10	5.22	4.50	4.88	4.42	4.15	4.02	3.44	4.82	4.65	4.18	4.68
4.42	5.68	4.82	5.46	4.66	4.46	4.34	3.77	5.14	5.19	4.50	5.65
4.74	6.21	5.14	6.01	4.98	4.91	4.66	4.14	5.46	5.77	4.82	6.64
5.06	6.79	5.46	6.57	5.30	5.39	4.74	4.26	5.78	6.33	5.14	7.52
5.38	7.42	5.78	7.18	5.62	5.90	4.82	4.35	6.10	6.91	5.46	8.27
5.70	8.07	6.10	7.76	5.94	6.42	5.14	4.79	6.42	7.44	5.78	8.93
6.02	8.73	6.42	8.33	6.26	6.93	5.46	5.25	6.74	7.95	6.10	9.49
6.34	9.35	6.74	8.87	6.58	7.43	5.78	5.72	7.06	8.41	6.42	9.97
6.66	9.96	7.06	9.37	6.90	7.92	6.10	6.22	7.38	8.82	6.74	10.39
6.99	10.50	7.38	9.84	7.22	8.37	6.42	6.71	7.70	9.20	7.06	10.73
7.31	11.03	7.70	10.28	7.54	8.79	6.74	7.20	8.02	9.55	7.38	11.04
7.63	11.52	8.02	10.67	7.86	9.18	7.06	7.64	8.34	9.87	7.70	11.34
7.95	11.98	8.34	11.04	8.18	9.54	7.38	8.08	8.66	10.15	8.02	11.57
8.27	12.39	8.66	11.39	8.50	9.87	7.70	8.49	8.98	10.42	8.34	11.78
8.59	12.78	8.98	11.72	8.82	10.18	8.02	8.86	9.30	10.65	8.66	11.97
8.91	13.15	9.30	12.01	9.14	10.47	8.34	9.19	9.62	10.87	8.98	12.13
9.23	13.49	9.62	12.30	9.46	10.75	8.66	9.51	9.94	11.07	9.30	12.27
9.55	13.82	9.94	12.55	9.78	11.00	8.98	9.81	10.26	11.26	9.63	12.40
9.87	14.11	10.26	12.81	10.10	11.22	9.30	10.05	10.58	11.42	9.95	12.52
10.19	14.38	10.58	13.03	10.42	11.43	9.62	10.30	10.90	11.56	10.27	12.63

Table B7 Cure characteristics of the compounds filled with various silica/CB hybrid ratios (cont.): (c) SSBR3626_HDSi

SSBR3626											
HDSi100/CB0		HDSi80/CB20		HDSi60/CB40		HDSi40/CB60		HDSi20/CB80		Silica0/CB100	
Time (min)	Torque (dN.m)	Time (min)	Torque (dN.m)	Time (min)	Torque (dN.m)	Time (min)	Torque (dN.m)	Time (min)	Torque (dN.m)	Time (min)	Torque (dN.m)
10.51	14.66	10.90	13.23	10.74	11.65	9.94	10.55	11.22	11.70	10.59	12.71
10.83	14.90	11.22	13.43	11.06	11.84	10.26	10.78	11.54	11.83	10.91	12.80
11.15	15.15	11.54	13.62	11.38	12.03	10.58	10.98	11.86	11.95	11.23	12.88
11.47	15.37	11.86	13.80	11.70	12.20	10.90	11.18	12.18	12.08	11.55	12.94
11.79	15.57	12.18	13.95	12.02	12.36	11.22	11.34	12.50	12.19	11.87	13.00
12.11	15.76	12.50	14.11	12.34	12.50	11.54	11.51	12.82	12.29	12.19	13.07
12.43	15.94	12.82	14.26	12.66	12.64	11.86	11.66	13.14	12.37	12.51	13.11
12.75	16.09	13.14	14.38	12.98	12.78	12.18	11.80	13.46	12.45	12.83	13.15
13.07	16.24	13.46	14.51	13.30	12.90	12.50	11.94	13.78	12.53	13.15	13.16
13.39	16.43	13.78	14.64	13.62	13.01	12.82	12.07	14.10	12.60	13.47	13.21
13.71	16.53	14.10	14.74	13.94	13.10	13.14	12.19	14.42	12.68	13.79	13.25
14.03	16.70	14.42	14.85	14.26	13.20	13.46	12.32	14.74	12.75	14.11	13.29
14.35	16.84	14.74	14.95	14.58	13.30	13.78	12.41	15.06	12.81	14.43	13.33
14.67	16.92	15.06	15.06	14.90	13.39	14.10	12.49	15.38	12.88	14.75	13.35
14.99	17.05	15.38	15.14	15.22	13.48	14.42	12.58	15.70	12.93	15.07	13.38
15.31	17.15	15.70	15.21	15.54	13.55	14.74	12.65	16.02	12.97	15.39	13.39
15.63	17.26	16.02	15.29	15.86	13.63	15.06	12.75	16.34	13.02	15.71	13.41
15.95	17.35	16.34	15.37	16.18	13.70	15.38	12.83	16.66	13.06	16.03	13.43
16.27	17.46	16.66	15.44	16.50	13.78	15.70	12.90	16.98	13.11	16.35	13.43
16.59	17.54	16.98	15.50	16.82	13.83	16.02	12.98	17.30	13.15	16.67	13.46
16.91	17.61	17.30	15.58	17.14	13.90	16.34	13.03	17.62	13.19	16.99	13.47
17.23	17.70	17.62	15.63	17.46	13.94	16.66	13.07	17.94	13.23	17.31	13.47
17.55	17.77	17.94	15.68	17.78	14.00	16.98	13.11	18.26	13.25	17.63	13.47
17.87	17.84	18.26	15.73	18.10	14.05	17.30	13.18	18.58	13.29	17.95	13.49
18.19	17.91	18.58	15.79	18.42	14.09	17.62	13.24	18.90	13.32	18.27	13.50
18.51	17.98	18.90	15.84	18.74	14.15	17.94	13.29	19.22	13.36	18.59	13.49
18.83	18.01	19.22	15.88	19.06	14.18	18.26	13.34	19.54	13.38	18.91	13.51
19.15	18.10	19.54	15.93	19.38	14.23	18.58	13.38	19.86	13.41	19.23	13.52
19.47	18.16	19.86	15.98	19.70	14.27	18.90	13.42	20.18	13.44	19.55	13.52
19.79	18.22	20.18	16.02	20.02	14.31	19.22	13.47	20.50	13.45	19.87	13.52
20.11	18.27	20.50	16.06	20.34	14.35	19.54	13.51	20.82	13.47	20.19	13.52
20.43	18.29	20.82	16.11	20.66	14.38	19.86	13.52	21.14	13.48	20.51	13.52
20.74	18.35	21.14	16.14	20.98	14.41	20.18	13.57	21.46	13.50	20.83	13.51
21.06	18.40	21.46	16.17	21.30	14.45	20.50	13.61	21.78	13.53	21.15	13.54
21.38	18.45	21.78	16.22	21.62	14.47	20.82	13.65	22.10	13.56	21.47	13.55

Table B7 Cure characteristics of the compounds filled with various silica/CB hybrid ratios (cont.): (c) SSBR3626_HDSi

SSBR3626											
HDSi100/CB0		HDSi80/CB20		HDSi60/CB40		HDSi40/CB60		HDSi20/CB80		Silica0/CB100	
Time (min)	Torque (dN.m)	Time (min)	Torque (dN.m)	Time (min)	Torque (dN.m)	Time (min)	Torque (dN.m)	Time (min)	Torque (dN.m)	Time (min)	Torque (dN.m)
21.70	18.51	22.10	16.25	21.94	14.51	21.14	13.67	22.42	13.58	21.79	13.55
22.02	18.55	22.42	16.28	22.26	14.54	21.46	13.71	22.74	13.59	22.11	13.54
22.34	18.58	22.74	16.32	22.58	14.57	21.78	13.71	23.06	13.61	22.43	13.54
22.66	18.63	23.06	16.34	22.90	14.59	22.10	13.79	23.38	13.63	22.75	13.54
22.98	18.66	23.38	16.36	23.22	14.62	22.42	13.77	23.70	13.64	23.07	13.54
23.30	18.70	23.70	16.38	23.54	14.65	22.74	13.81	24.02	13.66	23.39	13.55
23.62	18.74	24.02	16.40	23.86	14.66	23.06	13.82	24.34	13.68	23.71	13.54
23.94	18.78	24.34	16.45	24.18	14.68	23.38	13.85	24.66	13.70	24.03	13.55
24.26	18.80	24.66	16.47	24.49	14.70	23.70	13.87	24.98	13.71	24.35	13.54
24.58	18.82	24.98	16.47	24.81	14.73	24.02	13.90	25.30	13.71	24.67	13.54
24.90	18.84	25.30	16.52	25.13	14.75	24.34	13.93	25.62	13.73	24.99	13.55
25.22	18.88	25.62	16.52	25.45	14.77	24.66	13.93	25.94	13.74	25.31	13.55
25.54	18.92	25.94	16.56	25.77	14.77	24.98	13.97	26.26	13.75	25.63	13.54
25.86	18.94	26.26	16.58	26.09	14.81	25.30	13.98	26.58	13.75	25.95	13.56
26.18	18.97	26.58	16.61	26.41	14.83	25.62	14.00	26.90	13.77	26.27	13.55
26.50	18.98	26.90	16.64	26.73	14.85	25.94	14.00	27.22	13.78	26.59	13.55
26.82	19.02	27.22	16.64	27.05	14.87	26.26	14.02	27.54	13.78	26.91	13.55
27.14	19.04	27.54	16.66	27.37	14.87	26.58	14.03	27.86	13.79	27.23	13.55
27.46	19.07	27.86	16.67	27.69	14.90	26.90	14.06	28.18	13.80	27.55	13.54
27.78	19.08	28.18	16.70	28.01	14.89	27.22	14.06	28.50	13.82	27.86	13.55
28.10	19.10	28.50	16.72	28.33	14.91	27.54	14.10	28.82	13.82	28.18	13.54
28.42	19.14	28.82	16.72	28.65	14.94	27.86	14.11	29.14	13.84	28.50	13.55
28.74	19.14	29.14	16.73	28.97	14.95	28.18	14.11	29.46	13.86	28.82	13.56
29.06	19.16	29.46	16.76	29.29	14.98	28.50	14.14	29.78	13.86	29.14	13.54
29.38	19.18	29.78	16.77	29.61	14.98	28.81	14.15	30.10	13.87	29.46	13.53
29.70	19.19	30.10	16.78	29.93	15.00	29.13	14.16	30.42	13.86	29.78	13.55
30.02	19.22	30.42	16.82	30.25	15.00	29.45	14.16	30.74	13.88	30.10	13.55
30.34	19.26	30.74	16.82	30.57	15.02	29.77	14.17	31.06	13.89	30.42	13.53
30.66	19.25	31.06	16.82	30.89	15.03	30.09	14.20	31.38	13.90	30.74	13.54
30.98	19.26	31.38	16.84	31.21	15.04	30.41	14.21	31.70	13.90	31.06	13.56
31.30	19.28	31.70	16.85	31.53	15.06	30.73	14.21	32.02	13.92	31.38	13.56
31.62	19.30	32.02	16.87	31.85	15.07	31.05	14.22	32.34	13.92	31.70	13.55
31.94	19.32	32.34	16.89	32.17	15.07	31.37	14.23	32.66	13.91	32.02	13.55
32.26	19.33	32.66	16.90	32.49	15.08	31.69	14.23	32.98	13.94	32.34	13.54
32.58	19.35	32.98	16.90	32.81	15.09	32.01	14.26	33.30	13.93	32.66	13.54

Table B7 Cure characteristics of the compounds filled with various silica/CB hybrid ratios (cont.): (c) SSBR3626_HDSi

SSBR3626											
HDSi100/CB0		HDSi80/CB20		HDSi60/CB40		HDSi40/CB60		HDSi20/CB80		Silica0/CB100	
Time (min)	Torque (dN.m)	Time (min)	Torque (dN.m)	Time (min)	Torque (dN.m)	Time (min)	Torque (dN.m)	Time (min)	Torque (dN.m)	Time (min)	Torque (dN.m)
32.90	19.36	33.30	16.93	33.13	15.09	32.33	14.27	33.62	13.93	32.98	13.54
33.22	19.39	33.62	16.93	33.45	15.10	32.65	14.28	33.94	13.94	33.30	13.54
33.54	19.38	33.94	16.94	33.77	15.12	32.97	14.29	34.26	13.95	33.62	13.53
33.86	19.41	34.26	16.96	34.09	15.12	33.29	14.29	34.58	13.96	33.94	13.56
34.18	19.41	34.57	16.98	34.41	15.13	33.61	14.32	34.90	13.97	34.26	13.54
34.50	19.43	34.90	17.00	34.73	15.14	33.93	14.31	35.22	13.96	34.58	13.53
34.82	19.44	35.22	17.00	35.05	15.14	34.25	14.33	35.54	13.98	34.90	13.54
35.14	19.45	35.53	17.01	35.37	15.16	34.57	14.33	35.86	13.99	35.22	13.52
35.46	19.45	35.85	17.02	35.69	15.17	34.89	14.34	36.18	13.99	35.54	13.53
35.78	19.47	36.17	17.02	36.01	15.17	35.21	14.34	36.50	13.98	35.86	13.54
36.10	19.48	36.49	17.04	36.33	15.17	35.53	14.34	36.82	13.99	36.18	13.53
36.42	19.49	36.81	17.04	36.65	15.20	35.85	14.36	37.14	13.99	36.50	13.55
36.74	19.49	37.13	17.05	36.97	15.21	36.17	14.36	37.47	14.00	36.82	13.54
37.06	19.51	37.45	17.07	37.29	15.22	36.49	14.36	37.79	14.01	37.14	13.54
37.38	19.50	37.77	17.07	37.61	15.23	36.81	14.38	38.11	14.01	37.46	13.50
37.70	19.53	38.09	17.09	37.93	15.22	37.13	14.39	38.43	14.02	37.78	13.53
38.02	19.54	38.41	17.10	38.25	15.23	37.45	14.39	38.75	14.02	38.10	13.53
38.34	19.55	38.73	17.09	38.57	15.24	37.77	14.41	39.07	14.03	38.42	13.54
38.66	19.56	39.05	17.10	38.89	15.24	38.09	14.39	39.39	14.03	38.74	13.54
38.98	19.56	39.37	17.12	39.21	15.25	38.41	14.42	39.71	14.03	39.06	13.53
39.30	19.57	39.69	17.12	39.54	15.26	38.73	14.42	40.03	14.04	39.38	13.52
39.62	19.58	40.01	17.12	39.86	15.26	39.05	14.44	40.35	14.05	39.70	13.52
39.94	19.59	40.33	17.14	40.18	15.25	39.37	14.41	40.67	14.04	40.02	13.52
40.26	19.61	40.65	17.16	40.50	15.28	39.69	14.44	40.99	14.06	40.34	13.50
40.58	19.60	40.97	17.15	40.82	15.28	40.01	14.44	41.31	14.07	40.66	13.52
40.90	19.61	41.29	17.17	41.14	15.29	40.33	14.44	41.63	14.07	40.98	13.51
41.22	19.62	41.61	17.17	41.46	15.31	40.65	14.44	41.95	14.06	41.30	13.53
41.54	19.62	41.93	17.18	41.78	15.31	40.97	14.45	42.27	14.06	41.62	13.53
41.86	19.64	42.25	17.19	42.10	15.31	41.29	14.44	42.59	14.07	41.94	13.55
42.18	19.64	42.58	17.21	42.42	15.30	41.61	14.46	42.91	14.07	42.26	13.53
42.50	19.65	42.90	17.20	42.74	15.32	41.92	14.48	43.23	14.08	42.58	13.53
42.82	19.65	43.22	17.22	43.06	15.33	42.24	14.50	43.55	14.09	42.90	13.53
43.14	19.67	43.54	17.23	43.38	15.33	42.56	14.49	43.87	14.10	43.22	13.52
43.46	19.68	43.86	17.23	43.70	15.32	42.88	14.50	44.19	14.10	43.54	13.52
43.78	19.65	44.18	17.24	44.02	15.33	43.20	14.50	44.51	14.09	43.85	13.52

Table B7 Cure characteristics of the compounds filled with various silica/CB hybrid ratios (cont.): (c) SSBR3626_HDSi

SSBR3626											
HDSi100/CB0		**HDSi80/CB20**		**HDSi60/CB40**		**HDSi40/CB60**		**HDSi20/CB80**		**Silica0/CB100**	
Time (min)	**Torque (dN.m)**	**Time (min)**	**Torque (dN.m)**	**Time (min)**	**Torque (dN.m)**	**Time (min)**	**Torque (dN.m)**	**Time (min)**	**Torque (dN.m)**	**Time (min)**	**Torque (dN.m)**
44.10	19.67	44.50	17.23	44.34	15.33	43.52	14.50	44.83	14.09	44.17	13.51
44.42	19.68	44.82	17.24	44.66	15.34	43.84	14.49	45.15	14.09	44.49	13.50
44.74	19.69	45.14	17.28	44.98	15.33	44.16	14.50	45.47	14.12	44.81	13.50
45.06	19.70	45.46	17.26	45.34	15.34	44.48	14.50	45.79	14.11	45.13	13.51
45.38	19.68	45.78	17.25	45.66	15.35	44.80	14.52	46.11	14.12	45.45	13.49
45.70	19.68	46.10	17.25	45.98	15.37	45.12	14.52	46.43	14.12	45.77	13.52
46.02	19.69	46.42	17.25	46.30	15.36	45.44	14.53	46.75	14.13	46.09	13.53
46.34	19.71	46.74	17.26	46.62	15.36	45.76	14.55	47.07	14.11	46.41	13.52
46.66	19.71	47.06	17.29	46.94	15.38	46.08	14.52	47.39	14.12	46.73	13.50
46.98	19.72	47.38	17.30	47.26	15.40	46.40	14.53	47.71	14.12	47.05	13.48
47.30	19.73	47.70	17.29	47.58	15.40	46.72	14.52	48.03	14.14	47.37	13.52
47.62	19.74	48.02	17.32	47.90	15.39	47.04	14.53	48.35	14.14	47.69	13.51
47.94	19.75	48.34	17.30	48.22	15.39	47.36	14.55	48.67	14.14	48.01	13.50
48.26	19.75	48.66	17.31	48.53	15.41	47.68	14.56	48.99	14.15	48.33	13.52
48.58	19.75	48.98	17.34	48.85	15.42	48.00	14.56	49.31	14.15	48.65	13.53
48.90	19.75	49.30	17.33	49.17	15.41	48.32	14.57	49.64	14.15	48.97	13.51
49.22	19.77	49.62	17.33	49.49	15.41	48.64	14.56	50.00	14.18	49.29	13.50
49.54	19.75	50.00	17.32	49.81	15.42	48.96	14.56			49.61	13.52
49.86	19.77			49.99	15.44	49.28	14.57			49.99	13.51
50.00	19.75					49.60	14.59				
						49.91	14.58				
						49.99	14.57				

Table B8 Cure characteristics of the compounds filled with various silica/CB hybrid ratios: (d) SSBR3626_CSi

SSBR3626											
CSi100/CB0		CSi80/CB20		CSi60/CB40		CSi40/CB60		CSi20/CB80		Silica0/CB100	
Time (min)	Torque (dN.m)	Time (min)	Torque (dN.m)	Time (min)	Torque (dN.m)	Time (min)	Torque (dN.m)	Time (min)	Torque (dN.m)	Time (min)	Torque (dN.m)
0.02	2.48	0.02	2.29	0.02	2.31	0.02	3.21	0.02	3.41	0.02	1.59
0.34	2.03	0.34	2.04	0.34	2.05	0.34	2.24	0.34	2.47	0.34	2.61
0.66	2.31	0.38	2.04	0.66	2.08	0.66	2.21	0.66	2.40	0.62	2.55
0.98	2.56	0.42	2.05	0.98	2.19	0.98	2.27	0.74	2.39	0.90	2.59
1.30	2.78	0.74	2.23	1.30	2.30	1.30	2.35	0.82	2.40	1.22	2.64
1.62	2.93	1.06	2.42	1.62	2.40	1.62	2.42	1.14	2.46	1.54	2.68
1.94	3.07	1.38	2.56	1.94	2.49	1.94	2.48	1.46	2.51	1.86	2.75
2.26	3.19	1.70	2.70	2.26	2.57	2.26	2.53	1.78	2.57	2.18	2.79
2.58	3.32	2.02	2.79	2.58	2.67	2.58	2.62	2.10	2.62	2.50	2.88
2.90	3.50	2.34	2.91	2.90	2.80	2.90	2.70	2.42	2.67	2.82	2.98
3.22	3.71	2.66	3.03	3.22	2.95	3.22	2.83	2.74	2.76	3.14	3.13
3.54	3.95	2.98	3.20	3.54	3.19	3.54	2.99	3.06	2.86	3.46	3.36
3.86	4.26	3.30	3.41	3.86	3.46	3.86	3.21	3.38	2.99	3.78	3.77
4.18	4.64	3.62	3.67	4.18	3.80	4.18	3.51	3.70	3.19	4.10	4.45
4.50	5.06	3.94	3.99	4.50	4.19	4.50	3.85	3.94	3.39	4.14	4.55
4.82	5.54	3.98	4.05	4.82	4.63	4.78	4.19	4.18	3.63	4.18	4.68
5.14	6.08	4.02	4.09	5.14	5.10	5.06	4.56	4.50	4.03	4.50	5.65
5.46	6.69	4.34	4.48	5.46	5.61	5.38	4.99	4.74	4.39	4.82	6.64
5.62	7.01	4.66	4.95	5.78	6.14	5.70	5.45	4.98	4.79	5.14	7.52
5.78	7.34	4.98	5.46	6.10	6.67	6.02	5.93	5.30	5.33	5.46	8.27
6.10	8.03	5.30	6.02	6.42	7.21	6.34	6.40	5.62	5.89	5.78	8.93
6.42	8.71	5.62	6.62	6.74	7.72	6.66	6.88	5.94	6.44	6.10	9.49
6.74	9.36	5.94	7.24	7.06	8.20	6.98	7.33	6.26	6.99	6.42	9.97
7.06	9.98	6.26	7.86	7.38	8.65	7.30	7.76	6.50	7.39	6.74	10.39
7.38	10.53	6.58	8.45	7.70	9.05	7.62	8.17	6.74	7.76	7.06	10.73
7.70	11.05	6.90	9.01	8.02	9.44	7.94	8.54	7.06	8.20	7.38	11.04
8.02	11.55	7.22	9.52	8.34	9.79	8.26	8.88	7.38	8.62	7.70	11.34
8.34	11.99	7.54	10.01	8.66	10.11	8.58	9.19	7.70	8.99	8.02	11.57
8.66	12.41	7.86	10.46	8.98	10.41	8.90	9.50	8.02	9.31	8.34	11.78
8.98	12.80	8.18	10.86	9.30	10.70	9.22	9.76	8.34	9.62	8.66	11.97
9.30	13.15	8.50	11.24	9.62	10.97	9.54	10.03	8.66	9.88	8.98	12.13
9.62	13.47	8.82	11.59	9.94	11.21	9.86	10.25	8.98	10.15	9.30	12.27
9.94	13.78	9.14	11.90	10.26	11.45	10.18	10.48	9.30	10.37	9.63	12.40
10.26	14.06	9.46	12.22	10.58	11.64	10.50	10.67	9.62	10.58	9.95	12.52
10.58	14.32	9.78	12.49	10.90	11.83	10.82	10.88	9.94	10.77	10.27	12.63

Table B8 Cure characteristics of the compounds filled with various silica/CB hybrid ratios (cont.): (d) SSBR3626_CSi

SSBR3626											
CSi100/CB0		CSi80/CB20		CSi60/CB40		CSi40/CB60		CSi20/CB80		Silica0/CB100	
Time (min)	Torque (dN.m)	Time (min)	Torque (dN.m)	Time (min)	Torque (dN.m)	Time (min)	Torque (dN.m)	Time (min)	Torque (dN.m)	Time (min)	Torque (dN.m)
10.90	14.56	10.10	12.73	11.22	12.03	11.14	11.05	10.26	10.94	10.59	12.71
11.22	14.79	10.42	12.98	11.54	12.19	11.46	11.23	10.58	11.12	10.91	12.80
11.54	15.00	10.74	13.20	11.86	12.35	11.78	11.39	10.90	11.27	11.23	12.88
11.86	15.22	11.06	13.41	12.18	12.49	12.10	11.53	11.22	11.40	11.55	12.94
12.18	15.41	11.38	13.61	12.50	12.64	12.42	11.66	11.54	11.52	11.87	13.00
12.50	15.58	11.70	13.79	12.82	12.77	12.74	11.80	11.86	11.64	12.19	13.07
12.82	15.75	12.02	13.95	13.14	12.91	13.06	11.92	12.18	11.76	12.51	13.11
13.14	15.90	12.34	14.10	13.46	13.00	13.38	12.02	12.50	11.87	12.83	13.15
13.46	16.03	12.66	14.27	13.78	13.10	13.70	12.14	12.82	11.95	13.15	13.16
13.78	16.18	12.98	14.41	14.10	13.22	14.02	12.24	13.14	12.04	13.47	13.21
14.10	16.31	13.30	14.54	14.42	13.31	14.34	12.32	13.46	12.13	13.79	13.25
14.42	16.44	13.62	14.66	14.74	13.39	14.65	12.41	13.78	12.20	14.11	13.29
14.74	16.54	13.94	14.78	15.06	13.48	14.97	12.48	14.10	12.25	14.43	13.33
15.06	16.65	14.26	14.89	15.38	13.57	15.29	12.57	14.42	12.33	14.75	13.35
15.38	16.74	14.58	15.01	15.70	13.63	15.61	12.64	14.74	12.40	15.07	13.38
15.70	16.86	14.90	15.09	16.02	13.70	15.93	12.71	15.06	12.45	15.39	13.39
16.02	16.96	15.22	15.16	16.34	13.77	16.25	12.77	15.38	12.50	15.71	13.41
16.34	17.04	15.54	15.25	16.66	13.83	16.57	12.84	15.70	12.55	16.03	13.43
16.67	17.12	15.86	15.34	16.98	13.88	16.89	12.90	16.02	12.61	16.35	13.43
16.99	17.19	16.18	15.40	17.30	13.94	17.21	12.96	16.34	12.65	16.67	13.46
17.31	17.28	16.50	15.49	17.62	13.99	17.53	13.02	16.66	12.69	16.99	13.47
17.63	17.33	16.82	15.54	17.94	14.03	17.85	13.06	16.98	12.73	17.31	13.47
17.95	17.41	17.14	15.60	18.26	14.09	18.17	13.09	17.30	12.76	17.63	13.47
18.27	17.45	17.46	15.66	18.58	14.13	18.49	13.14	17.62	12.80	17.95	13.49
18.59	17.51	17.78	15.72	18.89	14.18	18.81	13.18	17.94	12.84	18.27	13.50
18.91	17.59	18.10	15.78	19.21	14.22	19.13	13.22	18.26	12.89	18.59	13.49
19.23	17.64	18.42	15.84	19.53	14.26	19.45	13.26	18.58	12.91	18.91	13.51
19.55	17.68	18.74	15.89	19.85	14.30	19.77	13.31	18.90	12.93	19.23	13.52
19.87	17.73	19.06	15.92	20.17	14.33	20.09	13.33	19.22	12.95	19.55	13.52
20.19	17.78	19.38	15.98	20.49	14.37	20.41	13.37	19.54	12.96	19.87	13.52
20.51	17.82	19.70	16.03	20.81	14.40	20.73	13.40	19.86	13.01	20.19	13.52
20.83	17.85	20.02	16.07	21.13	14.43	21.05	13.44	20.18	13.02	20.51	13.52
21.15	17.90	20.34	16.09	21.45	14.45	21.37	13.47	20.50	13.07	20.83	13.51
21.47	17.95	20.66	16.15	21.77	14.49	21.69	13.49	20.84	13.08	21.15	13.54
21.79	17.99	20.98	16.19	22.09	14.50	22.01	13.52	21.16	13.09	21.47	13.55

Table B8 Cure characteristics of the compounds filled with various silica/CB hybrid ratios (cont.): (d) SSBR3626_CSi

SSBR3626											
CSi100/CB0		CSi80/CB20		CSi60/CB40		CSi40/CB60		CSi20/CB80		Silica0/CB100	
Time (min)	Torque (dN.m)	Time (min)	Torque (dN.m)	Time (min)	Torque (dN.m)	Time (min)	Torque (dN.m)	Time (min)	Torque (dN.m)	Time (min)	Torque (dN.m)
22.11	18.03	21.30	16.22	22.41	14.54	22.33	13.56	21.48	13.11	21.79	13.55
22.43	18.05	21.62	16.26	22.73	14.58	22.65	13.57	21.80	13.14	22.11	13.54
22.75	18.09	21.94	16.28	23.05	14.60	22.97	13.58	22.12	13.16	22.43	13.54
23.07	18.12	22.26	16.32	23.37	14.61	23.29	13.61	22.44	13.19	22.75	13.54
23.39	18.15	22.58	16.34	23.69	14.64	23.61	13.64	22.76	13.19	23.07	13.54
23.71	18.17	22.90	16.37	24.01	14.66	23.93	13.64	23.08	13.22	23.39	13.55
24.03	18.21	23.22	16.40	24.33	14.68	24.25	13.66	23.40	13.23	23.71	13.54
24.35	18.25	23.54	16.43	24.65	14.70	24.57	13.70	23.72	13.24	24.03	13.55
24.67	18.26	23.86	16.45	24.97	14.72	24.89	13.73	24.04	13.26	24.35	13.54
24.99	18.29	24.18	16.48	25.29	14.74	25.21	13.75	24.36	13.27	24.67	13.54
25.31	18.31	24.50	16.51	25.61	14.77	25.53	13.76	24.68	13.29	24.99	13.55
25.63	18.33	24.82	16.52	25.93	14.79	25.85	13.77	25.00	13.30	25.31	13.55
25.95	18.37	25.14	16.54	26.25	14.80	26.17	13.79	25.32	13.31	25.63	13.54
26.27	18.37	25.46	16.58	26.57	14.80	26.49	13.81	25.64	13.32	25.95	13.56
26.60	18.39	25.78	16.60	26.89	14.82	26.81	13.83	25.96	13.33	26.27	13.55
26.92	18.41	26.10	16.61	27.21	14.83	27.13	13.84	26.28	13.34	26.59	13.55
27.24	18.43	26.42	16.63	27.53	14.86	27.45	13.85	26.60	13.33	26.91	13.55
27.56	18.45	26.74	16.66	27.85	14.88	27.77	13.86	26.92	13.35	27.23	13.55
27.88	18.46	27.06	16.66	28.17	14.89	28.09	13.87	27.24	13.39	27.55	13.54
28.20	18.49	27.38	16.68	28.49	14.90	28.41	13.88	27.56	13.38	27.86	13.55
28.52	18.50	27.70	16.69	28.81	14.92	28.73	13.90	27.88	13.39	28.18	13.54
28.84	18.51	28.02	16.72	29.13	14.93	29.05	13.92	28.20	13.41	28.50	13.55
29.16	18.51	28.34	16.73	29.45	14.94	29.37	13.92	28.52	13.42	28.82	13.56
29.48	18.53	28.66	16.75	29.77	14.96	29.69	13.94	28.84	13.42	29.14	13.54
29.80	18.56	28.98	16.77	30.09	14.97	30.01	13.94	29.16	13.44	29.46	13.53
30.12	18.57	29.30	16.78	30.41	14.97	30.33	13.97	29.48	13.44	29.78	13.55
30.44	18.59	29.62	16.79	30.73	14.99	30.65	13.98	29.80	13.46	30.10	13.55
30.76	18.62	29.94	16.81	31.05	15.01	30.97	13.97	30.12	13.47	30.42	13.53
31.08	18.62	30.26	16.84	31.37	15.01	31.29	13.98	30.44	13.47	30.74	13.54
31.40	18.63	30.58	16.85	31.69	15.01	31.61	13.99	30.76	13.47	31.06	13.56
31.72	18.65	30.90	16.86	32.01	15.03	31.93	14.01	31.08	13.48	31.38	13.56
32.04	18.67	31.22	16.88	32.33	15.05	32.25	14.02	31.40	13.48	31.70	13.55
32.36	18.67	31.54	16.88	32.65	15.04	32.57	14.02	31.72	13.50	32.02	13.55
32.68	18.68	31.86	16.90	32.97	15.06	32.89	14.03	32.04	13.51	32.34	13.54
33.00	18.69	32.18	16.91	33.29	15.10	33.21	14.04	32.36	13.51	32.66	13.54

Table B8 Cure characteristics of the compounds filled with various silica/CB hybrid ratios (cont.): (d) SSBR3626_CSi

SSBR3626											
CSi100/CB0		CSi80/CB20		CSi60/CB40		CSi40/CB60		CSi20/CB80		Silica0/CB100	
Time (min)	Torque (dN.m)	Time (min)	Torque (dN.m)	Time (min)	Torque (dN.m)	Time (min)	Torque (dN.m)	Time (min)	Torque (dN.m)	Time (min)	Torque (dN.m)
33.32	18.69	32.50	16.91	33.61	15.07	33.53	14.03	32.68	13.51	32.98	13.54
33.64	18.71	32.82	16.92	33.93	15.08	33.85	14.07	33.00	13.52	33.30	13.54
33.96	18.73	33.14	16.93	34.25	15.11	34.17	14.08	33.32	13.53	33.62	13.53
34.28	18.74	33.46	16.95	34.57	15.12	34.49	14.08	33.64	13.54	33.94	13.56
34.60	18.76	33.78	16.97	34.89	15.13	34.81	14.08	33.96	13.54	34.26	13.54
34.92	18.75	34.10	16.98	35.21	15.14	35.13	14.10	34.28	13.55	34.58	13.53
35.24	18.77	34.42	16.99	35.53	15.15	35.45	14.11	34.60	13.54	34.90	13.54
35.56	18.78	34.74	17.00	35.85	15.16	35.77	14.12	34.92	13.55	35.22	13.52
35.88	18.77	35.06	17.01	36.17	15.16	36.09	14.11	35.24	13.58	35.54	13.53
36.20	18.78	35.38	17.03	36.49	15.18	36.41	14.12	35.55	13.59	35.86	13.54
36.52	18.78	35.70	17.04	36.81	15.17	36.73	14.14	35.87	13.58	36.18	13.53
36.84	18.80	36.02	17.04	37.13	15.19	37.05	14.14	36.19	13.59	36.50	13.55
37.16	18.82	36.34	17.03	37.45	15.19	37.37	14.15	36.51	13.60	36.82	13.54
37.48	18.84	36.66	17.05	37.77	15.19	37.69	14.14	36.83	13.60	37.14	13.54
37.80	18.83	36.98	17.06	38.09	15.20	38.01	14.15	37.15	13.60	37.46	13.50
38.12	18.85	37.30	17.06	38.41	15.21	38.33	14.17	37.47	13.61	37.78	13.53
38.44	18.86	37.62	17.08	38.73	15.22	38.65	14.17	37.79	13.60	38.10	13.53
38.76	18.86	37.94	17.09	39.05	15.22	38.97	14.18	38.11	13.61	38.42	13.54
39.08	18.87	38.26	17.09	39.37	15.23	39.29	14.19	38.43	13.63	38.74	13.54
39.40	18.88	38.58	17.12	39.69	15.23	39.61	14.18	38.75	13.64	39.06	13.53
39.72	18.89	38.90	17.10	40.01	15.25	39.93	14.19	39.07	13.65	39.38	13.52
40.04	18.90	39.22	17.12	40.33	15.25	40.25	14.20	39.39	13.66	39.70	13.52
40.36	18.91	39.54	17.12	40.65	15.26	40.57	14.20	39.71	13.65	40.02	13.52
40.69	18.91	39.86	17.13	40.97	15.26	40.89	14.22	40.03	13.63	40.34	13.50
41.01	18.91	40.18	17.14	41.29	15.26	41.21	14.21	40.35	13.64	40.66	13.52
41.33	18.91	40.50	17.16	41.61	15.27	41.53	14.22	40.67	13.65	40.98	13.51
41.65	18.92	40.82	17.16	41.93	15.28	41.85	14.24	40.99	13.66	41.30	13.53
41.97	18.92	41.14	17.16	42.25	15.28	42.17	14.24	41.31	13.68	41.62	13.53
42.29	18.93	41.46	17.18	42.57	15.28	42.49	14.24	41.63	13.69	41.94	13.55
42.61	18.94	41.78	17.17	42.89	15.30	42.81	14.26	41.95	13.68	42.26	13.53
42.93	18.94	42.10	17.18	43.21	15.31	43.13	14.25	42.27	13.68	42.58	13.53
43.25	18.95	42.42	17.18	43.53	15.32	43.45	14.25	42.59	13.67	42.90	13.53
43.57	18.97	42.74	17.18	43.85	15.31	43.77	14.26	42.91	13.69	43.22	13.52
43.89	18.97	43.06	17.20	44.17	15.33	44.09	14.25	43.23	13.68	43.54	13.52
44.21	18.97	43.38	17.21	44.49	15.33	44.41	14.26	43.55	13.71	43.85	13.52

Table B8 Cure characteristics of the compounds filled with various silica/CB hybrid ratios (cont.): (d) SSBR3626_CSi

SSBR3626											
CSi100/CB0		**CSi80/CB20**		**CSi60/CB40**		**CSi40/CB60**		**CSi20/CB80**		**Silica0/CB100**	
Time (min)	**Torque (dN.m)**	**Time (min)**	**Torque (dN.m)**	**Time (min)**	**Torque (dN.m)**	**Time (min)**	**Torque (dN.m)**	**Time (min)**	**Torque (dN.m)**	**Time (min)**	**Torque (dN.m)**
44.53	18.97	43.70	17.21	44.81	15.33	44.73	14.27	43.87	13.71	44.17	13.51
44.85	18.99	44.02	17.21	45.13	15.34	45.05	14.28	44.19	13.70	44.49	13.50
45.17	18.98	44.34	17.23	45.45	15.34	45.37	14.28	44.51	13.71	44.81	13.50
45.49	18.99	44.66	17.24	45.77	15.33	45.69	14.30	44.83	13.71	45.13	13.51
45.81	18.98	44.98	17.26	46.09	15.36	46.01	14.29	45.15	13.71	45.45	13.49
46.13	18.98	45.30	17.25	46.41	15.37	46.33	14.29	45.47	13.72	45.77	13.52
46.45	19.00	45.62	17.26	46.72	15.36	46.65	14.29	45.79	13.72	46.09	13.53
46.77	19.01	45.94	17.27	47.04	15.36	46.97	14.29	46.11	13.72	46.41	13.52
47.09	19.04	46.26	17.28	47.36	15.37	47.29	14.31	46.43	13.74	46.73	13.50
47.41	19.04	46.58	17.27	47.68	15.37	47.61	14.31	46.75	13.75	47.05	13.48
47.73	19.04	46.90	17.27	48.00	15.38	47.93	14.31	47.07	13.74	47.37	13.52
48.05	19.05	47.22	17.28	48.32	15.41	48.24	14.33	47.39	13.74	47.69	13.51
48.37	19.04	47.54	17.27	48.64	15.42	48.56	14.33	47.71	13.75	48.01	13.50
48.69	19.06	47.86	17.29	48.97	15.41	48.88	14.34	48.03	13.74	48.33	13.52
49.01	19.05	48.18	17.31	49.29	15.41	49.20	14.34	48.35	13.75	48.65	13.53
49.33	19.07	48.50	17.30	49.61	15.41	49.52	14.33	48.67	13.75	48.97	13.51
49.65	19.08	48.82	17.32	49.99	15.42	49.84	14.33	48.99	13.74	49.29	13.50
49.99	19.08	49.14	17.32			49.98	14.31	49.31	13.76	49.61	13.52
		49.46	17.31					49.63	13.77	49.99	13.51
		49.78	17.31					49.99	13.75		
		50.00	17.32								

Table B9 Cure characteristics of the compounds filled with various silica/CB hybrid ratios: (e) ESBR1723_HDSi

ESBR1723											
HDSi100/CB0		HDSi80/CB20		HDSi60/CB40		HDSi40/CB60		HDSi20/CB80		Silica0/CB100	
Time (min)	Torque (dN.m)	Time (min)	Torque (dN.m)	Time (min)	Torque (dN.m)	Time (min)	Torque (dN.m)	Time (min)	Torque (dN.m)	Time (min)	Torque (dN.m)
0.02	1.89	0.02	1.22	0.02	1.56	0.02	2.64	0.02	2.47	0.02	1.96
0.34	1.31	0.34	1.41	0.34	1.50	0.34	1.60	0.34	1.88	0.34	2.15
0.66	1.30	0.66	1.39	0.66	1.46	0.66	1.57	0.66	1.86	0.60	2.14
0.98	1.32	0.74	1.38	0.82	1.45	0.98	1.58	0.78	1.85	0.84	2.16
1.30	1.35	0.82	1.39	0.98	1.47	1.30	1.61	0.90	1.88	1.16	2.18
1.62	1.38	1.14	1.41	1.30	1.50	1.62	1.64	1.22	1.90	1.48	2.22
1.94	1.42	1.46	1.44	1.62	1.52	1.94	1.67	1.54	1.94	1.80	2.26
2.26	1.46	1.78	1.47	1.94	1.56	2.26	1.71	1.86	1.98	2.12	2.30
2.58	1.49	2.10	1.51	2.26	1.58	2.58	1.76	2.18	2.03	2.44	2.32
2.90	1.55	2.42	1.53	2.58	1.63	2.90	1.82	2.50	2.06	2.76	2.36
3.22	1.59	2.74	1.57	2.90	1.69	3.22	1.91	2.82	2.13	3.08	2.43
3.54	1.67	3.06	1.63	3.22	1.76	3.54	2.03	3.14	2.22	3.40	2.50
3.86	1.75	3.38	1.69	3.54	1.84	3.86	2.19	3.46	2.36	3.72	2.62
4.18	1.86	3.70	1.77	3.86	1.96	4.18	2.39	3.78	2.56	4.04	2.83
4.50	1.96	4.02	1.88	4.18	2.11	4.42	2.58	4.10	2.86	4.36	3.18
4.82	2.10	4.34	2.00	4.50	2.27	4.66	2.76	4.42	3.21	4.68	3.68
5.14	2.25	4.66	2.15	4.82	2.47	4.98	3.05	4.74	3.60	4.96	4.14
5.22	2.30	4.98	2.28	5.14	2.68	5.30	3.37	4.94	3.87	5.24	4.62
5.30	2.33	5.14	2.40	5.46	2.92	5.62	3.68	5.14	4.15	5.56	5.18
5.62	2.52	5.30	2.50	5.78	3.19	5.94	4.07	5.46	4.63	5.88	5.72
5.94	2.71	5.62	2.69	6.10	3.48	6.26	4.46	5.78	5.09	6.20	6.23
6.26	2.93	5.94	2.91	6.42	3.79	6.58	4.80	6.10	5.54	6.52	6.72
6.58	3.17	6.26	3.17	6.74	4.10	6.90	5.16	6.42	5.98	6.84	7.18
6.74	3.29	6.58	3.44	7.06	4.41	7.22	5.50	6.74	6.37	7.16	7.59
6.90	3.42	6.90	3.72	7.38	4.72	7.54	5.82	7.06	6.75	7.48	7.99
7.22	3.67	7.22	4.01	7.70	5.02	7.86	6.13	7.38	7.10	7.80	8.33
7.54	3.94	7.54	4.29	8.02	5.31	8.18	6.41	7.70	7.42	8.12	8.63
7.86	4.19	7.86	4.57	8.34	5.60	8.34	6.58	8.02	7.70	8.44	8.92
8.18	4.44	8.18	4.84	8.66	5.86	8.50	6.71	8.34	7.99	8.76	9.16
8.50	4.73	8.50	5.11	8.98	6.12	8.82	6.94	8.66	8.23	9.08	9.40
8.82	4.93	8.82	5.36	9.30	6.34	9.14	7.19	8.98	8.46	9.40	9.61
9.14	5.18	9.14	5.60	9.62	6.56	9.46	7.42	9.30	8.66	9.72	9.79
9.46	5.39	9.46	5.84	9.94	6.80	9.78	7.59	9.62	8.86	10.04	9.95
9.78	5.61	9.78	6.07	10.26	7.00	10.10	7.80	9.95	9.05	10.36	10.11
10.10	5.83	10.10	6.28	10.58	7.20	10.41	7.98	10.27	9.21	10.68	10.25

Table B9 Cure characteristics of the compounds filled with various silica/CB hybrid ratios (cont.): (e) ESBR1723_HDSi

ESBR1723											
HDSi100/CB0		HDSi80/CB20		HDSi60/CB40		HDSi40/CB60		HDSi20/CB80		Silica0/CB100	
Time (min)	Torque (dN.m)	Time (min)	Torque (dN.m)	Time (min)	Torque (dN.m)	Time (min)	Torque (dN.m)	Time (min)	Torque (dN.m)	Time (min)	Torque (dN.m)
10.42	6.05	10.42	6.50	10.90	7.39	10.73	8.15	10.59	9.35	11.00	10.37
10.74	6.26	10.74	6.70	11.22	7.57	11.05	8.32	10.91	9.49	11.32	10.49
11.06	6.45	11.06	6.88	11.54	7.74	11.37	8.46	11.23	9.63	11.64	10.59
11.38	6.63	11.38	7.05	11.86	7.90	11.69	8.59	11.55	9.75	11.96	10.68
11.70	6.82	11.70	7.23	12.18	8.05	12.01	8.70	11.87	9.84	12.28	10.75
12.02	6.99	12.02	7.40	12.50	8.19	12.33	8.85	12.19	9.95	12.60	10.82
12.34	7.16	12.34	7.55	12.82	8.33	12.65	8.97	12.51	10.04	12.92	10.89
12.66	7.32	12.66	7.70	13.14	8.46	12.97	9.06	12.83	10.12	13.24	10.96
12.98	7.48	12.98	7.85	13.46	8.59	13.29	9.17	13.15	10.21	13.56	11.02
13.30	7.64	13.30	7.99	13.78	8.70	13.61	9.27	13.47	10.28	13.88	11.07
13.62	7.79	13.62	8.13	14.10	8.81	13.93	9.37	13.79	10.35	14.20	11.14
13.94	7.92	13.94	8.26	14.42	8.92	14.25	9.44	14.11	10.42	14.52	11.19
14.26	8.05	14.26	8.38	14.74	9.02	14.57	9.50	14.43	10.47	14.84	11.23
14.57	8.19	14.58	8.50	15.06	9.11	14.89	9.58	14.75	10.53	15.16	11.26
14.89	8.31	14.90	8.61	15.38	9.21	15.21	9.67	15.07	10.59	15.48	11.29
15.21	8.44	15.22	8.72	15.70	9.29	15.53	9.73	15.39	10.62	15.80	11.32
15.53	8.56	15.54	8.82	16.02	9.37	15.85	9.79	15.71	10.68	16.12	11.34
15.85	8.67	15.86	8.92	16.34	9.45	16.17	9.84	16.03	10.72	16.44	11.38
16.17	8.78	16.18	9.01	16.66	9.53	16.49	9.90	16.35	10.76	16.76	11.38
16.49	8.88	16.50	9.10	16.98	9.61	16.81	9.96	16.67	10.79	17.08	11.41
16.81	8.99	16.82	9.19	17.30	9.68	17.13	10.01	16.99	10.83	17.40	11.43
17.13	9.09	17.14	9.27	17.62	9.73	17.45	10.04	17.31	10.86	17.72	11.45
17.45	9.18	17.46	9.35	17.94	9.80	17.77	10.10	17.63	10.88	18.04	11.46
17.77	9.28	17.78	9.42	18.26	9.86	18.09	10.13	17.95	10.91	18.36	11.48
18.09	9.34	18.10	9.50	18.58	9.92	18.41	10.17	18.27	10.94	18.68	11.49
18.41	9.44	18.42	9.57	18.90	9.97	18.73	10.21	18.59	10.97	19.00	11.50
18.73	9.54	18.74	9.64	19.22	10.02	19.05	10.25	18.91	10.99	19.32	11.51
19.05	9.60	19.06	9.70	19.54	10.07	19.37	10.29	19.23	11.00	19.64	11.51
19.37	9.67	19.38	9.76	19.86	10.12	19.69	10.32	19.55	11.01	19.96	11.52
19.69	9.73	19.70	9.82	20.18	10.16	20.01	10.34	19.87	11.03	20.28	11.52
20.01	9.80	20.02	9.86	20.50	10.19	20.33	10.38	20.19	11.05	20.60	11.54
20.34	9.90	20.34	9.93	20.82	10.23	20.64	10.38	20.51	11.07	20.92	11.54
20.66	9.96	20.66	9.99	21.14	10.27	20.96	10.42	20.83	11.09	21.24	11.54
20.98	10.02	20.98	10.04	21.46	10.31	21.28	10.45	21.15	11.10	21.56	11.54
21.30	10.07	21.30	10.08	21.78	10.36	21.60	10.47	21.47	11.11	21.88	11.54

Table B9 Cure characteristics of the compounds filled with various silica/CB hybrid ratios (cont.): (e) ESBR1723_HDSi

ESBR1723											
HDSi100/CB0		HDSi80/CB20		HDSi60/CB40		HDSi40/CB60		HDSi20/CB80		Silica0/CB100	
Time (min)	Torque (dN.m)	Time (min)	Torque (dN.m)	Time (min)	Torque (dN.m)	Time (min)	Torque (dN.m)	Time (min)	Torque (dN.m)	Time (min)	Torque (dN.m)
21.61	10.12	21.62	10.13	22.10	10.41	21.92	10.50	21.79	11.12	22.20	11.54
21.93	10.19	21.94	10.17	22.42	10.43	22.24	10.51	22.11	11.14	22.52	11.55
22.25	10.25	22.26	10.22	22.74	10.45	22.56	10.53	22.43	11.15	22.84	11.54
22.57	10.30	22.58	10.27	23.06	10.48	22.88	10.55	22.75	11.14	23.16	11.53
22.89	10.35	22.90	10.30	23.38	10.50	23.20	10.58	23.08	11.16	23.48	11.54
23.21	10.40	23.22	10.34	23.70	10.54	23.52	10.59	23.40	11.17	23.80	11.55
23.53	10.45	23.54	10.37	24.02	10.57	23.84	10.61	23.72	11.18	24.12	11.53
23.85	10.50	23.86	10.40	24.34	10.59	24.16	10.63	24.06	11.19	24.44	11.54
24.17	10.54	24.18	10.44	24.66	10.61	24.48	10.65	24.38	11.18	24.76	11.54
24.50	10.59	24.50	10.48	24.98	10.63	24.80	10.65	24.70	11.19	25.08	11.54
24.82	10.63	24.82	10.50	25.30	10.65	25.12	10.66	25.02	11.20	25.40	11.54
25.14	10.67	25.14	10.54	25.62	10.67	25.44	10.68	25.34	11.21	25.72	11.53
25.46	10.70	25.46	10.58	25.94	10.70	25.76	10.70	25.66	11.20	26.04	11.53
25.78	10.74	25.78	10.60	26.26	10.72	26.08	10.71	25.98	11.21	26.36	11.54
26.10	10.77	26.10	10.63	26.58	10.73	26.40	10.71	26.30	11.21	26.68	11.53
26.41	10.80	26.42	10.65	26.90	10.75	26.72	10.73	26.62	11.21	27.00	11.52
26.73	10.84	26.74	10.67	27.22	10.77	27.04	10.72	26.94	11.22	27.32	11.51
27.05	10.89	27.06	10.69	27.54	10.79	27.36	10.73	27.26	11.22	27.64	11.51
27.37	10.91	27.38	10.73	27.86	10.81	27.68	10.75	27.58	11.22	27.96	11.52
27.69	10.94	27.70	10.75	28.18	10.82	28.00	10.76	27.90	11.23	28.28	11.52
28.01	10.98	28.02	10.77	28.50	10.83	28.32	10.78	28.22	11.23	28.60	11.51
28.33	11.00	28.34	10.79	28.82	10.84	28.64	10.79	28.54	11.23	28.92	11.51
28.66	11.03	28.66	10.81	29.14	10.87	28.96	10.77	28.86	11.23	29.24	11.50
28.98	11.06	28.98	10.83	29.46	10.88	29.28	10.77	29.18	11.23	29.56	11.50
29.30	11.08	29.30	10.85	29.78	10.88	29.60	10.79	29.50	11.23	29.89	11.51
29.62	11.10	29.62	10.86	30.10	10.90	29.92	10.80	29.82	11.24	30.21	11.49
29.94	11.13	29.94	10.87	30.42	10.90	30.24	10.82	30.14	11.22	30.53	11.50
30.26	11.16	30.26	10.91	30.74	10.92	30.56	10.82	30.46	11.23	30.85	11.50
30.58	11.17	30.58	10.92	31.06	10.94	30.88	10.83	30.78	11.23	31.17	11.49
30.90	11.19	30.90	10.95	31.38	10.94	31.20	10.83	31.10	11.24	31.49	11.49
31.22	11.22	31.22	10.95	31.70	10.94	31.52	10.84	31.42	11.22	31.81	11.47
31.54	11.23	31.54	10.96	32.02	10.97	31.84	10.83	31.74	11.22	32.13	11.48
31.86	11.25	31.86	10.98	32.34	10.97	32.16	10.83	32.06	11.23	32.45	11.46
32.18	11.27	32.18	10.99	32.66	10.97	32.48	10.84	32.38	11.24	32.77	11.47
32.50	11.28	32.50	11.00	32.98	11.00	32.80	10.85	32.70	11.24	33.09	11.47

Table B9 Cure characteristics of the compounds filled with various silica/CB hybrid ratios (cont.): (e) ESBR1723_HDSi

ESBR1723											
HDSi100/CB0		HDSi80/CB20		HDSi60/CB40		HDSi40/CB60		HDSi20/CB80		Silica0/CB100	
Time (min)	Torque (dN.m)	Time (min)	Torque (dN.m)	Time (min)	Torque (dN.m)	Time (min)	Torque (dN.m)	Time (min)	Torque (dN.m)	Time (min)	Torque (dN.m)
32.82	11.31	32.82	11.02	33.30	10.99	33.12	10.86	33.02	11.23	33.41	11.46
33.14	11.32	33.14	11.03	33.62	11.01	33.44	10.86	33.34	11.23	33.73	11.46
33.46	11.35	33.46	11.04	33.94	11.01	33.76	10.87	33.66	11.24	34.05	11.46
33.78	11.37	33.78	11.05	34.26	11.01	34.08	10.87	33.98	11.23	34.37	11.45
34.10	11.38	34.10	11.08	34.58	11.02	34.40	10.88	34.30	11.23	34.69	11.44
34.42	11.40	34.42	11.09	34.90	11.02	34.72	10.87	34.62	11.22	35.01	11.44
34.73	11.41	34.74	11.09	35.22	11.03	35.04	10.88	34.94	11.22	35.33	11.43
35.06	11.43	35.06	11.10	35.54	11.04	35.36	10.88	35.26	11.22	35.65	11.42
35.38	11.44	35.38	11.10	35.86	11.04	35.68	10.88	35.58	11.22	35.97	11.43
35.70	11.45	35.70	11.13	36.18	11.05	36.00	10.89	35.90	11.22	36.29	11.42
36.01	11.46	36.02	11.14	36.49	11.07	36.32	10.89	36.22	11.22	36.61	11.43
36.33	11.46	36.34	11.15	36.81	11.07	36.64	10.89	36.54	11.22	36.93	11.42
36.65	11.48	36.66	11.15	37.13	11.07	36.96	10.88	36.86	11.21	37.25	11.42
36.97	11.49	36.98	11.15	37.45	11.07	37.28	10.90	37.18	11.21	37.57	11.42
37.29	11.52	37.30	11.17	37.77	11.08	37.60	10.91	37.50	11.21	37.89	11.42
37.61	11.53	37.62	11.19	38.09	11.08	37.92	10.91	37.82	11.22	38.21	11.42
37.93	11.54	37.94	11.19	38.41	11.09	38.24	10.91	38.14	11.21	38.53	11.40
38.25	11.56	38.26	11.20	38.73	11.10	38.56	10.90	38.46	11.21	38.85	11.39
38.57	11.57	38.58	11.20	39.05	11.10	38.88	10.90	38.78	11.21	39.17	11.40
38.89	11.56	38.90	11.21	39.37	11.11	39.20	10.90	39.10	11.21	39.49	11.40
39.21	11.57	39.22	11.21	39.69	11.11	39.52	10.90	39.42	11.21	39.81	11.41
39.53	11.57	39.54	11.22	40.01	11.12	39.84	10.91	39.74	11.21	40.13	11.39
39.85	11.60	39.86	11.24	40.33	11.12	40.16	10.93	40.06	11.21	40.45	11.39
40.17	11.61	40.18	11.25	40.65	11.12	40.48	10.91	40.38	11.21	40.77	11.38
40.49	11.61	40.50	11.26	40.97	11.13	40.80	10.91	40.70	11.21	41.09	11.38
40.81	11.62	40.82	11.25	41.29	11.14	41.12	10.91	41.02	11.20	41.41	11.39
41.13	11.64	41.14	11.25	41.61	11.13	41.44	10.92	41.34	11.20	41.73	11.37
41.45	11.65	41.46	11.27	41.93	11.14	41.76	10.93	41.66	11.21	42.05	11.38
41.77	11.64	41.78	11.27	42.25	11.14	42.08	10.92	41.98	11.21	42.40	11.37
42.09	11.64	42.10	11.28	42.57	11.15	42.40	10.92	42.30	11.21	42.72	11.37
42.41	11.66	42.41	11.28	42.89	11.15	42.72	10.92	42.62	11.21	42.98	11.37
42.73	11.67	42.73	11.29	43.21	11.16	43.04	10.92	42.94	11.21		
43.05	11.68	43.05	11.29	43.53	11.16	43.36	10.94	43.26	11.20		
43.37	11.69	43.37	11.31	43.85	11.16	43.68	10.94	43.58	11.19		
43.69	11.69	43.69	11.31	44.19	11.16	44.00	10.94	43.90	11.20		

Table B9 Cure characteristics of the compounds filled with various silica/CB hybrid ratios (cont.): (e) ESBR1723_HDSi

ESBR1723											
HDSi100/CB0		HDSi80/CB20		HDSi60/CB40		HDSi40/CB60		HDSi20/CB80		Silica0/CB100	
Time (min)	Torque (dN.m)	Time (min)	Torque (dN.m)	Time (min)	Torque (dN.m)	Time (min)	Torque (dN.m)	Time (min)	Torque (dN.m)	Time (min)	Torque (dN.m)
44.01	11.69	44.01	11.32	44.51	11.17	44.32	10.92	44.22	11.20		
44.33	11.70	44.33	11.32	44.83	11.17	44.64	10.93	44.54	11.20		
44.65	11.70	44.65	11.32	45.15	11.17	44.96	10.92	44.86	11.19		
44.97	11.72	44.97	11.33	45.47	11.17	45.28	10.94	45.18	11.19		
45.29	11.73	45.29	11.34	45.79	11.18	45.60	10.92	45.50	11.19		
45.61	11.73	45.61	11.35	46.11	11.18	45.92	10.92	45.82	11.19		
45.93	11.73	45.93	11.34	46.43	11.18	46.24	10.92	46.14	11.18		
46.25	11.74	46.25	11.35	46.75	11.19	46.56	10.93	46.46	11.19		
46.57	11.75	46.57	11.35	47.07	11.19	46.88	10.92	46.78	11.19		
46.89	11.74	46.89	11.35	47.39	11.20	47.20	10.93	47.10	11.18		
47.21	11.75	47.21	11.37	47.71	11.19	47.52	10.93	47.42	11.18		
47.53	11.76	47.53	11.37	48.03	11.19	47.84	10.93	47.74	11.19		
47.85	11.77	47.85	11.38	48.35	11.20	48.16	10.94	48.06	11.20		
48.19	11.77	48.17	11.37	48.67	11.19	48.48	10.93	48.38	11.20		
48.51	11.78	48.49	11.38	48.99	11.20	48.80	10.93	48.70	11.18		
48.83	11.78	48.81	11.38	49.31	11.19	49.12	10.93	49.02	11.19		
49.15	11.79	49.13	11.39	49.63	11.20	49.44	10.92	49.34	11.17		
49.47	11.79	49.45	11.39	49.99	11.21	49.76	10.93	49.66	11.17		
49.79	11.79	49.77	11.40			49.98	10.93	49.98	11.17		
49.99	11.80	49.99	11.40								

Table B10 Cure characteristics of the compounds filled with various silica/CB hybrid ratios: (f) ESBR1723_CSi

ESBR1723											
CSi100/CB0		CSi80/CB20		CSi60/CB40		CSi40/CB60		CSi20/CB80		Silica0/CB100	
Time (min)	Torque (dN.m)	Time (min)	Torque (dN.m)	Time (min)	Torque (dN.m)	Time (min)	Torque (dN.m)	Time (min)	Torque (dN.m)	Time (min)	Torque (dN.m)
0.02	1.81	0.02	1.89	0.02	1.85	0.02	2.18	0.02	1.05	0.02	1.96
0.34	1.22	0.34	1.38	0.34	1.45	0.34	1.52	0.34	1.86	0.34	2.15
0.46	1.20	0.46	1.35	0.58	1.42	0.66	1.51	0.66	1.84	0.60	2.14
0.58	1.21	0.58	1.36	0.82	1.44	0.98	1.53	0.98	1.85	0.84	2.16
0.90	1.23	0.90	1.37	1.14	1.46	1.30	1.56	1.30	1.88	1.16	2.18
1.22	1.28	1.22	1.40	1.46	1.49	1.62	1.59	1.62	1.91	1.48	2.22
1.54	1.31	1.54	1.43	1.78	1.52	1.94	1.62	1.94	1.95	1.80	2.26
1.86	1.34	1.86	1.46	2.10	1.55	2.26	1.66	2.26	1.99	2.12	2.30
2.18	1.37	2.18	1.48	2.42	1.58	2.58	1.69	2.58	2.04	2.44	2.32
2.50	1.40	2.50	1.51	2.74	1.62	2.90	1.76	2.90	2.10	2.76	2.36
2.82	1.43	2.82	1.56	3.06	1.68	3.22	1.82	3.22	2.20	3.08	2.43
3.14	1.48	3.14	1.62	3.38	1.75	3.54	1.93	3.54	2.33	3.40	2.50
3.46	1.55	3.46	1.67	3.70	1.83	3.86	2.06	3.86	2.54	3.72	2.62
3.78	1.62	3.78	1.75	4.02	1.94	4.18	2.22	4.18	2.81	4.04	2.83
4.10	1.70	4.10	1.86	4.34	2.06	4.50	2.42	4.50	3.15	4.36	3.18
4.42	1.81	4.42	1.98	4.66	2.22	4.62	2.51	4.82	3.52	4.68	3.68
4.74	1.93	4.74	2.11	4.98	2.40	4.74	2.61	5.14	3.92	4.96	4.14
5.06	2.07	5.06	2.28	5.02	2.42	5.06	2.87	5.46	4.37	5.24	4.62
5.34	2.21	5.18	2.35	5.06	2.45	5.38	3.15	5.78	4.82	5.56	5.18
5.62	2.35	5.30	2.42	5.38	2.66	5.70	3.46	6.10	5.27	5.88	5.72
5.94	2.53	5.62	2.62	5.70	2.88	5.74	3.52	6.42	5.69	6.20	6.23
6.26	2.74	5.94	2.85	6.02	3.13	5.78	3.55	6.73	6.10	6.52	6.72
6.58	2.96	6.26	3.09	6.34	3.41	6.10	3.91	7.05	6.47	6.84	7.18
6.90	3.21	6.58	3.35	6.66	3.71	6.42	4.27	7.37	6.82	7.16	7.59
7.22	3.47	6.90	3.63	6.98	4.03	6.74	4.63	7.69	7.14	7.48	7.99
7.54	3.74	7.22	3.94	7.30	4.34	7.06	4.99	8.01	7.43	7.80	8.33
7.86	4.01	7.54	4.23	7.62	4.65	7.38	5.32	8.33	7.71	8.12	8.63
8.18	4.26	7.86	4.51	7.94	4.96	7.70	5.66	8.65	7.97	8.44	8.92
8.50	4.53	8.18	4.77	8.26	5.24	8.02	5.94	8.97	8.19	8.76	9.16
8.82	4.77	8.50	5.06	8.58	5.52	8.34	6.22	9.29	8.41	9.08	9.40
9.14	5.01	8.82	5.31	8.90	5.76	8.66	6.49	9.61	8.60	9.40	9.61
9.46	5.24	9.14	5.54	9.22	6.02	8.98	6.73	9.93	8.80	9.72	9.79
9.78	5.47	9.46	5.78	9.54	6.25	9.30	6.96	10.25	8.95	10.04	9.95
10.10	5.68	9.78	5.99	9.78	6.42	9.62	7.18	10.57	9.11	10.36	10.11
10.42	5.88	10.10	6.21	10.02	6.57	9.94	7.39	10.89	9.25	10.68	10.25

Table B10 Cure characteristics of the compounds filled with various silica/CB hybrid ratios (cont.): (f) ESBR1723_CSi

ESBR1723											
CSi100/CB0		CSi80/CB20		CSi60/CB40		CSi40/CB60		CSi20/CB80		Silica0/CB100	
Time (min)	Torque (dN.m)	Time (min)	Torque (dN.m)	Time (min)	Torque (dN.m)	Time (min)	Torque (dN.m)	Time (min)	Torque (dN.m)	Time (min)	Torque (dN.m)
10.74	6.08	10.42	6.42	10.34	6.78	10.26	7.58	11.21	9.38	11.00	10.37
10.94	6.20	10.74	6.60	10.66	6.97	10.58	7.75	11.53	9.50	11.32	10.49
11.18	6.34	11.06	6.78	10.98	7.16	10.90	7.92	11.87	9.62	11.64	10.59
11.50	6.52	11.38	6.95	11.30	7.33	11.22	8.07	12.19	9.72	11.96	10.68
11.82	6.69	11.70	7.13	11.62	7.50	11.54	8.22	12.51	9.81	12.28	10.75
12.14	6.85	12.02	7.30	11.94	7.66	11.86	8.36	12.83	9.90	12.60	10.82
12.46	7.00	12.34	7.44	12.26	7.81	12.18	8.50	13.15	9.99	12.92	10.89
12.78	7.16	12.66	7.59	12.58	7.95	12.50	8.62	13.47	10.06	13.24	10.96
13.10	7.30	12.98	7.73	12.90	8.08	12.82	8.73	13.79	10.14	13.56	11.02
13.42	7.43	13.30	7.85	13.22	8.21	13.14	8.82	14.11	10.21	13.88	11.07
13.74	7.57	13.62	7.97	13.54	8.34	13.46	8.93	14.43	10.27	14.20	11.14
14.06	7.71	13.94	8.10	13.86	8.46	13.78	9.04	14.75	10.32	14.52	11.19
14.38	7.83	14.26	8.22	14.18	8.57	14.10	9.12	15.07	10.38	14.84	11.23
14.70	7.95	14.58	8.33	14.50	8.66	14.42	9.22	15.39	10.43	15.16	11.26
15.02	8.06	14.90	8.44	14.82	8.76	14.74	9.29	15.71	10.47	15.48	11.29
15.34	8.17	15.22	8.53	15.14	8.85	15.06	9.36	16.03	10.52	15.80	11.32
15.66	8.29	15.54	8.64	15.46	8.96	15.37	9.43	16.35	10.57	16.12	11.34
15.98	8.39	15.86	8.74	15.78	9.04	15.69	9.51	16.67	10.60	16.44	11.38
16.30	8.50	16.18	8.82	16.10	9.13	16.01	9.57	16.99	10.63	16.76	11.38
16.62	8.59	16.50	8.90	16.42	9.20	16.33	9.62	17.31	10.67	17.08	11.41
16.94	8.68	16.82	8.99	16.74	9.26	16.65	9.68	17.63	10.69	17.40	11.43
17.26	8.76	17.14	9.06	17.06	9.34	16.97	9.72	17.95	10.73	17.72	11.45
17.58	8.85	17.46	9.14	17.38	9.40	17.29	9.78	18.27	10.76	18.04	11.46
17.90	8.93	17.78	9.20	17.70	9.49	17.61	9.83	18.59	10.78	18.36	11.48
18.22	9.01	18.10	9.27	18.02	9.54	17.93	9.87	18.90	10.79	18.68	11.49
18.54	9.09	18.42	9.35	18.34	9.60	18.25	9.92	19.22	10.83	19.00	11.50
18.86	9.15	18.74	9.41	18.66	9.66	18.57	9.95	19.54	10.84	19.32	11.51
19.18	9.23	19.06	9.47	18.98	9.72	18.89	10.00	19.86	10.86	19.64	11.51
19.50	9.29	19.38	9.52	19.30	9.76	19.21	10.02	20.18	10.88	19.96	11.52
19.82	9.36	19.70	9.58	19.62	9.81	19.53	10.07	20.50	10.89	20.28	11.52
20.14	9.43	20.02	9.63	19.94	9.86	19.85	10.11	20.82	10.92	20.60	11.54
20.46	9.48	20.34	9.68	20.26	9.92	20.17	10.14	21.15	10.93	20.92	11.54
20.78	9.54	20.66	9.75	20.58	9.96	20.49	10.16	21.47	10.94	21.24	11.54
21.10	9.59	20.98	9.79	20.90	9.99	20.81	10.19	21.78	10.95	21.56	11.54
21.42	9.66	21.30	9.84	21.22	10.03	21.13	10.23	22.10	10.96	21.88	11.54

Table B10 Cure characteristics of the compounds filled with various silica/CB hybrid ratios (cont.): (f) ESBR1723_CSi

ESBR1723											
CSi100/CB0		CSi80/CB20		CSi60/CB40		CSi40/CB60		CSi20/CB80		Silica0/CB100	
Time (min)	Torque (dN.m)	Time (min)	Torque (dN.m)	Time (min)	Torque (dN.m)	Time (min)	Torque (dN.m)	Time (min)	Torque (dN.m)	Time (min)	Torque (dN.m)
21.74	9.71	21.62	9.86	21.54	10.08	21.45	10.24	22.42	10.97	22.20	11.54
22.06	9.76	21.94	9.91	21.86	10.12	21.77	10.26	22.74	10.98	22.52	11.55
22.38	9.81	22.26	9.95	22.18	10.13	22.09	10.29	23.06	10.98	22.84	11.54
22.70	9.85	22.58	9.99	22.50	10.18	22.41	10.30	23.38	11.00	23.16	11.53
23.02	9.89	22.90	10.04	22.82	10.21	22.73	10.33	23.70	11.00	23.48	11.54
23.34	9.95	23.22	10.07	23.14	10.24	23.05	10.34	24.02	11.01	23.80	11.55
23.66	9.98	23.54	10.10	23.46	10.27	23.37	10.36	24.34	11.02	24.12	11.53
23.98	10.02	23.86	10.13	23.78	10.30	23.69	10.38	24.66	11.03	24.44	11.54
24.30	10.06	24.18	10.16	24.10	10.33	24.01	10.40	24.98	11.05	24.76	11.54
24.62	10.10	24.50	10.20	24.42	10.36	24.33	10.41	25.30	11.05	25.08	11.54
24.94	10.13	24.82	10.22	24.74	10.37	24.65	10.43	25.62	11.04	25.40	11.54
25.26	10.17	25.14	10.26	25.06	10.39	24.97	10.45	25.94	11.04	25.72	11.53
25.58	10.20	25.46	10.27	25.38	10.43	25.29	10.46	26.26	11.05	26.04	11.53
25.90	10.23	25.78	10.31	25.70	10.44	25.61	10.47	26.58	11.06	26.36	11.54
26.22	10.27	26.10	10.33	26.02	10.47	25.93	10.48	26.90	11.06	26.68	11.53
26.54	10.30	26.42	10.36	26.34	10.48	26.25	10.50	27.22	11.08	27.00	11.52
26.86	10.33	26.74	10.37	26.66	10.50	26.57	10.51	27.54	11.06	27.32	11.51
27.18	10.35	27.06	10.41	26.98	10.52	26.89	10.52	27.86	11.07	27.64	11.51
27.50	10.40	27.38	10.42	27.30	10.55	27.21	10.53	28.18	11.07	27.96	11.52
27.82	10.42	27.70	10.44	27.62	10.56	27.53	10.55	28.50	11.08	28.28	11.52
28.14	10.44	28.02	10.47	27.94	10.56	27.85	10.54	28.82	11.08	28.60	11.51
28.46	10.47	28.34	10.49	28.26	10.58	28.17	10.56	29.14	11.07	28.92	11.51
28.78	10.49	28.66	10.51	28.58	10.60	28.49	10.57	29.46	11.09	29.24	11.50
29.10	10.51	28.98	10.54	28.90	10.61	28.81	10.58	29.78	11.07	29.56	11.50
29.42	10.54	29.30	10.55	29.22	10.64	29.13	10.58	30.10	11.09	29.89	11.51
29.74	10.56	29.62	10.58	29.54	10.65	29.45	10.59	30.42	11.09	30.21	11.49
30.06	10.58	29.94	10.58	29.86	10.66	29.77	10.61	30.74	11.10	30.53	11.50
30.38	10.60	30.26	10.60	30.18	10.67	30.09	10.60	31.06	11.10	30.85	11.50
30.70	10.61	30.58	10.61	30.50	10.68	30.41	10.61	31.38	11.10	31.17	11.49
31.02	10.63	30.90	10.63	30.82	10.70	30.73	10.62	31.70	11.10	31.49	11.49
31.34	10.66	31.22	10.65	31.14	10.72	31.05	10.63	32.02	11.11	31.81	11.47
31.66	10.67	31.54	10.67	31.46	10.72	31.37	10.64	32.34	11.09	32.13	11.48
31.98	10.68	31.86	10.67	31.78	10.74	31.69	10.65	32.66	11.09	32.45	11.46
32.30	10.71	32.17	10.68	32.10	10.75	32.01	10.65	32.98	11.09	32.77	11.47
32.62	10.72	32.49	10.70	32.42	10.76	32.33	10.66	33.30	11.11	33.09	11.47

Table B10 Cure characteristics of the compounds filled with various silica/CB hybrid ratios (cont.): (f) ESBR1723_CSi

ESBR1723											
CSi100/CB0		CSi80/CB20		CSi60/CB40		CSi40/CB60		CSi20/CB80		Silica0/CB100	
Time (min)	Torque (dN.m)	Time (min)	Torque (dN.m)	Time (min)	Torque (dN.m)	Time (min)	Torque (dN.m)	Time (min)	Torque (dN.m)	Time (min)	Torque (dN.m)
32.94	10.74	32.81	10.72	32.73	10.76	32.65	10.66	33.62	11.10	33.41	11.46
33.26	10.74	33.13	10.74	33.05	10.78	32.97	10.66	33.94	11.10	33.73	11.46
33.58	10.78	33.45	10.76	33.37	10.79	33.29	10.68	34.26	11.11	34.05	11.46
33.90	10.79	33.77	10.76	33.69	10.80	33.61	10.68	34.58	11.10	34.37	11.45
34.22	10.80	34.09	10.77	34.01	10.81	33.93	10.68	34.90	11.10	34.69	11.44
34.54	10.81	34.41	10.78	34.33	10.81	34.25	10.68	35.22	11.11	35.01	11.44
34.86	10.81	34.73	10.78	34.65	10.82	34.57	10.68	35.54	11.09	35.33	11.43
35.18	10.83	35.05	10.80	34.97	10.82	34.89	10.69	35.86	11.11	35.65	11.42
35.50	10.85	35.37	10.81	35.29	10.84	35.21	10.71	36.18	11.10	35.97	11.43
35.82	10.87	35.69	10.82	35.61	10.84	35.53	10.71	36.50	11.11	36.29	11.42
36.14	10.87	36.01	10.83	35.93	10.85	35.85	10.71	36.82	11.11	36.61	11.43
36.46	10.89	36.33	10.83	36.25	10.86	36.17	10.72	37.14	11.10	36.93	11.42
36.78	10.89	36.65	10.85	36.57	10.88	36.49	10.72	37.46	11.10	37.25	11.42
37.10	10.89	36.97	10.86	36.89	10.88	36.81	10.72	37.78	11.09	37.57	11.42
37.42	10.92	37.29	10.88	37.21	10.89	37.13	10.72	38.10	11.10	37.89	11.42
37.74	10.93	37.61	10.88	37.53	10.90	37.45	10.73	38.42	11.10	38.21	11.42
38.06	10.94	37.93	10.90	37.85	10.91	37.77	10.73	38.74	11.09	38.53	11.40
38.38	10.94	38.25	10.90	38.17	10.91	38.09	10.74	39.06	11.10	38.85	11.39
38.70	10.95	38.57	10.91	38.49	10.92	38.41	10.75	39.38	11.08	39.17	11.40
39.02	10.97	38.89	10.91	38.81	10.92	38.73	10.75	39.70	11.10	39.49	11.40
39.34	10.98	39.21	10.92	39.13	10.93	39.05	10.75	40.02	11.09	39.81	11.41
39.66	10.98	39.53	10.93	39.45	10.92	39.37	10.74	40.34	11.10	40.13	11.39
39.98	10.99	39.85	10.94	39.77	10.94	39.69	10.74	40.66	11.09	40.45	11.39
40.30	11.00	40.17	10.93	40.09	10.95	40.00	10.75	40.98	11.10	40.77	11.38
40.62	11.00	40.49	10.96	40.41	10.95	40.32	10.76	41.30	11.10	41.09	11.38
40.94	11.02	40.81	10.96	40.73	10.95	40.64	10.76	41.62	11.09	41.41	11.39
41.26	11.02	41.13	10.96	41.05	10.96	40.96	10.77	41.94	11.09	41.73	11.37
41.58	11.03	41.45	10.97	41.37	10.96	41.28	10.77	42.26	11.09	42.05	11.38
41.90	11.05	41.77	10.98	41.69	10.98	41.60	10.77	42.58	11.08	42.40	11.37
42.22	11.06	42.09	10.97	42.01	10.96	41.92	10.78	42.90	11.08	42.72	11.37
42.54	11.07	42.41	10.99	42.33	10.97	42.24	10.77	43.22	11.09	42.98	11.37
42.86	11.06	42.73	11.00	42.65	10.98	42.56	10.77	43.54	11.10		
43.18	11.07	43.05	11.01	42.97	10.99	42.88	10.77	43.86	11.09		
43.50	11.08	43.37	11.00	43.29	11.00	43.20	10.77	44.18	11.08		
43.82	11.08	43.69	11.00	43.61	10.99	43.52	10.78	44.50	11.08		

Table B10 Cure characteristics of the compounds filled with various silica/CB hybrid ratios (cont.): (f) ESBR1723_CSi

ESBR1723											
CSi100/CB0		CSi80/CB20		CSi60/CB40		CSi40/CB60		CSi20/CB80		Silica0/CB100	
Time (min)	Torque (dN.m)	Time (min)	Torque (dN.m)	Time (min)	Torque (dN.m)	Time (min)	Torque (dN.m)	Time (min)	Torque (dN.m)	Time (min)	Torque (dN.m)
44.14	11.09	44.01	11.02	43.93	10.99	43.84	10.77	44.82	11.09		
44.46	11.10	44.33	11.02	44.25	11.01	44.16	10.78	45.14	11.08		
44.78	11.10	44.65	11.03	44.57	11.01	44.48	10.79	45.46	11.08		
45.10	11.11	44.97	11.04	44.89	11.01	44.80	10.79	45.78	11.06		
45.42	11.12	45.29	11.05	45.21	11.02	45.12	10.79	46.10	11.08		
45.74	11.12	45.61	11.05	45.53	11.01	45.44	10.78	46.42	11.08		
46.06	11.13	45.93	11.05	45.85	11.03	45.76	10.79	46.74	11.09		
46.38	11.13	46.25	11.06	46.17	11.04	46.08	10.80	47.06	11.08		
46.70	11.14	46.57	11.06	46.49	11.04	46.40	10.79	47.38	11.08		
47.02	11.15	46.89	11.07	46.81	11.04	46.72	10.79	47.70	11.06		
47.34	11.14	47.21	11.05	47.13	11.04	47.04	10.79	48.02	11.07		
47.66	11.15	47.53	11.07	47.45	11.04	47.36	10.79	48.34	11.07		
47.98	11.17	47.85	11.08	47.77	11.04	47.68	10.79	48.66	11.07		
48.30	11.16	48.17	11.08	48.09	11.05	48.00	10.80	48.98	11.06		
48.62	11.17	48.49	11.08	48.41	11.05	48.32	10.80	49.30	11.07		
48.94	11.17	48.81	11.09	48.73	11.05	48.64	10.80	49.62	11.07		
49.26	11.17	49.13	11.09	49.05	11.06	48.96	10.80	49.98	11.06		
49.58	11.18	49.45	11.10	49.37	11.06	49.28	10.81				
49.90	11.19	49.77	11.10	49.69	11.06	49.60	10.81				
50.00	11.17	49.99	11.10	49.99	11.07	49.92	10.81				
						50.00	10.81				

Table B11 Cure characteristics of the compounds filled with different filler and oil loading

F1		F2		F3		F4	
Time (min)	Torque (dN.m)	Time (min)	Torque (dN.m)	Time (min)	Torque (dN.m)	Time (min)	Torque (dN.m)
0.02	1.88	0.02	2.31	0.02	2.09	0.02	2.24
0.34	2.04	0.34	1.91	0.34	1.75	0.34	1.68
0.66	2.06	0.46	1.90	0.66	1.82	0.66	1.78
0.98	2.12	0.58	1.93	0.98	1.93	0.98	1.91
1.30	2.19	0.90	2.01	1.30	2.02	1.30	2.01
1.62	2.25	1.22	2.08	1.62	2.10	1.62	2.09
1.94	2.32	1.54	2.16	1.94	2.16	1.94	2.15
2.26	2.36	1.86	2.20	2.26	2.20	2.26	2.22
2.58	2.42	2.18	2.26	2.58	2.27	2.58	2.30
2.90	2.48	2.50	2.32	2.90	2.35	2.90	2.38
3.22	2.56	2.82	2.39	3.22	2.46	3.22	2.49
3.54	2.65	3.14	2.46	3.54	2.57	3.54	2.62
3.86	2.77	3.46	2.53	3.86	2.72	3.86	2.79
4.18	2.92	3.78	2.67	3.98	2.75	4.18	2.98
4.50	3.13	4.10	2.83	4.10	2.82	4.50	3.17
4.82	3.36	4.42	3.01	4.42	3.01	4.82	3.41
5.14	3.64	4.74	3.23	4.74	3.25	5.14	3.67
5.46	3.95	5.06	3.47	5.06	3.49	5.46	3.95
5.54	4.04	5.38	3.76	5.38	3.76	5.78	4.23
5.62	4.12	5.54	3.92	5.70	4.11	6.10	4.53
5.94	4.49	5.70	4.07	6.02	4.43	6.42	4.82
6.26	4.84	6.02	4.40	6.34	4.75	6.74	5.13
6.58	5.23	6.34	4.74	6.66	5.07	7.06	5.43
6.90	5.61	6.66	5.09	6.98	5.40	7.38	5.73
7.22	6.02	6.98	5.45	7.30	5.73	7.70	6.01
7.54	6.40	7.30	5.82	7.62	6.06	8.02	6.28
7.86	6.76	7.62	6.15	7.94	6.37	8.34	6.53
8.10	7.04	7.94	6.50	8.26	6.67	8.50	6.67
8.34	7.28	8.26	6.81	8.58	6.93	8.66	6.79
8.66	7.61	8.34	6.90	8.90	7.19	8.98	7.02
8.98	7.91	8.42	6.97	9.22	7.45	9.30	7.24
9.30	8.17	8.74	7.27	9.54	7.67	9.62	7.44
9.62	8.45	9.06	7.54	9.86	7.90	9.94	7.65
9.94	8.70	9.38	7.79	10.18	8.10	10.26	7.84
10.25	8.93	9.70	8.05	10.50	8.29	10.58	8.02

Table B11 Cure characteristics of the compounds filled with different filler and oil loading (cont.)

F1		F2		F3		F4	
Time (min)	Torque (dN.m)	Time (min)	Torque (dN.m)	Time (min)	Torque (dN.m)	Time (min)	Torque (dN.m)
10.57	9.16	10.02	8.28	10.82	8.47	10.90	8.18
10.89	9.37	10.34	8.49	11.14	8.65	11.22	8.35
11.21	9.56	10.66	8.70	11.46	8.80	11.54	8.51
11.53	9.74	10.98	8.89	11.78	8.94	11.86	8.64
11.85	9.90	11.30	9.08	12.10	9.09	12.18	8.78
12.17	10.05	11.62	9.23	12.42	9.22	12.50	8.89
12.49	10.22	11.94	9.39	12.74	9.34	12.82	9.01
12.81	10.36	12.26	9.52	13.06	9.46	13.14	9.13
13.13	10.50	12.58	9.67	13.38	9.59	13.46	9.25
13.45	10.61	12.90	9.82	13.70	9.69	13.78	9.33
13.77	10.75	13.22	9.95	14.02	9.79	14.10	9.44
14.09	10.85	13.54	10.06	14.34	9.88	14.42	9.55
14.41	10.98	13.86	10.17	14.66	9.99	14.74	9.64
14.73	11.06	14.18	10.28	14.98	10.08	15.06	9.71
15.05	11.16	14.50	10.38	15.30	10.16	15.38	9.80
15.37	11.26	14.82	10.47	15.62	10.24	15.70	9.88
15.69	11.36	15.14	10.56	15.94	10.32	16.02	9.96
16.01	11.43	15.46	10.65	16.26	10.39	16.34	10.02
16.33	11.50	15.78	10.73	16.58	10.45	16.66	10.08
16.65	11.57	16.10	10.80	16.90	10.52	16.98	10.16
16.97	11.64	16.42	10.89	17.22	10.58	17.30	10.22
17.29	11.71	16.75	10.96	17.54	10.63	17.62	10.28
17.61	11.77	17.07	11.02	17.86	10.69	17.94	10.33
17.93	11.84	17.39	11.07	18.18	10.74	18.26	10.38
18.25	11.90	17.71	11.13	18.50	10.79	18.58	10.42
18.57	11.95	18.03	11.19	18.82	10.83	18.90	10.47
18.89	11.99	18.35	11.24	19.14	10.88	19.21	10.52
19.21	12.04	18.67	11.30	19.46	10.92	19.53	10.57
19.53	12.08	18.99	11.35	19.78	10.96	19.85	10.61
19.85	12.13	19.31	11.39	20.10	11.01	20.17	10.65
20.17	12.17	19.63	11.44	20.42	11.05	20.49	10.68
20.49	12.21	19.95	11.47	20.74	11.08	20.81	10.72
20.81	12.25	20.27	11.51	21.06	11.11	21.13	10.76
21.13	12.28	20.59	11.54	21.38	11.15	21.45	10.80
21.45	12.32	20.91	11.59	21.70	11.16	21.77	10.83

Table B11 Cure characteristics of the compounds filled with different filler and oil loading (cont.)

F1		F2		F3		F4	
Time (min)	Torque (dN.m)	Time (min)	Torque (dN.m)	Time (min)	Torque (dN.m)	Time (min)	Torque (dN.m)
21.77	12.36	21.23	11.62	22.02	11.21	22.09	10.84
22.09	12.38	21.55	11.65	22.34	11.23	22.41	10.88
22.41	12.41	21.87	11.68	22.66	11.25	22.73	10.90
22.73	12.44	22.19	11.71	22.97	11.27	23.05	10.93
23.05	12.48	22.51	11.74	23.29	11.30	23.37	10.96
23.36	12.50	22.83	11.77	23.61	11.33	23.69	10.99
23.68	12.52	23.15	11.79	23.93	11.36	24.01	11.01
24.00	12.54	23.47	11.82	24.25	11.37	24.33	11.03
24.32	12.58	23.79	11.84	24.57	11.39	24.65	11.06
24.64	12.60	24.11	11.86	24.89	11.42	24.97	11.08
24.98	12.62	24.43	11.89	25.21	11.44	25.29	11.10
25.30	12.64	24.75	11.91	25.53	11.47	25.61	11.11
25.62	12.66	25.07	11.92	25.85	11.48	25.93	11.13
25.94	12.68	25.39	11.94	26.17	11.49	26.25	11.15
26.26	12.71	25.71	11.97	26.49	11.51	26.57	11.16
26.58	12.71	26.03	11.99	26.81	11.54	26.89	11.18
26.90	12.74	26.35	12.01	27.13	11.55	27.21	11.21
27.22	12.74	26.67	12.03	27.45	11.57	27.53	11.22
27.54	12.76	26.99	12.04	27.77	11.59	27.85	11.23
27.86	12.78	27.31	12.06	28.09	11.60	28.17	11.26
28.18	12.80	27.63	12.09	28.41	11.61	28.49	11.28
28.50	12.82	27.95	12.08	28.73	11.62	28.81	11.30
28.82	12.83	28.27	12.09	29.05	11.64	29.13	11.30
29.14	12.84	28.59	12.12	29.37	11.65	29.45	11.31
29.46	12.84	28.91	12.14	29.69	11.67	29.77	11.33
29.78	12.87	29.23	12.14	30.01	11.68	30.09	11.35
30.10	12.87	29.55	12.16	30.33	11.69	30.41	11.36
30.42	12.89	29.87	12.17	30.65	11.72	30.73	11.38
30.74	12.89	30.19	12.18	30.97	11.73	31.05	11.38
31.06	12.90	30.51	12.18	31.29	11.74	31.37	11.40
31.38	12.92	30.83	12.20	31.61	11.74	31.69	11.42
31.70	12.93	31.15	12.22	31.93	11.75	32.01	11.41
32.02	12.94	31.48	12.23	32.25	11.77	32.33	11.43
32.34	12.94	31.80	12.23	32.57	11.77	32.65	11.42
32.66	12.94	32.12	12.25	32.89	11.77	32.97	11.45

Table B11 Cure characteristics of the compounds filled with different filler and oil loading (cont.)

F1		F2		F3		F4	
Time (min)	Torque (dN.m)	Time (min)	Torque (dN.m)	Time (min)	Torque (dN.m)	Time (min)	Torque (dN.m)
32.98	12.95	32.44	12.25	33.21	11.78	33.29	11.46
33.30	12.97	32.76	12.26	33.53	11.79	33.61	11.47
33.62	12.99	33.08	12.27	33.85	11.79	33.93	11.47
33.94	12.99	33.40	12.28	34.17	11.80	34.25	11.47
34.26	12.99	33.72	12.28	34.49	11.83	34.57	11.50
34.58	12.99	34.04	12.29	34.81	11.83	34.89	11.51
34.90	13.00	34.36	12.30	35.13	11.84	35.21	11.53
35.22	13.01	34.68	12.32	35.45	11.86	35.53	11.53
35.54	13.03	35.00	12.33	35.77	11.86	35.85	11.52
35.86	13.04	35.32	12.34	36.09	11.87	36.17	11.56
36.18	13.03	35.64	12.34	36.41	11.87	36.49	11.56
36.50	13.05	35.96	12.35	36.73	11.88	36.81	11.57
36.81	13.05	36.28	12.35	37.05	11.89	37.13	11.58
37.13	13.05	36.60	12.36	37.37	11.90	37.45	11.59
37.45	13.06	36.92	12.37	37.69	11.90	37.77	11.58
37.77	13.06	37.24	12.37	38.01	11.91	38.09	11.60
38.09	13.06	37.56	12.37	38.33	11.92	38.41	11.62
38.41	13.07	37.88	12.39	38.65	11.93	38.73	11.60
38.73	13.07	38.20	12.38	38.97	11.93	39.05	11.60
39.05	13.10	38.52	12.41	39.29	11.92	39.37	11.63
39.37	13.09	38.84	12.41	39.61	11.95	39.69	11.64
39.69	13.10	39.16	12.43	39.93	11.95	40.01	11.62
40.01	13.11	39.48	12.42	40.25	11.95	40.33	11.63
40.33	13.11	39.80	12.42	40.57	11.96	40.65	11.65
40.65	13.11	40.13	12.44	40.89	11.96	40.97	11.67
40.97	13.10	40.45	12.43	41.21	11.99	41.29	11.67
41.29	13.12	40.77	12.44	41.53	11.99	41.61	11.67
41.61	13.12	41.09	12.44	41.85	11.98	41.93	11.68
41.93	13.12	41.41	12.45	42.17	11.99	42.25	11.68
42.25	13.12	41.73	12.46	42.49	11.99	42.57	11.70
42.57	13.13	42.05	12.45	42.81	11.99	42.89	11.69
42.89	13.15	42.37	12.46	43.13	12.01	43.21	11.71
43.21	13.15	42.69	12.47	43.45	12.02	43.53	11.71
43.53	13.15	43.01	12.48	43.77	12.01	43.85	11.72
43.85	13.15	43.33	12.48	44.09	12.02	44.17	11.71

Table B11 Cure characteristics of the compounds filled with different filler and oil loading (cont.)

F1		F2		F3		F4	
Time (min)	Torque (dN.m)	Time (min)	Torque (dN.m)	Time (min)	Torque (dN.m)	Time (min)	Torque (dN.m)
44.17	13.16	43.65	12.49	44.41	12.02	44.49	11.73
44.49	13.17	43.97	12.50	44.75	12.03	44.80	11.73
44.81	13.16	44.29	12.50	45.07	12.04	45.12	11.73
45.13	13.16	44.61	12.49	45.39	12.04	45.44	11.73
45.45	13.17	44.93	12.49	45.71	12.04	45.76	11.73
45.77	13.17	45.25	12.49	46.03	12.05	46.08	11.74
46.09	13.18	45.57	12.51	46.35	12.06	46.40	11.76
46.41	13.18	45.89	12.51	46.67	12.07	46.72	11.77
46.73	13.18	46.21	12.52	46.99	12.08	47.04	11.77
47.05	13.19	46.53	12.54	47.31	12.06	47.36	11.77
47.37	13.20	46.85	12.52	47.63	12.09	47.68	11.78
47.69	13.21	47.17	12.54	47.95	12.07	48.00	11.78
48.01	13.21	47.49	12.54	48.27	12.09	48.32	11.79
48.33	13.20	47.81	12.55	48.59	12.09	48.64	11.80
48.65	13.21	48.13	12.55	48.91	12.08	48.96	11.80
48.97	13.21	48.45	12.55	49.23	12.08	49.28	11.81
49.29	13.23	48.77	12.55	49.55	12.10	49.60	11.81
49.61	13.21	49.09	12.55	49.87	12.09	49.98	11.79
49.99	13.22	49.41	12.54	49.99	12.11		
		49.73	12.55				
		49.99	12.56				

Table B12 Cure characteristics of the compounds having different relative amount of curatives

CV_100%		CV_120%		CV_140%		semi-EV_100%		semi-EV_120%		semi-EV_140%	
Time (min)	Torque (dN.m)	Time (min)	Torque (dN.m)	Time (min)	Torque (dN.m)	Time (min)	Torque (dN.m)	Time (min)	Torque (dN.m)	Time (min)	Torque (dN.m)
0.02	2.99	0.02	2.88	0.02	2.29	0.02	2.27	0.02	2.73	0.02	2.84
0.34	2.21	0.34	2.22	0.06	2.76	0.34	2.33	0.34	2.23	0.34	2.21
0.42	2.19	0.38	2.21	0.10	2.53	0.50	2.33	0.66	2.28	0.66	2.25
0.50	2.21	0.42	2.22	0.42	2.21	0.66	2.36	0.98	2.36	0.98	2.33
0.82	2.28	0.76	2.28	0.74	2.27	0.98	2.45	1.30	2.45	1.30	2.42
1.14	2.36	1.10	2.37	1.06	2.35	1.30	2.52	1.62	2.52	1.62	2.49
1.46	2.43	1.42	2.44	1.38	2.42	1.62	2.59	1.94	2.57	1.94	2.55
1.78	2.50	1.74	2.51	1.70	2.49	1.94	2.64	2.26	2.63	2.26	2.60
2.10	2.55	2.06	2.58	2.02	2.57	2.26	2.70	2.58	2.69	2.58	2.67
2.42	2.61	2.38	2.66	2.34	2.63	2.58	2.75	2.90	2.77	2.90	2.76
2.74	2.69	2.71	2.74	2.66	2.74	2.90	2.82	3.22	2.86	3.22	2.86
3.06	2.78	3.03	2.86	2.98	2.89	3.22	2.87	3.54	2.96	3.54	3.01
3.38	2.89	3.35	3.02	3.30	3.11	3.54	2.97	3.86	3.10	3.86	3.22
3.70	3.03	3.67	3.23	3.42	3.24	3.86	3.08	4.18	3.30	4.18	3.50
4.02	3.23	3.99	3.54	3.54	3.35	4.18	3.20	4.50	3.53	4.50	3.86
4.34	3.47	4.31	3.93	3.86	3.79	4.50	3.36	4.82	3.82	4.82	4.28
4.66	3.75	4.63	4.41	4.10	4.24	4.82	3.53	5.14	4.12	5.14	4.75
4.98	4.07	4.95	4.92	4.34	4.73	5.14	3.72	5.46	4.48	5.46	5.23
5.10	4.20	5.27	5.48	4.66	5.50	5.46	3.94	5.78	4.84	5.78	5.74
5.22	4.33	5.59	6.06	4.98	6.33	5.78	4.15	6.10	5.19	6.10	6.19
5.54	4.69	5.91	6.64	5.30	7.18	6.02	4.33	6.42	5.55	6.42	6.64
5.86	5.08	6.23	7.21	5.62	8.01	6.26	4.51	6.74	5.88	6.74	7.09
6.18	5.46	6.55	7.74	5.94	8.77	6.58	4.74	7.06	6.21	7.06	7.50
6.50	5.86	6.87	8.23	6.26	9.45	6.90	4.98	7.38	6.53	7.38	7.91
6.82	6.25	7.19	8.67	6.58	10.01	7.22	5.21	7.70	6.84	7.70	8.27
7.14	6.65	7.51	9.09	6.90	10.56	7.54	5.43	8.02	7.14	8.02	8.60
7.46	7.03	7.83	9.46	7.22	11.01	7.86	5.65	8.14	7.25	8.34	8.90
7.78	7.39	8.15	9.79	7.54	11.42	8.18	5.88	8.30	7.38	8.66	9.17
8.10	7.72	8.47	10.11	7.86	11.76	8.50	6.09	8.62	7.64	8.98	9.41
8.42	8.01	8.79	10.39	8.18	12.08	8.82	6.29	8.97	7.93	9.30	9.64
8.74	8.30	9.11	10.65	8.50	12.37	9.14	6.50	9.29	8.14	9.62	9.83
9.06	8.58	9.43	10.90	8.82	12.62	9.46	6.70	9.61	8.35	9.94	10.02
9.38	8.83	9.75	11.11	9.14	12.86	9.78	6.89	9.93	8.54	10.26	10.19
9.70	9.06	10.07	11.31	9.46	13.07	10.10	7.06	10.25	8.73	10.58	10.35
10.02	9.28	10.39	11.50	9.78	13.27	10.42	7.24	10.57	8.91	10.90	10.47

Table B12 Cure characteristics of the compounds having different relative amount of curatives (cont.)

CV_100%		CV_120%		CV_140%		semi-EV_100%		semi-EV_120%		semi-EV_140%	
Time (min)	Torque (dN.m)	Time (min)	Torque (dN.m)	Time (min)	Torque (dN.m)	Time (min)	Torque (dN.m)	Time (min)	Torque (dN.m)	Time (min)	Torque (dN.m)
10.34	9.48	10.71	11.66	10.10	13.44	10.74	7.38	10.89	9.06	11.22	10.61
10.66	9.66	11.03	11.83	10.42	13.59	11.06	7.54	11.21	9.20	11.54	10.72
10.98	9.84	11.35	11.97	10.74	13.71	11.38	7.68	11.53	9.34	11.86	10.82
11.30	10.01	11.67	12.11	11.06	13.85	11.70	7.81	11.85	9.47	12.18	10.92
11.62	10.17	11.99	12.25	11.38	13.97	12.02	7.95	12.17	9.59	12.50	11.02
11.94	10.31	12.31	12.37	11.70	14.07	12.34	8.08	12.49	9.70	12.82	11.11
12.26	10.45	12.63	12.47	12.02	14.16	12.66	8.19	12.81	9.80	13.14	11.18
12.58	10.57	12.95	12.57	12.34	14.26	12.98	8.31	13.13	9.89	13.46	11.26
12.90	10.70	13.27	12.68	12.66	14.33	13.30	8.40	13.45	9.98	13.78	11.32
13.22	10.82	13.59	12.76	12.98	14.40	13.62	8.50	13.77	10.07	14.10	11.39
13.54	10.92	13.91	12.85	13.30	14.46	13.94	8.60	14.09	10.15	14.42	11.45
13.86	11.02	14.23	12.93	13.62	14.54	14.26	8.68	14.41	10.22	14.74	11.50
14.18	11.11	14.55	13.00	13.94	14.59	14.58	8.76	14.73	10.30	15.06	11.56
14.50	11.21	14.87	13.07	14.26	14.67	14.90	8.84	15.05	10.37	15.38	11.61
14.82	11.30	15.19	13.14	14.58	14.72	15.22	8.93	15.37	10.43	15.70	11.65
15.14	11.38	15.51	13.20	14.90	14.77	15.54	8.99	15.69	10.49	16.02	11.69
15.46	11.46	15.83	13.26	15.22	14.82	15.86	9.06	16.01	10.55	16.33	11.73
15.78	11.54	16.15	13.31	15.54	14.84	16.18	9.13	16.33	10.61	16.65	11.78
16.10	11.60	16.47	13.36	15.86	14.90	16.50	9.19	16.65	10.65	16.97	11.80
16.42	11.67	16.79	13.42	16.18	14.93	16.81	9.25	16.97	10.70	17.29	11.84
16.74	11.73	17.11	13.46	16.50	14.97	17.13	9.32	17.29	10.77	17.61	11.87
17.06	11.78	17.43	13.50	16.82	14.99	17.45	9.36	17.61	10.80	17.93	11.91
17.38	11.84	17.75	13.53	17.14	15.03	17.77	9.41	17.93	10.84	18.25	11.93
17.70	11.88	18.07	13.57	17.46	15.06	18.09	9.46	18.25	10.88	18.57	11.96
18.02	11.93	18.39	13.60	17.78	15.09	18.41	9.51	18.57	10.91	18.89	12.00
18.34	11.97	18.71	13.64	18.10	15.12	18.73	9.56	18.89	10.96	19.21	12.01
18.66	12.02	19.03	13.69	18.42	15.12	19.05	9.60	19.21	10.99	19.53	12.04
18.98	12.08	19.35	13.71	18.74	15.15	19.37	9.65	19.53	11.01	19.85	12.06
19.30	12.11	19.67	13.73	19.06	15.19	19.69	9.69	19.85	11.04	20.17	12.07
19.62	12.16	19.99	13.76	19.38	15.19	20.01	9.73	20.17	11.08	20.49	12.10
19.94	12.19	20.31	13.79	19.70	15.22	20.33	9.76	20.49	11.11	20.81	12.12
20.26	12.21	20.63	13.81	20.02	15.24	20.65	9.80	20.81	11.15	21.13	12.13
20.58	12.25	20.95	13.83	20.34	15.27	20.97	9.83	21.13	11.16	21.45	12.13
20.90	12.29	21.27	13.86	20.66	15.28	21.29	9.87	21.45	11.18	21.77	12.16
21.22	12.32	21.59	13.88	20.98	15.29	21.61	9.90	21.77	11.21	22.09	12.18

Table B12 Cure characteristics of the compounds having different relative amount of curatives (cont.)

CV_100%		CV_120%		CV_140%		semi-EV_100%		semi-EV_120%		semi-EV_140%	
Time (min)	Torque (dN.m)	Time (min)	Torque (dN.m)	Time (min)	Torque (dN.m)	Time (min)	Torque (dN.m)	Time (min)	Torque (dN.m)	Time (min)	Torque (dN.m)
21.54	12.36	21.91	13.89	21.30	15.32	21.93	9.94	22.09	11.23	22.41	12.19
21.86	12.37	22.23	13.90	21.62	15.33	22.25	9.95	22.41	11.25	22.73	12.21
22.18	12.40	22.55	13.91	21.94	15.35	22.57	9.98	22.73	11.27	23.05	12.22
22.50	12.42	22.87	13.95	22.26	15.36	22.89	10.01	23.05	11.29	23.37	12.23
22.82	12.45	23.19	13.95	22.58	15.37	23.21	10.04	23.37	11.32	23.69	12.25
23.14	12.48	23.51	13.98	22.90	15.39	23.53	10.05	23.69	11.34	24.01	12.25
23.46	12.49	23.83	13.98	23.22	15.40	23.85	10.08	24.01	11.35	24.33	12.27
23.78	12.51	24.15	14.01	23.54	15.40	24.17	10.11	24.33	11.37	24.65	12.27
24.10	12.54	24.47	14.02	23.86	15.43	24.49	10.14	24.65	11.38	24.97	12.30
24.42	12.56	24.79	14.03	24.18	15.43	24.81	10.15	24.97	11.39	25.29	12.29
24.74	12.58	25.11	14.06	24.50	15.44	25.13	10.17	25.29	11.42	25.61	12.31
25.05	12.60	25.43	14.07	24.82	15.47	25.45	10.19	25.61	11.42	25.93	12.33
25.37	12.61	25.75	14.06	25.14	15.48	25.77	10.22	25.93	11.45	26.25	12.33
25.69	12.62	26.07	14.09	25.46	15.46	26.09	10.23	26.25	11.45	26.57	12.35
26.01	12.65	26.39	14.11	25.78	15.48	26.41	10.25	26.56	11.46	26.89	12.34
26.33	12.66	26.71	14.11	26.10	15.49	26.73	10.26	26.88	11.47	27.21	12.36
26.65	12.68	27.03	14.11	26.42	15.51	27.05	10.26	27.20	11.50	27.53	12.37
26.97	12.69	27.35	14.13	26.74	15.51	27.36	10.31	27.52	11.51	27.85	12.38
27.29	12.71	27.67	14.14	27.06	15.53	27.68	10.31	27.84	11.52	28.17	12.39
27.61	12.72	27.99	14.14	27.38	15.54	28.00	10.33	28.16	11.51	28.49	12.39
27.93	12.73	28.31	14.15	27.70	15.54	28.32	10.35	28.48	11.53	28.81	12.39
28.25	12.74	28.65	14.15	28.02	15.55	28.64	10.36	28.80	11.56	29.13	12.40
28.57	12.76	28.97	14.17	28.34	15.57	28.96	10.38	29.12	11.56	29.45	12.39
28.89	12.77	29.29	14.18	28.66	15.58	29.28	10.38	29.44	11.58	29.77	12.41
29.21	12.77	29.61	14.18	28.98	15.59	29.60	10.41	29.76	11.58	30.09	12.44
29.53	12.78	29.93	14.19	29.30	15.58	29.92	10.42	30.08	11.60	30.41	12.44
29.85	12.80	30.25	14.20	29.62	15.59	30.24	10.44	30.40	11.60	30.73	12.44
30.17	12.82	30.57	14.21	29.94	15.61	30.56	10.43	30.72	11.62	31.05	12.45
30.49	12.82	30.89	14.21	30.26	15.62	30.88	10.46	31.04	11.61	31.37	12.46
30.81	12.84	31.21	14.22	30.58	15.62	31.20	10.45	31.36	11.62	31.69	12.47
31.13	12.83	31.53	14.22	30.90	15.61	31.52	10.48	31.68	11.63	32.01	12.48
31.45	12.84	31.85	14.23	31.22	15.63	31.84	10.48	32.00	11.64	32.33	12.48
31.77	12.86	32.17	14.24	31.54	15.63	32.16	10.50	32.32	11.64	32.65	12.48
32.09	12.87	32.49	14.24	31.86	15.64	32.48	10.51	32.64	11.66	32.97	12.49
32.41	12.88	32.81	14.25	32.18	15.65	32.80	10.51	32.96	11.66	33.29	12.49

Table B12 Cure characteristics of the compounds having different relative amount of curatives (cont.)

CV_100%		CV_120%		CV_140%		semi-EV_100%		semi-EV_120%		semi-EV_140%	
Time (min)	Torque (dN.m)	Time (min)	Torque (dN.m)	Time (min)	Torque (dN.m)	Time (min)	Torque (dN.m)	Time (min)	Torque (dN.m)	Time (min)	Torque (dN.m)
32.73	12.88	33.13	14.26	32.50	15.66	33.12	10.52	33.28	11.67	33.61	12.50
33.05	12.90	33.45	14.26	32.82	15.66	33.44	10.52	33.60	11.68	33.93	12.49
33.37	12.90	33.77	14.27	33.14	15.66	33.76	10.54	33.92	11.68	34.25	12.50
33.69	12.89	34.09	14.27	33.46	15.67	34.08	10.55	34.24	11.69	34.57	12.51
34.01	12.92	34.41	14.27	33.78	15.68	34.40	10.55	34.56	11.68	34.89	12.53
34.33	12.91	34.73	14.27	34.10	15.68	34.72	10.55	34.88	11.72	35.21	12.53
34.65	12.93	35.05	14.28	34.42	15.69	35.04	10.58	35.20	11.71	35.53	12.52
34.97	12.93	35.37	14.29	34.74	15.71	35.36	10.58	35.52	11.70	35.85	12.52
35.29	12.94	35.69	14.30	35.06	15.71	35.68	10.59	35.84	11.71	36.17	12.54
35.61	12.95	36.01	14.30	35.38	15.70	36.00	10.60	36.16	11.73	36.49	12.54
35.93	12.95	36.33	14.31	35.70	15.72	36.32	10.61	36.48	11.74	36.81	12.54
36.25	12.96	36.65	14.31	36.02	15.72	36.64	10.61	36.80	11.75	37.13	12.55
36.57	12.97	36.97	14.31	36.34	15.72	36.96	10.62	37.12	11.75	37.45	12.55
36.89	12.97	37.29	14.32	36.66	15.73	37.28	10.63	37.44	11.75	37.77	12.56
37.21	12.97	37.61	14.33	36.98	15.75	37.60	10.64	37.76	11.76	38.09	12.56
37.53	13.00	37.93	14.31	37.30	15.73	37.92	10.66	38.08	11.76	38.41	12.58
37.85	12.99	38.25	14.31	37.62	15.76	38.24	10.65	38.40	11.77	38.73	12.59
38.17	12.98	38.57	14.34	37.94	15.76	38.56	10.66	38.72	11.78	39.05	12.58
38.49	13.00	38.89	14.34	38.26	15.76	38.88	10.67	39.04	11.78	39.37	12.58
38.81	13.00	39.21	14.35	38.58	15.75	39.20	10.66	39.36	11.78	39.69	12.59
39.13	13.01	39.53	14.34	38.90	15.78	39.52	10.68	39.68	11.80	40.01	12.60
39.45	13.02	39.85	14.35	39.22	15.77	39.84	10.68	40.00	11.80	40.33	12.61
39.77	13.01	40.17	14.35	39.54	15.78	40.16	10.69	40.32	11.81	40.65	12.60
40.09	13.01	40.49	14.35	39.86	15.79	40.48	10.70	40.64	11.82	40.97	12.60
40.41	13.02	40.81	14.35	40.18	15.78	40.80	10.70	40.96	11.81	41.29	12.61
40.73	13.04	41.13	14.37	40.50	15.78	41.12	10.71	41.28	11.82	41.61	12.61
41.05	13.04	41.45	14.37	40.82	15.79	41.44	10.72	41.60	11.84	41.93	12.62
41.37	13.04	41.77	14.39	41.14	15.81	41.76	10.73	41.92	11.83	42.25	12.63
41.69	13.05	42.09	14.37	41.47	15.81	42.08	10.73	42.24	11.84	42.57	12.63
42.01	13.06	42.41	14.40	41.79	15.82	42.40	10.75	42.56	11.83	42.89	12.63
42.33	13.06	42.73	14.35	42.11	15.81	42.72	10.75	42.89	11.84	43.21	12.65
42.64	13.06	43.05	14.40	42.43	15.82	43.04	10.75	43.21	11.85	43.53	12.65
42.96	13.07	43.37	14.38	42.75	15.84	43.36	10.75	43.53	11.86	43.85	12.64
43.28	13.07	43.69	14.37	43.07	15.83	43.68	10.76	43.85	11.84	44.17	12.66
43.60	13.08	44.01	14.39	43.39	15.84	44.00	10.76	44.17	11.86	44.49	12.65

Table B12 Cure characteristics of the compounds having different relative amount of curatives (cont.)

CV_100%		CV_120%		CV_140%		semi-EV_100%		semi-EV_120%		semi-EV_140%	
Time (min)	Torque (dN.m)	Time (min)	Torque (dN.m)	Time (min)	Torque (dN.m)	Time (min)	Torque (dN.m)	Time (min)	Torque (dN.m)	Time (min)	Torque (dN.m)
43.92	13.08	44.33	14.40	43.71	15.83	44.32	10.77	44.49	11.87	44.81	12.65
44.24	13.08	44.65	14.38	44.03	15.84	44.64	10.77	44.81	11.87	45.13	12.66
44.56	13.09	44.97	14.45	44.35	15.85	44.96	10.78	45.13	11.88	45.45	12.66
44.88	13.09	45.29	14.39	44.67	15.84	45.28	10.78	45.45	11.87	45.77	12.67
45.20	13.10	45.61	14.40	44.99	15.85	45.60	10.79	45.77	11.88	46.09	12.66
45.52	13.11	45.93	14.40	45.31	15.86	45.92	10.79	46.09	11.88	46.41	12.67
45.84	13.10	46.25	14.40	45.63	15.86	46.24	10.79	46.41	11.90	46.73	12.67
46.16	13.10	46.57	14.42	45.95	15.86	46.56	10.79	46.73	11.89	47.05	12.68
46.48	13.11	46.89	14.40	46.27	15.87	46.88	10.81	47.05	11.90	47.37	12.68
46.80	13.12	47.21	14.41	46.59	15.87	47.20	10.81	47.37	11.90	47.69	12.70
47.12	13.12	47.53	14.41	46.91	15.86	47.52	10.82	47.69	11.91	48.01	12.71
47.44	13.13	47.85	14.42	47.23	15.87	47.84	10.80	48.01	11.91	48.33	12.70
47.76	13.13	48.17	14.41	47.55	15.87	48.16	10.81	48.33	11.91	48.65	12.70
48.08	13.14	48.49	14.42	47.87	15.87	48.48	10.82	48.65	11.91	48.97	12.70
48.40	13.13	48.81	14.43	48.19	15.87	48.80	10.84	48.97	11.92	49.29	12.69
48.72	13.14	49.12	14.42	48.51	15.88	49.12	10.83	49.29	11.92	49.61	12.71
49.04	13.14	49.44	14.43	48.83	15.88	49.44	10.84	49.61	11.93	49.99	12.72
49.36	13.14	49.76	14.43	49.15	15.88	49.76	10.85	49.99	11.93		
49.68	13.15	49.98	14.46	49.47	15.89	50.00	10.83				
50.00	13.15			49.79	15.91						
				49.99	15.88						

APPENDIX C
PAYNE EFFECT OF THE RUBBER COMPOUNDS

Table C1 Storage modulus (G') as a function of test strain of the compounds prepared at various silanization temperatures: (a) HDSi

Strain (%)	G' (kPa)				
	HDSi_120°C	HDSi_130°C	HDSi_140°C	HDSi_150°C	HDSi_160°C
0.56	520.66	437.78	403.78	380.46	365.53
0.98	470.04	403.39	370.35	363.40	340.22
1.95	414.08	356.00	329.20	324.17	309.09
5.02	325.04	287.11	273.22	264.83	270.33
10.04	248.59	229.04	234.95	240.86	242.94
19.95	191.03	192.68	194.77	202.82	208.65
49.94	131.72	120.81	134.46	141.42	146.66
100.02	82.67	81.22	84.97	88.41	91.02

Table C2 Storage modulus (G') as a function of test strain of the compounds prepared at various silanization temperatures: (b) CSi

Strain (%)	G' (kPa)				
	CSi_120°C	CSi_130°C	CSi_140°C	CSi_150°C	CSi_160°C
0.56	409.58	343.34	313.48	355.65	336.00
0.98	439.33	369.78	348.39	345.45	333.09
1.95	391.25	326.68	301.83	304.05	293.93
5.02	306.02	264.24	240.10	252.06	252.70
10.04	236.07	223.77	215.15	219.57	224.93
19.95	182.55	182.17	179.34	185.54	194.07
49.94	127.07	124.64	125.75	131.74	139.65
100.02	80.96	80.24	81.43	84.58	88.87

Table C3 Storage modulus (G') as a function of test strain of the compounds treated by various TESPT contents: (a) HDSi

Strain (%)	G' (kPa)				
	HDSi_without TESPT	HDSi_6wt%	HDSi_8wt%	HDSi_10wt%	HDSi_12wt%
0.56	1565.20	454.90	417.68	405.90	386.66
0.98	1571.90	449.62	405.48	379.00	372.52
1.95	1387.90	402.08	355.24	330.21	319.14
5.02	935.36	328.84	289.84	258.23	252.15
10.04	712.33	278.73	247.55	231.06	225.26
19.95	454.97	226.50	194.85	193.00	187.47
49.94	227.59	151.48	140.35	126.43	130.99
100.02	127.70	93.49	88.53	85.77	83.77

Table C4 Storage modulus (G') as a function of test strain of the compounds treated by various TESPT contents: (b) CSi

Strain (%)	G' (kPa)				
	CSi_without TESPT	CSi_6wt%	CSi_8wt%	CSi_10wt%	CSi_12wt%
0.56	1657.60	411.47	394.21	377.36	343.24
0.98	1679.50	391.66	360.50	364.87	333.68
1.95	1465.30	361.71	321.66	314.18	285.64
5.02	1018.60	297.02	263.81	254.31	234.86
10.04	696.79	252.13	225.84	218.72	202.72
19.95	436.22	196.20	187.73	174.01	169.45
49.94	217.59	140.83	132.03	127.65	120.72
100.02	123.93	89.58	85.27	82.71	79.04

Table C5 Storage modulus (G') as a function of test strain of the compounds filled with various silica/CB hybrid ratios: (a) HDSi

Strain (%)	G' (kPa)					
	SSBR6450SL					
	HDSi100/CB0	HDSi80/CB20	HDSi60/CB40	HDSi40/CB60	HDSi800/CB20	Silica0/CB100
0.56	429.05	467.30	476.61	591.85	687.48	978.63
0.98	410.77	443.14	443.73	532.01	615.03	834.98
1.95	357.21	379.15	374.59	403.14	473.77	574.93
5.02	285.77	297.56	276.57	316.44	329.66	347.93
10.04	241.88	250.24	242.69	255.71	259.23	255.51
19.95	197.95	205.15	199.61	205.71	204.80	193.43
49.94	135.89	141.13	139.89	142.35	140.04	129.61
100.02	86.02	90.00	90.61	91.48	89.54	84.38
Strain (%)	SSBR3626					
	HDSi100/CB0	HDSi80/CB20	HDSi60/CB40	HDSi40/CB60	HDSi800/CB20	Silica0/CB100
0.56	442.03	459.03	531.16	573.79	713.68	1026.10
0.98	439.60	429.61	500.42	565.64	678.51	935.28
1.95	377.31	377.60	404.43	409.50	507.21	634.28
5.02	275.84	289.00	299.74	314.86	318.70	370.61
10.04	244.39	232.56	246.50	254.09	264.50	267.18
19.95	191.40	191.26	194.10	204.09	199.42	202.00
49.94	139.92	132.14	134.64	134.68	145.18	137.60
100.02	90.49	86.34	93.97	94.49	95.41	89.96
Strain (%)	ESBR1723					
	HDSi100/CB0	HDSi80/CB20	HDSi60/CB40	HDSi40/CB60	HDSi800/CB20	Silica0/CB100
0.56	236.07	256.84	278.70	354.11	477.61	770.52
0.98	221.02	249.88	278.43	322.76	457.78	705.48
1.95	200.97	209.28	238.28	286.46	356.83	487.65
5.02	167.84	180.38	192.66	216.55	243.89	291.97
10.04	145.99	155.32	163.03	176.53	189.87	211.78
19.95	122.18	127.93	133.29	140.52	147.34	157.35
49.94	88.60	91.33	94.05	91.53	100.43	103.98
100.02	60.33	57.94	62.81	64.52	66.07	67.71

Table C6 Storage modulus (G') as a function of test strain of the compounds filled with various silica/CB hybrid ratios: (b) CSi

Strain (%)	G' (kPa)					
	SSBR6450SL					
	CSi100/CB0	CSi80/CB20	CSi60/CB40	CSi40/CB60	CSi800/CB20	Silica0/CB100
0.56	375.29	421.81	461.1	532.44	684.3	978.63
0.98	361.93	411.36	428.31	493.16	616.82	834.98
1.95	296.8	348.24	364.96	402.36	473.88	574.93
5.02	252.55	272.17	278.19	295.71	324.82	347.93
10.04	215.45	229.25	232.07	240.22	252.9	255.51
19.95	179.71	189.77	190.51	194.66	199.07	193.43
49.94	126.81	132.78	133.48	135.38	136.58	129.61
100.02	82.642	86.211	86.69	88.181	88.511	84.38
Strain (%)	SSBR3626					
	CSi100/CB0	CSi80/CB20	CSi60/CB40	CSi40/CB60	CSi800/CB20	Silica0/CB100
0.56	378.15	415.31	462.31	574.88	732.26	1026.10
0.98	375.63	392.09	443.35	554.35	686.04	935.28
1.95	318.29	342.23	363.55	433.04	513.93	634.28
5.02	252.04	264.31	272.62	309.69	343.19	370.61
10.04	216.35	223.41	227.54	249.23	265.95	267.18
19.95	181.89	186.18	188.21	200.34	208.85	202.00
49.94	132.06	126.71	135.99	133.18	144.89	137.60
100.02	88.01	89.77	90.88	93.85	95.21	89.96
Strain (%)	ESBR1723					
	CSi100/CB0	CSi80/CB20	CSi60/CB40	CSi40/CB60	CSi800/CB20	Silica0/CB100
0.56	224.05	255.75	290.72	350.83	452.47	770.52
0.98	219.03	250.21	289.09	332.55	432.07	705.48
1.95	197.35	223.38	249.08	284.00	355.93	487.65
5.02	166.37	175.86	197.96	215.47	225.84	291.97
10.04	144.34	158.10	166.06	176.88	185.23	211.78
19.95	120.16	130.57	130.23	140.54	144.99	157.35
49.94	87.79	93.97	94.85	97.18	99.55	103.98
100.02	61.13	64.12	63.82	64.53	65.84	67.71

Table C7 Storage modulus (G') as a function of test strain of the compounds filled with different filler and oil loading

Strain (%)	G' (kPa)			
	F1	F2	F3	F4
0.56	382.53	399.53	403.78	421.84
0.98	363.40	377.15	382.53	400.46
1.95	320.93	318.12	288.66	313.10
5.02	260.95	241.04	233.27	225.12
10.04	227.01	212.81	193.34	180.11
19.95	193.62	178.56	159.42	144.39
49.94	133.55	128.36	113.55	100.46
100.02	92.86	84.18	74.41	65.37

APPENDIX D
DYNAMIC MECHANICAL PROPERTIES OF RUBBER VULCANIZATES

Table D1 Loss factor (tanδ) as a function of test temperature of the vulcanizates prepared at various silanization temperatures: (a) HDSi

HDSi_120°C		HDSi_130°C		HDSi_140°C		HDSi_150°C		HDSi_160°C	
Temp. (°C)	Tan δ	Temp. (°C)	Tan δ	Temp. (°C)	Tan δ	Temp. (°C)	Tan δ	Temp. (°C)	Tan δ
-59.3	0.089	-59.1	0.098	-59.6	0.085	-59.4	0.082	-59.8	0.083
-59.0	0.089	-58.9	0.098	-59.1	0.084	-59.0	0.084	-59.4	0.084
-56.7	0.089	-56.5	0.098	-56.7	0.084	-56.7	0.085	-56.5	0.084
-54.6	0.089	-54.7	0.097	-54.7	0.084	-54.7	0.085	-54.7	0.083
-52.7	0.089	-52.8	0.098	-52.8	0.084	-52.7	0.085	-52.8	0.083
-50.8	0.090	-50.8	0.098	-50.8	0.084	-50.6	0.085	-50.9	0.083
-48.9	0.091	-48.9	0.100	-48.8	0.085	-48.8	0.085	-48.8	0.084
-46.8	0.092	-46.8	0.101	-46.8	0.086	-46.8	0.086	-46.6	0.085
-44.7	0.095	-44.8	0.104	-44.8	0.088	-44.8	0.087	-44.7	0.086
-42.7	0.098	-42.6	0.107	-42.7	0.090	-43.0	0.090	-42.6	0.088
-40.6	0.102	-40.7	0.111	-40.6	0.094	-40.9	0.093	-40.7	0.092
-38.7	0.108	-38.5	0.118	-38.8	0.101	-38.7	0.099	-38.7	0.099
-36.6	0.116	-36.8	0.126	-36.7	0.111	-36.7	0.107	-36.8	0.108
-34.8	0.128	-34.5	0.144	-34.7	0.125	-34.7	0.120	-34.6	0.120
-32.8	0.145	-32.5	0.163	-32.8	0.145	-32.8	0.138	-32.7	0.135
-30.5	0.175	-30.3	0.193	-30.3	0.184	-30.7	0.164	-30.6	0.164
-28.6	0.231	-28.5	0.235	-28.7	0.232	-28.6	0.220	-28.7	0.213
-26.8	0.277	-26.6	0.296	-26.6	0.286	-26.4	0.277	-26.8	0.268
-24.9	0.338	-24.7	0.348	-24.7	0.351	-24.5	0.358	-24.7	0.333
-21.9	0.506	-22.7	0.441	-22.8	0.436	-22.8	0.434	-22.5	0.431
-20.7	0.562	-20.8	0.540	-20.3	0.573	-20.4	0.567	-20.7	0.529
-18.4	0.681	-17.5	0.709	-18.8	0.658	-18.4	0.678	-18.8	0.644
-16.8	0.743	-16.7	0.747	-16.7	0.753	-16.8	0.748	-16.8	0.750
-14.8	0.783	-14.8	0.793	-14.7	0.814	-14.9	0.815	-14.8	0.829
-12.9	0.789	-12.8	0.806	-12.9	0.831	-12.7	0.842	-12.7	0.865
-10.8	0.757	-10.9	0.777	-10.8	0.803	-10.8	0.823	-10.9	0.856
-8.8	0.702	-8.8	0.721	-8.8	0.753	-8.8	0.774	-8.7	0.811
-6.8	0.638	-6.8	0.655	-6.8	0.687	-6.8	0.711	-6.9	0.748
-4.8	0.575	-4.7	0.590	-4.8	0.624	-4.8	0.645	-4.8	0.677

Table D1 Loss factor (tanδ) as a function of test temperature of the vulcanizates prepared at various silanization temperatures (cont.): (a) HDSi

HDSi_120°C		HDSi_130°C		HDSi_140°C		HDSi_150°C		HDSi_160°C	
Temp. (°C)	Tan δ	Temp. (°C)	Tan δ	Temp. (°C)	Tan δ	Temp. (°C)	Tan δ	Temp. (°C)	Tan δ
-2.7	0.517	-2.9	0.534	-2.8	0.562	-2.8	0.584	-2.8	0.611
-0.8	0.468	-0.9	0.482	-0.9	0.512	-0.7	0.527	-0.9	0.556
3.0	0.418	2.9	0.429	2.8	0.459	3.2	0.472	3.1	0.493
3.3	0.402	3.2	0.413	3.2	0.444	3.6	0.454	3.4	0.471
5.1	0.366	5.2	0.377	5.1	0.402	5.1	0.411	5.1	0.428
7.2	0.333	7.2	0.341	7.0	0.364	7.0	0.374	7.2	0.386
9.3	0.302	9.2	0.311	9.3	0.331	9.3	0.338	9.2	0.349
11.3	0.277	11.2	0.283	11.3	0.303	11.2	0.311	11.2	0.319
13.2	0.256	13.3	0.259	13.3	0.282	13.3	0.284	13.3	0.289
15.3	0.241	15.2	0.244	15.2	0.262	15.2	0.264	15.2	0.271
17.1	0.227	17.2	0.231	17.2	0.249	17.2	0.249	17.3	0.252
19.2	0.216	19.1	0.218	19.2	0.233	19.2	0.234	19.2	0.238
21.2	0.205	21.2	0.208	21.2	0.223	21.0	0.223	21.2	0.223
23.3	0.197	23.2	0.200	23.3	0.213	23.3	0.214	23.3	0.213
25.2	0.190	25.2	0.193	25.3	0.204	25.2	0.206	25.3	0.203
27.2	0.183	27.2	0.186	27.2	0.195	27.2	0.197	27.1	0.195
29.2	0.176	29.1	0.179	29.2	0.186	29.1	0.189	29.3	0.186
31.2	0.171	31.1	0.174	31.2	0.180	31.2	0.182	31.2	0.176
33.2	0.165	33.2	0.166	33.2	0.173	33.3	0.176	33.2	0.169
35.3	0.161	35.2	0.160	35.2	0.167	35.2	0.168	35.2	0.163
37.2	0.154	37.1	0.157	37.3	0.159	37.2	0.165	37.2	0.157
39.2	0.149	39.1	0.149	39.2	0.156	39.2	0.157	39.1	0.153
41.3	0.144	41.2	0.147	41.3	0.150	41.2	0.150	41.2	0.148
43.2	0.140	43.2	0.142	43.1	0.146	43.2	0.147	43.2	0.142
45.2	0.136	45.2	0.137	45.2	0.142	45.3	0.142	45.2	0.135
47.2	0.131	47.1	0.133	47.2	0.136	47.3	0.136	47.2	0.129
49.2	0.127	49.2	0.128	49.3	0.133	49.1	0.132	49.2	0.127
51.2	0.124	51.2	0.125	51.2	0.125	51.2	0.124	51.2	0.120
53.1	0.118	53.3	0.118	53.3	0.118	53.2	0.119	53.1	0.116
55.3	0.116	55.2	0.113	55.1	0.115	55.2	0.115	55.2	0.110
57.3	0.113	57.2	0.110	57.2	0.110	57.2	0.109	57.2	0.106
59.2	0.108	59.2	0.107	59.2	0.107	59.3	0.107	59.2	0.104
61.2	0.105	61.1	0.102	61.1	0.102	61.2	0.102	61.2	0.100
63.3	0.104	63.3	0.098	63.2	0.100	63.1	0.099	63.2	0.096
65.2	0.098	65.2	0.096	65.2	0.097	65.2	0.098	65.3	0.090
67.2	0.097	67.3	0.094	67.2	0.098	67.2	0.095	67.2	0.089
69.2	0.095	69.2	0.089	69.3	0.094	69.2	0.092	69.2	0.084
71.2	0.091	71.2	0.088	71.2	0.088	71.2	0.089	71.2	0.084
73.2	0.087	73.2	0.086	73.2	0.085	73.3	0.084	73.1	0.082
75.4	0.085	75.3	0.084	75.3	0.089	75.2	0.086	75.1	0.084
77.2	0.082	77.2	0.082	77.2	0.086	77.2	0.085	77.2	0.078
79.1	0.083	79.2	0.081	79.3	0.080	79.2	0.081	79.3	0.078

Table D2 Loss factor (tanδ) as a function of test temperature of the vulcanizates prepared at various silanization temperatures: (b) CSi

CSi_120°C		CSi_130°C		CSi_140°C		CSi_150°C		CSi_160°C	
Temp. (°C)	Tan δ	Temp. (°C)	Tan δ	Temp. (°C)	Tan δ	Temp. (°C)	Tan δ	Temp. (°C)	Tan δ
-59.7	0.080	-59.8	0.081	-59.9	0.085	-59.9	0.080	-59.8	0.090
-59.3	0.079	-59.4	0.080	-58.9	0.085	-58.9	0.078	-59.2	0.089
-56.7	0.079	-56.7	0.081	-56.7	0.085	-56.8	0.077	-56.6	0.089
-54.7	0.078	-54.8	0.080	-54.7	0.084	-54.7	0.077	-54.6	0.089
-52.7	0.079	-52.8	0.080	-52.7	0.084	-52.8	0.077	-52.7	0.089
-50.8	0.080	-50.7	0.081	-50.8	0.085	-50.8	0.078	-50.8	0.090
-48.9	0.081	-48.6	0.082	-48.8	0.086	-48.8	0.079	-48.8	0.091
-46.8	0.083	-46.7	0.083	-46.8	0.087	-46.7	0.081	-46.8	0.092
-44.7	0.085	-44.8	0.085	-44.8	0.089	-44.8	0.083	-44.8	0.094
-42.9	0.088	-42.8	0.087	-42.9	0.091	-42.7	0.085	-42.8	0.097
-40.6	0.092	-40.8	0.090	-40.8	0.095	-40.8	0.090	-40.6	0.102
-38.7	0.099	-38.6	0.097	-38.7	0.101	-38.7	0.096	-38.7	0.108
-36.6	0.108	-36.5	0.106	-36.8	0.110	-36.7	0.106	-36.8	0.117
-34.6	0.121	-34.6	0.120	-34.8	0.123	-34.7	0.121	-34.7	0.130
-32.8	0.140	-32.5	0.141	-32.5	0.145	-32.6	0.144	-32.7	0.150
-30.3	0.176	-30.5	0.172	-30.5	0.176	-30.6	0.174	-30.5	0.178
-28.6	0.219	-28.6	0.220	-28.5	0.223	-28.5	0.224	-28.5	0.222
-26.6	0.288	-26.6	0.279	-26.7	0.285	-26.7	0.279	-26.7	0.273
-24.8	0.347	-24.3	0.367	-23.9	0.395	-24.7	0.352	-24.7	0.343
-22.7	0.444	-22.7	0.441	-22.7	0.449	-22.3	0.480	-22.3	0.464
-20.6	0.555	-20.8	0.542	-20.7	0.552	-20.8	0.566	-20.7	0.550
-17.5	0.721	-18.8	0.651	-18.3	0.687	-17.6	0.752	-17.5	0.738
-16.7	0.755	-15.5	0.783	-16.7	0.757	-16.7	0.789	-16.6	0.780
-14.8	0.797	-14.8	0.804	-14.7	0.814	-14.8	0.843	-14.9	0.837
-12.8	0.804	-12.7	0.811	-12.8	0.830	-12.8	0.860	-12.8	0.868
-10.9	0.777	-10.8	0.785	-10.8	0.809	-10.8	0.838	-10.8	0.856
-8.8	0.723	-8.8	0.733	-8.8	0.757	-8.8	0.789	-8.8	0.811
-6.8	0.661	-6.8	0.670	-6.8	0.697	-6.8	0.724	-6.8	0.748
-4.8	0.598	-4.8	0.605	-4.8	0.632	-4.8	0.661	-4.9	0.682
-2.8	0.542	-2.8	0.549	-2.8	0.571	-2.7	0.597	-2.7	0.616
-0.8	0.491	-0.9	0.498	-0.8	0.517	-0.9	0.542	-0.8	0.558
2.4	0.443	2.0	0.450	2.3	0.466	2.2	0.488	2.4	0.503
2.8	0.429	2.7	0.431	2.8	0.451	2.6	0.471	2.8	0.485
5.2	0.386	5.1	0.388	5.2	0.402	5.1	0.421	5.1	0.435
7.2	0.349	7.2	0.354	6.9	0.369	7.3	0.385	7.3	0.395

Table D2 Loss factor (tanδ) as a function of test temperature of the vulcanizates prepared at various silanization temperatures (cont.): (b) CSi

CSi_120°C		CSi_130°C		CSi_140°C		CSi_150°C		CSi_160°C	
Temp. (°C)	Tan δ	Temp. (°C)	Tan δ	Temp. (°C)	Tan δ	Temp. (°C)	Tan δ	Temp. (°C)	Tan δ
9.2	0.323	9.2	0.329	9.2	0.339	9.2	0.355	9.1	0.363
11.3	0.298	11.2	0.305	11.2	0.315	11.2	0.328	11.2	0.333
13.2	0.279	13.2	0.288	13.3	0.295	13.2	0.306	13.2	0.309
15.1	0.261	15.2	0.270	15.2	0.275	15.1	0.288	15.2	0.289
17.2	0.247	17.3	0.252	17.1	0.259	17.2	0.268	17.2	0.272
19.1	0.234	19.2	0.238	19.2	0.245	19.1	0.252	19.3	0.253
21.3	0.220	21.3	0.224	21.2	0.231	21.2	0.238	21.2	0.242
23.3	0.211	23.2	0.215	23.3	0.217	23.3	0.224	23.3	0.224
25.2	0.200	25.2	0.203	25.2	0.207	25.2	0.211	25.2	0.213
27.2	0.193	27.1	0.194	27.1	0.198	27.1	0.204	27.2	0.204
29.2	0.185	29.2	0.187	29.2	0.189	29.2	0.196	29.2	0.194
31.2	0.179	31.3	0.180	31.1	0.182	31.3	0.186	31.2	0.187
33.3	0.172	33.2	0.175	33.2	0.175	33.1	0.180	33.2	0.178
35.2	0.168	35.1	0.169	35.2	0.171	35.2	0.174	35.2	0.171
37.2	0.162	37.1	0.162	37.2	0.165	37.2	0.170	37.1	0.165
39.2	0.156	39.2	0.157	39.2	0.158	39.2	0.159	39.1	0.159
41.2	0.151	41.2	0.151	41.4	0.152	41.2	0.155	41.3	0.150
43.1	0.146	43.3	0.147	43.1	0.149	43.0	0.148	43.3	0.144
45.2	0.139	45.3	0.139	45.2	0.141	45.3	0.143	45.1	0.138
47.2	0.134	47.2	0.134	47.1	0.133	47.2	0.133	47.1	0.132
49.2	0.132	49.2	0.131	49.2	0.129	49.1	0.128	49.2	0.128
51.1	0.127	51.2	0.125	51.1	0.125	51.2	0.121	51.1	0.118
53.2	0.118	53.2	0.120	53.3	0.118	53.2	0.117	53.3	0.116
55.1	0.113	55.3	0.117	55.2	0.113	55.3	0.111	55.2	0.109
57.2	0.108	57.1	0.111	57.0	0.109	57.1	0.107	57.2	0.105
59.2	0.105	59.2	0.110	59.2	0.105	59.2	0.106	59.2	0.104
61.2	0.101	61.2	0.105	61.2	0.103	61.3	0.099	61.1	0.099
63.2	0.100	63.2	0.098	63.3	0.100	63.2	0.100	63.3	0.094
65.0	0.096	65.3	0.098	65.2	0.097	65.1	0.098	65.1	0.093
67.1	0.094	67.2	0.096	67.2	0.092	67.2	0.094	67.2	0.089
69.2	0.093	69.2	0.092	69.2	0.095	69.2	0.089	69.2	0.089
71.1	0.090	71.1	0.093	71.2	0.090	71.1	0.087	71.1	0.085
73.2	0.087	73.2	0.089	73.0	0.087	73.2	0.087	73.2	0.085
75.3	0.086	75.1	0.088	75.3	0.087	75.1	0.093	75.2	0.079
77.3	0.084	77.0	0.086	77.1	0.087	77.2	0.081	77.3	0.079
79.2	0.080	79.2	0.082	79.2	0.083	79.1	0.081	79.0	0.076

Table D3 Loss factor (tanδ) as a function of test strain at 0°C of the vulcanizates prepared at various silanization temperatures: (a) HDSi

HDSi_120°C		HDSi_130°C		HDSi_140°C		HDSi_150°C		HDSi_160°C	
Strain (%)	Tan δ	Strain (%)	Tan δ	Strain (%)	Tan δ	Strain (%)	Tan δ	Strain (%)	Tan δ
0.031	0.346	0.030	0.364	0.030	0.375	0.031	0.397	0.030	0.422
0.035	0.347	0.035	0.364	0.035	0.378	0.036	0.407	0.037	0.426
0.041	0.349	0.040	0.368	0.041	0.382	0.041	0.405	0.041	0.427
0.048	0.351	0.048	0.370	0.048	0.385	0.049	0.408	0.048	0.430
0.056	0.354	0.056	0.373	0.057	0.387	0.056	0.412	0.056	0.431
0.066	0.357	0.066	0.376	0.065	0.390	0.066	0.415	0.065	0.434
0.077	0.362	0.076	0.379	0.077	0.394	0.077	0.419	0.076	0.438
0.089	0.365	0.089	0.383	0.088	0.398	0.089	0.422	0.089	0.442
0.104	0.370	0.105	0.388	0.104	0.402	0.103	0.427	0.103	0.446
0.122	0.375	0.122	0.393	0.122	0.407	0.122	0.433	0.122	0.452
0.142	0.381	0.142	0.399	0.142	0.414	0.142	0.438	0.142	0.457
0.166	0.388	0.166	0.406	0.167	0.420	0.166	0.445	0.166	0.463
0.195	0.396	0.195	0.414	0.194	0.428	0.194	0.452	0.194	0.470
0.227	0.405	0.227	0.423	0.227	0.437	0.227	0.461	0.227	0.479
0.266	0.416	0.266	0.433	0.266	0.447	0.265	0.471	0.266	0.488
0.311	0.428	0.310	0.445	0.310	0.458	0.310	0.482	0.310	0.499
0.364	0.440	0.363	0.458	0.363	0.471	0.363	0.494	0.363	0.511
0.425	0.454	0.424	0.473	0.424	0.485	0.424	0.507	0.424	0.524
0.496	0.469	0.496	0.488	0.494	0.500	0.495	0.520	0.496	0.538
0.581	0.485	0.579	0.504	0.578	0.515	0.579	0.534	0.579	0.553
0.678	0.501	0.677	0.521	0.678	0.532	0.677	0.548	0.677	0.568
0.792	0.518	0.792	0.538	0.791	0.548	0.790	0.563	0.791	0.584
0.927	0.533	0.926	0.555	0.925	0.564	0.924	0.577	0.924	0.599
1.082	0.549	1.082	0.571	1.077	0.580	1.081	0.591	1.081	0.613
1.265	0.564	1.264	0.587	1.264	0.595	1.263	0.604	1.263	0.626
1.460	0.576	1.477	0.601	1.476	0.609	1.475	0.615	1.475	0.638
1.720	0.588	1.713	0.612	1.705	0.619	1.722	0.624	1.721	0.645
1.993	0.596	1.992	0.620	1.998	0.628	1.997	0.630	1.992	0.649
2.337	0.602	2.327	0.626	2.335	0.634	2.327	0.633	2.334	0.652
2.733	0.605	2.719	0.628	2.718	0.635	2.719	0.632	2.733	0.650
3.184	0.604	3.190	0.627	3.189	0.634	3.177	0.626	3.190	0.644
3.719	0.598	3.712	0.619	3.712	0.625	3.712	0.616	3.711	0.629
4.339	0.584	4.345	0.610	4.337	0.612	4.336	0.602	4.336	0.612
5.068	0.567	5.066	0.592	5.066	0.596	5.068	0.584	5.065	0.592
5.921	0.547	5.918	0.570	5.918	0.575	5.919	0.560	5.918	0.566
6.917	0.524	6.913	0.546	6.916	0.551	6.916	0.534	6.914	0.537
8.068	0.498	8.076	0.518	8.067	0.521	8.075	0.504	8.074	0.505
9.424	0.468	9.431	0.488	9.422	0.491	9.431	0.473	9.431	0.473

Table D4 Loss factor (tanδ) as a function of test strain at 0°C of the vulcanizates prepared at various silanization temperatures: (b) CSi

CSi_120°C		CSi_130°C		CSi_140°C		CSi_150°C		CSi_160°C	
Strain (%)	Tan δ	Strain (%)	Tan δ	Strain (%)	Tan δ	Strain (%)	Tan δ	Strain (%)	Tan δ
0.030	0.361	0.029	0.382	0.030	0.391	0.030	0.411	0.030	0.408
0.035	0.364	0.034	0.383	0.034	0.390	0.035	0.413	0.034	0.412
0.041	0.366	0.041	0.385	0.041	0.392	0.041	0.414	0.041	0.417
0.048	0.368	0.048	0.387	0.047	0.395	0.047	0.415	0.047	0.420
0.055	0.370	0.056	0.387	0.056	0.396	0.056	0.416	0.055	0.423
0.066	0.372	0.065	0.388	0.065	0.399	0.065	0.419	0.065	0.427
0.076	0.376	0.077	0.391	0.076	0.401	0.077	0.422	0.076	0.431
0.089	0.380	0.089	0.394	0.090	0.406	0.090	0.426	0.089	0.434
0.104	0.383	0.105	0.398	0.104	0.410	0.104	0.430	0.105	0.439
0.122	0.388	0.122	0.402	0.122	0.416	0.122	0.436	0.122	0.443
0.142	0.394	0.141	0.408	0.142	0.422	0.142	0.441	0.143	0.450
0.167	0.400	0.167	0.414	0.166	0.428	0.166	0.448	0.166	0.456
0.195	0.407	0.194	0.422	0.194	0.436	0.194	0.456	0.194	0.463
0.227	0.415	0.227	0.431	0.227	0.445	0.227	0.465	0.227	0.471
0.266	0.425	0.266	0.441	0.265	0.455	0.266	0.474	0.266	0.480
0.311	0.436	0.310	0.452	0.311	0.466	0.310	0.485	0.310	0.490
0.363	0.449	0.363	0.465	0.363	0.479	0.363	0.498	0.363	0.502
0.424	0.462	0.423	0.478	0.424	0.493	0.424	0.511	0.423	0.514
0.496	0.476	0.496	0.493	0.496	0.508	0.496	0.526	0.495	0.528
0.579	0.492	0.580	0.509	0.579	0.524	0.580	0.541	0.578	0.542
0.678	0.508	0.678	0.524	0.678	0.540	0.677	0.558	0.677	0.557
0.792	0.525	0.792	0.540	0.792	0.557	0.792	0.574	0.790	0.572
0.925	0.541	0.925	0.556	0.925	0.573	0.925	0.590	0.923	0.587
1.082	0.557	1.082	0.571	1.081	0.589	1.081	0.606	1.080	0.603
1.264	0.572	1.263	0.585	1.264	0.605	1.263	0.621	1.261	0.617
1.478	0.587	1.477	0.598	1.476	0.619	1.475	0.635	1.475	0.630
1.710	0.597	1.720	0.608	1.719	0.632	1.711	0.645	1.723	0.641
1.998	0.607	1.998	0.616	1.999	0.639	1.992	0.652	1.998	0.647
2.336	0.614	2.328	0.621	2.336	0.644	2.328	0.657	2.338	0.651
2.731	0.618	2.720	0.622	2.731	0.645	2.730	0.660	2.722	0.651
3.192	0.618	3.177	0.620	3.191	0.642	3.177	0.654	3.192	0.647
3.712	0.610	3.713	0.614	3.712	0.632	3.712	0.646	3.712	0.634
4.337	0.600	4.337	0.602	4.336	0.618	4.337	0.632	4.336	0.619
5.067	0.585	5.067	0.585	5.067	0.601	5.067	0.614	5.065	0.600
5.919	0.566	5.919	0.565	5.918	0.578	5.921	0.592	5.918	0.577
6.914	0.543	6.915	0.540	6.913	0.552	6.914	0.562	6.913	0.548
8.075	0.517	8.075	0.513	8.076	0.524	8.067	0.533	8.072	0.518
9.432	0.489	9.422	0.482	9.431	0.492	9.423	0.500	9.422	0.487

Table D5 Loss factor (tanδ) as a function of test strain at 60°C of the vulcanizates prepared at various silanization temperatures: (a) HDSi

HDSi_120°C		HDSi_130°C		HDSi_140°C		HDSi_150°C		HDSi_160°C	
Strain (%)	Tan δ	Strain (%)	Tan δ	Strain (%)	Tan δ	Strain (%)	Tan δ	Strain (%)	Tan δ
0.030	0.087	0.030	0.077	0.030	0.080	0.030	0.079	0.030	0.076
0.036	0.091	0.034	0.074	0.035	0.085	0.035	0.076	0.035	0.071
0.041	0.084	0.040	0.076	0.042	0.082	0.042	0.080	0.041	0.079
0.048	0.089	0.048	0.082	0.048	0.080	0.047	0.074	0.048	0.078
0.056	0.084	0.055	0.076	0.057	0.078	0.056	0.079	0.056	0.078
0.066	0.081	0.064	0.075	0.064	0.078	0.064	0.080	0.062	0.077
0.076	0.084	0.076	0.076	0.077	0.079	0.077	0.074	0.075	0.076
0.089	0.079	0.089	0.074	0.089	0.078	0.088	0.080	0.088	0.077
0.104	0.080	0.104	0.075	0.104	0.081	0.103	0.080	0.105	0.077
0.122	0.083	0.121	0.073	0.121	0.080	0.122	0.078	0.121	0.078
0.142	0.085	0.142	0.078	0.142	0.081	0.142	0.078	0.142	0.077
0.166	0.087	0.166	0.079	0.166	0.079	0.166	0.080	0.166	0.076
0.196	0.088	0.194	0.080	0.194	0.082	0.194	0.081	0.194	0.079
0.226	0.089	0.226	0.082	0.229	0.081	0.227	0.082	0.226	0.080
0.265	0.092	0.264	0.085	0.264	0.083	0.265	0.084	0.264	0.081
0.309	0.095	0.309	0.087	0.309	0.086	0.309	0.086	0.309	0.082
0.361	0.098	0.361	0.089	0.361	0.089	0.361	0.088	0.361	0.085
0.422	0.101	0.421	0.092	0.421	0.089	0.422	0.090	0.421	0.086
0.493	0.103	0.493	0.095	0.492	0.092	0.493	0.093	0.493	0.089
0.576	0.106	0.575	0.098	0.575	0.095	0.576	0.095	0.575	0.091
0.671	0.109	0.672	0.100	0.672	0.097	0.672	0.097	0.672	0.092
0.786	0.111	0.786	0.103	0.785	0.099	0.785	0.099	0.787	0.094
0.918	0.114	0.918	0.106	0.917	0.101	0.918	0.101	0.918	0.096
1.073	0.116	1.072	0.108	1.069	0.103	1.074	0.103	1.072	0.098
1.253	0.118	1.252	0.110	1.255	0.105	1.253	0.105	1.252	0.099
1.464	0.119	1.466	0.112	1.464	0.106	1.464	0.106	1.463	0.100
1.709	0.120	1.710	0.114	1.710	0.108	1.710	0.108	1.711	0.101
1.999	0.121	1.997	0.115	1.998	0.109	1.998	0.109	1.996	0.103
2.333	0.121	2.334	0.116	2.333	0.111	2.333	0.110	2.334	0.104
2.729	0.122	2.727	0.118	2.726	0.112	2.726	0.110	2.724	0.104
3.184	0.123	3.188	0.119	3.185	0.112	3.184	0.111	3.183	0.105
3.722	0.123	3.721	0.120	3.718	0.113	3.721	0.112	3.718	0.105
4.338	0.125	4.346	0.121	4.347	0.114	4.346	0.112	4.344	0.106
5.067	0.125	5.067	0.122	5.073	0.116	5.071	0.114	5.075	0.107
5.920	0.126	5.918	0.123	5.919	0.117	5.919	0.114	5.918	0.108
6.908	0.127	6.914	0.125	6.909	0.118	6.915	0.115	6.914	0.109
8.077	0.127	8.076	0.126	8.068	0.119	8.068	0.115	8.074	0.110
9.431	0.129	9.422	0.127	9.423	0.120	9.427	0.116	9.428	0.110

Table D6 Loss factor (tanδ) as a function of test strain at 60°C of the vulcanizates prepared at various silanization temperatures: (b) CSi

CSi_120°C		CSi_130°C		CSi_140°C		CSi_150°C		CSi_160°C	
Strain (%)	Tan δ	Strain (%)	Tan δ	Strain (%)	Tan δ	Strain (%)	Tan δ	Strain (%)	Tan δ
0.029	0.079	0.030	0.072	0.029	0.076	0.030	0.075	0.032	0.080
0.035	0.077	0.036	0.080	0.035	0.084	0.035	0.080	0.035	0.080
0.042	0.074	0.041	0.079	0.041	0.081	0.041	0.079	0.042	0.074
0.047	0.077	0.048	0.077	0.049	0.079	0.048	0.078	0.048	0.076
0.056	0.075	0.055	0.076	0.055	0.076	0.057	0.081	0.057	0.074
0.065	0.074	0.064	0.077	0.065	0.079	0.066	0.080	0.066	0.073
0.076	0.074	0.076	0.076	0.075	0.080	0.077	0.080	0.076	0.075
0.088	0.075	0.089	0.078	0.090	0.079	0.089	0.080	0.091	0.078
0.104	0.075	0.103	0.078	0.104	0.080	0.103	0.080	0.104	0.075
0.121	0.077	0.122	0.079	0.122	0.081	0.121	0.081	0.120	0.074
0.142	0.078	0.142	0.078	0.142	0.082	0.142	0.081	0.142	0.076
0.166	0.080	0.166	0.081	0.165	0.082	0.165	0.081	0.166	0.077
0.194	0.082	0.194	0.081	0.195	0.083	0.194	0.084	0.193	0.078
0.227	0.084	0.226	0.084	0.226	0.085	0.226	0.085	0.227	0.078
0.265	0.086	0.265	0.086	0.265	0.087	0.261	0.086	0.265	0.079
0.309	0.089	0.309	0.089	0.310	0.089	0.309	0.088	0.309	0.081
0.361	0.092	0.361	0.091	0.361	0.091	0.361	0.090	0.361	0.082
0.422	0.095	0.421	0.094	0.422	0.094	0.421	0.092	0.421	0.084
0.493	0.098	0.492	0.097	0.493	0.096	0.492	0.095	0.492	0.086
0.576	0.101	0.576	0.100	0.575	0.098	0.575	0.097	0.575	0.088
0.673	0.105	0.672	0.102	0.673	0.101	0.672	0.100	0.673	0.090
0.786	0.108	0.786	0.105	0.786	0.104	0.785	0.102	0.785	0.093
0.918	0.111	0.917	0.108	0.917	0.107	0.918	0.105	0.918	0.094
1.072	0.113	1.072	0.110	1.072	0.109	1.072	0.107	1.071	0.096
1.253	0.116	1.252	0.112	1.252	0.111	1.252	0.109	1.252	0.098
1.464	0.118	1.463	0.114	1.463	0.113	1.463	0.111	1.463	0.099
1.711	0.119	1.705	0.115	1.709	0.114	1.709	0.112	1.708	0.100
1.999	0.121	1.998	0.117	1.990	0.115	1.997	0.113	1.995	0.101
2.336	0.122	2.334	0.117	2.334	0.116	2.334	0.114	2.333	0.102
2.730	0.124	2.726	0.118	2.726	0.117	2.726	0.115	2.724	0.103
3.189	0.126	3.187	0.119	3.184	0.118	3.183	0.116	3.182	0.103
3.713	0.128	3.723	0.120	3.722	0.119	3.717	0.116	3.718	0.104
4.348	0.128	4.346	0.120	4.344	0.120	4.343	0.116	4.344	0.104
5.061	0.131	5.067	0.122	5.065	0.121	5.074	0.117	5.074	0.105
5.913	0.132	5.919	0.122	5.921	0.121	5.917	0.118	5.917	0.106
6.916	0.133	6.914	0.123	6.913	0.122	6.912	0.118	6.913	0.106
8.068	0.136	8.068	0.124	8.068	0.124	8.074	0.119	8.071	0.107
9.424	0.137	9.429	0.124	9.428	0.124	9.426	0.120	9.426	0.107

Table D7 Loss factor (tanδ) as a function of test temperature of the vulcanizates treated by various TESPT contents: (a) HDSi

HDSi_without TESPT		HDSi_6wt%		HDSi_8wt%		HDSi_10wt%		HDSi_12wt%	
Temp. (^{O}C)	Tan δ	Temp. (^{O}C)	Tan δ	Temp. (^{O}C)	Tan δ	Temp. (^{O}C)	Tan δ	Temp. (^{O}C)	Tan δ
-59.3	0.122	-59.7	0.094	-59.7	0.095	-59.5	0.075	-59.9	0.074
-59.0	0.122	-59.3	0.095	-58.8	0.096	-58.5	0.073	-59.2	0.084
-56.8	0.125	-56.6	0.096	-56.7	0.097	-55.2	0.074	-56.7	0.088
-54.8	0.125	-54.6	0.096	-54.8	0.097	-52.7	0.073	-54.9	0.089
-52.8	0.126	-52.8	0.096	-52.8	0.097	-50.3	0.073	-52.8	0.089
-50.8	0.128	-50.7	0.096	-50.7	0.098	-48.0	0.074	-50.9	0.091
-48.8	0.131	-48.8	0.097	-48.8	0.098	-45.6	0.075	-48.7	0.092
-46.7	0.134	-46.8	0.098	-46.8	0.100	-43.3	0.078	-46.7	0.094
-44.7	0.138	-44.5	0.101	-44.9	0.101	-41.0	0.082	-44.7	0.096
-42.8	0.143	-42.7	0.105	-42.7	0.105	-39.1	0.087	-42.7	0.100
-40.7	0.150	-40.7	0.111	-40.7	0.110	-38.0	0.096	-40.7	0.105
-38.8	0.157	-38.6	0.119	-38.7	0.117	-37.0	0.103	-38.7	0.112
-36.8	0.167	-36.7	0.129	-36.6	0.127	-35.9	0.110	-36.8	0.122
-34.7	0.184	-34.6	0.146	-34.5	0.142	-34.7	0.118	-34.7	0.136
-32.8	0.208	-32.6	0.169	-32.5	0.165	-32.7	0.138	-32.6	0.157
-30.5	0.246	-30.3	0.207	-30.4	0.201	-30.5	0.174	-30.4	0.189
-28.5	0.301	-28.6	0.265	-28.6	0.254	-28.5	0.227	-28.5	0.242
-26.6	0.365	-25.8	0.363	-26.6	0.313	-26.7	0.285	-26.5	0.302
-24.7	0.428	-23.8	0.462	-23.5	0.430	-23.4	0.436	-24.3	0.380
-22.3	0.552	-22.7	0.508	-22.5	0.504	-21.2	0.555	-22.3	0.475
-20.7	0.623	-20.4	0.644	-20.3	0.624	-20.4	0.605	-19.5	0.623
-18.3	0.708	-18.9	0.722	-18.7	0.710	-18.4	0.713	-18.7	0.667
-16.8	0.736	-15.5	0.857	-16.8	0.803	-16.4	0.799	-16.8	0.741
-14.8	0.737	-14.8	0.871	-14.3	0.868	-14.0	0.858	-14.8	0.812
-12.8	0.703	-12.9	0.873	-12.8	0.877	-12.8	0.862	-12.8	0.843
-10.7	0.645	-10.8	0.837	-10.8	0.849	-10.8	0.839	-10.8	0.807
-8.8	0.580	-8.9	0.784	-8.8	0.794	-8.8	0.788	-8.8	0.760
-6.8	0.514	-6.8	0.716	-6.8	0.725	-6.9	0.722	-6.9	0.701
-4.8	0.455	-4.8	0.648	-4.8	0.658	-4.8	0.656	-4.8	0.638
-2.8	0.400	-2.8	0.584	-2.8	0.592	-2.7	0.591	-2.8	0.580
-0.8	0.355	-0.9	0.528	-0.9	0.538	-0.8	0.538	-0.8	0.527
2.7	0.313	2.6	0.474	2.4	0.482	2.6	0.484	2.4	0.476
3.1	0.303	3.0	0.458	2.8	0.466	2.9	0.472	2.7	0.463
5.1	0.269	5.1	0.409	5.2	0.415	5.1	0.421	5.1	0.415
7.2	0.240	7.3	0.370	7.3	0.378	7.2	0.384	7.2	0.380

Table D7 Loss factor (tanδ) as a function of test temperature of the vulcanizates treated by various TESPT contents (cont.): (a) HDSi

HDSi_without TESPT		HDSi_6wt%		HDSi_8wt%		HDSi_10wt%		HDSi_12wt%	
Temp. (^{O}C)	Tan δ	Temp. (^{O}C)	Tan δ	Temp. (^{O}C)	Tan δ	Temp. (^{O}C)	Tan δ	Temp. (^{O}C)	Tan δ
9.3	0.216	9.2	0.339	9.2	0.348	9.1	0.354	9.2	0.353
11.3	0.197	11.3	0.312	11.2	0.321	11.2	0.326	11.2	0.327
13.3	0.182	13.2	0.290	13.2	0.298	13.2	0.303	13.2	0.305
15.2	0.169	15.2	0.271	15.0	0.279	15.2	0.284	15.1	0.286
17.3	0.159	17.1	0.256	17.2	0.262	17.1	0.266	17.2	0.268
19.2	0.151	19.3	0.241	19.2	0.246	19.2	0.249	19.2	0.252
21.2	0.144	21.2	0.228	21.2	0.231	21.1	0.236	21.2	0.235
23.3	0.139	23.2	0.215	23.2	0.219	23.3	0.223	23.3	0.222
25.2	0.133	25.2	0.206	25.2	0.206	25.2	0.211	25.3	0.210
27.2	0.130	27.2	0.194	27.3	0.197	27.2	0.200	27.1	0.200
29.3	0.125	29.2	0.187	29.2	0.188	29.2	0.192	29.2	0.194
31.2	0.121	31.2	0.179	31.2	0.180	31.1	0.182	31.2	0.183
33.3	0.119	33.2	0.173	33.2	0.174	33.2	0.177	33.2	0.179
35.3	0.116	35.2	0.168	35.2	0.169	35.2	0.168	35.2	0.170
37.2	0.114	37.2	0.161	37.2	0.163	37.2	0.161	37.2	0.167
39.1	0.114	39.2	0.157	39.2	0.157	39.3	0.157	39.2	0.159
41.2	0.111	41.2	0.151	41.2	0.151	41.2	0.150	41.2	0.153
43.2	0.108	43.2	0.148	43.2	0.142	43.2	0.145	43.2	0.147
45.2	0.107	45.2	0.140	45.2	0.139	45.2	0.140	45.2	0.139
47.2	0.104	47.2	0.135	47.2	0.134	47.2	0.136	47.2	0.133
49.2	0.102	49.2	0.129	49.3	0.127	49.1	0.129	49.2	0.129
51.3	0.100	51.1	0.126	51.3	0.120	51.3	0.123	51.2	0.124
53.2	0.098	53.3	0.119	53.1	0.115	53.2	0.118	53.3	0.120
55.2	0.095	55.3	0.114	55.0	0.109	55.0	0.115	55.0	0.113
57.2	0.091	57.1	0.110	57.2	0.106	57.3	0.108	57.1	0.107
59.2	0.090	59.1	0.107	59.1	0.103	59.2	0.107	59.3	0.107
61.2	0.087	61.2	0.104	61.4	0.101	61.2	0.103	61.2	0.101
63.2	0.086	63.2	0.099	63.3	0.098	63.1	0.097	63.1	0.099
65.2	0.083	65.2	0.098	65.2	0.094	65.1	0.092	65.1	0.097
67.1	0.081	67.2	0.094	67.2	0.089	67.2	0.093	67.2	0.092
69.3	0.080	69.2	0.093	69.2	0.088	69.1	0.092	69.2	0.088
71.1	0.077	71.2	0.088	71.1	0.086	71.3	0.087	71.2	0.086
73.2	0.076	73.3	0.087	73.1	0.083	73.3	0.085	73.1	0.085
75.0	0.074	75.2	0.085	75.2	0.086	75.3	0.085	75.2	0.085
77.2	0.073	77.2	0.083	77.2	0.080	77.1	0.081	77.2	0.080
79.2	0.071	79.2	0.082	79.3	0.075	79.2	0.080	79.1	0.078

Table D8 Loss factor (tanδ) as a function of test temperature of the vulcanizates treated by various TESPT contents: (b) CSi

CSi_without TESPT		CSi_6wt%		CSi_8wt%		CSi_10wt%		CSi_12wt%	
Temp. (^{O}C)	Tan δ	Temp. (^{O}C)	Tan δ	Temp. (^{O}C)	Tan δ	Temp. (^{O}C)	Tan δ	Temp. (^{O}C)	Tan δ
-59.5	0.083	-59.7	0.098	-59.8	0.089	-59.7	0.101	-59.6	0.096
-59.2	0.127	-59.3	0.102	-59.3	0.095	-59.1	0.104	-59.3	0.098
-55.0	0.128	-56.8	0.103	-56.6	0.096	-56.6	0.104	-56.5	0.099
-52.6	0.128	-54.6	0.103	-54.8	0.096	-54.7	0.104	-54.6	0.100
-50.2	0.127	-52.9	0.104	-52.8	0.097	-52.8	0.104	-52.7	0.101
-47.8	0.128	-50.8	0.105	-50.7	0.097	-50.7	0.105	-50.8	0.102
-45.4	0.130	-48.8	0.107	-48.7	0.098	-48.7	0.106	-48.7	0.103
-43.0	0.130	-46.8	0.109	-46.6	0.099	-46.8	0.107	-46.8	0.105
-40.5	0.133	-44.8	0.112	-44.7	0.101	-44.8	0.109	-44.7	0.107
-38.1	0.139	-42.4	0.115	-42.7	0.104	-42.7	0.111	-42.7	0.110
-35.8	0.153	-40.6	0.119	-40.6	0.110	-40.7	0.115	-40.6	0.115
-33.3	0.186	-38.8	0.126	-38.6	0.117	-38.7	0.122	-38.5	0.121
-32.3	0.216	-36.8	0.138	-36.7	0.127	-36.7	0.132	-36.5	0.131
-31.2	0.229	-34.8	0.155	-34.6	0.142	-34.6	0.145	-34.6	0.146
-30.0	0.258	-32.7	0.178	-32.4	0.163	-32.5	0.166	-32.6	0.167
-28.8	0.301	-30.6	0.218	-30.3	0.196	-30.3	0.200	-30.2	0.200
-27.5	0.342	-28.7	0.274	-28.4	0.250	-28.5	0.250	-28.6	0.242
-26.4	0.395	-26.4	0.334	-26.5	0.305	-25.3	0.378	-26.5	0.315
-24.6	0.470	-23.4	0.479	-23.9	0.421	-24.3	0.393	-24.6	0.363
-22.3	0.596	-22.5	0.531	-22.2	0.511	-22.3	0.489	-22.7	0.447
-20.7	0.665	-20.4	0.659	-20.7	0.588	-20.8	0.575	-20.7	0.555
-17.9	0.747	-18.8	0.739	-18.8	0.694	-18.7	0.689	-18.7	0.663
-16.7	0.759	-15.5	0.856	-15.5	0.830	-15.5	0.835	-15.5	0.810
-14.7	0.749	-14.7	0.871	-14.7	0.854	-14.7	0.860	-14.7	0.837
-12.8	0.710	-12.7	0.869	-12.7	0.863	-12.7	0.875	-12.7	0.852
-10.7	0.649	-10.8	0.834	-10.8	0.838	-10.8	0.852	-10.8	0.830
-8.7	0.581	-8.8	0.777	-8.8	0.785	-8.8	0.798	-8.8	0.780
-6.8	0.517	-6.8	0.709	-6.8	0.719	-6.8	0.735	-6.8	0.714
-4.8	0.456	-4.8	0.643	-4.8	0.651	-4.8	0.665	-4.8	0.647
-2.7	0.403	-2.7	0.578	-2.7	0.585	-2.8	0.602	-2.7	0.582
-0.8	0.359	-0.8	0.525	-0.8	0.530	-0.8	0.546	-0.8	0.529
2.6	0.316	2.9	0.469	2.4	0.475	2.7	0.489	2.2	0.476
2.9	0.306	3.4	0.453	2.8	0.460	3.0	0.473	2.8	0.461
5.1	0.271	5.1	0.408	5.2	0.410	5.1	0.424	5.2	0.412
7.3	0.244	7.0	0.369	7.3	0.371	7.3	0.386	7.4	0.376

Table D8 Loss factor (tanδ) as a function of test temperature of the vulcanizates treated by various TESPT contents (cont.): (b) CSi

CSi_without TESPT		CSi_6wt%		CSi_8wt%		CSi_10wt%		CSi_12wt%	
Temp. (^{O}C)	Tan δ	Temp. (^{O}C)	Tan δ	Temp. (^{O}C)	Tan δ	Temp. (^{O}C)	Tan δ	Temp. (^{O}C)	Tan δ
9.3	0.223	9.3	0.333	9.3	0.341	9.3	0.353	9.3	0.346
11.2	0.206	11.3	0.307	11.2	0.317	11.2	0.327	11.3	0.322
13.3	0.191	13.4	0.285	13.1	0.296	13.2	0.304	13.3	0.300
15.3	0.178	15.2	0.268	15.1	0.277	15.1	0.284	15.1	0.280
17.2	0.168	17.2	0.251	17.2	0.258	17.2	0.265	17.2	0.261
19.2	0.158	19.2	0.237	19.2	0.241	19.2	0.248	19.2	0.245
21.2	0.151	21.3	0.226	21.2	0.228	21.1	0.236	21.2	0.231
23.3	0.144	23.3	0.214	23.3	0.213	23.4	0.221	23.2	0.217
25.2	0.138	25.2	0.206	25.2	0.204	25.3	0.211	25.3	0.205
27.1	0.134	27.1	0.195	27.2	0.194	27.2	0.202	27.2	0.195
29.2	0.130	29.2	0.187	29.3	0.185	29.1	0.193	29.2	0.187
31.2	0.125	31.2	0.181	31.2	0.179	31.3	0.186	31.2	0.182
33.2	0.123	33.2	0.174	33.3	0.170	33.2	0.178	33.3	0.173
35.2	0.121	35.3	0.167	35.1	0.164	35.3	0.169	35.3	0.168
37.2	0.118	37.2	0.163	37.3	0.159	37.2	0.162	37.2	0.161
39.3	0.116	39.1	0.155	39.1	0.152	39.2	0.158	39.2	0.156
41.2	0.114	41.3	0.151	41.3	0.151	41.2	0.152	41.2	0.148
43.3	0.112	43.3	0.146	43.2	0.143	43.2	0.144	43.2	0.142
45.2	0.109	45.2	0.140	45.2	0.137	45.2	0.138	45.1	0.136
47.1	0.107	47.2	0.137	47.1	0.133	47.2	0.132	47.2	0.128
49.3	0.105	49.3	0.130	49.3	0.127	49.2	0.126	49.2	0.124
51.1	0.102	51.1	0.125	51.2	0.122	51.2	0.120	51.2	0.117
53.2	0.099	53.2	0.120	53.2	0.117	53.2	0.117	53.2	0.113
55.3	0.096	55.2	0.115	55.3	0.111	55.2	0.110	55.3	0.106
57.1	0.094	57.1	0.111	57.2	0.106	57.2	0.106	57.1	0.104
59.2	0.092	59.2	0.106	59.2	0.107	59.1	0.100	59.2	0.097
61.2	0.091	61.2	0.103	61.2	0.101	61.2	0.097	61.3	0.094
63.2	0.088	63.1	0.100	63.1	0.097	63.3	0.094	63.1	0.091
65.3	0.085	65.2	0.096	65.3	0.094	65.2	0.092	65.3	0.089
67.3	0.084	67.2	0.094	67.2	0.091	67.0	0.088	67.3	0.089
69.1	0.081	69.2	0.094	69.4	0.092	69.3	0.088	69.2	0.084
71.1	0.082	71.1	0.090	71.3	0.086	71.1	0.084	71.3	0.078
73.4	0.079	73.1	0.086	73.1	0.083	73.2	0.080	73.3	0.077
75.2	0.078	75.3	0.084	75.1	0.082	75.1	0.079	75.2	0.077
77.2	0.074	77.1	0.083	77.2	0.080	77.2	0.076	77.2	0.075
79.1	0.074	79.3	0.081	79.1	0.081	79.1	0.071	79.4	0.070

Table D9 Loss factor (tanδ) as a function of test strain at 0°C of the vulcanizates treated by various TESPT contents: (a) HDSi

HDSi_without TESPT		HDSi_6wt%		HDSi_8wt%		HDSi_10wt%		HDSi_12wt%	
Strain (%)	Tan δ	Strain (%)	Tan δ	Strain (%)	Tan δ	Strain (%)	Tan δ	Strain (%)	Tan δ
0.029	0.213	0.029	0.370	0.030	0.384	0.029	0.384	0.029	0.378
0.036	0.220	0.035	0.375	0.035	0.386	0.035	0.385	0.034	0.378
0.041	0.224	0.041	0.376	0.040	0.388	0.041	0.386	0.040	0.382
0.048	0.229	0.048	0.377	0.047	0.392	0.047	0.390	0.047	0.385
0.055	0.233	0.055	0.379	0.055	0.395	0.056	0.394	0.056	0.389
0.065	0.237	0.066	0.382	0.066	0.398	0.066	0.397	0.065	0.391
0.076	0.241	0.076	0.385	0.076	0.401	0.077	0.400	0.077	0.395
0.089	0.247	0.089	0.389	0.090	0.406	0.088	0.403	0.089	0.400
0.104	0.252	0.104	0.393	0.104	0.411	0.104	0.408	0.104	0.404
0.122	0.258	0.122	0.399	0.122	0.416	0.122	0.413	0.122	0.408
0.143	0.265	0.143	0.405	0.143	0.422	0.142	0.418	0.142	0.414
0.167	0.272	0.167	0.413	0.166	0.428	0.166	0.425	0.167	0.421
0.195	0.280	0.194	0.420	0.194	0.435	0.195	0.432	0.195	0.428
0.228	0.289	0.228	0.429	0.228	0.444	0.227	0.440	0.228	0.437
0.266	0.298	0.266	0.440	0.266	0.454	0.266	0.451	0.266	0.448
0.311	0.307	0.311	0.451	0.311	0.465	0.311	0.462	0.310	0.459
0.364	0.317	0.363	0.463	0.363	0.477	0.363	0.474	0.363	0.472
0.425	0.327	0.425	0.476	0.425	0.490	0.425	0.488	0.424	0.486
0.497	0.337	0.496	0.490	0.496	0.504	0.494	0.502	0.497	0.502
0.581	0.348	0.579	0.504	0.580	0.518	0.580	0.518	0.580	0.518
0.679	0.358	0.677	0.519	0.678	0.534	0.678	0.533	0.679	0.535
0.794	0.369	0.792	0.534	0.792	0.549	0.792	0.549	0.793	0.551
0.927	0.379	0.925	0.548	0.925	0.565	0.926	0.564	0.928	0.569
1.085	0.390	1.082	0.562	1.081	0.580	1.082	0.579	1.084	0.585
1.268	0.401	1.264	0.576	1.264	0.595	1.264	0.594	1.267	0.601
1.451	0.409	1.478	0.588	1.477	0.609	1.478	0.607	1.474	0.616
1.717	0.417	1.720	0.600	1.713	0.621	1.721	0.618	1.722	0.629
1.993	0.424	2.001	0.608	2.000	0.631	2.009	0.625	2.002	0.636
2.342	0.431	2.337	0.614	2.328	0.636	2.337	0.630	2.339	0.642
2.721	0.436	2.720	0.615	2.720	0.638	2.730	0.634	2.734	0.643
3.182	0.438	3.178	0.614	3.177	0.635	3.178	0.628	3.191	0.641
3.718	0.439	3.712	0.606	3.712	0.629	3.717	0.624	3.713	0.630
4.343	0.436	4.338	0.594	4.337	0.617	4.337	0.607	4.337	0.616
5.074	0.432	5.066	0.577	5.065	0.601	5.066	0.589	5.066	0.597
5.916	0.423	5.919	0.556	5.919	0.579	5.917	0.567	5.917	0.575
6.912	0.412	6.915	0.532	6.915	0.553	6.915	0.540	6.914	0.548
8.075	0.398	8.077	0.504	8.077	0.525	8.077	0.511	8.076	0.518
9.432	0.382	9.423	0.473	9.420	0.493	9.420	0.480	9.423	0.488

Table D10 Loss factor (tanδ) as a function of test strain at 0°C of the vulcanizates treated by various TESPT contents: (b) CSi

CSi_without TESPT		CSi_6wt%		CSi_8wt%		CSi_10wt%		CSi_12wt%	
Strain (%)	Tan δ	Strain (%)	Tan δ	Strain (%)	Tan δ	Strain (%)	Tan δ	Strain (%)	Tan δ
0.030	0.253	0.030	0.381	0.030	0.390	0.029	0.388	0.030	0.379
0.035	0.254	0.035	0.386	0.035	0.391	0.035	0.391	0.036	0.380
0.040	0.257	0.041	0.387	0.041	0.394	0.040	0.392	0.041	0.382
0.048	0.259	0.047	0.391	0.047	0.397	0.047	0.395	0.047	0.385
0.057	0.262	0.055	0.391	0.055	0.399	0.056	0.399	0.056	0.387
0.066	0.265	0.066	0.395	0.065	0.403	0.065	0.403	0.065	0.390
0.076	0.268	0.075	0.398	0.076	0.407	0.076	0.406	0.077	0.394
0.087	0.273	0.090	0.402	0.090	0.411	0.090	0.411	0.090	0.398
0.104	0.278	0.103	0.406	0.103	0.415	0.105	0.415	0.104	0.402
0.122	0.283	0.122	0.410	0.122	0.419	0.122	0.419	0.120	0.407
0.143	0.289	0.142	0.416	0.142	0.426	0.142	0.425	0.142	0.413
0.167	0.295	0.166	0.422	0.166	0.432	0.167	0.431	0.166	0.420
0.195	0.302	0.194	0.430	0.194	0.439	0.195	0.438	0.194	0.428
0.228	0.310	0.228	0.438	0.228	0.448	0.227	0.446	0.228	0.436
0.266	0.319	0.265	0.448	0.265	0.457	0.266	0.456	0.266	0.445
0.312	0.328	0.311	0.458	0.311	0.468	0.310	0.466	0.310	0.456
0.364	0.337	0.363	0.470	0.363	0.480	0.363	0.479	0.363	0.468
0.425	0.347	0.424	0.483	0.424	0.493	0.424	0.491	0.424	0.481
0.497	0.358	0.496	0.497	0.496	0.507	0.496	0.505	0.496	0.496
0.581	0.368	0.579	0.511	0.579	0.522	0.580	0.520	0.578	0.511
0.678	0.379	0.677	0.526	0.678	0.538	0.677	0.536	0.678	0.527
0.793	0.389	0.792	0.542	0.792	0.554	0.792	0.551	0.793	0.544
0.927	0.399	0.925	0.557	0.926	0.570	0.926	0.567	0.927	0.561
1.083	0.410	1.082	0.573	1.081	0.586	1.081	0.584	1.083	0.578
1.267	0.420	1.264	0.587	1.264	0.601	1.265	0.599	1.264	0.594
1.459	0.424	1.477	0.601	1.478	0.615	1.478	0.614	1.478	0.610
1.721	0.433	1.711	0.613	1.697	0.627	1.706	0.627	1.721	0.624
2.000	0.440	2.008	0.624	2.001	0.637	1.999	0.637	2.000	0.634
2.338	0.447	2.335	0.630	2.329	0.642	2.337	0.644	2.339	0.642
2.736	0.452	2.730	0.633	2.719	0.644	2.732	0.647	2.720	0.643
3.179	0.451	3.191	0.632	3.192	0.644	3.177	0.645	3.184	0.645
3.715	0.449	3.712	0.623	3.712	0.635	3.712	0.637	3.716	0.638
4.341	0.447	4.336	0.612	4.337	0.621	4.337	0.626	4.337	0.624
5.072	0.442	5.065	0.596	5.066	0.604	5.065	0.609	5.065	0.608
5.925	0.435	5.917	0.575	5.917	0.581	5.917	0.587	5.917	0.587
6.911	0.424	6.911	0.550	6.913	0.555	6.913	0.561	6.914	0.561
8.072	0.409	8.074	0.523	8.067	0.526	8.075	0.531	8.075	0.531
9.430	0.393	9.422	0.490	9.421	0.494	9.422	0.500	9.422	0.500

Table D11 Loss factor (tanδ) as a function of test strain at 60°C of the vulcanizates treated by various TESPT contents: (a) HDSi

HDSi_without TESPT		HDSi_6wt%		HDSi_8wt%		HDSi_10wt%		HDSi_12wt%	
Strain (%)	Tan δ	Strain (%)	Tan δ	Strain (%)	Tan δ	Strain (%)	Tan δ	Strain (%)	Tan δ
0.030	0.088	0.030	0.094	0.030	0.087	0.031	0.080	0.030	0.083
0.035	0.087	0.034	0.087	0.035	0.084	0.035	0.076	0.036	0.077
0.042	0.086	0.041	0.085	0.042	0.081	0.041	0.076	0.041	0.078
0.048	0.086	0.047	0.086	0.047	0.089	0.048	0.079	0.048	0.080
0.055	0.084	0.056	0.088	0.056	0.082	0.055	0.076	0.055	0.077
0.065	0.086	0.066	0.092	0.065	0.084	0.065	0.079	0.065	0.081
0.077	0.087	0.077	0.091	0.076	0.082	0.076	0.076	0.077	0.076
0.090	0.087	0.090	0.089	0.089	0.082	0.089	0.078	0.089	0.079
0.104	0.086	0.104	0.090	0.103	0.081	0.104	0.077	0.104	0.079
0.122	0.085	0.121	0.089	0.121	0.085	0.122	0.079	0.122	0.079
0.142	0.084	0.142	0.090	0.142	0.084	0.142	0.080	0.142	0.081
0.166	0.085	0.166	0.091	0.166	0.083	0.166	0.081	0.166	0.083
0.194	0.085	0.194	0.092	0.194	0.084	0.193	0.083	0.194	0.084
0.227	0.086	0.226	0.093	0.226	0.087	0.227	0.085	0.227	0.085
0.265	0.087	0.265	0.095	0.264	0.089	0.265	0.087	0.264	0.087
0.309	0.087	0.308	0.098	0.309	0.091	0.308	0.088	0.309	0.089
0.361	0.089	0.361	0.100	0.361	0.093	0.361	0.090	0.361	0.092
0.424	0.090	0.422	0.103	0.422	0.096	0.420	0.093	0.420	0.094
0.494	0.091	0.493	0.106	0.492	0.098	0.493	0.095	0.493	0.097
0.577	0.092	0.576	0.109	0.576	0.101	0.575	0.098	0.575	0.100
0.674	0.094	0.672	0.112	0.672	0.104	0.672	0.100	0.672	0.102
0.788	0.096	0.785	0.114	0.786	0.107	0.786	0.103	0.785	0.105
0.920	0.098	0.918	0.117	0.917	0.110	0.918	0.105	0.917	0.107
1.075	0.100	1.072	0.119	1.073	0.112	1.072	0.107	1.072	0.109
1.257	0.103	1.252	0.121	1.253	0.115	1.253	0.110	1.253	0.111
1.469	0.106	1.463	0.123	1.463	0.117	1.464	0.111	1.463	0.113
1.717	0.110	1.709	0.124	1.710	0.119	1.710	0.113	1.710	0.115
2.007	0.114	1.996	0.126	1.996	0.121	1.998	0.114	1.996	0.116
2.338	0.118	2.332	0.127	2.332	0.122	2.333	0.116	2.332	0.117
2.723	0.122	2.724	0.128	2.724	0.124	2.725	0.117	2.725	0.119
3.181	0.126	3.186	0.129	3.183	0.125	3.184	0.118	3.185	0.120
3.719	0.132	3.719	0.130	3.720	0.127	3.720	0.119	3.721	0.122
4.335	0.138	4.345	0.131	4.346	0.128	4.345	0.121	4.347	0.123
5.061	0.145	5.066	0.132	5.067	0.130	5.066	0.123	5.074	0.126
5.916	0.151	5.925	0.132	5.917	0.131	5.925	0.124	5.925	0.127
6.912	0.157	6.912	0.133	6.905	0.133	6.907	0.125	6.906	0.129
8.075	0.162	8.053	0.134	8.066	0.134	8.067	0.127	8.068	0.130
9.428	0.166	9.423	0.134	9.424	0.134	9.424	0.128	9.425	0.131

Table D12 Loss factor (tanδ) as a function of test strain at 60°C of the vulcanizates treated by various TESPT contents: (b) CSi

CSi_without TESPT		CSi_6wt%		CSi_8wt%		CSi_10wt%		CSi_12wt%	
Strain (%)	Tan δ	Strain (%)	Tan δ	Strain (%)	Tan δ	Strain (%)	Tan δ	Strain (%)	Tan δ
0.031	0.081	0.030	0.082	0.030	0.084	0.029	0.074	0.030	0.080
0.035	0.078	0.035	0.084	0.035	0.077	0.036	0.075	0.034	0.080
0.042	0.082	0.041	0.081	0.041	0.076	0.040	0.073	0.041	0.067
0.048	0.082	0.050	0.087	0.048	0.084	0.049	0.072	0.047	0.077
0.056	0.079	0.056	0.085	0.056	0.077	0.056	0.077	0.056	0.080
0.064	0.081	0.064	0.088	0.066	0.080	0.066	0.077	0.065	0.076
0.076	0.081	0.077	0.085	0.076	0.082	0.076	0.079	0.076	0.077
0.088	0.081	0.089	0.082	0.088	0.080	0.088	0.075	0.088	0.079
0.103	0.080	0.104	0.085	0.104	0.078	0.104	0.080	0.104	0.078
0.121	0.081	0.120	0.085	0.121	0.078	0.121	0.077	0.121	0.077
0.142	0.081	0.142	0.085	0.142	0.080	0.142	0.078	0.142	0.079
0.166	0.082	0.166	0.086	0.166	0.081	0.166	0.078	0.166	0.082
0.194	0.082	0.193	0.086	0.194	0.083	0.194	0.080	0.194	0.083
0.227	0.083	0.226	0.089	0.226	0.085	0.226	0.081	0.226	0.084
0.265	0.083	0.264	0.091	0.265	0.086	0.264	0.083	0.263	0.086
0.309	0.085	0.309	0.093	0.309	0.088	0.309	0.086	0.309	0.088
0.361	0.086	0.361	0.096	0.361	0.091	0.361	0.087	0.361	0.090
0.422	0.087	0.421	0.097	0.422	0.092	0.422	0.090	0.421	0.093
0.493	0.089	0.494	0.100	0.493	0.096	0.493	0.092	0.492	0.095
0.576	0.091	0.576	0.103	0.576	0.099	0.575	0.094	0.575	0.098
0.673	0.093	0.672	0.105	0.672	0.101	0.672	0.097	0.672	0.101
0.787	0.095	0.786	0.108	0.784	0.104	0.784	0.099	0.785	0.104
0.920	0.098	0.917	0.110	0.917	0.106	0.917	0.101	0.917	0.106
1.075	0.101	1.071	0.112	1.072	0.109	1.072	0.103	1.072	0.109
1.256	0.105	1.253	0.114	1.252	0.111	1.252	0.105	1.252	0.110
1.468	0.109	1.463	0.116	1.464	0.113	1.464	0.107	1.463	0.112
1.716	0.113	1.711	0.118	1.709	0.115	1.709	0.108	1.709	0.114
2.006	0.118	1.997	0.119	1.998	0.116	1.997	0.110	1.997	0.116
2.343	0.124	2.335	0.121	2.332	0.117	2.334	0.111	2.334	0.117
2.723	0.129	2.725	0.122	2.725	0.118	2.724	0.113	2.725	0.119
3.181	0.134	3.184	0.123	3.185	0.119	3.184	0.114	3.183	0.120
3.719	0.140	3.721	0.125	3.719	0.120	3.719	0.115	3.721	0.122
4.335	0.145	4.346	0.126	4.345	0.121	4.345	0.117	4.345	0.123
5.075	0.152	5.071	0.127	5.071	0.123	5.066	0.119	5.066	0.125
5.916	0.158	5.924	0.128	5.924	0.124	5.911	0.120	5.911	0.127
6.912	0.163	6.913	0.129	6.906	0.125	6.913	0.122	6.906	0.128
8.074	0.168	8.066	0.130	8.074	0.126	8.067	0.124	8.067	0.130
9.427	0.171	9.423	0.130	9.428	0.127	9.424	0.125	9.427	0.131

Table D13 Loss factor (tanδ) as a function of test temperature of the vulcanizates filled with various silica/CB hybrid ratios: (a) SSBR6450SL_HDSi

SSBR6450SL											
HDSi100/CB0		HDSi80/CB20		HDSi60/CB40		HDSi40/CB60		HDSi20/CB80		Silica0/CB100	
Temp. (^{O}C)	Tan δ	Temp. (^{O}C)	Tan δ	Temp. (^{O}C)	Tan δ	Temp. (^{O}C)	Tan δ	Temp. (^{O}C)	Tan δ	Temp. (^{O}C)	Tan δ
-59.6	0.111	-59.6	0.112	-59.6	0.095	-59.4	0.114	-59.6	0.112	-59.4	0.108
-59.1	0.111	-59.2	0.110	-59.2	0.096	-59.1	0.113	-59.3	0.111	-59.0	0.107
-56.7	0.111	-56.4	0.109	-56.5	0.096	-56.7	0.112	-56.7	0.110	-56.7	0.107
-54.8	0.110	-54.5	0.109	-54.5	0.095	-54.7	0.111	-54.8	0.109	-54.5	0.107
-52.7	0.110	-52.6	0.108	-52.6	0.095	-52.7	0.111	-52.8	0.110	-52.6	0.106
-50.6	0.110	-50.5	0.109	-50.7	0.095	-50.5	0.112	-50.8	0.109	-50.7	0.106
-48.8	0.110	-48.8	0.110	-48.7	0.096	-48.7	0.113	-48.8	0.111	-48.6	0.106
-46.7	0.111	-46.8	0.110	-46.8	0.096	-46.8	0.113	-46.9	0.112	-46.8	0.107
-44.6	0.111	-44.9	0.111	-44.5	0.098	-44.7	0.115	-44.9	0.113	-44.8	0.109
-42.7	0.112	-42.6	0.114	-42.7	0.100	-42.7	0.117	-42.7	0.115	-42.7	0.110
-40.7	0.114	-40.6	0.116	-40.6	0.105	-40.7	0.120	-40.7	0.117	-40.6	0.113
-38.5	0.119	-38.6	0.122	-38.6	0.111	-38.6	0.125	-38.6	0.123	-38.6	0.119
-36.5	0.129	-36.6	0.132	-36.5	0.120	-36.4	0.135	-36.6	0.132	-36.6	0.128
-34.4	0.143	-34.6	0.146	-34.6	0.134	-34.5	0.148	-34.5	0.146	-34.5	0.143
-32.4	0.163	-32.6	0.166	-32.4	0.156	-32.5	0.168	-32.4	0.166	-32.5	0.163
-30.4	0.195	-30.3	0.198	-30.4	0.187	-30.5	0.197	-30.2	0.198	-30.3	0.194
-28.4	0.243	-28.5	0.240	-28.5	0.235	-28.4	0.243	-28.3	0.242	-28.4	0.242
-26.5	0.302	-26.6	0.294	-26.6	0.291	-26.5	0.297	-26.6	0.295	-26.5	0.305
-23.8	0.403	-23.4	0.410	-23.8	0.384	-24.2	0.379	-23.3	0.412	-23.8	0.401
-22.6	0.445	-22.5	0.465	-21.3	0.523	-21.4	0.473	-22.4	0.475	-22.7	0.463
-19.5	0.612	-20.7	0.549	-20.4	0.579	-20.1	0.592	-20.8	0.553	-20.3	0.580
-18.6	0.657	-18.7	0.659	-18.3	0.686	-18.7	0.658	-18.7	0.665	-18.8	0.652
-16.4	0.742	-15.5	0.789	-16.8	0.751	-15.5	0.772	-16.8	0.741	-16.7	0.716
-14.8	0.788	-14.6	0.810	-14.4	0.802	-14.6	0.792	-13.5	0.775	-14.8	0.737
-12.8	0.808	-12.9	0.819	-12.8	0.806	-12.7	0.788	-12.7	0.776	-12.8	0.719
-10.8	0.786	-10.9	0.794	-10.9	0.770	-10.8	0.752	-10.8	0.728	-10.8	0.669
-8.8	0.738	-8.8	0.738	-8.9	0.714	-8.8	0.694	-8.7	0.666	-8.8	0.606
-6.9	0.675	-6.8	0.675	-6.7	0.646	-6.9	0.627	-6.8	0.603	-6.7	0.546
-4.7	0.610	-4.9	0.612	-4.8	0.583	-4.8	0.561	-4.8	0.540	-4.8	0.491
-2.8	0.550	-2.8	0.552	-2.7	0.524	-2.8	0.506	-2.7	0.485	-2.8	0.443
-0.9	0.500	-0.8	0.499	-0.8	0.473	-0.8	0.457	-0.8	0.441	-0.7	0.401
2.5	0.446	2.7	0.448	2.6	0.426	2.6	0.411	2.7	0.396	2.5	0.364
2.9	0.432	3.0	0.433	2.8	0.415	2.8	0.399	3.0	0.385	2.9	0.356
5.2	0.388	5.1	0.392	5.1	0.372	5.2	0.362	5.2	0.352	5.1	0.324
7.3	0.354	7.3	0.357	7.3	0.341	7.2	0.332	7.3	0.324	7.3	0.302

Table D13 Loss factor (tanδ) as a function of test temperature of the vulcanizates filled with various silica/CB hybrid ratios (cont.): (a) SSBR6450SL_HDSi

SSBR6450SL											
HDSi100/CB0		HDSi80/CB20		HDSi60/CB40		HDSi40/CB60		HDSi20/CB80		Silica0/CB100	
Temp. (^{O}C)	Tan δ	Temp. (^{O}C)	Tan δ	Temp. (^{O}C)	Tan δ	Temp. (^{O}C)	Tan δ	Temp. (^{O}C)	Tan δ	Temp. (^{O}C)	Tan δ
9.3	0.328	9.2	0.332	9.3	0.317	9.3	0.311	9.2	0.305	9.2	0.286
11.2	0.306	11.2	0.308	11.2	0.295	11.3	0.293	11.2	0.287	11.2	0.271
13.3	0.284	13.3	0.288	13.3	0.279	13.2	0.277	13.2	0.272	13.2	0.260
15.2	0.267	15.2	0.271	15.3	0.262	15.3	0.262	15.3	0.260	15.2	0.251
17.2	0.254	17.3	0.258	17.2	0.250	17.2	0.249	17.1	0.250	17.2	0.240
19.2	0.237	19.1	0.245	19.2	0.239	19.2	0.238	19.3	0.241	19.2	0.233
21.2	0.225	21.2	0.234	21.2	0.227	21.1	0.228	21.2	0.232	21.3	0.227
23.4	0.215	23.3	0.224	23.2	0.217	23.3	0.220	23.2	0.224	23.3	0.220
25.2	0.205	25.1	0.215	25.2	0.211	25.2	0.212	25.2	0.218	25.1	0.217
27.2	0.197	27.2	0.206	27.3	0.204	27.2	0.207	27.2	0.212	27.2	0.211
29.2	0.191	29.1	0.200	29.1	0.200	29.2	0.202	29.1	0.207	29.2	0.207
31.2	0.183	31.3	0.193	31.2	0.192	31.2	0.194	31.2	0.205	31.2	0.202
33.2	0.176	33.1	0.188	33.2	0.185	33.2	0.190	33.1	0.198	33.3	0.201
35.2	0.172	35.1	0.183	35.2	0.183	35.2	0.186	35.2	0.196	35.2	0.196
37.2	0.167	37.1	0.180	37.3	0.176	37.2	0.184	37.2	0.193	37.2	0.193
39.1	0.161	39.2	0.174	39.3	0.175	39.2	0.180	39.2	0.189	39.2	0.191
41.2	0.156	41.3	0.169	41.1	0.169	41.2	0.176	41.3	0.185	41.1	0.188
43.3	0.150	43.2	0.163	43.2	0.166	43.2	0.168	43.2	0.183	43.2	0.184
45.1	0.142	45.1	0.156	45.3	0.160	45.2	0.168	45.2	0.176	45.2	0.182
47.3	0.137	47.2	0.153	47.2	0.153	47.3	0.161	47.2	0.175	47.3	0.177
49.1	0.132	49.2	0.145	49.2	0.150	49.1	0.160	49.1	0.169	49.2	0.174
51.2	0.127	51.2	0.143	51.3	0.144	51.3	0.157	51.2	0.167	51.2	0.168
53.2	0.122	53.1	0.134	53.3	0.143	53.1	0.151	53.2	0.161	53.2	0.168
55.1	0.117	55.1	0.130	55.2	0.134	55.2	0.146	55.2	0.158	55.2	0.165
57.3	0.113	57.2	0.124	57.2	0.131	57.1	0.143	57.2	0.153	57.3	0.160
59.1	0.108	59.1	0.121	59.1	0.126	59.2	0.139	59.2	0.149	59.1	0.157
61.2	0.103	61.3	0.115	61.1	0.122	61.3	0.133	61.2	0.145	61.3	0.152
63.2	0.098	63.2	0.109	63.1	0.117	63.2	0.130	63.2	0.141	63.2	0.150
65.2	0.094	65.3	0.106	65.2	0.117	65.2	0.127	65.3	0.133	65.3	0.147
67.2	0.091	67.1	0.104	67.3	0.113	67.3	0.122	67.2	0.134	67.1	0.143
69.2	0.090	69.2	0.102	69.1	0.109	69.1	0.119	69.2	0.127	69.2	0.144
71.2	0.089	71.3	0.096	71.3	0.108	71.1	0.115	71.2	0.126	71.3	0.139
73.2	0.085	73.3	0.096	73.2	0.107	73.0	0.112	73.3	0.120	73.1	0.137
75.1	0.082	75.1	0.093	75.2	0.104	75.3	0.114	75.3	0.120	75.3	0.136
77.1	0.082	77.2	0.094	77.1	0.105	77.2	0.111	77.2	0.119	77.1	0.137
79.1	0.075	79.2	0.090	79.2	0.101	79.3	0.110	79.2	0.117	79.2	0.128

Table D14 Loss factor (tanδ) as a function of test temperature of the vulcanizates filled with various silica/CB hybrid ratios: (b) SSBR6450SL_CSi

SSBR6450SL											
CSi100/CB0		CSi80/CB20		CSi60/CB40		CSi40/CB60		CSi20/CB80		Silica0/CB100	
Temp. (^{O}C)	Tan δ	Temp. (^{O}C)	Tan δ	Temp. (^{O}C)	Tan δ	Temp. (^{O}C)	Tan δ	Temp. (^{O}C)	Tan δ	Temp. (^{O}C)	Tan δ
-59.4	0.108	-59.5	0.100	-59.5	0.109	-59.4	0.101	-59.7	0.110	-59.4	0.108
-59.1	0.108	-59.1	0.100	-59.2	0.108	-59.2	0.101	-59.1	0.109	-59.0	0.107
-56.5	0.107	-56.3	0.100	-56.6	0.108	-56.5	0.100	-56.6	0.108	-56.7	0.107
-54.6	0.107	-54.5	0.100	-54.7	0.108	-54.7	0.099	-54.4	0.108	-54.5	0.107
-52.6	0.106	-52.7	0.100	-52.6	0.108	-52.6	0.099	-52.5	0.107	-52.6	0.106
-50.5	0.107	-50.7	0.100	-50.7	0.108	-50.7	0.099	-50.6	0.108	-50.7	0.106
-48.7	0.107	-48.8	0.100	-48.7	0.109	-48.7	0.100	-48.6	0.109	-48.6	0.106
-46.6	0.107	-46.8	0.100	-46.7	0.109	-46.9	0.101	-46.7	0.109	-46.8	0.107
-44.7	0.108	-44.6	0.101	-44.8	0.110	-44.7	0.101	-44.6	0.111	-44.8	0.109
-42.7	0.110	-42.6	0.103	-42.6	0.113	-42.8	0.104	-42.6	0.112	-42.7	0.110
-40.6	0.113	-40.6	0.107	-40.7	0.117	-40.8	0.106	-40.5	0.115	-40.6	0.113
-38.6	0.119	-38.4	0.114	-38.6	0.122	-38.7	0.113	-38.6	0.119	-38.6	0.119
-36.9	0.128	-36.5	0.124	-36.7	0.130	-36.6	0.122	-36.6	0.129	-36.6	0.128
-34.8	0.141	-34.5	0.137	-34.4	0.145	-34.5	0.137	-34.6	0.143	-34.5	0.143
-32.5	0.164	-32.4	0.159	-32.5	0.162	-32.7	0.158	-32.5	0.166	-32.5	0.163
-30.5	0.192	-30.3	0.191	-30.4	0.191	-30.3	0.193	-30.4	0.195	-30.3	0.194
-28.6	0.234	-28.4	0.247	-28.6	0.241	-28.4	0.239	-28.4	0.241	-28.4	0.242
-26.7	0.286	-25.2	0.359	-26.2	0.324	-26.5	0.295	-26.6	0.291	-26.5	0.305
-23.8	0.381	-24.2	0.390	-24.2	0.367	-23.3	0.416	-24.1	0.386	-23.8	0.401
-22.6	0.441	-21.5	0.530	-21.4	0.524	-22.3	0.477	-22.6	0.454	-22.7	0.463
-20.8	0.543	-20.5	0.581	-20.5	0.580	-20.7	0.560	-20.3	0.589	-20.3	0.580
-18.4	0.680	-18.8	0.666	-18.8	0.669	-18.4	0.694	-17.5	0.724	-18.8	0.652
-15.5	0.804	-15.5	0.803	-15.5	0.802	-16.8	0.760	-16.6	0.761	-16.7	0.716
-14.7	0.828	-14.7	0.826	-14.7	0.822	-14.8	0.811	-14.8	0.787	-14.8	0.737
-12.8	0.846	-12.8	0.834	-12.8	0.824	-12.8	0.813	-12.8	0.777	-12.8	0.719
-10.8	0.823	-10.8	0.804	-10.8	0.791	-10.8	0.773	-10.8	0.732	-10.8	0.669
-8.8	0.770	-8.8	0.750	-8.8	0.732	-8.9	0.713	-8.8	0.670	-8.8	0.606
-6.8	0.702	-6.8	0.684	-6.8	0.666	-6.9	0.645	-6.8	0.607	-6.7	0.546
-4.9	0.638	-4.8	0.615	-4.9	0.600	-4.8	0.579	-4.8	0.545	-4.8	0.491
-2.8	0.574	-2.8	0.556	-2.8	0.538	-2.8	0.521	-2.7	0.490	-2.8	0.443
-0.9	0.519	-0.8	0.501	-0.7	0.484	-0.9	0.472	-0.9	0.444	-0.7	0.401
2.8	0.461	2.6	0.449	2.9	0.434	2.5	0.424	2.4	0.401	2.5	0.364
3.3	0.443	2.8	0.437	3.0	0.420	2.8	0.413	2.8	0.391	2.9	0.356
5.2	0.402	5.2	0.390	5.1	0.380	5.2	0.373	5.2	0.355	5.1	0.324
7.2	0.365	7.3	0.357	7.2	0.347	7.2	0.343	7.3	0.327	7.3	0.302

Table D14 Loss factor (tanδ) as a function of test temperature of the vulcanizates filled with various silica/CB hybrid ratios (cont.): (b) SSBR6450SL_CSi

SSBR6450SL											
CSi100/CB0		CSi80/CB20		CSi60/CB40		CSi40/CB60		CSi20/CB80		Silica0/CB100	
Temp. (^{O}C)	Tan δ	Temp. (^{O}C)	Tan δ	Temp. (^{O}C)	Tan δ	Temp. (^{O}C)	Tan δ	Temp. (^{O}C)	Tan δ	Temp. (^{O}C)	Tan δ
9.2	0.333	9.2	0.331	9.3	0.321	9.2	0.320	9.2	0.308	9.2	0.286
11.2	0.302	11.3	0.308	11.2	0.298	11.2	0.298	11.2	0.289	11.2	0.271
13.3	0.275	13.1	0.287	13.2	0.277	13.2	0.281	13.3	0.275	13.2	0.260
15.2	0.259	15.3	0.270	15.3	0.262	15.2	0.267	15.3	0.262	15.2	0.251
17.2	0.244	17.2	0.255	17.1	0.249	17.2	0.254	17.2	0.252	17.2	0.240
19.2	0.229	19.1	0.246	19.3	0.238	19.2	0.243	19.3	0.242	19.2	0.233
21.2	0.218	21.2	0.231	21.0	0.226	21.3	0.232	21.1	0.233	21.3	0.227
23.3	0.210	23.4	0.218	23.3	0.219	23.3	0.225	23.3	0.225	23.3	0.220
25.2	0.201	25.2	0.211	25.2	0.209	25.3	0.217	25.2	0.220	25.1	0.217
27.2	0.195	27.2	0.204	27.2	0.202	27.1	0.211	27.2	0.215	27.2	0.211
29.2	0.187	29.2	0.195	29.2	0.196	29.1	0.205	29.2	0.208	29.2	0.207
31.2	0.178	31.2	0.190	31.2	0.190	31.1	0.198	31.1	0.205	31.2	0.202
33.2	0.173	33.2	0.185	33.2	0.186	33.3	0.194	33.3	0.201	33.3	0.201
35.2	0.168	35.2	0.179	35.2	0.183	35.2	0.191	35.1	0.196	35.2	0.196
37.2	0.160	37.1	0.174	37.2	0.177	37.3	0.183	37.3	0.195	37.2	0.193
39.2	0.158	39.3	0.168	39.2	0.169	39.2	0.180	39.2	0.188	39.2	0.191
41.2	0.153	41.2	0.163	41.3	0.168	41.3	0.176	41.2	0.185	41.1	0.188
43.2	0.150	43.2	0.156	43.3	0.163	43.3	0.173	43.1	0.181	43.2	0.184
45.2	0.144	45.2	0.151	45.3	0.159	45.1	0.167	45.3	0.175	45.2	0.182
47.1	0.140	47.3	0.148	47.1	0.154	47.2	0.165	47.2	0.175	47.3	0.177
49.2	0.131	49.2	0.142	49.2	0.148	49.1	0.159	49.1	0.169	49.2	0.174
51.3	0.127	51.1	0.135	51.3	0.145	51.2	0.153	51.1	0.165	51.2	0.168
53.2	0.119	53.2	0.130	53.2	0.140	53.2	0.149	53.3	0.161	53.2	0.168
55.2	0.120	55.2	0.127	55.1	0.137	55.2	0.148	55.3	0.153	55.2	0.165
57.1	0.109	57.2	0.123	57.3	0.128	57.2	0.141	57.2	0.151	57.3	0.160
59.2	0.102	59.2	0.116	59.2	0.120	59.1	0.136	59.1	0.147	59.1	0.157
61.2	0.098	61.2	0.114	61.1	0.120	61.2	0.134	61.2	0.142	61.3	0.152
63.2	0.095	63.1	0.106	63.2	0.114	63.2	0.127	63.2	0.136	63.2	0.150
65.2	0.090	65.3	0.106	65.1	0.113	65.2	0.125	65.3	0.133	65.3	0.147
67.2	0.085	67.3	0.103	67.4	0.115	67.3	0.122	67.2	0.129	67.1	0.143
69.3	0.085	69.2	0.105	69.3	0.109	69.3	0.118	69.1	0.129	69.2	0.144
71.1	0.081	71.1	0.097	71.1	0.108	71.2	0.117	71.3	0.124	71.3	0.139
73.3	0.080	73.2	0.095	73.3	0.101	73.2	0.115	73.2	0.122	73.1	0.137
75.2	0.079	75.2	0.096	75.2	0.098	75.2	0.110	75.2	0.121	75.3	0.136
77.1	0.076	77.2	0.093	77.2	0.096	77.1	0.110	77.1	0.119	77.1	0.137
79.2	0.075	79.2	0.091	79.1	0.095	79.2	0.108	79.3	0.114	79.2	0.128

Table D15 Loss factor (tanδ) as a function of test temperature of the vulcanizates filled with various silica/CB hybrid ratios: (c) SSBR3626_HDSi

SSBR3626											
HDSi100/CB0		HDSi80/CB20		HDSi60/CB40		HDSi40/CB60		HDSi20/CB80		Silica0/CB100	
Temp. (^{O}C)	Tan δ	Temp. (^{O}C)	Tan δ	Temp. (^{O}C)	Tan δ	Temp. (^{O}C)	Tan δ	Temp. (^{O}C)	Tan δ	Temp. (^{O}C)	Tan δ
-59.5	0.111	-59.7	0.112	-59.6	0.112	-59.6	0.117	-59.7	0.102	-59.8	0.101
-59.2	0.109	-58.8	0.112	-59.3	0.112	-59.3	0.116	-59.0	0.101	-58.7	0.102
-56.5	0.109	-56.6	0.112	-56.6	0.112	-56.5	0.115	-56.5	0.101	-56.6	0.103
-54.5	0.109	-54.6	0.112	-54.6	0.111	-54.7	0.115	-54.7	0.101	-54.7	0.103
-52.7	0.109	-52.8	0.111	-52.5	0.112	-52.6	0.116	-52.8	0.101	-52.7	0.103
-50.7	0.110	-50.6	0.111	-50.4	0.111	-50.5	0.117	-50.7	0.101	-50.5	0.102
-48.7	0.111	-48.6	0.111	-48.7	0.112	-48.9	0.118	-48.8	0.101	-48.7	0.103
-46.3	0.112	-46.7	0.111	-46.7	0.112	-46.9	0.118	-46.8	0.101	-46.9	0.103
-44.9	0.113	-44.7	0.112	-44.7	0.113	-44.7	0.120	-44.9	0.102	-44.6	0.103
-42.8	0.115	-42.6	0.112	-42.7	0.114	-42.6	0.121	-42.7	0.102	-42.5	0.105
-40.6	0.116	-40.6	0.115	-40.7	0.114	-40.5	0.123	-40.6	0.104	-40.6	0.106
-38.7	0.119	-38.7	0.116	-38.7	0.117	-38.7	0.125	-38.6	0.106	-38.6	0.109
-36.6	0.123	-36.5	0.122	-36.6	0.122	-36.6	0.130	-36.6	0.111	-36.6	0.116
-34.6	0.130	-34.6	0.129	-34.6	0.131	-34.7	0.137	-34.6	0.120	-34.6	0.125
-32.6	0.142	-32.5	0.142	-32.6	0.144	-32.7	0.149	-32.6	0.135	-32.5	0.138
-30.7	0.161	-30.6	0.157	-30.5	0.162	-30.5	0.169	-30.4	0.156	-30.5	0.160
-28.4	0.190	-28.5	0.184	-28.5	0.189	-28.5	0.196	-28.3	0.190	-28.4	0.192
-26.6	0.230	-26.4	0.233	-26.4	0.236	-26.4	0.235	-26.3	0.236	-26.4	0.240
-24.7	0.285	-24.6	0.292	-24.5	0.300	-24.5	0.291	-24.5	0.292	-24.6	0.306
-22.7	0.341	-22.2	0.366	-21.4	0.400	-21.8	0.367	-22.5	0.349	-21.7	0.406
-20.2	0.440	-20.8	0.408	-20.3	0.448	-20.7	0.419	-19.8	0.476	-20.6	0.450
-18.7	0.503	-18.2	0.541	-18.3	0.543	-18.7	0.502	-18.7	0.516	-18.7	0.529
-16.3	0.615	-16.7	0.605	-16.8	0.610	-16.6	0.593	-16.3	0.612	-16.3	0.619
-14.8	0.675	-14.8	0.683	-14.8	0.687	-13.9	0.687	-14.7	0.662	-14.3	0.665
-11.6	0.767	-12.7	0.735	-12.0	0.751	-12.8	0.714	-12.4	0.704	-12.8	0.680
-10.8	0.781	-10.7	0.768	-10.8	0.760	-10.8	0.729	-10.8	0.710	-10.8	0.669
-8.8	0.771	-8.8	0.754	-8.8	0.746	-8.7	0.712	-8.8	0.688	-8.7	0.637
-6.7	0.735	-6.7	0.711	-6.8	0.705	-6.8	0.674	-6.8	0.648	-6.8	0.589
-4.8	0.683	-4.8	0.659	-4.8	0.651	-4.7	0.620	-4.8	0.598	-4.8	0.538
-2.9	0.625	-2.8	0.600	-2.7	0.595	-2.8	0.567	-2.8	0.546	-2.8	0.488
-0.9	0.572	-0.7	0.543	-0.8	0.539	-0.8	0.516	-0.8	0.495	-0.8	0.444
3.5	0.508	3.0	0.486	2.7	0.485	2.9	0.463	2.8	0.447	2.4	0.401
3.7	0.490	3.3	0.471	3.0	0.472	3.1	0.451	3.1	0.436	2.8	0.392
5.1	0.445	5.1	0.426	5.1	0.422	5.2	0.405	5.1	0.395	5.2	0.353
7.2	0.401	7.3	0.385	7.3	0.383	7.0	0.371	6.8	0.364	7.3	0.327

Table D15 Loss factor (tanδ) as a function of test temperature of the vulcanizates filled with various silica/CB hybrid ratios (cont.): (c) SSBR3626_HDSi

SSBR3626											
HDSi100/CB0		HDSi80/CB20		HDSi60/CB40		HDSi40/CB60		HDSi20/CB80		Silica0/CB100	
Temp. (^{O}C)	Tan δ	Temp. (^{O}C)	Tan δ	Temp. (^{O}C)	Tan δ	Temp. (^{O}C)	Tan δ	Temp. (^{O}C)	Tan δ	Temp. (^{O}C)	Tan δ
9.4	0.365	9.3	0.354	9.2	0.353	9.3	0.342	9.4	0.336	9.2	0.304
11.2	0.334	11.2	0.328	11.3	0.328	11.3	0.318	11.3	0.315	11.2	0.290
13.2	0.309	13.2	0.306	13.2	0.305	13.3	0.300	13.2	0.298	13.2	0.274
15.2	0.286	15.2	0.286	15.3	0.288	15.2	0.281	15.3	0.280	15.2	0.261
17.1	0.268	17.3	0.264	17.1	0.270	17.2	0.267	17.1	0.269	17.2	0.250
19.3	0.252	19.3	0.250	19.2	0.255	19.1	0.256	19.2	0.256	19.3	0.241
21.2	0.237	21.2	0.237	21.2	0.243	21.3	0.244	21.2	0.245	21.2	0.232
23.3	0.224	23.3	0.225	23.3	0.231	23.3	0.234	23.2	0.238	23.4	0.225
25.3	0.214	25.2	0.213	25.2	0.221	25.2	0.225	25.2	0.229	25.2	0.219
27.2	0.203	27.2	0.203	27.1	0.214	27.2	0.216	27.2	0.222	27.2	0.213
29.2	0.195	29.1	0.197	29.2	0.203	29.2	0.210	29.2	0.216	29.2	0.209
31.3	0.188	31.3	0.189	31.2	0.196	31.2	0.202	31.2	0.209	31.2	0.203
33.2	0.184	33.2	0.182	33.1	0.192	33.2	0.198	33.3	0.204	33.3	0.201
35.2	0.173	35.2	0.178	35.3	0.186	35.1	0.195	35.3	0.199	35.1	0.196
37.3	0.170	37.1	0.172	37.2	0.182	37.3	0.190	37.2	0.197	37.1	0.195
39.2	0.162	39.2	0.167	39.3	0.178	39.1	0.187	39.2	0.192	39.3	0.190
41.2	0.159	41.2	0.167	41.2	0.174	41.2	0.184	41.2	0.188	41.2	0.190
43.2	0.154	43.2	0.160	43.1	0.168	43.2	0.177	43.2	0.183	43.2	0.186
45.2	0.148	45.3	0.156	45.2	0.167	45.2	0.175	45.3	0.179	45.2	0.184
47.2	0.144	47.2	0.150	47.2	0.159	47.2	0.172	47.1	0.176	47.2	0.180
49.0	0.140	49.1	0.145	49.1	0.154	49.3	0.165	49.1	0.173	49.3	0.177
51.3	0.135	51.3	0.139	51.2	0.149	51.2	0.160	51.3	0.168	51.3	0.171
53.2	0.131	53.1	0.138	53.2	0.147	53.1	0.158	53.3	0.163	53.2	0.170
55.2	0.125	55.3	0.131	55.2	0.141	55.2	0.152	55.2	0.160	55.1	0.168
57.3	0.120	57.2	0.127	57.3	0.134	57.2	0.148	57.2	0.156	57.1	0.165
59.2	0.117	59.2	0.124	59.2	0.130	59.3	0.145	59.3	0.151	59.3	0.162
61.3	0.108	61.2	0.119	61.3	0.127	61.2	0.143	61.2	0.145	61.3	0.159
63.1	0.105	63.2	0.114	63.2	0.124	63.2	0.135	63.2	0.145	63.2	0.155
65.3	0.099	65.2	0.114	65.0	0.123	65.2	0.133	65.2	0.144	65.3	0.155
67.0	0.101	67.1	0.107	67.3	0.116	67.1	0.131	67.2	0.139	67.2	0.152
69.3	0.092	69.3	0.107	69.1	0.118	69.4	0.128	69.4	0.136	69.1	0.148
71.1	0.089	71.2	0.106	71.1	0.113	71.3	0.127	71.2	0.134	71.3	0.146
73.3	0.086	73.3	0.099	73.2	0.112	73.2	0.122	73.2	0.130	73.1	0.146
75.1	0.086	75.3	0.097	75.1	0.111	75.3	0.121	75.1	0.131	75.2	0.144
77.1	0.081	77.3	0.096	77.1	0.107	77.2	0.119	77.1	0.124	77.0	0.141
79.0	0.081	79.3	0.094	79.3	0.106	79.2	0.113	79.1	0.123	79.1	0.139

Table D16 Loss factor (tanδ) as a function of test temperature of the vulcanizates filled with various silica/CB hybrid ratios: (d) SSBR3626_CSi

SSBR3626											
CSi100/CB0		CSi80/CB20		CSi60/CB40		CSi40/CB60		CSi20/CB80		Silica0/CB100	
Temp. (^{O}C)	Tan δ	Temp. (^{O}C)	Tan δ	Temp. (^{O}C)	Tan δ	Temp. (^{O}C)	Tan δ	Temp. (^{O}C)	Tan δ	Temp. (^{O}C)	Tan δ
-59.8	0.109	-59.8	0.100	-59.6	0.097	-59.5	0.108	-59.6	0.091	-59.8	0.101
-59.2	0.108	-58.7	0.099	-59.2	0.096	-59.4	0.107	-59.3	0.090	-58.7	0.102
-56.5	0.108	-56.4	0.099	-56.7	0.095	-56.6	0.107	-56.6	0.090	-56.6	0.103
-54.7	0.107	-54.5	0.099	-54.7	0.095	-54.4	0.107	-54.6	0.089	-54.7	0.103
-52.6	0.108	-52.5	0.099	-52.7	0.096	-52.7	0.106	-52.7	0.090	-52.7	0.103
-50.6	0.108	-50.6	0.099	-50.8	0.096	-50.6	0.106	-50.6	0.090	-50.5	0.102
-48.7	0.109	-48.6	0.099	-48.7	0.097	-48.6	0.107	-48.7	0.090	-48.7	0.103
-46.7	0.109	-46.5	0.099	-46.8	0.098	-46.8	0.107	-46.6	0.090	-46.9	0.103
-44.6	0.110	-44.6	0.099	-44.7	0.099	-44.7	0.107	-44.8	0.090	-44.6	0.103
-42.6	0.112	-42.6	0.101	-42.8	0.099	-42.7	0.108	-42.8	0.091	-42.5	0.105
-40.7	0.113	-40.6	0.102	-40.6	0.102	-40.6	0.109	-40.5	0.093	-40.6	0.106
-38.5	0.116	-38.7	0.105	-38.5	0.105	-38.6	0.112	-38.4	0.096	-38.6	0.109
-36.6	0.121	-36.6	0.112	-36.6	0.111	-36.6	0.116	-36.6	0.102	-36.6	0.116
-34.7	0.129	-34.6	0.121	-34.6	0.121	-34.4	0.125	-34.5	0.113	-34.6	0.125
-32.6	0.143	-32.6	0.135	-32.6	0.137	-32.5	0.139	-32.5	0.128	-32.5	0.138
-30.7	0.161	-30.5	0.154	-30.6	0.158	-30.4	0.157	-30.6	0.147	-30.5	0.160
-28.4	0.191	-28.4	0.184	-28.3	0.193	-28.4	0.183	-28.2	0.183	-28.4	0.192
-26.4	0.234	-26.5	0.227	-26.5	0.238	-26.5	0.227	-26.5	0.225	-26.4	0.240
-24.5	0.295	-24.6	0.293	-24.6	0.294	-24.6	0.290	-24.5	0.279	-24.6	0.306
-21.8	0.383	-22.2	0.376	-22.2	0.369	-20.5	0.444	-22.6	0.342	-21.7	0.406
-20.7	0.425	-19.8	0.484	-20.6	0.432	-18.7	0.513	-18.5	0.530	-20.6	0.450
-18.7	0.511	-18.8	0.528	-18.8	0.519	-16.8	0.610	-16.3	0.620	-18.7	0.529
-16.7	0.610	-16.8	0.617	-16.3	0.639	-14.7	0.687	-14.7	0.670	-16.3	0.619
-14.8	0.689	-14.0	0.729	-14.3	0.713	-11.9	0.744	-11.6	0.715	-14.3	0.665
-12.3	0.765	-12.8	0.762	-12.4	0.759	-10.7	0.751	-10.7	0.724	-12.8	0.680
-10.8	0.784	-10.7	0.778	-10.8	0.775	-8.8	0.730	-8.8	0.695	-10.8	0.669
-8.8	0.776	-8.9	0.771	-8.8	0.761	-6.8	0.689	-6.8	0.653	-8.7	0.637
-6.9	0.738	-6.8	0.738	-6.8	0.720	-4.8	0.631	-4.7	0.601	-6.8	0.589
-4.8	0.682	-4.8	0.683	-4.8	0.666	-2.7	0.572	-2.8	0.549	-4.8	0.538
-2.8	0.621	-2.7	0.620	-2.7	0.604	-0.8	0.519	-0.7	0.496	-2.8	0.488
-0.9	0.567	-0.7	0.562	-0.8	0.551	2.6	0.467	2.8	0.449	-0.8	0.444
3.1	0.503	2.8	0.503	2.7	0.492	2.9	0.455	3.0	0.438	2.4	0.401
3.6	0.486	3.1	0.488	3.1	0.479	5.2	0.406	5.2	0.396	2.8	0.392
5.1	0.438	5.1	0.438	5.1	0.430	7.2	0.373	7.3	0.364	5.2	0.353
7.2	0.395	6.9	0.396	7.3	0.391	9.2	0.345	9.2	0.339	7.3	0.327

Table D16 Loss factor (tanδ) as a function of test temperature of the vulcanizates filled with various silica/CB hybrid ratios (cont.): (d) SSBR3626_CSi

SSBR3626											
CSi100/CB0		CSi80/CB20		CSi60/CB40		CSi40/CB60		CSi20/CB80		Silica0/CB100	
Temp. (^{O}C)	Tan δ	Temp. (^{O}C)	Tan δ	Temp. (^{O}C)	Tan δ	Temp. (^{O}C)	Tan δ	Temp. (^{O}C)	Tan δ	Temp. (^{O}C)	Tan δ
9.3	0.359	9.3	0.358	9.3	0.360	11.1	0.321	11.2	0.316	9.2	0.304
11.3	0.327	11.3	0.335	11.2	0.335	13.2	0.299	13.2	0.297	11.2	0.290
13.2	0.302	13.3	0.313	13.2	0.312	15.2	0.283	15.2	0.281	13.2	0.274
15.1	0.277	15.3	0.291	15.2	0.292	17.2	0.267	17.2	0.266	15.2	0.261
17.3	0.258	17.3	0.273	17.3	0.276	19.1	0.253	19.2	0.257	17.2	0.250
19.2	0.241	19.1	0.257	19.2	0.260	21.2	0.240	21.2	0.244	19.3	0.241
21.2	0.226	21.2	0.244	21.1	0.246	23.2	0.230	23.2	0.237	21.2	0.232
23.3	0.217	23.3	0.231	23.3	0.235	25.2	0.220	25.2	0.229	23.4	0.225
25.2	0.206	25.2	0.220	25.3	0.226	27.2	0.212	27.2	0.222	25.2	0.219
27.1	0.197	27.2	0.208	27.2	0.214	29.3	0.205	29.1	0.215	27.2	0.213
29.2	0.189	29.2	0.199	29.2	0.208	31.1	0.198	31.2	0.209	29.2	0.209
31.2	0.182	31.2	0.192	31.3	0.201	33.2	0.194	33.1	0.203	31.2	0.203
33.2	0.174	33.2	0.186	33.3	0.194	35.1	0.189	35.2	0.199	33.3	0.201
35.3	0.167	35.3	0.178	35.2	0.188	37.2	0.184	37.2	0.197	35.1	0.196
37.2	0.160	37.2	0.172	37.1	0.185	39.2	0.182	39.2	0.192	37.1	0.195
39.2	0.161	39.1	0.169	39.3	0.180	41.2	0.177	41.2	0.189	39.3	0.190
41.2	0.153	41.2	0.164	41.2	0.174	43.2	0.171	43.2	0.183	41.2	0.190
43.1	0.147	43.1	0.161	43.2	0.171	45.1	0.169	45.2	0.180	43.2	0.186
45.3	0.141	45.3	0.155	45.3	0.165	47.2	0.165	47.2	0.177	45.2	0.184
47.2	0.137	47.2	0.149	47.3	0.160	49.1	0.159	49.1	0.171	47.2	0.180
49.3	0.136	49.1	0.143	49.2	0.155	51.3	0.155	51.2	0.167	49.3	0.177
51.1	0.130	51.2	0.141	51.3	0.149	53.2	0.151	53.1	0.163	51.3	0.171
53.2	0.125	53.2	0.132	53.1	0.143	55.2	0.145	55.2	0.160	53.2	0.170
55.3	0.120	55.1	0.126	55.2	0.142	57.1	0.144	57.2	0.156	55.1	0.168
57.1	0.115	57.2	0.125	57.1	0.136	59.2	0.138	59.2	0.150	57.1	0.165
59.4	0.107	59.2	0.121	59.0	0.132	61.1	0.133	61.1	0.145	59.3	0.162
61.3	0.104	61.2	0.117	61.1	0.127	63.3	0.129	63.0	0.142	61.3	0.159
63.3	0.095	63.1	0.113	63.2	0.123	65.2	0.128	65.4	0.138	63.2	0.155
65.3	0.097	65.3	0.107	65.4	0.122	67.2	0.129	67.3	0.139	65.3	0.155
67.2	0.097	67.2	0.109	67.1	0.116	69.1	0.124	69.2	0.136	67.2	0.152
69.2	0.091	69.2	0.103	69.2	0.113	71.2	0.118	71.2	0.131	69.1	0.148
71.3	0.087	71.1	0.103	71.3	0.114	73.1	0.121	73.1	0.127	71.3	0.146
73.3	0.083	73.4	0.100	73.2	0.110	75.3	0.114	75.2	0.128	73.1	0.146
75.2	0.083	75.1	0.097	75.3	0.108	77.2	0.112	77.2	0.124	75.2	0.144
77.2	0.078	77.3	0.096	77.2	0.106	79.3	0.113	79.2	0.121	77.0	0.141
79.3	0.080	79.3	0.094	79.2	0.103					79.1	0.139

Table D17 Loss factor (tanδ) as a function of test temperature of the vulcanizates filled with various silica/CB hybrid ratios: (e) ESBR1723_HDSi

ESBR1723											
HDSi100/CB0		HDSi80/CB20		HDSi60/CB40		HDSi40/CB60		HDSi20/CB80		Silica0/CB100	
Temp. (^{O}C)	Tan δ	Temp. (^{O}C)	Tan δ	Temp. (^{O}C)	Tan δ	Temp. (^{O}C)	Tan δ	Temp. (^{O}C)	Tan δ	Temp. (^{O}C)	Tan δ
-59.6	0.117	-59.7	0.107	-59.7	0.118	-59.7	0.098	-59.7	0.106	-59.8	0.091
-59.3	0.109	-58.7	0.102	-58.7	0.111	-59.4	0.095	-58.9	0.095	-59.0	0.082
-56.5	0.106	-56.5	0.100	-56.5	0.109	-56.7	0.092	-56.7	0.091	-56.5	0.078
-54.4	0.110	-54.4	0.104	-54.7	0.112	-54.8	0.095	-54.5	0.095	-54.5	0.084
-52.6	0.117	-52.3	0.113	-52.9	0.117	-52.8	0.101	-52.7	0.105	-52.5	0.096
-50.5	0.128	-50.5	0.125	-50.9	0.126	-50.8	0.113	-50.9	0.118	-50.7	0.115
-48.6	0.146	-48.5	0.146	-48.5	0.147	-48.5	0.134	-48.6	0.147	-48.6	0.147
-46.6	0.177	-46.4	0.181	-46.6	0.176	-46.6	0.171	-46.4	0.186	-46.6	0.184
-44.7	0.208	-44.6	0.225	-44.4	0.227	-44.6	0.223	-44.8	0.227	-44.6	0.228
-42.5	0.264	-42.9	0.273	-42.4	0.282	-41.4	0.349	-42.4	0.305	-42.7	0.291
-39.3	0.430	-40.5	0.364	-39.2	0.430	-40.4	0.394	-40.9	0.372	-40.2	0.396
-37.1	0.557	-37.5	0.545	-37.2	0.569	-37.6	0.558	-38.3	0.490	-38.6	0.475
-36.0	0.614	-36.2	0.629	-36.4	0.624	-36.5	0.614	-36.5	0.582	-36.2	0.594
-33.7	0.754	-34.8	0.704	-34.2	0.728	-34.5	0.718	-34.4	0.675	-34.8	0.643
-32.8	0.800	-32.5	0.793	-32.6	0.778	-32.8	0.765	-33.0	0.710	-32.9	0.663
-30.8	0.837	-30.8	0.814	-30.7	0.796	-30.8	0.775	-30.8	0.705	-30.8	0.642
-28.9	0.824	-28.7	0.789	-28.8	0.770	-28.8	0.740	-28.7	0.667	-28.7	0.597
-26.8	0.772	-26.9	0.737	-26.9	0.718	-26.7	0.679	-26.7	0.610	-26.6	0.541
-24.8	0.708	-24.7	0.668	-24.8	0.654	-24.8	0.618	-24.9	0.556	-24.7	0.491
-22.7	0.638	-22.8	0.605	-22.7	0.586	-22.7	0.554	-22.7	0.500	-22.8	0.445
-20.7	0.573	-20.7	0.542	-20.8	0.533	-20.9	0.503	-20.7	0.452	-20.7	0.402
-18.8	0.517	-18.9	0.493	-18.7	0.481	-18.6	0.451	-18.8	0.411	-18.9	0.368
-16.8	0.467	-17.0	0.447	-16.7	0.438	-16.9	0.412	-16.7	0.375	-16.7	0.334
-14.8	0.422	-14.7	0.404	-14.8	0.400	-14.7	0.374	-14.7	0.342	-14.8	0.309
-12.9	0.386	-12.8	0.370	-12.7	0.366	-12.8	0.343	-12.7	0.315	-12.8	0.287
-10.8	0.350	-10.8	0.340	-10.8	0.337	-10.9	0.316	-10.7	0.292	-10.9	0.268
-8.8	0.322	-8.7	0.313	-8.7	0.311	-8.7	0.292	-8.8	0.273	-8.8	0.251
-6.8	0.298	-7.0	0.293	-6.8	0.291	-6.8	0.274	-6.8	0.256	-6.8	0.239
-4.8	0.276	-4.9	0.273	-4.8	0.272	-4.8	0.258	-4.8	0.243	-4.8	0.228
-2.8	0.259	-2.8	0.256	-2.7	0.257	-2.8	0.244	-2.8	0.232	-2.7	0.219
-0.9	0.245	-0.9	0.243	-0.9	0.244	-0.9	0.234	-0.8	0.223	-0.9	0.212
2.5	0.230	2.2	0.231	2.4	0.233	2.2	0.223	2.3	0.216	2.4	0.206
2.9	0.228	2.7	0.227	2.8	0.230	2.7	0.219	2.8	0.213	2.8	0.204
5.2	0.218	5.2	0.217	5.2	0.222	5.2	0.213	5.1	0.208	5.2	0.201
7.3	0.211	6.8	0.211	7.2	0.215	7.3	0.208	7.3	0.204	7.3	0.198

Table D17 Loss factor (tanδ) as a function of test temperature of the vulcanizates filled with various silica/CB hybrid ratios (cont.): (e) ESBR1723_HDSi

ESBR1723											
HDSi100/CB0		HDSi80/CB20		HDSi60/CB40		HDSi40/CB60		HDSi20/CB80		Silica0/CB100	
Temp. (^{O}C)	Tan δ	Temp. (^{O}C)	Tan δ	Temp. (^{O}C)	Tan δ	Temp. (^{O}C)	Tan δ	Temp. (^{O}C)	Tan δ	Temp. (^{O}C)	Tan δ
9.3	0.204	9.3	0.205	9.3	0.210	9.2	0.205	9.2	0.202	9.3	0.197
11.1	0.201	11.4	0.203	11.2	0.206	11.2	0.202	11.2	0.200	11.2	0.195
13.2	0.195	13.3	0.199	13.3	0.204	13.2	0.200	13.2	0.198	13.1	0.193
15.3	0.192	15.2	0.194	15.2	0.200	15.2	0.197	15.3	0.195	15.3	0.193
17.2	0.187	17.2	0.193	17.2	0.197	17.1	0.194	17.2	0.194	17.0	0.192
19.1	0.186	19.2	0.189	19.2	0.194	19.2	0.192	19.2	0.193	19.2	0.191
21.2	0.183	21.2	0.186	21.2	0.191	21.2	0.190	21.2	0.190	21.2	0.190
23.3	0.178	23.2	0.184	23.2	0.190	23.2	0.188	23.3	0.189	23.3	0.188
25.3	0.175	25.3	0.179	25.2	0.187	25.3	0.185	25.2	0.187	25.2	0.188
27.2	0.171	27.2	0.177	27.3	0.184	27.2	0.183	27.3	0.186	27.2	0.187
29.2	0.168	29.1	0.173	29.2	0.182	29.2	0.180	29.2	0.183	29.2	0.186
31.1	0.163	31.1	0.171	31.1	0.177	31.3	0.176	31.2	0.182	31.2	0.184
33.2	0.161	33.3	0.167	33.2	0.174	33.2	0.173	33.1	0.179	33.2	0.182
35.2	0.158	35.2	0.165	35.2	0.172	35.1	0.172	35.2	0.176	35.3	0.181
37.2	0.152	37.1	0.161	37.3	0.169	37.3	0.169	37.2	0.175	37.2	0.180
39.2	0.149	39.1	0.158	39.2	0.166	39.1	0.167	39.2	0.172	39.1	0.177
41.3	0.147	41.2	0.156	41.2	0.162	41.2	0.162	41.1	0.170	41.1	0.175
43.2	0.145	43.3	0.151	43.1	0.160	43.2	0.158	43.2	0.166	43.2	0.172
45.2	0.142	45.3	0.146	45.3	0.156	45.3	0.157	45.2	0.164	45.2	0.170
47.1	0.137	47.2	0.142	47.1	0.151	47.2	0.151	47.3	0.161	47.1	0.168
49.3	0.132	49.2	0.139	49.3	0.148	49.2	0.149	49.3	0.157	49.2	0.166
51.2	0.128	51.2	0.137	51.2	0.144	51.2	0.145	51.2	0.155	51.1	0.164
53.2	0.124	53.2	0.132	53.2	0.141	53.1	0.144	53.2	0.150	53.2	0.160
55.3	0.121	55.2	0.128	55.3	0.138	55.2	0.140	55.2	0.150	55.2	0.159
57.1	0.117	57.3	0.124	57.2	0.134	57.2	0.137	57.2	0.147	57.2	0.158
59.4	0.112	59.3	0.121	59.2	0.130	59.1	0.136	59.2	0.144	59.3	0.155
61.2	0.110	61.2	0.119	61.1	0.129	61.2	0.134	61.4	0.143	61.2	0.153
63.1	0.107	63.3	0.117	63.2	0.122	63.2	0.131	63.3	0.142	63.1	0.151
65.1	0.104	65.4	0.113	65.4	0.123	65.2	0.129	65.2	0.139	65.2	0.152
67.2	0.103	67.2	0.111	67.2	0.120	67.2	0.128	67.2	0.137	67.3	0.149
69.4	0.102	69.1	0.109	69.1	0.119	69.2	0.126	69.0	0.135	69.1	0.148
71.1	0.102	71.2	0.108	71.2	0.117	71.3	0.123	71.2	0.135	71.1	0.146
73.1	0.100	73.2	0.106	73.3	0.115	73.0	0.121	73.2	0.132	73.1	0.144
75.2	0.099	74.9	0.103	75.1	0.113	75.1	0.121	75.1	0.129	75.0	0.145
77.3	0.096	77.1	0.104	77.1	0.112	77.3	0.119	77.2	0.129	77.3	0.142
79.1	0.096	79.0	0.103	79.4	0.111	79.2	0.117	79.0	0.127	79.1	0.140

Table D18 Loss factor (tanδ) as a function of test temperature of the vulcanizates filled with various silica/CB hybrid ratios: (f) ESBR1723_CSi

ESBR1723											
CSi100/CB0		CSi80/CB20		CSi60/CB40		CSi40/CB60		CSi20/CB80		Silica0/CB100	
Temp. (^{O}C)	Tan δ	Temp. (^{O}C)	Tan δ	Temp. (^{O}C)	Tan δ	Temp. (^{O}C)	Tan δ	Temp. (^{O}C)	Tan δ	Temp. (^{O}C)	Tan δ
-59.5	0.121	-59.4	0.107	-59.5	0.103	-59.5	0.113	-59.6	0.101	-59.8	0.091
-59.4	0.114	-59.1	0.106	-59.4	0.098	-59.4	0.112	-59.1	0.095	-59.0	0.082
-56.4	0.105	-56.7	0.099	-56.7	0.084	-56.5	0.105	-56.6	0.089	-56.5	0.078
-54.5	0.105	-54.7	0.102	-54.7	0.087	-54.2	0.109	-54.6	0.094	-54.5	0.084
-52.5	0.110	-52.7	0.109	-52.8	0.094	-52.5	0.119	-52.5	0.106	-52.5	0.096
-50.7	0.122	-50.6	0.121	-50.7	0.110	-50.5	0.133	-50.6	0.122	-50.7	0.115
-48.7	0.143	-48.6	0.141	-48.7	0.133	-48.6	0.154	-48.7	0.147	-48.6	0.147
-46.5	0.181	-46.6	0.173	-46.6	0.175	-46.5	0.188	-46.4	0.188	-46.6	0.184
-44.6	0.223	-44.8	0.221	-44.8	0.212	-44.5	0.233	-44.6	0.230	-44.6	0.228
-42.2	0.301	-42.8	0.280	-42.8	0.266	-42.7	0.294	-42.6	0.288	-42.7	0.291
-39.2	0.441	-39.6	0.419	-39.5	0.424	-39.3	0.446	-39.3	0.451	-40.2	0.396
-37.1	0.561	-38.5	0.473	-38.5	0.467	-37.9	0.525	-38.4	0.486	-38.6	0.475
-36.4	0.620	-36.7	0.586	-36.3	0.603	-36.8	0.589	-36.2	0.608	-36.2	0.594
-34.4	0.732	-34.4	0.724	-34.8	0.688	-34.7	0.690	-34.5	0.676	-34.8	0.643
-32.7	0.803	-32.9	0.790	-32.6	0.768	-32.8	0.751	-32.8	0.716	-32.9	0.663
-30.9	0.845	-30.8	0.821	-30.8	0.784	-30.9	0.761	-30.6	0.713	-30.8	0.642
-28.7	0.840	-28.9	0.805	-28.8	0.758	-28.7	0.730	-28.8	0.674	-28.7	0.597
-26.8	0.795	-26.7	0.754	-26.8	0.707	-26.8	0.677	-26.8	0.624	-26.6	0.541
-24.9	0.733	-24.7	0.691	-24.8	0.643	-24.7	0.615	-24.8	0.565	-24.7	0.491
-22.8	0.663	-22.8	0.629	-22.9	0.585	-22.9	0.558	-22.8	0.510	-22.8	0.445
-20.8	0.597	-20.8	0.567	-20.9	0.529	-20.8	0.503	-20.8	0.461	-20.7	0.402
-18.9	0.540	-19.0	0.516	-18.8	0.478	-18.8	0.456	-18.6	0.417	-18.9	0.368
-16.8	0.485	-16.8	0.465	-16.9	0.435	-16.8	0.415	-16.9	0.384	-16.7	0.334
-14.8	0.439	-14.8	0.423	-14.7	0.397	-14.7	0.379	-14.7	0.350	-14.8	0.309
-12.8	0.399	-12.8	0.385	-12.8	0.364	-12.8	0.348	-12.7	0.323	-12.8	0.287
-10.7	0.364	-10.8	0.353	-10.9	0.336	-10.9	0.322	-10.8	0.300	-10.9	0.268
-8.9	0.334	-8.8	0.325	-8.7	0.311	-8.7	0.298	-8.9	0.279	-8.8	0.251
-6.8	0.307	-6.7	0.300	-6.8	0.289	-6.8	0.278	-6.7	0.263	-6.8	0.239
-4.8	0.285	-4.8	0.280	-4.9	0.272	-4.9	0.261	-4.8	0.249	-4.8	0.228
-2.8	0.267	-2.8	0.263	-2.7	0.256	-2.8	0.248	-2.8	0.237	-2.7	0.219
-0.9	0.251	-0.9	0.249	-0.8	0.244	-0.9	0.236	-0.8	0.227	-0.9	0.212
2.6	0.237	2.5	0.235	2.2	0.233	2.5	0.225	2.4	0.219	2.4	0.206
2.8	0.234	2.8	0.232	2.7	0.227	2.9	0.224	2.8	0.217	2.8	0.204
5.2	0.223	5.1	0.222	5.2	0.221	5.2	0.216	5.1	0.212	5.2	0.201
7.2	0.214	7.2	0.215	6.9	0.214	6.8	0.211	7.0	0.207	7.3	0.198

Table D18 Loss factor (tanδ) as a function of test temperature of the vulcanizates filled with various silica/CB hybrid ratios (cont.): (f) ESBR1723_CSi

ESBR1723											
CSi100/CB0		CSi80/CB20		CSi60/CB40		CSi40/CB60		CSi20/CB80		Silica0/CB100	
Temp. (^{O}C)	Tan δ	Temp. (^{O}C)	Tan δ	Temp. (^{O}C)	Tan δ	Temp. (^{O}C)	Tan δ	Temp. (^{O}C)	Tan δ	Temp. (^{O}C)	Tan δ
9.2	0.209	9.2	0.209	9.2	0.209	9.3	0.207	9.2	0.205	9.3	0.197
11.2	0.203	11.2	0.203	11.2	0.206	11.3	0.205	11.2	0.201	11.2	0.195
13.2	0.198	13.1	0.198	13.3	0.202	13.2	0.201	13.3	0.200	13.1	0.193
15.1	0.195	15.2	0.195	15.2	0.200	15.1	0.199	15.2	0.198	15.3	0.193
17.2	0.190	17.3	0.192	17.2	0.197	17.3	0.198	17.2	0.196	17.0	0.192
19.3	0.186	19.0	0.188	19.3	0.195	19.2	0.195	19.1	0.194	19.2	0.191
21.1	0.182	21.1	0.186	21.2	0.191	21.2	0.192	21.2	0.194	21.2	0.190
23.3	0.179	23.3	0.183	23.4	0.187	23.3	0.191	23.3	0.191	23.3	0.188
25.2	0.175	25.2	0.180	25.2	0.185	25.1	0.188	25.1	0.188	25.2	0.188
27.3	0.171	27.2	0.175	27.1	0.182	27.2	0.185	27.2	0.187	27.2	0.187
29.2	0.167	29.1	0.170	29.3	0.181	29.2	0.184	29.2	0.185	29.2	0.186
31.1	0.165	31.2	0.168	31.2	0.176	31.3	0.180	31.1	0.183	31.2	0.184
33.2	0.161	33.2	0.166	33.2	0.175	33.1	0.178	33.1	0.180	33.2	0.182
35.3	0.158	35.2	0.161	35.2	0.170	35.2	0.175	35.2	0.177	35.3	0.181
37.2	0.154	37.2	0.158	37.1	0.167	37.1	0.173	37.1	0.177	37.2	0.180
39.1	0.148	39.1	0.155	39.1	0.164	39.2	0.169	39.1	0.173	39.1	0.177
41.3	0.147	41.2	0.150	41.2	0.161	41.1	0.165	41.1	0.170	41.1	0.175
43.1	0.143	43.2	0.148	43.2	0.157	43.1	0.163	43.2	0.168	43.2	0.172
45.2	0.139	45.1	0.146	45.2	0.153	45.1	0.159	45.1	0.164	45.2	0.170
47.2	0.135	47.2	0.140	47.2	0.149	47.3	0.156	47.2	0.163	47.1	0.168
49.2	0.132	49.3	0.136	49.1	0.146	49.1	0.153	49.2	0.158	49.2	0.166
51.1	0.129	51.2	0.133	51.3	0.144	51.3	0.150	51.2	0.156	51.1	0.164
53.3	0.127	53.2	0.131	53.2	0.140	53.2	0.146	53.3	0.153	53.2	0.160
55.2	0.122	55.1	0.128	55.2	0.136	55.1	0.143	55.1	0.152	55.2	0.159
57.1	0.118	57.1	0.123	57.3	0.132	57.1	0.138	57.3	0.146	57.2	0.158
59.2	0.114	59.3	0.119	59.2	0.129	59.4	0.136	59.2	0.143	59.3	0.155
61.2	0.111	61.3	0.118	61.2	0.126	61.3	0.134	61.1	0.143	61.2	0.153
63.2	0.110	63.2	0.116	63.1	0.126	63.2	0.131	63.3	0.138	63.1	0.151
65.2	0.106	65.2	0.113	65.2	0.123	65.2	0.129	65.2	0.136	65.2	0.152
67.3	0.103	67.2	0.108	67.1	0.120	67.2	0.126	67.1	0.135	67.3	0.149
69.2	0.104	69.2	0.108	69.0	0.119	69.2	0.124	69.3	0.135	69.1	0.148
71.2	0.103	71.2	0.108	71.2	0.117	71.3	0.123	71.2	0.132	71.1	0.146
73.0	0.099	73.1	0.106	73.0	0.114	73.2	0.121	73.1	0.129	73.1	0.144
75.4	0.099	75.1	0.104	75.4	0.112	75.2	0.119	75.2	0.130	75.0	0.145
77.1	0.097	77.3	0.104	77.2	0.111	77.2	0.117	77.1	0.127	77.3	0.142
79.5	0.097	79.3	0.101	79.3	0.109	79.4	0.116	79.1	0.127	79.1	0.140

Table D19 Loss factor (tanδ) as a function of test strain at 0°C of the vulcanizates filled with various silica/CB hybrid ratios: (a) SSBR6450SL_HDSi

SSBR6450SL											
HDSi100/CB0		HDSi80/CB20		HDSi60/CB40		HDSi40/CB60		HDSi20/CB80		Silica0/CB100	
Strain (%)	Tan δ	Strain (%)	Tan δ	Strain (%)	Tan δ	Strain (%)	Tan δ	Strain (%)	Tan δ	Strain (%)	Tan δ
0.029	0.390	0.030	0.357	0.030	0.360	0.029	0.343	0.030	0.315	0.030	0.290
0.035	0.393	0.035	0.356	0.035	0.358	0.035	0.346	0.035	0.318	0.036	0.290
0.041	0.395	0.041	0.358	0.041	0.361	0.041	0.348	0.041	0.318	0.041	0.291
0.048	0.394	0.047	0.360	0.047	0.364	0.048	0.348	0.048	0.320	0.048	0.292
0.056	0.396	0.056	0.362	0.056	0.366	0.056	0.350	0.056	0.322	0.056	0.293
0.065	0.397	0.065	0.364	0.065	0.368	0.065	0.352	0.065	0.324	0.066	0.296
0.076	0.400	0.076	0.367	0.076	0.371	0.077	0.356	0.076	0.328	0.076	0.298
0.089	0.403	0.089	0.370	0.089	0.376	0.090	0.359	0.089	0.332	0.089	0.301
0.104	0.406	0.104	0.374	0.104	0.380	0.104	0.364	0.104	0.335	0.104	0.306
0.121	0.410	0.122	0.378	0.122	0.385	0.122	0.370	0.122	0.342	0.122	0.311
0.142	0.415	0.142	0.383	0.142	0.391	0.143	0.377	0.143	0.350	0.143	0.319
0.166	0.421	0.167	0.391	0.167	0.399	0.167	0.386	0.167	0.358	0.167	0.327
0.195	0.428	0.195	0.399	0.194	0.408	0.195	0.396	0.195	0.369	0.195	0.338
0.227	0.438	0.227	0.409	0.227	0.418	0.227	0.408	0.228	0.383	0.229	0.351
0.266	0.448	0.265	0.420	0.266	0.431	0.266	0.422	0.267	0.398	0.267	0.367
0.311	0.460	0.310	0.433	0.311	0.445	0.311	0.438	0.312	0.415	0.313	0.385
0.363	0.473	0.363	0.447	0.364	0.461	0.363	0.456	0.365	0.435	0.366	0.406
0.424	0.487	0.425	0.463	0.425	0.478	0.425	0.476	0.427	0.457	0.428	0.430
0.496	0.502	0.497	0.480	0.497	0.497	0.497	0.497	0.499	0.480	0.501	0.456
0.579	0.518	0.581	0.498	0.581	0.517	0.582	0.520	0.583	0.505	0.581	0.482
0.677	0.534	0.678	0.516	0.676	0.537	0.676	0.542	0.678	0.530	0.679	0.510
0.791	0.551	0.792	0.535	0.789	0.557	0.790	0.565	0.791	0.555	0.792	0.539
0.922	0.567	0.918	0.556	0.918	0.580	0.923	0.588	0.925	0.581	0.916	0.573
1.076	0.583	1.073	0.574	1.077	0.597	1.073	0.613	1.070	0.611	1.073	0.601
1.258	0.598	1.258	0.589	1.259	0.616	1.250	0.634	1.254	0.634	1.248	0.629
1.461	0.611	1.461	0.606	1.465	0.635	1.464	0.653	1.465	0.656	1.466	0.653
1.711	0.622	1.711	0.619	1.707	0.649	1.711	0.670	1.712	0.675	1.713	0.675
1.995	0.629	1.995	0.629	1.994	0.660	1.999	0.684	1.995	0.689	1.995	0.690
2.330	0.634	2.330	0.636	2.330	0.667	2.330	0.691	2.330	0.699	2.330	0.702
2.723	0.635	2.723	0.639	2.722	0.670	2.722	0.695	2.722	0.704	2.723	0.708
3.181	0.632	3.181	0.638	3.181	0.668	3.180	0.694	3.180	0.704	3.181	0.708
3.711	0.621	3.712	0.629	3.711	0.658	3.715	0.687	3.715	0.698	3.712	0.699
4.335	0.607	4.336	0.616	4.335	0.645	4.334	0.672	4.334	0.683	4.335	0.686
5.064	0.588	5.064	0.599	5.063	0.627	5.063	0.653	5.063	0.665	5.064	0.667
5.916	0.564	5.915	0.577	5.913	0.604	5.914	0.630	5.914	0.641	5.914	0.645
6.910	0.538	6.910	0.551	6.908	0.577	6.908	0.603	6.908	0.615	6.909	0.619
8.070	0.508	8.069	0.521	8.069	0.547	8.068	0.572	8.069	0.585	8.068	0.590
9.424	0.477	9.436	0.489	9.425	0.514	9.423	0.541	9.423	0.554	9.424	0.560

Table D20 Loss factor (tanδ) as a function of test strain at 0°C of the vulcanizates filled with various silica/CB hybrid ratios: (b) SSBR6450SL_CSi

SSBR6450SL											
CSi100/CB0		CSi80/CB20		CSi60/CB40		CSi40/CB60		CSi20/CB80		Silica0/CB100	
Strain (%)	Tan δ	Strain (%)	Tan δ	Strain (%)	Tan δ	Strain (%)	Tan δ	Strain (%)	Tan δ	Strain (%)	Tan δ
0.030	0.398	0.030	0.364	0.030	0.350	0.030	0.341	0.031	0.326	0.030	0.290
0.035	0.395	0.035	0.366	0.035	0.350	0.035	0.343	0.035	0.326	0.036	0.290
0.041	0.400	0.041	0.369	0.041	0.353	0.041	0.343	0.041	0.324	0.041	0.291
0.048	0.400	0.047	0.369	0.048	0.357	0.048	0.345	0.048	0.326	0.048	0.292
0.056	0.403	0.056	0.374	0.056	0.358	0.056	0.347	0.057	0.328	0.056	0.293
0.066	0.404	0.066	0.375	0.065	0.360	0.065	0.350	0.065	0.330	0.066	0.296
0.076	0.406	0.076	0.378	0.076	0.363	0.077	0.351	0.077	0.333	0.076	0.298
0.089	0.410	0.089	0.382	0.089	0.368	0.089	0.356	0.089	0.336	0.089	0.301
0.104	0.414	0.104	0.385	0.104	0.372	0.104	0.361	0.105	0.340	0.104	0.306
0.122	0.418	0.122	0.391	0.121	0.376	0.122	0.366	0.122	0.344	0.122	0.311
0.142	0.424	0.143	0.397	0.142	0.383	0.142	0.373	0.143	0.351	0.143	0.319
0.166	0.430	0.167	0.404	0.166	0.390	0.166	0.381	0.167	0.360	0.167	0.327
0.195	0.437	0.194	0.411	0.194	0.399	0.195	0.391	0.195	0.370	0.195	0.338
0.227	0.445	0.227	0.421	0.227	0.409	0.228	0.402	0.228	0.382	0.229	0.351
0.265	0.455	0.266	0.432	0.265	0.422	0.266	0.416	0.267	0.397	0.267	0.367
0.310	0.466	0.311	0.444	0.311	0.436	0.311	0.432	0.312	0.413	0.313	0.385
0.363	0.479	0.363	0.459	0.364	0.451	0.364	0.449	0.365	0.433	0.366	0.406
0.424	0.492	0.424	0.474	0.425	0.469	0.425	0.468	0.427	0.455	0.428	0.430
0.495	0.507	0.496	0.490	0.497	0.488	0.498	0.489	0.499	0.478	0.501	0.456
0.579	0.522	0.580	0.508	0.581	0.508	0.581	0.510	0.584	0.503	0.581	0.482
0.677	0.538	0.677	0.526	0.679	0.528	0.680	0.533	0.677	0.528	0.679	0.510
0.790	0.554	0.788	0.545	0.793	0.549	0.792	0.561	0.786	0.559	0.792	0.539
0.923	0.570	0.924	0.563	0.924	0.574	0.925	0.584	0.924	0.581	0.916	0.573
1.076	0.588	1.072	0.584	1.077	0.591	1.078	0.602	1.074	0.611	1.073	0.601
1.253	0.603	1.250	0.601	1.254	0.614	1.254	0.626	1.249	0.636	1.248	0.629
1.464	0.616	1.464	0.616	1.461	0.632	1.464	0.646	1.465	0.657	1.466	0.653
1.713	0.628	1.707	0.630	1.711	0.648	1.711	0.663	1.712	0.677	1.713	0.675
1.994	0.637	1.994	0.640	2.000	0.662	1.994	0.674	1.995	0.691	1.995	0.690
2.330	0.644	2.330	0.648	2.330	0.669	2.330	0.683	2.330	0.701	2.330	0.702
2.722	0.648	2.722	0.652	2.722	0.673	2.722	0.688	2.722	0.706	2.723	0.708
3.180	0.647	3.180	0.651	3.180	0.672	3.180	0.688	3.181	0.706	3.181	0.708
3.711	0.639	3.711	0.642	3.711	0.661	3.710	0.677	3.715	0.699	3.712	0.699
4.334	0.627	4.335	0.630	4.335	0.648	4.335	0.664	4.335	0.683	4.335	0.686
5.064	0.610	5.063	0.613	5.063	0.629	5.063	0.645	5.064	0.664	5.064	0.667
5.914	0.589	5.915	0.591	5.919	0.605	5.915	0.623	5.915	0.640	5.914	0.645
6.908	0.564	6.908	0.565	6.909	0.579	6.908	0.596	6.909	0.613	6.909	0.619
8.068	0.535	8.067	0.536	8.070	0.549	8.068	0.565	8.068	0.583	8.068	0.590
9.425	0.503	9.424	0.504	9.424	0.516	9.423	0.532	9.424	0.550	9.424	0.560

Table D21 Loss factor (tanδ) as a function of test strain at 0°C of the vulcanizates filled with various silica/CB hybrid ratios: (c) SSBR3626_HDSi

SSBR3626											
HDSi100/CB0		**HDSi80/CB20**		**HDSi60/CB40**		**HDSi40/CB60**		**HDSi20/CB80**		**Silica0/CB100**	
Strain (%)	**Tan δ**	**Strain (%)**	**Tan δ**	**Strain (%)**	**Tan δ**	**Strain (%)**	**Tan δ**	**Strain (%)**	**Tan δ**	**Strain (%)**	**Tan δ**
0.030	0.434	0.030	0.416	0.030	0.396	0.030	0.389	0.030	0.373	0.030	0.337
0.035	0.432	0.036	0.416	0.036	0.398	0.035	0.390	0.035	0.375	0.036	0.337
0.041	0.434	0.041	0.417	0.041	0.399	0.041	0.391	0.041	0.376	0.041	0.340
0.047	0.436	0.048	0.419	0.049	0.400	0.049	0.393	0.048	0.376	0.048	0.341
0.056	0.437	0.056	0.419	0.056	0.402	0.056	0.394	0.056	0.380	0.057	0.342
0.065	0.440	0.065	0.423	0.065	0.405	0.065	0.397	0.066	0.381	0.065	0.343
0.076	0.442	0.076	0.425	0.076	0.407	0.076	0.399	0.076	0.383	0.077	0.346
0.089	0.445	0.089	0.428	0.090	0.412	0.090	0.403	0.089	0.388	0.089	0.350
0.104	0.449	0.104	0.432	0.105	0.416	0.104	0.407	0.104	0.392	0.104	0.354
0.122	0.453	0.122	0.437	0.122	0.421	0.122	0.412	0.122	0.397	0.122	0.359
0.143	0.458	0.143	0.443	0.143	0.427	0.143	0.419	0.143	0.404	0.143	0.366
0.167	0.465	0.166	0.451	0.167	0.435	0.167	0.427	0.167	0.412	0.168	0.375
0.194	0.473	0.195	0.460	0.195	0.445	0.194	0.437	0.196	0.423	0.196	0.385
0.228	0.483	0.228	0.471	0.228	0.457	0.228	0.449	0.228	0.435	0.229	0.398
0.266	0.495	0.267	0.484	0.267	0.470	0.267	0.464	0.267	0.450	0.268	0.414
0.312	0.508	0.312	0.499	0.312	0.486	0.312	0.479	0.313	0.468	0.313	0.432
0.364	0.523	0.365	0.516	0.364	0.504	0.366	0.499	0.366	0.488	0.367	0.452
0.426	0.540	0.426	0.534	0.427	0.523	0.427	0.519	0.428	0.511	0.429	0.476
0.498	0.558	0.498	0.554	0.499	0.544	0.497	0.541	0.501	0.535	0.501	0.501
0.579	0.577	0.583	0.575	0.579	0.567	0.584	0.565	0.581	0.562	0.582	0.528
0.678	0.601	0.673	0.600	0.673	0.594	0.678	0.591	0.679	0.588	0.681	0.557
0.791	0.619	0.790	0.620	0.792	0.615	0.792	0.618	0.784	0.622	0.784	0.593
0.916	0.642	0.924	0.643	0.915	0.643	0.919	0.648	0.919	0.651	0.922	0.623
1.070	0.661	1.075	0.667	1.070	0.666	1.070	0.674	1.068	0.680	1.070	0.654
1.251	0.680	1.251	0.686	1.250	0.689	1.248	0.699	1.250	0.705	1.256	0.685
1.462	0.695	1.462	0.704	1.462	0.710	1.461	0.721	1.462	0.727	1.462	0.711
1.709	0.707	1.708	0.718	1.709	0.727	1.708	0.739	1.704	0.747	1.703	0.735
1.997	0.715	1.996	0.728	1.997	0.739	1.996	0.754	1.992	0.762	1.991	0.754
2.333	0.718	2.333	0.735	2.333	0.746	2.333	0.762	2.333	0.770	2.333	0.767
2.722	0.712	2.721	0.733	2.726	0.748	2.721	0.761	2.721	0.770	2.725	0.773
3.176	0.703	3.182	0.730	3.182	0.743	3.179	0.755	3.180	0.767	3.178	0.769
3.713	0.688	3.713	0.714	3.713	0.727	3.710	0.744	3.713	0.752	3.713	0.760
4.337	0.668	4.336	0.695	4.337	0.708	4.336	0.726	4.336	0.733	4.336	0.743
5.064	0.642	5.064	0.671	5.065	0.683	5.065	0.701	5.066	0.708	5.065	0.721
5.917	0.612	5.916	0.642	5.916	0.655	5.917	0.671	5.916	0.678	5.916	0.693
6.912	0.578	6.910	0.608	6.911	0.620	6.911	0.637	6.912	0.645	6.910	0.661
8.072	0.542	8.070	0.572	8.072	0.584	8.070	0.602	8.073	0.609	8.071	0.628
9.427	0.505	9.427	0.533	9.425	0.547	9.426	0.563	9.426	0.571	9.426	0.592

Table D22 Loss factor (tanδ) as a function of test strain at 0°C of the vulcanizates filled with various silica/CB hybrid ratios: (d) SSBR3626_CSi

SSBR3626											
CSi100/CB0		CSi80/CB20		CSi60/CB40		CSi40/CB60		CSi20/CB80		Silica0/CB100	
Strain (%)	Tan δ	Strain (%)	Tan δ	Strain (%)	Tan δ	Strain (%)	Tan δ	Strain (%)	Tan δ	Strain (%)	Tan δ
0.030	0.441	0.030	0.418	0.029	0.411	0.030	0.395	0.030	0.369	0.030	0.337
0.035	0.443	0.035	0.421	0.036	0.414	0.035	0.396	0.035	0.368	0.036	0.337
0.041	0.445	0.041	0.421	0.041	0.416	0.041	0.396	0.041	0.371	0.041	0.340
0.047	0.446	0.048	0.425	0.048	0.417	0.048	0.398	0.048	0.373	0.048	0.341
0.056	0.450	0.055	0.426	0.056	0.418	0.056	0.400	0.056	0.373	0.057	0.342
0.065	0.451	0.065	0.428	0.065	0.423	0.065	0.403	0.066	0.376	0.065	0.343
0.077	0.455	0.077	0.432	0.076	0.425	0.077	0.407	0.076	0.378	0.077	0.346
0.089	0.458	0.089	0.435	0.089	0.428	0.089	0.411	0.090	0.382	0.089	0.350
0.104	0.462	0.104	0.439	0.105	0.433	0.104	0.416	0.104	0.386	0.104	0.354
0.122	0.466	0.122	0.444	0.122	0.438	0.122	0.421	0.122	0.391	0.122	0.359
0.142	0.472	0.142	0.451	0.143	0.444	0.143	0.428	0.143	0.397	0.143	0.366
0.166	0.478	0.167	0.459	0.167	0.453	0.167	0.436	0.167	0.405	0.168	0.375
0.194	0.486	0.195	0.468	0.195	0.462	0.195	0.447	0.195	0.415	0.196	0.385
0.227	0.495	0.228	0.478	0.228	0.474	0.228	0.459	0.228	0.427	0.229	0.398
0.266	0.506	0.266	0.491	0.267	0.488	0.267	0.473	0.267	0.442	0.268	0.414
0.311	0.519	0.311	0.505	0.311	0.504	0.313	0.491	0.313	0.459	0.313	0.432
0.363	0.534	0.365	0.522	0.365	0.521	0.365	0.509	0.365	0.478	0.367	0.452
0.425	0.549	0.425	0.540	0.426	0.541	0.427	0.530	0.428	0.500	0.429	0.476
0.497	0.566	0.498	0.559	0.498	0.562	0.499	0.553	0.497	0.524	0.501	0.501
0.581	0.584	0.582	0.580	0.579	0.584	0.580	0.577	0.580	0.550	0.582	0.528
0.678	0.603	0.678	0.601	0.679	0.612	0.678	0.603	0.678	0.577	0.681	0.557
0.784	0.624	0.790	0.624	0.786	0.635	0.786	0.633	0.793	0.606	0.784	0.593
0.923	0.642	0.924	0.647	0.924	0.656	0.925	0.657	0.916	0.638	0.922	0.623
1.071	0.661	1.070	0.671	1.074	0.683	1.070	0.686	1.070	0.667	1.070	0.654
1.254	0.678	1.254	0.693	1.250	0.705	1.254	0.711	1.255	0.695	1.256	0.685
1.462	0.693	1.461	0.711	1.466	0.726	1.461	0.733	1.459	0.720	1.462	0.711
1.709	0.705	1.708	0.727	1.708	0.743	1.708	0.752	1.708	0.741	1.703	0.735
1.997	0.714	1.996	0.739	1.995	0.756	1.996	0.766	1.996	0.759	1.991	0.754
2.333	0.717	2.332	0.748	2.331	0.764	2.332	0.776	2.333	0.771	2.333	0.767
2.721	0.713	2.724	0.750	2.725	0.767	2.725	0.779	2.725	0.776	2.725	0.773
3.179	0.704	3.178	0.742	3.178	0.759	3.178	0.771	3.178	0.772	3.178	0.769
3.713	0.690	3.712	0.730	3.712	0.747	3.712	0.760	3.710	0.763	3.713	0.760
4.336	0.671	4.336	0.712	4.337	0.728	4.336	0.742	4.336	0.747	4.336	0.743
5.065	0.645	5.065	0.687	5.065	0.703	5.064	0.718	5.065	0.725	5.065	0.721
5.916	0.616	5.916	0.657	5.916	0.672	5.915	0.689	5.916	0.696	5.916	0.693
6.909	0.581	6.909	0.624	6.910	0.638	6.910	0.655	6.910	0.665	6.910	0.661
8.069	0.544	8.071	0.587	8.071	0.602	8.069	0.618	8.070	0.628	8.071	0.628
9.426	0.507	9.425	0.548	9.425	0.564	9.426	0.578	9.423	0.591	9.426	0.592

Table D23 Loss factor (tanδ) as a function of test strain at 0°C of the vulcanizates filled with various silica/CB hybrid ratios: (e) ESBR1723_HDSi

ESBR1723											
HDSi100/CB0		HDSi80/CB20		HDSi60/CB40		HDSi40/CB60		HDSi20/CB80		Silica0/CB100	
Strain (%)	Tan δ	Strain (%)	Tan δ	Strain (%)	Tan δ	Strain (%)	Tan δ	Strain (%)	Tan δ	Strain (%)	Tan δ
0.030	0.181	0.030	0.175	0.030	0.175	0.030	0.169	0.030	0.163	0.030	0.157
0.035	0.182	0.035	0.176	0.035	0.176	0.036	0.170	0.035	0.166	0.034	0.159
0.041	0.183	0.041	0.181	0.041	0.179	0.041	0.169	0.042	0.167	0.041	0.160
0.048	0.180	0.048	0.180	0.047	0.178	0.048	0.172	0.048	0.168	0.048	0.161
0.056	0.183	0.056	0.181	0.056	0.178	0.055	0.173	0.056	0.170	0.056	0.162
0.066	0.186	0.065	0.184	0.066	0.181	0.065	0.175	0.065	0.171	0.065	0.163
0.076	0.187	0.076	0.185	0.076	0.183	0.076	0.176	0.076	0.174	0.077	0.165
0.089	0.190	0.089	0.188	0.089	0.186	0.089	0.180	0.089	0.177	0.089	0.169
0.104	0.194	0.104	0.191	0.104	0.190	0.104	0.184	0.104	0.180	0.104	0.173
0.122	0.196	0.122	0.196	0.122	0.194	0.122	0.188	0.122	0.185	0.122	0.178
0.143	0.202	0.143	0.201	0.142	0.200	0.143	0.194	0.142	0.191	0.143	0.184
0.166	0.206	0.166	0.207	0.166	0.206	0.166	0.201	0.167	0.198	0.167	0.192
0.195	0.213	0.195	0.214	0.195	0.214	0.195	0.209	0.196	0.207	0.196	0.201
0.228	0.220	0.228	0.222	0.228	0.223	0.228	0.219	0.228	0.217	0.229	0.212
0.265	0.227	0.266	0.231	0.266	0.232	0.266	0.230	0.266	0.229	0.268	0.226
0.311	0.237	0.311	0.241	0.311	0.244	0.311	0.242	0.312	0.243	0.313	0.241
0.363	0.246	0.363	0.252	0.364	0.256	0.364	0.255	0.364	0.257	0.366	0.258
0.424	0.257	0.424	0.263	0.425	0.269	0.425	0.270	0.427	0.274	0.428	0.276
0.495	0.268	0.497	0.275	0.496	0.282	0.497	0.286	0.498	0.290	0.500	0.295
0.578	0.279	0.579	0.287	0.580	0.296	0.581	0.301	0.583	0.308	0.584	0.315
0.676	0.290	0.677	0.299	0.678	0.310	0.679	0.317	0.676	0.325	0.677	0.335
0.790	0.300	0.790	0.311	0.792	0.323	0.789	0.333	0.786	0.346	0.791	0.355
0.923	0.311	0.924	0.322	0.921	0.336	0.918	0.352	0.915	0.364	0.924	0.374
1.078	0.321	1.079	0.333	1.075	0.349	1.076	0.362	1.072	0.378	1.070	0.399
1.259	0.330	1.251	0.346	1.257	0.361	1.253	0.379	1.258	0.388	1.252	0.415
1.463	0.342	1.462	0.355	1.462	0.374	1.467	0.388	1.463	0.406	1.463	0.429
1.707	0.349	1.707	0.363	1.713	0.381	1.705	0.402	1.708	0.417	1.709	0.443
1.999	0.354	1.994	0.370	1.995	0.392	1.995	0.411	1.997	0.427	1.992	0.456
2.330	0.362	2.330	0.376	2.326	0.398	2.327	0.419	2.331	0.435	2.332	0.464
2.721	0.366	2.721	0.381	2.721	0.402	2.722	0.424	2.723	0.441	2.724	0.471
3.175	0.369	3.179	0.384	3.180	0.406	3.180	0.427	3.175	0.445	3.176	0.476
3.714	0.370	3.715	0.385	3.715	0.407	3.710	0.429	3.710	0.445	3.711	0.477
4.333	0.369	4.333	0.384	4.333	0.407	4.333	0.427	4.334	0.444	4.335	0.477
5.062	0.367	5.062	0.382	5.062	0.404	5.063	0.425	5.063	0.440	5.064	0.473
5.913	0.363	5.913	0.377	5.913	0.399	5.914	0.419	5.914	0.434	5.915	0.467
6.908	0.357	6.905	0.369	6.905	0.392	6.906	0.410	6.906	0.425	6.906	0.458
8.064	0.348	8.065	0.360	8.065	0.381	8.066	0.400	8.065	0.414	8.066	0.446
9.419	0.336	9.420	0.348	9.420	0.368	9.420	0.387	9.420	0.401	9.421	0.432

Table D24 Loss factor (tanδ) as a function of test strain at 0°C of the vulcanizates filled with various silica/CB hybrid ratios: (f) ESBR1723_CSi

ESBR1723											
CSi100/CB0		CSi80/CB20		CSi60/CB40		CSi40/CB60		CSi20/CB80		Silica0/CB100	
Strain (%)	Tan δ	Strain (%)	Tan δ	Strain (%)	Tan δ	Strain (%)	Tan δ	Strain (%)	Tan δ	Strain (%)	Tan δ
0.030	0.181	0.030	0.177	0.030	0.177	0.029	0.174	0.030	0.168	0.030	0.157
0.035	0.180	0.036	0.181	0.035	0.177	0.035	0.173	0.035	0.166	0.034	0.159
0.042	0.180	0.041	0.179	0.041	0.179	0.041	0.173	0.041	0.168	0.041	0.160
0.048	0.181	0.047	0.183	0.047	0.179	0.048	0.177	0.047	0.169	0.048	0.161
0.056	0.182	0.056	0.183	0.057	0.180	0.056	0.177	0.056	0.169	0.056	0.162
0.066	0.185	0.065	0.184	0.065	0.182	0.066	0.179	0.065	0.172	0.065	0.163
0.077	0.186	0.076	0.187	0.076	0.183	0.077	0.181	0.076	0.174	0.077	0.165
0.089	0.189	0.089	0.190	0.090	0.188	0.089	0.184	0.089	0.177	0.089	0.169
0.104	0.194	0.104	0.193	0.104	0.191	0.104	0.187	0.104	0.182	0.104	0.173
0.121	0.196	0.122	0.197	0.122	0.195	0.122	0.193	0.122	0.186	0.122	0.178
0.142	0.201	0.142	0.202	0.143	0.200	0.143	0.198	0.143	0.191	0.143	0.184
0.166	0.206	0.167	0.207	0.166	0.206	0.166	0.205	0.167	0.199	0.167	0.192
0.195	0.212	0.194	0.213	0.195	0.214	0.195	0.214	0.195	0.207	0.196	0.201
0.227	0.219	0.227	0.222	0.228	0.222	0.227	0.222	0.228	0.217	0.229	0.212
0.266	0.227	0.266	0.231	0.266	0.232	0.266	0.233	0.267	0.229	0.268	0.226
0.311	0.236	0.311	0.240	0.311	0.243	0.311	0.245	0.312	0.241	0.313	0.241
0.362	0.246	0.363	0.252	0.364	0.256	0.364	0.258	0.365	0.256	0.366	0.258
0.424	0.256	0.424	0.263	0.425	0.269	0.425	0.273	0.426	0.271	0.428	0.276
0.495	0.267	0.496	0.275	0.496	0.283	0.497	0.288	0.498	0.288	0.500	0.295
0.578	0.278	0.579	0.287	0.580	0.297	0.580	0.303	0.582	0.305	0.584	0.315
0.676	0.289	0.676	0.300	0.675	0.311	0.678	0.318	0.679	0.322	0.677	0.335
0.789	0.300	0.790	0.312	0.788	0.325	0.789	0.334	0.786	0.344	0.791	0.355
0.922	0.311	0.923	0.324	0.921	0.339	0.921	0.348	0.917	0.361	0.924	0.374
1.077	0.322	1.078	0.335	1.077	0.355	1.071	0.367	1.077	0.373	1.070	0.399
1.258	0.331	1.259	0.346	1.255	0.364	1.256	0.377	1.252	0.392	1.252	0.415
1.466	0.341	1.462	0.358	1.462	0.378	1.462	0.392	1.469	0.402	1.463	0.429
1.707	0.351	1.707	0.366	1.713	0.385	1.705	0.402	1.705	0.419	1.709	0.443
1.999	0.356	2.000	0.372	1.991	0.396	1.994	0.411	1.995	0.428	1.992	0.456
2.329	0.364	2.330	0.380	2.330	0.402	2.330	0.419	2.331	0.437	2.332	0.464
2.718	0.368	2.721	0.385	2.718	0.407	2.722	0.424	2.717	0.443	2.724	0.471
3.175	0.371	3.179	0.388	3.175	0.410	3.180	0.428	3.175	0.448	3.176	0.476
3.709	0.372	3.714	0.389	3.709	0.410	3.714	0.429	3.715	0.449	3.711	0.477
4.332	0.372	4.333	0.388	4.333	0.409	4.333	0.428	4.333	0.449	4.335	0.477
5.061	0.370	5.062	0.385	5.062	0.406	5.061	0.424	5.062	0.445	5.064	0.473
5.913	0.365	5.913	0.380	5.913	0.401	5.913	0.419	5.913	0.439	5.915	0.467
6.907	0.359	6.908	0.373	6.904	0.392	6.908	0.411	6.905	0.430	6.906	0.458
8.064	0.349	8.064	0.364	8.064	0.382	8.064	0.399	8.065	0.419	8.066	0.446
9.418	0.338	9.419	0.352	9.418	0.370	9.419	0.386	9.420	0.406	9.421	0.432

Table D25 Loss factor (tanδ) as a function of test strain at 60°C of the vulcanizates filled with various silica/CB hybrid ratios: (a) SSBR6450SL_HDSi

SSBR6450SL											
HDSi100/CB0		HDSi80/CB20		HDSi60/CB40		HDSi40/CB60		HDSi20/CB80		Silica0/CB100	
Strain (%)	Tan δ	Strain (%)	Tan δ	Strain (%)	Tan δ	Strain (%)	Tan δ	Strain (%)	Tan δ	Strain (%)	Tan δ
0.030	0.073	0.030	0.081	0.030	0.092	0.030	0.089	0.030	0.094	0.030	0.110
0.034	0.071	0.034	0.079	0.036	0.084	0.035	0.096	0.035	0.108	0.035	0.106
0.041	0.070	0.041	0.084	0.041	0.089	0.041	0.086	0.041	0.102	0.041	0.107
0.047	0.068	0.045	0.092	0.048	0.089	0.047	0.102	0.049	0.105	0.048	0.108
0.056	0.077	0.056	0.080	0.056	0.090	0.056	0.094	0.055	0.102	0.056	0.106
0.065	0.075	0.065	0.089	0.066	0.097	0.065	0.096	0.066	0.103	0.065	0.107
0.077	0.077	0.076	0.089	0.077	0.091	0.077	0.097	0.076	0.105	0.076	0.110
0.089	0.076	0.090	0.084	0.089	0.090	0.088	0.101	0.089	0.104	0.089	0.114
0.104	0.073	0.105	0.086	0.104	0.096	0.102	0.100	0.104	0.109	0.104	0.116
0.122	0.079	0.121	0.085	0.121	0.096	0.122	0.106	0.122	0.111	0.122	0.120
0.142	0.078	0.142	0.089	0.142	0.100	0.142	0.106	0.142	0.114	0.142	0.123
0.166	0.079	0.166	0.091	0.166	0.100	0.166	0.110	0.166	0.118	0.166	0.128
0.194	0.082	0.194	0.093	0.194	0.102	0.194	0.112	0.194	0.121	0.194	0.134
0.226	0.084	0.227	0.097	0.227	0.104	0.227	0.115	0.227	0.128	0.228	0.142
0.264	0.086	0.265	0.099	0.264	0.108	0.265	0.121	0.265	0.134	0.266	0.149
0.309	0.088	0.310	0.103	0.310	0.113	0.310	0.126	0.311	0.141	0.310	0.160
0.361	0.091	0.362	0.106	0.362	0.120	0.361	0.132	0.362	0.148	0.363	0.171
0.422	0.095	0.422	0.110	0.422	0.126	0.422	0.138	0.423	0.157	0.424	0.182
0.493	0.096	0.494	0.115	0.492	0.131	0.493	0.145	0.494	0.166	0.495	0.194
0.576	0.100	0.576	0.118	0.576	0.138	0.576	0.152	0.580	0.175	0.578	0.206
0.673	0.102	0.673	0.123	0.673	0.144	0.673	0.159	0.674	0.183	0.675	0.218
0.786	0.105	0.786	0.127	0.787	0.151	0.787	0.166	0.787	0.192	0.788	0.230
0.918	0.108	0.918	0.132	0.918	0.157	0.918	0.172	0.919	0.199	0.921	0.242
1.072	0.111	1.072	0.135	1.073	0.163	1.074	0.179	1.074	0.208	1.076	0.253
1.253	0.113	1.253	0.139	1.253	0.169	1.254	0.185	1.254	0.216	1.254	0.262
1.463	0.115	1.464	0.142	1.464	0.174	1.464	0.191	1.465	0.223	1.467	0.271
1.709	0.118	1.710	0.145	1.709	0.179	1.710	0.195	1.709	0.229	1.713	0.278
1.998	0.120	1.998	0.149	1.996	0.183	1.996	0.200	1.996	0.233	1.997	0.284
2.334	0.121	2.332	0.151	2.332	0.186	2.333	0.204	2.335	0.237	2.325	0.290
2.713	0.124	2.725	0.153	2.725	0.190	2.716	0.208	2.724	0.241	2.719	0.293
3.180	0.126	3.177	0.156	3.180	0.194	3.182	0.208	3.182	0.243	3.182	0.293
3.708	0.127	3.714	0.157	3.714	0.195	3.713	0.211	3.713	0.245	3.711	0.296
4.336	0.129	4.336	0.158	4.331	0.197	4.331	0.212	4.331	0.245	4.331	0.294
5.061	0.131	5.060	0.159	5.059	0.198	5.060	0.212	5.060	0.244	5.064	0.291
5.911	0.133	5.912	0.160	5.911	0.198	5.911	0.212	5.911	0.243	5.910	0.290
6.904	0.136	6.905	0.161	6.904	0.198	6.904	0.211	6.904	0.241	6.905	0.286
8.064	0.138	8.065	0.161	8.066	0.198	8.062	0.209	8.063	0.238	8.064	0.282
9.418	0.140	9.419	0.161	9.417	0.196	9.418	0.207	9.416	0.234	9.421	0.275

Table D26 Loss factor (tanδ) as a function of test strain at 60°C of the vulcanizates filled with various silica/CB hybrid ratios: (b) SSBR6450SL_CSi

SSBR6450SL											
CSi100/CB0		CSi80/CB20		CSi60/CB40		CSi40/CB60		CSi20/CB80		Silica0/CB100	
Strain (%)	Tan δ	Strain (%)	Tan δ	Strain (%)	Tan δ	Strain (%)	Tan δ	Strain (%)	Tan δ	Strain (%)	Tan δ
0.030	0.069	0.030	0.086	0.031	0.091	0.030	0.094	0.030	0.100	0.030	0.110
0.036	0.074	0.035	0.079	0.035	0.080	0.036	0.097	0.035	0.101	0.035	0.106
0.041	0.075	0.040	0.078	0.041	0.081	0.041	0.096	0.041	0.101	0.041	0.107
0.048	0.077	0.048	0.086	0.048	0.088	0.049	0.097	0.048	0.102	0.048	0.108
0.055	0.076	0.056	0.084	0.056	0.085	0.056	0.095	0.056	0.102	0.056	0.106
0.065	0.079	0.063	0.078	0.065	0.090	0.066	0.092	0.065	0.104	0.065	0.107
0.076	0.088	0.076	0.084	0.076	0.091	0.076	0.098	0.076	0.105	0.076	0.110
0.089	0.082	0.089	0.084	0.090	0.093	0.089	0.100	0.089	0.107	0.089	0.114
0.104	0.075	0.104	0.085	0.104	0.092	0.104	0.100	0.103	0.110	0.104	0.116
0.122	0.073	0.122	0.086	0.122	0.092	0.122	0.103	0.121	0.111	0.122	0.120
0.142	0.079	0.142	0.085	0.143	0.096	0.142	0.104	0.143	0.116	0.142	0.123
0.166	0.080	0.166	0.086	0.166	0.097	0.166	0.107	0.166	0.119	0.166	0.128
0.194	0.081	0.194	0.089	0.194	0.100	0.194	0.111	0.194	0.122	0.194	0.134
0.226	0.083	0.226	0.090	0.226	0.103	0.227	0.115	0.228	0.127	0.228	0.142
0.265	0.085	0.265	0.093	0.265	0.108	0.265	0.119	0.267	0.135	0.266	0.149
0.309	0.087	0.309	0.098	0.310	0.112	0.310	0.125	0.310	0.141	0.310	0.160
0.361	0.090	0.360	0.100	0.362	0.116	0.362	0.131	0.362	0.149	0.363	0.171
0.421	0.091	0.422	0.105	0.422	0.121	0.423	0.138	0.423	0.157	0.424	0.182
0.492	0.094	0.493	0.108	0.493	0.126	0.494	0.144	0.494	0.166	0.495	0.194
0.576	0.097	0.575	0.112	0.576	0.133	0.577	0.152	0.577	0.175	0.578	0.206
0.672	0.099	0.672	0.117	0.673	0.138	0.672	0.158	0.674	0.183	0.675	0.218
0.786	0.101	0.785	0.121	0.786	0.144	0.787	0.166	0.787	0.193	0.788	0.230
0.917	0.104	0.915	0.124	0.918	0.149	0.919	0.173	0.919	0.202	0.921	0.242
1.071	0.106	1.072	0.129	1.073	0.155	1.073	0.180	1.074	0.211	1.076	0.253
1.249	0.108	1.252	0.132	1.253	0.160	1.253	0.186	1.251	0.218	1.254	0.262
1.459	0.110	1.463	0.135	1.463	0.165	1.465	0.192	1.464	0.226	1.467	0.271
1.708	0.112	1.709	0.138	1.705	0.169	1.709	0.198	1.709	0.232	1.713	0.278
1.997	0.113	1.996	0.140	1.998	0.173	1.998	0.202	1.996	0.238	1.997	0.284
2.331	0.114	2.332	0.142	2.332	0.177	2.334	0.206	2.333	0.243	2.325	0.290
2.723	0.116	2.725	0.144	2.722	0.179	2.723	0.209	2.724	0.246	2.719	0.293
3.179	0.117	3.169	0.146	3.177	0.183	3.169	0.213	3.181	0.248	3.182	0.293
3.714	0.118	3.714	0.147	3.714	0.184	3.711	0.212	3.710	0.252	3.711	0.296
4.337	0.119	4.332	0.148	4.335	0.185	4.335	0.214	4.334	0.251	4.331	0.294
5.061	0.121	5.060	0.148	5.060	0.186	5.064	0.214	5.064	0.250	5.064	0.291
5.911	0.122	5.911	0.149	5.911	0.186	5.911	0.214	5.911	0.250	5.910	0.290
6.905	0.124	6.905	0.150	6.904	0.186	6.904	0.213	6.908	0.247	6.905	0.286
8.063	0.125	8.064	0.150	8.062	0.185	8.066	0.210	8.065	0.245	8.064	0.282
9.418	0.127	9.419	0.150	9.418	0.184	9.420	0.208	9.419	0.240	9.421	0.275

Table D27 Loss factor (tanδ) as a function of test strain at 60°C of the vulcanizates filled with various silica/CB hybrid ratios: (c) SSBR3626_HDSi

SSBR3626											
HDSi100/CB0		**HDSi80/CB20**		**HDSi60/CB40**		**HDSi40/CB60**		**HDSi20/CB80**		**Silica0/CB100**	
Strain (%)	**Tan δ**	**Strain (%)**	**Tan δ**	**Strain (%)**	**Tan δ**	**Strain (%)**	**Tan δ**	**Strain (%)**	**Tan δ**	**Strain (%)**	**Tan δ**
0.030	0.084	0.030	0.085	0.030	0.094	0.030	0.095	0.030	0.100	0.030	0.106
0.035	0.083	0.035	0.088	0.036	0.091	0.035	0.096	0.036	0.097	0.035	0.106
0.041	0.089	0.041	0.087	0.041	0.091	0.041	0.102	0.041	0.101	0.041	0.106
0.048	0.083	0.048	0.085	0.048	0.092	0.048	0.098	0.048	0.105	0.048	0.110
0.056	0.090	0.056	0.085	0.056	0.096	0.056	0.100	0.055	0.104	0.056	0.112
0.066	0.085	0.065	0.091	0.066	0.090	0.065	0.097	0.065	0.100	0.066	0.107
0.077	0.087	0.077	0.086	0.076	0.097	0.076	0.099	0.076	0.103	0.076	0.113
0.090	0.090	0.089	0.090	0.090	0.092	0.089	0.101	0.090	0.106	0.089	0.115
0.105	0.089	0.104	0.089	0.105	0.099	0.105	0.101	0.104	0.108	0.104	0.118
0.122	0.091	0.121	0.090	0.121	0.099	0.122	0.106	0.122	0.110	0.122	0.121
0.143	0.091	0.142	0.094	0.142	0.103	0.142	0.110	0.142	0.115	0.143	0.126
0.166	0.094	0.166	0.096	0.166	0.105	0.166	0.111	0.166	0.119	0.167	0.132
0.194	0.095	0.195	0.097	0.194	0.109	0.194	0.116	0.195	0.124	0.195	0.139
0.225	0.097	0.227	0.102	0.227	0.113	0.227	0.122	0.227	0.131	0.228	0.147
0.265	0.100	0.265	0.106	0.265	0.118	0.266	0.128	0.266	0.138	0.266	0.156
0.310	0.103	0.310	0.109	0.310	0.124	0.310	0.134	0.310	0.146	0.309	0.166
0.362	0.107	0.363	0.114	0.362	0.129	0.362	0.141	0.363	0.155	0.363	0.178
0.425	0.110	0.422	0.119	0.423	0.135	0.423	0.150	0.423	0.165	0.425	0.191
0.495	0.114	0.494	0.124	0.494	0.142	0.494	0.157	0.495	0.174	0.496	0.204
0.579	0.117	0.577	0.129	0.577	0.149	0.578	0.166	0.579	0.184	0.579	0.217
0.676	0.119	0.671	0.133	0.674	0.156	0.675	0.175	0.675	0.194	0.677	0.230
0.788	0.122	0.787	0.138	0.787	0.162	0.788	0.183	0.788	0.204	0.790	0.243
0.921	0.125	0.920	0.143	0.920	0.168	0.921	0.191	0.921	0.213	0.922	0.255
1.077	0.127	1.074	0.147	1.074	0.174	1.074	0.198	1.076	0.222	1.077	0.267
1.256	0.129	1.255	0.151	1.254	0.179	1.255	0.206	1.256	0.231	1.258	0.277
1.466	0.130	1.464	0.155	1.465	0.184	1.466	0.213	1.467	0.238	1.462	0.290
1.711	0.131	1.711	0.158	1.712	0.189	1.711	0.218	1.713	0.244	1.714	0.294
2.000	0.132	1.998	0.161	2.000	0.193	1.997	0.223	1.997	0.250	1.993	0.303
2.334	0.133	2.334	0.164	2.333	0.196	2.332	0.227	2.333	0.253	2.333	0.307
2.723	0.134	2.724	0.167	2.711	0.200	2.725	0.230	2.718	0.259	2.725	0.308
3.175	0.134	3.178	0.168	3.169	0.201	3.173	0.233	3.177	0.260	3.182	0.313
3.709	0.135	3.713	0.169	3.712	0.202	3.708	0.234	3.711	0.260	3.711	0.313
4.332	0.135	4.337	0.170	4.332	0.203	4.336	0.234	4.332	0.261	4.331	0.313
5.062	0.137	5.061	0.171	5.060	0.203	5.066	0.234	5.065	0.259	5.060	0.311
5.913	0.138	5.912	0.171	5.911	0.203	5.910	0.234	5.911	0.258	5.911	0.307
6.908	0.139	6.907	0.171	6.906	0.201	6.906	0.232	6.905	0.255	6.905	0.303
8.065	0.140	8.065	0.170	8.064	0.199	8.064	0.228	8.064	0.251	8.065	0.297
9.419	0.140	9.420	0.169	9.419	0.197	9.417	0.224	9.418	0.246	9.418	0.289

Table D28 Loss factor (tanδ) as a function of test strain at 60°C of the vulcanizates filled with various silica/CB hybrid ratios: (d) SSBR3626_CSi

SSBR3626											
CSi100/CB0		CSi80/CB20		CSi60/CB40		CSi40/CB60		CSi20/CB80		Silica0/CB100	
Strain (%)	Tan δ	Strain (%)	Tan δ	Strain (%)	Tan δ	Strain (%)	Tan δ	Strain (%)	Tan δ	Strain (%)	Tan δ
0.030	0.078	0.030	0.080	0.030	0.087	0.030	0.094	0.030	0.103	0.030	0.106
0.035	0.070	0.035	0.087	0.035	0.089	0.035	0.095	0.035	0.103	0.035	0.106
0.040	0.076	0.041	0.083	0.041	0.092	0.042	0.099	0.041	0.097	0.041	0.106
0.048	0.069	0.048	0.087	0.047	0.095	0.048	0.100	0.048	0.100	0.048	0.110
0.056	0.076	0.056	0.091	0.056	0.090	0.056	0.098	0.056	0.105	0.056	0.112
0.066	0.076	0.065	0.088	0.066	0.090	0.065	0.098	0.066	0.105	0.066	0.107
0.076	0.079	0.075	0.085	0.076	0.092	0.076	0.102	0.076	0.108	0.076	0.113
0.089	0.079	0.089	0.087	0.089	0.094	0.090	0.102	0.089	0.109	0.089	0.115
0.104	0.078	0.103	0.089	0.104	0.096	0.104	0.105	0.105	0.110	0.104	0.118
0.122	0.078	0.122	0.092	0.122	0.097	0.122	0.105	0.122	0.113	0.122	0.121
0.142	0.079	0.142	0.093	0.142	0.099	0.142	0.108	0.142	0.117	0.143	0.126
0.166	0.083	0.168	0.096	0.166	0.102	0.166	0.111	0.166	0.120	0.167	0.132
0.196	0.084	0.194	0.097	0.194	0.106	0.194	0.116	0.193	0.125	0.195	0.139
0.226	0.087	0.227	0.100	0.227	0.109	0.227	0.121	0.227	0.131	0.228	0.147
0.264	0.088	0.265	0.103	0.265	0.114	0.265	0.126	0.266	0.138	0.266	0.156
0.310	0.090	0.309	0.108	0.310	0.120	0.310	0.133	0.310	0.146	0.309	0.166
0.361	0.094	0.362	0.111	0.363	0.125	0.362	0.139	0.363	0.155	0.363	0.178
0.422	0.097	0.422	0.116	0.422	0.131	0.423	0.147	0.424	0.164	0.425	0.191
0.493	0.100	0.493	0.121	0.493	0.137	0.494	0.156	0.495	0.174	0.496	0.204
0.576	0.103	0.576	0.126	0.577	0.143	0.577	0.163	0.577	0.184	0.579	0.217
0.673	0.107	0.673	0.131	0.674	0.150	0.673	0.172	0.675	0.194	0.677	0.230
0.786	0.110	0.787	0.135	0.787	0.156	0.787	0.180	0.788	0.204	0.790	0.243
0.915	0.113	0.919	0.140	0.920	0.162	0.922	0.188	0.921	0.213	0.922	0.255
1.073	0.116	1.073	0.145	1.073	0.168	1.074	0.196	1.075	0.222	1.077	0.267
1.253	0.118	1.254	0.149	1.253	0.174	1.254	0.202	1.255	0.230	1.258	0.277
1.464	0.120	1.464	0.153	1.465	0.179	1.466	0.209	1.467	0.238	1.462	0.290
1.709	0.122	1.709	0.157	1.711	0.184	1.711	0.215	1.713	0.244	1.714	0.294
1.996	0.124	1.998	0.159	1.997	0.188	1.999	0.219	1.999	0.250	1.993	0.303
2.334	0.125	2.334	0.162	2.328	0.193	2.332	0.223	2.333	0.254	2.333	0.307
2.725	0.126	2.725	0.164	2.719	0.195	2.719	0.228	2.725	0.257	2.725	0.308
3.178	0.128	3.179	0.166	3.177	0.197	3.180	0.229	3.181	0.260	3.182	0.313
3.712	0.129	3.715	0.167	3.712	0.198	3.715	0.230	3.711	0.261	3.711	0.313
4.332	0.130	4.331	0.168	4.336	0.199	4.335	0.230	4.331	0.261	4.331	0.313
5.065	0.131	5.060	0.169	5.065	0.200	5.064	0.230	5.060	0.259	5.060	0.311
5.911	0.133	5.911	0.169	5.911	0.200	5.911	0.230	5.911	0.258	5.911	0.307
6.907	0.135	6.906	0.169	6.905	0.199	6.906	0.228	6.905	0.255	6.905	0.303
8.066	0.136	8.065	0.169	8.065	0.198	8.063	0.225	8.064	0.251	8.065	0.297
9.418	0.137	9.418	0.168	9.419	0.195	9.422	0.221	9.417	0.245	9.418	0.289

Table D29 Loss factor (tanδ) as a function of test strain at 60°C of the vulcanizates filled with various silica/CB hybrid ratios: (e) ESBR1723_HDSi

ESBR1723											
HDSi100/CB0		HDSi80/CB20		HDSi60/CB40		HDSi40/CB60		HDSi20/CB80		Silica0/CB100	
Strain (%)	Tan δ	Strain (%)	Tan δ	Strain (%)	Tan δ	Strain (%)	Tan δ	Strain (%)	Tan δ	Strain (%)	Tan δ
0.029	0.092	0.030	0.095	0.030	0.099	0.030	0.106	0.030	0.114	0.030	0.118
0.037	0.090	0.035	0.094	0.035	0.111	0.035	0.109	0.035	0.111	0.035	0.118
0.041	0.092	0.041	0.098	0.041	0.102	0.041	0.109	0.041	0.116	0.040	0.112
0.047	0.093	0.048	0.093	0.048	0.102	0.048	0.108	0.046	0.108	0.048	0.122
0.056	0.089	0.056	0.096	0.056	0.101	0.056	0.102	0.056	0.111	0.057	0.118
0.065	0.088	0.065	0.095	0.066	0.101	0.065	0.109	0.065	0.112	0.065	0.119
0.076	0.093	0.076	0.094	0.077	0.103	0.076	0.109	0.076	0.110	0.076	0.120
0.089	0.095	0.089	0.094	0.089	0.105	0.089	0.105	0.089	0.114	0.089	0.123
0.104	0.093	0.104	0.097	0.105	0.104	0.104	0.107	0.104	0.114	0.104	0.124
0.122	0.095	0.122	0.097	0.122	0.106	0.122	0.110	0.122	0.116	0.122	0.128
0.143	0.096	0.143	0.100	0.142	0.106	0.142	0.112	0.143	0.120	0.142	0.133
0.166	0.095	0.167	0.100	0.166	0.109	0.165	0.114	0.166	0.122	0.167	0.136
0.194	0.097	0.194	0.101	0.194	0.112	0.195	0.117	0.194	0.127	0.195	0.143
0.227	0.100	0.227	0.105	0.227	0.114	0.227	0.121	0.227	0.131	0.228	0.148
0.265	0.104	0.266	0.107	0.265	0.118	0.265	0.126	0.266	0.137	0.266	0.156
0.310	0.106	0.310	0.110	0.309	0.122	0.309	0.131	0.310	0.144	0.310	0.165
0.363	0.108	0.362	0.114	0.362	0.124	0.362	0.136	0.363	0.152	0.363	0.175
0.423	0.112	0.423	0.117	0.423	0.130	0.423	0.142	0.423	0.159	0.423	0.185
0.495	0.114	0.494	0.121	0.494	0.136	0.494	0.149	0.494	0.167	0.495	0.196
0.578	0.118	0.577	0.125	0.577	0.141	0.577	0.155	0.577	0.175	0.579	0.207
0.673	0.122	0.674	0.130	0.674	0.146	0.675	0.162	0.675	0.184	0.675	0.218
0.788	0.126	0.787	0.134	0.787	0.152	0.787	0.169	0.788	0.192	0.789	0.229
0.921	0.129	0.919	0.138	0.920	0.157	0.919	0.175	0.920	0.200	0.922	0.239
1.074	0.132	1.074	0.142	1.074	0.163	1.074	0.182	1.075	0.208	1.072	0.248
1.255	0.136	1.255	0.146	1.254	0.168	1.255	0.188	1.255	0.215	1.256	0.257
1.466	0.139	1.466	0.151	1.466	0.174	1.466	0.194	1.466	0.221	1.468	0.265
1.713	0.142	1.712	0.154	1.712	0.178	1.712	0.199	1.712	0.227	1.711	0.272
1.998	0.144	1.998	0.158	1.997	0.183	2.000	0.204	1.999	0.232	1.993	0.280
2.330	0.148	2.329	0.163	2.328	0.188	2.328	0.210	2.335	0.237	2.328	0.283
2.721	0.149	2.712	0.165	2.724	0.189	2.719	0.213	2.725	0.240	2.723	0.286
3.178	0.151	3.177	0.167	3.181	0.193	3.177	0.215	3.181	0.243	3.176	0.287
3.713	0.152	3.708	0.168	3.711	0.195	3.705	0.216	3.715	0.244	3.708	0.288
4.336	0.154	4.336	0.169	4.336	0.196	4.331	0.217	4.331	0.244	4.336	0.287
5.060	0.155	5.065	0.170	5.065	0.197	5.060	0.217	5.061	0.243	5.065	0.285
5.910	0.155	5.911	0.171	5.915	0.198	5.915	0.216	5.915	0.241	5.911	0.283
6.904	0.155	6.906	0.170	6.906	0.197	6.905	0.215	6.905	0.239	6.906	0.279
8.066	0.155	8.064	0.169	8.067	0.195	8.064	0.212	8.064	0.234	8.064	0.274
9.420	0.154	9.420	0.167	9.418	0.192	9.421	0.208	9.422	0.230	9.422	0.267

Table D30 Loss factor (tanδ) as a function of test strain at 60°C of the vulcanizates filled with various silica/CB hybrid ratios: (f) ESBR1723_CSi

ESBR1723											
CSi100/CB0		CSi80/CB20		CSi60/CB40		CSi40/CB60		CSi20/CB80		Silica0/CB100	
Strain (%)	Tan δ	Strain (%)	Tan δ	Strain (%)	Tan δ	Strain (%)	Tan δ	Strain (%)	Tan δ	Strain (%)	Tan δ
0.030	0.091	0.030	0.093	0.030	0.108	0.030	0.102	0.030	0.110	0.030	0.118
0.035	0.087	0.035	0.088	0.035	0.099	0.035	0.104	0.035	0.108	0.035	0.118
0.041	0.091	0.041	0.096	0.042	0.102	0.041	0.102	0.042	0.110	0.040	0.112
0.048	0.091	0.048	0.100	0.048	0.098	0.048	0.107	0.048	0.116	0.048	0.122
0.056	0.091	0.056	0.092	0.055	0.099	0.057	0.109	0.055	0.118	0.057	0.118
0.065	0.090	0.065	0.095	0.066	0.100	0.065	0.107	0.066	0.112	0.065	0.119
0.076	0.090	0.076	0.096	0.076	0.100	0.076	0.105	0.076	0.114	0.076	0.120
0.089	0.091	0.089	0.093	0.089	0.103	0.089	0.105	0.089	0.118	0.089	0.123
0.104	0.091	0.104	0.097	0.104	0.103	0.104	0.109	0.105	0.118	0.104	0.124
0.122	0.093	0.122	0.097	0.122	0.106	0.122	0.110	0.122	0.119	0.122	0.128
0.142	0.093	0.142	0.100	0.142	0.107	0.142	0.111	0.143	0.121	0.142	0.133
0.166	0.094	0.166	0.101	0.166	0.108	0.166	0.115	0.166	0.125	0.167	0.136
0.194	0.096	0.194	0.102	0.194	0.111	0.195	0.118	0.194	0.129	0.195	0.143
0.226	0.096	0.227	0.104	0.227	0.114	0.227	0.121	0.227	0.132	0.228	0.148
0.265	0.099	0.265	0.106	0.265	0.118	0.265	0.125	0.265	0.138	0.266	0.156
0.309	0.101	0.310	0.110	0.310	0.122	0.310	0.131	0.309	0.144	0.310	0.165
0.361	0.104	0.362	0.113	0.362	0.126	0.362	0.135	0.362	0.150	0.363	0.175
0.422	0.107	0.423	0.116	0.423	0.131	0.422	0.141	0.424	0.158	0.423	0.185
0.494	0.110	0.494	0.121	0.494	0.136	0.493	0.148	0.495	0.167	0.495	0.196
0.576	0.113	0.576	0.125	0.577	0.141	0.576	0.154	0.577	0.175	0.579	0.207
0.673	0.117	0.673	0.129	0.673	0.147	0.673	0.160	0.674	0.183	0.675	0.218
0.787	0.121	0.786	0.133	0.787	0.153	0.787	0.167	0.787	0.191	0.789	0.229
0.919	0.124	0.919	0.138	0.919	0.158	0.919	0.174	0.920	0.199	0.922	0.239
1.074	0.128	1.073	0.142	1.073	0.164	1.074	0.180	1.075	0.207	1.072	0.248
1.254	0.131	1.253	0.147	1.253	0.169	1.254	0.186	1.255	0.213	1.256	0.257
1.465	0.135	1.463	0.151	1.465	0.174	1.465	0.192	1.461	0.219	1.468	0.265
1.710	0.138	1.711	0.154	1.712	0.178	1.710	0.197	1.710	0.226	1.711	0.272
2.000	0.141	1.997	0.158	1.998	0.183	1.997	0.202	1.999	0.231	1.993	0.280
2.333	0.144	2.334	0.161	2.328	0.188	2.328	0.208	2.333	0.235	2.328	0.283
2.725	0.147	2.722	0.166	2.719	0.191	2.724	0.210	2.725	0.238	2.723	0.286
3.181	0.151	3.176	0.167	3.177	0.191	3.176	0.214	3.176	0.242	3.176	0.287
3.715	0.152	3.711	0.169	3.715	0.195	3.711	0.215	3.711	0.243	3.708	0.288
4.332	0.154	4.336	0.170	4.332	0.196	4.335	0.216	4.331	0.243	4.336	0.287
5.060	0.154	5.060	0.171	5.060	0.196	5.060	0.217	5.064	0.242	5.065	0.285
5.911	0.155	5.911	0.171	5.911	0.195	5.915	0.215	5.915	0.241	5.911	0.283
6.905	0.156	6.905	0.171	6.906	0.194	6.905	0.214	6.905	0.238	6.906	0.279
8.064	0.155	8.063	0.169	8.063	0.191	8.063	0.211	8.064	0.234	8.064	0.274
9.418	0.155	9.417	0.167	9.421	0.188	9.420	0.207	9.421	0.229	9.422	0.267

Table D31 Loss factor (tanδ) as a function of test temperature of the vulcanizates filled with different filler and oil loading

F1		F2		F3		F4	
Temp. (^{O}C)	Tan δ	Temp. (^{O}C)	Tan δ	Temp. (^{O}C)	Tan δ	Temp. (^{O}C)	Tan δ
-59.5	0.089	-59.6	0.095	-59.6	0.087	-59.5	0.095
-59.3	0.087	-59.2	0.094	-59.3	0.086	-59.3	0.092
-56.5	0.087	-56.6	0.094	-56.5	0.085	-56.3	0.092
-54.4	0.087	-54.6	0.094	-54.4	0.085	-54.5	0.092
-52.5	0.087	-52.6	0.094	-52.6	0.086	-52.7	0.092
-50.7	0.088	-50.6	0.095	-50.6	0.087	-50.6	0.092
-48.7	0.088	-48.6	0.096	-48.5	0.088	-48.6	0.093
-46.7	0.090	-46.6	0.097	-46.5	0.090	-46.6	0.094
-44.6	0.092	-44.6	0.099	-44.6	0.092	-44.5	0.096
-42.6	0.095	-42.5	0.102	-42.6	0.096	-42.5	0.100
-40.5	0.098	-40.3	0.107	-40.5	0.102	-40.4	0.107
-38.5	0.103	-38.5	0.114	-38.5	0.110	-38.4	0.117
-36.4	0.112	-36.5	0.125	-36.5	0.122	-36.4	0.131
-34.4	0.124	-34.5	0.140	-34.4	0.141	-34.3	0.153
-32.3	0.141	-32.3	0.165	-32.3	0.171	-32.1	0.188
-30.3	0.169	-30.3	0.201	-30.3	0.209	-30.3	0.231
-28.2	0.209	-28.5	0.250	-28.5	0.260	-28.5	0.284
-26.5	0.257	-25.4	0.361	-25.3	0.359	-26.6	0.323
-23.3	0.372	-23.5	0.407	-23.5	0.433	-24.2	0.419
-21.5	0.430	-21.7	0.534	-22.6	0.510	-21.4	0.582
-19.3	0.624	-20.7	0.601	-19.9	0.660	-20.5	0.633
-18.4	0.685	-17.5	0.790	-18.7	0.724	-18.8	0.709
-16.8	0.784	-16.6	0.833	-16.8	0.802	-16.7	0.771
-14.8	0.880	-14.8	0.885	-14.7	0.845	-14.8	0.794
-12.8	0.926	-12.8	0.895	-12.8	0.840	-12.7	0.774
-10.8	0.914	-10.8	0.858	-10.8	0.797	-10.8	0.725
-8.8	0.860	-8.8	0.793	-8.8	0.733	-8.8	0.665
-6.7	0.785	-6.8	0.719	-6.8	0.665	-6.8	0.602
-4.8	0.707	-4.8	0.649	-4.8	0.601	-4.7	0.544
-2.7	0.635	-2.7	0.586	-2.8	0.544	-2.8	0.495
-0.8	0.569	-0.8	0.532	-0.7	0.492	-0.8	0.450
2.5	0.505	2.5	0.478	2.5	0.444	2.6	0.407
2.6	0.495	2.9	0.465	2.8	0.430	2.7	0.393
5.2	0.435	5.2	0.417	5.2	0.391	5.2	0.362
7.0	0.398	7.3	0.380	7.3	0.362	7.3	0.338

Table D31 Loss factor (tanδ) as a function of test temperature of the vulcanizates filled with different filler and oil loading (cont.)

F1		F2		F3		F4	
Temp. (^{O}C)	Tan δ	Temp. (^{O}C)	Tan δ	Temp. (^{O}C)	Tan δ	Temp. (^{O}C)	Tan δ
9.3	0.363	9.3	0.352	9.2	0.337	9.2	0.317
11.4	0.334	11.2	0.329	11.3	0.315	11.3	0.299
13.3	0.312	13.2	0.307	13.3	0.298	13.2	0.284
15.1	0.295	15.3	0.288	15.2	0.283	15.2	0.272
17.3	0.275	17.2	0.273	17.3	0.270	17.3	0.263
19.2	0.259	19.2	0.260	19.1	0.257	19.3	0.251
21.2	0.244	21.2	0.248	21.3	0.248	21.2	0.244
23.3	0.230	23.3	0.233	23.3	0.237	23.3	0.235
25.2	0.220	25.2	0.225	25.2	0.230	25.3	0.229
27.2	0.210	27.2	0.216	27.2	0.221	27.3	0.222
29.3	0.202	29.2	0.209	29.2	0.215	29.2	0.218
31.2	0.194	31.3	0.203	31.4	0.209	31.1	0.212
33.3	0.190	33.2	0.194	33.2	0.201	33.2	0.209
35.3	0.181	35.2	0.189	35.3	0.197	35.2	0.204
37.3	0.177	37.4	0.183	37.3	0.193	37.2	0.198
39.3	0.169	39.1	0.180	39.4	0.187	39.2	0.194
41.2	0.162	41.2	0.173	41.2	0.180	41.4	0.188
43.3	0.155	43.4	0.167	43.3	0.174	43.3	0.184
45.2	0.149	45.1	0.162	45.2	0.167	45.2	0.178
47.1	0.144	47.3	0.154	47.3	0.162	47.3	0.171
49.3	0.140	49.1	0.151	49.1	0.157	49.2	0.164
51.1	0.132	51.3	0.145	51.3	0.152	51.3	0.162
53.4	0.128	53.2	0.141	53.2	0.146	53.2	0.156
55.2	0.126	55.1	0.133	55.3	0.145	55.2	0.151
57.3	0.118	57.2	0.130	57.2	0.140	57.1	0.148
59.1	0.116	59.2	0.129	59.3	0.134	59.3	0.142
61.4	0.112	61.2	0.121	61.2	0.129	61.3	0.139
63.2	0.109	63.1	0.117	63.2	0.126	63.2	0.135
65.3	0.108	65.3	0.115	65.3	0.122	65.3	0.133
67.3	0.105	67.2	0.115	67.3	0.120	67.2	0.129
69.2	0.101	69.2	0.111	69.2	0.120	69.3	0.128
71.3	0.097	71.3	0.107	71.3	0.116	71.2	0.122
73.3	0.100	73.3	0.106	73.3	0.108	73.1	0.122
75.2	0.094	75.1	0.102	75.2	0.108	75.4	0.116
77.0	0.092	77.3	0.102	77.3	0.110	77.2	0.115
79.3	0.092	79.4	0.097	79.2	0.103	79.3	0.116

Table D32 Loss factor (tanδ) as a function of test strain at 0°C of the vulcanizates filled with different filler and oil loading

F1		F2		F3		F4	
Strain (%)	**Tan δ**	**Strain (%)**	**Tan δ**	**Strain (%)**	**Tan δ**	**Strain (%)**	**Tan δ**
0.030	0.413	0.030	0.372	0.030	0.354	0.030	0.325
0.035	0.416	0.035	0.372	0.035	0.353	0.036	0.322
0.041	0.416	0.041	0.376	0.041	0.356	0.041	0.326
0.048	0.418	0.048	0.379	0.049	0.355	0.048	0.326
0.056	0.420	0.056	0.380	0.056	0.356	0.056	0.328
0.065	0.421	0.065	0.383	0.065	0.358	0.065	0.329
0.077	0.426	0.076	0.386	0.077	0.361	0.076	0.332
0.089	0.429	0.089	0.390	0.089	0.364	0.089	0.336
0.104	0.434	0.105	0.395	0.104	0.367	0.104	0.339
0.122	0.439	0.122	0.401	0.122	0.372	0.122	0.344
0.143	0.445	0.142	0.408	0.142	0.379	0.143	0.351
0.166	0.453	0.166	0.415	0.167	0.386	0.167	0.359
0.195	0.460	0.195	0.425	0.195	0.395	0.195	0.370
0.227	0.470	0.227	0.435	0.228	0.407	0.228	0.382
0.266	0.480	0.266	0.448	0.266	0.420	0.267	0.397
0.311	0.493	0.311	0.462	0.310	0.436	0.312	0.415
0.363	0.507	0.363	0.478	0.364	0.454	0.365	0.434
0.424	0.523	0.425	0.496	0.425	0.473	0.426	0.456
0.496	0.540	0.497	0.515	0.497	0.495	0.498	0.479
0.580	0.558	0.580	0.535	0.581	0.518	0.579	0.504
0.677	0.577	0.678	0.556	0.676	0.541	0.677	0.530
0.788	0.595	0.792	0.578	0.784	0.570	0.786	0.561
0.924	0.615	0.918	0.603	0.919	0.593	0.923	0.583
1.072	0.636	1.076	0.621	1.078	0.613	1.079	0.609
1.257	0.652	1.258	0.642	1.259	0.635	1.254	0.638
1.469	0.669	1.464	0.663	1.464	0.660	1.461	0.661
1.706	0.682	1.710	0.679	1.706	0.677	1.706	0.681
1.998	0.694	1.998	0.692	1.993	0.691	1.999	0.698
2.329	0.697	2.334	0.702	2.335	0.704	2.329	0.710
2.721	0.698	2.720	0.704	2.721	0.709	2.721	0.718
3.179	0.695	3.178	0.704	3.179	0.710	3.179	0.720
3.714	0.686	3.713	0.698	3.714	0.705	3.714	0.717
4.334	0.667	4.338	0.687	4.334	0.691	4.334	0.704
5.062	0.646	5.062	0.666	5.062	0.674	5.062	0.688
5.913	0.620	5.913	0.643	5.913	0.653	5.914	0.666
6.906	0.590	6.905	0.616	6.906	0.626	6.906	0.641
8.066	0.557	8.066	0.585	8.066	0.596	8.067	0.612
9.423	0.522	9.422	0.551	9.421	0.564	9.424	0.580

Table D33 Loss factor (tanδ) as a function of test strain at 60°C of the vulcanizates filled with different filler and oil loading

F1		F2		F3		F4	
Strain (%)	**Tan δ**	**Strain (%)**	**Tan δ**	**Strain (%)**	**Tan δ**	**Strain (%)**	**Tan δ**
0.030	0.086	0.030	0.086	0.030	0.097	0.030	0.095
0.035	0.082	0.036	0.092	0.035	0.100	0.035	0.104
0.041	0.083	0.041	0.089	0.041	0.099	0.041	0.101
0.048	0.080	0.047	0.089	0.048	0.097	0.048	0.099
0.056	0.088	0.056	0.093	0.056	0.096	0.056	0.102
0.065	0.088	0.066	0.096	0.066	0.099	0.066	0.103
0.076	0.087	0.076	0.092	0.076	0.097	0.076	0.105
0.089	0.091	0.089	0.095	0.089	0.100	0.089	0.105
0.104	0.092	0.104	0.093	0.104	0.100	0.104	0.109
0.122	0.088	0.120	0.096	0.122	0.104	0.122	0.110
0.142	0.093	0.142	0.097	0.143	0.104	0.142	0.111
0.165	0.095	0.166	0.100	0.166	0.108	0.166	0.115
0.194	0.097	0.194	0.102	0.194	0.110	0.194	0.119
0.227	0.099	0.227	0.104	0.227	0.114	0.227	0.123
0.265	0.102	0.265	0.108	0.265	0.119	0.265	0.129
0.309	0.105	0.309	0.113	0.309	0.125	0.310	0.136
0.360	0.109	0.362	0.116	0.362	0.129	0.360	0.142
0.422	0.113	0.422	0.122	0.423	0.135	0.423	0.149
0.493	0.118	0.493	0.128	0.492	0.140	0.494	0.156
0.575	0.123	0.576	0.133	0.577	0.147	0.577	0.164
0.673	0.128	0.673	0.138	0.673	0.154	0.675	0.171
0.786	0.134	0.786	0.144	0.786	0.160	0.787	0.179
0.918	0.139	0.918	0.149	0.919	0.167	0.919	0.187
1.072	0.144	1.073	0.155	1.073	0.173	1.074	0.193
1.252	0.149	1.253	0.159	1.253	0.178	1.255	0.200
1.462	0.154	1.464	0.164	1.464	0.184	1.464	0.205
1.709	0.158	1.710	0.168	1.709	0.189	1.711	0.210
1.996	0.162	1.995	0.172	1.990	0.193	1.997	0.215
2.333	0.166	2.330	0.175	2.334	0.196	2.332	0.219
2.725	0.169	2.724	0.178	2.724	0.199	2.720	0.224
3.176	0.172	3.182	0.180	3.182	0.202	3.181	0.223
3.714	0.172	3.708	0.183	3.714	0.204	3.714	0.227
4.334	0.175	4.331	0.185	4.335	0.205	4.335	0.227
5.059	0.176	5.059	0.186	5.060	0.207	5.065	0.228
5.909	0.176	5.909	0.186	5.911	0.207	5.910	0.229
6.906	0.177	6.902	0.187	6.906	0.207	6.902	0.229
8.060	0.176	8.063	0.187	8.064	0.207	8.060	0.228
9.418	0.175	9.420	0.186	9.418	0.206	9.422	0.226

Table D34 Loss factor (tanδ) as a function of test temperature of the vulcanizates having different relative amount of curatives

CV_100%		CV_120%		CV_140%		semi-EV_100%		semi-EV_120%		semi-EV_140%	
Temp. (^{O}C)	Tan δ	Temp. (^{O}C)	Tan δ	Temp. (^{O}C)	Tan δ	Temp. (^{O}C)	Tan δ	Temp. (^{O}C)	Tan δ	Temp. (^{O}C)	Tan δ
-59.8	0.109	-59.8	0.094	-59.8	0.100	-59.9	0.083	-59.7	0.105	-59.8	0.092
-58.7	0.107	-58.9	0.094	-59.0	0.100	-58.9	0.080	-59.2	0.104	-58.7	0.095
-56.5	0.108	-56.7	0.093	-56.5	0.100	-56.4	0.080	-56.4	0.104	-56.5	0.096
-54.6	0.108	-54.7	0.093	-54.5	0.099	-54.6	0.080	-54.7	0.104	-54.6	0.096
-52.7	0.108	-52.7	0.094	-52.6	0.099	-52.7	0.080	-52.6	0.104	-52.7	0.096
-50.7	0.108	-50.6	0.093	-50.7	0.100	-50.6	0.081	-50.7	0.105	-50.6	0.096
-48.6	0.108	-48.6	0.093	-48.7	0.100	-48.7	0.082	-48.7	0.105	-48.7	0.097
-46.8	0.108	-46.6	0.093	-46.6	0.101	-46.8	0.083	-46.6	0.106	-46.7	0.098
-44.7	0.108	-44.5	0.093	-44.7	0.100	-44.8	0.090	-44.5	0.106	-44.7	0.098
-42.7	0.109	-42.7	0.093	-42.7	0.101	-42.6	0.091	-42.5	0.108	-42.7	0.100
-40.5	0.110	-40.6	0.096	-40.5	0.102	-40.6	0.095	-40.4	0.112	-40.5	0.103
-38.5	0.113	-38.7	0.096	-38.6	0.105	-38.5	0.101	-38.4	0.116	-38.4	0.109
-36.6	0.118	-36.5	0.101	-36.7	0.108	-36.4	0.110	-36.4	0.124	-36.5	0.115
-34.5	0.127	-34.6	0.108	-34.5	0.117	-34.4	0.124	-34.4	0.139	-34.4	0.127
-32.5	0.140	-32.5	0.119	-32.4	0.126	-32.3	0.145	-32.1	0.165	-32.3	0.148
-30.2	0.166	-30.5	0.137	-30.3	0.143	-30.4	0.182	-30.2	0.199	-30.3	0.180
-28.5	0.199	-28.4	0.172	-28.2	0.172	-28.4	0.241	-28.4	0.254	-28.5	0.224
-26.1	0.268	-26.5	0.216	-26.5	0.208	-25.3	0.356	-26.0	0.313	-26.1	0.292
-24.2	0.319	-23.7	0.333	-24.5	0.265	-23.1	0.484	-23.4	0.438	-23.4	0.401
-21.3	0.467	-21.4	0.416	-22.2	0.364	-21.9	0.566	-21.2	0.581	-21.3	0.534
-20.4	0.524	-20.5	0.464	-19.4	0.459	-20.7	0.638	-20.3	0.648	-20.5	0.598
-18.8	0.628	-18.7	0.573	-18.1	0.551	-18.3	0.791	-18.8	0.741	-18.4	0.728
-16.8	0.756	-16.4	0.734	-16.7	0.630	-16.9	0.859	-16.7	0.849	-16.9	0.812
-14.8	0.858	-14.8	0.819	-14.3	0.770	-14.7	0.903	-14.7	0.909	-14.7	0.889
-12.8	0.905	-12.7	0.892	-12.8	0.838	-12.7	0.891	-12.9	0.913	-12.8	0.907
-10.8	0.902	-10.8	0.907	-10.8	0.881	-10.8	0.838	-10.8	0.868	-10.8	0.875
-8.8	0.853	-8.8	0.874	-8.8	0.871	-8.8	0.768	-8.7	0.799	-8.8	0.816
-6.8	0.782	-6.8	0.811	-6.8	0.822	-6.7	0.694	-6.8	0.722	-6.8	0.742
-4.8	0.709	-4.8	0.739	-4.8	0.757	-4.7	0.626	-4.8	0.649	-4.8	0.669
-2.7	0.637	-2.7	0.667	-2.7	0.678	-2.7	0.561	-2.7	0.583	-2.8	0.600
-0.8	0.574	-0.9	0.601	-0.8	0.615	-0.9	0.508	-0.8	0.527	-0.8	0.540
2.5	0.516	1.9	0.542	2.6	0.549	2.5	0.454	2.5	0.472	2.4	0.484
3.0	0.507	3.0	0.511	3.0	0.540	2.8	0.444	2.8	0.460	2.7	0.475
5.2	0.450	5.2	0.466	5.1	0.473	5.1	0.394	5.2	0.406	5.2	0.418
7.1	0.403	6.9	0.423	7.2	0.427	7.0	0.361	6.9	0.375	7.3	0.380

Table D34 Loss factor (tanδ) as a function of test temperature of the vulcanizates having different relative amount of curatives (cont.)

CV_100%		CV_120%		CV_140%		semi-EV_100%		semi-EV_120%		semi-EV_140%	
Temp. (^{O}C)	Tan δ	Temp. (^{O}C)	Tan δ	Temp. (^{O}C)	Tan δ	Temp. (^{O}C)	Tan δ	Temp. (^{O}C)	Tan δ	Temp. (^{O}C)	Tan δ
9.3	0.367	9.3	0.387	9.3	0.389	9.3	0.329	9.3	0.342	9.2	0.352
11.3	0.342	11.2	0.360	11.2	0.356	11.3	0.307	11.3	0.320	11.7	0.318
13.2	0.317	13.2	0.332	13.3	0.326	13.4	0.289	13.8	0.294	13.3	0.303
15.2	0.297	15.2	0.309	15.3	0.300	15.3	0.272	15.1	0.283	15.3	0.283
17.2	0.279	18.5	0.274	17.1	0.280	17.2	0.263	17.2	0.268	17.3	0.268
19.4	0.264	19.3	0.268	19.2	0.265	19.2	0.250	19.3	0.254	19.3	0.255
21.3	0.252	21.6	0.247	21.3	0.247	21.3	0.238	21.2	0.242	21.2	0.242
24.7	0.223	23.4	0.236	23.3	0.231	23.3	0.227	23.3	0.232	23.3	0.234
26.7	0.219	25.3	0.224	25.2	0.220	25.3	0.219	25.3	0.222	25.6	0.220
27.6	0.216	27.2	0.212	27.2	0.207	27.2	0.211	27.3	0.212	27.2	0.213
29.3	0.210	30.0	0.195	29.2	0.197	29.1	0.205	29.2	0.205	29.3	0.205
32.6	0.194	32.0	0.187	31.2	0.193	31.2	0.198	31.3	0.198	32.2	0.192
34.7	0.184	33.7	0.182	33.3	0.186	33.4	0.192	33.2	0.192	33.2	0.191
36.7	0.179	35.2	0.179	35.3	0.179	35.2	0.189	35.3	0.186	36.5	0.177
38.9	0.172	37.3	0.172	37.2	0.173	37.2	0.184	37.3	0.181	37.8	0.172
39.7	0.169	39.1	0.167	39.3	0.167	39.3	0.180	39.2	0.173	39.2	0.176
41.3	0.171	41.3	0.162	42.5	0.155	41.2	0.172	41.2	0.169	42.5	0.160
44.6	0.158	43.1	0.155	43.7	0.149	43.2	0.171	43.2	0.165	43.7	0.158
45.4	0.160	45.3	0.147	45.2	0.149	45.2	0.164	45.2	0.160	45.2	0.157
48.4	0.145	47.2	0.141	47.2	0.143	47.3	0.160	47.2	0.156	47.1	0.154
49.3	0.147	49.3	0.135	49.3	0.135	49.6	0.150	49.4	0.149	49.6	0.143
49.3	0.145	51.2	0.132	51.2	0.130	51.3	0.149	51.2	0.144	51.3	0.142
53.1	0.139	53.2	0.125	54.6	0.120	53.2	0.147	53.2	0.140	53.1	0.136
55.2	0.131	55.1	0.122	56.1	0.112	55.2	0.143	55.3	0.134	55.2	0.129
57.3	0.126	57.3	0.115	57.1	0.111	57.1	0.140	57.1	0.132	57.3	0.124
59.2	0.126	59.3	0.115	59.2	0.111	59.4	0.140	59.2	0.131	59.1	0.123
61.2	0.118	61.1	0.108	61.3	0.104	62.4	0.130	61.2	0.126	61.3	0.120
63.3	0.118	63.2	0.103	63.2	0.101	63.2	0.133	63.2	0.122	64.5	0.116
65.2	0.114	65.1	0.101	65.1	0.098	65.2	0.129	65.3	0.120	65.4	0.116
67.2	0.109	67.3	0.101	67.3	0.097	67.2	0.128	67.3	0.117	67.2	0.113
69.2	0.110	69.2	0.097	69.2	0.091	69.4	0.124	69.1	0.117	69.2	0.111
71.2	0.103	71.2	0.097	71.2	0.089	71.2	0.127	71.3	0.116	71.8	0.105
73.1	0.102	73.2	0.093	73.3	0.090	73.2	0.124	73.3	0.111	73.3	0.109
75.1	0.102	75.3	0.093	76.5	0.082	75.3	0.124	75.3	0.111	75.3	0.103
77.3	0.101	77.4	0.088	77.4	0.085	77.3	0.122	77.3	0.105	78.6	0.085
79.3	0.099	79.1	0.086	79.2	0.082	79.4	0.122	79.3	0.102	80.0	0.100

Table D35 Loss factor (tanδ) as a function of test strain at 0°C of the vulcanizates having different relative amount of curatives

CV_100%		CV_120%		CV_140%		semi-EV_100%		semi-EV_120%		semi-EV_140%	
Strain (%)	Tan δ	Strain (%)	Tan δ	Strain (%)	Tan δ	Strain (%)	Tan δ	Strain (%)	Tan δ	Strain (%)	Tan δ
0.029	0.429	0.030	0.442	0.030	0.485	0.040	0.386	0.032	0.394	0.029	0.407
0.032	0.420	0.036	0.444	0.035	0.485	0.035	0.386	0.036	0.396	0.038	0.411
0.041	0.423	0.040	0.446	0.040	0.486	0.065	0.400	0.041	0.404	0.043	0.408
0.049	0.424	0.048	0.447	0.049	0.487	0.043	0.386	0.048	0.403	0.045	0.407
0.057	0.428	0.056	0.448	0.055	0.488	0.068	0.403	0.055	0.402	0.059	0.409
0.064	0.427	0.066	0.449	0.066	0.490	0.079	0.403	0.066	0.406	0.063	0.411
0.077	0.432	0.075	0.451	0.076	0.493	0.095	0.406	0.077	0.407	0.080	0.416
0.088	0.434	0.089	0.457	0.088	0.495	0.111	0.405	0.090	0.410	0.089	0.418
0.104	0.435	0.104	0.460	0.105	0.498	0.128	0.408	0.103	0.411	0.103	0.420
0.122	0.443	0.122	0.465	0.123	0.501	0.142	0.412	0.122	0.415	0.123	0.424
0.142	0.448	0.143	0.470	0.143	0.506	0.165	0.415	0.141	0.420	0.143	0.431
0.167	0.455	0.166	0.476	0.165	0.513	0.194	0.421	0.166	0.426	0.166	0.436
0.194	0.462	0.195	0.485	0.195	0.521	0.229	0.429	0.195	0.435	0.195	0.444
0.227	0.471	0.228	0.494	0.228	0.530	0.267	0.438	0.228	0.443	0.227	0.452
0.267	0.482	0.267	0.504	0.266	0.540	0.312	0.448	0.266	0.453	0.265	0.463
0.310	0.493	0.309	0.517	0.310	0.552	0.365	0.461	0.309	0.465	0.309	0.474
0.363	0.507	0.363	0.531	0.363	0.565	0.424	0.474	0.361	0.478	0.362	0.488
0.423	0.523	0.423	0.546	0.425	0.581	0.496	0.489	0.423	0.493	0.424	0.503
0.496	0.539	0.496	0.563	0.496	0.597	0.579	0.505	0.495	0.509	0.497	0.519
0.580	0.557	0.579	0.581	0.579	0.616	0.677	0.521	0.577	0.525	0.577	0.535
0.677	0.574	0.676	0.599	0.677	0.635	0.791	0.537	0.677	0.543	0.674	0.553
0.792	0.592	0.791	0.618	0.788	0.654	0.925	0.553	0.790	0.561	0.790	0.571
0.924	0.610	0.924	0.636	0.923	0.673	1.078	0.569	0.922	0.578	0.923	0.589
1.078	0.627	1.072	0.656	1.072	0.693	1.258	0.584	1.078	0.595	1.078	0.607
1.253	0.646	1.253	0.673	1.256	0.709	1.464	0.599	1.255	0.612	1.254	0.624
1.466	0.659	1.460	0.687	1.468	0.726	1.708	0.609	1.461	0.627	1.460	0.641
1.714	0.674	1.709	0.700	1.712	0.740	1.997	0.618	1.712	0.639	1.713	0.654
1.993	0.680	1.998	0.710	1.998	0.749	2.333	0.625	1.993	0.649	1.989	0.666
2.329	0.685	2.329	0.713	2.329	0.751	2.719	0.626	2.328	0.654	2.332	0.673
2.720	0.685	2.721	0.714	2.721	0.750	3.177	0.624	2.720	0.656	2.725	0.677
3.179	0.682	3.179	0.710	3.179	0.744	3.711	0.618	3.177	0.655	3.177	0.672
3.714	0.672	3.714	0.700	3.714	0.732	4.337	0.608	3.712	0.648	3.712	0.665
4.333	0.654	4.334	0.680	4.334	0.710	5.062	0.590	4.338	0.637	4.337	0.653
5.061	0.632	5.062	0.657	5.063	0.685	5.912	0.570	5.061	0.618	5.060	0.632
5.913	0.607	5.913	0.630	5.911	0.656	6.904	0.547	5.911	0.596	5.911	0.610
6.906	0.577	6.906	0.598	6.906	0.621	8.066	0.520	6.905	0.572	6.905	0.584
8.067	0.543	8.066	0.562	8.066	0.581	9.422	0.490	8.066	0.542	8.065	0.553
9.440	0.506	9.421	0.523	9.421	0.539			9.422	0.508	9.423	0.518

Table D36 Loss factor (tanδ) as a function of test strain at 60°C of the vulcanizates having different relative amount of curatives

CV_100%		CV_120%		CV_140%		semi-EV_100%		semi-EV_120%		semi-EV_140%	
Strain (%)	Tan δ	Strain (%)	Tan δ	Strain (%)	Tan δ	Strain (%)	Tan δ	Strain (%)	Tan δ	Strain (%)	Tan δ
0.062	0.089	0.062	0.076	0.060	0.074	0.057	0.107	0.054	0.093	0.056	0.083
0.063	0.091	0.065	0.077	0.063	0.072	0.066	0.105	0.067	0.101	0.066	0.085
0.076	0.092	0.074	0.078	0.076	0.071	0.077	0.103	0.073	0.101	0.077	0.086
0.089	0.093	0.090	0.082	0.091	0.072	0.090	0.105	0.090	0.102	0.089	0.086
0.104	0.095	0.105	0.082	0.102	0.074	0.104	0.104	0.103	0.102	0.104	0.087
0.122	0.096	0.124	0.082	0.124	0.075	0.122	0.104	0.123	0.101	0.122	0.087
0.143	0.096	0.143	0.083	0.143	0.076	0.141	0.107	0.144	0.101	0.143	0.088
0.166	0.096	0.170	0.083	0.165	0.077	0.167	0.110	0.168	0.101	0.165	0.091
0.197	0.100	0.198	0.084	0.194	0.078	0.195	0.114	0.196	0.104	0.193	0.094
0.230	0.100	0.229	0.086	0.227	0.080	0.226	0.113	0.226	0.106	0.226	0.094
0.269	0.104	0.268	0.089	0.266	0.082	0.264	0.118	0.267	0.106	0.265	0.098
0.306	0.106	0.312	0.092	0.308	0.085	0.308	0.120	0.310	0.110	0.309	0.101
0.362	0.109	0.366	0.095	0.364	0.087	0.361	0.124	0.360	0.113	0.362	0.104
0.424	0.113	0.424	0.098	0.420	0.090	0.420	0.128	0.419	0.118	0.422	0.108
0.493	0.119	0.496	0.102	0.493	0.093	0.493	0.133	0.492	0.120	0.492	0.112
0.574	0.122	0.577	0.105	0.577	0.096	0.576	0.138	0.575	0.125	0.576	0.118
0.674	0.127	0.676	0.110	0.672	0.101	0.673	0.142	0.671	0.129	0.672	0.122
0.788	0.133	0.785	0.114	0.786	0.104	0.781	0.147	0.783	0.134	0.786	0.127
0.920	0.137	0.919	0.118	0.918	0.108	0.918	0.151	0.916	0.138	0.917	0.131
1.074	0.141	1.075	0.122	1.073	0.112	1.070	0.156	1.070	0.142	1.072	0.136
1.256	0.146	1.254	0.125	1.255	0.116	1.252	0.160	1.248	0.147	1.252	0.140
1.466	0.150	1.463	0.129	1.464	0.120	1.464	0.164	1.461	0.151	1.465	0.144
1.713	0.153	1.708	0.133	1.712	0.123	1.710	0.167	1.707	0.155	1.712	0.148
1.998	0.155	1.997	0.136	1.999	0.127	1.996	0.170	1.995	0.158	1.998	0.152
2.334	0.158	2.328	0.141	2.330	0.129	2.330	0.173	2.333	0.161	2.331	0.155
2.720	0.161	2.719	0.141	2.725	0.130	2.724	0.175	2.720	0.165	2.724	0.157
3.178	0.163	3.175	0.143	3.177	0.133	3.176	0.178	3.178	0.167	3.181	0.160
3.713	0.164	3.713	0.145	3.709	0.135	3.712	0.179	3.710	0.169	3.709	0.163
4.338	0.165	4.332	0.147	4.336	0.136	4.332	0.181	4.332	0.171	4.336	0.164
5.060	0.166	5.060	0.148	5.060	0.138	5.061	0.181	5.064	0.171	5.065	0.165
5.913	0.165	5.913	0.148	5.913	0.138	5.915	0.181	5.911	0.173	5.914	0.165
6.902	0.165	6.906	0.148	6.902	0.139	6.902	0.182	6.901	0.173	6.908	0.166
8.067	0.163	8.067	0.148	8.062	0.139	8.066	0.181	8.067	0.173	8.067	0.166
9.421	0.161	9.417	0.146	9.417	0.138	9.415	0.180	9.421	0.172	9.419	0.165

Table D37 Loss factor (tanδ) as a function of test strain at 0°C of the vulcanizates prepared from the best PCR tire tread formulation as compared with the tread of commercial PCR tires

The best formulation		Commercial tire A		Commercial tire B		Commercial tire C		Commercial tire D		Commercial tire E	
Strain (%)	Tan δ	Strain (%)	Tan δ	Strain (%)	Tan δ	Strain (%)	Tan δ	Strain (%)	Tan δ	Strain (%)	Tan δ
0.030	0.485	0.030	0.239	0.030	0.193	0.030	0.230	0.030	0.172	0.030	0.134
0.035	0.485	0.035	0.240	0.035	0.198	0.035	0.231	0.035	0.172	0.035	0.133
0.040	0.486	0.041	0.242	0.041	0.196	0.040	0.231	0.041	0.173	0.041	0.134
0.049	0.487	0.048	0.243	0.048	0.197	0.048	0.233	0.049	0.173	0.049	0.134
0.055	0.488	0.056	0.243	0.056	0.198	0.056	0.234	0.056	0.174	0.056	0.136
0.066	0.490	0.065	0.245	0.065	0.198	0.066	0.236	0.065	0.176	0.066	0.138
0.076	0.493	0.076	0.247	0.077	0.198	0.076	0.237	0.077	0.178	0.076	0.140
0.088	0.495	0.090	0.251	0.089	0.201	0.089	0.239	0.089	0.181	0.090	0.143
0.105	0.498	0.104	0.253	0.105	0.203	0.104	0.241	0.105	0.185	0.105	0.146
0.123	0.501	0.122	0.257	0.121	0.205	0.121	0.245	0.122	0.189	0.122	0.151
0.143	0.506	0.142	0.262	0.142	0.209	0.142	0.249	0.143	0.195	0.143	0.157
0.165	0.513	0.167	0.268	0.166	0.213	0.166	0.256	0.167	0.202	0.167	0.164
0.195	0.521	0.195	0.275	0.195	0.218	0.195	0.263	0.196	0.210	0.196	0.173
0.228	0.530	0.228	0.283	0.227	0.224	0.228	0.272	0.229	0.221	0.229	0.183
0.266	0.540	0.267	0.292	0.265	0.231	0.266	0.282	0.268	0.232	0.268	0.196
0.310	0.552	0.311	0.303	0.311	0.239	0.311	0.293	0.313	0.245	0.313	0.210
0.363	0.565	0.363	0.314	0.363	0.248	0.364	0.306	0.365	0.259	0.367	0.225
0.425	0.581	0.425	0.325	0.424	0.258	0.424	0.319	0.428	0.274	0.429	0.242
0.496	0.597	0.497	0.337	0.495	0.268	0.497	0.333	0.501	0.290	0.500	0.259
0.579	0.616	0.580	0.349	0.579	0.279	0.580	0.347	0.576	0.309	0.574	0.284
0.677	0.635	0.678	0.361	0.676	0.290	0.677	0.361	0.678	0.321	0.671	0.301
0.788	0.654	0.791	0.372	0.790	0.301	0.791	0.375	0.792	0.337	0.792	0.312
0.923	0.673	0.924	0.382	0.922	0.311	0.921	0.389	0.925	0.353	0.916	0.336
1.072	0.693	1.079	0.393	1.077	0.321	1.076	0.404	1.070	0.372	1.074	0.350
1.256	0.709	1.254	0.404	1.258	0.331	1.256	0.415	1.253	0.385	1.250	0.367
1.468	0.726	1.467	0.410	1.465	0.339	1.466	0.424	1.460	0.397	1.461	0.380
1.712	0.740	1.710	0.419	1.707	0.349	1.711	0.433	1.707	0.408	1.711	0.389
1.998	0.749	1.995	0.424	1.999	0.353	1.997	0.439	1.993	0.416	1.999	0.398
2.329	0.751	2.327	0.428	2.327	0.360	2.331	0.444	2.329	0.423	2.329	0.406
2.721	0.750	2.718	0.431	2.718	0.363	2.718	0.447	2.721	0.427	2.721	0.410
3.179	0.744	3.182	0.432	3.175	0.365	3.176	0.447	3.178	0.429	3.178	0.412
3.714	0.732	3.711	0.430	3.709	0.365	3.710	0.445	3.713	0.429	3.712	0.411
4.334	0.710	4.334	0.426	4.333	0.363	4.335	0.441	4.338	0.426	4.337	0.408
5.063	0.685	5.063	0.421	5.062	0.359	5.064	0.434	5.062	0.420	5.061	0.404
5.911	0.656	5.911	0.411	5.915	0.353	5.911	0.424	5.914	0.412	5.913	0.398
6.906	0.621	6.906	0.401	6.905	0.345	6.905	0.412	6.909	0.402	6.908	0.390
8.066	0.581	8.065	0.387	8.065	0.335	8.065	0.398	8.069	0.390	8.068	0.381
9.421	0.539	9.421	0.372	9.420	0.323	9.420	0.380	9.425	0.375	9.424	0.370

Table D38 Loss factor (tanδ) as a function of test strain at 60°C of the vulcanizates prepared from the best PCR tire tread formulation as compared with the tread of commercial PCR tires

The best formulation		Commercial tire A		Commercial tire B		Commercial tire C		Commercial tire D		Commercial tire E	
Strain (%)	Tan δ	Strain (%)	Tan δ	Strain (%)	Tan δ	Strain (%)	Tan δ	Strain (%)	Tan δ	Strain (%)	Tan δ
0.030	0.065	0.030	0.103	0.030	0.087	0.030	0.085	0.030	0.115	0.030	0.139
0.034	0.080	0.035	0.100	0.036	0.093	0.035	0.080	0.034	0.118	0.035	0.147
0.041	0.079	0.041	0.103	0.041	0.086	0.041	0.082	0.041	0.120	0.041	0.144
0.048	0.083	0.047	0.099	0.049	0.086	0.049	0.085	0.048	0.118	0.047	0.148
0.060	0.074	0.056	0.107	0.056	0.086	0.056	0.079	0.056	0.120	0.056	0.144
0.063	0.072	0.065	0.104	0.066	0.088	0.065	0.079	0.065	0.122	0.066	0.153
0.076	0.071	0.076	0.107	0.076	0.085	0.077	0.081	0.077	0.122	0.077	0.148
0.091	0.072	0.089	0.108	0.090	0.088	0.089	0.083	0.090	0.123	0.090	0.154
0.102	0.074	0.104	0.107	0.104	0.086	0.104	0.081	0.104	0.126	0.104	0.155
0.124	0.075	0.121	0.109	0.122	0.089	0.122	0.083	0.122	0.128	0.122	0.158
0.143	0.076	0.142	0.110	0.142	0.091	0.142	0.085	0.143	0.131	0.143	0.164
0.165	0.077	0.166	0.111	0.166	0.090	0.163	0.086	0.167	0.135	0.167	0.168
0.194	0.078	0.194	0.112	0.194	0.096	0.194	0.088	0.194	0.140	0.195	0.176
0.227	0.080	0.227	0.116	0.227	0.096	0.227	0.090	0.228	0.145	0.228	0.185
0.266	0.082	0.265	0.119	0.265	0.099	0.265	0.094	0.266	0.153	0.266	0.194
0.308	0.085	0.309	0.124	0.309	0.102	0.310	0.097	0.310	0.159	0.311	0.204
0.364	0.087	0.362	0.127	0.359	0.105	0.362	0.101	0.364	0.168	0.364	0.216
0.420	0.090	0.423	0.132	0.423	0.110	0.423	0.105	0.425	0.176	0.425	0.227
0.493	0.093	0.494	0.135	0.493	0.114	0.493	0.109	0.496	0.185	0.497	0.238
0.577	0.096	0.579	0.140	0.577	0.118	0.576	0.113	0.579	0.193	0.580	0.249
0.672	0.101	0.674	0.144	0.673	0.123	0.673	0.118	0.676	0.202	0.678	0.261
0.786	0.104	0.787	0.148	0.784	0.128	0.786	0.123	0.791	0.210	0.791	0.269
0.918	0.108	0.918	0.152	0.919	0.133	0.919	0.127	0.923	0.219	0.924	0.279
1.073	0.112	1.074	0.155	1.076	0.137	1.073	0.132	1.078	0.225	1.074	0.287
1.255	0.116	1.254	0.158	1.254	0.141	1.253	0.136	1.255	0.232	1.254	0.294
1.464	0.120	1.465	0.162	1.464	0.146	1.463	0.139	1.466	0.238	1.461	0.302
1.712	0.123	1.709	0.164	1.711	0.149	1.711	0.142	1.712	0.243	1.707	0.306
1.999	0.127	1.999	0.166	1.998	0.153	1.996	0.145	1.990	0.249	1.991	0.310
2.330	0.129	2.333	0.168	2.331	0.155	2.332	0.147	2.334	0.249	2.328	0.311
2.725	0.130	2.719	0.170	2.725	0.157	2.724	0.148	2.717	0.252	2.724	0.310
3.177	0.133	3.181	0.171	3.176	0.161	3.177	0.150	3.174	0.252	3.179	0.312
3.709	0.135	3.711	0.171	3.710	0.161	3.711	0.150	3.708	0.251	3.712	0.310
4.336	0.136	4.332	0.171	4.335	0.161	4.331	0.150	4.335	0.250	4.332	0.309
5.060	0.138	5.066	0.171	5.065	0.162	5.065	0.149	5.061	0.248	5.060	0.305
5.913	0.138	5.911	0.172	5.910	0.162	5.910	0.148	5.912	0.245	5.911	0.301
6.902	0.139	6.905	0.172	6.904	0.161	6.905	0.147	6.904	0.240	6.906	0.296
8.062	0.139	8.064	0.171	8.064	0.159	8.064	0.146	8.066	0.235	8.065	0.290
9.417	0.138	9.419	0.170	9.418	0.157	9.418	0.143	9.420	0.229	9.421	0.283

APPENDIX E

PUBLICATION

JOURNAL OF Applied Polymer SCIENCE

Effects of silanization temperature and silica type on properties of silica-filled solution styrene butadiene rubber (SSBR) for passenger car tire tread compounds

Puchong Thaptong,[1,2] Pongdhorn Sae-Oui,[2,3] Chakrit Sirisinha[1,3]
[1]Department of Chemistry, Faculty of Science, Mahidol University, Rama VI Rd, Rajdhevee, Bangkok 10400, Thailand
[2]MTEC, National Science and Technology Development Agency, 114 Thailand Science Park, Paholyothin Rd, Klong 1, Klong-Luang, Pathumthani 12120, Thailand
[3]Rubber Technology Research Centre (RTEC), Faculty of Science, Mahidol University, Phutthamonthon 4 Rd, Salaya, Nakornprathom 73170, Thailand
Correspondence to: C. Sirisinha (E-mail: chakrit.sir@mahidol.ac.th)

ABSTRACT: Influence of silanization temperature on properties of silica-filled solution polymerized styrene butadiene rubber was investigated. Two types of silica, i.e., highly dispersible silica (HDSi) and conventional silica (CSi), were compared. Results show that the increased silanization temperature leads to the enhanced rubber–filler interaction, filler dispersion, and cross-link density giving rise to the improvement in vulcanizate properties such as modulus, heat build-up (HBU), and dynamic set, as well as tire performance, e.g., wet grip (WG), rolling resistance (RR), and abrasion resistance. Great care, however, must be taken to avoid the scorching phenomenon during the mixing process at too high temperature. Taken as a whole, the balanced properties are found at the silanization temperature of 140°C. Surprisingly, HDSi provides insignificant differences in degree of filler dispersion, WG, and RR, compared to CSi, despite its claimed greater dispersability. Probably, the relatively long mixing time used in this experiment may override the influence of silica type. © 2016 Wiley Periodicals, Inc. J. Appl. Polym. Sci. **2016**, *133*, 43342.

KEYWORDS: elastomers; mechanical properties; rubber; synthesis and processing; viscosity and viscoelasticity

Received 17 September 2015; accepted 11 December 2015
DOI: 10.1002/app.43342

INTRODUCTION

Tread is one of the most important parts of tire because it is the outer part of tire that contacts the road surface, and protects the inner casing from road hazards. Apart from tread pattern, tire performance depends strongly on tire tread properties.[1] Generally, tire performance is evaluated based on three main properties namely "the magic triangle", i.e., fuel efficiency related to the rolling resistance (RR),[2] wet grip (WG) corresponding to an efficiency of car control and breaking performance on a wet road,[3] and wear resistance.

Many attempts have been made to investigate the properties of tire tread compounds based on carbon black (CB),[4,5] silica,[4,6–8] CB/silica hybrid filler,[4,9–11] and CB/clay hybrid filler.[12,13] It has been reported that the replacement of CB by silica in passenger car tire tread leads to a significantly reduced RR without sacrificing WG and wear resistance.[14] Unlike CB, silica surfaces are densely covered by silanol groups (-Si-O-H) which can facilitate strong transient filler network formation through intermolecular hydrogen bonding,[15] leading to the difficulty to achieve good filler dispersion. Moreover, because of its hydrophilic nature, silica is less compatible with most rubbers used in the production of tire tread such as natural rubber (NR), styrene butadiene rubber (SBR), and butadiene rubber (BR), leading to negative effect on tire performance. However, after the advent of silane coupling agents (SCAs), silica has become more popular in tire industry. It has been reported that the addition of organosilane, e.g., bis-(3-(triethoxysilyl)-propyl)-tetrasulfide (TESPT), into silica-filled rubber, not only improves silica dispersion but also enhances rubber–silica interaction leading to the improvement in RR and WG.[16] To gain maximum benefit from SCAs, the reaction between silanol groups on silica surfaces and alkoxy groups of SCAs, so-called silanization, must take place sufficiently during the mixing process. Several attempts have been made to investigate the effect of mixing conditions on properties of silica-filled rubber for tire tread compounds.[17–19] However, comparison has not yet been made between conventional silica (CSi) and highly dispersible silica (HDSi), a new generation of silica claimed to be easily dispersible because of its greater branched structure (higher structure) leading to the higher shear force during the mixing process.[20]

It is therefore the intention of this work to compare the effect of silanization temperature on properties of silica-filled solution polymerized styrene butadiene rubber (SSBR) reinforced by CSi and HDSi for passenger car tire tread compounds. Comparison of tire performance between CSi-filled and HDSi-filled tread compounds at various silanization temperatures is also reported.

EXPERIMENTAL

Materials

All mixing ingredients were used as-received. Oil extended SSBR (SOLC6450SL with 54.5 of ML(1 + 4)@100°C, 27.1% of treated distillate aromatic extract (TDAE) content, 34.6% of styrene content and 40.1% of vinyl content) was produced by Kumho Petrochemical, South Korea. HDSi (Zeosil 1165MP with the average primary particle size of 20 nm and BET specific surface area of 153 m^2/g) was manufactured by Rhodia Silica Korea, South Korea. CSi (Tokusil 255), having the average primary particle size of 20 nm and BET specific surface area of 166 m^2/g, was obtained from OSC Siam Silica, Thailand. TESPT (Si-69) was supplied by Innova (Tianjin) Chemical, China. N-(1,3-dimethylbutyl)-N′-phenyl-p-phenylenediamine (6PPD), 2,2,4-trimethyl-1,2-dihydroquinoline (TMQ) and N-tert-butyl-2-benzothiazyl sulfenamide (TBBS) were purchased from Monflex Pte., Singapore. Other chemicals were obtained from suppliers in Thailand. Zinc oxide (ZnO, white seal) was supplied by Thai-Lysaght. Stearic acid was purchased from Kij Paiboon Chemical, Part. Paraffin wax was supplied by Petch Thai Chemical. TDAE oil was obtained from PSP Specialties. Tetrabenzylthiuram disulfide (TBzTD) and sulfur were purchased from Behn Meyer Chemicals (Thailand) and The Siam Chemical Public, respectively.

Preparation and Testing of Rubber Compounds

The formulation employed in this study is given in Table I. Mixing was carried out using a laboratory-sized internal mixer (Brabender Plasticorder 350E, Germany). Fill factor and rotor speed were kept constant at 0.75 and 40 rpm, respectively. Three-step mixing was used in this experiment. In the first step, SSBR was mixed with all ingredients, except for curatives (TBBS, TBzTD and sulfur), at the mixing temperature of 60°C for 10 min to gain satisfactory degree of filler dispersion. The compounds were then sheeted on a two-roll mill (Labtech LRM150, Thailand) and cooled down to the room temperature. In the second step, the so-called silanization step, the compounds were re-mixed at high temperature (the silanization temperature was varied from 120°C to 160°C) for 6 min to promote the silanization reaction between TESPT and silica. Again, the compounds were then sheeted and cooled down to room temperature. In the final step, the compounds were mixed with the curatives at the mixing temperature of 60°C for 3 min. After mixing, the compounds were sheeted and kept overnight at room temperature prior to testing.

Table I. The Compound Formulation (Unit: Parts per Hundred Rubber; phr)

Ingredient	Content (phr)
SSBR	137.5
ZnO	3.0
Stearic acid	2.0
6PPD	1.5
TMQ	1.0
Paraffin wax	2.0
TDAE	10.0
Silica (Zeosil 1165MP or Tokusil 255)	80.0
TESPT (8% w/w of silica)	6.4
TBBS	1.2
TBzTD	0.2
Sulfur	2.2

Measurement of Mooney viscosity (ML(1 + 4)@100°C) was carried out in accordance with ISO 289-1 using a Mooney viscometer (TechPro viscTECH+, USA). Cure characteristics were investigated using a moving die rheometer (MDR, TechPro MD+, USA) at 160°C following ISO 6502. Payne effect was determined by the use of a rubber process analyzer (RPA, Alpha Technologies RPA2000, USA) at frequency of 1.7 Hz and temperature of 100°C. The dynamic strain was varied from 0.56% to 100.02%. The difference between storage moduli at 0.56% and 100.02% (or $\Delta G'$) was used to determine the Payne magnitude of the compounds. Measurement of bound rubber content (BRC) was carried out by extracting the unbound rubber with toluene. Approximately 0.5 g of rubber test piece was extracted by 100 mL of toluene for 168 h at room temperature. After filtering with filter paper, the insoluble part was dried in an oven at 70°C until a constant weight was gained. The BRC was calculated by the following equation:

Table II. Dump Temperature and Temperature Rise of the Compounds

	HDSi		CSi	
Silanization temperature (°C)	Dump temperature (°C)	Temperature rise (°C)	Dump temperature (°C)	Temperature rise (°C)
120	135	15	134	14
130	142	12	142	12
140	147	7	146	6
150	154	4	154	4
160	166	6	165	5

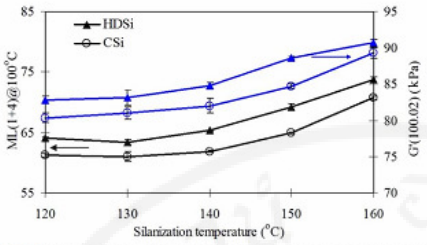

Figure 1. G' at high strain and Mooney viscosity of the compounds. [Color figure can be viewed in the online issue, which is available at wileyonlinelibrary.com.]

$$\text{BRC}\,(\%) = \left[\frac{(W_d - F)}{R}\right] \times 100 \quad (1)$$

where W_d is the weight of dry gel, F is the weight of filler in the test piece, and R is the weight of rubber in the test piece. It is generally accepted that BRC measured at room temperature is formed by both physical and chemical interactions.[21] As physically bound rubber could be destroyed at high temperature,[22] the amount of chemically bound rubber could therefore be determined by the above procedure, except that, the extraction was carried out at 85°C for 36 h. Determination of molecular weight of the rubber matrix was carried out using gel permeation chromatography technique (GPC, WatersTM 150-CV plus, USA).

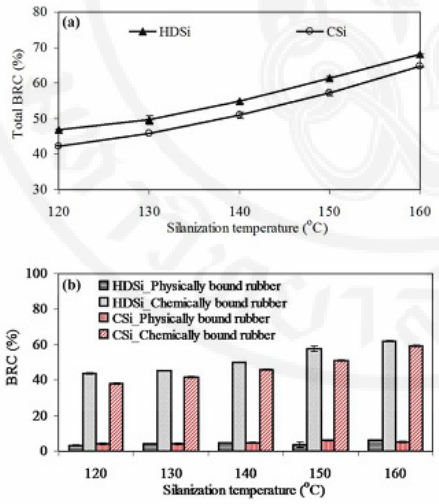

Figure 2. Types of BRC of the compounds prepared with various silanization temperature: (a) total BRC and (b) physically and chemically bound rubber. [Color figure can be viewed in the online issue, which is available at wileyonlinelibrary.com.]

Approximately 5 mg of rubber compound was dissolved in 5 mL of tetrahydrofuran (THF) for 5 days. The solution (100 μL) was filtrated prior to being injected into the GPC instrument. The mobile phase was THF, and the flow rate of 1 mm/min was used.

Testing of Rubber Vulcanizates

Vulcanization was carried out in a hydraulic hot press (Wabash MPI G30-15-0X, USA) at 160°C based on the optimum cure time measured from MDR. Cross-link density was reported in terms of a swelling ratio. Rubber test pieces were immersed in toluene for 5 days. After the immersion, the specimens were blotted off with filter paper prior to the determination of mass change. The swelling ratio was calculated based on the equation as follows:

$$\text{Swelling ratio}\,(\%) = \frac{(W_1 - W_0)}{W_0} \times 100 \quad (2)$$

where W_0 and W_1 are the weights of the test specimen before and after swelling, respectively.

Determination of hardness was carried out using a Shore A durometer (Wallace H17A, UK) according to ISO 7619 Part 1. Tensile properties were determined using a universal testing machine (Instron 3366 series, USA) following ISO 37 (die type 1). Abrasion resistance test was performed by Akron abrasion tester (Gotech GT-7012-A, Taiwan) according to BS 903: Part A9, Method B. Heat build-up (HBU) was evaluated in terms of temperature rise at specimen base following ISO 4666 by the use of a Goodrich flexometer (BF Goodrich Model II, USA). After the HBU test, dynamic set was also evaluated. The specimens were taken from the test chamber and left at room temperature for 30 min before the measurement of their final height. The dynamic set is calculated using the following equation.

$$\text{Dynamic set}\,(\%) = \frac{(H_0 - H_f)}{H_0} \times 100 \quad (3)$$

where H_0 and H_f are the original and final heights of the specimen, respectively. Dynamic properties were evaluated in tension mode using a dynamic mechanical thermal analyzer (DMTA: Gabo Qualimeter Eplexor 25N, Germany). For temperature sweep test, the test conditions were as follows: static strain of 1%, dynamic strain of 0.15%, frequency of 10 Hz, and heating rate of 2°C/min. The temperature was scanned from −60°C to

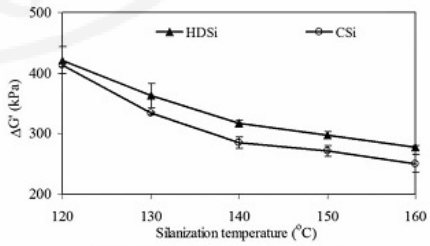

Figure 3. Payne effect of the compounds.

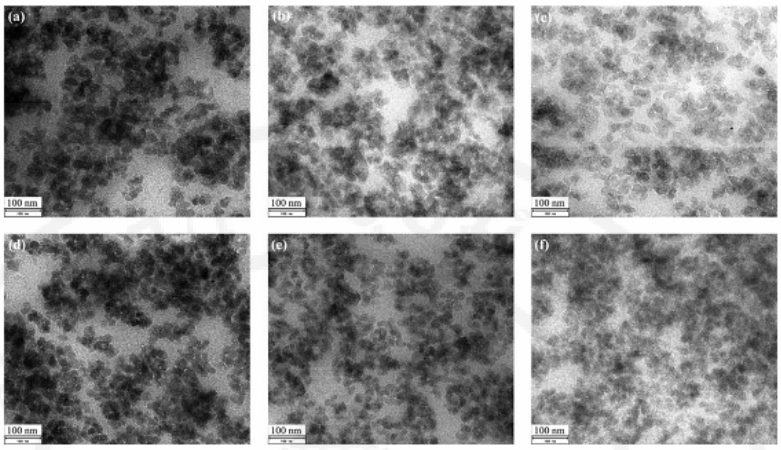

Figure 4. TEM micrographs (x20,000) of the silica-filled vulcanizates at various silanization temperatures: (a) HDSi_120°C, (b) HDSi_140°C, (c) HDSi_160°C, (d) CSi_120°C, (e) CSi_140°C, and (f) CSi_160°C.

80°C. To perform the strain sweep test, the static strain and frequency were set at 12% and 10 Hz, respectively. The dynamic strain was varied from 0.03% to 10% at both 0°C and 60°C. The degree of filler dispersion was examined by transmission electron microscopy (TEM, JEOL JEM-2010, Japan) under an accelerating voltage of 200 kV. TEM images were taken on the ultra-thin sections of the specimens prepared under cryogenic condition at −70°C using an ultra-microtome (Leica EM FCS, Austria).

RESULTS AND DISCUSSION

Mixing Behavior in Silanization Step

Table II represents dump temperature and temperature rise of the compounds recorded during the silanization step. As expected, the dump temperature increases continuously with increasing silanization temperature whereas the temperature rise remarkably decreases with increasing silanization temperature up to 140°C and then tends to level off. Such decrease in temperature rise with increasing silanization temperature is explained as follows; with increasing silanization temperature, bulk viscosity is reduced and, thus the shear heating during the mixing process. However, at high silanization temperatures (≥140°C), the effect of scorching phenomenon, because of the released sulfur from TESPT, on bulk viscosity is more dominant leading to the insignificant changes of viscosity and, thus, temperature rise. Similar observation is also reported in which the scorch could be found in the SSBR/BR blend when mixed with TESPT at high temperature.[17] It is also found that dump temperature and temperature rise are independent of silica type.

Compound and Vulcanizate Properties

Figure 1 discloses storage modulus (G') at high strain of 100% measured by RPA2000 and Mooney viscosity of the compounds. As can be seen, G' at high strain and Mooney viscosity increase slightly with increasing silanization temperature up to 140°C and then dramatically increase thereafter. The possible explanations are given to the enhancement in magnitude of rubber–filler interaction (see Figure 2) and the scorching phenomenon induced by TESPT which is more pronounced at high temperature as previously discussed. The findings imply the decreased mobility of rubber molecules with increasing silanization temperature. Results presented in

Table III. Cure Characteristics of the Compounds

	HDSi		CSi	
Silanization temperature (°C)	t_s1 (min)	t_c90 (min)	t_s1 (min)	t_c90 (min)
120	0.85 ± 0.04	15.45 ± 0.16	0.54 ± 0.04	15.02 ± 0.12
130	0.86 ± 0.02	16.55 ± 0.06	0.82 ± 0.03	16.63 ± 0.45
140	1.11 ± 0.04	17.56 ± 0.05	1.00 ± 0.04	18.26 ± 0.28
150	1.43 ± 0.09	19.40 ± 0.06	1.26 ± 0.05	19.32 ± 0.49
160	2.46 ± 0.01	20.88 ± 0.08	2.03 ± 0.06	21.60 ± 0.59

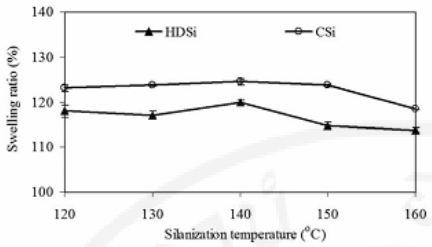

Figure 5. Relationship between swelling ratio of the vulcanizates and silanization temperature.

Figure 1 also reveal that HDSi-filled compounds possess considerably higher G' at high strain and Mooney viscosity than CSi-filled compounds. The greater rubber–filler interaction and the higher structure level of HDSi could be the reasonable explanations for this finding.

The relationship between BRC and silanization temperature is given in Figure 2. With increasing silanization temperature, both total BRC and chemically bound rubber consecutively increase. Moreover, the portion of chemically bound rubber is obviously higher than that of physically bound rubber. The results imply that the increased silanization temperature can improve the rubber–filler interaction via the coupling reaction, resulting in the strong chemical interaction between rubber and silica. At a given silanization temperature, HDSi provides greater total BRC and chemically bound rubber content, compared to CSi, suggesting the stronger rubber–filler interaction.

Figure 3 depicts Payne effect of the compounds as a function of silanization temperature. Generally, the greater the Payne effect magnitude, the larger the amount of filler network. As expected, with increasing silanization temperature, the Payne magnitude tends to decrease revealing a reduction in filler network caused by the silanization reaction between ethoxysilyl groups of TESPT and silanol groups on silica surfaces. Since the Payne magnitude is greater in the system filled with HDSi, it could be said that HDSi gives stronger filler–filler interaction than CSi, possibly because of its higher structure.

Figure 4 represents TEM micrographs (×20,000) of the vulcanizates. As expected, the dispersion of silica is improved with increasing silanization temperature regardless of silica type. The results are in good accordance with the Payne effect results. The decreased hydrophilicity of silica surfaces after silanization reaction and the enhancement in rubber–filler interaction via the coupling reaction are believed to be responsible for such finding. Unexpectedly, at any given silanization temperature, both HDSi and CSi demonstrate comparable degree of dispersion. The relatively long mixing time used in this experiment which might override the silica type effect is proposed to explain such findings.

Cure characteristics of the compounds are exhibited in Table III. It can evidently be seen that both scorch time (t_s1) and optimum cure time (t_c90) tend to increase with increasing silanization temperature, attributed mainly to the reduced concentration of curatives in the rubber matrix caused by the increase in the amount of mobilized rubber because of the improved filler dispersion. Results also reveal that cure characteristics of the compounds are independent of silica type.

The relationship between swelling ratio and silanization temperature is shown in Figure 5. Change of swelling ratio is not noticeable with increasing silanization temperature up to 140°C. However, at higher silanization temperatures, swelling ratio tends to decrease significantly due possibly to the increased rubber–filler interaction. It has been reported that the tightly bound rubber could restrict the rubber molecules from swelling and, thus, could behave as cross-link points in rubber vulcanizates.[23] Again, as HDSi provides considerably higher magnitude of rubber–filler interaction, the HDSi-filled vulcanizates therefore shows lower swelling ratio than the CSi-filled vulcanizates.

Table IV summarizes mechanical properties of the vulcanizates. In spite of the enhanced rubber–filler interaction and cross-link density (particularly at silanization temperature >140°C), the reduction in hardness with increasing silanization temperature is found, possibly because of the dominant effects of the reduced magnitude of filler network and molecular weight of rubber matrix (see Table V), as measured by a GPC technique. The results obtained from GPC exhibit that the molecular weight of rubber in the compounds tends to decrease with increasing silanization temperature, revealing the thermal degradation of rubber at high silanization temperature. Because of the combined consequences of the greater magnitudes of rubber–filler interaction, filler network, and cross-link density, the HDSi-filled vulcanizate shows significantly higher hardness than the CSi-filled vulcanizate.

Table IV. Mechanical Properties of the Vulcanizates

	HDSi				CSi			
Silanization temperature (°C)	Hardness (Shore A)	TS (MPa)	M100 (MPa)	Volume loss (mm^3)	Hardness (Shore A)	TS (MPa)	M100 (MPa)	Volume loss (mm^3)
120	69.3 ± 0.6	19.8 ± 0.2	3.2 ± 0.1	39.2 ± 0.5	67.4 ± 0.7	20.4 ± 1.7	3.0 ± 0.1	30.5 ± 0.8
130	67.1 ± 0.2	20.3 ± 0.7	3.3 ± 0.1	38.4 ± 1.8	66.1 ± 0.4	19.7 ± 1.9	3.0 ± 0.1	29.9 ± 1.0
140	66.1 ± 0.4	20.2 ± 1.0	3.3 ± 0.1	35.5 ± 0.8	64.7 ± 0.6	19.0 ± 1.0	3.1 ± 0.2	28.8 ± 0.7
150	63.9 ± 0.4	19.8 ± 0.6	3.8 ± 0.1	32.2 ± 0.7	63.4 ± 0.2	19.1 ± 0.8	3.1 ± 0.1	25.7 ± 0.5
160	63.0 ± 0.5	19.8 ± 0.7	4.0 ± 0.1	30.5 ± 0.8	61.3 ± 0.3	20.6 ± 1.4	3.8 ± 0.3	25.4 ± 0.8

Table V. Molecular Weight of Rubber Portion in the Compounds

	HDSi			CSi		
Silanization temperature (°C)	M_n (Daltons)	M_w (Daltons)	M_p (Daltons)	M_n (Daltons)	M_w (Daltons)	M_p (Daltons)
120	440,709	713,072	855,512	447,183	708,343	859,915
130	405,666	691,584	846,044	411,515	710,093	870,939
140	347,774	630,732	799,340	356,733	670,704	840,166
150	341,641	616,347	758,408	354,700	640,499	804,040
160	325,272	541,949	667,836	361,976	635,933	756,510

Unexpectedly, tensile strength (TS) does not significantly change with increasing silanization temperature, possibly because of the counter-balance between the reduced molecular weight and the increased filler dispersion and rubber–filler interaction. Results also suggest little effect of silica type on tensile strength.

Unlike hardness, modulus at 100% strain (M100) is found to increase with increasing silanization temperature. This might be attributed to the dominant effects of the enhanced cross-link density and rubber–filler interaction. As expected, the higher modulus is observed in the HDSi-filled systems, because of the greater cross-link density and stronger rubber–filler interaction.

Results presented in Table IV also show that, with increasing silanization temperature, the volume loss is found to decrease meaning the improved abrasion resistance. The enhancements of rubber–filler interaction and degree of filler dispersion could be used to explain the results. Unexpectedly, the greater abrasion resistance is observed in the CSi-filled vulcanizates.

The effect of silanization temperature on HBU and dynamic set is displayed in Table VI. Because of the reduced magnitude of filler network and the increased rubber–filler interaction and cross-link density, HBU and dynamic set decrease slightly with increasing silanization temperature. Results also suggest that the silica type does not significantly influence HBU and dynamic set of the vulcanizates.

Figure 6 illustrates effect of silanization temperature on loss factor (tan δ). Glass transition temperature (T_g), tan δ_{max} and tan δ area extracted from Figure 6 are summarized in Table VII. The T_g of the vulcanizates tends to increase with increasing silanization temperature. This is understandable because, with increasing silanization temperature, the magnitude of rubber–filler interaction is enhanced, leading to the increased restriction of the molecular motion. It is also found that the values of tan δ_{max} and tan δ area increase consecutively with increasing silanization temperature indicating the greater amount of rubber chains participating in the glass transition which results from the improved filler dispersion. It has been reported that the tan δ value of filled polymer can be calculated using the following equation[24,25]:

$$\tan\delta_f = \frac{\tan\delta_u}{(1+B\varphi)} \quad (4)$$

where tan δ_f and tan δ_u are the tan δ_{max} values of filled and unfilled polymer, respectively, B is the phenomenological

Table VI. Heat Build-Up (HBU) and Dynamic Set of the Vulcanizates

	HDSi		CSi	
Silanization temperature (°C)	Heat build-up (°C)	Dynamic set (%)	Heat build-up (°C)	Dynamic set (%)
120	13.5 ± 0.5	4.64 ± 0.34	13.0 ± 0.0	4.39 ± 0.50
130	13.0 ± 0.0	4.50 ± 0.14	13.0 ± 0.0	4.44 ± 0.12
140	13.0 ± 0.0	4.30 ± 0.09	13.0 ± 0.0	4.18 ± 0.37
150	13.0 ± 0.0	4.37 ± 0.18	12.5 ± 0.7	4.00 ± 0.11
160	12.5 ± 0.7	3.76 ± 0.06	12.0 ± 0.0	3.68 ± 0.12

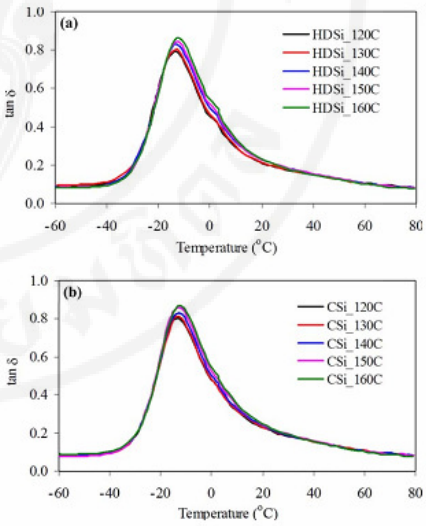

Figure 6. Loss factor (tan δ) as a function of test temperature of the vulcanizates at various silanization temperatures: (a) HDSi and (b) CSi. [Color figure can be viewed in the online issue, which is available at wileyonlinelibrary.com.]

Table VII. Glass Transition Temperature (T_g), Tan δ_{max} and Tan δ Area of the Vulcanizates

	HDSi			CSi		
Silanization temperature (°C)	T_g (°C)	tanδ_{max}	tanδ area (°C)	T_g (°C)	tanδ_{max}	tanδ area (°C)
120	−14.0	0.787	15.36	−13.7	0.787	15.95
130	−13.5	0.803	15.71	−13.3	0.802	16.06
140	−12.9	0.828	16.35	−12.8	0.828	16.55
150	−12.8	0.842	16.77	−12.6	0.840	17.42
160	−12.2	0.862	17.35	−12.1	0.864	17.38

interaction parameter which is directly related to the polymer–filler interaction, and φ is the effective volume fraction of filler. As tan δ_{max} increases continuously with increasing silanization temperature, the results indicate that the multiple of $B\varphi$ must be decreased. However, since B is increased with increasing silanization temperature as evidenced from the BRC results, φ must be greatly decreased. The reduction of φ with increasing silanization temperature arises from the improved filler dispersion. Results also demonstrate that silica type provides little effect on T_g and tan δ_{max} values. However, it is observed that CSi gives slightly higher tan δ area than HDSi, possibly attributed to its lower structure and, thus, trapped rubber.

In tire application, tan δ values at 0°C and 60°C are usually used to predict WG and RR, respectively.[2,7,8] The higher the tan δ at 0°C, the better the WG of vulcanizates. The lower the tan δ at 60°C, the lower the RR of vulcanizates. The tan δ values of the vulcanizates as a function of dynamic strain from 0.03% to 10% at 0°C are represented in Figure 7. It is found that, at a given strain, WG of the vulcanizates as indicated from the tan δ at 0°C increases continuously with increasing silanization temperature. Unexpectedly, both HDSi and CSi demonstrate comparable WG. Results in Figure 7 also show that the tan δ value increases with increasing dynamic strain up to 3% strain and, then decreases afterwards. The initial increase of tan δ is caused mainly by the increased destruction of filler network whereas the reduced tanδ at high strain results from the disappearance of filler network.

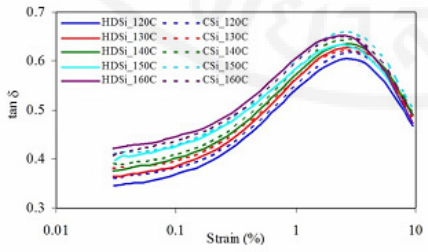

Figure 7. Loss factor (tan δ) as a function of dynamic strain at 0°C of the vulcanizates. [Color figure can be viewed in the online issue, which is available at wileyonlinelibrary.com.]

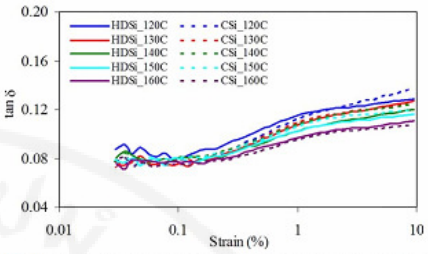

Figure 8. Loss factor (tan δ) as a function of dynamic strain at 60°C of the vulcanizates. [Color figure can be viewed in the online issue, which is available at wileyonlinelibrary.com.]

Figure 8 discloses the tan δ at 60°C of the vulcanizates as a function of dynamic strain. As expected, RR tends to decrease with increasing silanization temperature. Explanation is given by the improved rubber–filler interaction, leading to the lower magnitude of molecular slippage on the filler surfaces during the deformation and, hence, the lower energy dissipation. Similar to WG, RR of the vulcanizates is independent of the silica type. Although HDSi gives greater rubber–filler interaction and cross-link density than CSi, in the meantime, it provides higher

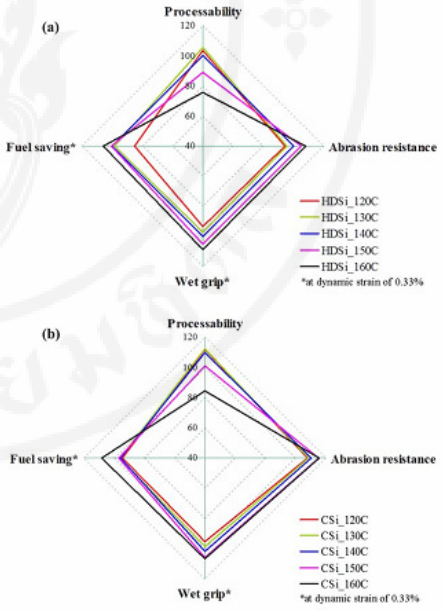

Figure 9. Normalized graph of processability and tire performance at various silanization temperatures (a) HDSi and (b) CSi. [Color figure can be viewed in the online issue, which is available at wileyonlinelibrary.com.]

magnitude of filler network available for energy dissipation. HDSi and CSi therefore give comparable RR.

Figure 9 represents the effect of silanization temperature on processability (evaluated from Mooney viscosity) and tire performance in terms of the normalized graph. Clearly, the balanced properties are found at the silanization temperature of 140°C.

CONCLUSIONS

With increasing silanization temperature, the tire performance, e.g., WG, RR, and abrasion resistance are significantly improved with the sacrifice of processability. Such improvements arise from the enhanced rubber–filler interaction, improved filler dispersion and increased cross-link density. Overall, the silanization temperature of 140°C provides a good balance between tire performance and processability. Surprisingly, HDSi and CSi demonstrate comparable degree of filler dispersion, scorch time (t_s1), optimum cure time (t_c90), tensile strength, HBU, dynamic set, including WG and RR. The results reveal that silica type has little effect on tire performance, as long as the sufficiently long mixing time is employed.

ACKNOWLEDGMENTS

The authors thank the Thailand Research Fund (TRF) through the Research and Researchers for Industries (RRi) and Siam Rubber Ltd., Part (Grant PHD56I0074) for financial support throughout this study.

REFERENCES

1. Hirata, Y.; Kondo, H.; Ozawa, Y. In Chemistry, Manufacture and Applications of Natural Rubber; Kohjiya, S.; Ikeda, Y., Eds.; Woodhead Publishing: UK, **2014**; Chapter 12, p 325.
2. Muraki, T.; Ishikawa, Y. U.S. Patent 5,500,482, **1996**.
3. Rao, G. V.; Mouli, S. C.; Boddeti, N. K. *Int. J. Eng. Technol.* **2010**, *2*, 87.
4. Wang, Y. X.; Wu, Y. P.; Li, W. J.; Zhang, L. Q. *Appl. Surf. Sci.* **2011**, *257*, 2058.
5. Karak, N.; Gupta, B. R. K. *Kautsch. Gummi Kunstst.* **2000**, *53*, 30.
6. Saeed, F.; Ansarifar, A.; Ellis, R. J.; Haile-Meskel, Y.; Irfan, M. S. *J. Appl. Polym. Sci.* **2012**, *123*, 1518.
7. Liu, X.; Zhao, S.; Zhang, X.; Li, X.; Bai, Y. *Polymer* **2014**, *55*, 1964.
8. Ko, J. Y.; Prakashan, K.; Kim, J. K. *J. Elastom. Plast.* **2012**, *44*, 549.
9. Lee, H. G.; Kim, H. S.; Cho, S. T.; Jung, I. T.; Cho, C. T. *Asian J. Chem.* **2013**, *25*, 5251.
10. Zafarmehrabian, R.; Gangali, S. T.; Ghoreishy, M. H. R.; Davallu, M. *E J. Chem.* **2012**, *9*,
11. Rattanasom, N.; Saowapark, T.; Deeprasertkul, C. *Polym. Test.* **2007**, *26*, 369.
12. Liu, Y.; Li, L.; Wang, Q. *J. Appl. Polym. Sci.* **2010**, *118*, 1111.
13. Ayippadath Gopi, J.; Patel, S.; Chandra, A.; Tripathy, D. *J. Polym. Res.* **2011**, *18*, 1625.
14. Rauline, R. Patent EP 0 501227 A1, **1992**.
15. Waddell, W. H.; Evans, L. R. In Rubber Technology: Compounding and Testing for Performance; Dick, J. S., Ed.; Hanser Publishers: Munich, **2001**; Chapter 13, p 325.
16. Goerl, U.; Hunsche, A.; Mueller, A.; Koban, H. G. *Rubber Chem. Technol.* **1997**, *70*, 608.
17. Reuvekamp, L. A. E. M.; Brinke, J. W.; Swaaij, P. J.; Noordermeer, J. W. M. *Kautsch. Gummi Kunstst.* **2002**, *55*, 41.
18. Kaewsakul, W.; Sahakaro, K.; Dierkes, W. K.; Noordermeer, J. W. M. *Rubber Chem. Technol.* **2012**, *85*, 277.
19. Wolff, S. *Rubber Chem. Technol.* **1982**, *55*, 967.
20. Chakraborty, S.; Shah, D.; Silica, M. *Rubber World* **2013**, 37. pp
21. Wolff, S.; Wang, M. J.; Tan, E. H. *Chem. Technol.* **1993**, *66*, 163.
22. Wolff, S. *Rubber Chem. Technol.* **1996**, *69*, 325.
23. Valentín, J. L.; Mora-Barrantes, I.; Carretero-González, J.; López-Manchado, M. A.; Sotta, P.; Long, D. R.; Saalwächter, K. *Macromolecules* **2010**, *43*, 334.
24. Ziegel, K. D.; Romanov, A. *J. Appl. Polym. Sci.* **1973**, *17*, 1119.
25. Qu, L.; Yu, G.; Xie, X.; Wang, L.; Li, J.; Zhao, Q. *Polym. Compos.* **2013**, *34*, 1575.

BIOGRAPHY

NAME	Mr. Puchong Thaptong
DATE OF BIRTH	6 January 1979
PLACE OF BIRTH	Kanchanaburi, Thailand
INSTITUTIONS ATTENDED	Mahidol University, 1998 – 2002: Bachelor of Science (Chemistry) Mahidol University, 2012 – 2016: Doctor of Philosophy (Polymer Science and Technology)
RESEARCH GRANTS	Thailand Research Fund (TRF): Research and Researcher for Industries (RRi), Siam Rubber Ltd., Part. Grant number: PHD56I0074
HOME ADDRESS	429 Moo 2 Nongri Bophloi Kanchanaburi, 71220 Tel. +66-3464-6131
EXPERIENCE	Rubber Chemist, October 2002 – January 2004 Research Assistant, February 2004 – Present
PRESENTATION	RRi congress I: Bangkok, Thailand July 22, 2015 Global Rubber, Latex & Tire Expo 2016 (GRTE 2016) Bangkok, Thailand March 9 – 11, 2016

PUBLICATION

Sae-oui P, Sirisinha C, Thepsuwan U, **Thapthong P**. Influence of Accelerator Type on Properties of NR/EPDM Blends. Polymer Testing (2007);26:1062-67.

Sae-oui P, Sirisinha C, **Thaptong P**. Utilization of Limestone Dust Waste as Filler in Natural Rubber. Journal of Material Cycles and Waste Management (2009);11:166-71.

Sae-oui P, Sirisinha C, Sa-nguanthammarong P, **Thaptong P.** Properties and Recyclability of Thermoplastic Elastomer Prepared from Natural Rubber Powder (NRP) and High Density Polyethylene (HDPE). Polymer Testing (2010);29:346-51.

Sae-oui P, Sirisinha C, **Thaptong P**, Intiya W. Possible Use of Ultra Fine Acrylonitrile Butadiene Rubber Powder (UFNBRP) as Filler in Natural Rubber (NR) Vulcanizates. Journal of Applied Polymer Science (2010);118:353-58.

Sae-oui P, Sirisinha C, Intiya W, **Thaptong P.** Properties of Natural Rubber Filled with Ultrafine Carboxylic Acrylonitrile Butadiene Rubber Powder. Advance in Polymer Technology (2011);30(3):183-90.

Sae-oui P, Thepsuwan U, Sirisinha C, **Thaptong P.** Comparison of Reinforcing Efficiency of Carbon Black, Conductive Carbon Black, and Carbon Nanotube in Natural Rubber. Advance in Polymer Technology (2014);33(4):21422.

Thaptong P, Sirisinha C, Thepsuwan U, Sae-oui P. Properties of Natural Rubber Reinforced by Carbon Black-based Hybrid Fillers. Polymer-Plastics Technology and Engineering (2014);53:818-23.

Thaptong P, Sirisinha C, Sae-oui P. Effects of Silanization Temperature and Silica Type on Properties of Silica-filled Solution Styrene Butadiene Rubber (SSBR) for Passenger Car Tire Tread Compounds. Journal of Applied Polymer Science (2016);133:43342.

Thaptong P, Sirisinha C, Sae-oui P. Influences of Styrene Butadiene Rubber (SBR) and Silica Types on Performance of Passenger Car Radial (PCR) Tire Tread. Rubber Chemistry and Technology. **(Submitted)**